Analysis of abovementioned results shows that suggestion of instantaneous injection allows to describe propagation of scr when function $\varkappa_r(r,R)$ can not be factorized with respect to r and R and of $\varkappa_r \sim r^{\delta} R^{\alpha}$,then $\partial\delta/\partial R > 0$ and at r=1 A.U. α=0.3-0.6 that is in good agreement with the data on frequency power spectrum of interplanetary magnetic field fluctuation.

REFERENCES

Dolginov A.Z., Toptygin I.N., ZHETF,1966,v.51,p.1771-1783.

Jokipii J.R.,Levy E.H., Astrophys. J.,1977,v.213, p.L85-L88.

Kolomeets E.V., Sevos'tyanov V.N., Stekol'nikov N.V.,17 ICRC, 1981, v.3, p.322-325.

Krylov V.I.,Bobkov V.V.,Monastyrsky P.I. Vychislitel'nye metody, M., 1977, v.2, p.155.

Lanzerotti L.J. YII Leninrgrad Mezhdun. Sem.,L., p.161.

Palmeira R.A.R., et al., Leningrad Mezhdun. Sem., 1971,p. 76-151.

C-6

N85-34825

SH 3.2-10

DIFFUSION-CONVECTION FUNCTION OF COSMIC RAYS

Gongliang Zhang and Guang Yang*
Institute of Space Physics, Academia Sinica
Beijing, China

ABSTRACT

This paper presents the fundamental properties and some numerical results of the solution of the diffusion equation of an impulsive cosmic-ray point source in an uniform, unbounded and spherically symmetrical moving medium.

I. INTRODUCTION The diffusion-convection(D-C) function is an elementary composite function of the solution of the D-C equation for the particles injected impulsively from a diffusive point source into a uniform, unbounded and spherically symmetrical medium. It is the analytic solution derived by the dimensional method for the propagation equation of solar cosmic rays in the heliosphere, i.e. the interplanetary space. Because of the introduction of convection effect of solar wind, a nonhomogeneous term appears in the propagation equation, it is difficult to express its solution in terms of the ordinary special functions. The research made so far has led to a solution containing only the first order approximation of the convection effect. Undoubtedly it is insufficient to study only the propagation of the particle with not too high energy. The solution we get with the dimensional method, up to date, is the most general solution of propagation equation in a uniform, unbounded and spherically symmetrical medium. It includes the higher orders of approximation for the convection effect, and has been used in discussing various kinds of propagation effects of solar cosmic ray, making propagation corrections and evaluating the equivalent diffusion coefficients.[1] The solution may also have its value for reference in the discussion of the diffusion in the ordinary moving medium.

It is necessary to point out that this solution is valid only in the case of a constant K. For the low energy particles, the energy of particles and also their diffusion coefficients change as a result of the adiabatic expension loss and other processes. In this case, such limitations can be retrieved by the equivalent diffusion coefficient reflecting the average nature of propagation space.

The diffusion equation in a uniform, unbounded and spherically symmetrical medium is

$$r^2\frac{\partial^2 U}{\partial r^2}+2r\frac{\partial U}{\partial r}-\frac{r^2}{K}\frac{\partial U}{\partial t}=\frac{Vr^2}{K}\frac{\partial U}{\partial r}+\frac{2CVr}{K}U \qquad (1.1)$$

where U is the number density of diffusing particle, C is a constant relating to the energy spectrum index. In the space far from the source, the solution satisfying condition

---

* Presently at Department of Physics, University of New Hampshire, Durham, NH 03824, U.S.A.

$U(r,t=0)=\frac{N}{4\pi r^2}\delta(r-r_0)$ and Eq. (1.1) is[1]

$$U(r,t)=\frac{N}{(4\pi r^2)^{3/2}}Z^{1/2}\exp\left[-\frac{(r-Vt)^2}{4Kt}\right]\phi(X,Z), \qquad (1.2)$$

where ϕ is 'diffusion-convection function' which the paper is going to discuss in detail. It can be expressed as a function of two dimensionless parameters as follows: Diffusion parameter $Z=r^2/(4Kt)$, Convection parameter for time $X=(2C-1)V(t/K)^{1/2}$. Disregarding ϕ, solution (1.2) is like a kind of the diffusion caused by a source moving outward with the convective velocity V. The equation of ϕ is

$$r^2\frac{\partial^2\phi}{\partial r^2}+r\frac{\partial\phi}{\partial r}\left(2-\frac{r^2}{Kt}\right)-\frac{r^2}{K}\frac{\partial\phi}{\partial t}=(2C-1)\frac{Vr}{K}\phi \qquad (1.3)$$

In case of no convection, $V=0$ and $\phi=1$, solution(1.2) is a function of a single parameter Z. When convective effect is not too strong, ϕ can be expanded into a power series of power series of parameter X: $\phi(X,Z)=\sum_{l=0}^{\infty}X^l F(l,Z)$, (1.4)

$F(l,Z)$ is called the l-th order influence function of convection, and its equation is

$$F''(l,Z)+\left[-1+\frac{3}{2}Z^{-1}\right]F'(l,Z)-\frac{1}{2}Z^{-1}F(l,Z)=\frac{1}{2}Z^{-3/2}F(l-1,Z) \qquad (1.5)$$

Seeing that the solution must be finite at the origin, $Z\sim0$, expression of $F(l,Z)$ can be taken as

$$F(l,Z)=\sum_{m=0}^{l}Z^{-m/2}\sum_{k=0}^{\infty}A(n,m,k)Z^k,\quad n=l-m. \qquad (1.6)$$

II. MAIN METHODS A(n,m,k) is a multiple series relating to m,and k, the lowest recurrence values for m and k are all zero. For the derivation of the general recurrence formula of A(n,m,k), it is instructive to evaluate first from the lower-order coefficient A(n,m-1,k) the next one A(n,m,k) byrecurring k. Then, the general formula of A(n,m,k) can be yielded as:

$$A(n,m,k)=A(n)Q(n,m)\left[\begin{matrix}\frac{n}{2}+m\\ \frac{m+1}{2},\ \frac{m+2}{2}\end{matrix}\right]_k S(n,m,k) \qquad (2.1)$$

$$Q(n,m)=\frac{(\frac{n}{2})_m}{(m+1)!},\ n\neq0;\quad Q(0,m)=\frac{2(m-1)!}{(m+1)},\ m\neq0;\ Q(0,0)=1 \qquad (2.2)$$

$$S(n,m,k)=\sum_{k_1=0}^{k}\frac{S(n,m-1,k_1)}{(\frac{n}{2}+m-1+k_1)(\frac{m}{2}+k_1)} \qquad (2.3)$$

$$S(n,m_0,k)=1,\ k=0,1,2,\cdots,\ m_0=0,\ n\neq0,\ m_0=1,\ n=0, \qquad (2.4)$$

where coefficient A(n) is determined by the initial condition.

The multiple series s(n,m,k) can be transformed into a series composed of the higher-order Γ function (function Ψ and G).

From the initial condition at $t=0$ and the asymptotic value (2.7) of function as $Z\to\infty$, the recurrence formula of coefficient A(l) can be yielded :

$$G_l=\sum_{m=0}^{l-1}\frac{A(n)}{\Gamma(\frac{n}{2})}\left(\frac{1}{2}\right)^m S(n,m)+A(0)\left(\frac{1}{2}\right)^{l-1}S(0,l)=0,\quad n=l-m,\ A(0)=1 \qquad (2.7)$$

The higher order coefficient A is difficult to express in a simple form. However, it is quite convenient to calculate A(1) with the recurrence formulae (2.3) and (2.5) by computer. It can be shown that A(1) is an alternative sequence, and its absolute value decreases when 1 increases.

Formula (1.5) is a nonhomogeneous equation. Its nonhomogeneous terms are composed of the same functions of lower order. The formula of function F(1,Z) can be derived from formulae (1.6) and (2.1):

$$F(l,Z)=\sum_{m=0}^{l} Z^{m/2}\, a(n,m)\, A(n)\, f(n,m,Z) \qquad (2.6)$$

The asymptotic value of f(n,m,Z) when t = o or $Z\to\infty$ is

$$f(n,m,Z)_{Z\to\infty} \sim \Gamma(\tfrac{1}{2})\, Z^{\frac{n-1}{2}} \exp(Z)\, \frac{(m+1)!}{\Gamma(n/2+m)} (\tfrac{1}{2})^{m} S(n,m) \qquad (2.7)$$

Therefrom the recurrence formula (2.5) of coefficient A(1) can be formulated.

III. DIFFUSION-CONVECTION FUNCTION $\phi(X,Z)$

For convenience of discussion, function ϕ can be rewritten as

$$\phi=\sum_{n+m=0}^{\infty} A(n)\, a(n,m)\, X^{n} Y^{m} f(n,m,Z) \qquad (3.1)$$

where Y is another dimensionless parameter, namely, the convection parameter for space: $Y = (2C-1)\frac{Vr}{2K} = XZ^{\frac{1}{2}}$ (3.2)

Fig. 1. illustrates the value of n for calculation of ϕ as a function of Y and T, when the relative magnitude of the last term os less than 10 . It can be seen that the term number of convergence increases with the value of Y and T. Function ϕ is probably divergent as X > 3.00. So, we often restrict our discussion to propagation problem within the range X ≤ 3.00.

Fig. 1.

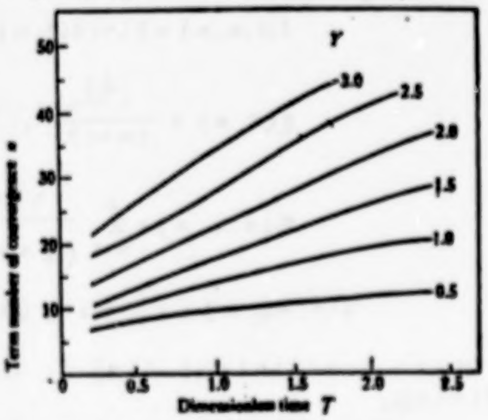

Abscissa is the dimensionless time T, ordinate is the number of terms summing up the function ϕ accurate to 10^{-7}.

IV. VARIATION OF DENSITY U Variation of D-C function with the convection parameter for space Y and thedimensionless time $T(=4Kt/r^2)$ have already been shown in Fig. 1. of [2] . Plotted here is the variation of diffusing particles density U with T under the different conditions of solar wind convections (Fig. 2.). A set of curves on the left side are the results calculated by Formula (1.2), taking $2C - 1 = 4$, or the differential-momentum-spectrum index of particles to be 5.5. Such case corresponds to that of the isotropic propagation. But in fact, propagation of cosmic rays particles in interplanetary space is anisotropic, the diffusion coefficient along the magnetic line $K_{\parallel}$ is different from the transverse one $K_{\perp}$. In this case, propagation equation becomes

$$U = \frac{N}{(4\pi r^2)^{3/2}} Z^{5/2} \frac{K_{\parallel}}{K_{\perp}} \left(\frac{\theta}{\sin\theta}\right)^{\frac{1}{2}} \exp\left[-Z\left(1+\frac{K_{\parallel}}{K_{\perp}}\theta^2\right)\right] \cdot \exp\left[H-\frac{H^2}{4Z}\right] \Phi(X,Z) \quad (4.1)$$

where is the magnetic azimuth of observation point from the source, and H is the modulation parameter, $H = \frac{Vr}{2K_{\parallel}}$ (4.2)

Substitute $k_{\parallel}$ for K when Z is calculated.

Solution (4.1) of the anisotropic propagation equation is drawn by a set of curves of the right side of Fig2 when $\theta = 0°$. It can be shown that the intensity of diffusing particles decreases and the maximum time moves up as the convection effect intensifies. Besides, the time scale of the isotropic D-C propagation is longer than that of the anisotropic one. Hence, it is possible to form an over estimation of equivalent diffusion coefficient if observational data is fitted merely by the former. However, better results can be got by using the model of anisotropic propagation.

Fig. 2.

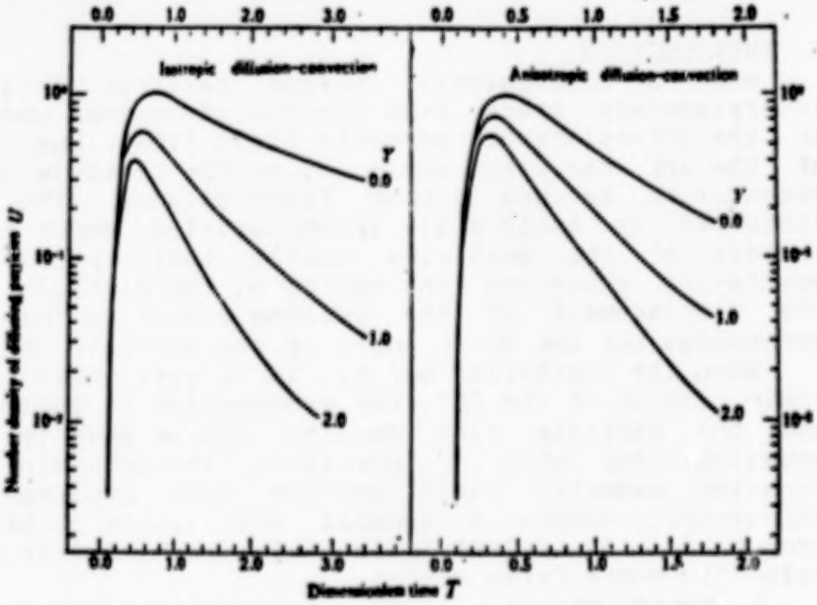

(a) Isotropic D-C (b) anisotropic D-C

REFERENCES

[1] Zhang, Gongliang, (1978), HIGH ENERGY PHYSICS AND NUCLEAR PHYSICS, 2, 200.

[2] Zhang, Gongliang, SCIENTIA SINICA, 22(1979), 934.

N85-34826

SH 3.2-11

MONTE CARLO CALCULATIONS OF RELATIVISTIC SOLAR PROTON PROPAGATION IN INTERPLANETARY SPACE

M.Lumme, J.J.Torsti, E.Vainikka, J.Peltonen,
M.Nieminen, E.Valtonen, and H.Arvela

Department of Physical Sciences, University of Turku, and
Wihuri Physical Laboratory, University of Turku
SF-20500 Turku, Finland

ABSTRACT

Particle fluxes and pitch angle distributions of relativistic solar protons at 1 AU have been determined by Monte Carlo calculations. The analysis covers two hours after the release of the particles from the Sun and total of $8 \cdot 10^6$ particle trajectories were simulated. The pitch angle scattering was assumed to be isotropic and the scattering mean free path was varied from 0.1 to 4 AU.

As an application, the solar injection time and interplanetary scattering mean free path of particles that gave rise to the GLE on May 7, 1978 were determined. Assuming exponential form, the injection decay time was found to be about 11 minutes. The m.f.p. of pitch angle scattering during the event was about 1 AU.

1. INTRODUCTION

When a relativistic charged particle is injected into the interplanetary space from the Sun it becomes under the influence of the interplanetary magnetic field (IMF). Due to the divergence of the IMF, the pitch angle, α, of the particle decreases and the propagation becomes almost field-aligned. The nominal IMF is disturbed by small-scale irregularities, which act as scattering centers of the particles during their propagation. In these scattering processes the energy of the particle is conserved and the displacement of the guiding center is only of order of the gyroradius but the pitch angle of the particle changes.

When the scattering m.f.p., λ, is very small compared with the scale lenght of the IMF, the propagation is dominantly stochastic and the particle flux density can be described by a diffusion equation. But when λ increases, the deterministic role of the focusing magnetic field becomes more important. During highly anisotropic events a general description of the interplanetary propagation of relativistic solar particles is possible only by using the Monte Carlo method.

Lockwood et al. (1982) have applied the particle distributions calculated by Monte Carlo method in an analysis of the GLE on May 7, 1978. They found an average scattering m.f.p. of 5 AU during this event.

2. PARTICLE PROPAGATION IN THE IMF

2.1. Magnetic Focusing. In this work we have approximated the interplanetary magnetic field by the classical Archimedean spiral field. The angular velocity of the Sun was $2.865 \cdot 10^{-6}$ rad/s and the solar wind speed was 450 km/s, which is slightly above its average quiet time value.

The conservation of both the magnetic moment and the momentum of a particle during its propagation in a magnetic field of strength B, states that $\sin^2\alpha/B$ remains constant.

2.2. Pitch Angle Scattering. The scattering of a particle from magnetic irregularities depends, in addition to the rigidity of the particle, also on the strength and structure of the scattering centers. If the distribution is forward with respect to the direction of motion before scattering, there is less backscattering and consequently the total particle flux decreases faster, than if the scattering were isotropic. In this work we chose the pitch angle scattering to be isotropic.

2.3. The Monte Carlo Method. The particles were injected isotropically from the solar corona at a distance of 0.02 AU from the center of the Sun. The distance to the first scattering along the field line was taken to be $\Delta s = -\lambda \ln x$, where x is a random number evenly distributed between 0 and 1. After the scattering, a new pitch angle was given by $\alpha = \arccos(1 - 2x)$, where x is a new random number. Then the distance Δs to the next scattering center was determined as above. During two hours after the injection, the time elapsed and the pitch angle were recorded every time the particle passed 1 AU in either direction.

The number of trajectories calculated in this analysis varied from $5 \cdot 10^5$ (λ=0.1 AU) to $2 \cdot 10^6$ (λ=4 AU).

2.4. Anisotropy. Let us denote by $F(\alpha)$ the pitch angle distribution and by $I(\alpha_0)$ the average density of particles having the pitch angle $\alpha \leq \alpha_0$, and by $I(\overline{\alpha}_0)$ the average density for $\alpha > \alpha_0$. The anisotropy of the solar particle flux is conventionally defined by either

$$A = \frac{F(0^\circ) - F(180^\circ)}{F(0^\circ) + F(180^\circ)} \qquad \text{or} \qquad A = \frac{I(90^\circ) - I(\overline{90^\circ})}{I(90^\circ) + I(\overline{90^\circ})}$$

During solar particle events, the detectors at Earth, having their asymptotic directions of approach near the IMF field line, receive the majority of solar particles from a very narrow but finite cone. Therefore, we defined the anisotropy between two stations as

$$A = \frac{I_1 - I_2}{I_1 + I_2}$$

where I_1 and I_2 are the average particle densities in the asymptotic cones to which the stations 1 and 2 mainly respond.

3. RESULTS AND DISCUSSION

3.1. Intensity at 1 AU. The intensity-time profiles of particles at 1 AU after a delta-like injection are shown in Figure 1. The particles arriving during the first minute are, in addition to the unscattered particles, also those which are scattered either near the Sun, where the focusing is very rapid, or near 1 AU, where the distance to be travelled at large pitch angles is short, and also those scattered almost in the forward direction. Thus, the relative number of particles arriving during the first minute is higher than $\exp(-1.13/\lambda)$, which represents the theoretical unscattered component.

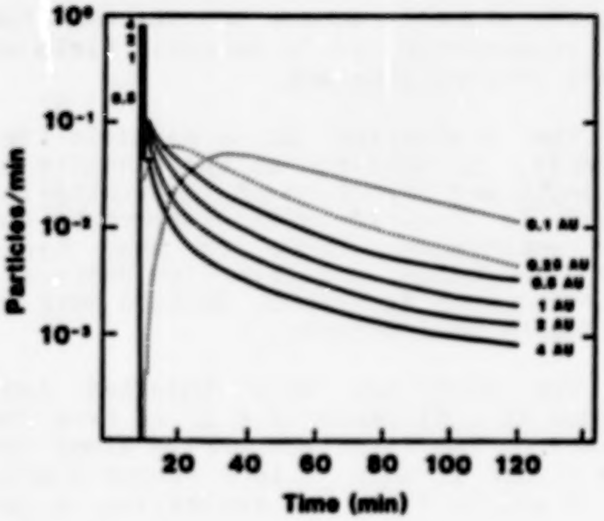

Fig. 1. Intensity-time profiles at 1 AU for various scattering mean free paths.

3.2. The May 7, 1978 Solar Particle Event. On May 7, 1978, an increase in the counting rates of ground level neutron monitors was recorded starting in the time interval 0335-0340 UT. The increase exceeded 50 % at several stations. At Kerguelen, which had its asymptotic directions of approach ideally connected with the apparent source direction, the increase was more than 200 %.

The apparent source direction, which is the direction of the IMF line at Earth, was chosen to be 5 N, 90 E. This was estimated using data from the world-wide network of neutron monitors (Shea et al. 1979). The co-rotational acceptance cone of Kerguelen was calculated by trajectory tracing method. The rigidities ranged from 3 to 10 GV, and also non-vertical directions were included.

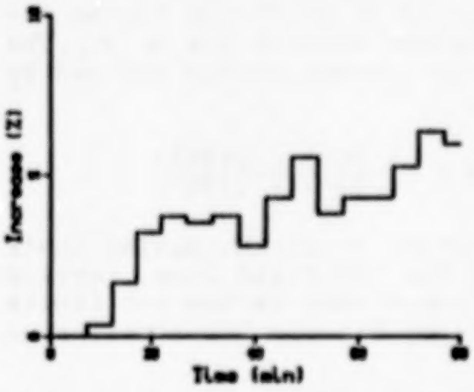

Fig. 2. Increase at "DRI".

Due to the large fluctuations at stations receiving only back-scattered particles, we introduced a fictive station "DRI", where both the counting rate increase and the asymptotic directions are averages of the stations Deep River and Inuvik. The increase at this station is shown in Figure 2. The pitch angle interval it responds to was taken to range from 120° to 160° during the entire event.

An observed intensity profile can be related to several injection profiles depending on the scattering mean free path. By increasing λ, also the injection time has to be increased, since the particle flux decreases faster (see Fig. 1). In the following we illustrate a method, where both injection time and mean free path of pitch angle scattering are deduced simultaneously.

We first parametrize the injection profile as $\exp(-t/\tau)$. At each of the scattering mean free paths, 0.5, 1, 2, and 4 AU, we then calculate the theoretical intensity profiles at Kerguelen for various values of τ. By comparing these profiles with the observed intensity profile we deduce the proper injection profile for each λ. In Figure 3 we show this comparison for $\lambda = 1$ AU. The best fit of the (λ, τ) pairs deduced in this way are (0.5 AU, 9 min), (1 AU, 11 min), (2 AU, 12 min), and (4 AU, 13 min).

Using these (λ, τ) pairs we then calculate the anisotropy Kerguelen vs. DRI. In Figure 4 we show these anisotropy curves together with the observed anisotropy. The figure indicates that λ = 1 AU and that the decay time of exponential injection is 11 minutes. This scattering mean free path is significantly smaller than the previously published 3 - 5 AU (Debrunner and Lockwood, 1980; Lockwood at al., 1982).

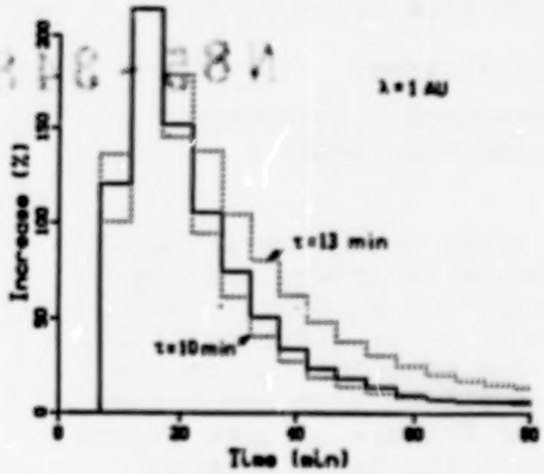

Fig. 3. Comparison between observed increase at Kerguelen (solid line) and increases deduced from Monte Carlo distributions at 1 AU (dotted, normalised at max increase).

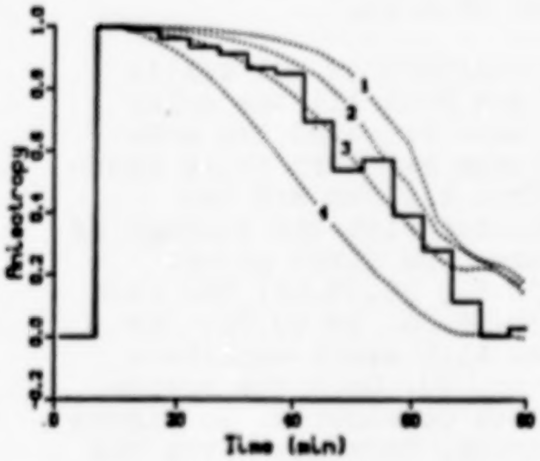

Fig. 4. Anisotropy Kerguelen vs. DRI during the GLE on May 7, 1978. Solid line: observed, dotted lines: theoretical curves: 1. λ = 4 AU, τ = 13 min; 2. 2 AU, 12 min ; 3. 1 AU, 11 min ; 4. 0.5 AU, 9 min.

4. CONCLUSIONS

The intensity profiles of the particles after a delta-like injection from the Sun show that the interplanetary propagation is diffusive only at scattering mean free paths below 0.5 AU.

The scattering mean free path during the May, 7, 1978 solar particle event was about 1 AU and represented by exponential form, the injection had a decay time of about 11 minutes.

5. ACKNOWLEDGEMENTS

We are grateful to D. Fouassier and to Margaret D. Wilson for providing us the data from Kerguelen and the Canadian stations.

REFERENCES

Debrunner H and Lockwood J A, J. Geophys. Res. 85, 6853(1990)
Lockwood J A, Debrunner H, Flückiger E, Neuenschwander H, and Schubnell M, J.Geophys. Res. 87, 4338(1982)
Shea M A et al., Proc. 18th Int. Cosmic Ray Conf. 5, 226(1979)

ON REFLECTING BOUNDARY BEHIND THE EARTH'S ORBIT AT PROPAGATION OF FAST PARTICLES FROM SOLAR FLARES

N85-34827

A.S.Niskovskikh, A.T.Filippov
Institute of Cosmophysical Research & Aeronomy,
Lenin Ave., 31, 677891 Yakutsk, USSR

1. Introduction. The flares of solar cosmic rays (SCR) associated with the presence of shocks in interplanetary magnetic field and with their propagation at significant heliocentric distances were always of great interest [1,2].

Here we consider some events and problems concerning the peculiarities of propagation of flare CR in the interplanetary medium. The distinguishing feature of such events is the presence of shock front behind the Earth's orbit having formed either directly in the process of shock generation on the Sun or at large heliocentric distances as a result of the interaction of fast and slow quasistationary recurrent solar wind (SW) streams. Based on the experimental material we show here that the significant nonlinear disturbances in IMF behind the Earth's orbit can yield the occurence of the additional SCR flux from shock front region as a result of the interaction of flare flux with shock and a partial reflection from it.

2. Method and Results. For the analysis on the available data of superneutron monitor net from all the solar proton events (SPE) for 1968-1984 were selected two main groups: the events at Forbush-decrease recovery phase associated with the passage of shock from the Sun and the events at GCR decrease phase associated with the passage of the interacting recurrent SW streams. The first group: 18,11.68, 07.08.72, 07.05.78, 12.10.81, 26.11.82; the second one: 25.02.69, 24-25.01.71, 30.04.76, 23.09.78. The identification of recurrent streams with small-amplitude Forbush-decreases was carried out on [3]. Only the events with reliable observational data were considered. In Figure are shown the examples from each group. Here are given the hourly intensity values for Alert (top) and 5-minute values for two stations having the oppositely directed "receiving cones" . Also are shown the asymptotic directions of particle arrival [4] for the following stations: Ap-Apatity, MG-Magadan, NS-Novosibirsk, Ya-Yakutsk, CAL-Calgary, D-R - Deep River, G-B - Goose Bay, CH-Churchill, D-Dallas, T-B - Tixie Bay, R-B - Resolute Bay. The length of vector is proportional to SCR increase amplitude. At the bottom is shown the qualitative picture of the reflecting boundary of two types. For all the events were built the analogous graphs and "receiving cones". The examples in Figure are typical for each group. In the Table are presented the onset time of increase (t_{ons}) for pairs of stations; the maximum ampli-

ORIGINAL PAGE IS
OF POOR QUALITY

tude (A, %); the vertical cut-off rigidity (R_c); the mean angle between asymptotic longitudes of energetic particles arrival for pairs of stations ($\Delta \varphi$) and the mean φ_{me} angle between the direction of "Receiving cone" and the mean IMF direction in helioequator plane (OX-axis is sunward directed) for the station having the earlier time of increase onset. As is seen from the Table t_{ons} difference for the stations "looking" field-aligned sunward and in the opposite direction is significant and it reaches 30–40 min (for the event not under consideration here 16.02.84 it is ~ 60 min). The differences in A, % are also available.

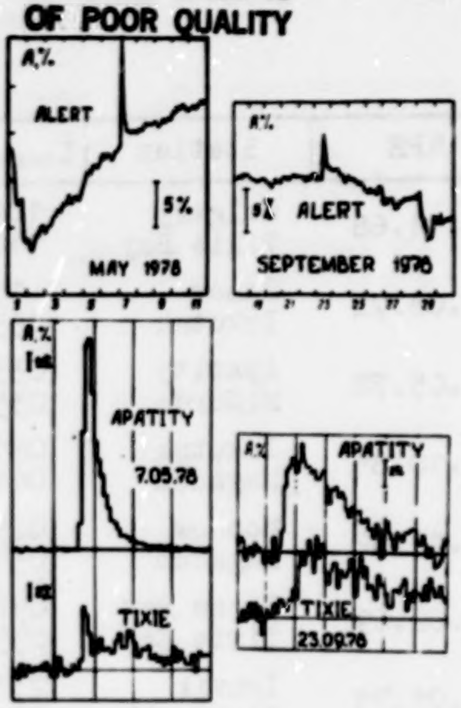

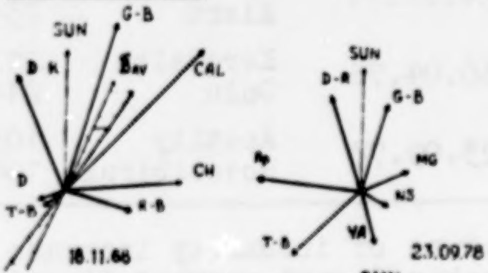

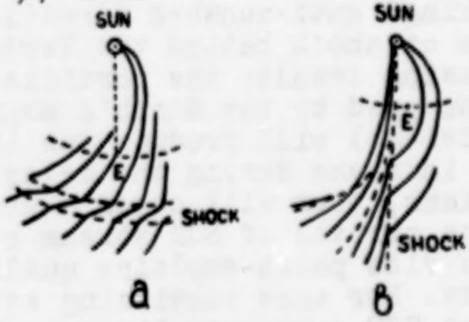

3. Discussion. Similar delays for particles with $E > 1$ GeV can hardly be explained by the diffusion process within the Earth's orbit. Therefore one can assume that shocks accompanying all these events are responsible for the time difference of SCR intensity increase onset. I.e. the delay was caused by the fact that after the passage of shock beyond 1 a.u. the IMF becomes a regular one [5] and flare SCR injected in such a medium being not inclined in the Earth's magnetosphere pass behind its orbit and be reflected from the shock reverse front (for recurrent streams a higher regularity degree of IMF was shown in [6]). In favour of the such argument is a positive correlation between the duration of delay of SCR increase onset and the time between Forbush-decrease onset and flare onset (i.e. the farther is shock behind the Earth's orbit, the longer is the delay time). The calculations [1] show that on the average the reflected particles change their pitch-angle by ~ 20°. This value mainly is independent of the initial particle velocity or of shock parameters. We can conclude that the most SCR streams and shock interactions (reflections) are with no particle isotropization. If to try to recover the

Table

SPE	Station	t_{ons}, UT	A,%	R_c,GV	Δ φ	φ_{mt}
18.11.68	Calgary	1045	17	1.07	~170°	~15°
	Tixie Bay	1105	2	0.45		
07.08.72	Sanae	1525	8	0.91	~170°	~15°
	Irkutsk	1555	1.5	3.56		
07.05.78	Apatity	0330	120	0.6	~180°	~15°
	McMurdo	0355	4	0.0		
12.10.81	Irkutsk	0610	4	3.56	~70°	-
	Magadan	0640	7.7	2.11		
26.11.82	Moscow	0250	4	2.39	~180°	-
	Magadan	0310	2	2.11		
25.02.69	Goose Bay	0920	16	0.6	~170°	~15°
	Tixie Bay	0950	2	0.45		
24.01.71	Inuvik	2330	14	0.16	~140°	~20°
	Alert	2340	15	0.0		
30.04.76	Kerguelen	2125	11	1.1	~110°	~45°
	Oulu	2140	4	0.77		
23.09.78	Apatity	1030	14	0.6	~150°	-
	Novosibirsk	1040	5	2.78		

picture of intensity increase change on SPE at the station "looking" anti-sunward direction taking into account the presence of shock behind the Earth's orbit, one can obtain the following result: the particles of direct SCR stream from the Sun trapped by the Earth's magnetosphere (if their number is sufficient) will produce the insignificant "diffusive" intensity increase during the delay of two oppositely "looking" stations, then will occur a sharp intensity increase caused by the arrival of SCR stream reflected from the shock. The above view point explains qualitatively both groups of events. For more convincing evidence of existence of the reflected SCR component the energy spectrum of reflected particles is of great interest. But its finding is impossible yet because of lack of data on stations "looking" strictly in the direction of the arrival of the reflected component.

At a detailed investigation in groups of each event were found the peculiarities which can be explained not only by the presence of shock behind the Earth's orbit, but also by the existence of "corks" near the Sun caused by thickening of IMF force lines in the direction towards photosphere. The similar peculiarities were manifested in "two-humped" change of SCR intensity increase. The first increase corresponds to the reflection from shock behind the Earth's orbit and has a delay ~ 20-25 min and the second one corresponds to the secondary reflection from the "cork" already with the delay ~ 50-60 min (such a phenomenon was observed for Tixie Bay on May 7, 1978).

4. Conclusion. From the above analysis one can conclude: it is most probable that for the peculiarities of SCR increase change in SPE on ground-based data (the delay of SCR increase onsets with E > 1 GeV at various stations; the significant difference in amplitudes; "two-humped" structure of increase etc) are responsible strong non-linear IMF disturbances (shocks) playing a role of the reflecting boundary for energetic particles.

References

1. Pesses, M.E., (1982), *Invited Paper Cospar Symposium on the Solar Maximum Year*, Canada.
2. Scholer, M., (1982), *Invited Talks 8-th European Cosmic Ray Symposium*, Roma, 1.
3. King, J.H., (1977), *Interplanetary Medium Data Book Appendix*. Report WDC-A, Maryland, USA.
4. *Cosmic Ray Tables*, *No.1*, (1983), WDC-C2, Tokyo, Japan.
5. Samsonov, I.S. i dr., (1979), *Kosmicheskiye Luchi Sverkhvysokikh Energii*, Yakutsk, 85.
6. Kozlov, V.I. i dr., (1974), *Izv. AN SSSR, Ser.Fiz.*, No.9, 1908.

N85-34828

THE DISPERSIVE EVOLUTION OF CHARGED-PARTICLE BUNCHES IN RANDOM MAGNETIC FIELDS

J.A. Earl

Dept. of Physics & Astronomy, Univ. of MD, College Park, MD 20742

ABSTRACT

Shortly after a strongly anisotropic beam of charged particles is injected along a guiding magnetic field on which is superimposed a small random component, the particle density can be represented by a Gaussian profile whose center moves with the coherent velocity V_* and whose width increases with time at a rate controlled by the coefficient of dispersion D_*. Both parameters depend upon the mean free path λ, which characterizes scattering by the random fields, and the focusing length L, which characterizes spatial variations of the guiding field. These dependences are known explicitly for V_*. Formulae for D_* are available only in the limits of very weak and very strong focusing. This paper presents a new expression for D_*, which spans this gap.

1. Introduction. The equation which describes particle transport along a guiding field under the combined influences of scattering by magnetic turbulence and focusing by spatial inhomogenieties of the guiding field is

$$\frac{\partial f}{\partial t} + \mu V \frac{\partial f}{\partial z} = \frac{1}{2} e^{G} \frac{\partial}{\partial \mu} \phi e^{-G} \frac{\partial f}{\partial \mu}, \tag{1}$$

where f is particle density in phase space, z is distance along the guiding field, μ is the pitch-angle cosine and V is particle velocity. If the coefficient of pitch-angle scattering is given by the standard form

$$\phi = \frac{3(V/\lambda)}{(2-q)(4-q)} (1-\mu^2) |\mu|^{q-1}, \tag{2}$$

where q is an index that measures the anisotropy of scattering, then the odd function G is given by

$$G(z,\mu) = -\frac{V}{B} \frac{\partial B}{\partial z} \int_0^\mu \frac{1-\nu^2}{\phi(z,\nu)} d\nu = \frac{(4-q)}{3} \frac{\lambda}{L} \mu |\mu|^{1-q}, \tag{3}$$

where L is the focusing length and B is the guiding field. Throughout this paper both λ and L will be assumed to be constant.

Even with these assumptions, it is not possible to solve the transport equation in closed form. However, there are approximations that provide considerable insight into phenomena, such as those outlined in the abstract, that do not fit into the familiar picture of purely diffusive transport. A first-order analysis (Earl, 1981; Kunstmann, 1979) leads to simplified transport equations which describe coherent propagation in terms of infinitely narrow pulses, but which do not include the dispersive spreading of these disturbances. This paper presents a second-order analysis which includes this effect.

In the context of new possibilities for numerical solutions opened up by advances in computer technology, the phenomenon of dispersion takes on special significance, for there is an artifact, which I call "numerical dispersion", and which can obscure the physical effect. (See Paper SH 4.1-4) Numerical dispersion is an artifact of the Boltzmann operator that appears on the left hand side of equation (1). Consequently, it is not affected by focusing. To avoid inaccuracies, it is necessary to specify sufficiently fine spatial resolution in the numerical implementation so that the numerical dispersion coefficient is much smaller than the physical one. This paper provides the quantitative knowledge of $D_\star$ needed to make this specification.

2. The Coefficient of Dispersion. The second approximation to the distribution function takes a form

$$f = F_\psi\{z,t\} + Be^G H_\phi\{z,t\} + W\{\mu\}\frac{\partial F_\psi}{\partial z} - Be^G W\{-\mu\}\frac{\partial H_\phi}{\partial z}, \quad (4)$$

in which the first two terms represent supercoherent and pseudodiffusive components that appeared in the first-order approximation and the second two are anisotropic components that are proportional to the spatial gradients of F_ψ and H_ϕ. Both of these additions involve the same function $W\{\mu\}$, but the sign of its argument is different in the two new terms. This relationship reflects a fundamental symmetry of focused transport that I call the "principle of complementarity". When equation (4) is substituted in the transport equation, and when the first-order transport equations are satisfied, the following equation for W is obtained:

$$\frac{1}{2}\frac{\partial}{\partial\mu} e^{-G}\frac{\partial W\{\mu\}}{\partial\mu} - \frac{V_\phi K}{L(K^2-1)} W\{-\mu\} = \left(\mu V + \frac{V_\phi^2 K}{(K^2-1)}\right) e^{-G} - \frac{V_\phi K}{(K^2-1)}, \quad (5)$$

where

$$K = \frac{1}{2}\int_{-1}^{+1} e^G \, d\mu, \quad (6)$$

is a normalization constant that goes from K = 1 in the limit of weak focusing ($\lambda/L \ll 1$) to $K = \infty$ in the limit of strong focusing, and

$$V_\phi = \frac{V}{2K}\int_{1}^{+1} \mu e^G \, d\mu, \quad (7)$$

is a characteristic velocity that I call the pseudodiffusive velocity. Note that this is not the coherent velocity $V_\star$, which is given by

$$V_\star = \frac{V_\phi K}{(K^2-1)^{1/2}} \,. \quad (8)$$

Although the presence of the term in $W\{-\mu\}$ complicates equation (5), it can be solved for W with the aid of the method of eigenfunctions. In fact, because this term is relatively small, W can be evaluated fairly accurately by a simple double integration.

When the additional terms in f are taken into account, the second-order transport equations take the forms

$$\frac{\partial F_\phi}{\partial t} - V_\phi \frac{\partial F_\phi}{\partial z} + \frac{B}{K} \frac{\partial H_\phi}{\partial t} = D_* \frac{\partial^2 F_\phi}{\partial z^2}, \tag{9}$$

and

$$\frac{\partial H_\phi}{\partial t} + V_\phi \frac{\partial H_\phi}{\partial z} + \frac{1}{BK} \frac{\partial F_\phi}{\partial t} = D_* \frac{\partial^2 H_\phi}{\partial z^2}, \tag{10}$$

in which the left hand sides reproduce the first-order transport equations and the right hand sides are second-order terms. Here, the coefficient of dispersion, given by

$$D_* = -\frac{1}{2K} \int_{-1}^{+1} d\mu \quad \left(\left(\mu V + \frac{V_\phi K^2}{K^2-1}\right) e^{-G} - \frac{V_\phi K}{K^2-1}\right) \; W(\mu), \tag{11}$$

determines the size of the new terms, which involve the second spatial derivatives of the supercoherent and pseudodiffusive components. They describe the dispersive aspect of coherent propagation, in which the delta function pulses of the first-order description are more accurately described as Gaussian disturbances whose centers move with the coherent velocity V_* while their widths increase with time at a rate controlled by the coefficient D_*.

In the figure, separate curves show how D_* depends upon (λ/L) when the function $W(\mu)$ is evaluated in three different ways. The dashed curve gives the exact result, in which the term in $W(-\mu)$ is retained in equation (5). The solid curve gives a much simpler result obtained from an approximate evaluation in which this term is ignored. For most applications, in which its ~20% deviation from the exact result is not important,

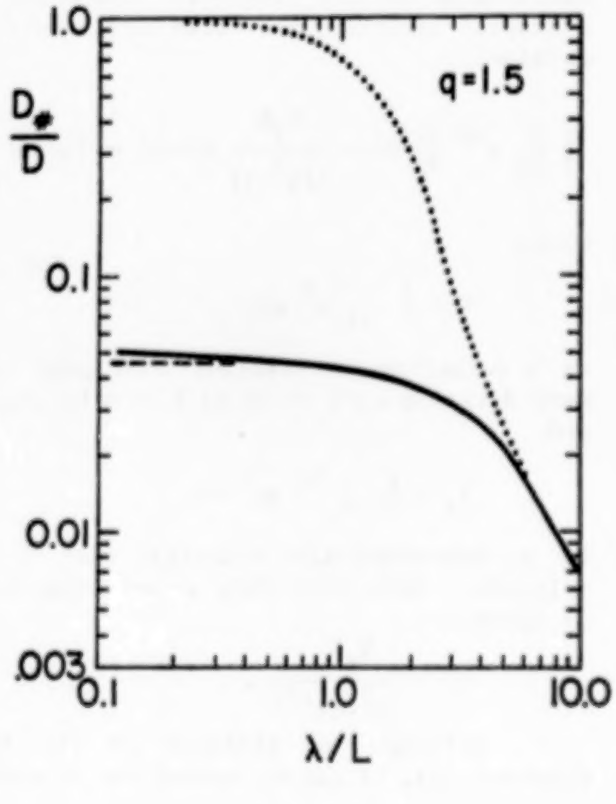

this approximation is adequate. In contrast, the dotted curve, which gives a result obtained by Kunstmann (1979) and by Bieber (1977) deviates by a factor of ~20 at small values of (λ/L). These results grew out of an analysis which describes correctly the strong focusing regime, but which does not take into account the coupling between components embodied in equations (9) and (10). Unless focusing is very strong, this neglect leads to a large overestimate of the dispersive effect.

3. Summary. The coefficient of dispersion given by equation (11) is a basic parameter needed to implement numerical solutions of the transport equation. In this context, where great accuracy is not required, the limitations of the present analysis to constant λ and L are not important.

4. Acknowledgements. This research was supported by the National Aeronautics and Space Administration through grant NGR-21-002-066.

References

Bieber, J.W. 1977, Ph.D. thesis, University of Maryland.
Earl, J.A. 1981, Ap.J., 251, 739.
Kunstmann, J. 1979, Ap.J., 229, 812.

N85-34829

NUMERICAL DESCRIPTIONS OF COSMIC-RAY TRANSPORT

J.A. Earl
Dept. of Physics & Astronomy, Univ. of MD, College Park, MD 20742

J.R. Jokipii
Dept. of Planetary Sciencies, Univ. of Arizona, Tucson, AZ 85721

ABSTRACT

The behavior of energetic particles in the solar system is described by a well known Fokker-Planck equation. Although analytic methods yield insight into the nature of its solutions, especially in the diffusion regime, calculations that go beyond diffusion are very complicated. Under these circumstances, numerical computations offer the only feasible way to obtain concrete results. However, the reliability of these calculations is of concern, because numerical methods are notorious for their errors and artifacts. To address this concern, the well known Milne problem of classical transport theory has been analyzed with the aid of three different numerical methods. These are:

1. The method of eigenfunctions in which the distribution function is approximated by a sum of eigenfunctions of the scattering operator. Its complexity limits the practicality of this approach, but it is closely related to the analytic and classical approaches.

2. Numerical solutions of a finite-difference equation. This is the most practical approach, but it is subject to subtle errors.

3. Direct simulation of the scattering and streaming of individual particles with the aid of Monte Carlo methods. The accuracy of this approach is limited by statistical considerations, but it is closely related to the physics.

If proper precautions are taken to ensure its validity, the second method gives results that are in precise quantitative agreement with those of the first. Results of Monte Carlo calculations are not accurate enough to define non-diffusive effects, but in the diffusion regime, they are consistent with diffusion theory.

1. Introduction. According to Weinberg and Wigner (1958), the Milne problem is "the touchstone of classical transport theory". It is in this traditional role as a test for new developments that this famous problem is addressed here. More specifically, the steady-state diffusion of particles to a free escape boundary from a planar source deep within a one-dimensional medium, which is the configuration assumed in the Milne problem, is treated under the further assumptions that the diffusing medium is magnetic turbulence superimposed upon a uniform guiding field and that the particles are cosmic rays whose pitch-angles

relative to the guiding field undergo scattering that is described by the Fokker-Planck formalism. Within this framework, the algebra needed to obtain analytic solutions in terms of eigenfunctions becomes manageable, because temporal variations are absent. These solutions, which embody non-diffusive effects, provide a convenient and well understood standard for judging the accuracy with which numerical methods describe these effects.

Some basic aspects of this picture are outlined within these proceedings in Paper SH4.1-4, and this paper deals with the same transport equation, invokes the same definitions and notation, and insofar as possible, uses the same numbers.

2. The Method of Eigenfunctions. This approach follows exactly the classical treatment in terms of spherical harmonics (Case and Zweifel, 1967, sec 8.4), except that the distribution function is expanded in terms of the scattering eigenfunctions tabulated by Bieber (1977) rather than in terms of Legendre polynomials. In the diffusion approximation, the distribution function $f(z,\mu)$ is approximated essentially by the first two eigenfunctions. In this case, the isotropic density is finite at the surface, and if it is extrapolated beyond the boundary along the same uniform slope that applies to diffusion deep within the medium, it reaches zero at a distance of $(2/3)\lambda$ outside the boundary. This result is exactly the one obtained from the classical P_1 approximation. To obtain a better description, assume that solutions of the form

$$T(\mu)\exp(-z/\Lambda)$$

can be expanded as a finite sum of four or more scattering eigenfunctions. Then the matrix form of the transport equation can be solved only for certain specific values of Λ that correspond to a distinct set of transient eigenfunctions. (Note that the term "transient", which derives from classical transport theory, has nothing to do with temporal variations.) These are summed in such a way that the returning intensity at the surface is as near as possible to zero over the outward facing hemisphere. In practice, only the first transient is significant. For the examples computed with $q = 1.8$, which are discussed below, the first characteristic length is $\Lambda = \lambda/40$.

3. Numerical Solutions of a Finite-Difference Equation. These computations invoke the same formulation and scattering operator as in Paper SH4.1-4, except that steady injection was accomplished by specifying at a fixed value of z a constant angular distribution. Starting from the diffusion solution, computations were carried out for a time sufficient to allow a particle moving in a straight line to traverse ten times the distance between injection point and boundary. At this time, the flux was essentially independent of z, which means that the solution was very close to the steady state. (See Earl, 1974b, eq. 24.)

In the figures below, results are plotted for two different values of the spatial increment, $\Delta z = \lambda/21$ (solid curves) and $\Delta z = \lambda/210$ (dotted curves), which are, respectively, substantially larger and

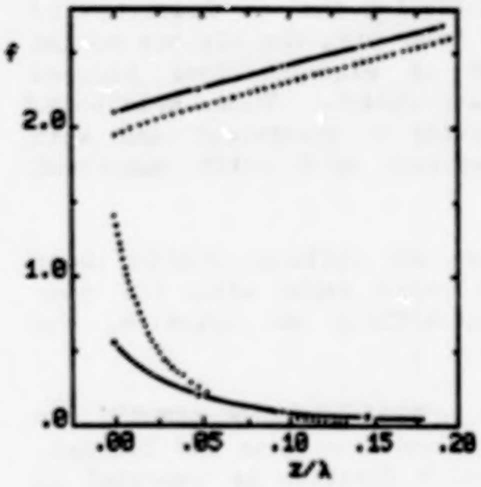

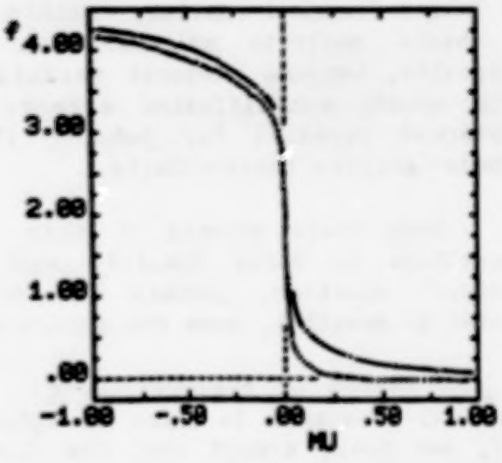

smaller than the characteristic length Λ. Note that both increments are much less than the value $(3/4)\lambda$ derived by Kota et al. (1982) as a condition for validity of the diffusive picture. The analytical solution described above was computed separately, but it cannot be plotted, because its deviations from the dotted curves are smaller than the dots. In the figure at the left, the curves at the top give the isotropic density and those below give ten times the coefficient f_2 of the second scattering eigenfunction, which was obtained by expanding computed angular distributions as a series of four eigenfunctions. The surface density predicted at $z = 0$ by the solid curve is ~8% larger than expected. This discrepancy can be attributed to inaccuracies in the description of non-diffusive effects that can be seen in the curves below, which describe an even component that appears in the transient anisotropy, but not in the diffusion approximation. Here, the dotted curve follows exactly the expected exponential dependence characterized by $\Lambda = \lambda/40$, while the solid curve, whose spatial resolution is too coarse to describe this strong gradient, follows instead an exponential which has only 40% of the amplitude expected at the surface, and whose decay is characterized by $\Delta z = \lambda/21$.

In the figure to the right, the intensity at the surface is plotted as a function of pitch-angle cosine μ. The eigenfunction solution is again indistinguishable from the dotted curve, whose rms deviation from expected values is 2.2%. Except for the point nearest to $\mu = 0$, the intensity predicted by the dotted curve within the hemisphere $\mu > 0$ is essentially zero, while in contrast, the solid curve, which refers to an inappropriate choice of Δz, exhibits here a small but finite intensity. Because scattering cannot turn back escaping particles beyond the boundary, no returning intensity is expected, and its degree of absence can be taken as a figure of merit for comparison of different calculations.

4. The Monte Carlo Method. The Fokker-Planck formalism derives from a statistical model in which scattering results from many tiny deflections of particle trajectories by turbulent fields. With the aid of

computers, these random deflections can be simulated directly, and the history of individual particles can be traced through space and time. Two crucial points of this approach are to choose the amplitudes of the deflections to be consistent with the Fokker-Planck coefficient ψ, and to adjust time increments so that the systematic drift in pitch-angle is compatible with the random spreading.

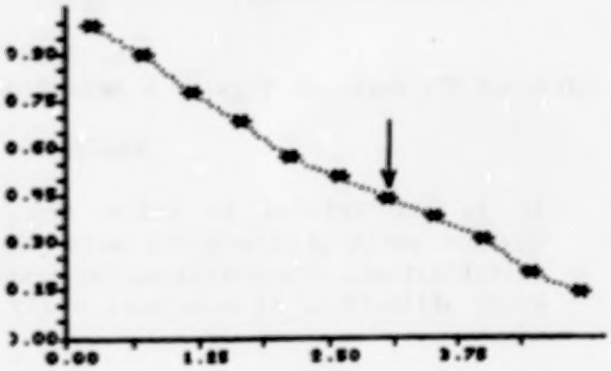

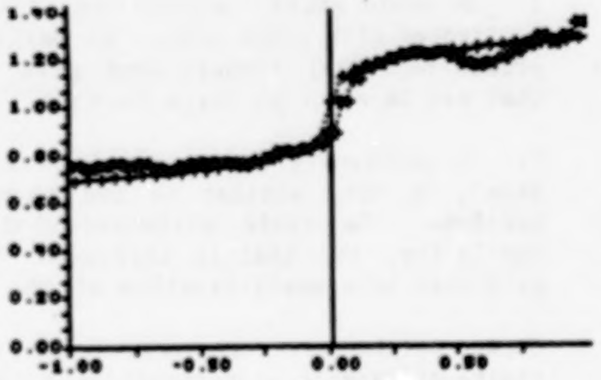

Because of the limitations on accuracy imposed on this method by statistical considerations, it is very difficult to study the non-diffusive effects considered above. However, the figures to the right show results obtained in the diffusion regime from a Monte Carlo simulation of the Milne problem. Plotted above is the isotropic density as a function of distance, which shows the expected uniform slope downward to a finite density on the boundary at the right. The arrow here designates the point at which the angular distribution plotted below was obtained. This angular distribution is in good agreement with the one expected from diffusion theory, whose points are designated by + symbols.

5. Conclusions. The non-diffusive effects discussed above are miniscule, but the precision with which they are described numerically leaves little doubt that finite-difference calculations can give valid results, provided that their parameters are chosen appropriately. In the diffusion regime, Monte Carlo methods offer a useful alternative.

References

Bieber, J.W. 1977, Ph.D. thesis, University of Maryland.
Case, K.M. and Zweifel, P.F. 1967, Linear Transport Theory (Reading: Addison-Wesley).
Earl, J.A. 1974a, Ap.J., 188, 379 (Paper II).
Earl, J.A. 1974b, Ap.J., 193, 231 (Paper III).
Earl, J.A. 1976, Ap.J., 205, 900 (Paper IV).
Kota, J., et al. 1982, Ap.J., 254, 398.
Weinberg, A.M. and Wigner, E.P. 1958, The Physical Theory of Neutron Chain Reactors (Chicago: University of Chicago Press).

N85-34830

SH 4.1-4

NUMERICAL AND ANALYTIC DESCRIPTIONS OF COSMIC-RAY TRANSPORT

J.A. Earl
Univ. of MD, Dept. of Physics & Astronomy, College Park, MD 20742

ABSTRACT

It is not trivial to solve the equations that describe charged particle transport with the aid of computers, for instabilities, inaccuracies, and subtle artifacts are well known afflictions of numerical analysis. Two specific points are:

1. To avoid gross inaccuracies, pitch-angle scattering must be treated with great care. In particular, slightly inappropriate numerical formulations give rise to mean free paths that are in error by large factors.

2. A previously unrecognized artifact, "numerical dispersion", is very similar to the physical phenomenon of dispersion. To avoid misinterpretations arising from this similarity, the spatial increment of the finite-difference grid must be a small fraction of the mean free path.

These points are illustrated by calculations based upon finite-difference approximations to the transport equation.

1. Introduction. The diffusive idealization, which has been almost universally invoked in discussions of cosmic-ray transport is easy to treat analytically. However, many observed phenomena give clear evidence for the presence of non-diffusive effects. One example is the so-called "scatter-free" propagation of kilovolt solar electrons which is inconsistent with diffusion, but which can readily be interpreted in terms of the coherent mode of propagation. Although the qualitative features of these effects have been outlined (Earl, 1974a, 1976), the theory is very complicated. Consequently, there is a need for reliable numerical computations which bypass these complexities and yield concrete results that are well suited for comparison with observations. This paper explores such methods within the limited context of rectilinear propagation of cosmic-ray along a uniform guiding field on which are superimposed random fields.

Under these circumstances, transport is described by

$$\frac{\partial f}{\partial s} + \mu\frac{\partial f}{\partial z} = \frac{\partial}{\partial \mu}\,\psi\,\frac{\partial f}{\partial \mu} \qquad (1)$$

in which f is particle density in phase space, μ is the pitch-angle cosine, and z is distance parallel to the guiding field. The parameter $s = Vt$, where V is particle velocity, plays the role of a temporal variable. The coefficient of pitch-angle scattering is given by

$$\psi = \frac{(3/2\lambda)}{(2-q)(4-q)}\,(1-\mu^2)\,|\mu|^{q-1}, \qquad (2)$$

where λ is the mean free path, and q is an index that measures the anisotropy of scattering.

Diffusion refers to a configuration of slow temporal variations of the anisotropy and weak spatial inhomogenities of the isotropic density F_o (Earl, 1974b), which act as the source of a diffusive anisotropy given by

$$F_1 = -V \frac{\partial F_o}{\partial z} g, \qquad (3)$$

where

$$g(\mu) = [(4-q)\lambda/3]\ \mu|\mu|^{1-q} \qquad (4)$$

is a solution of

$$\frac{\partial}{\partial \mu} \psi \frac{\partial g}{\partial \mu} = -\mu. \qquad (5)$$

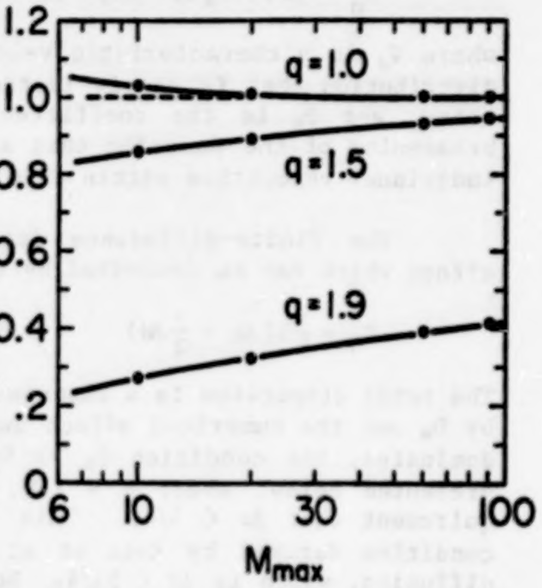

2. Finite-Difference Approximations to the Scattering Operator. In the discrete formulation, the continuous variables are replaced by a three-dimensional grid whose spacings are Δz, $\Delta \mu$, and $\Delta s = V\Delta t$, and the derivatives appearing in equation (1) are replaced by their finite-difference analogs. A test of the relationships implied by diffusion can be made without extensive calculations by replacing the differential operator in equation (5) by its finite version and solving numerically for the diffusive anisotropy. This procedure should give an answer consistent with equation (4), and if it does not, the effective mean free path is given by

$$\lambda = (3/2) \int_{-1}^{+1} \mu g \, d\mu. \qquad (6)$$

Kota et al. (1982) gave an explicit finite-difference form for the scattering operator. Although this derivation seems eminently reasonable from the standpoint of both mathematics and physics, the resulting scattering operator does not pass this test near the threshold at $q = 2$ for pure coherent propagation.

Mean free paths derived from this operator are given in the figure above, where the ratio of the actual value of λ obtained from equation (6) to the nominal value that appears in equation (2) is plotted against the number $M = 2/\Delta\mu$ of increments in pitch-angle. The correspondence is close for $q = 1$ and fairly close for $q = 1.5$, but for $q = 1.9$, λ is a factor of ~2.5 too small and shows little indication of converging to the nominal value as M increases. These inaccuracies are a consequence of the fact that weak scattering near $\mu = 0$ gives rise to large deviations from the analytic behavior. To avoid these deviations, I use a finite operator constructed so that equation (5) is satisfied exactly when g is described by the analytic expression. Far from $\mu = 0$, this operator behaves the same as Kota's operator, but it also gives the correct diffusive anisotropy and makes the actual mean free path identical to the nominal one.

3. Numerical Dispersion. In a configuration of weak scattering, particle bunches propagate coherently in a moving Gaussian profile given by

$$F_o = 1/(4\pi D_* t)^{1/2} \exp\{-(z - V_* t)^2/4D_* t\} \qquad (7)$$

where V_* is a characteristic velocity, which corresponds to an angular distribution that is nearly isotropic in one hemisphere and zero in the other, and D_* is the coefficient of dispersion, which describes the broadening of the Gaussian that arises from statistical fluctuations of individual velocities within this distribution. (Earl, 1974a).

The finite-difference implementation leads to a very similar effect which can be described by equation (7) with D_* replaced by

$$D_{\dagger} = \frac{1}{4}V(\Delta z - \frac{1}{2}\Delta s) \qquad (8)$$

The total dispersion is a superposition of the physical effect described by D_* and the numerical effect described by $D_{\dagger}$. To ensure that physics dominates, the condition $D_* \gg D_{\dagger}$ must be satisfied. In the examples presented below, where $q = 1.8$, this condition translates into a requirement that $\Delta z < \lambda/40$. This condition is similar in concept to the condition derived by Kota et al. for the validity of calculations of diffusion, which is $\Delta z < 3\lambda/4$. However, the required spatial resolution is much finer in the coherent regime that it is in the diffusion regime.

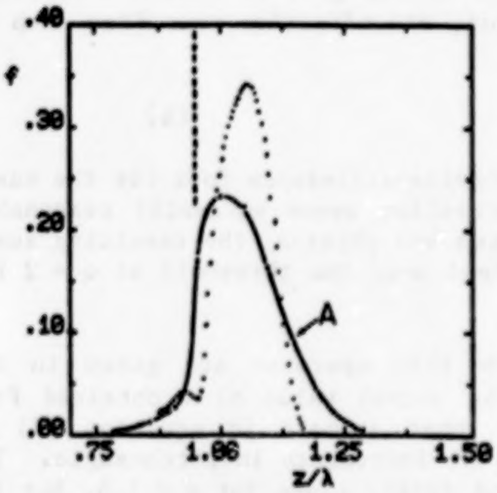

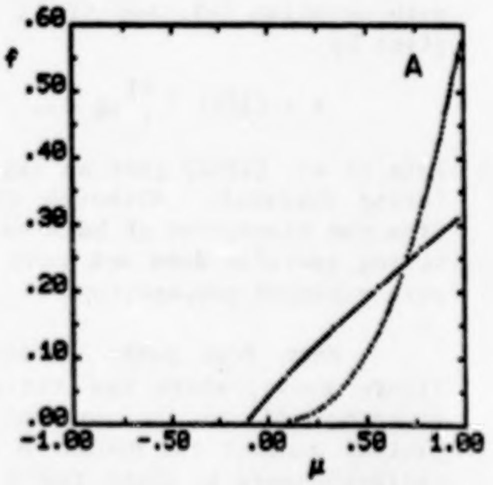

4. A Specific Example. To illustrate the points made above, two calculations were made which had identical values of λ and $\Delta\mu = 0.22$, but which had values $\Delta z = \lambda/21$ (plotted as solid lines) and $\Delta z = \lambda/210$ (plotted as dotted lines) that are, respectively, well below and well above the required spatial resolution. In the figure to the left, snapshots of the density profiles at the instant $s = 0.19\lambda$, display the familiar coherent pulses followed by small but perceptible wakes. At this time, the dotted peak has moved a distance of 0.105λ to the right of the point indicated by a vertical dotted line at which a localized coherent angular distribution was injected at $s = 0$. This corresponds

to a coherent velocity $V_* = 0.55V$ that is in good agreement with the corresponding velocity of $0.53V$ tabulated by Bieber (1977). Similarly, the FWHM width of the pulse 0.135λ is in good agreement with the width 0.125λ expected from a combination of physical dispersion with $D_* = 0.0064\lambda V$ and numerical dispersion with $D_\dagger = 0.001\lambda V$.

The coherent velocity of the solid line peak is less than that of the dotted one and its dispersion, which is dominated by the numerical effect, is larger. To the right of point A, significant solid density appears in regions where the dotted density is zero. This discrepancy is relevant to descriptions of the early onset phase of solar particle events, for it means that the numerical dispersion can bring particles from the sun faster than the physics can, and this could lead to significant errors in the timing of flare events.

The angular distributions in the figure that appears at the right above add weight to this point. They refer to point A where the two profiles have equal densities and, consequently, can be directly compared without normalization. The dotted distribution is much more collimated in the forward direction near $\mu = 1$ than the solid one is. It is clear that any attempts to interpret observed angular distributions of the first few particles arriving in a flare event should take rigorous measures to exclude the effect of numerical dispersion.

5. Conclusions. Before non-diffusive transport can even be considered, the scattering operator must be carefully tailored to give valid results in the diffusion regime. Once this has been done, calculations that take proper account of numerical dispersion give results in good agreement with those expected from the theory of coherent propagation, but not with those calculated with inadequate spatial resolution. This situation can lead to insidious errors, for the invalid results appear to be qualitatively reasonable, and can be detected only by quantitative tests.

6. Acknowledgements. This research was supported by NASA under Grant NGR 21-002-066.

References

Bieber, J.W. 1977, Ph.D. thesis, University of Maryland.
Earl, J.A. 1974a, Ap.J., 188, 379 (Paper II).
Earl, J.A. 1974b, Ap.J., 193, 231 (Paper III).
Earl, J.A. 1976, Ap.J., 205, 900 (Paper IV).
Kota, J., *et al.* 1982, Ap.J., 254, 398.

N85-34831

SH 4.1-7

THE ROLE OF SHOCK WAVES IN MODULATION OF GALACTIC COSMIC RAYS

R.Gall[1], B.T. Thomas[2] and H. Durand[1]

1. Instituto de Geofísica, Universidad Nacional Autónoma de México,MEXICO.

2. Computer Sciences Department, University of Bristol, Bristol, ENGLAND.

INTRODUCTION

In the last decade our understanding of modulation of the galactic cosmic rays has considerably progressed by the exploration by space probes of mayor heliospheric structures, such as the Coratating Interaction Regions, the neutral sheet, and the compression regions of intense heliospheric magnetic fields. Also relevant in this context were the detections in the outer heliosphere of long lasting Forbush type decreases of cosmic ray intensity (1,2,3).

In this paper we shall present the results of our recent theoretical studies on the changes in intensity and energy, at different locations from the sun, induced by the passage of shocks across the heliosphere. In this short version of our research we shall deal mainly with the simplest cases of modulation of 1GV and 2GV particles by single or several shocks during periods of positive and negative solar field polarity.

We shall report here the results of the theoretical aspects of our research. The comparison of the theoretical predictions with space probe data (4,5) will allow us to draw conclusions on the role of shocks on the modulation on both the 11 and 22 year galactic cosmic ray cycles in the outer heliosphere and on the plausibity of the models and parameters used.

METHOD AND MODELS

The modulation that the galactic relativistic cosmic rays undergo during their propagation across the heliosphere all the way to the observer, is studied by means of Liouville's theorem that states that the six dimensional phase space density $f(\underline{r},\underline{p})$ is conserved along the particle trajectories. In order to follow the past history of a particle of momentum $\underline{p}$, detected at $\underline{r}$, one must trace the trajectory of the particle all the way to the boundary.

The method which we used in our studies of shock induced Forbush Decreases (6,7),(the FdM method), consists of integration of full differential equation of motion $d\underline{p}/dt = e(\underline{E}+\underline{v}\times\underline{B}/c)$ of a large mumber of particles moving in both Parkerian and magnetic field shock model, scattered also by small irregularities achieved by random angular deflection corresponding to a chosen diffusion coefficient. The trajectory of each individual particle is integrated back in time, all the way from the observer at $\underline{r}$ to the chosen spherical boundary, keeping all along a detailed account, of the changing particle momentum. Tne intensity of the particle is inferred from the relation $j=fp^2$. We determine the associated intensity at the boundary by a power law in total particle energy of spectral index -2.6.

The FdM method allowed us to prove that the principal mechanism of Forbush decreases is simply the additional adiabatic cooling of the relativistic cosmic rays during their prolongued containment by magnetic field between the shock and the sun.

In the present research we use a method designed by B. Thomas (the BTM -

method, wich saves much computer time. It differs from FdM in that instead of solving the full differential equation we now solve the Boltzman equation and deal with the GC. We compute the focussing and all the drift velocities and evaluate the diffusion and the energy loss by the FdM method. Just as in FdM we impose a $k_{\parallel}$ and $k_{\perp}$ and follow the trajectory integration of 50 particles, back in time, from the position of the observer all the way to the boundary; at every step size of the integration we compute the "average particle" position and pitch angle.

The momentum $\underline{p}_o$ at the boundary, averaged over all individual particles estimates is used to compute the intensity and particle energy loss at $\underline{r}$. (For better understanding of FbM and TBM methods we refer the reader to reference 7)

We use the semispherical shock model of Dryer's type (8), a Parkerian-magnetic field model autside the shocks, and a magnetic field model inside the shock, given by $B = B_o/r^2$; $B\phi=(B_o/r)V_w\Omega\sin\Theta\{3+3\cos\pi(r-r_o)/d\}$, where d is the width of the shock and r_o is the heliospheric distance of the shock interface.

In our elementary studies on the shocks influence of cosmic ray modulation we asume that all the shocks propagate with the same velocity of 400 klm/sec, its width changing with the position of the shock, given by $d=0.2xr_o$. The shocks are placed at sufficiently large distance, (20AU), from each other to avoid shock-shock interaction. Moreover the shock's loss of energy is not considered. A flat ecliptic neutral sheet-model is used; we place the observers at $\lambda=0$, $\varphi=0$ and $\lambda=5°$, $\varphi=0°$, for positive and negative polarity periods, respectively.

RESULTS AND COMMENTS

Figure 1A exhibits the 22 years modulation of 1GV protons in the outer heliosphere induced by the diffusive propagation in a merely Parkerian magnetic field; $k_{\parallel}=.219\times10^{21} r\,cm^2/sec$ and $7.68\times10^{21} r\,cm^2/sec$, for 1 and 2GV respectively. As seen by observers located at different r, the intensities for negative polarity are not only higher that for positive polarity, but exhibit a relatively constant radial gradient. In the table below we list some of the modulation characteristics.

1	2	3	- 4 +	
1GV	80 UA: 42% 20 UA: 2.4%	0.7%/AU	25%	41.9%
2GV	80 UA: 30% 29 UA: 21%	.16%/AU	3.5%	9.1%

1. Proton rigidity.
2. The % ratio of negative to positive polarity intensities at 80 and 20 UA
3. Average intensity gradient of $20<r<80$ AU (negative polarity)
4. % of total energy (E_T) loss by adiabatic cooling for 20 AU observer.

Obviously the theoretical data on propagation in Parkerian field is rather elementary as it does not include the effects induced by large magnetic heliospheric structures. Still it serves as a usefull tool, as a first approximation, to which the effect of shocks, CIR or inclined neutral sheet can be separately added.

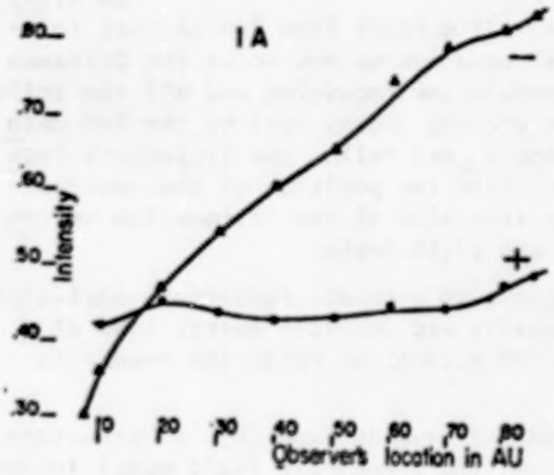

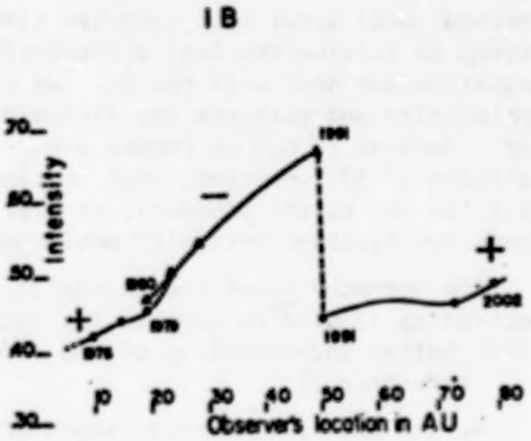

Fig.1A: Intensity of 1GV protons, detected by observers located along the cliptic at different distances from the sun, for A- and A+ periods.

Fig.1B: The computed intensities of 1GV protons for 1976-2002 period. The sign of solar field polarity is marked.

Finally we shall discuss the modulation of cosmic rays induced by - -- shocks. Using the BTM method and the shock and shock associated magnetic-field models, se have computed the intensities of 2 GV protons for the - - cases of 1, 2, and 4 shocks propagating across the outer heliosphere. - - Notice that it takes aproximately 13 months for the shocks to propagate - from the sun to the boundery. For the period of positive solar field polarity. An observer located at 17 AU will detect as illustrated in Fig.2A a similar pattern of intensity vs time, for the three cases mentioned. A- typical Forbush type 15% intensity decrease, lasting aproximately 100 days of equal decrease and recovery time, followed by a 40 days period of 5% - intensity increase above the Parkerian propagation intensity level (which we shall call here PI). This increase is due to an acceleration,during -- the temporal trapping of particles between the shocks is followed by a recovery to practicaly PI level. Only in the case of 4 shocks one detects- as slow intensity decrease of less than 4%.

This intensity vs time pattern, during A- period is very different from the one described above, which obviously implies an important 22 years -- cosmic rays intensity cycle.

As seen in figure 2B, the observer at 24 AU, sees a slight increase of- intensity, lasting 40 and 80 days for 1 shock and 2 shocks, respectively; this is probably due to the typical PI increase during the A- periods.

This increase is followed by an abrupt 50% decrease that occurs at 30- AU for the case of 1 shock and at 50 AU for 2 shocks propagating across - the outer heliosphere. Necesarily the intensity level will rise as the - particles aproach the vecinity of the boundery.

One must keep in mind that the pattern I just used, corresponds to a -- rather simple model of shocks, described before. We plan to continue - - this research using a much more realistic shock models.

ORIGINAL PAGE IS
OF POOR QUALITY

2 A

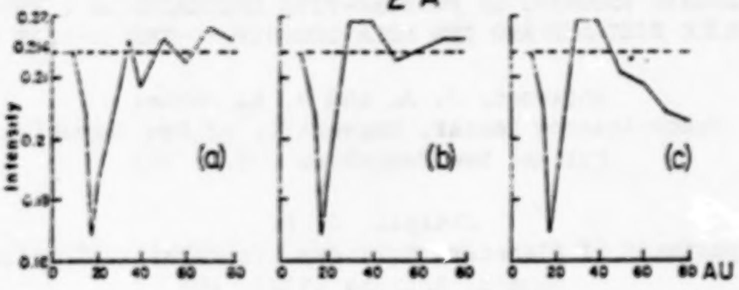

2 B

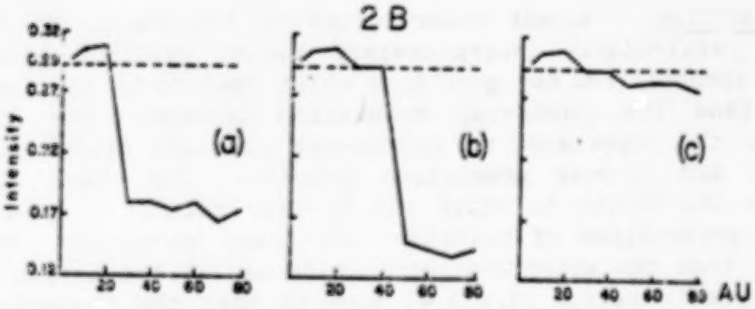

Fig.2A and 2B show the intensity variations during 340 days of observations by an observer located along the ecliptic at fixed distance from the sun. The variations are induced by one(a),two(b)or four(c)shocks. The abcissa-marks the position r_o of the most advanced shock; it also provides the --time:(t)x4.33 r_o days, measured from the day of emision of the mentioned-shock. (Fig.2A: observer at 17 AU, A-; Fig.2B observer at 24 AU, A+)

Aknowledgments

R.Gall is indebted to the UNAM Programe Universitario de Cómputo (PUC) where all the computation was carried out; thanks are especially due to - Ing.Strassburger, PUC's research director, for his unconditional assistance. Thanks are also due to CONACYT for their economic cooperation.

H. Durand expresses his thanks to the local committee for their generosity that made possible his personal participation in the 19th. ICRC.

References

1.Pyle,K.R., et al, (1979),Large Scale Modulation of Galactic Cosmic Rays and Anomalous. He Observed at 16 AU with Pioneer 10,Proc.16th.ICRC,5, - 345-350, Kyoto, Japan, 1979.
2.Van Allen.,(1979),Propagation of a Forbush Decrease in Cosmic Ray Intensity to 15.9 AU, Goephys.Res.Lttrs. 6(1),566-568.
3.Fillius,W.,et al,(1983),Cosmic Ray Gradients in the Outer Heliosphere - 18th. ICRC,3,55-58.
4.Fillius,W., and I. Axford, J.Geophys. Res. 90,(A1),517-520, 1985.
5.Gall, R., and B.T. Thomas,(1981), A Theoretical Interpretation of - - Forbush Decreases, 17th. ICRC, 4,1-4, 1981.
6.Thomas,B.T., and R.Gall,(1984),Solar Flare-Induced Forbush Decreases: - Dependence on shock Wave Geometry,J.Geophys.Res.,89 (A5),2991-2996,1984.
7.Kóta,J. (1984), Time Reversed Method in Cosmic Ray Modulation Theory, - Proc. Int. Symp. Cosmic Ray Modulation in the Heliosphere, 153, Marioka, Japan, 1985.
8.Dryer M., Interplanetary Shock Waves Generated by Solar Flares Space, - Sci. Rev. 13, 401, 1974.

N85-34832

SH4.1-9

THE INTENSITY RECOVERY OF FORBUSH-TYPE DECREASES AS A FUNCTION OF HELIOCENTRIC DISTANCE AND ITS RELATIONSHIP TO THE 11-YEAR VARIATION

Lockwood, J. A. and W. R. Webber
Space Science Center, University of New Hampshire
Durham, New Hampshire 03824 USA

Jokipii, J. R.
Department of Planetary Sciences, University of Arizona
Tucson, Arizona 95721 USA

1. Introduction. Recent observations of the cosmic-ray modulation, including particularly interplanetary radial gradient studies, have helped to identify two key questions which need to be answered in order to understand the cosmic-ray modulation process. One question is related to the importance of cosmic-ray particle drifts in both the short-term and 11-year modulation process. The other question is related to the degree to which the 11-year modulation process represents a superposition of transient (Forbush) decreases. Recent data indicating that the solar modulation effects are propagated outward in the heliospheric cavity [1,2,3,4] suggest that the 11-year cosmic-ray modulation can best be described by a dynamic time-dependent model.

In this context an understanding of the recovery characteristics of large transient Forbush-type decreases is important. This includes the typical recovery time at a fixed energy at 1 AU as well as at larger heliocentric radial distances, the energy dependence of the recovery time at 1 AU, and the dependence of the time for the intensity to decrease to the minimum in the transient decrease as a function of distance. We characterize these transient decreases by their asymmetrical decrease and recovery times, generally 1-2 days and 3-10 days respectively at ~ 1 AU. Near earth these are referred to as Forbush decreases, associated with a shock or blast wave passage. At R $\gtrsim$ 10 AU, these transient decreases may represent the combined effects of several shock waves that have merged together.

2. Observations. About thirty transient decreases from 1972-1984 observed at 1 AU (Fig. 1) for which data were available from the IMP spacecraft (P median ~ 1.7 GV) and the Mt. Washington neutron monitor (P median ~ 5 GV) were analyzed to determine the characteristic recovery time t_o at earth. Certain selection criteria were applied to these decreases: a) magnitude $\gtrsim$ 3% as seen in daily average count rate of the Mt. Washington neutron monitor; and, b) effects of solar particles in the IMP cosmic-ray data should be small or negligible. The fractional decrease ($\Delta N/N$) was calculated from the logarithmic difference of the daily average counting rates recorded for three days before the decrease and at the minimum. For the recovery it is assumed that $n = n_o \exp(-t/t_o)$, where $n = \ln N_o - \ln N$ and $n_o = \ln N_o - \ln N_m$. N_o is the 3-day average intensity before the event, N is the intensity on day t and N_m is the minimum intensity (for details see [5]). In all cases the recovery could be fitted well by this form.

In Fig. 2 we have plotted the characteristic recovery time, t_o, derived in the manner described above for the IMP detector versus that for the neutron monitor at Mt. Washington. Clearly the data are fitted by $t_o(\mathrm{MW}) = t_o(\mathrm{IMP})$ with an average $\approx$ 5 days which implies that the decay time in these events is on the average the same for the two instruments differing by a factor of 3 in the rigidity of their mean responses. We also observe that: 1) there is no significant difference in recovery times for events classed as Co-rotating Interaction Regions (CIR), having a more symmetrical decrease and recovery time, and the classical Forbush-type transients; 2) t_o does not depend upon the magnitude of the decrease; 3) t_o does not change significantly before and after the solar magnetic field reversal in 1980; and 4) t_o is the same in the decreasing phase of the solar cycle (before 1981-1982) and in the recovery part of the cycle.

We have investigated the heliocentric radial dependence of t_o for 19 transient decreases, of which 16 were included in the analysis of the energy dependence of t_o above, utilizing additional data from cosmic-ray telescopes (E > 60 MeV) on Voyagers 1 and 2, and Pioneer 10. An additional criterion imposed for this latter study is that (ΔN/N) of the transient must be $\gtrsim$ 10% as seen in the daily average count rate of the IMP detector at 1 AU. This latter criterion enables the transient events to be more clearly identified as they move outward and possibly coalesce with other decreases at R ~ 10 AU [6]. For 13 of the 19 events examined we believe that there is little doubt about the association at various radial distances. For only one transient decrease is t_o less at larger R. In Fig. 3 we show an example of a transient decrease which has been traced from 1 AU to 21 AU. The dependence of t_o upon heliocentric radial distance for the ensemble of all 16 events is shown in Fig. 4. It is evident that on the average the magnitude of t_o becomes much longer as R increases [see 7]. The data shown is Fig. 4 can be fitted by $t_o(R)/t_o(1) = 1.26 \exp(0.090R)$, where R is the radial distance in AU.

From a comparison of the magnitude of the "same" event (ΔN/N) at different R we find no strong dependence of (ΔN/N) upon R. A possible reason for this behavior as opposed to a more rapid decrease in magnitude expected for a single shock is that, as suggested by [6], the transients seen at R ~ 10 AU probably represent the coalescence of several smaller transients seen at 1 AU.

For 10 out of 19 transient decreases we also determined the time T from onset to the minimum intensity as a function of R. We find $T(R)/T(1) = 1.10 \exp(0.055R)$ where T(R) is the value at R and T(1) at earth. This means that at R $\gtrsim$ 10 AU it takes about twice as long to reach minimum. We find that from 1 to 30 AU the ratio (t_o/T) increases slowly, due to the longer recovery time at larger R. The fact that this ratio is >> 1 clearly indicates that we are observing asymmetrical transient decreases at large R, however.

3. Physical Model for the Observed Energy and Spatial Dependence of the Recovery Time.

A physical model based upon a time-dependent, two-dimensional numerical solution to the cosmic-ray transport with a single shock weakening with distance has been developed by one of us (JRJ) to study these transient events [8]. The transient is represented by a disturbance propagated into the steady-state cosmic-ray distribution. The intensities at several radii and energies are studied. This model predicts that there should be only a small dependence of t_o upon energy at a given R as is observed. The variation of intensity with R depends mainly on the decay of the disturbance as it propagates through the heliosphere. For an e-folding distance of 5-7 AU for the weakening of the shock, the variation of the recovery time with energy and heliocentric radius is given in Table 1.

Table 1: Variation of Recovery Time t_o With Energy and Heliocentric Radius.

Energy [GeV]	Distance [AU]		
	1.7	3.3	5.0
1.3	5.3	7.5	9.7
3.6	5.0	7.0	8.6
9.1	4.5	5.9	7.6

These properties are in excellent qualitative agreement with the observations reported here. Precise quantitative agreement is not expected at this stage given that the model is only two-dimensional and the evolution of the disturbance is quite simple.

We conclude that for the transient decreases observed here:

1) the average recovery time t_o from transient decreases at 1 AU is energy independent and t_o is $\sim$ 5 days;
2) t_o is essentially the same before as after the solar magnetic field reversed in 1980;
3) t_o is constant throughout the solar modulation cycle;
4) the ratio of recovery times $t_o(R)/t_o(1)$ increases with R and is about 5 times longer at 20 AU than at 1 AU;
5) the time for the decrease to reach minimum, T, increases about 10%/AU out to 20 AU; so that at 20 AU it is $\sim$ 2 times longer than at 1 AU;
6) these results are well described by a two-dimensional numerical solution to the cosmic-ray transport equation which incorporates an outward moving weakening shock.

6. Acknowledgments.

The authors want to thank F.B. McDonald and T. von Rosenvinge for making data available from Pioneer and Voyager spacecraft and IMP satellite respectively. The studies by JAL, WRW and JRJ were supported, in part, by grants from NSF (ATM-8304486), NASA/GSFC (NAS5-24354) and NSF (ATM-8317701) and NASA (NSG-7101) respectively.

References

1. McDonald, F.B., et al., (1981), Ap. J., 249, L71.
2. Webber, W.R. and J.A. Lockwood, (1981), J. Geophys. Res. 86, 11458.
3. McKibben, R.B., et al., (1982), Ap. J., 254, L23.
4. Lockwood, J.A. and W.R. Webber, (1984), J. Geophys. Res., 89, 17.
5. Lockwood, J.A. and W.R. Webber, (1985), to be pub. J.Geophys. Res.
6. Burlaga, L., et al., (1984), J. Geophys. Res., 89, 6579.
7. Van Allen, J.A., (1979), Geophys. Res. Lett., 6, 566.
8. Jokipii, J.R., and J. Kota, (1983), Ap. J., 265, 573.

Figure Captions

Fig. 1 Mt. Washington neutron monitor monthly average count rate. Upper panel indicates transient decreases > 3% observed at Mt. Washington.

Fig. 2 t_o for IMP vs. t_o for Mt. Washington neutron monitor.

Fig. 3 Count rate of IMP8, V1,V2, and P10 for transient decrease on July 12, 1982.

Fig. 4 Ratio $t_o(R)/t_o(R = 1)$ vs. radial distance R.

N85-34833

ORIGINAL PAGE IS
OF POOR QUALITY

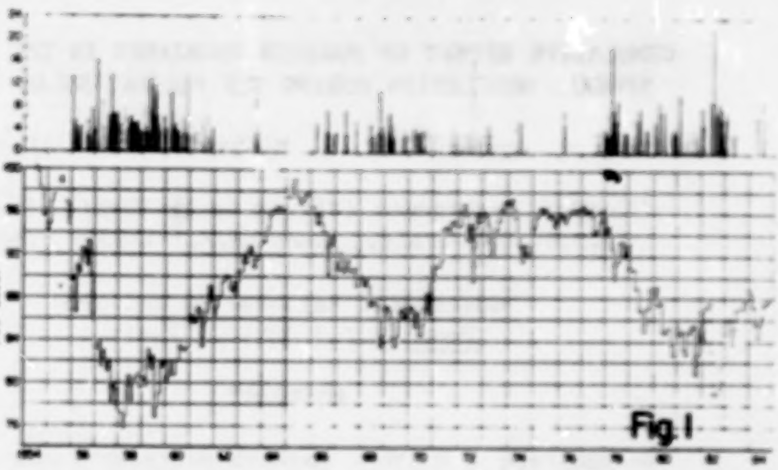

Fig.1

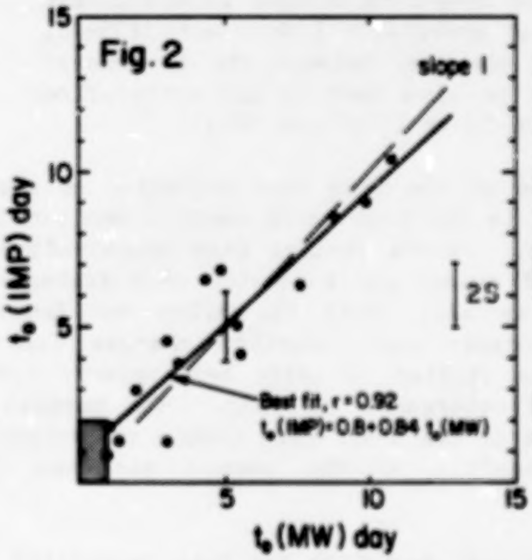

Fig. 2

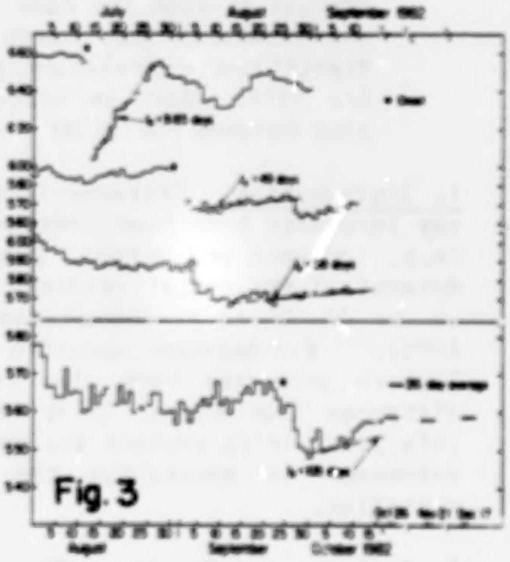

Fig. 3

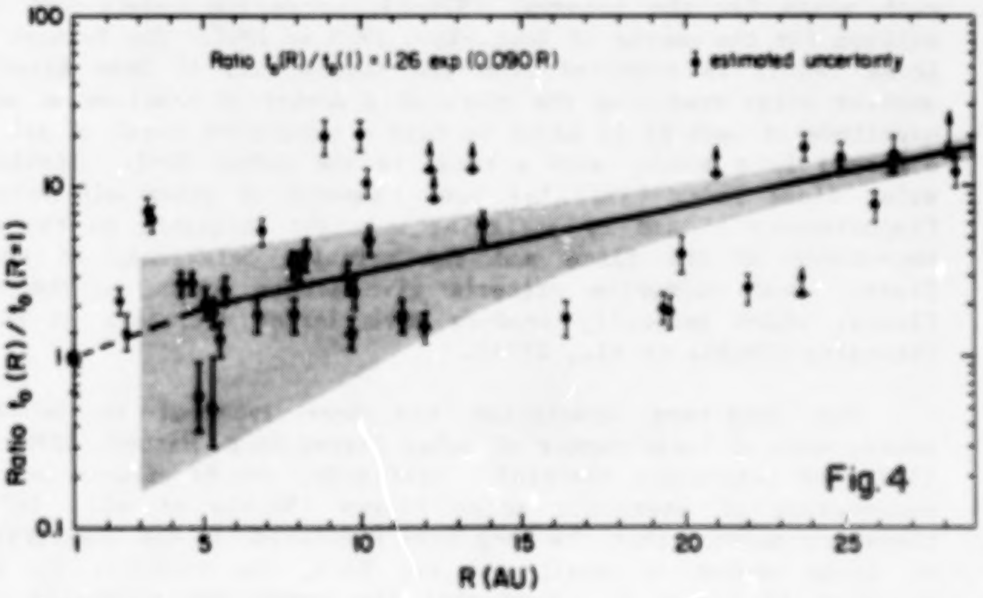

Fig. 4

N85-34833

SH4.1-10

CUMULATIVE EFFECT OF FORBUSH DECREASES IN THE HELIOSPHERIC MODULATION DURING THE PRESENT SOLAR CYCLE

S. P. Agrawal[1], B. L. Mishra[1], A. K. Jain[1,2]

[1]Physics Department (Vikram Space Physics Centre)
A.P.S. University, Rewa (M.P.) 486003, India

[2]Government Engineering College
Rewa (M.P.) 486002, India

ABSTRACT

We generate a monthly Forbush decrease index (Fd-I) and compare it with the observed long-term changes in the cosmic ray intensity near earth at energies > 1 Gev over 1976-83. Significant correlation is observed between the two except for 1978. Such an effect is also seen in the correlation plot between the solar flare index (SFI) and Fd-I.

1. Introduction. Characteristics of the long term variation of cosmic ray intensity have been obtained in the past using neutron monitor data (e.g. Lockwood and Webber, 1984). Recent studies from spacecraft have determined the radial gradient of cosmic ray intensity to a distance of up to 30 AU (e.g. Venkatesan et al., 1984; Van Allen and Randall, 1985). Furthermore specific cosmic ray intensity changes such as Forbush decreases have also been studied to large heliospheric radial distances (Van Allen, 1979; and references therein). The purpose of this paper is to explore the role of the short-term cosmic ray intensity decreases in generating the profile of the cosmic ray long-term variation.

2. Analysis and Results. The percent deviation has been calculated for each month for the interval 1976-83, using the cosmic ray intensity maximum for the months of Sept.-Nov. 1976 as 100%. The Forbush decrease index (Fd-I) is computed from the hourly data of Deep River neutron monitor after examining the plots of a number of stations as well. The magnitude of each Fd is added to form a cumulative total of all the Fd's observed in a month; such a total is the index, Fd-I. Similarly, the solar flare index (SFI) has been computed by using all solar flares (importance > 1) and by assigning a weight according to the numerical importance of the flare and the relative brightness of each solar flare. Such objective criteria give proper weight to the energetic flares, which generally produce much larger decreases in cosmic ray intensity (Shukla et al., 1978).

The long-term modulation has been reported to be a direct consequence of large number of solar flares (e.g. Hatton, 1980; Agrawal, 1983; and references therein). Similarly, the Fd effects are also the consequence of energetic solar flares (Shukla et al., 1978). We therefore suggest that the long term modulation is the cumulative effect of large number of small and big Fd's, the validity for which is examined in Figure 1. Note that the cosmic ray intensity reaches a maximum in 1976, and a minimum in 1982. However, the Fd-I changes very abruptly, with a very large peak in 1978, and with a conspicuous minimum in 1980. The anomalous behaviour of low Fd activity during 1980 is being investigated separately in a paper (SH 5.1-15). Moreover, the peak value of Fd-I in 1978, is of considerable interest, and will be discussed further.

Note from Fig. 1 that both R_z and SFI are still increasing during 1978, while Fd-I shows a very large peak in 1978. Geomagnetic disturbance index Ap also shows moderately low values till 1981, after which it increases, (probably associated with the dominating effect of coronal holes).

The correlation between the long term cosmic ray variations and the Forbush decrease index, is investigated by a cross-plot (Fig. 2) using monthly values for the two quantities during 1976-83. Note that in spite of significant correlation, many points lie close to X-axis. Opposite is true for the year 1978, when most of the points lie close to y-axis, indicating large Fd-I without any associated cosmic ray decreases. Nevertheless, correlated changes observed during other periods show that the long term modulation of cosmic ray intensity can be understood in terms of the cumulative effect of Fd's. We believe that the exception during 1978 of Fd-I on %-deviation of cosmic rays is perhaps attributable to the faster recovery of cosmic rays during 1978. This needs further investigation as also why during certain months of high solar activity no Forbush decreases are seen.

The correlation between Fd-I and percent cosmic ray deviations, with SFI during 1976-83, is shown in Figure 3(a) and (b). Note again that large Fd-I's are associated with small SFI during 1978. Reverse is true for certain months in 1980. The correlation is poor in 1980 and during the recovery of cosmic ray intensity in 1983, when large cosmic ray intensity deviations are observed for low values of SFI. Nevertheless, Figure 3(a) indicates a correlated variation in the cosmic ray intensity with the observed changes in SFI. Thus, from Fig. 3(a) and 3(b), we observe the effect of SFI on both Fd-I and cosmic ray intensity (except for certain specific periods mentioned earlier), which also in turn justify the correlation shown in Fig. 2. It is therefore, reasonable to presume that the long term cosmic ray variation is generated by the cumulative effect of Forbush decreases, and the departure is quite significant during 1978 and 1980, in the present sunspot cycle.

4. References.

Agrawal, S. P., (1983), Space Sci. Rev., 34, 127.
Hatton, C. J., (1980), Solar Phys.66, 159.
Lockwood, J. A., and W. R. Webber, (1984), J. Geophys. Res., 89, 17.
Shukla, A. K., J. P. Shukla, S. M. Sharma, R. L. Singh, and S. P. Agrawal (1978), Ind. J. Radio & Space Phys. 7, 179.
Van Allen, J. A., (1979), Geophys. Res. Lett., 6, 566.
Van Allen, J. A. and B. A. Randall, (1985), J. Geophys. Res. 90, 1399.
Venkatesan, D., R. B. Decker and S. M. Krimigis, (1984), J. Geophys. Res. 89, 3735.

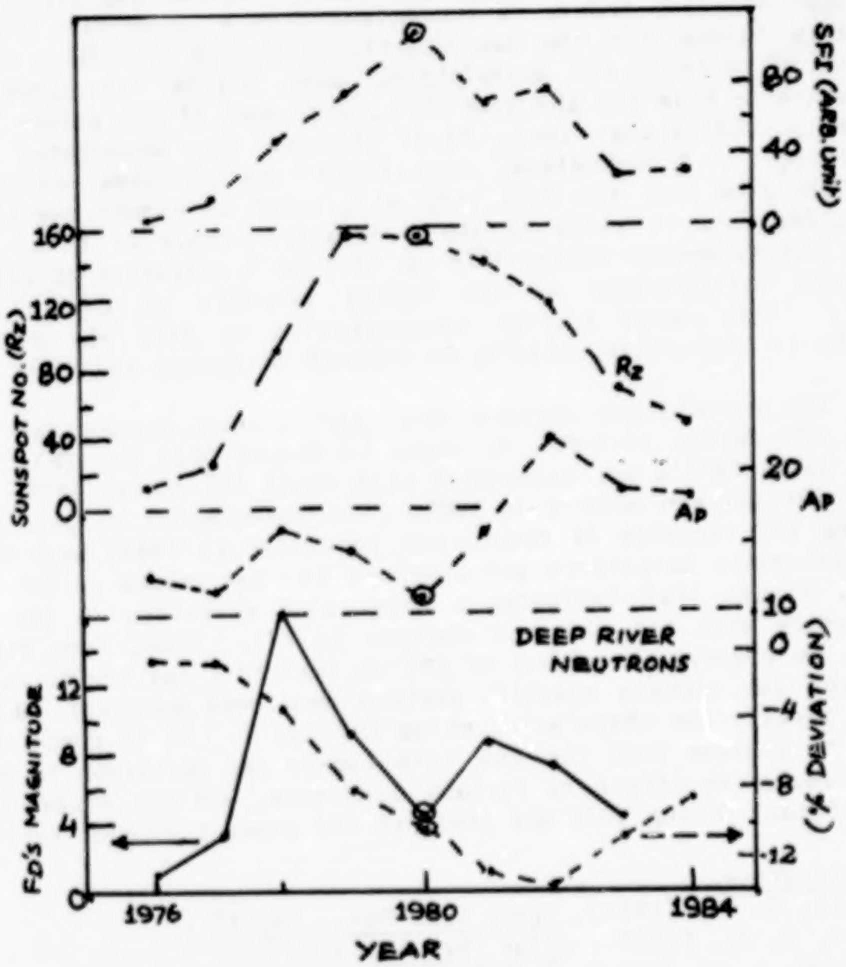

Figure 1 Yearly means of the solar flare index, sunspot number, Ap index, Forbush decrease index (Fd-I) and the cosmic ray intensity deviations from its maximum value, for 1976-84. The annual average values for 1984 are derived from limited number of monthly values. A large peak in Fd-I in 1978 is clearly evident.

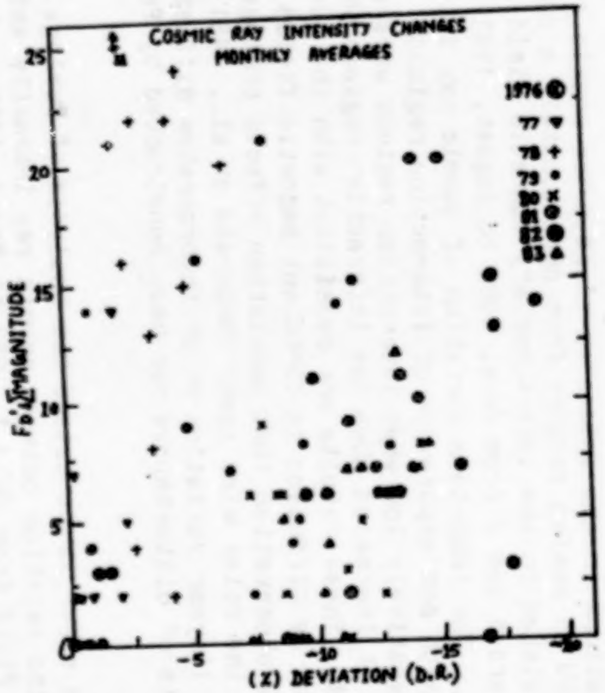

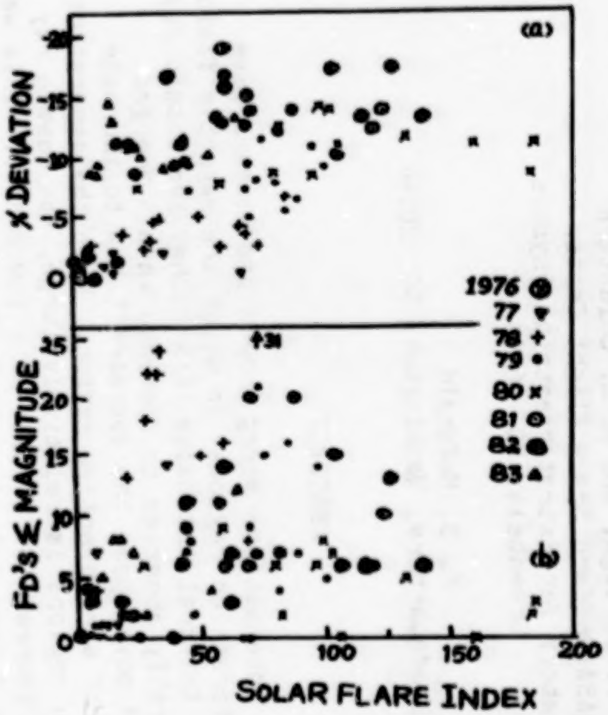

Figure 2 Cross-plot of monthly values of Z deviation of cosmic ray intensity and Fd-I during 1976-83 with various symbols for different years.

Figure 3 (a,b) Crossplot of monthly values of SFI and (Fd-I)/percent deviation of cosmic rays during 1976-83. Symbols are the same as used in Figure 2.

N85-34834

SH 4.1-11

COSMIC RAY MODULATION AND MERGED INTERACTION REGIONS

L. F. Burlaga, and M. L. Goldstein
NASA/Goddard Space Flight Center
Laboratory for Extraterrestrial Physics
Greenbelt, MD 20771

F. B. McDonald
NASA Headquarters, Washington, DC 20546

ABSTRACT

Beyond several AU, interactions among shocks and streams give rise to "merged interaction regions" in which the magnetic field is turbulent. The integral intensity of > 75 MeV/Nuc cosmic rays at Voyager is generally observed to decrease when a "merged interaction region" moves past the spacecraft and to increase during the passage of a rarefaction region. When the separation between interaction regions is relatively large, the cosmic ray intensity tends to increase on a scale of a few months. This was the case at Voyager 1 from July 1, 1983 to May 1, 1984, when the spacecraft moved from 16.7 to 19.6 AU. Changes in cosmic ray intensity were related to the magnetic field strength in a simple way. It is estimated that the diffusion coefficient in merged interaction regions at this distance is $\sim 0.6 \times 10^{22}$ cm^2/s.

1. Introduction. Variations in the intensity of galactic cosmic rays > 75 MeV/nucleon near 11 AU on scales ranging from approximately a day to a year were found to be related to the interplanetary magnetic field in observations from Voyagers 1 and 2 from June, 1982 to August, 1983 (Burlaga et al., 1985a). The long-term variation of cosmic ray intensity was related to the strength and separation of interaction regions. It decreased or remained relatively low when interaction regions were strong and closely spaced, and it increased when the interaction regions were weaker and widely spaced. These results are consistent with the idea that modulation is caused by diffusion in turbulent magnetic fields (Morrison, 1956) and the observation that modulation effects propagate outward from the sun at the solar wind speed (McDonald et al., 1981). A non-steady model of the 11-year variation which incorporates diffusion and propagation of shells of disturbances has been constructed by Perko and Fisk (1983).

The purpose of this paper is to extend the analysis of Burlaga et al. (1985a) to examine the relation between cosmic ray intensity and the interplanetary magnetic field from July 1, 1983 to May 1, 1984, using Voyager 1 data. During this interval the spacecraft moved from a heliocentric distance of 16.7 AU to 19.6 AU and from a heliographic latitude of 20° to 23°.

2. Observations. The intensity of cosmic rays > 75 MeV/nucleon, measured by the CalTech/University of New Hampshire/Goddard Space Flight Center experiment is shown in Figure 1, together with the strength of the interplanetary magnetic field measured by the GSFC magnetometer (N. Ness, Principal Investigator). The magnetic field strength was normalized by the spiral magnetic field strength, $B_p = 4.75 \times (1 + r^2)^{1/2}/r^2$. Thus, the magnetic field fluctuations in Figure 1 are perturbations on the large-scale average magnetic field, which are produced by dynamical interplanetary processes.

Figure 1 shows a correlation between B/B_p and the cosmic ray intensity C: C generally decreases during the passage of an interaction region or merged interaction region ($B/B_p > 1$) and it increases during the passage of a rarefaction region ($B/B_p < 1$). A similar relation was observed near 11 AU by Burlaga et al. The net effect in the period shown in Figure 1 is an overall increase in cosmic ray intensity. The cosmic ray intensity profile is the result of a competition between the effects of interaction regions and those of rarefaction regions. In this interval, the interaction regions were relatively weak $(B/B_o)_{max} \lesssim 2.5$ and the corresponding decreases in C were relatively small, while the rarefaction regions were large in extent, allowing more than enough time to recover from the individual decreases.

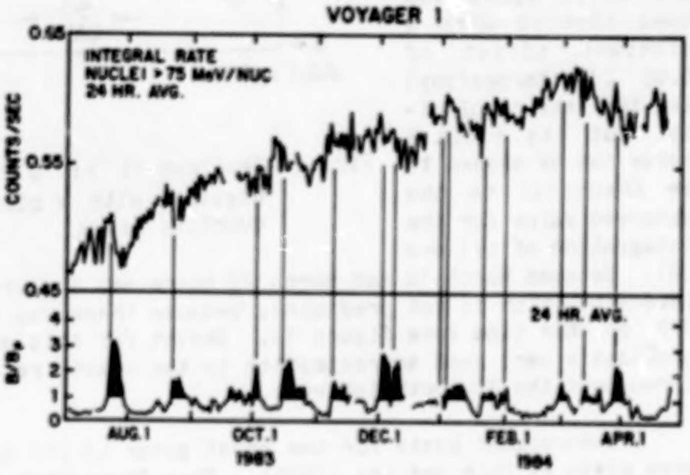

Fig. 1 Intensity of cosmic rays > 75 MeV/nuclei versus time (top) and magnetic field strength relative to the spiral field strength versus time (bottom).

3. Model. Burlaga et al. (1985a) modeled the variation of cosmic ray intensity observed near 11 AU from July, 1982 to August, 1983 with the following set of equations:

$$\frac{dC}{dt} = -D\,(B/B_p - 1) \quad \text{when } B/B_p > 1 \qquad (1)$$

$$\frac{dC}{dt} = R \quad \text{when } B/B_p \leq 1 \qquad (2)$$

where D and R are constants and B/B_p is the measured magnetic field strength as a function of time. Using the 24-hour averages of $B/B_p(t)$ shown in Figure 1, choosing D = 0.004 (counts/sec/day) and R = 0.002 (counts/sec/day) and taking the initial value of C at July 1, 1983, these

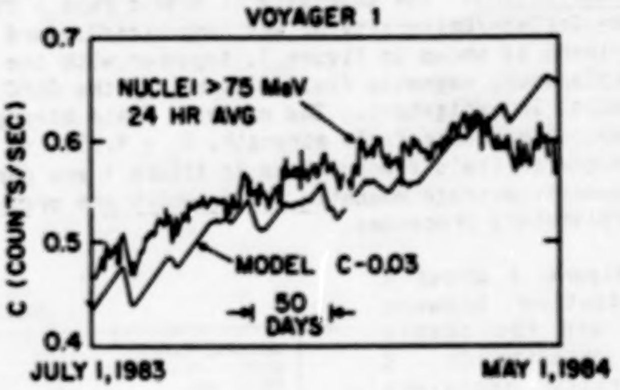

Fig. 2 The result of a model (see text) together with a plot of the observed counting rates.

equations were integrated to obtain the model cosmic ray intensity profile shown in Figure 2. The observed 24-hour averages of C(t) for > 75 MeV/nucleon cosmic rays are also plotted in Figure 2, for comparison. Note that the model curve has been plotted with a constant offset of 0.03 (counts/sec/day) for the sake of clarity, but its initial value can be chosen to be identical to the observed value for the integration of (1) and (2). Between March 10 and March 20 there was a decrease in cosmic ray intensity which is not predicted, because there was no large increase in B/B_o at this time (see Figure 1). Except for this anomaly, the model provides a very good approximation to the cosmic ray observations throughout the 10-month interval.

A theoretical basis for the model given by (1) and (2) has recently been given by Chih and Lee (1985). They found that under certain assumptions

$$\frac{dC}{dt} = -\frac{V}{L}(C-C_o) - \frac{V^2}{K} C_o \frac{\delta B}{B_o}, \tag{3}$$

where K is the diffusion coefficient, V is the solar wind speed, L is a characteristic length and δB is a measure of the fluctuations of B. It has been observed that $\delta B/B = 0.3$ between 1 AU and 5 AU, varying slowly with distance as $\propto r^{-1/3}$ (Burlaga et al., 1982), so it is reasonable to take $\delta B/B_o = 0.3\ B/B_o$ in (3). In this case the second term on the RHS of (3) has the same form as (1), and one can use our value of D to estimate the diffusion coefficient K. With $D = 0.004$ (counts/sec/day), $V = 400$ km/s, $C_o = 0.55$ counts/sec and $\delta B/B = 0.3$ one finds $K = 0.6 \times 10^{22}\ cm^2 s^{-1}$. This is somewhat smaller than the value chosen by Chih and Lee (because we used $\delta B/B = 0.3$), but it is close to the value for the diffusion coefficient used by Perko and Fisk (1983) to describe the 11-year variation. Identifying the first term on the RHS of (3) with R in (2), and taking $C-C_o = 0.03$ counts/sec, one finds that $R = 0.002$ (counts/sec/day) implies $L = 4$ AU.

In Figure 3 we show spectra of the components of B (upper curve), the magnitude of B (lower curve) and the magnetic helicity times frequency (fH_m) computed from one hour average Voyager 1 data from July 1, 1983 to May 1, 1984, using the fast Fourier transform method with 26 degrees of freedom, without detrending or filtering the data (Matthaeus and

Goldstein, 1982). Positive values of magnetic helicity are denoted as circles, negative values as triangles. Assuming that plasma is convected past the spacecraft at the mean solar wind speed in the interval, $\bar{V}$, the frequency f_c corresponding to the correlation length L, is $f_c = \bar{V}/L$, and this is shown by the arrow in Figure 3.

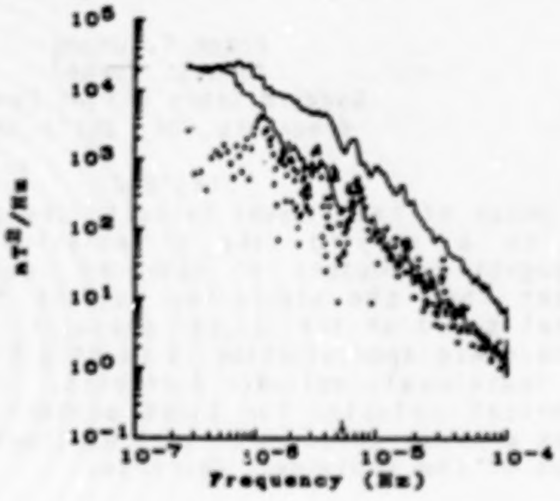

Fig. 3 Power spectra of the magnetic field (see text).

The spectrum of power in the components of $\underset{\sim}{B}$ has the form $f^{-5/3}$ expected for homogeneous turbulenge in the range 4×10^{-6} Hz to 2×10^{-5} Hz, corresponding to periods from 14 hours to 3 days. This is consistent with earlier results showing that the fluctuations in interaction regions are turbulent. At periods between 4 days and 15 days, the spectrum of power in the components of $\underset{\sim}{B}$ was $\sim f^{-1}$, which is probably either a remnant of the spectrum of fluctuations introduced at the source (Goldstein et al., 1984; Burlaga et al., 1985b) or evidence of an inverse cascade of magnetic helicity expected in fully developed MHD turbulence (Frisch et al., 1975; Montgomery and Matthaeus, 1981). If the former interpretation is correct, its presence is another indication that turbulence did not develop sufficiently to modify the initial spectrum in this quasi-stationary flow system, despite the long time available for evolution, viz. $\sim$18 AU/400 km/s $\approx$ 78 days.

References

Burlaga, L., (1984), Space Sci. Rev., 39, 255.
Burlaga, L. F. and J. King, (1979), J. Geophys. Res., 84, 6633.
Burlaga, L. F. et al., (1982), J. Geophys. Res., 87, 4345.
Burlaga, L. F. et al., (1984), J. Geophys. Res., 89, 6579.
Burlaga, L. F. et al., (1985a), NASA/GSFC TM 86193.
Burlaga, L. F. et al., (1985b), NASA TM 86213.
Chih, P. P. and M. A. Lee, preprint, (1985), submitted to J. Geophys. Res.
Frisch et al., (1975), J. Fluid Mech., 68, 769.
Goldstein, M. L. et al., (1982), J. Geophys. Res., 87, 6011.
Matthaeus, W. H. and M. L. Goldstein, (1984), J. Geophys. Res., 89, 3747.
Matthaeus, W. H. and D. Montgomery, (1981) J. Plasma Phys., 25, 11.
McDonald, F. B. et al., (1981), Ap. J. (Letters), 249, L71.
Morrison, P., (1956), Phys. Rev., 101, 1397.
Perko, J. S. and L. A. Fisk, (1983), J. Geophys. Res., 88, 9033.

N85-34835

SH 4.1-12

PROPAGATION OF THE PHASE OF SOLAR MODULATION

Miriam A. Forman
State University of New York
Stony Brook, NY 11794-2100 USA

Frank C. Jones
John S. Perko[1]
Goddard Space Flight Center
Greenbelt, MD 20771-0665

ABSTRACT

The phase of the 11-year galactic cosmic-ray variation, due to a varying rate of emission of long-lived, propagating regions of enhanced scattering, travels faster than the scattering regions themselves. The radial speed of the 11-year phase in the quasi-steady, force-field approximation is exactly twice the speed of the individual, episodic decreases. A time-dependent, numerical solution for 1-GeV protons at 1 and 30 AU gives a phase speed which is 1.85 times the propagation speed of the individual decreases.

1. Introduction. Sudden decreases in cosmic-ray intensity have been observed to propagate outward in the ecliptic plane at about 400-500 km/s, the solar wind speed [McDonald et. al., 1981; McKibben et. al., 1982; Van Allen, 1979; Venkatesan et. al., 1984; see review by Burlaga, 1983]. These decreases are related to regions of enhanced magnetic field strength and turbulence, which strongly suggests enhanced reflection and scattering of cosmic rays. Although these regions are very prominent near the ecliptic plane, it is not clear that all modulation can be ascribed to them. We do not know how their effects extend out of the ecliptic, nor how they may modify the expected modulation due to large-scale drift and the neutral sheet [Jokipii & Davila, 1981; Kota & Jokipii, 1982].

If the 11-year modulation cycle is due to an 11-year cycle in the emission of such propagating regions, as suggested in the references above and by Perko & Fisk [1983], then how would the phase of the 11-year modulation propagate? Venkatesan et. al. [1984] have remarked that "an unexpected result of [our] study is the apparent simultaneity (to within one solar rotation) of the occurrence of solar minimum at [1 and] 10 AU." This implies a phase speed of >700 km/s, which is distinctly faster than the 500 km/s of the observed episodic decreases. We show in this paper that the simplest episodic model of modulation predicts that the phase speed of the 11-year modulation moves outward at up to twice the speed of the individual intensity decreases.

---

[1] NAS/NRC Resident Research Associate

2. Heuristic Model. We consider propagating, episodic modulation in a quasi-steady, "Force-field" model [Gleeson & Axford, 1968]. The modulation parameter is defined as

$$\phi(r,t) = \int_r^R V\, dr'/K(r',t)$$

where "V" is the solar wind speed and "K(r',t)" is the radial diffusion coefficient for the cosmic rays. Since 1/K is proportional to the amount of turbulence, and regions of turbulence propagate at speed V,

$$\phi(r,t) = \int_r^R V\, dr'/K(0,t-r'/V)$$

ϕ then varies with the solar cycle because of the changing rate of emission from the Sun of scattering regions which propagate outward at speed V to a boundary at R, where their effect ceases.

A scattering region emitted from the Sun at time t_o causes a cosmic-ray decrease to begin at radius r_1 when the region passes at time $t_1=t_o+r_1/V$. At $r_2>r_1$, it begins at $t_2=t_o+r_2/V$. The *end* of the effect at both r_1 *and* r_2 occurs near the time $t_E=t_o+R/V$ when the region leaves the modulating sphere at radius R. For various reasons, the end is not clearly seen in observations. Still, the middle of the lasting effect on modulation at r_1 occurs at time $t_{m1}=(t_1+t_E)/2=t_o+(r_1+R)/2V$, and likewise at r_2, $t_{m2}=t_o+(r_2+R)/2V$. Thus, because the beginning of the effect travels at speed V, but the end of it occurs at the same time everywhere, the overall lasting effect of each scattering region propagates at speed 2V.

Alternatively, the solar cycle can be modelled by varying the averaged level of turbulence in the solar wind and propagating it outward. Then the modulation parameter $\phi(r,t)$ is the integral from r to R of V/K at the Sun at time (t-r'/V). If V/K varies as $\cos(\omega t)$ at the Sun, then ϕ varies with time as $\cos[\omega(t-(R+r)/2V)]$. Again, this shows that the phase velocity of the variation in modulation is 2V.

3. Numerical Results. Perko & Fisk [1983] modelled an 11-year cycle in modulation based on episodic events. They assumed the Sun emits spherically-symmetric regions in which scattering is enhanced by a maximum factor of 10 over a band 2 AU wide. The regions travel outward at a speed of 400 km/s until they reach a boundary at 100 AU, where they disappear. The rate of emission was made to vary from one every 4 months at solar minimum to one every 2 weeks at solar maximum. The recovery phase of the cycle was modelled by reversing that behavior. The diffusion coefficient in the undisturbed solar wind (outside the discrete scattering regions) was set at

ORIGINAL PAGE IS
OF POOR QUALITY

$$K = 4.3\beta(2 + P^2)\ 10^{21}\ \text{cm}^2/\text{s}$$

where "β" is the ratio of particle speed to the speed of light and "P" is particle rigidity. For boundary conditions and other details of the calculation, see Perko & Fisk [1983]. The result (Fig. 1) of their numerical integration of the time-dependent transport equations reproduces many of the features of the 11-year modulation. In particular, the episodic decreases propagate at the same speed as the scattering regions (see solid bar at the base of Fig. 1, which shows the propagation time of a scattering region and its accompanying intensity decrease going from 1 to 30 AU). The general level of modulation increases as the rate of emission of these regions increases; but as the rate decreases, the total number of regions in the heliosphere goes down, and there is a cosmic-ray minimum and recovery.

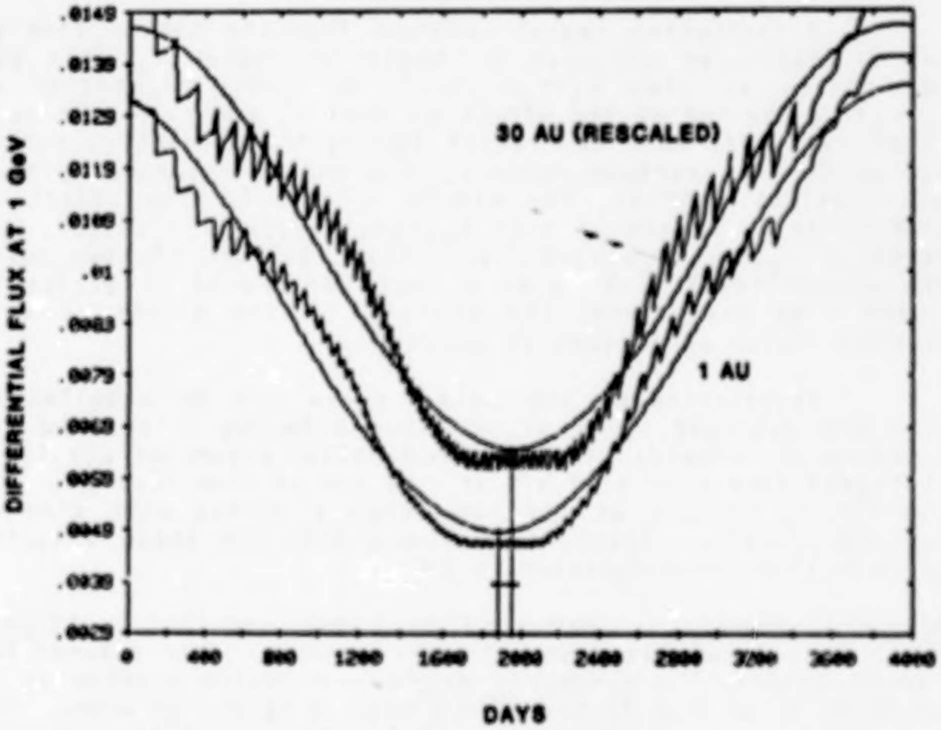

Fig. 1. Numerical calculation of flux (arbitrary units) of 1-GeV protons over the solar cycle, from one sunspot minimum to the next, at 1 and 30 AU. Individual decreases in intensity propagate from 1 to 30 AU in 125 days, shown by the bar at the base of the figure, but the time delay between cosmic-ray minima is only 68 days, shown by the vertical lines.

The smooth curves superposed on the numerical results are sine functions fitted to the results by a least-squares algorithm. The fitted parameters of the sine curves yielded the times of cosmic-ray minimum at 1 and 30 AU. These are indicated by the vertical lines connecting the curves with the abscissa.

It is a remarkable new result that the cosmic-ray minimum at 30 AU shown in Figure 1 occurred only 68 days after the minimum at 1 AU, which implies a propagation speed of 740 km/s, 1.85 times faster than the 400 km/s speed of individual decreases.

4. Conclusions. This simple model demonstrates that the phase of the 11-year cosmic-ray cycle, including recovery, propagates outward even under the simplified assumption of spherical symmetry. This outward propagation may not, therefore, be considered as a signature of models that allow preferential access to the solar cavity via the polar regions. Furthermore, this modulation phase moves at approximately twice the solar wind speed because the flux at a given radius depends on the average state of the heliosphere in the region between this radius and the outer boundary.

5. Acknowledgements. This work was supported by the Solar-Terrestrial Theory Program of the National Aeronautics and Space Administration.

References

Burlaga, L. F., 1983, Proc. 18 ICRC, Bangalore, 12, 21.
Gleeson, L. J., and W. I. Axford, 1968, Astrophys. J., 154, 1011.
Jokipii, J. R., and J. M. Davila, 1981, Astrophys. J., 248, 1156.
Kota, J., and J. R. Jokipii, 1982, Geophys. Res. Lett., 9, 656.
McDonald, F. B., N. Lal, J. H. Trainor, M. A. I. Van Hollebeke, and W. R. Webber, 1981, Astrophys. J., 249, L71.
McKibben, R. B., K. R. Pyle, and J. A. Simpson, 1982, Astrophys. J., 254, L23.
Perko, J. S., and L. A. Fisk, 1983, J. Geophys. Res., 88, 9033.
Van Allen, J. A., 1979, Geophys. Res. Lett., 6, 656.
Venkatesan, D., R. B. Decker, and S. M. Krimigis, 1984, J. Geophys. Res., 89, 3735.
Webber, W. R., and J. A. Lockwood, 1981, J. Geophys. Res., 86, 11458.

N85-34836

SH 4.1-13

LATITUDE VARIATION OF RECURRENT FLUXES IN THE OUTER SOLAR SYSTEM

S. P Christon and E. C. Stone
California Institute of Technology, USA

(Confirming Abstract)

Recurrent low-energy (≳ 0.5 MeV) proton flux enhancements, reliable indicators of corotating plasma interaction regions, were observed on the Voyager 1 and 2 and Pioneer 11 spacecraft in the heliographic latitude range 2°S to 23°N and the heliocentric radial range 11 to 20 AU [Christon and Stone, 1985]. After a period of rather high correlation between fluxes at different latitudes in early 1983, distinct differences developed in the fluxes during an overall flux decrease. The flux intensities returned to higher levels in early 1984 and differences in both the recurrence frequency and flux intensity persisted into 1985, as Voyager 1 traveled to 23 AU and 25°N latitude. Intercomparison of data from the three spacecraft indicates that the flux differences are most likely due to latitudinal, rather than radial or temporal, variations.

References.

Christon, S.P. and E.C. Stone [1985], *Geophys. Res. Lett.*, *12*, 109.

N85-34837

SH 4.1-14

LONGITUDINAL DISTRIBUTION OF COSMIC RAYS IN THE HELIOSPHERE

R. E. Gold[1] and D. Venkatesan[1,2]

[1]The Johns Hopkins University, Applied Physics Laboratory
Laurel, MD 20707
USA

[2]University of Calgary
Calgary, Alberta, T2N 1N4
Canada

ABSTRACT

The longitudinal distribution of cosmic ray intensity has been examined during the years 1974-1976 when the persistent high speed solar wind stream structures produced a well-ordered inner heliosphere. Solar wind velocity is mapped back to the sun and compared with cosmic ray intensity which is represented relative to the solar rotation average. Low solar wind velocity is observed to be a necessary, but not sufficient, condition for the occurrence of higher cosmic ray intensities at 1 AU. These relative enhancements cover a restricted range of heliographic longitudes and persist for several solar rotations. The observed solar wind and cosmic ray intensity relationships are consistent with a simple model suggested here in which cosmic ray modulation is very weak in the inner heliosphere, sunward of the first shock crossing on each field line and more intense in the outer heliosphere.

1. Introduction. The extremely well-ordered and persistent high speed solar wind stream structure during the years 1974 through 1976 provide us with a unique opportunity to compare cosmic ray intensity with solar wind velocity. Earlier studies [1, 2, 3, 4] have shown that no simple relationship exists at 1 AU; but, direct correlations between velocity and intensity may hold only over restricted time periods. The very persistent streams in the ecliptic plane that resulted from extensions of the solar polar coronal holes in the years 1974-76 provide us with a new perspective in which the relative cosmic ray intensity changes over restricted longitude ranges may be compared because the average cosmic ray intensity was only changing slowly over the time scale of many solar rotations. This quasi-equilibrium in the cosmic ray intensity is disturbed during the rest of the solar cycle by transient phenomena related to solar activity; hence the choice of this period for study.

2. Observations. The solar wind data used in this study were from the near-earth observations in the Omni Tape of J. King (NSSDC) supplemented with the isolated data points available from Pioneers 6 through 9. The solar wind observations were mapped back to the sun using the approximation of radial propagation at constant velocity as described in [5, 6]. Each solar wind observation is assumed to have originated at the subsolar point and propagated to the spacecraft with the observed speed. The emission longitude from the sun is therefore $\phi_E = \phi_o - \Omega_{\odot} R/V$

where ϕ_o is the subsolar longitude at the time of observation, $\Omega_\odot$ is the solar sidereal rotation rate, R is the heliocentric radial distance of the observing spacecraft and V is the solar wind velocity. Each of the observed velocities was assigned to the mapped longitude, which is also the foot point of its field line, and plotted in Figure 1 at the emission time (t_E) resulting from the constant velocity approximation $t_E = t_{OBS} - R/V$, where t_{OBS} is the observation time. The near-earth cosmic ray intensity was determined from the CPME experiment on IMP-8. The M scintillator channel responds to all ions $\gtrsim$ 35 MeV/nuc. Details of the CPME experiment are contained in [7]. Each M scintillator observation was associated with the mapped heliographic longitude of the solar wind observed at the same time. These cosmic ray intensities were then plotted in Figure 2 as a function of ϕ_E and t_E. The intensities are represented as the ratio to the average intensity at all longitudes with the same emission day (i.e., each vertical cut through Figure 2 averages to a value of 1.0).

3. Discussion and Conclusions. The cosmic ray intensity in Figure 2 shows relative enhancements over restricted ranges of heliographic longitude that extend over several months in 1975. The largest increases are seen between 150-240° in April through June and 270-330° in September through December. These correspond to the regions between the high speed streams seen in Figure 1. Similar periods are found in the 1974 and 1976 data as well. The 1975 data are shown here because they are free of large solar flare effects and Forbush decreases which disturb some of the solar rotation averages during high activity periods in 1974 and 1976. However, there are well defined cosmic ray enhancement periods during each of the years in the study period. During each of the cosmic ray enhancements, the observed solar wind velocity is low. These enhancements tend to fall in the gaps between the high speed streams and near the edges of the stream seen at 1 AU. However, low solar wind velocity is not always associated with enhanced cosmic ray intensity on the corresponding field lines within the study period. Thus, low solar wind velocity appears to be a necessary, but not sufficient, condition for relative cosmic ray enhancements of restricted azimuthal size that persist for several solar rotations.

The relationship between solar wind velocity and cosmic ray intensity during the interval 1974-76 can be clarified by referring to the solar wind mapping in Figure 3. This is an R-ϕ plot with radial distance increasing downward and heliographic longitude increasing to the right, modulo 360°. The line at the top shows the approximate solar wind velocity profile at the high corona that would produce a stream configuration like that observed between April and July 1974. The mapping was constructed using the observed velocities in May 1974. The CIR boundaries in the figure were determined by connecting the appropriate points in the mapped solar wind data from near-earth and Pioneer 11. The field lines were drawn by extrapolating the near-earth velocity outward until it encountered a CIR boundary. The CIR's are shaded and note that beyond ~ 10 AU all field lines from the inner heliosphere have intersected at least one shock. The region of enhanced cosmic ray intensity in May 1974 is shown as the heavy bar at 1 AU centered near 180°. The enhanced cosmic rays are seen on field lines that extend to large radial distances before they intersect a shock. This suggests a very simple model for relative variation of cosmic ray intensities in the inner heliosphere.

In the outer heliosphere, from the heliopause all the way inward to the innermost shock boundary, all of the plasma has been through a shock. Now imagine that this "shocked" plasma defines a uniformly modulating region for cosmic rays. This is the shaded region in Figure 3 and it determines the long term intensity variations throughout the heliosphere. Let the inner heliosphere (where the field lines are visible in Figure 3) modulate the cosmic rays only very weakly. Then we would expect a general pattern in which the relative intensity within a solar rotation at 1 AU would be enhanced on field lines that extend far out into the heliosphere before they encounter a CIR shock boundary. This condition is generally found in the trailing edge of large solar wind streams where the velocity is relatively low. The theoretical implications of this model are discussed by Roelof [8] in this conference.

4. Acknowledgements. This work has been supported in part by NASA under Task I of Contract N00024-85-C-5301 between The Johns Hopkins University and the Department of the Navy and in part by NSF under Grant ATM 83-05537.

References

1. Mathews, T., J. J. Quenby and J. Sear, (1971), Nature, 229, 246.
2. Hedgecock, P. C., J. J.Quenby and S. Webb, (1972), Nature Physical Science, 240, 173.
3. Intriligator, D. S., (1975), Proc. of the 14th International Cosmic Ray Conference, Munich, 3, 1033.
4. Barichello, J. C., (1978), M. Sc. Thesis, University of Calgary.
5. Synder, C. W. and M. Neugebauer, (1966), Solar Wind, Pergamon, New York.
6. Nolte, J. T. and E. C. Roelof, (1973), Solar Phys., 33, 241.
7. Krimigis, S. M., T. P. Armstrong and J. W. Kohl, (1973), Proc. Int. Conf. Cosmic Rays, 13th, 2, 1656.
8. Roelof, E. C., (1985), Proc. Int. Conf. Cosmic Rays, 19th, Paper SH 4.1-21.

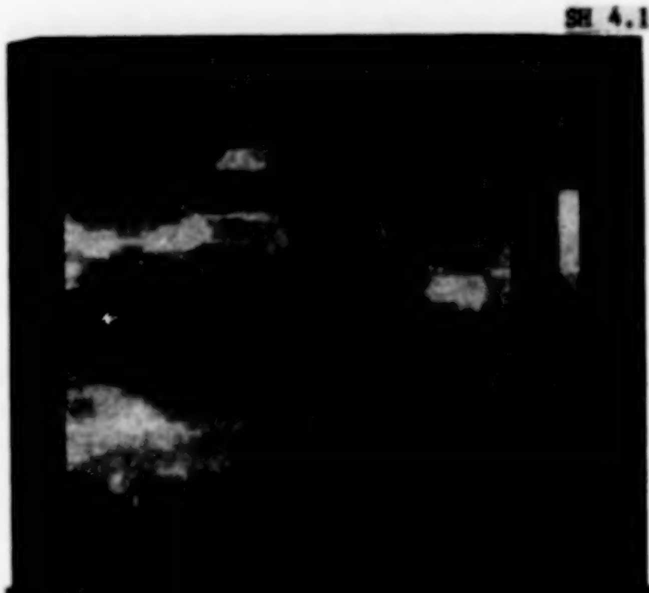

Fig. 1. Solar wind velocity during 1975 expressed as a grey shade from 250-800 km/sec. The data are plotted at the heliographic longitude of the foot point of the field line on which they were observed and at their emission time from the sun.

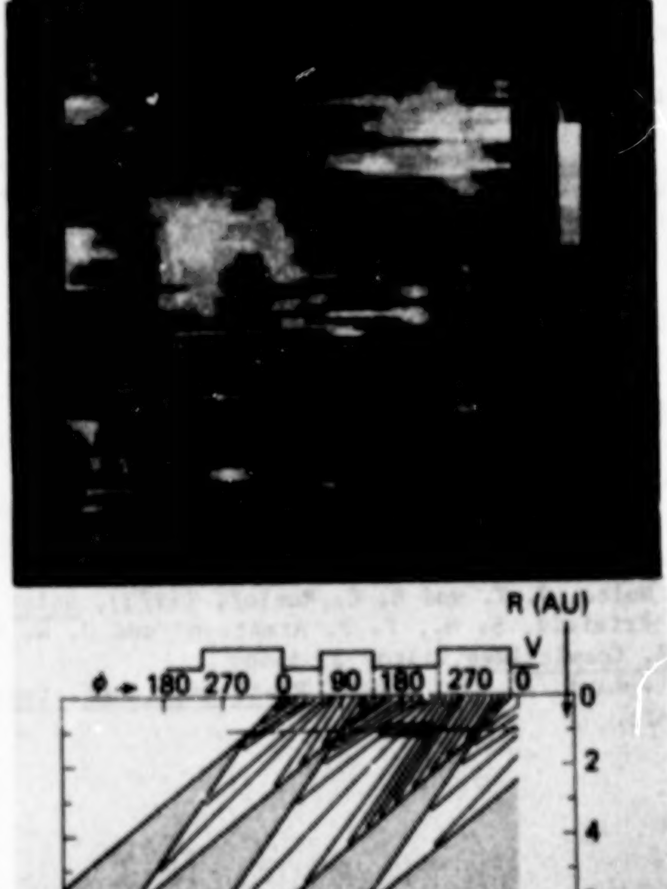

Fig. 2. Cosmic ray intensity (≳ 35 MeV) from the M scintillator channel of the CPME experiment on IMP-8. The data are plotted at the same coordinates as the solar wind velocity observed at the same time. Intensity is expressed as a ratio to the average over all longitudes for the corresponding emission time. Thus any vertical stripe in the figure will average to unity.

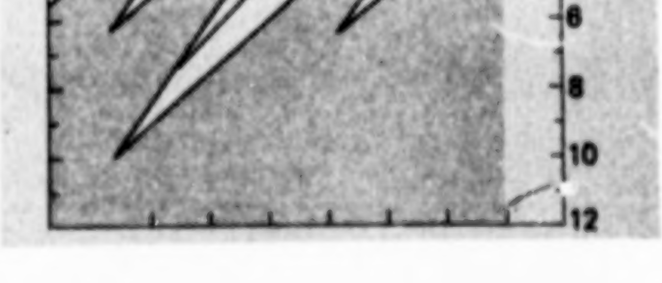

Fig. 3. A radius-longitude plot of the solar wind streams during May 1974. The line at the top is the approximate velocity profile at the sun that would produce the observed speeds at 1 AU. The field lines are extrapolated from the observed solar wind speeds at 1 AU. The shaded area is CIR. The CIR boundaries are reconstructed from Pioneer 11 and near-earth data. The cross-hatched area at 1 AU near 180° shows the region of enhanced cosmic ray intensity.

N85-34838

THE 1973-1984 SOLAR MODULATION OF COSMIC RAY NUCLEI

M. Garcia-Munoz, K.R. Pyle and J.A. Simpson*
Enrico Fermi Institute, University of Chicago
Chicago, IL, USA

ABSTRACT. As a continuation of our program of solar modulation studies we have carried out new measurements, with the University of Chicago cosmic ray telescope on the Earth satellite IMP-8, of the intensity time variations and the energy spectra of galactic cosmic ray protons, helium, carbon and oxygen from 1980 through 1984 including the recent solar maximum. In order to test the applicability of a steady state model of solar modulation during a period which includes times of rapidly changing modulation, we have compared these fluxes with the predictions of a conventional model of solar modulation which assumes equilibrium between modulation mechanisms. It is found that for a reasonable range of variations of the diffusion coefficient the model predictions can be made to agree with the measurements at essentially all times during the studied period. The model can account also for the observed hysteresis effects between cosmic rays of different rigidities.

1. **Introduction.** It has been observed that during the recent solar maximum the decreases and increases in cosmic ray intensity due to modulation level variations propagate outward from the Sun at approximately the solar wind velocity. (McDonald et al., 1981; McKibben, Pyle, and Simpson, 1982, 1985; Fillius and Axford, 1985). This fact together with the evidence that the radius of the modulation region is certainly greater than 30 A.U. and possibly as large as 50 to 150 A.U. implies that it takes to the disturbances responsible for these variations a time of the order of one year or more for propagation to the outer limits of the heliosphere. Therefore, at times of rapidly changing modulation, the modulation mechanisms may not be in equilibrium.

This work is a study of the modulation of cosmic ray nuclei in a time interval from 1973 through 1984, including the recent solar maximum. Measurements of the intensity time variations and differential energy spectra during this period are interpreted in the frame of a conventional model of solar modulation which assumes steady state (i.e. equilibrium) and absence of drifts. By using empirical diffusion coefficients and their time variations it is found that the model can reproduce at 1 A.U. the main features of time intensity variations and differential energy spectra of cosmic ray nuclei through the entire solar modulation cycle.

2. **The Modulation Model.** The model is described in Evenson *et al.* (1983). In it the solar wind velocity, V, is constant, and equal to 400 km/sec, and the diffusion coefficient is given by

$$k = \beta P^{\alpha} k(r); \qquad k(r) = k_0 \exp\left[(r-1)/29\right] \qquad (1)$$

---

*and Department of Physics

ORIGINAL PAGE IS
OF POOR QUALITY

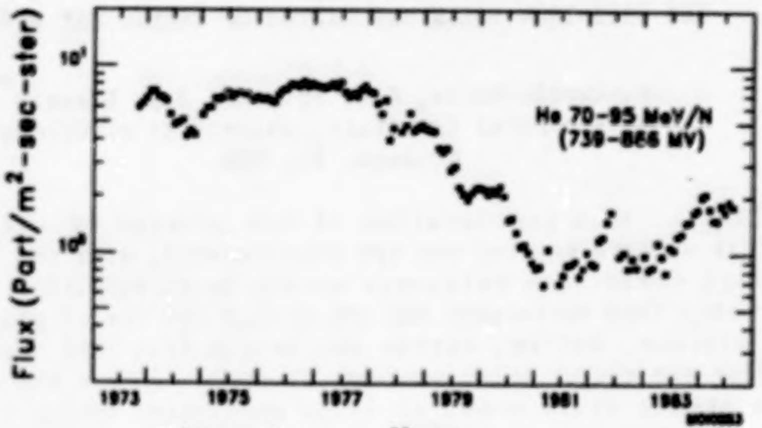

Figure 1

where P is particle magnetic rigidity, r distance from the Sun in A.U., β particle velocity in units of velocity of light and k_0 and α are functions of rigidity and time. It is assumed that the local interstellar electron differential spectrum is as deduced from synchrotron radiation by Cummings *et al*. (1973). Comparison with measured differential nuclear and electron spectra at 1 A.U. during solar minimum leads to the local interstellar nuclear spectra. In this model the depth of modulation at a point r is given, for a heliosphere of radius R, by the force-field parameter, or modulation parameter

$$\phi(r) = \frac{1}{3}\int_r^R \frac{V}{k(r)}\,dr \qquad (2)$$

and thus it is independent of the specific functional form of k(r). Therefore, other k(r) functions different from the one selected in (1) could lead also to the same modulation depth.

Perko and Fisk (1983) have developed a time-dependent model of solar modulation in which the parameter varying with time is the frequency of outward propagating depressions in k(r) which simulate zones of increased scattering associated with solar flare shocks. In our calculations of cosmic ray intensities at 1 AU, k(r) appears only in integral form in the determination of the modulation depth ϕ.

3. **Measurements and Calculations.** Figure 1 shows the time dependence from 1973 through 1984 of the 70-95 MeV/n quiet time cosmic ray ^{4}He flux measured at 1A.U., averaged in solar rotation intervals. The data are from the University of Chicago instrument onboard the IMP 8 spacecraft. Note that the 70-95 MeV/n ^{4}He flux does not contain anomalous helium, even at times of solar minimum. The anomalous helium, when present, extends below about 60

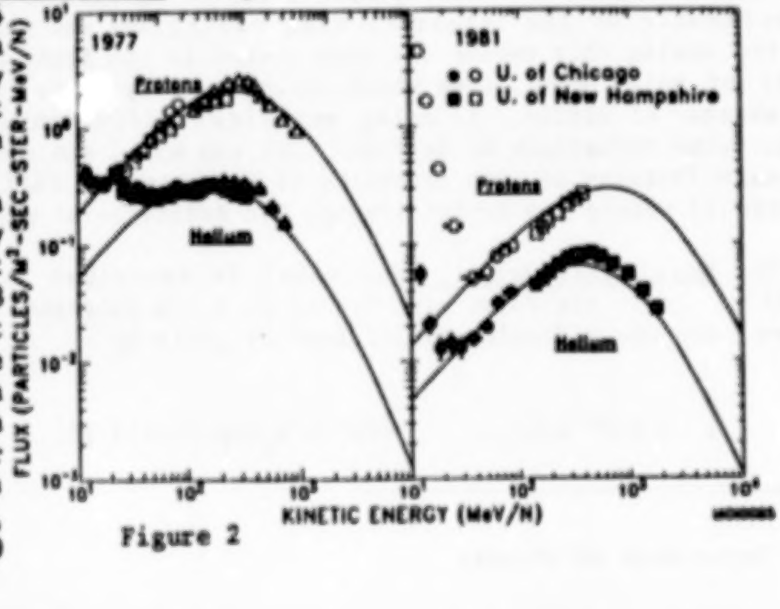

Figure 2

MeV/n. We have continued measuring the differential energy spectra of 10-95 MeV/n protons and helium from 1980 through 1984, adding to our previous measurements which extended up to 1979 (Evenson et al., 1983). Figure 2 shows the 1977 differential energy spectra at solar minimum, as reported by Evenson et al. (1983), and the 1981 spectra at solar maximum, where we have added the University of New Hampshire data (Webber et al., 1983). The curves in the figure are the fluxes predicted by the modulation model. Spectral measurements and theoretical fits have been obtained in this way from 1977 through 1984. The corresponding diffusion coefficients from solar minimum 1977 through solar maximum 1981, as the adjustable parameters, are shown in Figure 3. Each of these diffusion coefficients corresponds to a modulation depth ϕ and gives a modulated helium spectrum with a value for the 70-95 MeV/n helium flux. Therefore, there is a one-to-one relationship between ϕ and the 70-95 MeV/n helium flux.

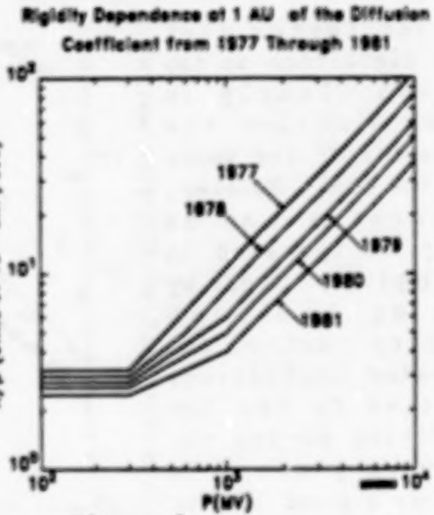

Figure 3

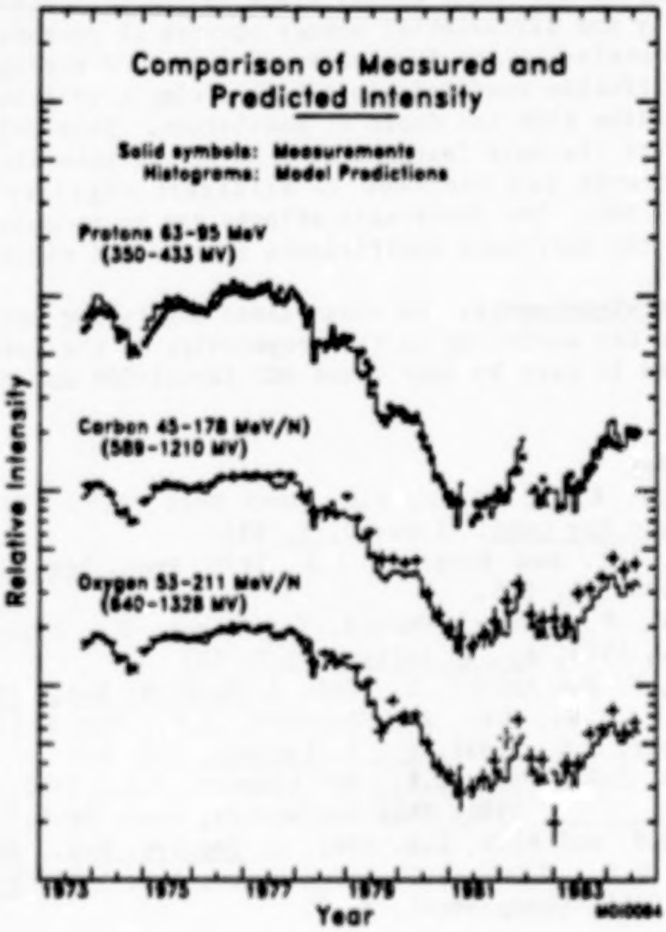

Figure 4

The next step is to use this relationship and use as input the 70-95 MeV/n He flux, from 1973 through 1984, in order to deduce the model predictions of the fluxes of protons, carbon, and oxygen cosmic rays in other energy (rigidity) intervals through the same period and compare these predictions with the IMP 8 measurements. Figure 4 shows, for the 1973-1984 time interval, the comparison of model predictions (histograms) and measurements (data points) for 63-95 MeV/n protons, 45-178 MeV/n carbon and 53-211 MeV/n oxygen. It can be seen that in general there is good agreement between model and measurements. The larger disagreements can be immediately traced to the very well known phenomenon of hysteresis (Cooper and Simpson, 1979) by which higher rigidities

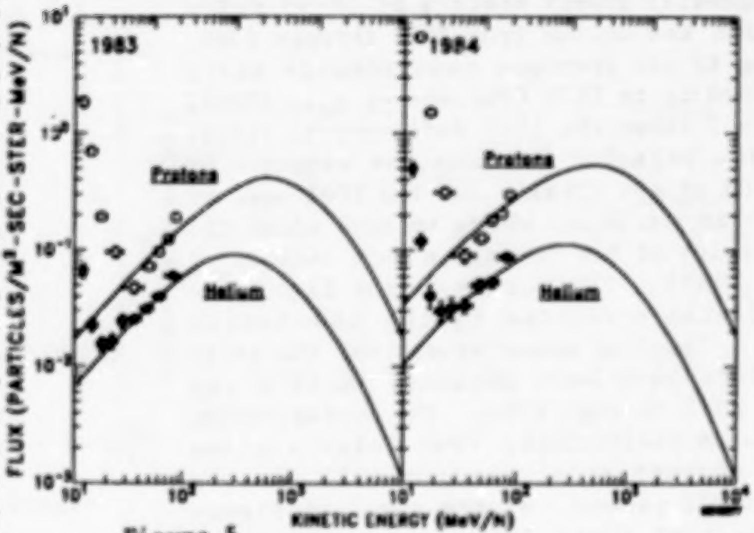

Figure 5

recover faster that lower rigidities as can by seen clearly in Figure 4 during the recoveries of the years 1982 and 1984. However, hysteresis can be easily incorporated in our simplified model by raising the high rigidity part of the diffusion coefficient relative to the low rigidities during the recovery phase. In this way a good fit to the 1983 and 1984 spectra is obtained, as is shown, for the particular case of protons and helium, in Figure 5.

4. **Conclusions**. Empirical diffusion coefficients can be obtained by assuming at all times steady state in the heliosphere and fitting simultaneously the differential energy spectra of protons and helium at 1 AU in successive years from solar minimum 1977 through solar maximum 1981. These diffusion coefficients define a simple relationship between 70-95 MeV/n helium flux and depth of modulation. This relationship can be used to predict the main features at 1 AU of the intensity time dependence of other cosmic ray nucleons in different rigidity intervals from 1973 through 1984. The hysteresis effects can be accounted for by modification of the diffusion coefficients in selected rigidity intervals.

5. **Acknowledgements**. We thank James Beatty for data analysis and Scott Marusak for assisting in the preparation of the data. This research was supported in part by NASA Grant NGL 14-001-006 and NASA Contract NAS 5-28442.

References

Cummings, A.C., Stone, E.C., and Vogt, R.E. 1973., Proc. 13th Int. Cosmic Ray Conf. (Denver), 1, 335.
Cooper, J.F. and Simpson, J.A. 1979, Proc. 16th Intl. Cosmic Ray Conf. (Kyoto) 12, 176.
Evenson, P., Garcia-Munoz, M., Meyer, P., Pyle, K.R. and Simpson, J.A., 1983, Ap. J. Letters, 275, L15
Fillius, W. and Axford, I. 1985, J. Geophys. Res., 90, 517
McDonald, F.B., Lal, N., Trainor, J.H., Van Hollebeke, M.A.I, and Webber, W.R., 1981, Ap. J. Letters, 249, L71
McKibben, R.B., Pyle, K.R., and Simpson, J.A., 1982, Ap. J. Letters, L23
_______________, 1985, This conference, Paper SH 4.7-7.
Perko, J.S. and Fisk, L.A. 1983, J. Geophys. Res., 88, 9033
Webber, W.R., Kish, J.C. and Schrier, D.A. 1983, Proc. 18th Int. Cosmic Ray Conf. (Bangalore), 3, 35

SH 4.1-20

N85-34839

COSMIC RAY MODULATION IN A RANDOM ANISOTROPIC MAGNETIC FIELD

L.I.Dorman

Institute of Terrestrial Magnetism, Ionosphere and Radio
Wawe Propagation of the USSR Academy of Sciences, 142092
Troitsk, Moscow Region, USSR

Yu.I.Fedorov, M.I.Katz, S.F.Nosov, B.A.Shakhov

The Astronomical Observatory of the Ukrainian Academy of
Sciences, 252127, Kiev, Goloseevo

Inhomogeneities of the interplanetary magnetic field can be divided into small-scale and large-scale ones/I,2/, as may be required by the character of the problem of cosmic ray (CR) propagation. CR propagation in stochastic magnetic fields is of diffusion character. The main contribution into the scattering of CR particles is made by their interaction with inhomogeneities of the magnetic field H(r,t) which have characteristic dimensions l of the order of Larmor radius R=cp/eH of particle (p is the absolute value of particle momentum, e is particle charge, c is velocity of light). Scattering of particles on such inhomogeneities leads to their diffusion mostly along a magnetic field with characteristic dimensions of variation in space exceeding the mean free path Λ of particles before their scattering. In view of this fact the inhomogeneities of the interplanetary field can be divided into small-scale (l   ) and large-scale ($l<\Lambda$) ones, and the random magnetic field can be represented as a sum of the small-scale $\mathcal{H}_1$ (r,t) and the large-scale $\mathcal{H}$ (r,t) fields. The boundary value l_0 of the inhomogeneities can be determined by several lengths Λ of the mean free path of particles and l_0 can be taken as the principal scale of the small-scale turbulence. The choice of the scale L_0 of the large-scale turbulence depends on a concrete formulation of the problem.

It is necessary to divide a random field into small-scale and large-scale parts because one cannot describe the whole of the magnetic field turbulence spectrum on a single basis in terms of the local isotropy. As the scale of fluctuations increases, the statistic distribution of these fluctuations becomes, apparently, nonisotropic in space.

The diffusion coefficient along the large-scale field H for $R\ll l_0$ can be written in the form /2/

$$\varkappa_{\parallel}=\frac{v\Lambda_{\parallel}}{3}, \quad \Lambda_{\parallel}=\frac{\nu(\nu+2)\,\Gamma\left(\frac{\nu-1}{2}\right)}{3\sqrt{\pi}\,(\nu+1)\,\Gamma(\nu/2)}(cp/e)^{2-\nu}\,l_0^{\nu-1}\,\frac{\tilde{H}^{\nu}}{\langle\mathcal{H}_1^2\rangle};\ \nu>1 \qquad (I)$$

where $\tilde{H} = |\tilde{\tilde{H}}| = |\bar{H}_0 + \bar{\mathcal{H}}|$, H_0 is a regular magnetic field, ν is the index of the frequency spectrum of the small-scale turbulence, (x) is gamma-function, V is particle velocity, $\Lambda_\parallel$ is the mean free path of a particle along the field H before scattering.

The transport equation in the case of the field $\tilde{\tilde{H}}$ has the form /2,3/

$$\frac{\partial N}{\partial t} = \nabla_\alpha \varkappa_{\alpha\lambda} \nabla_\lambda N - (\bar{u}\bar{\nabla})N + (\bar{\nabla}\bar{u})\frac{p}{3}\frac{\partial N}{\partial p} \tag{2}$$

where N(r,p,t) is CR particle concentration, u is solar wind velocity, $\nabla_\alpha \equiv \partial/\partial r_\alpha$, $\varkappa_{\alpha\lambda}$ is tensor diffusion coefficient which for a strong field $H^2 \gg \langle \mathcal{H}_1^2 \rangle$ $R \ll \Lambda_\parallel$, can be written as

$$\varkappa_{\alpha\lambda} = \varkappa_\parallel h_\alpha h_\lambda \tag{3}$$

where $\bar{h} = \bar{\tilde{H}}/\tilde{H}$. If the field $\tilde{\tilde{H}}$ is represented by a sum of the random $\mathcal{H}$ and the regular $\bar{H}_0$ fields, the expression (3) for $\langle \mathcal{H}_1^2 \rangle \ll H_0$ can be rewritten as

$$\varkappa_{\alpha\lambda} = \varkappa_\parallel^0 (n_\alpha n_\lambda + n_\alpha \mathcal{H}_\lambda H_0^{-1} + n_\lambda \mathcal{H}_\alpha H_0^{-1} + (\nu - 2) n_\alpha n_\lambda n_\mu H_0^{-1} \mathcal{H}_\mu) \tag{4}$$

where $\bar{n} = \bar{H}_0/H_0$, $\varkappa_0^\parallel = \varkappa_\parallel \tilde{H}^{-\nu}/H_0^\nu$.

The coefficient $\varkappa_{\alpha\lambda}$ in (2) depends on the random field $\mathcal{H}$ (r,t) and, hence, the function $N[\mathcal{H}(r,t)$; $(r,p,t)]$ itself is a functional of the random field, and if eq. (2) is averaged over a large-scale random field, we can use the standard averaging procedure /4/. As a result, we are led to the following equation for the mean CR concentration $\langle N \rangle$

$$\frac{\partial \langle N \rangle}{\partial t} = \nabla_\alpha \bar{\varkappa}_{\alpha\lambda} \nabla_\lambda \langle N \rangle - (\bar{u}\bar{\nabla})\langle N \rangle + \frac{p}{3}\bar{\nabla}\bar{u}\frac{\partial \langle N \rangle}{\partial p}, \tag{5}$$

where

$$\bar{\varkappa}_{\alpha\lambda} = \varkappa_\parallel n_\alpha n_\lambda + \bar{\varkappa}^\perp_{\alpha\lambda} + \varkappa^{\parallel,\perp}_{\alpha\lambda},$$

$$\bar{\varkappa}_\parallel = \varkappa_\parallel^0 \left\{1 + H_0^{-2}(\nu - 1)^2 n_\beta n_\gamma \int d\bar{k}\, \mathcal{B}_{\beta\gamma}(\bar{k})\right\}, \tag{6}$$

$$\bar{\varkappa}^\perp_{\alpha\lambda} = \varkappa_\parallel^0 H_0^{-2} \Delta_{\alpha\beta} \Delta_{\lambda\gamma} \int d\bar{k}\, \mathcal{B}_{\beta\gamma}(\bar{k});\ \Delta_{\alpha\beta} = \delta_{\alpha\beta} - n_\alpha n_\beta, \tag{7}$$

$$\overline{\varkappa}^{\parallel\perp}_{\alpha\lambda} = \varkappa^{0}_{\parallel}(\Delta_{\alpha\beta} n_\gamma n_\lambda + \Delta_{\lambda\gamma} n_\beta n_\alpha)\int d\vec{k}\,\mathcal{B}_{\beta\gamma}(\vec{k}) \qquad (8)$$

Here $\mathcal{B}_{\alpha\lambda}(\vec{k})$ is a Fourier-transform of the correlation tensor of a random magnetic field. When deriving (5), we used the hypothesis of frozen turbulence.

For an isotropic probability distribution of fluctuations of the field $\mathcal{H}$ (r,t) we have

$$\overline{\varkappa}_{\parallel} = \varkappa^{0}_{\parallel}\left(1+\frac{(\nu-1)^2}{3}\frac{\langle\mathcal{H}^2\rangle}{H_0^2}\right), \qquad (9)$$

$$\overline{\varkappa}^{\perp}_{\alpha\lambda} = \frac{1}{3}\varkappa^{0}_{\parallel}\frac{\langle\mathcal{H}^2\rangle}{H_0^2}\Delta_{\alpha\lambda};\ \varkappa^{\parallel,\perp}_{\alpha\lambda} = 0, \qquad (10)$$

$$\langle\mathcal{H}^2\rangle = 8\pi\int_{L_0}^{l_0^{-1}} dk\,k^2\mathcal{B}(k). \qquad (11)$$

Here L$_0$ is the maximum dimension of large-scale inhomogeneities.

The coefficient $\varkappa^{\perp}_{\alpha\lambda}$ describes particle transport across a regular magnetic field under the action of a large-scale random field. Its expression for the isotropic case agrees with the analogous expression obtained in the papers by Toptygin /2/ in the averaging of the kinetic equation for $\varkappa^{0}_{\parallel} = \varkappa_{\parallel}$. In our case, however $\varkappa_{\parallel}$ depends on the random field $\mathcal{H}$, and to compare it with the value of $\varkappa^{0}_{\parallel}$ one should average $\varkappa_{\parallel}$ over an ensemble of a large-scale random field. As a result we have $\langle\varkappa_{\parallel}\rangle = \varkappa^{0}_{\parallel}(1+\nu\langle\mathcal{H}^2\rangle/H_0^2$ /H$_0$). Such a renormalization of the diffusion coefficient will not affect noticeably the values of $\varkappa^{\perp}_{\alpha\lambda}$ and $\varkappa^{\parallel,\perp}_{\alpha\lambda}$ in which $\varkappa^{0}_{\parallel}$ is replaced by $\langle\varkappa_{\parallel}\rangle$ without an essential change in their values, but the coefficient of longitudinal diffusion changes the form. So, for the expression (9) we have

$$\overline{\varkappa}_{\parallel} = \langle\varkappa_{\parallel}\rangle\left\{1-\frac{1}{3}\frac{\langle\mathcal{H}^2\rangle}{H_0^2}\left(3\nu-(\nu-1)^2\right)\right\}, \qquad (12)$$

from which one can conclude that an isotropic large-scale turbulence changes particle diffusion along the regular field if the spectrum of small-scale turbulence does not fall very rapidly, namely, if the index of the spectrum ν is not larger than $\nu \propto 4.8$. Usually ν = I - 2/2/.

Large-scale turbulence of a magnetic field in interplanetary space is apparently anisotropic, i.e. spatial probability distribution of a random magnetic field has a distinguished direction e. As working models of anisotropic tur-

ORIGINAL PAGE IS
OF POOR QUALITY

bulence we take its two limiting cases: two-dimensional and one-dimensional fluctuation distribution. In the case of two-dimensional turbulence, the correlation tensor $\mathcal{B}_{\alpha\lambda}$ will be written in the form

$$\mathcal{B}^{\perp}_{\alpha\lambda}(\bar{k}) = \mathcal{B}^{\perp}(k_{\perp}^{2})\left(\delta_{\alpha\lambda} - \frac{k^{\perp}_{\alpha}k^{\perp}_{\lambda}}{k_{\perp}^{2}}\right)\delta(\bar{k}_{\parallel}); \quad (13)$$

and for the one-dimensional model we have

$$\mathcal{B}^{\parallel}_{\alpha\lambda}(\bar{k}) = \mathcal{B}^{\parallel}(k_{\parallel}^{2})\,\delta(k_{\perp}^{2})\,(\delta_{\alpha\lambda} - e_{\alpha}e_{\lambda}); \; k_{\parallel} = \bar{k}\bar{e}, \; k_{\perp} = |\bar{k} - \bar{k}_{\parallel}| \quad (14)$$

where $\mathcal{B}^{\perp}$ and $\mathcal{B}^{\parallel}$ are corresponding spectral functions.

For two-dimensional turbulence with a distinguished direction $\bar{e} \parallel \bar{n}$ the values of the diffusion coefficient are

$$\bar{\varkappa}_{\parallel} = \langle \varkappa_{\parallel} \rangle \left\{1 - \nu \frac{\langle \mathcal{H}^{2} \rangle}{H_0^{2}}\right\}; \; \bar{\varkappa}^{\perp}_{\alpha\lambda} = \langle \varkappa_{\parallel} \rangle \frac{\langle \mathcal{H}_{\parallel}^{2} \rangle}{H_0^{2}} \Delta_{\alpha\lambda} \quad (15)$$

$$\varkappa^{\parallel,\perp}_{\alpha\lambda} = 0; \; \langle \mathcal{H}_{\parallel}^{2} \rangle = 2\pi \int_{L_0^{-1}}^{l_0} dk_{\perp} k_{\perp} \mathcal{B}^{\perp}(k_{\perp}^{2})$$

L_0 is the principal scale of inhomogeneities in the direction transverse to H_0.

In the model of one-dimensional turbulence with a distinguished direction along the solar wind velocity, $\bar{e} \parallel \bar{u}$, we have

$$\bar{\varkappa}^{\parallel} = \langle \varkappa_{\parallel} \rangle \left\{1 - \left(\nu(\nu-1)^{2} \frac{u_{\perp}^{2}}{u^{2}}\right) \frac{\langle \mathcal{H}_{\perp}^{2} \rangle}{H_0^{2}}\right\}; \; \bar{\varkappa}^{\perp}_{\alpha\lambda} = \langle \varkappa_{\parallel} \rangle \frac{\langle \mathcal{H}_{\perp}^{2} \rangle}{H_0^{2}} \left\{\frac{1}{3}\Delta_{\alpha\lambda} - \frac{u^{\perp}_{\alpha}u^{\perp}_{\lambda}}{u^{2}}\right\},$$

$$\bar{\varkappa}^{\parallel,\perp}_{\alpha\lambda} = \langle \varkappa_{\parallel} \rangle \frac{\langle \mathcal{H}_{\perp}^{2} \rangle}{H_0^{2}} (\nu - 1) \frac{u_{\parallel}}{u^{2}} (u^{\perp}_{\alpha} n_{\lambda} + n_{\alpha} u^{\perp}_{\lambda}); \; \langle \mathcal{H}_{\perp}^{2} \rangle = 2\pi \int_{(L_0^{u})^{-1}}^{l_0} dk_{\parallel} \mathcal{B}^{\parallel}(k_{\parallel}^{2});$$

$$k_{\parallel} = (\bar{k}\bar{u})u,$$

where $u_{\parallel}$ and $\bar{u}_{\perp}$ are a parallel and a perpendicular components of the solar wind velocity vector relative to the regular magnetic field direction, L_0^{u} is the principal scale of inhomogeneities along u. In this case the cross diffusion coefficient $\varkappa^{\parallel,\perp}_{\alpha\lambda}$ is nonzero, whereas in all the rest of the considered cases it is equal to zero. The latter model of large-scale turbulence is apparently a most realistic reflection of the situation in interplanetary space with fluctuations going radially from the Sun, with systems of discontinuities and waves following one another in the far regions of solar wind.

REFERENCES

1. Toptygin I.N. Fast particles interaction with a magnetohydrodynamic turbulence. Astrophys. Space Sci., vol.20, 1973, p. 329-350.
2. Toptygin I.N. Cosmic rays in interplanetary fields.M.: Nauka, 1983.
3. Dorman L.I. Exper.and Theoret.bases of CR astroph. M.: Nauka, 1971.
4. Rytov S.M.,Kravtsov Yu.A.,Tatarsky V.I.Introduction to statistical radiophysics.P.2.Random Fields.M.:Nauka,1971.

N85-34840

SH 4.1-21

EVIDENCE FOR REGIONS OF NEGLIGIBLE COSMIC-RAY MODULATION IN THE INNER HELIOSPHERE (< 10 AU)

E. C. Roelof

The Johns Hopkins University, Applied Physics Laboratory
Laurel, Maryland, 20707, U.S.A.

ABSTRACT

Gold and Venkatesan [1] report observations of periods during 1974-1976 when extended regions of heliolongitude that emitted lower-than-average solar wind velocities at 1 AU also exhibited higher-than-average cosmic-ray intensities as measured by the E > 35 MeV CPME anti-coincidence scintillator (28 cm^2 omnidirectional geometric factor) on IMP-8. Their observations can be reproduced by a simple model, based on the observed steady solar wind structure, wherein there is little modulation of cosmic rays in the inner heliosphere until they reach the shocked plasma beyond the stream interactions in the outer heliosphere (~ 5-10 AU). Beyond the interaction boundary, the intensity exhibits a constant radial gradient (~ 2%/AU). The model also offers an explanation for the irregular behavior of the rotation-averaged radial gradients observed by inside 10 AU, as well as the significant, but often ephemeral, latitude gradients observed by Voyagers 1 and 2 and IMP-8 [2].

1. Introduction. Gold and Venkatesan [1] present correlated IMP-8 observations of integral cosmic ray intensity (> 35 MeV) and solar wind velocity during the previous minimum in solar activity (1974-6). The use of the anti-coincidence scintillator of the JHU/APL Charged Particle Measurements Experiment (CPME) as a cosmic ray detector was described in detail by Roelof, Decker and Krimigis [2]. They note that long-lived recurrent regions of enhanced cosmic ray intensity fall within recurrent regions of low speed solar wind (although they state that the converse is not necessarily so). They offer a qualitative explanation based on a sketch (reproduced here in Panel (b) of the Figure) of the quasi-stable solar wind structure deduced by extrapolating solar wind velocities outward with constant speed from IMP-8 and Pioneer-11, a technique observationally validated for this period in the study of Mitchell, Roelof and Wolfe [3]. The cosmic ray intensity enhancement of May 1974 occurred on extrapolated stream lines that intersected the furthest reaches of the "cavity" formed by the reverse shock of the preceding co-rotating interaction region (CIR) and the forward shock of the succeeding CIR. Gold and Venkatesan therefore suggest that the modulation is weaker in the "cavity" than in the shocked plasma beyond its boundary.

2. Analysis. Suppose the cosmic ray modulation beyond the cavities formed by the CIR's is described by a uniform radial gradient g (%/AU) so that the intensity j may be written $j = j_o \exp(gr)$. Here j_o would be the intensity at the sun if the modulation region extended uniformly inward to $r = 0$. However, we shall assume that $g = 0$ inside the

cavities; we could chose a small, but non-zero value of g inside the shocks, but the simplicity of the suggested model calls for a simple treatment. We assume that the cosmic ray populations are ordered along field lines in the inner heliosphere, as was demonstrated by the Voyager/IMP comparisons in 1977-8 [2]. In a steady solar wind structure, the large-scale interplanetary magnetic field lines follow the solar wind stream-lines, as viewed in a frame co-rotating with the sun. Then the intensity at the Earth when its heliolongitude is ϕ should be the intensity at the cavity boundary where the solar wind stream, extrapolated outward from 1 AU, intersects the forward or reverse shock bounding a CIR. Call the helioradial distance of this intersection $r_s(\phi)$. Then the cosmic ray intensity at Earth at heliolongitude ϕ is simply $j(\phi) = j_o \exp[r_s(\phi)]$.

The calculation of $r_s(\phi)$ is not difficult; the values could actually just be scaled off Panel (b) of the Figure. An extrapolated idealized field line has the equation $r(\phi') = a + V(\phi)(\phi - \phi')/\Omega$, where ϕ is the heliolongitude of the line at 1 AU ($r = a$), $V(\phi)$ is the velocity there, and Ω is the solar sidereal rotation rate. The CIR boundaries can be parametrized by a pseudo-field line with the velocities of the forward (V_F) or reverse (R_R) shock and the extrapolated crossings of those lines at 1 AU (ϕ_F and ϕ_R). The lines in the rarefaction between high (V_H) and low (V_L) speed regions can be idealized as a "dwell" in which the lines appear to emanate from a single coronal longitude (ϕ_o): $r(\phi') = a(\phi_o - \phi')/\phi_o - \phi)$. We compute $r_s(\phi)$ for the four regions of the idealized stream structure shown in Panel (c) of the Figure: I, $V(\phi) = V_H$, intersection of high speed solar wind with reverse shock $V = V_R$; II and III, rarefaction, as shown in Panel (b); and IV, $V(\phi) = V_L$, intersection of low speed solar wind with forward shock $V = V_F$. The resulting formulas are:

$$r_s(\phi) = a + (V_H V_R/\Omega)\ \frac{\phi_R - \phi}{V_H - V_R} \qquad \text{Region I}$$

$$r_s(\phi) = a\ \frac{1 + (V_R/\Omega a)(\phi_R - \phi_o)}{1 - (V_R/\Omega a)(\phi_o - \phi)} \qquad \text{Region II}$$

The corresponding formulas for Regions III and IV are obtained by replacing V_R with V_F, V_H with V_L and ϕ_R with ϕ_F. The result of the calculation is plotted in Panel (a) of the Figure with dashed lines indicating the regions where the over-simplification of the model is most extreme.

3. Comments. As could have been seen directly from Panel (b), the cosmic ray enhancement falls in the longitudes of high values of $r_s(\phi)$ shown in Panel (a); not so evident in Panel (a) is the sharpness of the peak within the rarefaction region. Since $d\phi/dt = -\Omega'$, the synodic rotation rate, the $r_s(\phi)$ plot is just a time plot running backwards (see lower scale). The intensity history, if treated as a fractional change, is $\ln(j/j_1) = g(r_s - a)$ where j_1 would be the minimum intensity predicted by the model. A peak radial distance of 9

AU beyond the Earth with a radial gradient of 2%/AU would give a fractional enhancement of $j/j_1 = 1.20$. This is within the range of maximum/minimum intensities presented in Figure 2 of [1]; note that Figure 2 and Figure 3 of that paper are from different years. Also, the longitude used in Figure 2 of [1] is not the Earth heliolongitude used here, but rather the estimated source longitude of the observed solar wind stream. The latter longitude is inappropriate for galactic cosmic ray studies - for example, it would compress the entire rarefaction region of Panel (a), with its attendant intensity enhancements, into a single longitude on their plot. A more appropriate longitude for labelling field lines in the outer heliosphere is the heliolongitude of the innermost spacecraft being used, as was done here and was discussed in [2].

The exercise of this paper is intended mainly to illustrate the very plausible circumstance that cosmic ray modulation in the inner heliosphere ($r \lesssim 10$ AU) may be quite variable (depending on stream structure evolution) with radial gradients much smaller than in the very different plasma/field regimes of the outer heliosphere. An extremely significant result from the VGR/IMP high time resolution (1 h) intensity comparisons [2] was that there were entire solar rotations devoid of significant gradients between 1 and 3-5 AU! Equally important were the ephemeral latitudinal gradients ~ 1%/deg lasting $\lesssim 1$ rotation (which would go essentially undetected if gradients are computed from 25-day averages as in other measurements done with less sensitive instruments). Our present study suggests an intriguing explanation for latitude gradients in the inner heliosphere. Suppose we compare intensities on two field lines passing through the same longitude (ϕ) at 1 AU, but at different latitudes (θ); this was the technique by which field-aligned latitudinal gradients were found in [2]. If the boundaries of the "cavity" were inclined to the solar equatorial plane owing to latitudinal shears described by terms like $(\partial V/\partial\theta)$ or $(\partial\phi_o/\partial\theta)$ in solar wind velocity structure, then we would have a latitudinal intensity gradient $\partial(\ln j)/\partial\theta = g[(\partial r_s/\partial V_i)(\partial V_i/\partial\theta) + (\partial r_s/\partial\phi_k)(\partial\phi_k/\partial\theta)]$ where, for example, $V_i = V_H$, V_R and $\phi_k = \phi_R$, ϕ_o. A shear of $\partial V/\partial\theta \approx (100 \text{ km/s})/(10 \text{ deg})$ is not unreasonable [3], and from Panel (a), we see that $\partial r_s/\partial V \approx (5 \text{ AU})/(100 \text{ km/s})$ in the peak. Consequently, a latitudinal gradient $\partial(\ln j)\partial\theta \approx (2\%/\text{AU})[(5 \text{ AU})/(100 \text{ km/s})][(100 \text{ km/s})/(10 \text{ deg})] = 1\%/\text{deg}$, as observed [2], could be produced by shears in the stream/shock structure.

4. Acknowledgements. This work was encouraged by my valued colleagues R. E. Gold and D. Venkatesan, and supported in part by the Air Force Geophysics Laboratory under Task 2F10 of Contract N00024-85-C-5301 between The Johns Hopkins University and the Department of the Navy.

5. References.

1. Gold, R. E., and D. Venkatesan, (1985), Proc. Int. Conf. Cosmic Rays, 19th, Paper SH 4.1-14.

2. Roelof, E. C., Decker, R. B. and S. M. Krimigis, (1983), J. Geophys. Res., 88, 9889.

ORIGINAL PAGE IS
OF POOR QUALITY

3. Mitchell, D. G., E. C. Roelof and J. H. Wolfe, (1981), J. Geophys. Res., 86, 165.

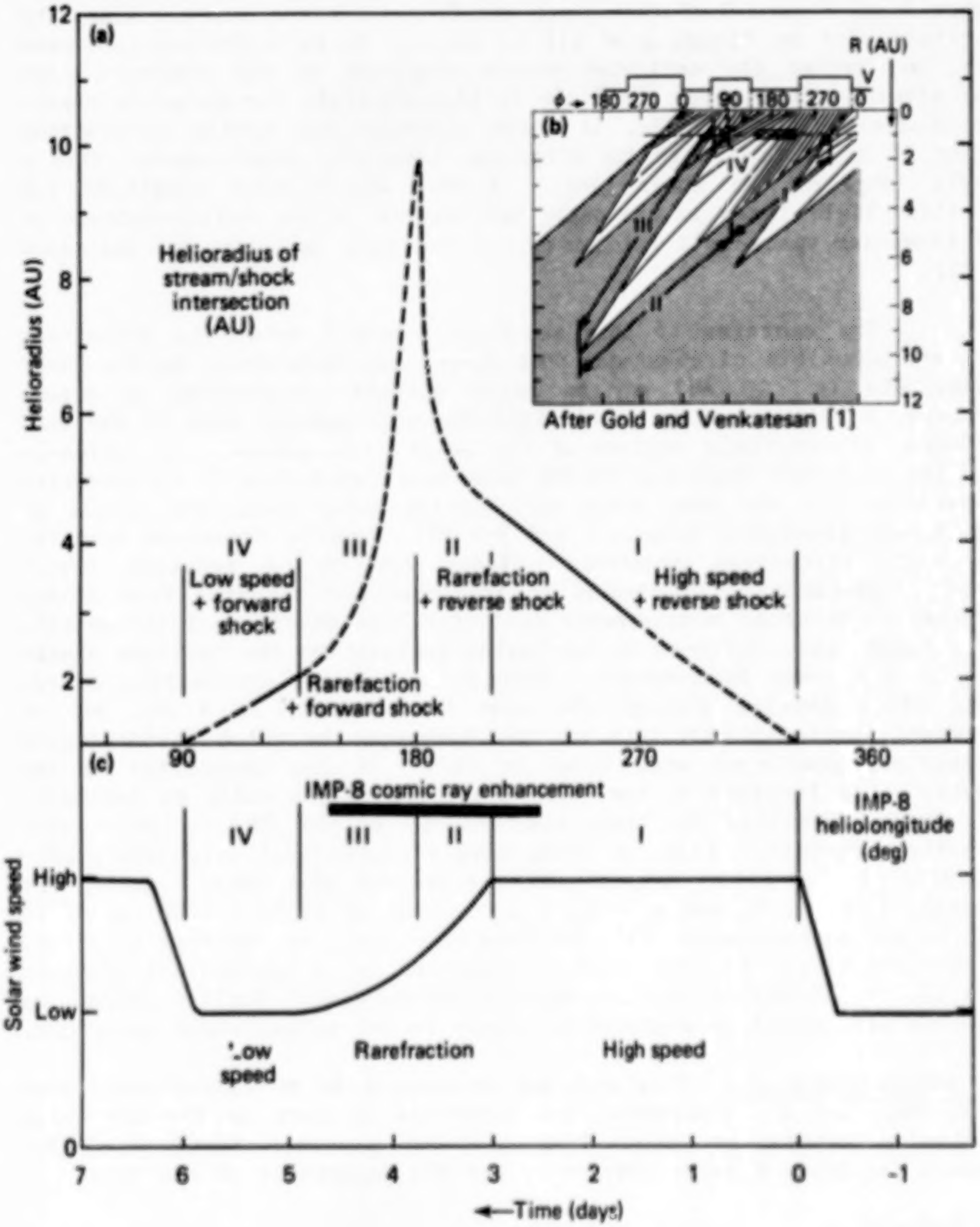

After Gold and Venkatesan [1]

Figure: (a) Outer helioradius $r_s(\phi)$ of intersection of interplanetary field lines from IMP-8 heliolongitude (ϕ) with "cavity" boundary formed by interacting CIR's sketched in (b), as proposed in [1], for the steady solar wind speed profile shown in (c). If there is no cosmic-ray radial gradient within the "cavity" and a constant radial gradient (g) beyond it, the intensity profile at $r = a = 1$ AU is $j = j_1 \exp\ [gr_s(\phi) - a]$.

N85-34841

SH 4.2-3

NOTES ON DRIFT THEORY

R.A. Burger, H. Moraal: PU-CSIR Cosmic Ray Research Unit, Dept. of Physics,
Potchefstroom University, Potchefstroom, 2520
South Africa

G.M. Webb: Dept. of Planetary Sciences, Univ. of Arizona, AZ 85721, U.S.A.

ABSTRACT

It is shown that there is a simpler way to derive the average guiding centre drift of a distribution of particles than via the so-called "single particle" analysis. Based on this derivation it is shown that the entire drift formalism can be considerably simplified, and that results for low order anisotropies are more generally valid than is usually appreciated. This drift analysis leads to a natural alternative derivation of the drift velocity along a neutral sheet. Full derivations are given in Burger, Moraal and Webb (1985; referred to as BMW), of which copies will be available at the Conference.

1. Alternative Derivation of Drift Velocity. A particle at position $\underline{x}$, with momentum $\underline{p}$, velocity $\underline{v}$, in a magnetic field $\underline{B}$ has a gyroradius $\underline{R} = \underline{b} \times \underline{p}/q$, where $\underline{b} = \underline{B}/B^2$. Its guiding centre is at $\underline{x}_g \equiv \underline{x} - \underline{R}$. Differentiation of $\underline{x}_g$ w.r.t. time in the steady state ($\partial/\partial t = 0$), with employment of the Lorentz force $\dot{\underline{p}} = q(\underline{E} + \underline{v} \times \underline{B})$ then gives

$$< \underline{v}_g > = < \underline{v}_{\parallel} > + \underline{E} \times \underline{b} + < \underline{p} \times (\underline{v}\cdot\underline{\nabla})\underline{b} >/q, \tag{1}$$

for the instantaneous, average drift velocity of particles inside a volume element d^3x around $\underline{x}$. For a particle distribution function $F(\underline{x}, \underline{p}, t)$ with density N, this average is defined as

$$<\cdots> = (1/N) \int \cdots Fd^3p = (1/N) \int dpp^2 \int \cdots Fd\Omega, \tag{2a}$$

where $d\Omega = \sin\Theta d\Theta d\phi$. We shall also use differential (omnidirectional) averages in momentum space in the interval $(p, p + dp)$ denoted by

$$<\cdots>_\Omega = \int \cdots Fd\Omega / \int Fd\Omega \tag{2b}$$

In terms of directions in momentum space, $\underline{p}$ may be written as

$$\underline{p} = p(\cos\Theta \underline{e}_1 + \sin\Theta \cos\phi \underline{e}_2 + \sin\Theta \sin\phi \underline{e}_3), \tag{3}$$

with Θ the pitch and ϕ the phase angle relative to $\underline{B}$. In index notation the last term of (1) is $\epsilon_{ijk} < p_j v_\ell > b_{k,\ell}/q$ and determination of $< \underline{v}_g >$ or $< \underline{v}_g >_\Omega$ only requires finding the components $< p_j v_\ell >$ of the $< \underline{p}\underline{v} >$ tensor, given a particular F. In BMW it is shown that the most complicated F which gives a tractable expression for $\underline{v}_g$ is

$$F(\underline{x},\underline{p},t) = F_{00} + (F_{10}\cos\Theta + F_{11}\sin\Theta\cos\phi + F_{1,-1}\sin\Theta\sin\phi) + \sum_{\ell=2}^{\infty} F_{\ell 0}P_\ell(\cos\Theta), \tag{4}$$

where P_ℓ are the Legendre polinomials. The $< \underline{p}\, \underline{v} >$ tensor is of the form:

$$< \underline{p}\, \underline{v} > = \begin{bmatrix} <p_\parallel v_\parallel> & 0 & 0 \\ 0 & \tfrac{1}{2}<p_\perp v_\perp> & 0 \\ 0 & 0 & \tfrac{1}{2}<p_\perp v_\perp> \end{bmatrix}, \quad \begin{aligned} < p_\parallel v_\parallel > &= \frac{1}{3}< pv(1 + \frac{2}{5}\frac{F20}{F00}) > \\ \tfrac{1}{2}<p_\perp v_\perp> &= <p_2 v_2> = <p_3 v_3> \\ &= \frac{1}{3}< pv\,(1 - \frac{1}{5}\frac{F20}{F00}) > \end{aligned} \tag{5}$$

N85-34841

For this form of F, the average drift velocity (1) becomes

$$\langle \underline{v}_g \rangle = \langle \underline{v}_\parallel \rangle + \underline{E}\times\underline{b} + \frac{1}{q}\left[\tfrac{1}{2}\langle p_\perp v_\perp \rangle \underline{\nabla}\times b + \underline{(\langle p_\parallel v_\parallel \rangle - \tfrac{1}{2}\langle p_\perp v_\perp \rangle)\frac{1}{B}\left(\underline{\nabla}\times\frac{\underline{B}}{B}\right)_\perp} \right] \tag{6}$$

There are six noteworthy points about this seemingly familiar result: (i) It is the *instantaneous* average guiding centre velocity of particles in the volume element d^3x in terms of the fields $\underline{E}$ and $\underline{B}$ *inside* d^3x. The usual "single particle" derivations (e.g. Rossi and Olbert, 1970) give a similar result, but for the *time* (gyroperiod) averaged drift velocity in terms of the fields $\underline{E}_g$ and $\underline{B}_g$ *at the guiding centres.* (ii) Our analysis does not need the usual "single particle condition that $R \ll L$ (where L is the smallest scale length of variation of $\underline{E}$ and $\underline{B}$). *But*, this does not mean that (6) is valid for any ratio R/L, as is discussed in Section 3. (iii) The result (6) is usually interpreted to hold only for gyrotropic distributions, in which $F_{11} = F_{1,-1} = 0$ in (4), (e.g. Rossi and Olbert, 1970; Lee and Fisk, 1981). This too strict condition on F stems from imprudent mixing of the $\langle \underline{p}\,\underline{v} \rangle$ tensor with the pressure tensor $\underline{\underline{P}} = N(\langle \underline{p}\,\underline{v} \rangle - \langle \underline{p} \rangle\langle \underline{v} \rangle)$. (iv) If F is of the simple form $F = (1+\cos\theta)^\gamma$, the underlined term in (6) exceeds the first one in $[\;]$ only if $\gamma \geq 3.56$. This represents a much higher anisotropy than usually found in Astrophysical applications, because then fully 95% of the particles have pitch angles in the forward range $0 \geq \theta \geq \pi/2$. (v) For first order anisotropies, $F_{\ell j}(\ell \geq 2) = 0$, the exact guiding centre velocity is form (5):

$$\langle \underline{v}_g \rangle = \langle \underline{v}_\parallel \rangle + \underline{E}\times\underline{b} + (P/qN)\,\underline{\nabla}\times\underline{b} \tag{7a}$$

or

$$\langle \underline{v}_g \rangle_\Omega = \langle \underline{v}_\parallel \rangle_\Omega + \underline{E}\times\underline{b} + (pv/3q)\,\underline{\nabla}\times\underline{b} \tag{7b}$$

where $P = (N/3)\langle pv \rangle$ is the scalar pressure. Because of the error mentioned in (iii), this is usually quoted as an approximate result, strictly valid for isotropic distributions only. (vi) Since

$$\underline{\nabla}\times\underline{b} = \frac{1}{B}\left[\frac{\underline{B}\times\underline{\nabla}B}{B^2} + \underline{\nabla}\times\frac{\underline{B}}{B}\right], \tag{8}$$

the last term in (7) is the sum of the usual gradient and curvature drift.

2. Average Particle Velocity $\langle \underline{v} \rangle$ and Nomenclature. From the first moment of the Vlasov Equation $\partial F/\partial t + \underline{v}\cdot\underline{\nabla}F + \dot{\underline{p}}\cdot\underline{\nabla}_p F = 0$, it is readily shown that in the steady state the average particle velocity for a distribution of the form (4) is

$$\langle \underline{v} \rangle = \langle \underline{v}_\parallel \rangle + \underline{E}\times\underline{b} + \frac{1}{q}\left[\frac{\underline{b}}{N}\times\underline{\nabla}(N\langle \tfrac{1}{2}p_\perp v_\perp \rangle) + \underline{(\langle p_\parallel v_\parallel \rangle - \tfrac{1}{2}\langle p_\perp v_\perp \rangle)\frac{1}{B}\left(\underline{\nabla}\times\frac{\underline{B}}{B}\right)_\perp} \right] \tag{9}$$

The underlined term is identical to the one in (6). For first order anisotropies this reduces to the well-known form

$$\langle \underline{v} \rangle = \langle \underline{v}_\parallel \rangle + \underline{E}\times\underline{b} + 1/(qN)\,\underline{b}\times\underline{\nabla}P, \tag{10a}$$

or in the differential case

$$\langle \underline{v} \rangle_\Omega = \langle \underline{v}_\parallel \rangle_\Omega + C\underline{E}\times\underline{b} + pv/(3qU)\,\underline{b}\times\underline{\nabla}U \tag{10b}$$

where $U = p^2(1/4\pi)\int F\,d\Omega$ is the differential number density in (p,p+dp), and $C = 1-(1/3U)\partial/\partial p(pU)$ the Compton-Getting factor. The results (10) are standard in cosmic ray literature.

From the definition $\underline{x}_g = \underline{x} - \underline{R}$ it follows that $\langle \underline{v}_g \rangle = \langle \underline{v} \rangle - \langle d\underline{R}/dt \rangle$. The average circulation velocity $\langle d\underline{R}/dt \rangle$ is usually called the diamagnetic drift, and together with $\langle \underline{v} \rangle$, these two velocities are frequently referred to as *collective plasma drifts.* This is in opposition to the guiding centre drift which is called a "single particle drift". The average guiding centre drift seems equally collective to us. We also argue that the guiding centre drift is the *only* drift, because it is designed to tell you where the distribution goes after the troublesome, typically dominant circular motion of each particle has been subtracted.

In BMW these arguments are extended to the non-steady state ($\partial/\partial t = 0$). After multiplication of all velocities with qN it is easily shown that for first order anisotropies

$$\underline{J} = \underline{J}_g + \underline{J}_b + \underline{J}_p = \underline{J}_g + \underline{\nabla} \times \underline{M} + \partial\underline{\Pi}/\partial t, \qquad (11)$$

where $\underline{M}=-N\langle\frac{1}{2}p_\perp v_\perp\rangle\underline{b}$ is the diamagnetic moment per unit volume and $\underline{\Pi}=\underline{b}\times N\langle\underline{p}\rangle$ the polarisation vector of the plasma. The total plasma current density is therefore the sum of the guiding centre (or free) current density, the diamagnetic (or bound) current density and the polarisation current density. When standard "single particle" drift analyses are used, the equivalent result for (11) can only be written down readily for the perpendicular components (e.g. Parker, 1957). Northrop (1961, 1963) also included the parallel components but he needed the introduction of a distribution function F_g for guiding centres in addition to F, and elaborate algebra to do it. By contrast our result is essentially true per definition.

3. Neutral Sheet Drift. Standard drift theory breaks down at neutral sheets ($B=0$) because the condition $R/L\ll1$ is violated. Our derivations are independent of this ratio but they still break down. The reason follows from Figure 1 which shows a field $\underline{B}=B(x)\underline{e}_z$, with $B(x)$ homogeneous in x, and dB/dx any arbitrary large positive value. The drift of particles such as (a) and (b) is perfectly well described by the last term of (7), independent of the magnitude of dB/dx. However (8) shows that at $x=0$, $\underline{\nabla}\times\underline{b}\to\infty$, while Figure 1 suggests that individuals drift with finite velocity. Consequently $\langle\underline{v}_g\rangle$ cannot be infinite (as it was used by Jokipii and Thomas (1981, and references therein)). The obvious reason for this breakdown is that the drift velocity at $x=0$ *depends on the phase angle at the point of crossing.*

The drift in and around a neutral sheet is readily calculated if $\underline{B}$ is given by $\underline{B}(x)=[2H(x)-1]B_o\underline{e}_z$, where B_o is a constant and H the unit step function at $x=0$. Figure 2 shows the orbit of a particle with velocity $\underline{v}=(v,\Theta,\phi)$, projected onto the plane $\Theta=\pi/2$. It last crossed the sheet at point a under phase angle ϕ_c, and will again do so at point b after having completed a projected arc length $s=2R_o(\pi-\phi_c)\sin\Theta$, where $R_o=p/(qB_o)$. At that time the guiding centre abruptly jumps a distance $\ell=2R_o\sin\Theta\sin\phi_c$ in the direction of $-\underline{e}_y$. Therefore the component of the (time averaged) guiding centre velocity in the direction $-\underline{e}_y$ may be taken as

$$v_{gy} = \ell/\Delta t = (\ell/s)\,v\sin\Theta = [v/(\Pi-\phi_c)]\sin\Theta\sin\phi_c \qquad (12)$$

From the relation $\cos\phi_c=\cos\phi+x/(R_o\sin\Theta)$ it follows that of all the particles momentarily inside d^3x, at a distance x from the sheet, only those with

$$\Theta_1<\Theta<\Pi-\Theta_1 \text{ and } \phi_1<\phi<2\Pi-\phi_1, \text{ where } \sin\Theta_1=x/(2R_o) \text{ and } \cos\phi_1=1-x/(R_o\sin\Theta) \qquad (13)$$

can cross the sheet before completing a full orbit. Therefore the directionally averaged drift velocity over an isotropic particle distribution inside d^3x is

$$\langle\underline{v}_g\rangle_\Omega = -\underline{e}_y(v/4\Pi)\int_{\Theta_1}^{R-\Theta_1} d\Theta\sin^2\Theta \int_{\phi_1}^{2\Pi-\phi_1} d\phi\sin\phi_c(\Theta,\phi)/[\Pi-\phi_c(\Theta,\phi)] \qquad (14)$$

The x-component of the drift velocity oscillates and does not contribute to the average, while the z-component of the average is zero for an isotropic distribution. The integral (14) can be evaluated as a series at $x=0$ to give $\langle\underline{v}_g\rangle=-0.463\underline{e}_y$ while its numerically calculated value in the range $-2R_o\leq x\leq2R_o$ is shown in Figure 2.

This interpretation of guiding centre drift at a neutral sheet differs considerably from previous ones. Firstly, there is no sheet current density of the form $\underline{J}(x)=J_o\delta(x)\underline{e}_y$ as is sometimes suggested. In fact the assumed isotropy implies $\underline{J}=0$ everywhere, even in a volume element d^3x at $x=0$. Secondly, the distribution in the entire range $-2R_o<x<2R_o$ progresses (drifts) in the direction $-\underline{e}_y$, instead of the infinite sheet drift current $\underline{J}_g=J_{go}\delta(x)\underline{e}_y$ derived by Jokipii *et al.* (1977) from the $\underline{\nabla}\times B/B^2$ term in (F).

As an example we consider the motion of cosmic rays in the interplanetary magnetic field.

$$\underline{B} = B_0(r_0/r)^2\left[e_r - (\Omega r \sin\Theta/V)\underline{e}_\phi\right]\left[1 - 2H(\Theta-\pi/2)\right], \qquad (15)$$

where $\underline{\Omega}$ is the angular velocity of the Sun, $\underline{V}$ is the radial solar wind velocity and the function (1-2H) models a flat neutral plane at $\Theta=\pi/2$. The neutral sheet drift (14) will be experienced by cosmic ray particles within an angle $\Delta\Theta=2R_0/r$ from the plane. If $V=400\ \mathrm{kms}^{-1}$, $\Omega=(2\pi/27)\ \mathrm{day}^{-1}$, r=1 A.U., and $B_0=5/\sqrt{2}$ nT ($|\ B\ |=5$ nT at Earth), it is readily shown that

$$\Delta\Theta = 0.72\ (P/P_0)r(r^2 + r_0^2)^{-\frac{1}{2}}\ \text{degrees}, \qquad (16)$$

where P is particle rigidity with $P_0=1$ GV. Typical cosmic ray protons with kinetic energy T=250 MeV, P=0.75 GV are therefore convected along the neutral plane in a region with thickness $2\Delta\Theta=1$ degree. This neutral plane drift effect is not included in existing drift models of cosmic ray modulation. Jokipii and Thomas (1981, and references therein) used the δ-function type drift velocity at the neutral plane, derived from the $\underline{\nabla}\times\underline{B}/B^2$ term. Potgieter and Moraal (1985) used a finite neutral plane drift velocity pattern, similar to that of Figure 2, but not based on the fundamental arguments used here. In their model the angular region $\Delta\Theta$ in (16) could i.a. be varied in an empirical and unjustified way, and it is significant that cosmic ray observations were better explained with finite neutral plane drift in a region $\Delta\Theta \geq 1°$, than with a δ-function type drift at $\Theta=\pi/2$ only.

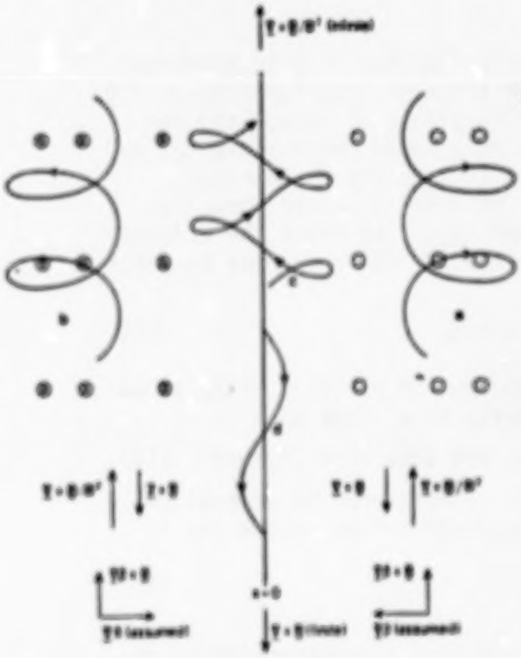

Figure 1

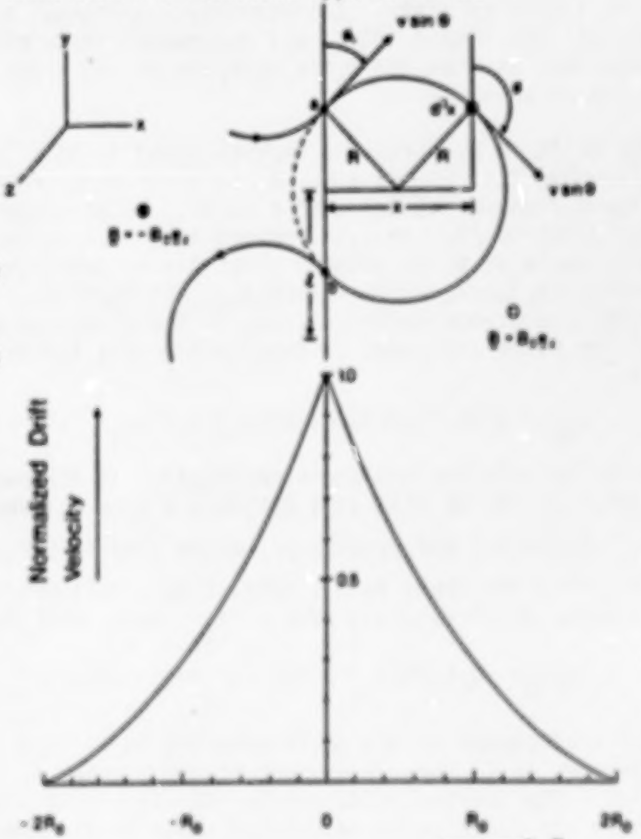

Figure 2

References

Burger, R.A., Moraal, H., & Webb, G.M.: 1985, Preprint available at Conference.
Jokipii, J.R., Levy, E.H., & Hubbard, W.B.: 1977, Ap. J., 213, 861.
Jokipii, J.R., & Thomas, B.: 1981, Ap.J., 243, 1115.
Lee, M.A., & Fisk, L: 1981, Ap.J., 248, 836.
Northrop, T.G.: 1961, Ann. Phys., 15, 79.
Northrop, T.G.: 1963, Adiabatic Motion of Charged Particles, Interscience, N.Y.
Parker, E.N.: 1957, Phys. Rev., 107, 924.
Potgieter, M.S., & Moraal, H.: 1985, Ap. J., 294, (July 15 issue).
Rossi, B., & Olbert, S.: 1970, Intr. to the Phys. of Space, Mc Graw-Hill, N.Y.

N85-34842

SH 4.2-4

DRIFT AND OBSERVATIONS IN COSMIC-RAY MODULATION. I.

M. S. Potgieter[1]
Space Science Center, University of New Hampshire,
Durham, NH 03824, USA

1. Introduction

Gradient and curvature drift, which are explicitly contained in standard cosmic-ray transport theories, were neglected until the mid-1970's. It was then realized that the sector structure of the interplanetary magnetic field (IMF) observed in the ecliptic plane does not pervade the whole heliosphere (e.g., Smith et al., 1978), but has a topology corresponding closely to that of a dipole at the Sun. Since then, several drift models based on the numerical solution of the cosmic-ray transport equation were published (Jokipii and Kopriva, 1979; Kota and Jokipii, 1983, and references therein). These models, mostly concerned with proton modulation, illustrate the general features of drift and show that drift has a rather dominant effect on solutions over a wide range of parameters.

The independently developed drift model of Potgieter and Moraal (1983, 1985) in general confirms these results, according to which the four basic effects - convection, diffusion, drift and energy change - each contribute to the modulation of cosmic rays in the heliosphere. The relative importance of drift has, however, not yet been established. In order to do so, observational evidence of effects primarily dependent on drift are required.

The change in polarity of the large-scale IMF is of fundamental importance in drift models. A major implication of this reversal in polarity is that protons and electrons should, due to drift, exhibit different behavior during consecutive solar activity cycles. A charge-sign dependent effect should therefore be observable, the magnitude of which may indicate the relative contribution of drift to the modulation of cosmic rays.

In this paper we report on our investigation of this effect using observed solar minimum spectra (Webber et al., 1983) and on the change in phase and amplitude of the diurnal anisotropy observed after the IMF polarity reversals in 1969-71 and 1980 (Potgieter and Moraal, 1983).

2. Model Calculations

We solved the steady-state transport equation numerically assuming azimuthal symmetry. The solar wind is assumed to increase rapidly as a function of radial distance r to 400 km s^{-1} in a spherical heliosphere with an outer boundary at r_b = 50 AU. The interstellar input spectra, boundary conditions, the spatial and energy dependence of the diffusion coefficients are given and motivated by Potgieter and Moraal (1985).

The IMF is assumed an Archimedean spiral with reversal of polarity across a flat neutral sheet. The reversal can be made either abrupt or smooth using a transition parameter $\theta_t = 90°$ and $85° \le \theta_t < 90°$ respectively. The drift velocity field calculated with $\theta_t = 86°$ is schematically presented for protons in Fig. 1.

---

[1] Also: Dept. of Physics, Potchefstroom University, South Africa

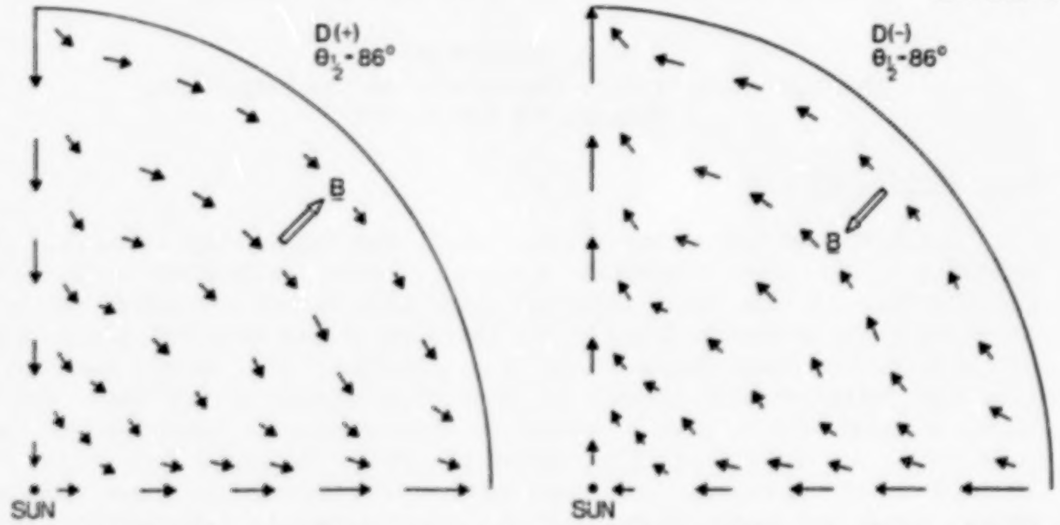

Fig. 1: Drift velocities for protons in the meridional plane with the transition parameter $\theta_{\frac{1}{2}} = 86°$. D(+): ∿ 1970-1980. D(-): ∿ 1959-1970; 1980-1991. The drift velocities reverse direction for electrons.

According to Fig. 1 positively charged particles are transported from the polar regions to the inner heliosphere during the D(+) epoch (including 1976-77) but from the outer equatorial regions to the inner heliosphere during the D(-) epoch (including 1965). This effect is quantitatively illustrated in Fig. 2 of Part 2 (Paper SH4.2-5). In contrast with the no-drift case, protons and electrons reaching Earth should traverse different regions of the heliosphere during consecutive solar minimum periods, causing a charge-sign dependent effect.

3. Results and Discussion

No-drift models have become less successful to simultaneously fit proton and electron spectra observed before and after IMF polarity reversals, e.g., the 1965 and 1977 spectra (Evenson et al., 1983). This indicates that the detailed behavior of low energy electrons and protons cannot be fully understood within the framework of numerical solutions to the spherically symmetric transport equation (see e.g., Rockstroh, 1977).

Recently, Evenson and Meyer (1984) reported that although protons and electrons responded to the onset of less modulation in much the same way in 1981-82, there is a systematic difference between the two sets of data. The electrons recovered more rapidly than the protons and were not as strongly modulated with increased activity in late 1982. Moreover, this effect is totally different from that observed by Burger and Swanenburg (1973) in 1968-72 when the electron recovery lagged behind that of protons. Perko (1984) used a time-dependent spherically symmetric model, doing calculations for an entire solar cycle, to establish to what extent the difference in rigidity between the data sets of Evenson and Meyer could produce the observed hysteresis. He found that the hysteresis went in the sense of the Burger-Swanenburg data. No-drift models can therefore neither explain the observed effect nor the higher electron intensities, but lower proton intensities observed in 1965 compared to that observed in 1976-77.

Our model, based on the assumption of steady-state and a flat neutral sheet, is applicable only to periods of minimum solar activity. This is, however, also the time for the best ordered large-scale IMF and the most likely period for drifts to occur. We therefore concentrated on a simultaneous fit to the observed 1965 and 1977 proton and electron spectra compiled by Evenson et al. (1983).

In contrast with the no-drift models, we could fit the mentioned spectra using one single set of modulation parameters, except for a change in the polarity of the IMF. Our result is best illustrated when compared to the ratio of the 1977 and 1965-66 data for protons and electrons respectively (Webber, et al., 1983). This is shown in Fig. 2.

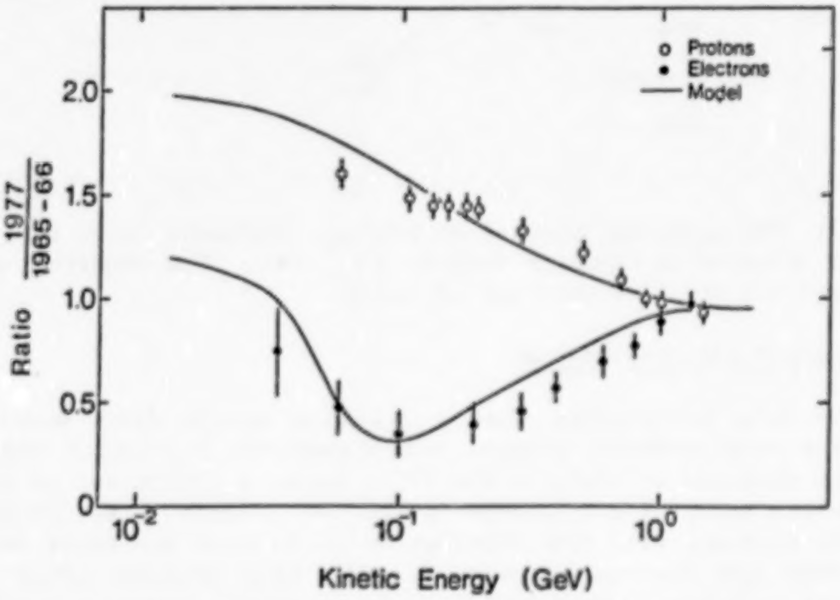

Fig. 2: Drift model calculations compared to proton and electron ratios for 1977 relative to 1965-66 (Webber, et al., 1983). The parameters used are given by Potgieter and Moraal (1985).

We want to emphasize that, other than perhaps less sophisticated equipment, there is no reason to doubt the validity of the 1965-66 electron data (Webber, private communication). We therefore interpret the result of Fig. 2 as a charge dependent effect due to drift, causing a factor of ∿ 2 difference at 500 MeV between consecutive solar minimum electron spectra.

An observation which is also unambiguously related to the reversal of the IMF polarity, is the shift in phase and amplitude of the diurnal anisotropy observed in 1969-71 and again in 1980-81 (Swinson, 1983). Fig. 3 shows, on a harmonic dial, the observed geomagnetically corrected anisotropy vector, calculated from the diurnal variation in the Hermanus neutron monitor (4.55 GV) counting rate. The vectors are averaged for 1964-66 and 1975-77; also for the entire period between polarity reversals, i.e., 1959-70 and 1971-79 respectively. These are compared to the calculated anisotropies at 1 GeV, using the same single set of modulation parameters used in Fig. 2. Our model is at least consistent with the observed shift in both phase and amplitude of the diurnal anisotropy following the 1969-71 polarity reversal, an effect which cannot be simulated by conventional spherically symmetric models.

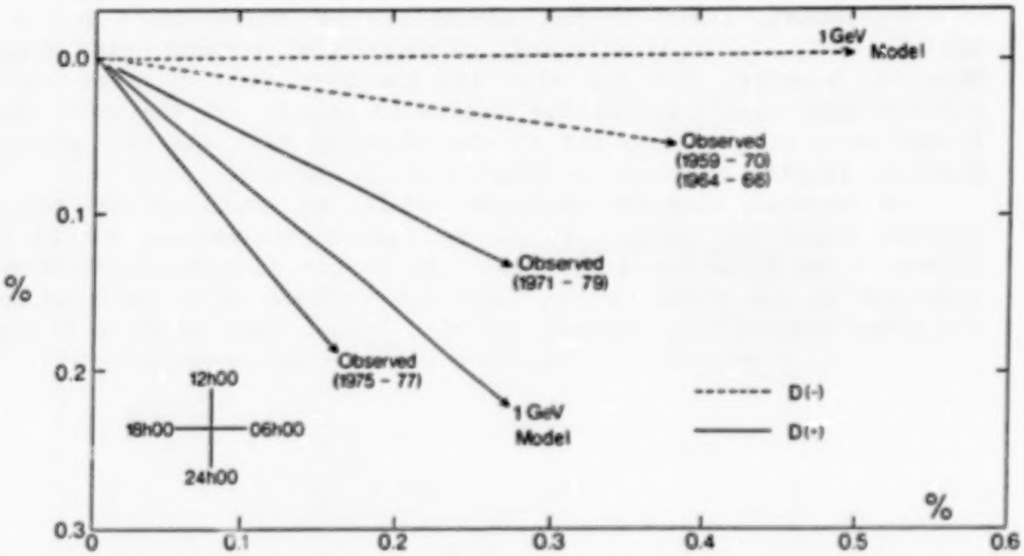

Fig. 3: The observed diurnal anisotropy (Hermanus, 4.55 GV), compared to the computed anisotropy vectors at 1 GeV. The observed values are averaged for the time periods indicated.

4. Summary and Conclusions

We have illustrated that a relative simple drift model can, in contrast with no-drift models, simultaneously fit proton and electron spectra observed in 1965-66 and 1977, using a single set of modulation parameters except for a change in the IMF polarity. We interpret this result, together with the observation of Evenson and Meyer (1984) that electrons are recovering more rapidly than protons after 1980, in contrast with what Burger and Swanenburg (1973) observed in 1968-72, as a charge-sign dependent effect due to the occurrence of drift in cosmic-ray modulation. The same set of parameters produces a shift in the phase and amplitude of the diurnal anisotropy vector, consistent with observations in 1969-71 and 1980-81.

5. Acknowledgements

This work was supported, in part, by the Space Science Center, University of New Hampshire and by the South African CSIR.

References

Burger, J.J. and Swanenburg, B.N., 1973, J. Geophys. Res., 78, 292.
Evenson, P., et al., 1983, Ap. J., 275, L15.
Evenson, P., and Meyer, P., 1984, J. Geophys. Res., 89, 1647.
Jokipii, J.R., and Kopriva, D.A., 1979, Ap. J., 234, 384.
Kota, J., and Jokipii, J.R., 1983, Ap. J., 265, 573.
Perko, J.S., 1984, Ph.D. Thesis, Univ. of New Hampshire, Durham, NH.
Potgieter, M.S., and Moraal, H., 1983, 18th ICRC (Bangalore), 10, 5.
Potgieter, M.S., and Moraal, H., 1985, Ap. J., in press.
Rockstroh, J.M., 1977, Ph.D. Thesis, Univ. of New Hampshire, Durham, NH.
Smith, E.J., et al., 1978, J. Geophys. Res., 83, 717.
Swinson, D.B., 1983, Proc. 18th ICRC (Bangalore), 10, 55.
Webber, W.R., et al., 1983, Proc. 18th ICRC (Bangalore), 3, 35.

N85-34843

SH 4.2-5

DRIFT AND OBSERVATIONS IN COSMIC-RAY MODULATION. II.

M.S. Potgieter
Space Science Center, University of New Hampshire,
Durham, NH 03824 USA

1. Introduction

In Part 1 (SH4.2-4) we have quantitatively shown that our drift model can simultaneously fit the observed 1965-66 and 1977 electron and proton spectra, in contrast with spherically symmetric models. We interpret this result as evidence of a charge-sign dependent effect due to particle drift. Using the same set of parameters, we could also simulate a shift in the phase and amplitude of the diurnal variation in the cosmic-ray (CR) intensity by reversing the polarity of the interplanetary magnetic field (IMF).

In this paper, again using the same set of parameters, we show that drift can cause significant differences in the radial and latitudinal dependence of cosmic rays for consecutive solar minimum periods. We also searched the literature for additional modulation features related to the IMF polarity reversal and therefore relevant to determining the role of particle drift in the modulation of cosmic rays.

2. Model Calculations

Using the parameters of Part 1, we calculated the radial and latitudinal dependence of the 100 MeV proton intensity for two consecutive solar minimum periods. The radial dependence, with the radial gradient G_r in %/AU, is shown in Fig. 1a. The latitudinal dependence, with the latitudinal gradient G_θ in %/degree, is shown for 1 AU and 20 AU in Fig. 1b and Fig. 1c respectively. For the D(+) period (1976), G_r remains almost constant for most of the heliosphere with a rapid increase near the boundary, and G_θ almost identical at 1 AU and 20 AU. For the D(-) period (1965), G_r is overall larger and decreases toward the boundary, while G_θ differs significantly for the two drift cases at 1 AU, and at 20 AU. (Note the difference in the intensity for the two drift solutions at 1 AU and 20 AU). The general behavior of the density gradients displayed in Fig. 1a-c is a feature of all drift models.

One of the best manifestations of the effect of drift becomes apparent when the transport equation is solved using θ-(polar angle) dependent Gaussian spectra at the outer boundary instead of the full θ-independent interstellar spectrum. By shifting these spectra (half-width of 10°) consecutively in 10° intervals from the heliospheric poles to the equator, the results shown in Fig. 2 were obtained. Protons reaching Earth from a particular region on the outer boundary are expressed as percentage of those that would have reached Earth if a full interstellar spectrum was used. The calculations were repeated for increasing values of the parallel diffusion coefficient $K_\parallel$ with other parameters unchanged. Solution (b) in Fig. 2 corresponds to the solutions in Fig. 1a-c. (Note that $(K_\parallel)_0$ is a constant in the expression for $K_\parallel$ given by Potgieter and Moraal, 1985). These results show, in contrast with the no-drift case, that drift causes positively charged particles reaching Earth to predominantly come from the outer equatorial regions during a D(-) period (1965), but from the outer polar regions when the IMF changes polarity. A factor 3 increase in K_w extends this region to include mid-latitudes, while the situation remains virtually unchanged for the D(-) period. In general these calculations show that oppositely charged particles should traverse different regions of the heliosphere (Part 1). Another implication is that the (anti) correlation between variations in the CR intensity and solar activity parameters should exhibit a 22-year cycle.

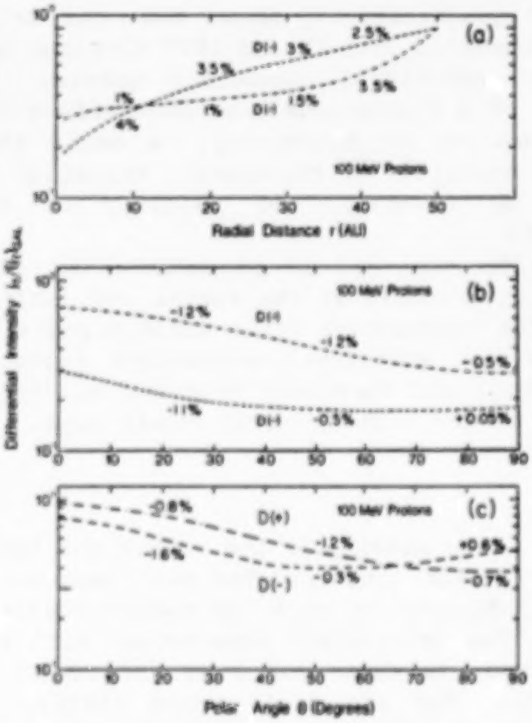

Fig. 1: (a) The radial dependence in the equatorial plane (θ = 90°), (b) the latitudinal dependence at 1 AU and (c) at 20 AU, of the 100 MeV proton intensity. (The differential gradients are in %/AU; -latitudinal gradients are in %/degree).

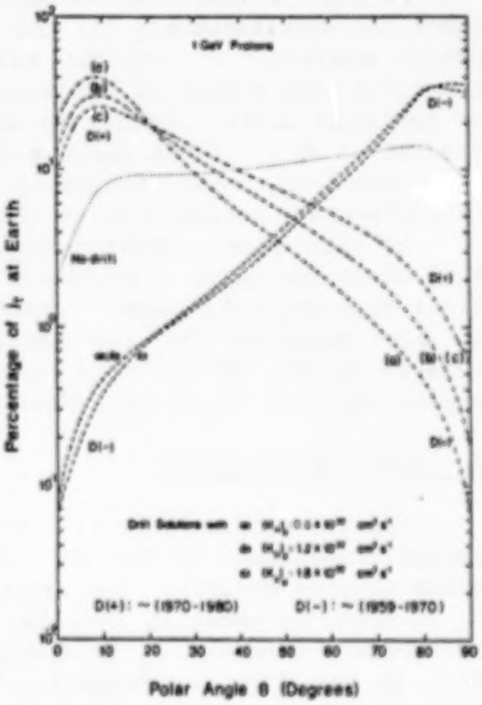

Fig. 2: The calculated percentage of 1 GeV protons reaching Earth from a particular region at the outer boundary for the two drift cases compared to the no-drift situation. The equatorial plane is at θ = 90°.

3. Discussion of Results and Observations

Fig. 1a-c show that drift can cause significant differences in the radial and latitude dependence of cosmic rays during consecutive solar minimum periods. Compared to our results, the observed integral latitudinal gradient (Decker et al., 1984) is as yet inconclusive about the role of drift. Jokipii (1984), however, by carefully simulating the exact observational conditions near the neutral sheet using a three-dimension drift model, found excellent agreement with the results of Newkirk and Fisk (1985), who studied the statistical dependence of CR intensity on the distance from the neutral sheet.

Less encouraging are observed integral radial gradients recently reported by Webber and Lockwood (1985) and McKibben et al. (1985). The radial gradient seems to decrease since 1981, which is not expected from a drift point of view. It also appears that our model predicts the radial gradient too small for the 1976 solar minimum period. Since both the radial and latitudinal gradients are rather insensitive to parameter variations in drift models, these observations may become an interesting challenge to these models. It is also a complicating factor in explaining the role of drift concerning the anomalous components. However, the near constancy of the integral radial gradient observed before 1980, despite large changes in solar activity (Webber and Lockwood, 1985), is consistent with our model, but not with time-independent spherically symmetric models. In these models a direct relation exists for variations in $K_\parallel$ and the radial gradient.

Potgieter et al. (1980) calculated neutron monitor differential response functions from latitude survey data for 1954, 1965 and 1976, and found that the 1965 response function deviates significantly from those for 1954 and 1976. Using the parameters of Part 1, which fit the low-energy 1965-66 and 1977 proton and electron data, we could not simulate the observed large difference between the corresponding response functions, although we obtained a split in the right direction. The complicating factor here is that the low-energy proton fluxes were higher in 1976-77 than in 1965, while the neutron monitor counting rates were lower in 1976-77 compared to 1965.

Another relevant observation is the change in direction of the annual wave vector, derived from the yearly variations in CR intensity, in 1958-59 and again in 1968-69 (e.g., Antonucci et al., 1978; Nosaka, et al., 1984). Whether drift effects are the predominant cause of this observation, is not yet clear and has to await more detailed studies.

From 1972-77 the CR intensity was an extended, rather flat plateau preceded by a fast recovery over 2 years in 1970-72. (See the correlation study of Akasofu et al., 1985 regarding this period). During the 1965 solar minimum the intensity was peaked, preceded by an extended recovery period of ∿ 7 years. This behavior is consistent with the feature of drift models that the proton intensity is less sensitive to variation in modulation parameters during a D(+) cycle (1970-80) compared to the 11-years before and after this period (Jokipii and Thomas, 1981; Kota and Jokipii, 1983; Potgieter and Moraal, 1985).

Shea and Smart (1981) found a correlation coefficient of -0.86 between the geomagnetic aa-index - a measure of disturbance in the ecliptic plane - and the CR intensity for the years around 1965. For this period Aldagarova et al. (1979) found that the CR intensity correlates best to coronal green line (CGL) intensity in the -20° to +20° heliolatitude range. However, for the years around 1976, Shea and Smart found a correlation coefficient of +0.28 and Aldagarova et al. the best correlation for +30° to +50°, and to a lesser extent for -20° to -30° heliolatitude. In combination these observations indicate that during a D(+) cycle (1976), variations in the CR intensity correlate better with solar activity parameters in a much wider heliolatitude range compared to a D(-) period (1965) when cosmic rays are predominantly transported to the inner heliosphere via the equatorial regions. (See also Jokipii, 1981). The same conclusion can be reached from the observations of Nagashima and Morishita (1980), Pandey et al. (1983) and Vernov et al. (1983), despite different data and techniques used by them. These observations are consistent with our calculations shown in Fig. 2 and the drift velocities shown in Part 1.

4. Summary and Conclusion

In Part 1 we discussed two key observations relevant to determining the relative importance of drift in cosmic-ray modulation. In the present paper, using the same set of parameters, we have illustrated the significant effect of drift on the radial and latitudinal dependence of cosmic rays for consecutive solar minimum periods. Compared with the integral radial gradient observed in 1976 (Webber and Lockwood, 1985), the calculated value seems too small. A detailed comparison will however have to await the forthcoming solar minimum. The same applies to the latitudinal gradient which is as yet inconclusive about drift effects.

Searching the literature for observations related to the IMF polarity reversal (in addition to Part 1), we found distinct difference in neutron monitor response functions for consecutive solar minimum periods, and also in the annual variations of cosmic rays observed before and after polarity reversals. Whether drift is the predominant effect is however not yet clear. We also found several reports which indicate better correlation between variations in the cosmic-ray intensity and solar activity parameters (e.g., the corona green line intensity) over a much wider range of heliolatitude during 1970-80 compared to before this period. These observations are consistent with drift models according to which cosmic ray protons primarily come via the polar regions during a D(+) period (1970-80), but primarily via the equatorial regions during D(-) periods. The observed peak vs. plateau in cosmic-ray intensity for the years around 1965 and 1976 respectively is also consistent with the general feature of drift models according to which the proton intensity is more sensitive to changes in modulation conditions during 1970-80 compared to before 1970.

5. Acknowledgements

This work was supported in part by the South African CSIR and the Space Science Center, University of New Hampshire.

References

Akasofu, S.I., et al., 1985, J. Geophys. Res., 90, 4439.
Aldagarova, Kh.Z., et al., 1979, Proc. 16th ICRC (Kyoto), 3, 343.
Antonucci, E., et al., 1978, Ap. J., 220, 712.
Decker, R.B., et al., 1984, Ap. J., 278, L119.
Jokipii, J.R., 1981, Geophys. Res. Lett., 8, 837.
Jokipii, J.R., 1984, Proc. Int. Symp. C.R., Morioka, Japan.
Jokipii, J.R., and Thomas, B., 1981, Ap. J., 243, 1115.
Kota, J., and Jokipii, J.R., 1983, Ap. J., 265, 573.
McKibben, R.B., et al., 1985, Ap. J., 289, L35.
Nagashima, K., and Morishita, I., 1980, Plant. Space Sci., 28, 195.
Newkirk, G., and Fisk, L.A., 1985, J. Geophys. Res., 90, 2391.
Nosaka, T., et al., 1984, J. Geomagn. Geoelectr., 36, 73.
Pandey, P.K., et al., 1983, Proc. 18th ICRC (Bangalore), 3, 91.
Potgieter, M.S., et al., 1980, South Afr. J. Phys., 3, 90.
Potgieter, M.S., and Moraal, H., 1985, Ap. J., in press.
Shea, M.A., and Smart, D.F., 1981, Adv. Space Res., 1, 47.
Vernov, S.N., et al., 1983, Proc. 18th ICRC (Bangalore), 3, 187.
Webber, W.R., and Lockwood, J.A., 1985, Paper SH4.3-1, this conference.

SH 4.2-6

N85-34844

COSMIC RAY NORTH-SOUTH ANISOTROPY 1961-1983

J. W. Bieber and M. A. Pomerantz
Bartol Research Foundation of The Franklin Institute
University of Delaware, Newark, DE 19716
USA

ABSTRACT

Measurements from neutron monitors in Thule (Greenland) and McMurdo (Antarctica) have been used to determine yearly values of the cosmic ray north-south anisotropy over the period 1961-1983. The results strongly suggest that superposed upon the mean anisotropy of 0.05% is a solar cycle variation of amplitude 0.03%. No evidence for a dependence of the anisotropy upon polarity of the solar poloidal magnetic field is found.

1. Introduction. Detailed information on the spatial distribution of cosmic rays in the heliosphere is essential for testing theories of the solar cycle modulation of galactic cosmic rays. An invaluable tool for probing the spatial distribution is the steady-state north-south anisotropy of cosmic rays, which has been found to be intimately related to the cosmic ray radial gradient (Swinson, 1969; Bercovitch, 1970; Iucci and Storini, 1972; Yasue, 1980; Pomerantz et al., 1982). Most investigations of this effect, however, have been limited to intervals of a few years, or else have combined data from many years, such that yearly variations were not evident. As a result, possible solar cycle or solar polarity dependences of the north-south anisotropy, and hence of the radial gradient at > 1 GV rigidities, are not well determined.

With the availability of neutron monitor data from north and south polar stations from 1961 to the present, an interval of more than 2 solar cycles, a comprehensive analysis of long-term changes in the north-south anisotropy is now feasible. The information gained through this analysis will provide important observational constraints that models of cosmic ray modulation must satisfy.

2. Results. Previous investigations of the steady-state north-south anisotropy have typically reported magnitudes ~ 0.1% or less. In order to extract this exceedingly small signal from the neutron monitor data, the method of analysis was designed with these goals in mind: (1) to reduce the effect of unrelated cosmic ray variations of much larger amplitude, (2) to take into account possible systematic variations in the relative efficiencies of the north and south polar detectors, and (3) to obtain reliable error estimates, which are essential for proper interpretation of the results. In essence, the method involved calculating, separately for toward and away polarity of the interplanetary magnetic field, the ratio of counts recorded at Thule to counts

recorded at McMurdo. The anisotropy was calculated for each solar rotation period from these ratios and from the relative efficiency of the two detectors, which was also determined separately for each solar rotation period. Finally, a yearly average of the anisotropy and an error estimate were calculated from this set of solar rotation values.

Results of the analysis appear in Figure 1, where yearly averages of the north-south anisotropy ξ_{NS} are plotted with $\pm$ 1σ error bars. By convention, ξ_{NS} is taken to be the value determined for toward sector polarity, with a positive value indicating that the observed cosmic ray intensity was larger at the north polar station than at the south polar station. With this convention, a positive value of ξ_{NS} is expected if the anisotropy arises from a positive radial gradient.

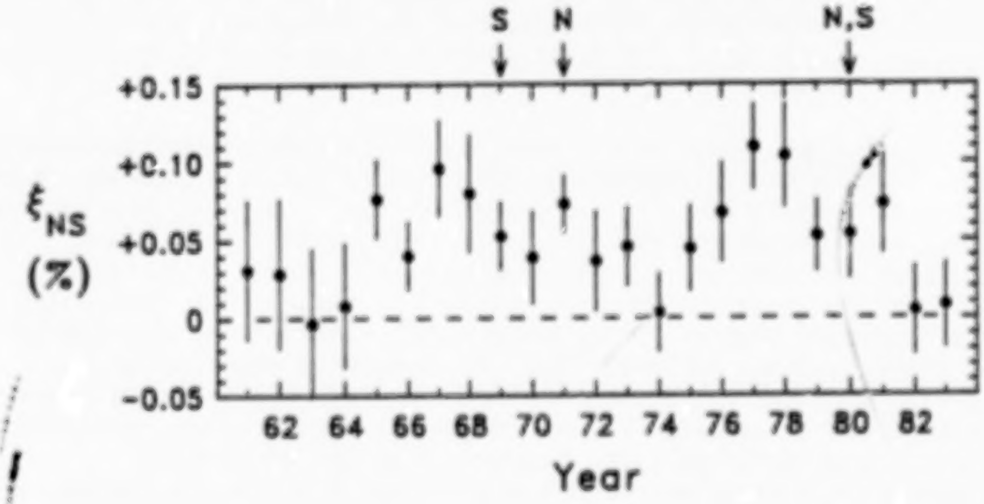

Fig. 1. Cosmic ray north-south anisotropy over a period of two solar cycles, as determined from neutron monitor observations at Thule and McMurdo. Arrows indicate years in which the sun's north (N) and/or south (S) pole changed magnetic polarity.

Note that there is no a priori reason that the method of analysis would preferentially yield positive values of anisotropy over negative ones. Thus, Figure 1 provides strong support for the interpretation that the steady-state north-south anisotropy results from a positive radial gradient via the $\vec{B} \times \vec{\nabla} n$ drift, with most points indicating positive values of anisotropy that differ significantly from zero.

3. Discussion.

Solar Cycle Variation of ξ_{NS}:

The value of the steady-state north-south anisotropy averaged over the 23-year period of this study is $\xi_{NS} = 0.052\%$. However, a possible solar cycle variation with period ~ 10 years is strongly suggested by Figure 1. To test this possibility quantitatively, the data of Figure 1 were assumed to be described by a constant plus a 10-year sinusoidal variation, with the phase and amplitude of the 10-year wave and the constant to be determined according to goodness-of-fit. The resulting constant term and wave amplitude were 0.053% and 0.028%, respectively, with the wave peaking in 1968 and 1978. Statistical tests indicate that there is only a 0.6% probability that a wave of this amplitude would occur by chance. Thus, a solar cycle variation of the cosmic ray north-south anisotropy is established with a high degree of confidence.

Effect of Drifts in Cosmic Ray Transport:

As illustrated in Figure 2, modulation models in which drifts play a predominant role predict that the radial profile of cosmic ray density will differ substantially between epochs of positive and negative polarity of the solar poloidal magnetic field (Jokipii and Kopriva, 1979). At a radial distance of 1 AU, the radial gradient — i.e., the slope of the curves in Figure 2 — is predicted to be substantially larger during epochs of negative solar polarity ($A < 0$) than during epochs of positive solar polarity ($A > 0$). This, in turn, would imply that the north-south anisotropy should show a corresponding dependence upon solar polarity.

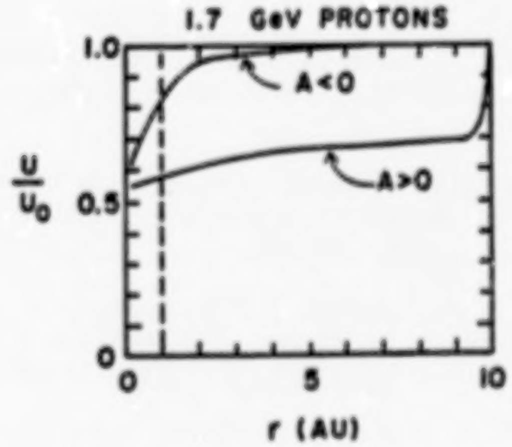

Fig. 2. Predicted relative intensity of cosmic rays as a function of radial distance (r) from the sun. Adapted from Figures 8 and 9 of Jokipii and Kopriva (1979).

The data of Figure 1 are inconsistent with this theoretical expectation. The average value of ζ_{NS} for the period 1961-1968, an epoch of negative solar polarity, was found to be 0.053%. Similarly, the value for the period 1972-1979, an epoch of positive solar polarity, was found to be 0.055%. A solar polarity dependence of the north-south anisotropy is not evident.

Cosmic Ray Radial Gradient:

The equations of cosmic ray transport permit information on the cosmic ray radial gradient to be inferred from a measurement of the north-south anisotropy. Since the relevant technique has been discussed by other investigators (e.g., Yasue, 1980), only results will be presented here. The average value of north-south anisotropy (0.053%) determined above corresponds to a radial gradient of 1.7%/AU at a rigidity of 10 GV, while the 10-year variation of the anisotropy suggests that the gradient actually oscillates between values ~ 0.8%/AU and ~ 2.6%/AU, the peaks occurring in 1968 and 1978. These inferred values of radial gradient appear to be generally consistent with recent spacecraft determinations of the integral radial gradient and its variation at lower energies (e.g., McKibben et al., 1985; Van Allen and Randall, 1985).

4. Acknowledgments. C. H. Tsao contributed significantly to the extensive computer analysis involved in this work. This research was supported by the National Science Foundation under grants ATM-8303758 and DPP-8300544.

References

Bercovitch, M., (1970), Determination of the heliocentric cosmic ray density gradient using neutron monitor data, Acta Physica Academiae Scientiarum Hungaricae, 29, Suppl. 2, 169.

Iucci, N., and M. Storini, (1972), The north-south anisotropy and the cosmic-ray radial gradient in the vicinity of the earth, Il Nuovo Cim., 10B, 325-333.

Jokipii, J. R., and D. A. Kopriva, (1979), Effects of particle drift on the transport of cosmic rays. III. Numerical models of galactic cosmic-ray modulation, Astrophys. J., 234, 384-392.

McKibben, R. B., K. R. Pyle, and J. A. Simpson, (1985), Changes in radial gradients of low-energy cosmic rays between solar minimum and maximum: Observations from 1 to 31 AU, Astrophys. J., 289, L35-L39.

Pomerantz, M. A., S. P. Duggal, A. J. Owens, M. F. Tolba, and C. H. Tsao, (1982), Cosmic ray north-south anisotropy: The role of the interplanetary magnetic field, J. Geophys. Res., 87, 10325-10330.

Swinson, D. B., (1969), 'Sidereal' cosmic-ray diurnal variations, J. Geophys. Res., 74, 5591-5598.

Van Allen, J. A., and B. A. Randall, (1985), Interplanetary cosmic ray intensity: 1972-1984 and out to 32 AU, J. Geophys. Res., 90, 1399-1412.

Yasue, S., (1980), North-south anisotropy and radial density gradient of galactic cosmic rays, J. Geomag. Geoelectr., 32, 617-635.

C-7

N85-34845

NORTH-SOUTH ASYMMETRY IN ACTIVITY ON THE SUN AND COSMIC RAY DENSITY GRADIENTS

D.B. Swinson[1], M.A. Shea[2], and J.E. Humble[3]

[1] Department of Physics and Astronomy, The University of New Mexico, 800 Yale N.E., Albuquerque, New Mexico 87131.

[2] Air Force Geophysics Lab., Hanscom AFB, Bedford, MA 01731.

[3] Department of Physics, University of Tasmania, Hobart, Tasmania, Australia 7001.

INTRODUCTION. One method of detecting a perpendicular cosmic ray density gradient ($\vec{\nabla} Np$) is to make use of the contribution of the drift term $\vec{B} \times \vec{\nabla} Np$ to the solar cosmic ray diurnal variation. This method has been described by Swinson [1970, 1976] and by Hashim and Bercovitch [1972]. The $\vec{B} \times \vec{\nabla} Np$ term produces a flow in the ecliptic plane perpendicular to the IMF $\vec{B}$, with the sense of the flow depending upon the sense of $\vec{B}$; this field-dependent flow adds vectorially to the usual azimuthal streaming which produces a cosmic ray intensity maximum at 18 hours solar time (after correction for geomagnetic bending). In the case of a southward perpendicular gradient, when the IMF is away from the sun, the resultant diurnal variation should have a larger amplitude, and the time of maximum should occur a little earlier, whereas if the IMF is toward the sun, the resultant diurnal variation should have a smaller amplitude with a later time of maximum. Swinson and Kananen [1982] have used this method to analyze neutron monitor and underground muon data, separated according to IMF sense, from 1965 to 1975, to show that there is a perpendicular cosmic ray gradient that pointed southward prior to 1969, and a suggested northward pointing gradient after the reversal of the sun's polar magnetic field in 1969-71.

DATA. In this paper we will consider data from four underground cosmic ray telescopes, two in the northern and two in the southern hemisphere. The telescopes are Embudo Cave (35.20°N, threshold rigidity 19 GV, median rigidity 132 GV), Socorro (34.04°N, threshold rigidity 45 GV, median rigidity 305 GV), Bolivia (16.31°S, threshold rigidity 16 GV, median rigidity 125 GV) and Hobart, (42.85°S, threshold rigidity 30 GV, median rigidity 162 GV). The data presented are for the periods 1965-83, 1968-83, 1965-76 and 1965-83, respectively. The yearly average solar diurnal variation for each telescope has been determined for days when the IMF was toward (T) and away from (A) the sun. The amplitude data are presented (the A amplitude should exceed the T amplitude for a southward gradient).

In Figure 1 the annual A and T amplitudes for each station, for all available data, are plotted for 1965 to

N85-34845

1983. The A amplitude points are joined by solid lines and the T amplitude points by dashed lines; shading occurs when A amplitudes are greater than T amplitudes, indicating a southward perpendicular gradient. The vertical lines on the diagram indicate the end of the solar polar field reversals of 1969-71 and 1980-81. Prior to 1971 there is a consistent predominance of A amplitudes over T amplitudes in both hemispheres, which is consistent with a southward perpendicular gradient during this period. After 1971, the northern hemisphere telescopes (Embudo and Socorro) show some dominance of T-amplitudes, while the southern hemisphere telescopes (Bolivia and Hobart) show little change from the pre-reversal situation. The average annual errors for the amplitudes plotted in Figure 1 are ±.014% for Embudo, ±0.165% for Socorro, ±0.16% for Bolivia and ±0.125% for Hobart.

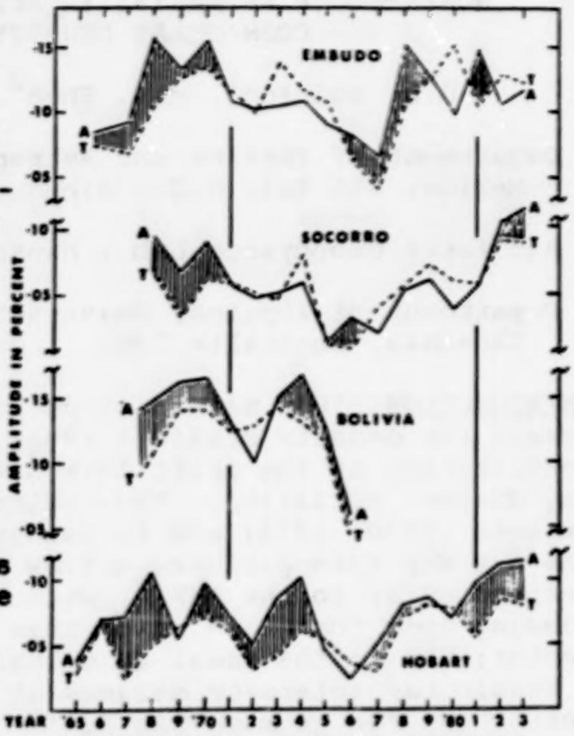

Figure 1. Yearly average amplitudes of away polar-polarity days (solid line) and toward polarity days (dashed line) for underground muon telescopes in Embudo, Socorro, Bolivia, and Hobart, 1965-1983.

The shaded areas occur when the amplitude for the away polarity exceeds that for the toward polarity.

In order to look for a possible cause for a perpendicular cosmic ray gradient we have examined data on the N-S asymmetry in activity on the sun. One might expect that when activity is greater on the sun's northern hemisphere, that activity might be more effective in sweeping cosmic rays out of the heliosphere above the ecliptic plane or in preventing galactic cosmic rays from entering, leading to a S-pointing perpendicular gradient. Here, we extend a study by Roy [1977], which used the "major" flares as defined by the comprehensive flare index, CFI, [Dodson and Hedeman, 1971] to show that between 1959 and 1970 there was a greater frequency of flares in the northern hemisphere of the sun than in the southern hemisphere; this northern hemisphere asymmetry was not evident from 1971 to 1974. This paper extends the results of Roy through 1980.

The number of flares in each hemisphere was counted as a function of month and year, using observations from the worldwide network of solar optical and radio patrol stations. From these data, an annual average for the per-

ORIGINAL PAGE IS
OF POOR QUALITY

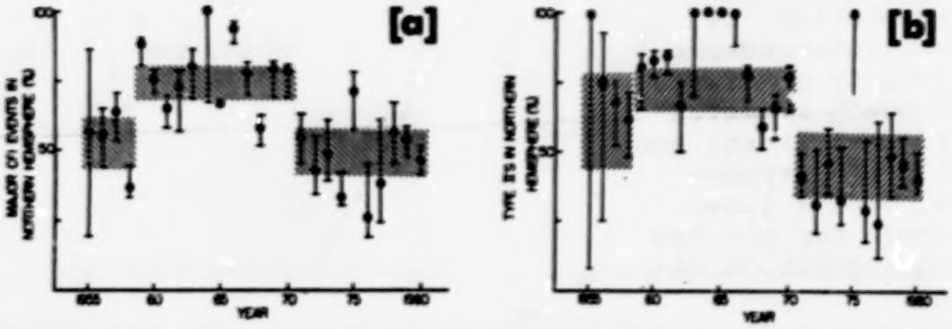

Figure 2(a) The percentage of "major" flares, as defined by the comprehensive flare index, that occurred in the northern hemisphere of the sun from 1955 through 1980, and (b) the percentage of flares with Type II radio emission that occurred in the northern hemisphere of the sun from 1955 through 1980. See text for further explanation.

centage of major events in the northern solar hemisphere was determined, and these annual averages are displayed as solid dots in Figure 2(a). The data have also been arranged into groups of years, and the average for each group of years falls within the shaded regions in Figure 2(a). It is clear that there is a strong, statistically significant dominance of solar northern hemisphere activity from 1959 to 1970, with an essentially even distribution of activity between the two solar hemispheres before and after that period.

This same method was applied to a sub-set of these "major" events -- the events for which metric Type II solar radio emission has been associated. These events were selected primarily because a Type II radio burst is indicative of a shock passing through the corona between 1.5 and 2 solar radii, which could subsequently effect the cosmic ray intensity in the inner heliosphere, particularly at that latitude. This sub-set of Type II events is displayed in Figure 2(b), where the results are comparable to those in Figure 2(a). Data in Figure 2 are preliminary; a complete analysis will be published later.

DISCUSSION AND CONCLUSION: The marked N-S asymmetry in solar activity (with predominant activity in the sun's northern hemisphere) during the 1960's could certainly account for a S-pointing cosmic ray gradient. It is also clear from the data in Figure 1 that the response to this change in solar activity asymmetry, and the related change in the perpendicular cosmic ray density gradient, is different for cosmic ray telescopes in the earth's northern and southern hemispheres. Northern hemisphere detectors see a S-pointing gradient in the 60's and a N-pointing gradient after 1971, while southern hemisphere telescopes see a S-pointing gradient both before and after the reversal.

These results can be accounted for by a combination of a

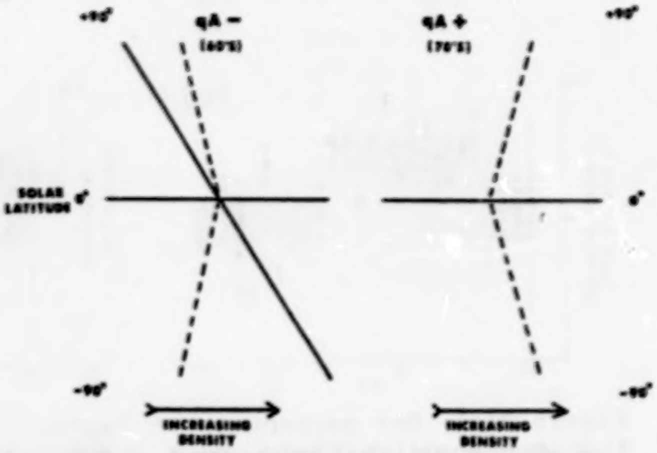

Figure 3. Schematic representation of perpendicular cosmic ray density gradients. North-South symmetrical (dashed lines) and North-South asymmetrical (solid lines) are shown for the two IMF configuration qA- and qA+.

N-S symmetrical gradient, and a significantly larger N-S asymmetrical gradient that is present only during the 1960's (dashed lines and solid lines, respectively, in Figure 3). The N-S symmetrical gradient arises naturally as the result of cosmic ray trajectories in the heliosphere [Erdos and Kota, 1981; Kota and Jokipii, 1983]; for these symmetric gradients, the cosmic ray intensity decreases with increasing heliolatitude before the 1969-71 reversal, and increases with increasing heliolatitude after the reversal as shown schematically in Figure 3. The N-S asymmetrical gradient is greater in magnitude than the symmetrical gradients, and is S-pointing above and below the equator before the reversal, as shown schematically by the solid line in Figure 3; the asymmetrical gradient is attributed to the N-S asymmetry in solar activity demonstrated in Figure 2. After the reversal there is no N-S solar activity asymmetry and therfore no N-S asymmetrical cosmic ray density gradient. Cosmic ray telescopes in the northern hemisphere therefore see a density gradient above the ecliptic plane that is S-pointing before the reversal and N-pointing after it, while telescopes in the southern hemisphere see a gradient below the ecliptic plane whose resultant effect is S-pointing before and after the reversal, leading to the cosmic ray effects seen in Figure 1.

ACKNOWLEDGEMENTS. The work of one of the authors (DBS) was supported by the Atmospheric Sciences Section, National Science Foundation, under grant ATM-8305098.

REFERENCES.

Dodson, H.W. & E.R. Hedeman, UAG-14, World Data Center A, 1971.
Erdos, G. & J. Kota, Proc. 17th ICRC (Paris), 10, 105, 1981.
Hashim, A & M. Bercovitch, Planet. Space Sci., 20, 791, 1972.
Kota, J. & J.R. Jokipii, Astrophys. J., 256, 573, 1983.
Roy, J.-R., Solar Physics, 52, 53, 1977.
Swinson, D.B., J. Geophys. Res., 75, 7303, 1970.
Swinson, D.B., J. Geophys. Res., 81, 2075, 1976.
Swinson, D.B. & H. Kananen, J. Geophys. Res., 87, 1685, 1982.

N85-34846

COSMIC RAY INTENSITY AND THE TILT OF THE NEUTRAL SHEET

T. Saito[1] and D. B. Swinson[2]

[1] Onagawa Magnetic Observatory and Geophysical Institute,
Tohoku University, Sendai 980, JAPAN

[2] Department of Physics and Astronomy, The University of
New Mexico, 800 Yale N.E., Albuquerque, NM 87131

ABSTRACT

Recent publications have related long-term variations in cosmic ray intensity at the earth with long term variations in the tilt of the neutral sheet in the inner heliosphere. In this paper we compare the tilt of the neutral sheet from 1971 to 1974 with the cosmic ray intensity at earth, recorded by the Mt. Washington neutron monitor. The remarkable large decreases in cosmic ray intensity which occurred in 1973 and 1974 correlate well with excursions in the tilt of the neutral sheet which occurred earlier during these same two years.

INTRODUCTION: Recently Hoeksema et al. [1982, 1983] have determined the structure of the heliospheric current sheet, computed on a source surface at 2.35 solar radii, using solar magnetograph data from the Stanford Solar Observatory. They note that the extent in latitude of the neutral sheet slowly increased from ~15° near sunspot minimum in 1976, to ~50° by 1978, and extending nearly to the poles by solar maximum. Similar behavior has been noted earlier by Saito [1975, 1984]; in Figure 1 examples of the neutral sheet configuration near solar minimum (1954) and close to solar maximum (1968-69) are shown. The sheet is obtained by drawing the Parker spirals from the interplanetary neutral line on the solar source surface (the central sphere), where the source surface sphere with real radius of 2.6 solar radii is exaggerated in the figure to a radius of 30 solar radii for clarity. The outer sphere, which has a radius of one astronomical unit, shows the neutral sheet configuration near the earth.

The neutral sheet, as displayed in Figure 1, will of course extend well beyond the earth, presumably to the limits of the heliosphere, and will therefore influence the trajectories of incoming galactic cosmic rays which will eventually be detected at the earth. It would seem probable that a greater inclination of the current sheet (from its position at solar minimum), with its accompanying enhanced warping, would present a potentially longer path for galactic cosmic rays between the heliopause and the earth, and would lead to a reduction in cosmic ray intensity at the earth. Kota and Jokipii [1983] have calculated particle trajectories in a 3-dimensional IMF, incorporating a wavy neutral sheet,

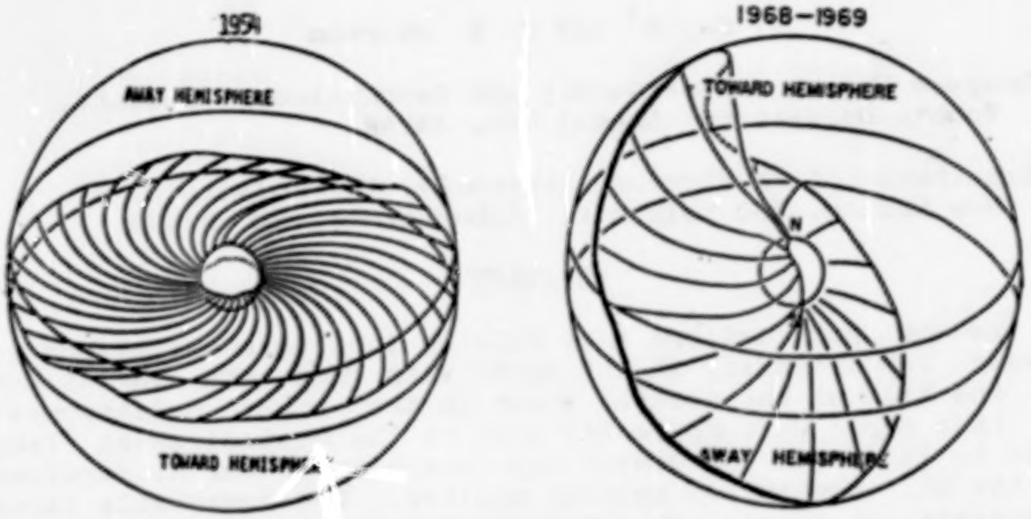

FIG. 1. Neutral sheet configuration between the sun and the earth near solar minimum (1954) aand near solar maximum (1968-69).

for both polarities of the sun's polar magnetic field. They find that, when the field is away from the sun in the sun's northern hemisphere (qA+), cosmic rays enter the heliosphere preferentially by way of the poles, while for the opposite magnetic configuration (qA-) cosmic rays enter preferentially via the neutral sheet. By incorporating a tilt angle for the neutral sheet that is small near solar minimum and larger at solar maximum, they are able to account for the variation in cosmic ray intensity at the earth during the two solar cycles from 1958 to 1980.

Smith and Thomas [1985] have used the data of Hoeksema et al. [1982, 1983] to determine the inclination of the neutral sheet from 1976 to 1982, and they have compared the inclination with cosmic ray intensity at earth measured by the Deep River neutron monitor, and with cosmic ray intensity measurements in space made by Pioneer 10 as it proceeded from 10 to 30 AU. They note, as was predicted by Kota and Jokipii [1983], that the sensitivity of the cosmic ray intensity to changes in the tilt of the neutral sheet was significantly different before and after the reversal of the heliospheric magnetic field. They observed a good correlation between increasing tilt angle and decreasing cosmic ray intensity, with the sensitivity being enhanced when the field was inward in the northern solar hemisphere (qA-).

In this paper we examine the correlation between the inclination of the neutral sheet between 1971 and 1974 and the cosmic ray intensity at the earth as measured by the Mt. Washington neutron monitor during that period.

ORIGINAL PAGE IS
OF POOR QUALITY

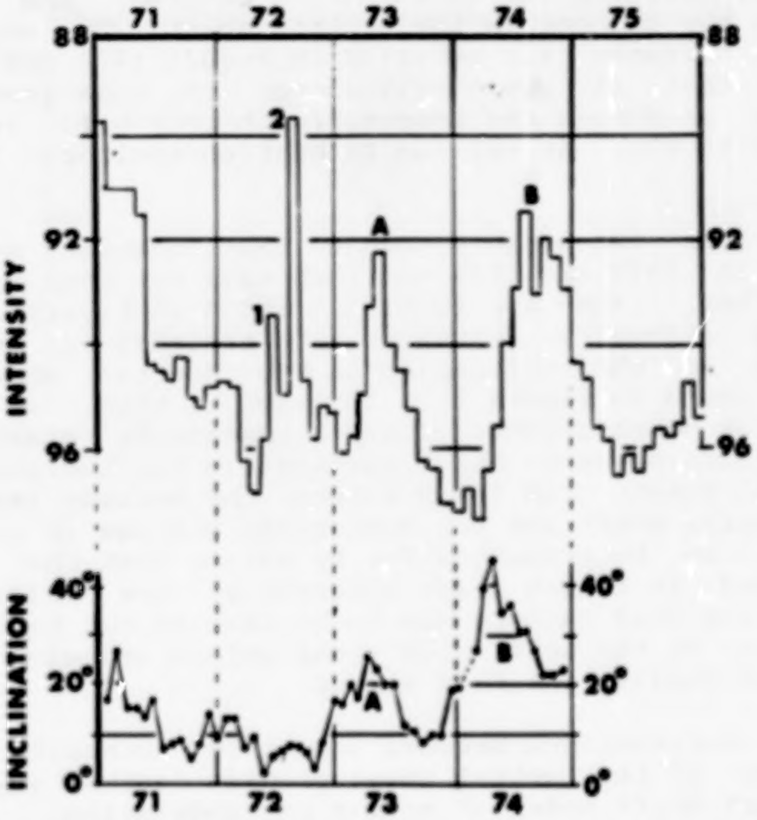

FIG. 2. (Top) Mt. Washington Neutron Monitor monthly average counting rate for 1971-1975, with intensity scale inverted, and (bottom) the average inclination of the neutral sheet for each solar rotation for 1971-1974.

DATA: K-Corona data have been used to determine the configuration of the heliomagnetospheric neutral sheet, and the inclination has been obtained for every Carrington rotation from 1971 to 1974. The basic data are the synoptic charts of K-corona intensity from 1971 to 1974. The latitude of the neutral line $\Lambda_o(\Phi)$ for a certain longitude Φ is obtained as $\Lambda_o(\Phi) = 1/2\ (\Lambda_N(\Phi) + \Lambda_S(\Phi))$, where Λ_N and Λ_S indicate the latitudes of the northern and southern borders of the bright K-coronal belt at longitude Φ. We define the tilt of the neutral sheet as the angle between the plane fitted to the various values of $\Lambda_o(\Phi)$, for one rotation, and the heliographic equator. The average inclination angles for each rotation are displayed at the bottom of Figure 2. At the top of the Figure the monthly average Mt. Washington neutron monitor counting rate is displayed [Lockwood and Webber, 1984], with the scale inverted i.e., intensity increases in the downward direction. The rate is normalized to 100 = 2506. In addition to the general correlation between the cosmic ray intensity and the inclination angle over the entire period, we note two very marked decreases in cosmic ray intensity in 1972; these are labeled 1 and 2 in Figure 2.

ORIGINAL PAGE IS
OF POOR QUALITY

These decreases are due to events on the sun, and are not related to any changes in the neutral sheet. The most marked of these decrases (#2) occurred in August 1972 and was so energetic that it was observed even by underground muon telescopes at Embudo and Socorro (with threshold regidities 19 GV and 45 GV), as well as by neutron monitors [Swinson, 1973].

The other two notable cosmic ray intensity decreases occurred in 1973 and 1974 and they have not thus far been accounted for. They are labeled A and B in Figure 2. These two large intensity decreases were preceded by two large excursions in the inclination of the neutral sheet, also labeled A and B in Figure 2. In light of this, as well as the previous observations, it seems reasonable to ascribe the intensity decreases to the excursions in the inclination of the neutral sheet. The delay between the maximum inclination of the neutral sheet and the subsequent minimum in cosmic ray intensity can be accounted for by noting that the inclinations noted in Figure 2 are observed at the solar source surface, and this pattern has to be carried out to the outer heliosphere at the solar wind speed before incoming galactic cosmic rays realize its full effect.

These correlations between cosmic ray intensity and the inclination of the neutral sheet provide further support for the gradient drift model of cosmic ray modulation.

ACKNOWLEDGMENTS: The authors express their thanks to J. R. Jokipii and E. J. Smith for valuable discussions, and to E. J. Smith for communicating the Smith and Thomas [1985] results prior to their publication. The work of one of the authors (DBS) was supported by the Atmospheric Sciences Section, National Science Foundation, under grant ATM-8305098.

REFERENCES

Hoeksema, J. T., J. M. Wilcox, and P. H. Sherrer, J. Geophys. Res., 87, 10, 331, 1982.
Hoeksema, J. T., J. M. Wilcox, and P. H. Sherrer, J. Geophys. Res., 88, 9910, 1983.
Kota, J. and J. R. Jokipii, Astrophys. J., 265, 573, 1983.
Lockwood, J. A. and W. R. Webber, J. Geophys. Res., 89, 17, 1984.
Saito, T., Sci. Rept. Tohoku Univ., Ser. 5, Geophys., 23, 37, 1975.
Saito, T., Extended Abstracts of Joint U.S.-Japan Seminar on the Heliomagnetosphere, 35, Kyoto, 1984.
Smith, E. J. and B. T. Thomas, Preprint, submitted to J. Geophys. Res., 1985.
Swinson, D. B., J. Geophys. Res., 78, 1707, 1973.

N85-34847

DIFFERENTIAL MEASUREMENT OF COSMIC-RAY GRADIENT WITH RESPECT TO INTERPLANETARY CURRENT SHEET

S. P. Christon, A. C. Cummings, and E. C. Stone
California Institute of Technology

K. W. Behannon, and L. F. Burlaga
Goddard Space Flight Center

ABSTRACT

Simultaneous magnetic field and charged particle measurements from the Voyager spacecraft at heliographic latitude separations from 10° to 21° are used to determine the latitude gradient of the galactic cosmic ray flux with respect to the interplanetary current sheet. By comparing the ratio of cosmic ray flux at Voyager 1 to that at Voyager 2 during periods when both spacecraft are first north and then south of the interplanetary current sheet, we find an estimate of the latitudinal gradient with respect to the current sheet of approximately -0.15 ± 0.05 %/deg under restricted interplanetary conditions.

1. Introduction. Organization of cosmic ray flux about the heliographic equator should result from symmetries in the interplanetary magnetic field produced by the sun's rotation. However, if particle drifts are important in cosmic ray transport, the cosmic ray flux should be organized with respect to the interplanetary current sheet. This symmetrizing property of the current sheet has been demonstrated in a three-dimensional model of cosmic ray transport including particle drifts [Kota and Jokipii, 1983]. At 1 AU, gradients with respect to the current sheet G_θ of up to ~ -0.33 %/deg have been identified for cosmic ray protons with energies >100 MeV in various integral energy ranges [Newkirk et al., 1984; Newkirk and Fisk, 1985].

The interplanetary current sheet is a surface separating regions of magnetic field pointing generally toward or away from the sun. In its least complicated configuration, the near-sun current sheet is essentially a circle tilted with respect to the heliographic equator. As the rotating sun's magnetic field is drawn out by the solar wind, warping of the current sheet ensues, thus allowing two spacecraft separated in latitude to sample fluxes on either side of it (Figure 1). The near-sun current sheet extends up to ~60° north N and south S of the equator and produces an interplanetary sector pattern that varies between two and four sectors during the period of this study [Hoeksema, 1984].

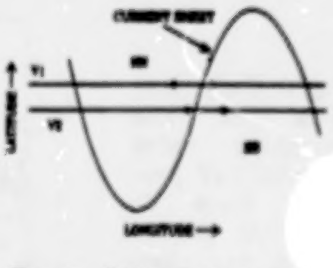

Fig. 1. Schematic representation of NN and SS configuration.

We determine G_θ using spacecraft trajectory information, the ratio of cosmic ray flux, and observations of the current sheet (magnetic field sector boundaries) at Voyager 1 (V1) and Voyager 2 (V2), separated in latitude by 10° to 21°. Such a differential measurement has significantly smaller non-latitudinal intensity variations than a single-point measurement such as the type employed by Newkirk et al. and Newkirk and Fisk. The cosmic ray flux at an observation point in the heliosphere is $j = j_b \exp(G_r(r-R_b))\exp(G_\theta(\theta-\theta_{cs}))$, where G_r is the radial gradient, G_θ is the colatitude gradient with respect to the current sheet, R_b is the radius of the boundary of the heliosphere, j_b is the cosmic ray flux at R_b, assumed constant, θ_{cs} is the colatitude of the current sheet, and r and θ are the radius and colatitude of the observation point. Heliographic colatitudes θ from 0° to 180° correspond to heliographic latitudes from 90°N to 90°S. Time series of simultaneous observations at two points in interplanetary space well separated in latitude allow estimates of G_θ to be obtained for each interval in the series. These individual estimates of $G_\theta = (\ln\Gamma - G_r\,(r_1 - r_2))/(\theta_1 - \theta_2)$, where the subscripts 1 and 2 refer to V1 and V2, respectively, and Γ is the ratio of the flux at V1 to that at V2, are independent of variations in the separation of the observation points. Statistically weighted averages of $\langle G_\theta \rangle_{NN(SS)} = \sum_{i(j)} w_{\theta i(j)} G_{\theta i(j)} / \sum_{i(j)} w_{\theta i(j)}$ and $\langle G_\theta \rangle = \left[\sum_i w_{\theta i} G_{\theta i} - \sum_j w_{\theta j} G_{\theta j}\right] / (\sum_i w_{\theta i} + \sum_j w_{\theta j})$, where i(j) runs from 1 to $n_{NN}(n_{SS})$, the number of observations when both spacecraft are north (NN) or both south (SS) of the current sheet. The first character of the two character identifier represents the magnetic field region for V1, the second for V2. Data for NS and SN configurations are also collected and are used independently, and in combination with the NN and SS data, to estimate G_r.

2. Data Selection.

This study covers the period from day 240, 1981 until day 190, 1983, while the V1-V2 separation increased from 1.9 to 4.7 AU in radial distance from the sun and from 10° to 21° in latitude. V1 traveled from 11 to 17 AU and from 6°N to 20°N. V1-V2 longitude separation was ≤16°. Daily samples of counting rates of protons with energies >75 MeV and a median energy ~1.1 GeV measured by the nearly identical High Energy Telescopes of the Voyager Cosmic Ray Subsystem [Stone et al., 1977], and Γ the ratio of V1 to V2 counting rate samples are plotted in Figure 2. Calendar days for the NN and SS data sets are highlighted in the upper panel by underscoring. We have compared measurements taken at both spacecraft on the same day under the assumptions that convective effects are unimportant on the average, consistent with long-interval average observations [Venkatesan et al, 1983], and that local variations in the cosmic ray intensity, after eliminating solar flare transient effects, are due to variations in the distance to the current sheet [Newkirk and Fisk, 1985].

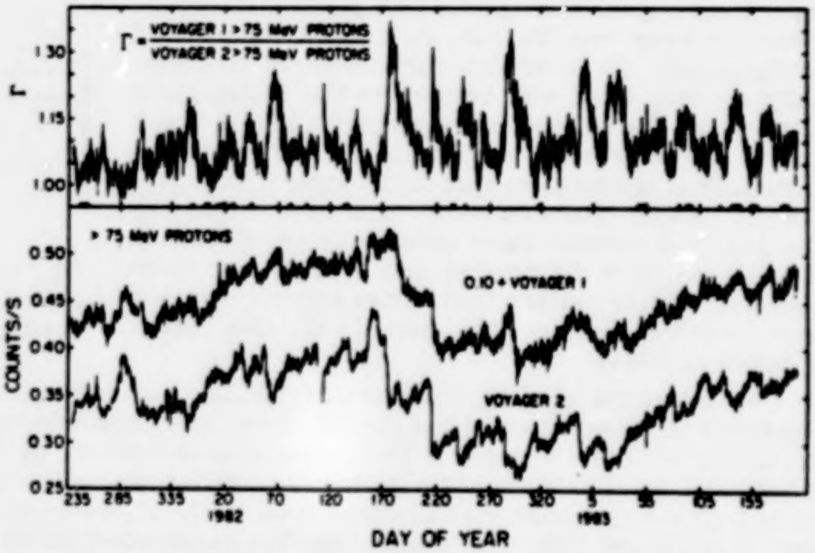

Fig. 2. Daily samples of the counting rates of >75 MeV protons from V1 and V2 (V1 is offset for clarity) and Γ the ratio of V1 to V2 counting rate samples. Uncertainties are due to counting statistics.

The counting rates of >75 MeV and ~1 MeV protons were used to eliminate periods possibly contaminated by solar flare particles and Forbush decreases. Proton energy spectra and elemental abundance measurements at lower energies were also used for this purpose. Hourly averages of the interplanetary magnetic field azimuth and elevation angles (Figure 3) measured by the Voyager Magnetic Field Experiment were used to determine the less active magnetic field periods, sector

ORIGINAL PAGE IS
OF POOR QUALITY

polarities, and transition regions between sectors. Time blocks of data were identified when V1 and V2 were in regions of magnetic field pointing generally toward or away from the sun along the expected field direction, which is generally perpendicular to the radial direction in the outer solar system and parallel to the equatorial plane near the equator. The minimum sector length used herein is 4.5 days, so that V1 and V2 were most likely in field regions associated with plasma flows from the sun's polar coronal holes. This produced Data Set (DS) I. Then days with a poorly defined transition region at either end of the magnetic sector and days with azimuthal turbulence were eliminated in order to produce DS II. Finally, days with elevation angles pointing away from the equatorial region and days with elevation angle turbulence were collected into subset DS IIb. When the elevation angle changes by a large amount in less than a day or two as in DS IIb, it is likely to represent a dynamical effect such as the passage of transient material or perhaps reconnection at a sector boundary, either of which could alter the cosmic ray gradient. Those quietest days remaining are subset DS IIa.

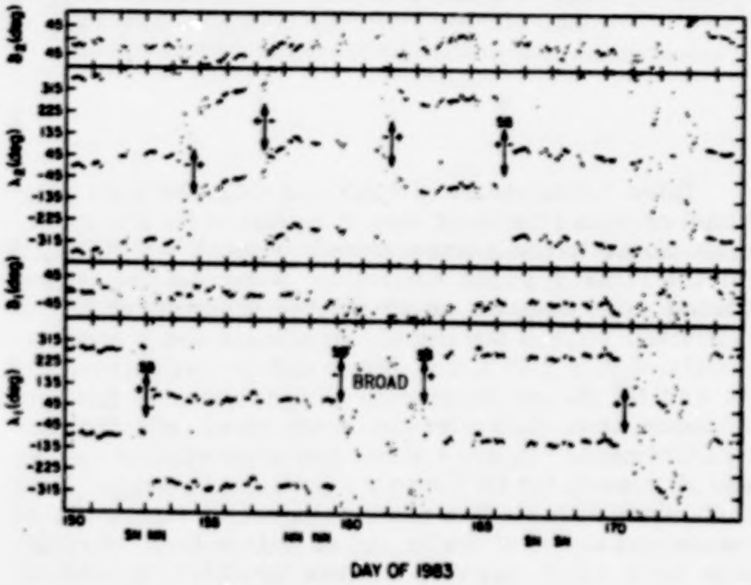

Fig. 3. Magnetic field azimuth and elevation angles from V1 and V2. The azimuth, λ, is 0° when the field is directed away from the sun and the elevation, δ, is 0° when the field is along the spacecraft-sun line. Two cycles of λ are plotted. Arrows highlight transition regions interpreted as current sheet crossings. Those labeled "SB" are similar to sector boundaries at 1 AU.

3. Observations and Discussion. Determination of $<G_\theta>$ requires knowledge of the value of G_r, which can be estimated from NS and SN data sets, since the latitude gradients, which have opposite signs in the two hemispheres should average to zero. Averaged over NS and SN, $<G_r>_{NSSN} = 2.21 \pm 0.11$ %/AU, consistent with radial gradients reported by [Venkatesan et al., 1983]. G_r can also be determined by averaging the NN and SS data sets, assuming that G_θ is negligible. This results in $<G_r>_{NNSS} = 2.29 \pm 0.13$ %/AU, consistent with $<G_r>_{NS,SN}$, and suggesting that the best estimate is the average over all 152 days of data which yields $<G_r> = 2.25 \pm 0.08$ %/AU. Note that an uncertainty of 0.1 %/AU in the assumed G_r introduces an error of only 0.01 %/deg in the derived $<G_\theta>$.

$<G_\theta>$ and $<G_\theta>$ have been calculated both without restrictions on spacecraft position (unrestricted average), and with restrictions on spacecraft position with respect to the current sheet based upon time to or from the closest sector boundary crossing (restricted average). Requiring V2 to be closer to the current sheet than V1 for NN data and V1 closer than V2 for SS data (see e.g., Figure 1), should enhance the measured $<G_\theta>$.

#48

Table 1. $\langle G_\theta \rangle$ and $\langle G_\phi \rangle$ (# : days of observation)

unrestricted average

DS	$\langle G_\theta \rangle_{NN}$ (%/deg)	$\langle G_\theta \rangle_{SS}$ (%/deg)	$\langle G_\phi \rangle$ (%/deg)
I	0.02 ± 0.03 (52)#	-0.02 ± 0.04 (22)	0.02 ± 0.03 (74)
II	0.03 ± 0.04 (29)	-0.01 ± 0.04 (19)	0.02 ± 0.03 (48)
IIa	-0.02 ± 0.05 (21)	-0.06 ± 0.03 (6)	-0.01 ± 0.04 (27)
IIb	0.14 ± 0.09 (8)	0.01 ± 0.05 (13)	0.06 ± 0.05 (21)

restricted average

DS	$\langle G_\theta \rangle_{Nn}$ (%/deg)	$\langle G_\theta \rangle_{sS}$ (%/deg)	$\langle G_\phi \rangle$ (%/deg)
I	-0.12 ± 0.04 (21)	0.09 ± 0.07 (7)	-0.11 ± 0.03 (28)
II	-0.18 ± 0.05 (10)	0.12 ± 0.09 (5)	-0.16 ± 0.04 (15)
IIa	-0.18 ± 0.05 (10)	-0.06 ± 0.08 (1)	-0.15 ± 0.05 (11)
IIb	------------- (0)	0.20 ± 0.09 (4)	-0.20 ± 0.09 (4)

Table 1 lists values of $\langle G_\theta \rangle$ and $\langle G_\phi \rangle$ for both positional criteria (the lower case subscript is for the spacecraft closer to the current sheet) using G_r = 2.25 %/AU for the radial gradient correction. Note that the unrestricted $\langle G_\phi \rangle$ displays no observable gradient, while the restricted $\langle G_\phi \rangle$ is statistically significant and is approximately -0.15 ± 0.05 %/deg. Since differences between DS IIa and DS IIb are statistically insignificant, we have no evidence that field elevation turbulence affected our measurements. Figure 4 shows the separation of the Nn and sS subsets for DS II with the restricted average. Note that, even with such a small data set, a separation of means and modes of the Nn and sS distributions, attributable to a small, negative latitude gradient, is evident. Further studies are required to determine whether such gradients are typical of other time periods.

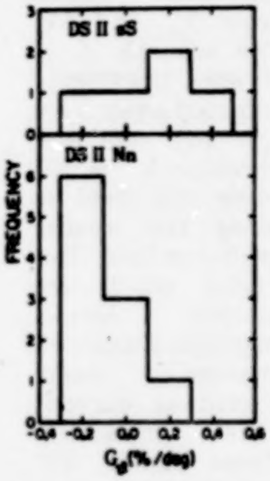

Fig. 4. $\langle G_\phi \rangle$ for DS II, restricted average.

4. Acknowledgements. We are grateful for the contributions of R.E. Vogt, other Voyager Cosmic Ray Subsystem team members, and N.F. Ness. Work at Caltech was supported in part by the National Aeronautics and Space Administration under contract JPL 49-556-63120-0-2600 and grant NGR 05-002-160.

References

Decker, R. B., S. M. Krimigis, and D. Venkatesan [1984], *Astrophys. J. Lett.*, *278*, L119.
Hoeksema, J. T. [1984], *Ph.D. Thesis*, Stanford University, Stanford CA.
Kota, J and J. R. Jokipii [1983], *Astrophys. J.*, *265*, 573.
Newkirk, G., J. Lockwood, M. Garcia-Munoz, and J. A. Simpson [1984], *EOS, Trans, Am. Geophys. U.*, *65*, 1034.
Newkirk, G. and L. A. Fisk [1985], *J. Geophys. Res.*, *90*, 3391.
Venkatesan, D., Decker, R. B., and S. M. Krimigis [1984], *J. Geophys. Res.*, *89*, 3735.

SPATIAL VARIATION OF COSMIC RAYS NEAR THE HELIOSPHERIC CURRENT SHEET

J. R. Jokipii
University of Arizona, Tucson, Az.
and
J. Kota
Central Research Institute for Physics, Budapest

N85-34848

ABSTRACT. We report a quantitative comparison between theoretical predictions and observations of the intensity of galactic cosmic rays near the interplanetary current sheet. Comparison of our model calculations is made with a statistical analysis of observations of galactic cosmic rays at Earth and the simultaneous position of the current sheet. We use an ensemble of different current sheet inclinations, in order to make the analysis of the computations approximate the method used to analyse the data.

1. **INTRODUCTION.** The transport of cosmic rays in the interplanetary magnetic field is the consequence of four basic effects - diffusion, convection, cooling and gradient and curvature drifts. The resulting transport equation for the distribution function f may be written:

$$\frac{\partial f}{\partial t} = \nabla\cdot(\underset{\sim}{\underline{K}}\cdot\nabla f) - \underline{V}\cdot\nabla f + \frac{1}{3}\nabla\cdot\underline{V}\,\frac{\partial f}{\partial \ln p} \qquad (1)$$

where P is momentum, $\underline{V}$ is wind velocity and $\underset{\sim}{\underline{K}}$ is the diffusion tensor.

A variety of solutions of this equation has appeared in the literature. A straightforward application of the equation leads to a situation in which the particle drifts play a very important and perhaps dominant role in the modulation of galactic cosmic rays (see, e.g. Jokipii and Kopriva, 1979, Jokipii and Davila, 1981, and Kota and Jokipii, 1982). The problem of the intensity near the interplanetary current sheet was first addressed observationally by Newkirk and Lockwood (1981). Subsequently, Kota and Jokipii (1982) showed that the Newkirk and Lockwood results were consistent with their three-dimensional code.

More-sophisticated analyses of the observations were reported by Newkirk and Fisk (1985) and Newkirk, Asbridge and Lockwood (1985). Here we determine the agreement of these observations with our model.

2. **The Model Calculations.** We have developed a 3-dimensional code to solve the full transport equation. We use a straightforward extrapolation of observations taken near the ecliptic plane. The model is static in a coordinate frame corotating with the Sun. The numerical technique and details of the model are described elsewhere (Kota and Jokipii 1982). The interplanetary magnetic field is the same as that used by Jokipii and Thomas (1981). The field at the solar surface is assumed to be uniform and radial, with opposite signs on either side of a magnetic equator. This magnetic equator is a tilted plane at the sun, which is a wavy neutral sheet at larger heliocentric radii in interplanetary space (see Figure 2 of Jokipii and Thomas 1981). The degree of waviness increases from a minimum near solar minimum to a large value near 90 near sunspot maximum. The field on either side of the current sheet is an Archimedean spiral. The case in which the northern hemisphere field is outward corresponds to the field parameter A being positive. The solar wind speed was taken radial and constant in magnitude at 400 km s^{-1}. We are not yet able to use a spatially-varying solar wind speed.

The parallel diffusion coefficient, $K_\parallel$, was assumed to be inversely proportional to the magnetic field strength, B ,

$$K_\parallel = K_0 P^t \beta \left(B_{earth}/B\right) \qquad (2)$$

with P being the particle rigidity in GV, is the particle velocity in units of velocity of light, and K_0 is a normalization constant in the range 10^{21} - 10^{23} if is expressed in cm^2/sec (see, eg., Jokipii and Davila, 1981). The ratio of perpendicular and parallel diffusion coefficients was kept constant at $\kappa_\perp/\kappa_\parallel$ = 0.05-0.10. To reduce computing requirements the outer boundary was set at r = 15 AU, with some runs carried out for a 30 A.U. boundary. The general features of the solutions have been discussed in detail elsewhere (Kota and Jokipii, 1982), and their discussion will not be repeated here, except to reiterate that the solutions are clearly affected by the particle drifts. Of most interest here is the dependence of the intensity on the structure of the interplanetary current sheet illustrated in the contour plot in figure (1). It is clear that the magnetic field organizes the cosmic-ray intensity in a characteristic manner relative to the current sheet, and that this organization is different for the two signs of the interplanetary magnetic field. Note also, for future reference, that the intensity is not simply dependent on the distance from the current sheet.

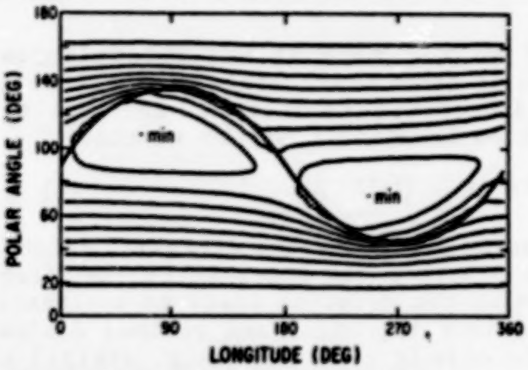

Fig. 1 Computed contours of equal intensity at a radius of 1 A.U., for protons of energy 2.36 GeV. Inclination of current sheet = 45°. K_0=1.0x10^{22} cm^2/sec, and the outer boundary was at 15 A.U. All other parameters as in Jokipii and Kota, 1982.

3. Comparison With Observations

a. The Data.

Given the above, it is of interest to study observationally the relationship between the current sheet and cosmic rays. The analyses carried out by Newkirk and Lockwood (1981) and Newkirk and Fisk (1985a) and Newkirk, Asbridge and Lockwood (1985) attacked this problem statistically, in order to minimize the problem of transient, time-dependent effects. They studied the dependence of the intensity of the Mt. Washington neutron monitor (to protons of about 5.3 GeV energy) on the distance from the current sheet, for data obtained in the years 1973-1978. Data from the years around sunspot maximum were not included. The determined the position of the current sheet from coronal white light data, which has been determined to be quite accurate. Their figure (9) shows a scatter plot of the daily intensity vs. the heliomagnetic latitude at the point of observation (defined as the angular distance in degrees along a meridian to the current sheet, which defines the heliomagnetic equator). The data show considerable scatter, which is to be expected since effects of transient disturbances, etc. may be expected to disrupt the pattern. Nontheless, there is a clear trend in the data, and the solid line gives the best fit of the function

$$I = a_0 + a_1 \sin^2(\lambda_{mg}) \qquad (3)$$

to the data, where λ_{mg} is heliomagnetic latitude. The fit to the data, with a_0 = 2407 and a_1 = - 117 is quite well-determined. In a subsequent paper, Newkirk, Asbridge and Lockwood examined the energy dependence of the ratio a_1/a_0 by analysing data from a variety of other sources. These data show that the effect depends inversely on energy, scaling approximately as $T^{-0.8}$. It should be noted, however, that this observational result is still consistent with there being no instantaneous latitudinal gradient. For, since all of the observations are taken near the solar equatorial plane, the large values of λ_{mg} occurred when the current sheet was far from the equatorial plane, and the inclination of

ORIGINAL PAGE IS
OF POOR QUALITY

the current sheet was large. Hence, if the intensity of cosmic rays globally were small when the current-sheet inclination was large, then a scatter plot of $_{mg}$ vs intensity would tend to be lower at large $_{mg}$, as is observed. We will not discuss this possibility any further here, as it does not affect the analysis.

b. The Model Calculations.

In order to compare these data with the model, it is important to simulate the methods used to analyse the data very accurately.

First, we note that the inclination of the current sheet varied considerably over the time period spanned by the data set, so it would not be appropriate to use only one simulation, with one current sheet inclination. Second, the orbit of the Earth carries the point of observation sinusoidally seven degrees above and below the heliographic equator. Since the maximum value of $_{mg}$ in the data set shown in figure (9) of Newkirk and Fisk is approximately 55°, a maximum current sheet inclination of 45° would give a maximum λ_{mg} of 52°. The work of Jokipii and Thomas (1981) suggests a minimum inclination of the order of 15° Hence, three different inclinations, 15, 30, and 45 degrees were computed for each parameter set. A fourth inclination of 0 degrees was also used in some of the runs, with little change in the results. Then, to simulate the motion of the Earth in its orbit, the intensity was determined at a number of points, which were spaced in heliographic latitude and longitude just as the Earth is in its orbit. For each such point, in addition to the computed intensity, j, the heliomagnetic latitude $_{mg}$ as defined by Newkirk and Fisk was calculated.

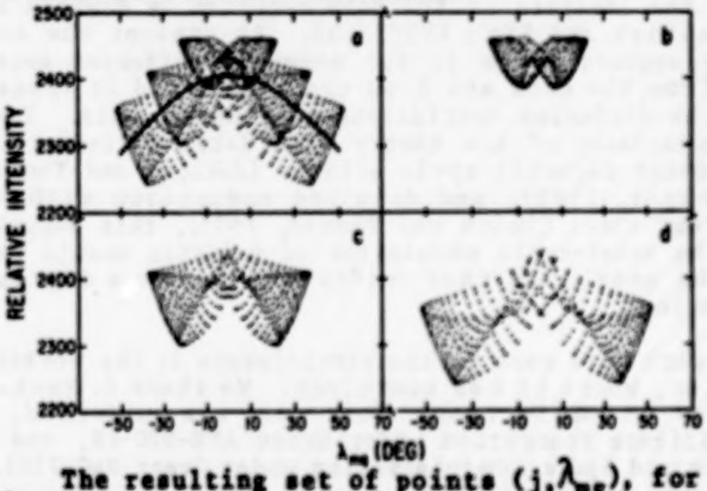

Fig. 2 a. Scatter plot of intensity vs λ_{mg} summed over three inclinations 15, 30 and 45 degrees, for the parameters of fig 1. b,c,d give the individual contributions for the three inclinations.

The resulting set of points (j,λ_{mg}), for three inclinations and along the Earth's orbit is illustrated in figure (2a) for one set of parameters. Note that there is considerable scatter in the points, reflecting the fact that the computed intensity depend[illegible]n other parameters as well as λ_{mg}. Nontheless, the calculated val[illegible] show a trend toward decreasing intensity as λ_{mg} increases, similar to that found in the data by Newkirk and Fisk. Figures (2 b,c,d) show the scatter plot obtained for the individual inclinations.

Finally, a least squares fit of equation (3) to the synthesized scatter plot was made to obtain the "theoretical value" of the coefficients a_0 and a_1 for each given set of parameters. This procedure was repeated for each set of parameters (diffusion coefficient normalization, energy, etc). As mentioned above, the absolute values are irrelevant, so the ratio a_1/a_0 is used in what follows. Illustrated in figure (3) gives the variation of this ratio for a range of diffusion-coefficient normalizations for particles of energy 2.36 GeV, together with the value for this energy given by Newkirk, Asbridge and Lockwood (1985). Clearly, there is a broad range of plausible diffusion coefficients for which the computed value is close to that observed.

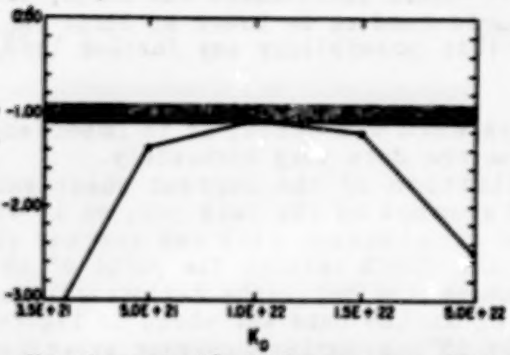

Fig. 3 Dependence of computed a_1/a_2 on K_0 for the parameters in figures 1 and 2. Horizontal band is observed value.

We also studied the energy dependence of the ratio a_1/a_0. We found that although the calculated value does indeed decrease with increasing particle energy, and agrees well with the data at a few GeV energy, the functional dependence is not the simple power law seen in the data. We expect that changing the energy dependence of the diffusion tensor could improve agreement here, but have not been able to verify this.

4. Summary and Interpretation The analysis presented above demonstrates that a model of modulation, in which the dominant physical effect is the large-scale structure of the interplanetary magnetic field, is quantitatively consistent with the analysis of the data reported by Newkirk and Lockwood (1981) and Newkirk and Fisk (1985a,b). At present the only significant discrepancy appears to be in the somewhat different energy dependences obtained from the data and from the model, and it appears likely that modifying the diffusion coefficient may improve this. Taken together with other comparisons of the theory with data, including the prediction of 22-year solar magnetic cycle effects (Jokipii and Thomas, 1981, and Kota and Jokipii, 1982), and detailed comparison with the inclination of the current sheet (Smith and Thomas, 1985), this suggests that many features of the solar-cycle modulation of galactic cosmic rays are a consequence of the model, and that drifts may well be a dominant process in solar modulation.

Acknowledgements. This work owes much to the participants in the Workshop on Cosmic Ray Modulation, where it was conceived. We thank G. Newkirk for providing data prior to publication. This work was supported, in part, by the National Science Foundation under Grant ATM-220-18, and by the National Aeronautics and Space Administration under Grant NsG-7101.

REFERENCES

Jokipii, J. R., Geophys. Res. Lett., 8, 837, 1981.
Jokipii, J. R., Levy, E. H., and Hubbard, W. B., Astrophys. J., 213, 861, 1977.
Jokipii, J. R., and Kopriva, David A., Astrophys. J., 234, 384, 1979.
Jokipii, J. R., and Davila, J. M. , Astrophys. J., 248, 1156, 1981.
Jokipii, J. R., and Thomas, B., Astrophys. J. , 243, 1115, 1981.
Kota, J., and Jokipii, J. R., Astrophys. J., 265, 573, 1982.
Newkirk, G., and Lockwood, J. A., Geophys. Res. Lett., 8, 619, 1981.
Newkirk, G. and Fisk, Lennard A., J. Geophys. Res. , in press, 1985.
Newkirk, G., Asbridge, John, and Lockwood, John A., J. Geophys. Res. , in press, 1985.
Shea, M. A., and Smart, D. F. , Advances in Space Research, Vol. 1, #3, 147, 1981.
Thomas, Barry T., and Smith, Edward J., J. Geophys. Res., 86, 11105, 1981.

N85-34849

EFFECTS OF A WAVY NEUTRAL SHEET ON COSMIC RAY ANISOTROPIES

J. Kota (1,2) and J.R. Jokipii (1)
(1) The University of Arizona, Tucson, Arizona, USA
(2) Central Research Institute for Physics, Budapest, Hungary

Abstract. We present the first results of our 3-D numerical code calculating cosmic ray anisotropies. The code includes diffusion, convection, adiabatic cooling, and drift in an interplanetary magnetic field model containing a wavy neutral sheet. We find that the 3-D model can reproduce all the principal observations for a resonable set of parameters.

Introduction. In the last decade, the effects of curvature and gradient drifts became a central issue in the theory of cosmic ray transport. It has been suggested that drift may play an important, and perhaps dominant, role in cosmic ray propagation in the heliosphere, and it may be responsible for the asymmetries appearing in consecutive 11-year cycles (Jokipii, Levy and Hubbard 1977; Jokipii and Kopriva 1980; Kota 1979; Jokipii and Thomas 1981; Kota and Jokipii 1983). The first success of drift models in explaining galactic cosmic-ray phenomena was the explanation of the phase shift of the solar daily variation (Levy 1976) observed in the years of the seventies, following the polarity reversal of the solar magnetic field. The first quantitative 2-dimensional (2-D) calculation was carried out by Jokipii and Kopriva (1980). In this work, however, the too small value of the diffusion coefficient, κ, led to unreasonable anisotropies in some cases. Kota (1981) derived an approximate force-field solution with a virtually perfect isotropy. This model, however, relied upon the too simple picture of 'hard-sphere' scattering.

The well known phase shift of the solar daily variation (Duggal and Pomerantz, 1975) is naturally explained by 2-D models (Levy 1976, Kadokura and Nishida 1984). The magnetic configuration of the seventies (A>0) yields a smaller radial density gradient which cannot balance the convection by the solar wind and thus results in a net outward streaming. Another well established observation is the presence of the polarity dependent N-S anisotropy associated with the $\underline{B} \times \underline{\nabla} n$ streaming (Bercovitch 1970, Pomerantz and Bieber 1984). In the seventies (A>0), this streaming is directed away from the neutral sheet. In a 2-D model, this pattern of streaming is hard to reconcile with the $\mathrm{div}\, \underline{S} < 0$ requirement, thus 2-D models are bound to encounter difficulties in explaining both observations.

The basic difficulty, in principle at least, may be removed if, violating the axial and N-S symmetries, a wavy neutral sheet is included. It is the purpose of this work to demonstrate that a 3-D model is indeed able to reproduce all components of the observed anisotropies. We present the first anisotropy results of our 3-D code incorporating a wavy neutral sheet.

The Model. We used a 3-D numerical code to solve the modulation equation including diffusion, convection, adiabatic deceleration and drift. The model and the scheme of calculation were described in detail elsewhere (Kota and Jokipii 1983, see also the preceding paper SH-4.2-10 in this issue). Briefly, a usual spiral field is adopted, the magnetic equator is a tilted plane at the sun, which then evolves into a wavy sheet (Jokipii and Thomas 1981). The case of A>0 corresponds to outward polarity above the sheet and inward polarity below the sheet while A<0 corresponds to the opposite configuration (sixties and eighties). Steady state is assumed in the frame corotating with the sun. The most serious limitation of the code is that it assumes constant solar wind speed thus many phenomena, like shocks, are precluded.

Calculations were carried out for protons in the 1 - 10 GV range. The parallel diffusion coefficient, $\kappa_\parallel$, was assumed to be inversely proportional to the magnetic field strength, B,

$$\kappa_\parallel = K_0 P^{1/2} \beta \, (B_{earth}/B)$$

with P being the particle rigidity in GV, ρ is the particle velocity in units of velocity of light, and K_0 is a normalization constant in the range of $10^{21} - 10^{23}$ cm^2/sec. The ratio of the perpendicular and parallel diffusion coefficients was kept constant at $\kappa_\perp/\kappa_\parallel = 0.05 - 0.20$.

Results and Discussion. Anisotropies were calculated at three heliocentric distances (0.5, 1, and 5 AU) over the full range of heliographic latitudes and longitudes. Here, we present the results near the earth. The anisotropies to be reported are obtained at the helioequator, at 1 AU, and averaged over longitudes in a magnetic sector.

The ecliptic components of the anisotropy responsible for the solar daily variation are given in Figures 1 and 2 ($P = 2.3$ GV; $\kappa_\perp/\kappa_\parallel = .05$). It should be noted that the anisotropies obtained for a flat sheet (dashed lines) show sharp changes at the neutral sheet. The actual values (dots) may considerably differ from the averages over a (-5°, 5°) latitude band (open circles). In most cases, A>0 gives an earlier phase and a smaller amplitude which is in general agreement with observations. Similar results were obtained for other rigidities, too. At large values of K_0, understandably, drift effects diminish and a near perfect corotation applies. The breaks in the lines in the $K_0 = 1.5 - 5.10^{22}$ cm^2/sec range indicate that corotation should be reached somewhere in this interval.

Figure 3 shows ξ_ϑ, the zenith angle component of the average near earth anisotropy above the neutral sheet for $P = 2.3$ GV. Consider first the case A>0, when the 'observed' value of ξ_ϑ is negative in accordance with the sense of the $\underline{B} \times \nabla n$ streaming. Curve (a) corresponding to $\kappa_\perp/\kappa_\parallel = .05$ and $\alpha = 15°$ yields the correct sign for ξ_ϑ. Larger tilt angle ($\alpha = 30°$, curve (b)), however, may already give positive values, too. If we take, on the other hand, a larger perpendicular diffusion (curve (c): $\kappa_\perp/\kappa_\parallel = .20, \alpha = 30°$) ξ_ϑ will again point in the proper direction for all values of K_0. The underlying physical picture is that, in the case of large tilt angles and small perpendicular diffusion, most particles reach the earth without having interacted with the neutral sheet. Being too far from the earth, the neutral sheet becomes irrelevant for A>0. As for A<0, particles intersect the sheet several times before reaching the earth. As a result, the calculated ξ_ϑ always shows the proper sense and is fairly independent of the tilt angle, α.

Figure 4 indicates that the magnitude of ξ_ϑ increases and its sign becomes more distinctive with increasing rigidities. This finding can also be anticipated since drift effects are expected to be more pronounced at higher rigidities.

The typical azimuthal dependence of the N-S anisotropy is presented in Figure 5. In most cases, we cannot find a one-to-one correspondence between the sign of ξ_ϑ and the polarity of the field. In general, smaller tilt angle, and larger $\kappa_\perp$ results in a better correlation; the correlation also improves at higher rigidities. At 5 AU heliocentric distance, virtually all our runs gave a 100 percent correlation. To interpret this, we note that the waves in the neutral sheet become relatively tighter at larger distances from the sun. Thus we expect the effects of waviness to be more direct there.

Conclusion. Our numerical results demonstrate that the inclusion of a wavy neutral sheet may explain all components of the observed anisotropies. We find a general agreement between 'theoretical' and 'observed' anisotropies for a wide range of parameters. At high latitudes, well above or below the sheet, however, we predict the anisotropy to point toward the equator in the case of A>0. This is in contrast to the poleward direction expected from the $\underline{B} \times \nabla n$ term only.

Acknowledgement. This work was supported by the National Science Foundation under Grants ATM-220-18 and INT-8400591.

References.

Bercovitch, M. 1970: Acta Phys. Hung., 29, Suppl 2, 169

Duggal, S. P. and Pomerantz, M. A. 1975: Proc. 14th ICRC, Munich, 4, 1209

Jokipii, J. R. and Kopriva, D. A. 1980: Ap. J., 234, 384

Jokipii, J. R. and Thomas, B. T. 1981: Ap. J., 243, 1115

Jokipii, J. R., Levy, E. H. and Hubbard, W. B. 1977: Ap. J., 213, 861

Kóta, J. 1979: Proc. 16th ICRC, Kyoto, 3, 13

Kóta, J. 1981: Adv. Space Res., 1, no. 3, 135

Kóta, J. and Jokipii, J. R. 1983: Ap. J., 265, 573

Levy, E. H. 1976: J. Geophys. Res., 81, 2082

Kadokura, A. and Nishida, A. 1984: Proc. Int. Symp. on CR Modulation, Morioka, Japan 1984, p177

Pomerantz, M. A. and Bieber, I. W. 1984: Proc. Int. Symp. on CR Modulation, Morioka, Japan 1984, p39

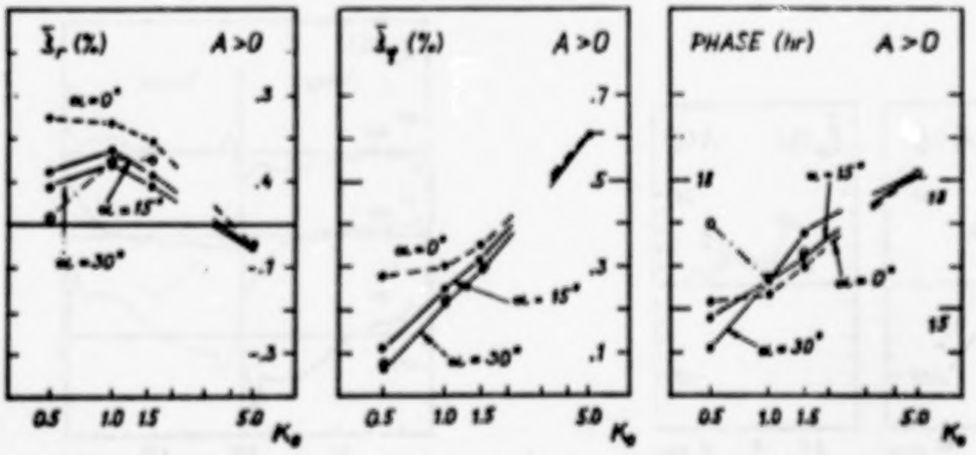

Figure 1. Radial and azimuthal components of the average near earth anisotropy calculated for A>0, P=2.3 GV, $\kappa_\perp/\kappa_\parallel$=.05. Dashed and solid lines refer to flat (see text) and wavy sheets, respectively. K_0 is in units of 10^{22} cm^2/sec. The phases of the resulting daily waves are also shown.

ORIGINAL PAGE IS
OF POOR QUALITY

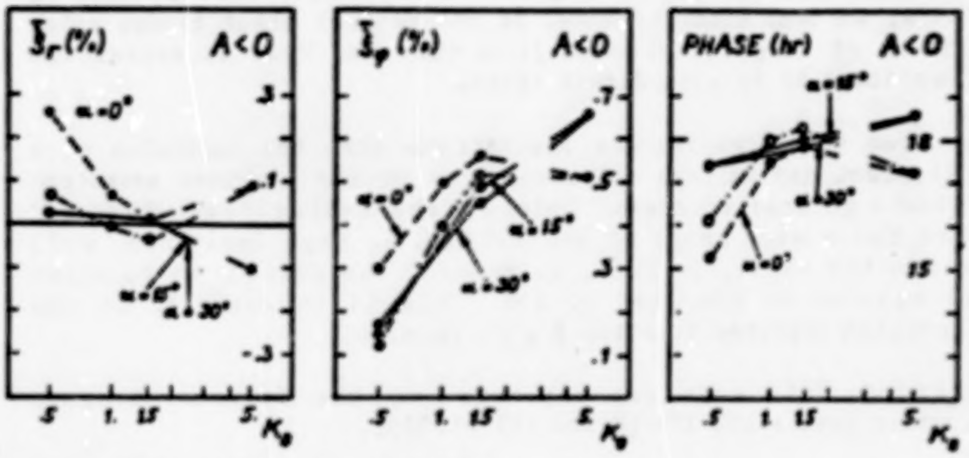

Figure 2. Same as Fig. 1., for A<0.

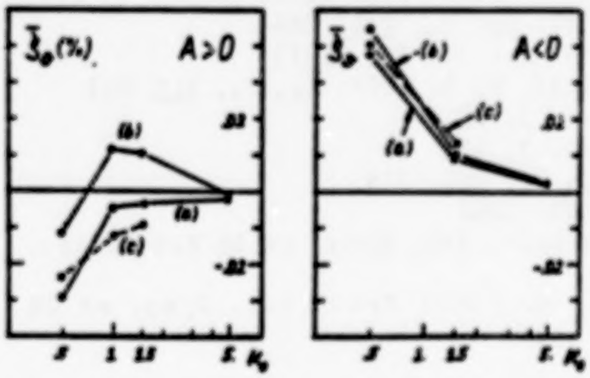

Figure 3. The average value of ξ_ϕ for the earth being above the neutral sheet. P=2.3 GV, K_0 is in units of 10^{22} cm^2/sec.
(a) $\kappa_\perp/\kappa_\parallel$=.05, α =15°;
(b) $\kappa_\perp/\kappa_\parallel$=.05, α =30°;
(c) $\kappa_\perp/\kappa_\parallel$=.20, α =30°.

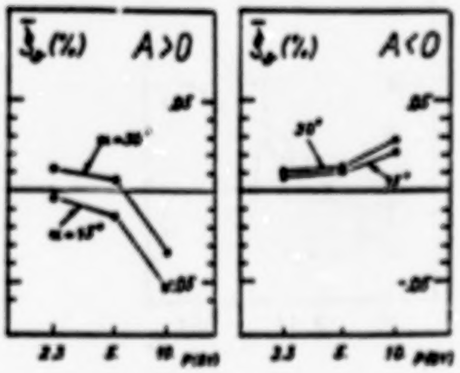

Figure 4. ξ_ϕ vs rigidity calculated for $K_0=10^{22}$ cm^2/sec, $\kappa_\perp/\kappa_\parallel$=0.05.

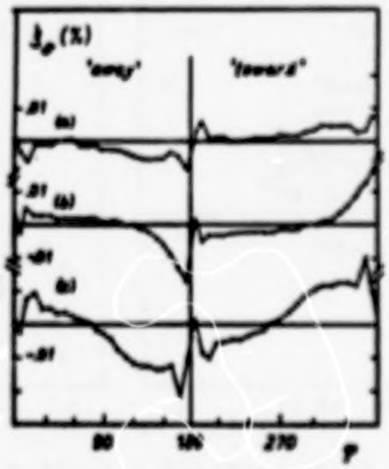

Figure 5. Azimuthal dependence of ξ_ϕ calculated for P=2.3 GV, $\kappa_\perp/\kappa_\parallel$=.05.
(a) A>0, α=15°; (b) A>0, α=30°;
(c) A<0, α=15°.

N85-34850

EFFECTS OF SOLAR MAGNETIC FIELD ON COSMIC RAYS

Goncher G.A., Kolomeets E.V.,
Lyakhova A.Kh., Slyunyaeva N.V., Stekol'nikov N.V.
Kazakh State University, Timiryazeva St. 46,
Alma-Ata 480121, USSR

The paper is devoted to some aspects of problem of galactic cosmic ray (gcr) propagation including inversion of solar total magnetic field (stmf) and to analysis of experimental facts related to heliomagnetic cycle.

It is known (Jokipii I.R., et al., 1977, Krainev M.V., 1979, Erkhov V.I., et al., 1983) that the global structure of solar total magnetic field (Parker's field) results in additional flux of gcr generated by curvature and gradient drifts. Velocity of charged particles drift is

$$\mathcal{D}_i = \frac{\partial \varkappa_{ij}^{(A)}}{\partial x_j} \qquad (1)$$

where $\varkappa_{ij}^{(A)}$ - antisymmetric part of diffusion tensor. It can be written for stmf in the form

$$\vec{\mathcal{D}} = \vec{\mathcal{D}}_1 + \delta(\theta - \pi/2)\vec{\mathcal{D}}_2 \qquad (2)$$

where $\vec{\mathcal{D}}_1$ is regular part and $\vec{\mathcal{D}}_2$ - singular part of velocity. Delta function is connected with the fact of existence of boudary between inward and outward lines of force of magnetic field of the Sun that is neutral current sheet.

The main equation including diffusion, convection, energy changes and drifts in heliocentric system of coordinate is of the form:

$$\frac{1}{r^2}\frac{\partial}{\partial r}\left[r^2\left(\varkappa_{rr}\frac{\partial n}{\partial r} - nu - n\mathcal{D}_r\right)\right] + \frac{1}{r\sin\theta}\frac{\partial}{\partial\theta}\left[\sin\theta\left(\frac{\varkappa_{\theta\theta}}{r}\frac{\partial n}{\partial\theta} - n\mathcal{D}_\theta\right)\right] + \frac{2u}{3r}\frac{\partial}{\partial\varepsilon}(\alpha\varepsilon n) = 0 \qquad (3)$$

where $\alpha = \frac{\varepsilon + 2m_0}{\varepsilon + m_0}$, n is density of galactic cosmic rays, ε - kinetic energy. To analyse effects related to redistribution of galactic cosmic rays due to drift motion let's consider the equation including only convection, diffusion along lines of force of magnetic field and drift. We obtain

$$\frac{1}{r^2}\frac{\partial}{\partial r}\left[r^2\left(\varkappa\frac{\partial n}{\partial r} - nu - n\mathcal{D}_r\right)\right] - \frac{1}{r\sin\theta}\frac{\partial}{\partial\theta}\left[\sin\theta\, n\mathcal{D}_\theta\right] = 0 \qquad (4)$$

Integration of equation (4) over θ within the limits of $\pi/2 - \varepsilon$ and $\pi/2 + \varepsilon$ and approaching ε to zero gives following condition:

$$n(r, \varepsilon, \theta = \pi/2) = n_0(\varepsilon) \qquad (5)$$

where $n_0(\varepsilon)$-density of galactic cosmic rays out of modulation region that is for $r \geqslant r_0$.

It shoud be noted that on the basis of general mathematical considerations (Mors F.M.,Feshbach G.,1958) condition(5) has sense only for odd cycles of solar activity. In order to solve parabolic equation (4) we used traditional boundary conditions for this kind of the problems (Ashirov R.R. et al.,1979,Krylov V.I.,et al.,1977)

$$n(z=z_0,\varepsilon,\theta)=n_0(\varepsilon)\,;\quad \left[\sigma n+(1-\sigma)\frac{\partial n}{\partial z}\right]\Big|_{z=0}=0 \qquad (6)$$

where σ - parameter.

The set of boundary conditions (5) and (6) allows to solve equation (4) correctly. Grid technique and Crank Nicholson schemes (Krylov V.I.,Bobkov V.V.,Monastyrsky V.I.,1977) were employed for solution. Equation (4) was solved for the energy range ε>1GeV.Figure 1 shows radial variation of n/n_o at the heliolatitude -7 for energies 1 and 10 GeV. Figure 2 illustrates latitudinal variations of $n/n_o$for the energies. Following values of latitudinal gradient of gcr were obtained at the orbit of the Earth:

$$\frac{1}{n}\frac{\partial n}{\partial\theta}(\varepsilon=1\,\mathrm{GeV})=1.9\%/a.u. \qquad \frac{1}{n}\frac{\partial n}{\partial\theta}(\varepsilon=10\,\mathrm{GeV})=0.16\%/a.u.$$

Hence including in the equation of gcr propagation the term describing drift of particles results in redistribution of density ,appearance of latitudinal gradient and reduction of modulation depth.

Let's consider and analyse experimental data connected with heliomagnetic cycle. As follows from abovementioned facts latitudinal gradient results in N-S asymmetry (Kolomeets E.V.,et al.,1977) . Let's consider asymmetry of cosmic rays and solar activity. Figure 3 shows amplitude of north-south asymmetry in the stratosphere data of Mirny and Murmansk at the depths of 20 g/cm^2 (a) and 480 g/cm^2 (b). One can see that amplutude of the effect grows with the depth in the atmosphere, this fact demonstrates rigid energy spectrum of the effect.

The investigation of solar activity during the last magnetic cycle reveals pronounced N-S asymmetry at all heliolatitudes. Figure 4 shows north-south asymmetry for the ranges of heliolatitudes (20-30) (a); (30-40) (b); (40-50) (c). One can see 22-year wave in N-S asymmetry. The change of the sign of north-south asymmetry occurs during the periods of inversion of solar total magnetic field. Periods of inversion are shaded.

In order to study nature of 22-year variation of neutron component of cosmic rays we analysed continuous set of the data of neutron monitors of the worldwide network for the last magnetic cycle. The wave averaged over two eleven-year cycles was substructed from original data to exclude 11-year variation. Figure 5(a) shows obtained 22-year variation for Deep River station.

Taking into account 22-year wave in solar activity we

ORIGINAL PAGE IS
OF POOR QUALITY

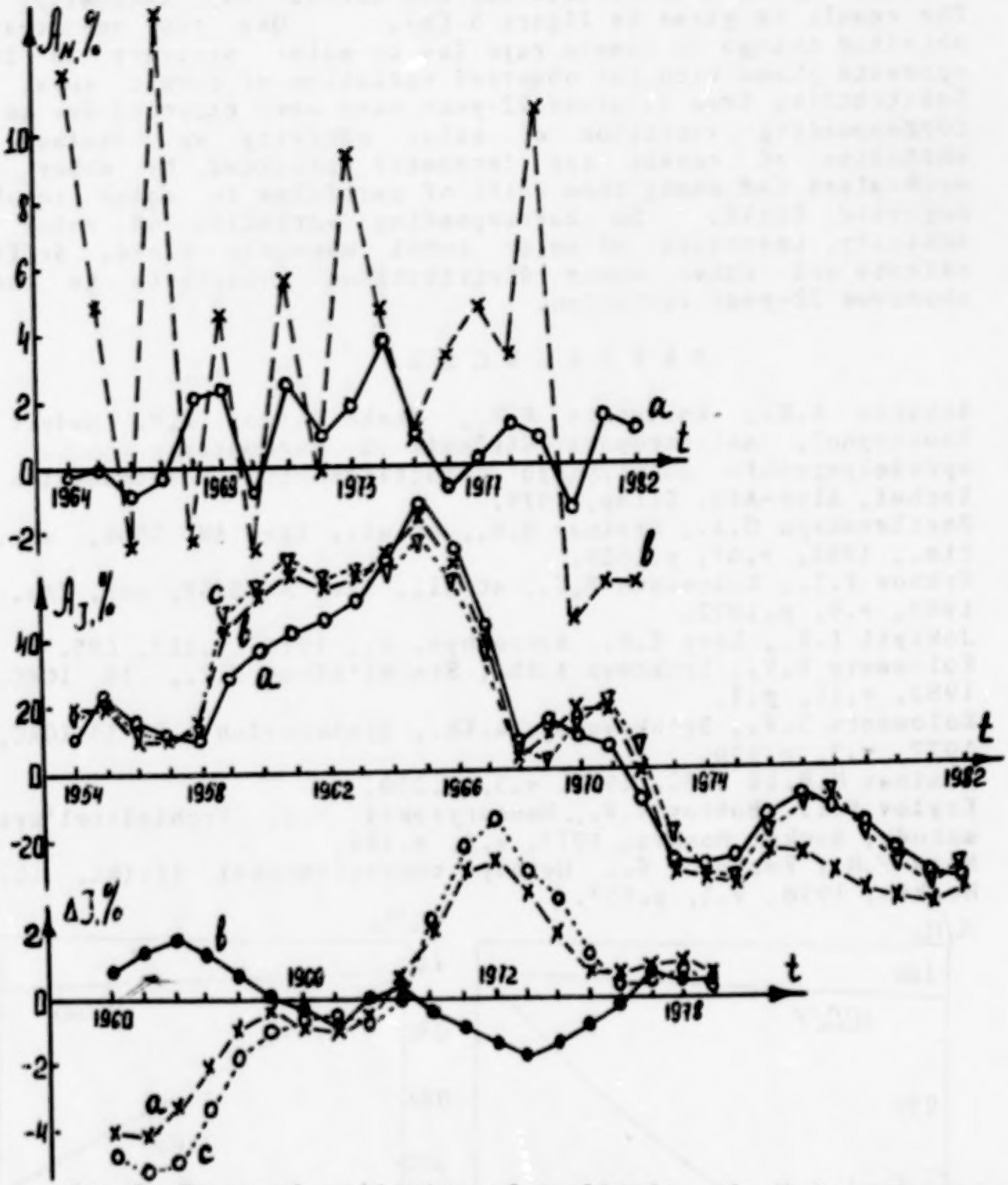

Fig.3. Temporal variation of amplitude of N-S asymmetry stratosphere data of Mirny and Murmansk).

Fig.4. Temporal variation of N-S asymmetry of solar activity at various heliolatitude regions.

Fig 5. 22-year variation of cosmic ray intensity, observed at Deep River. (a) -22-year wave in cosmic rays expected due to corresponding variation of solar activity. (b)- variation of cosmic ray intensity due to drift effects.

determined contribution of the wave to cosmic ray intensity. 22-year wave in cosmic rays expected due to 22-year variation of solar activity was found on the basis of empirical relation between solar activity and cosmic ray intensity. The result is given in figure 5 (b). One can see that obtained change in cosmic rays due to solar activity is in opposite phase with the observed variation of cosmic rays. Substructing from obtained 22-year wave wave expected due to corresponding variation of solar activity we obtained variation of cosmic ray intensity produced by other mechanisms and among them drift of particles in solar total magnetic field. So corresponding variation of solar activity, inversion of solar total magnetic field, drift effects and other space distributions contribute to the observed 22-year variation.

REFERENCES

Ashirov R.R., Kolomeets E.V., Stekol'nikov N.V. Modeli izotropnoi, anizotropnoi diffuzii i parametry, opredelyayushie modulyaziyu galacticheskich kosmicheskich luchei, Alma-Ata, Kitap, 1979.

Bazilevskaya G.A., Krainev M.B., et al., Izv. AN SSSR, ser. fiz., 1983, v.47, p.1669.

Erkhov V.I., Kolomeets E.V., et al., Izv. AN SSSR, ser. fiz., 1983, v.9, p.1822.

Jokipii I.R., Levy E.N., Astrophys. J., 1977, v.213, L85.

Kolomeets E.V., Lyskhova A.Kh., Stekol'nikov N.V., 18 ICRC, 1983, v.11, p.1.

Kolomeets E.V., Bychkovskaya A.Kh., Zysmanovich A.G. 15 ICRC, 1977, v.3, p.170.

Krainev M.B.16 ICRC, 1979, v.3, p.230.

Krylov V.I., Bobkov V.V., Monastyrskii V.I. Vychislitel'nye metody, Nauka, Moskva, 1977, v.2, p.146.

Mors F.M., Feshbach G., Metody teoreticheskoi fiziki, IL, Moskva, 1958, v.1, p.657.

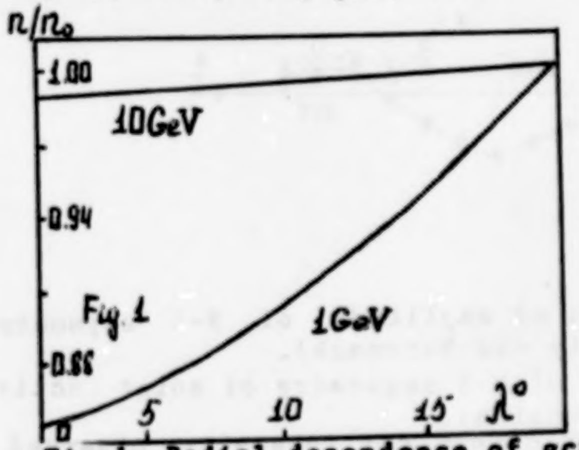

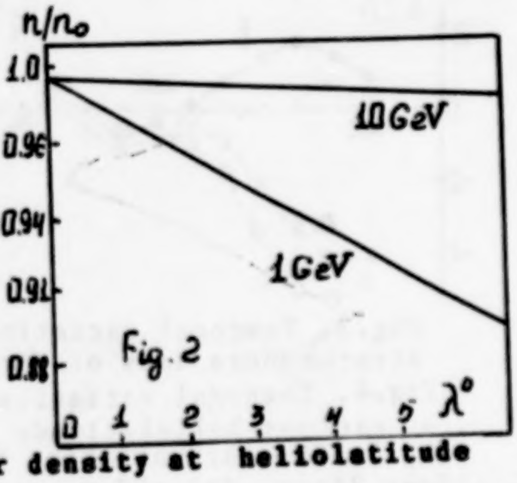

Fig.1. Radial dependence of gcr density at heliolatitude at energy 1 and 10 GeV.

Fig.2. Latitudinal dependence of gcr density at energies 1 and 10 GeV.

N85-34851

SH 4.2-13

DETERMINATION OF GALACTIC COSMIC RAY LATITUDINAL GRADIENT USING EARTH BASED DETECTORS

Badruddin and R.S.Yadav
Space Science Group,Dept. of Phys.,A.M.U.,Aligarh(India)

ABSTRACT

Using cosmic ray intensity data of Deep River Neutron monitor and relation between solar wind velocity and heliomagnetic latitude,an attempt has been made to evaluate quantitatively the latitudinal gradient of cosmic ray intensity during the periods dominated by a two sector pattern.Assuming a constant orientation of the heliospheric current sheet on a time scale of the order of a year,arelationship is determined between the cosmic ray intensity and the heliomagnetic latitude.

I.Introduction. Galactic cosmic ray intensity gradients play an important role in guiding theoretical models of cosmic ray transport in the heliosphere.The behaviour of radial and latitudinal intensity gradients with time and heliocentric radial distance is of interest for the overall understanding of the cosmic ray modulation.Most of the earlier studies of latitudinal gradients were made with respect to heliographic equator or the ecliptic plane.However,with the realization of the importance of heliospheric current sheet,two recent studies(Badruddin et al.,I985;Newkirk & Fisk,I985)have addressed this problem by assuming the heliospheric current sheet to be the heliomagnetic equator.

In this extension,of our earlier analysis,we shall give a quantitative relationship for determing the heliomagnetic latitudinal gradient at IAU during a period (I974) dominated by two sector pattern.

2.Method. We have calculated the heliomagnetic latitude(θ) using the relationship,given by Zhao and Hundhausen(I98I), between the solar wind velocity and heliomagnetic latitude both before and after the earth's crossing of the heliospheric current sheet (sector crossing),assuming the minimum velocity near the current sheet.Thus knowing the heliomagnetic latitude on days before and after the sector crossing, the latitudinal gradient of cosmic ray intensity with respect to zero latitude is calculated.Since the heliospheric current sheet(sector boundary) is thought to constitute a basic 'plane' of symmetry (Smith and Barnes,I983),the distance of the observations above or below the current sheet was considered more appropriate to a search for latitude dependence than the distance from the solar equator.

3.Results and Discussion. In Fig.I we have shown the average latitude gradient in I974 with respect to heliomagnetic equator, which we have assumed to be the heliospheric current sheet.We have not considered the solar rotations in which there was any sharp increase or decrease of cosmic ray intensity.It can be seen from Fig.I that the cosmic ray

ORIGINAL PAGE IS
OF POOR QUALITY

intensity decreases as the heliomagnetic latitude of the earth from the heliospheric current sheet increases.The relation between the gradient and the latitude for I974 can be expressed as:

$$G_\theta\ (\%) = -0.036\ |\theta| \qquad \text{for}\ 0^\circ \leq |\theta| \lesssim 30^\circ$$

Further,the maximum gradient from -I% to -3% has been found in different solar rotations.

The heliomagnetic latitude determined on different days using the relation between the solar wind velocity and heliomagnetic latitude(Zhao & Hundhansen,I98I) before and after the sector crossing and the corresponding gradient in cosmic ray intensity and solar wind velocity variations are shown in Fig.2. It is seen that during this period the cosmic ray gradient closely follows the solar wind velocity which increases away from the current sheet.The presence of such a latitudinal gradient of cosmic ray intensity indicate that some of the time variations observed at the earth are caused by the spacial variation of solar wind velocity with respect to heliomagnetic latitude(current sheet).Hakamada and Munakata(I984) suggested that solar wind speed depend on the angular distance from the magnetic neutral line(current sheet) and does not depend on the heliographic latitude of the Earth.

Roelof et al.(I983) using the data from IMP-8 and the closely spaced Voyager-I and 2 spacecrafts found heliolatitudinal gradient in $\gtrsim$35 Mev protons of $\sim$2% -5% per degree in short lived (I0-30 days) structures,and I% -2% per degree in structures recurring over a few solar rotations.From an analysis of IMP-8 and Voyager-I and 2 data from I972 through early I982, Venkatesan et al.(I984) concluded that,when corrected for radial gradients of 3% per AU, the intensity difference between either Voyager-I or Voyager-2 and IMP-8 was consistent with a heliolatitudinal gradient 0.00% per degree for $\gtrsim$70Mev protons.In another study,Decker et al.(I984) examined the integral cosmic ray intensities (proton energy $\gtrsim$70Mev) between Voyager-I and Voyager-2 in the 8-I3 AU helioradial range and over 3°- I6° heliolatitude separation during the first I7 months of the cosmic ray recovery in I98I -82.These data are also cosistent with the heliolatitude gradient $\sim$0 to $-$0.4% per degree.They admit that this null result is apparently still at least cosistent with either model of Fisk(I976) or Kota and Jokipii (I983),however,due to non availability of the location of Voyager-I & 2 relative to the heliospheric current sheet a detailed comparision with either the Fisk or Kota & Jokipii model is not possible.A preliminary analysis by Lockwood and Webber(I984) using the 26 days average Voyager-I and 2 counting rate gives less than -0.I% per degree heliolatitudinal gradient during I98I-82 period for more than 60Mev particles.

From neutron monitor observations in I975,Newkirk and Lockwood(I98I) found a value of about-0.04% per degree at 5Gev for latitudinal gradient.The theoretical prediction, including a warped current sheet yield about -0.06% per degree (Kota and Jokipii,I982).For I970-79 period the symmetric latitudinal gradient away from the current sheet is estimated to be -.06% per degree (Newkirk and Fisk,1985) which is not much different from our estimate of $\simeq$ -.04% per degree for the year 1974.

4.Conclusion: It has been found that the cosmic ray intensity decreases as the angular distance of the earth from the heliospheric current sheet(heliomagnetic equator)increases. During 1974 (for solar rotations in which there is no transient decrease of large amplitude) the maximum(negative) gradient from -1% to -3% has been found in different solar rotations assuming the heliospheric current sheet to be the heliomagnetic equator.The relation between the cosmic ray gradient and the heliomagnetic latitude can be expressed as:

$$G_{\theta}\ (\%) = -0.36\,|\theta| \qquad \text{for} \qquad 0^{\circ} \leq |\theta| \leq 30^{\circ}$$

The presence of such a latitudinal gradient indicates that some of the time variations of cosmic rays observed at the earth are caused by the spacial variation of the solar wind velocity with respect to current sheet.It may be possible that it is the heliospheric current sheet and not the helioequatorial plane that is of physical signifcance when one is calculating the heliolatitudinal gradients of galactic cosmic ray(Venkatesan et al.,1984).Since the relation between cosmic ray intensity and the heliomagnetic latitude may vary during the course of a solar cycles, aclear picture of heliomagnetic latitudinal gradient will emerge when the precise knowledge of heliospheric current sheet position during different epoch of solar activity cycle is available .

5.Acknowledgement. One of the authors(Badruddin)acknowledges the financial support from C.S.I.R., New Delhi.

References

Badruddin,R.S.Yadav,and K.R.Yadav,Planet.Space Sci.,33,191, (1985).
Decker,R.B.,Krimigis,S.M. and Venkatesan,D.,Astrophys.J.,278, L119,(1984).
Fisk,L.A.,J.Geophys.Res.,81,4646,(1976).
Hakamada,K. and Munakala,Y.,J.Geophys.Res.,89,357,(1974).
Kota,J.and Jokipii,J.R.,Geophys.Res.Lett.,9,656,(1982).
Kota,J.and Jokipii,J.R.,Astrophys.J.,265,573,(1983).
Newkirk,G.Jr.and Lockwood,J.A.,Geophys.Res.Lett.,8,619,(1981)
Newkirk,G.Jr.and Fisk,L.A.,J.Geophys.Res.,90,3391,(1985).
Roelof,E.C.,Decker,R.B.and Krimigis,S.M.,J.Geophys.Res.,88, 9889,(1983).
Smith,E.J. and Barnes,A.,Solar wind Five (Ed.M.Neugebaur) NASA Publ. 2280,521,(1983).
Venkatesan,D.,Decker,R.B.and Krimigis,SM.,J.Geophys.Res.,89, 3735,(1984).
Zhao,X.-P. and Hundhausen,A.J.,J.Geophys.Res.,86,5423,(1981).

ORIGINAL PAGE IS
OF POOR QUALITY

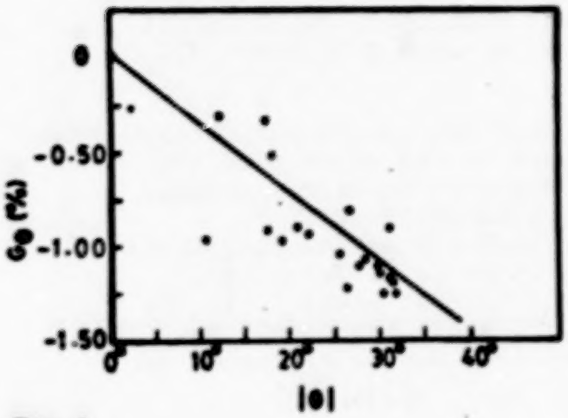

Fig._1

Fig.1 shows the average heliomagnetic latitude gradient calculated from Deep River neutron intensity for 1974.

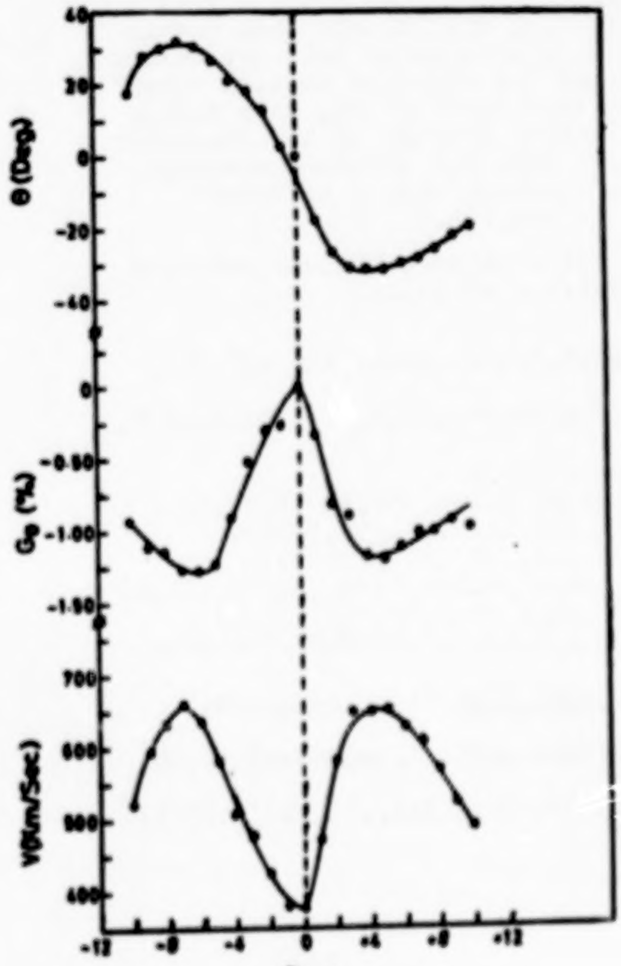

Fig._2

Fig.2 shows the variation of heliomagnetic latitude, the cosmic ray gradient and the solar wind velocity on the days before and after sector crossing for 1974.

N85-34852

SH 4.2-14

THE EXPECTED COSMIC RAY DENSITY AND STREAM DISTRIBUTIONS AT THE HELIOLATITUDINAL ASYMMETRY OF SOLAR WIND

Alania M.V., Aslamazashvili R.G., Dorman L.I., Iskra K.
Institute of Geophysics, Georgian Academy of Sciences USSR, IZMIRAN, Moscow Region, USSR, Agriculture - Teacher University, Physics and Biophysics Dep., Siedlce POLAND

ABSTRACT

The results of the spatial distribution of cosmic ray density, gradients and anisotropy obtained on the basis of the numerical solution of the anisotropic diffusion equation with an account of solar wind velocity change depending on the latitudinal angle θ of the form $U = U_0 e^{\alpha\theta}$ and the diffusion coefficient depending on the spatial coordinates and the particle rigidity are presented. It is shown theat the increase of the solar wind velocity and the diffusion coefficient with the heliolatitude leads to the gradient distributions that are in accord with the experimental data observation in cosmic space. In the paper the results of the energetic spectrum od 11 and 22-year cosmic ray variations obtained with an account of direction of the general magnetic field of the Sun are presented.

1. Introduction. The measurements by radio-astronomic methods show that solar wind velocity remains almost stable at medium heliolatitudes and increases in high areas. /1/
In all probability this is connected with coronal holes in the sun, which occur predominantly at medium and high heliolatitude. /2/ The open structures of the magnetic field in coronal holes contributes to the free exit of solar wind plasma from these areas and is thus a cause of high speed streams. Furthermore the strength of the magnetic inhomogeneities in these streams decreasesand because of this the cosmic ray diffusion coefficient increases.

2. The theoretical model. Cosmic ray diffusion in interplanetary space is described by the equation. /3/

$$\frac{\partial n}{\partial t} = \nabla_i(\chi_{ik}\nabla_k n) - \nabla_i(n \cdot U_i) + \frac{1}{3R^2}\frac{\partial}{\partial R}(R^3 n) \cdot \nabla_i U_i \qquad (1)$$

We assumed that solar wind velocity U changes depending on heliolatitudes as follows:

$$U = U_0\left(2 - e^{\alpha(\theta - \frac{\pi}{2})}\right)$$

where α = 0.44 and is independant of radial distance within the modulation boundaries. The diffusion coefficient χ depends on particle rigidity R and spatial coordinates as follows:

$$\chi = \chi_0 (1 + r) \cdot e^{R_1/R} (R_2 + R)^2 \cdot (1 + \beta(1 - \sin\theta))$$

where R1 = 0.05 GV, R2 = 3 GV, r is distance from the sun, β = 19. Equation (1) is solved with spherical coordinates r, θ, φ for a steady state situation $\left(\frac{\partial n}{\partial t} = 0, \frac{\partial n}{\partial \varphi} = \frac{\partial n}{\partial \varphi^2} = 0\right)$

The definedassumptions are valid for long-period variations when the galactic cosmic ray diffusion time is considerably less than the time needed for a change in the surrounding conditions. Equation (1) is solved by a network method for boundary conditions where $\rho=\frac{r}{r_0}$ and r is the distance from the sun, r_0 the radius of the extent of modulation. $B=\frac{n}{n_0}$, where n and n_0 are the cosmic ray particle density in interplanetary space and in the galaxy.

3. Results. Equation (1) is solved with regard to the anti symetrical part of tenzor diffusion, that is to say with regard to the particle drift in a regular interplanetary field of the sun under two conditions: a/ When the lines of force of the magnetic field go from the northern hemisphere of the sun to the southern hemisphere /H^+/ and b/ when the opposite is true /H^-/.
Fig.1 shows the distribution of radial gradients of cosmic rays on depending to the distance for 10 Gev energy particles.

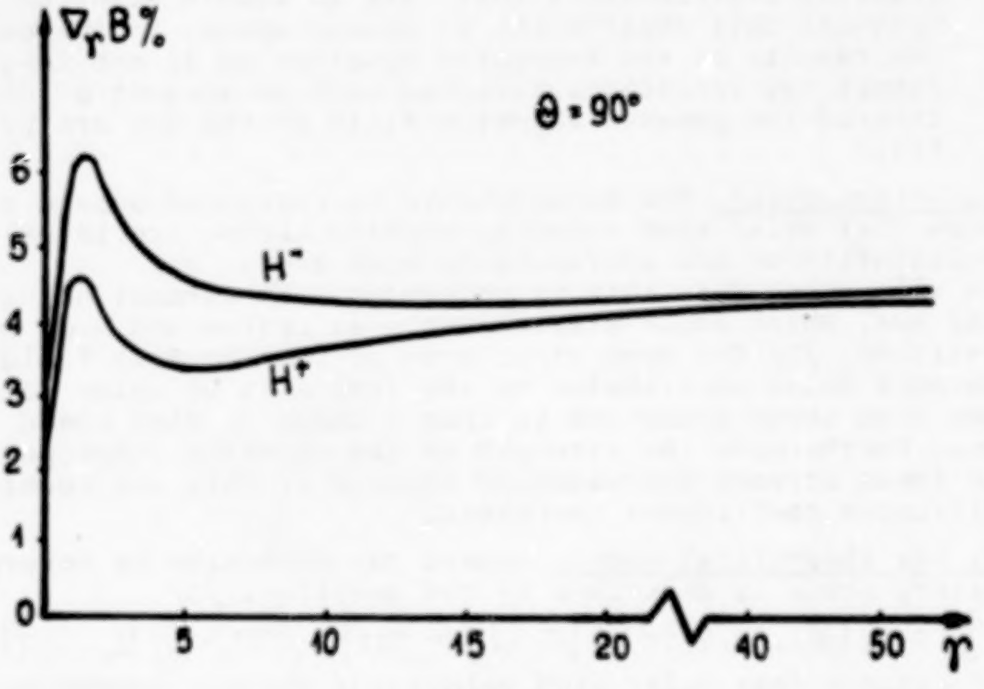

Fig. 1

Fig.2 shows the expected energy spectra for the 11-year variation in the event of /H^+/ and /H^-/ and also the 22-year variation caused by cosmic ray particle drift. /$H^+ - H^-$/

4. Discussion and conclusion. For all other conditions being equal the cosmic ray density is greater for an 11-year cycle solar activity when the lines of force go from the northern hemisphere of the sun to the south /H^+/. In this event the hemisphere sucks in cosmic-ray particles inwards from its external surroundings. It is interseting to compare the expected radial grandient distribution with the experimental

ORIGINAL PAGE IS
OF POOR QUALITY

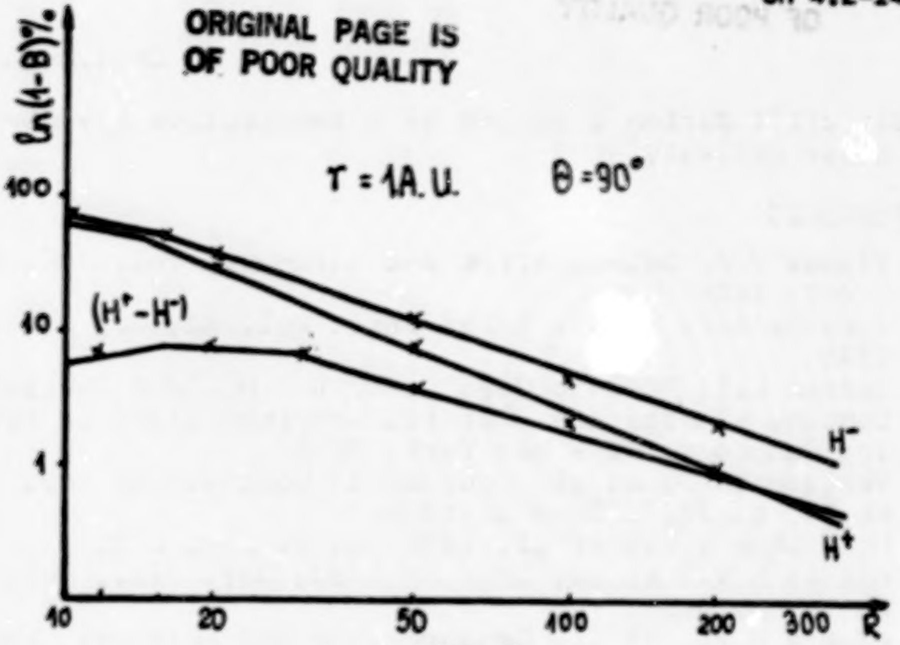

Fig. 2

data obtained from the American space station. /4/
At a distance of 1-5 AU sufficiently good coincidence can be observed. It is especially worth noticing the existance of the maximum radial gradient in the region of 2-5 AU which coincides with the observed experimental data.
In the data of Pioneer 10 and 11 no maximum was observed in the radial gradient distribution in the region of 2-5 AU /5/ and in relation to this, a divergence from the expected distribution can be noticed, obtained on the basis of a solution of the anizotropic diffusion equation type (1) with the boundary conditions $\frac{\partial B}{\partial \rho}\Big|_{\rho=0} = 0$ /6/
A solution of equation (1) with boundary conditions of the type $\frac{\partial B}{\partial \rho}\Big|_{\rho=0} \neq 0$ shows a small maximum. /7/

In this way it appears that the expected radial gradient distribution with distance depends on the choice of boundary conditions near the sun, that is to say on the physical conditions around the sun. The boundary condition $\frac{\partial B}{\partial \rho}\Big|_{\rho=0} = 0$ actually corresponds with the symmetrical distribution of density B, when for $\rho = 0$, B = minimum.

The boundary condition $\frac{\partial B}{\partial \rho}\Big|_{\rho=0} \neq 0$ does not impose any demands on the distribution B, it results from the fact that all cosmic ray particle streams are at an equal zero for $\rho = 0$. Accordingly, it is seen that the anizotropic diffusion equation type (1) describes the behaviour of cosmic ray particles $\gg$ 2-3 GV in interplanetary space, however in soloving it the physical conditions around the sun must be taken into consideration as these are effected considerably by the boundary conditions for $\rho = 0$. It is especially worth noticing the fact the energy spectrum for an 11-year variation in the case of H⁺ is softer than for H⁻. Apart from this it would be an unusually important experimental confirmation of 22-year variation spectrum caused by particle drift during a period of 2 consecutive 11-year cycles of solar activity.

REFERENCES

1. Vlasov V.I. Geomagnetism and Aeronomy, Vol. XIX, No 3, P 401, 1979
2. Timothy A.F. et al, Solar Phys. Vol. 42, NL, p. 135, 1975
3. Dorman L.I. "Cosmic Rays", North - Holland Publishing Company - Amsterdam, Oxford, American Elsevier Publishing Company, INC - New York, 1974
4. Venkatesan D. et al, Journal of Geophysical Res. Vol.89, No 6A, p. 3735, June 1, 1984
5. Mc Kibben R.B., et al, 1982 Ap. J. 254, L 23
6. Alania M.V., et al, Izv. AN SSSR, Ser. fiz., Vol. 48, No 11, p. 2103.
7. Alania M.V., et al, Geomagnetism and Aeronomy, Vol. 17, No 2, p. 131, 1977

N85-34853

LATITUDINAL GRADIENTS OF COSMIC RAYS AND THE POLARITY REVERSAL OF THE HELIOSPHERIC MAGNETIC FIELD: A PRELIMINARY EVALUATION

G. Newkirk, Jr.
National Center for Atmospheric Research, Boulder, Colorado

J. A. Lockwood
University of New Hampshire, Durham, New Hampshire

M. Garcia-Muñoz
and
J. A. Simpson
University of Chicago, Chicago, Illinois

1. Introduction. A central uncertainty in understanding the propagation and modulation of galactic cosmic rays is whether or not the cross-field drift of particles in the large-scale heliospheric magnetic field plays an important role (Burlaga, 1983; Jones, 1983). Studies of measured differences in various cosmic ray properties between epochs having positive and negative polarity of the heliospheric field have led to inconclusive results. A major uncertainty is the interpretation to be placed on differences in behavior between successive solar cycles separated by approximately 11 years; accidental differences from cycle to cycle may be confused with differences which are truly dependent upon the polarity of the field.

Since theoretical models of cosmic ray propagation including drifts predict the presence of an unambiguous latitudinal gradient of particle flux with respect to the heliospheric current sheet, one might expect that observation of this parameter could provide a means of resolving the question. However, neither analyses of the latitudinal gradient at one rigidity (Newkirk and Fisk, 1985) nor of the rigidity dependence of this parameter during the last solar minimum (Newkirk *et al.*, 1985) have done so. The reason for this failure is that models both with and without large-scale drifts can be adjusted within reasonable limits to provide agreement with the observations.

However, if drift effects are significant, the gradient of cosmic rays with respect to the current sheet should exhibit a *strong* sensitivity to the polarity of the large-scale magnetic field in the heliosphere (Jokipii and Kopriva, 1979; Kota and Jokipii, 1982). For example, at 2 GV and an inclination of the current sheet to the solar equator of 30°, the latitudinal gradient should increase from -3% AU^{-1} in the 1969-80 cycle to -13% AU^{-1} in the 1980-90 cycle. Even though the current sheet is usually more complex than a plane inclined to the solar equator and the observations represent the average of a variety of inclinations, this four-fold increase in the magnitude should provide unambiguous evidence for the importance of drifts. Naturally, models without drifts are insensitive to the polarity of the large-scale field.

This investigation provides preliminary answers to the questions: (1) Does the latitudinal gradient change as predicted by the drift-dominated models? and (2) Does the rigidity dependence of the latitudinal gradient display any sensitivity to the polarity of the field?

2. Data Analysis Our approach is to examine the gradient of cosmic ray flux in ecliptic latitude with respect to the current sheet at 1 AU for equivalent epochs before and after the reversal of the large-scale solar magnetic field in late 1980. We use synoptic K-coronameter observations to locate the position of the coronal current sheet, which we assume projects radially out to 1 AU according to the locally observed solar wind speed. The methodology is described in detail in Newkirk and Fisk (1985) and Newkirk *et al.* (1985). Cosmic ray fluxes between 0.9 GV and 35 GV (see Table) provide the basic data. The epochs chosen for the comparison are DOY 1 1971 to DOY 250 1972 and DOY 1 1983 to DOY 140 1984. Both periods include the early recovery stage of cosmic ray modulation and occur when the configurations of polar coronal holes and the current sheet were roughly similar (Figure 1). Daily mean fluxes were used throughout the study and, since we are concerned with the steady-state distribution of cosmic rays, days when the

ORIGINAL PAGE IS
OF POOR QUALITY

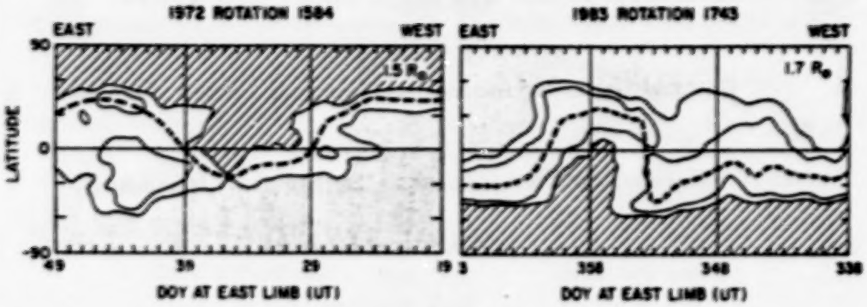

Fig. 1. Synoptic contour maps of the polarization-brightness product of the K-corona allow the "band of coronal streamers" and the assumed location of the coronal current sheet (heavy dashed) to be located for typical rotations in 1972 and 1983. For clarity only two contour levels are shown. Cross hatched and stippled areas indicate positive and negative magnetic polarities of the dominant magnetic field in the polar coronal holes as inferred from either a potential extrapolation of the photospheric fields or the polarity of the interplanetary field. During both epochs, the current sheet extends up to 35° from the equator.

interplanetary medium was disturbed or when solar energetic particles contaminated the record were excluded from the analysis. For the purposes of this study we have defined as disturbed any day influenced by a classical Forbush decrease in the Mt. Washington neutron monitor data. Days contaminated by solar energetic particles were identified in the IMP (> 106 MeV) channel and, to insure homogeneity, the same days were eliminated from all three records.

3. Results Figure 2 contains an example of the profile of cosmic ray flux with respect to the heliospheric current sheet. The scatter of the individual daily values indicates that considerable variation unrelated to the separation of the earth from the current sheet is present. However, a least-means-square fit of the form

$$U = a_0 + a_1 \sin^2\lambda_{mg} ,$$

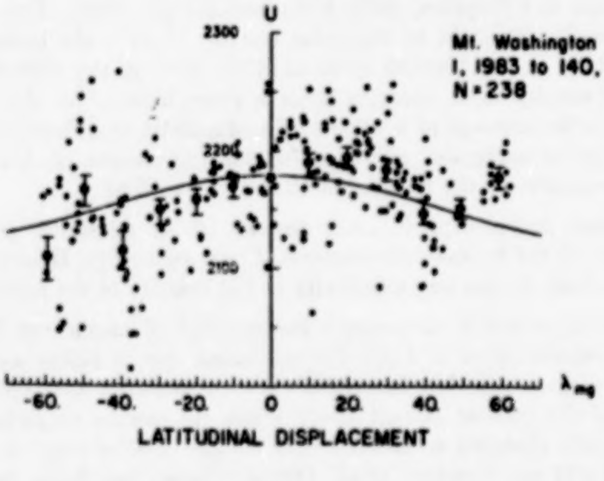

Fig. 2. An example of the latitudinal variation detected in the individual daily values of cosmic ray flux (•) and in the means of each 10° interval (●). Range lines give the standard deviations of the means. The smooth curve is the least-mean-square fit of the equation to the daily values. For this example $a_o = 2179 \pm 3$, $a_1 = -56 \pm 13$.

where $\lambda_{m\epsilon}$ is the inferred separation in ecliptic latitude between the Earth and the current sheet, is able to define the parameter a_1 with a precision of 20 to 30% for most cases. Of course, longer data intervals containing more points would produce a more precise result; however, the additional data are not yet available for the post-1980 interval and the pre-1980 interval has been limited deliberately to include approximately the same number of data points in both sets. The relative latitudinal gradients a_1/a_0 appear in the Table along with P_F, the probability that the coefficient a_1 is zero according to Fisher's F-test of the deviations of the daily points from the curve (Bevington, 1969). Although the data are noisy, all except the Huancayo value for 1971-72 are reasonably well established. The rigidity dependence of the latitudinal variation is displayed graphically in Figure 3. Vertical range lines indicate the standard error of estimate of the quantity a_1/a_0 while horizontal range lines delineate the limits within which 50% of the cosmic ray counting ray is generated. The straight line indicates the variation $P^{-0.72}$ estimated from a larger rigidity range for the four year period 1974-77 (Newkirk, *et al.* 1985).

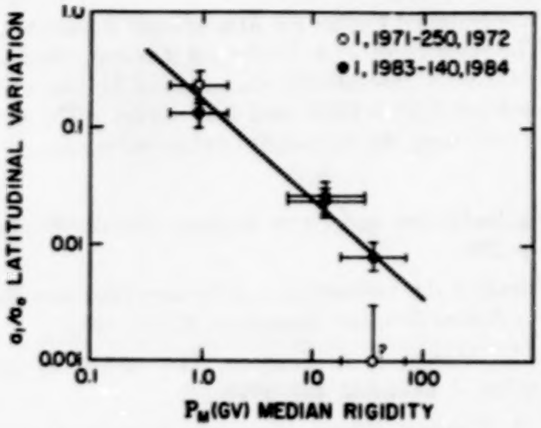

Fig. 3. The rigidity dependence of the relative latitudinal gradient $-a_1/a_0$ shows no significant difference between the 1971-72 and the 1983-84 intervals.

Table
Parameters of the Cosmic Ray Monitors
and
Relative Latitudinal Gradients

Detector System	Reference	$P_M(GV)$	1971-72 $-a_1/a_0$	 P_F	1983-84 $-a_1/a_0$	 P_F
Huancayo	Simpson and Wang, 1970	35 (18-70)	0.001 ± 0.002	6×10^{-1}	0.008 ± 0.002	8×10^{-5}
Mt. Washington	Lockwood and Webber, 1967; 1979	13 (6-30)	0.026 ± 0.008	1×10^{-3}	0.024 ± 0.006	10^{-6}
IMP-8(≥06 MeV)	Garcia-Muñoz *et al.*, 1975	0.9 (0.5-1.7)	0.23 ± 0.07	5×10^{-4}	0.14 ± 0.03	2×10^{-6}

P_M = median rigidity (Newkirk, *et al.*, 1985), ( ) = 50% range

4. Conclusions and Discussion Within the statistical limits imposed by the currently available data and the noise inherent in the determination of the latitudinal gradient, no evidence for the expected change in the latitudinal gradient from pre-1980 to post-1980 epochs can be found. In addition, the rigidity dependence of the gradient appears to be the same in the two epochs. Thus, we can find no evidence for a sensitivity of the latitudinal gradient to the polarity of the large-scale heliospheric magnetic field such as has been predicted by models incorporating particle drifts.

5. Acknowledgements The National Center for Atmospheric Research is sponsored by the National Science Foundation. The research of J. A. Lockwood was supported in part by the National Science Foundation under Grant ATM-8304486 while that of M. Garcia-Munoz and J. Simpson was supported by NASA contract NAS-5-25731 and NSF Grant ATM-82-06418. The authors thank D. G. Sime reading and criticizing the manuscript before submission.

6. References

Bevington, P. R., Data Reduction and Error Analysis for the Physical Sciences, McGraw-Hill, New York, 1969, p. 200.

Burlaga, L. F., Understanding the heliosphere and its energetic particles, *Proc. 18th International Cosmic Ray Conf., Invited Reviews*, Bangalore, 12, 21, 1983.

Garcia-Muñoz, M., G. M. Mason, J. A. Simpson, The cosmic-ray age deduced form the ^{10}Be abundance, *Astrophys. J. Let., 201,* 145, 1975.

Jokipii, J. R., and D. A. Kopriva, Effects of particle drift on the transport of cosmic rays. III. Numerical models of galactic cosmic-ray modulation, *Astrophys. J., 234,* 384, 1979.

Jones, F. C., Cosmic ray modulation and anomalous component, *Rev. Geophys. and Space Physics, 21,* 318, 1983.

Kota, J., and J. R. Jokipii, Cosmic rays near the heliospheric current sheet, *Geophys. Res. Lett., 9,* 656, 1982.

Lockwood, J. A., and W. R. Webber, Differential response and specific yield functions of cosmic ray neutron monitors, *J. Geophys. Res., 72,* 3395, 1967.

Lockwood, J. A., and W. R. Webber, Cosmic ray modulation during solar activity cycle 20, *J. Geophys. Res., 84,* 120, 1979.

Newkirk, G., Jr., and L. A. Fisk, Variation of cosmic rays and solar wind properties with respect to the heliospheric current sheet, I: 5 GeV protons and solar wind speed, *J. Geophys. Res., 90,* 3391, 1985.

Newkirk, G., Jr., J. Asbridge, J. A. Lockwood, M. Garcia-Munoz and J. A. Simpson, Variations of cosmic rays and solar wind properties with respect to the heliospheric current sheet, II: Rigidity dependence of the latitudinal gradient of cosmic rays at 1 A.U., *J. Geophys. Res.*, submitted April 1985.

Simpson, J. A. and J. R. Wang, The eleven-year and residual solar modulation of cosmic rays (1952-1969) *Astrophys. J., 161,* 265, 1970.

N85-34854
SH 4.2-17

THE INFLUENCE OF NONSTATIONARITY OF THE SOLAR ACTIVITY AND GENERAL SOLAR FIELD ON MODULATION OF COSMIC RAYS

Zusmanovich A.G.,Kryakunova O.N.,Churunova L.F.,
Shvartsman Ya.E.

Institute of Ionosphere of AN KazSSR,480068,
Alma-Ata,USSR.

ABSTRACT. It was conducted numerical model of the propagation of galactic cosmic rays in the interplanetary space for the case when the modulation depth determined by the level of the solar activity changed in time.Also the contribution of the particles drift in the regular field was calculated and it was shown the agreement with experimental data about the ratio of protons and electrons in two solar activity minima.

The stationary spherical-symmetric approach of weak modulation was applied for the investigation of galactic cosmic ray modulation /1-3/.For the cosmic rays intensity at the Earth's orbite we write

$$n(r,t)=n_0 \exp\left[-\int_{r}^{r_0} \frac{u(r)}{\varkappa(r)}\,dr\right], \tag{1}$$

where U is the solar wind velocity, $\varkappa$ is the diffusion coefficient, r_0 is the dimension of modulation region.We'll consider the simple modelling problem.Let us break the integral in (1) for N equal parts assuming $u_i/\varkappa_i$ is constant for each interval Δr.Then we have for K-moment in case, when $\varkappa$ =const(r)

$$\frac{n_K}{n_0}=\exp\left[-\sum_{i=0}^{N} y_{iK}\right],\quad y_{iK}=\frac{u_{iK}}{\varkappa_{iK}}\Delta r \tag{2}$$

and for gradient g_{ik}

$$g_{iK}=\left\{\exp\left[-\sum_{i+1}^{N} y_{iK}\right]-\exp\left[-\sum_{i-1}^{N} y_{iK}\right]\right\}\Big/2\exp\left[-\sum_{i}^{N} y_{iK}\right]\Delta r;\qquad i\geq 1. \tag{3}$$

In case when $\varkappa\sim r$

$$\frac{n_K}{n_0}=\prod_{i=0}^{N}\left[\frac{1+6i}{1+6(i+1)}\right]^{y_{iK}},\quad y_{iK}=\frac{u_{iK}}{\varkappa_{iK}}r_1,\qquad r_1=1\,a.u.; \tag{4}$$

$$g_{iK}=\left\{\prod_{i+1}^{N}\left[\frac{1+6i}{1+6(i+1)}\right]^{y_{iK}}-\prod_{i-1}^{N}\left[\frac{1+6i}{1+6(i+1)}\right]^{y_{iK}}\right\}\times\left\{2\prod_{i}^{N}\left[\frac{1+6i}{1+6(i+1)}\right]^{y_{iK}}\Delta r\right\}^{-1} \tag{5}$$

The interval Δr was chosen equal to 6 a.u. The values y_{ik} were generated as follows: for t=0 (i.e. k=0) the sum of all terms of y_{ik} sub i was filled up by numbers a, which were chosen so as their sum is equal to 1.8 (that correspond to modulation coefficient at solar activity maximum). Hence it follows $a_0=0.164$. For the first column $y_{0k} = a_0 - kb$ to k=15 then $y_{0k} = y_{0\sigma} + kb$ ($15 < k < 30$) and again $y_{0k} = y_{0\varkappa} - kb$ ($k > 30$). The value b was chosen equal to 0.01. Thus the values y_{0k} (in Fig.1a) represent the solar activity cycle. The results obtained from (2) and (4) have been shown in Fig. 1a. One can see that the lag of cosmic rays intensity increase is bigger in case when the diffusion cuefficient is independent on the distance from the Sun. The results of the calculations of radial gradient for $\varkappa$ =const (r) (dotted line) and $\varkappa \sim r$ (solid line) have been shown in Fig.1b. We have constant gradient for uniform filling of modulation region (k= 0). Then gradient increases with distance at decreased "solar activity" branch and it decreases at the increased branch (k=30). The change of gradient with distance has complicated form at transition period (k=19). Introducing the dependence n_k/n_0 on the particle rigidity R through the dependence $\varkappa$ (R) in the form /4/

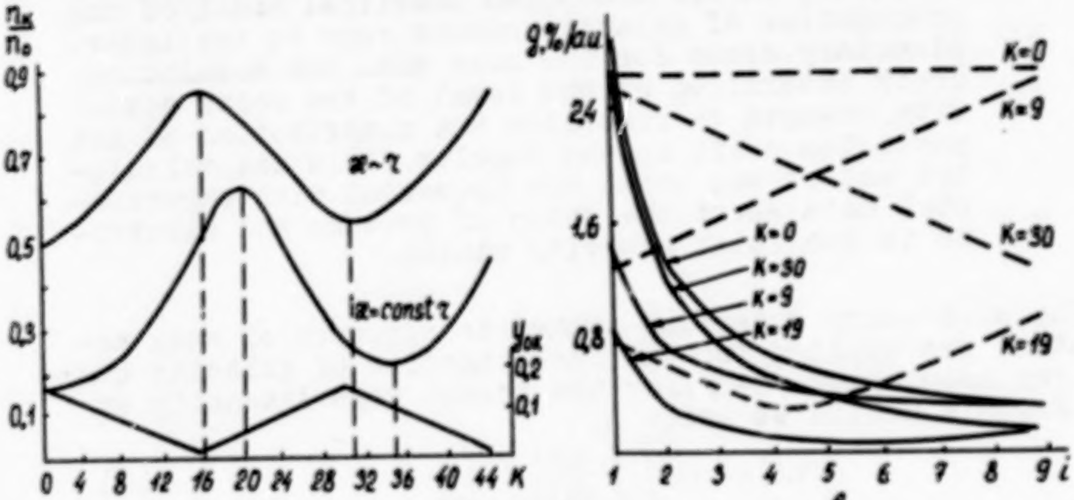

a

б

Figure 1.

$$\varkappa(R) = \varkappa_0 f(R), \text{ where } f(R) = \frac{R^{1.5}(R+R_0)^{1.5}}{(1+R_0)^{1.5}(R^2+0.88)^{1.5}}, \quad (6)$$

we have for $\varkappa$ =const(r)

$$\frac{n_k}{n_0} = \exp\left[-\frac{1}{f(R)}\sum_{i=0}^{N} y_{ik}\right] \quad (7)$$

and for $\varkappa \sim r$

$$\frac{n_k}{n_0} = \prod_{i=0}^{N}\left(\frac{1+6i}{1+6(i+1)}\right)^{\frac{y_{ik}}{f(R)}} \quad (8)$$

ORIGINAL PAGE IS
OF POOR QUALITY

Energy spectra of the cosmic rays intensity normalized at the solar activity minimum have been shown in Fig.2.The solid lines correspond to the case $\varkappa$ =const(r),dotted lines - $\varkappa \sim r$,symbols are values k-different moments of "solar activity" cycle.The curves with k=0 and k=30 correspond to the same "solar activity" level,however the curves differ greatly in appearance.Analogously the curves with k=7,37 and k=23 correspond to the same "solar activity" level.

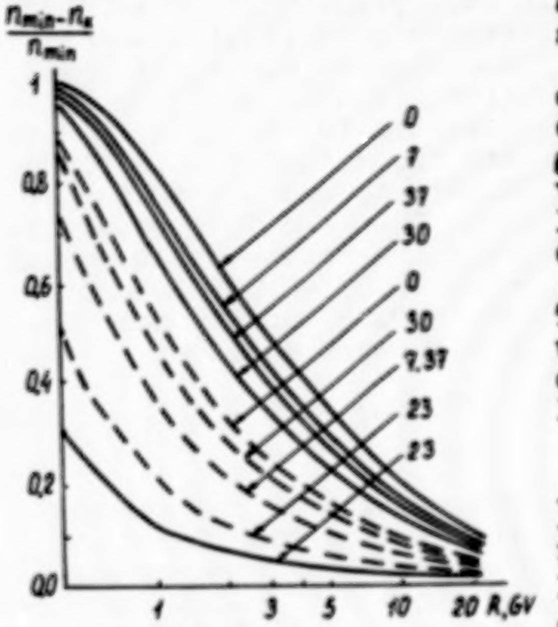

Figure 2.

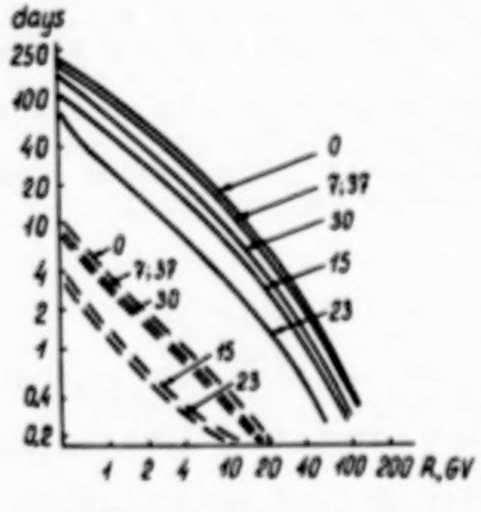

Figure 3.

The influence this factor on the lag time modulation effects relatively to changes of the solar activity level is shown in Fig.3 (solid lines for case $\varkappa$ =const(r), dotted lines for the case $\varkappa \sim r$,symbols are values k). The values of the lag time τ_i were calculated with method described in /5/,then total lag time determined by $\tau = \sum \tau_i$

Thus one can see that the nonstationarity of modulation properties of the solar wind and its distribution with distance from the Sun essentially influences on the energy spectra of particles,gradients of cosmic rays intensity in the interplanetary space and the lag time of modulation effects relatively to changes of the solar activity level observed near the Earth when the dimencion of the cosmic ray modulation region is greater than 50 a.u.

Moreover the particles drift in the regular magnetic field connected with general solar field /6-8/ gives certain contribution to the break of the relation between cosmic ray intensity and the observed solar activity level.

In /9/ the values of the absolute coefficients of "usual" convective-diffusion modulation (determined by the solar activity level) K_1 and effect of the influence of general solar fields K_2 were determined by investigation the con-

ORIGINAL PAGE IS
OF POOR QUALITY

nection between the cosmic ray intensity and HL-index of solar activity.On the whole the observed intensity is determined in this model by

$$J(\mathcal{E},K_1,K_2)=J_0(\mathcal{E})\exp\left[-\frac{K_1}{f(R)}+\frac{K_2}{f_2(R)}\right]. \qquad (9)$$

where f(R) is the same that in (6),$f_2(R)=\lambda\rho/(\lambda^2+\rho^2)$, ρ is Larmor radius, λ is determined from (6),($\varkappa=\lambda v/3$).

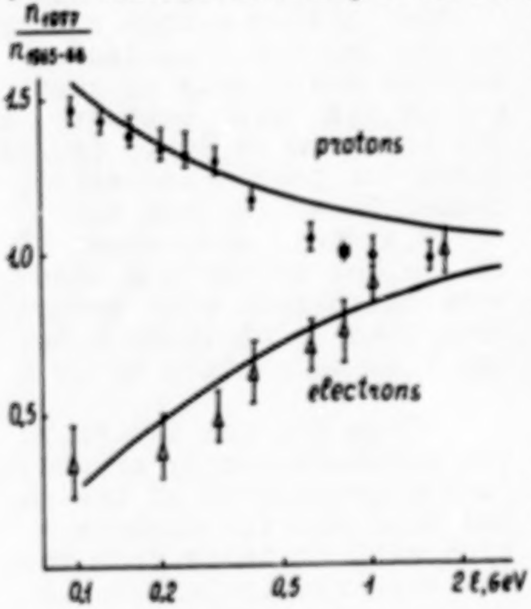

Figure 4.

The sign before K_2 is positive for 1954 and 1976,and negative for 1965.In /9/ it was found that $K_1=0.21\pm0.08$; 0.32 ± 0.10 and 0.35 ± 0.10 for 1954,1965 and 1976 respectively,the values K_2 are equal $+0.14\pm0.03$;-0.09 ± 0.04 and $+0.11\pm0.03$ for the same periods.Hence we have:

$$\frac{J_{1977}}{J_{1965}}=\exp\left[-\frac{0.03}{f(R)}+\frac{0.2}{f_2(R)}\right]. \qquad (10)$$

The results of the calculations using (10) for $R_0=15$ GV have been shown by curves in Fig.4 for protons and electrons.In this figure we have presented the direct experimental data from /10/ for these ratios in the energy interval 0.1 - 2 GeV.It is seems a good agreement between our calculations and the experimental ratios.

We have shown that the effects connected with nonstationarity of the modulation properties of the solar wind and the particles drift in the regular field exerts essential influence on galactic cosmic ray modulation.

REFERENCES.

1.Webber W.R. Proc.16th ICRC,Kyoto,1979,14,253.
2.Owens A.J. Rev.Geophys.Space Phys.,1979,17,560.
3.Antonova V.P.,et al. Izv.AN SSSR.Ser.fiz.,1981,45,1287.
4.Zusmanovich A.G. Proc.16th ICRC,Kyoto,1979,3,366.
5.Zusmanovich A.G.,Kryakunova O.N. Proc.18th ICRC,Bangalore,1983,3,19.
6.Krainev M.B.,Stozhkov Yu.I. Izv.AN SSSR.Ser.fiz.,1979,43,N 12,2603.
7.Alania M.V.,Dorman L.I.Proc.16thICRC,Kyoto,1979,3,57.
8.Zusmanovich A.G. Proc.18th ICRC,Bangalore,1983,3,118.
9.Zusmanovich A.G. et al. Proc 18th ICRC,Bangalore,1983,3,102.
10.Webber W.R. et al. Proc. 18th ICRC,Bangalore,1983,3,35.

N85-34855

SH 4.2-18

THE EFFECT OF THE NEUTRAL SHEET STRUCTURE OF THE INTERPLANETARY MAGNETIC FIELD ON COSMIC RAY DISTRIBUTION IN SPACE

Alania M.V., Aslamazashvili R.G., Bochorishvili T.B.,
Djapiashvili T.V., Tkemaladze V.S.

The Institute of Geophysics, Georgian Academy of
Science, Z.Rukhadze str.1, 380093, Tbilisi

ABSTRACT

I.The results of the numerical solution of the anisotropic diffusion equation are presented in the paper. It is shown that the modulation depth of galactic cosmic rays is defined by degree of curvature of the neutral current sheet in Heliosphere. 2.The effect of the regular interplanetary magnetic field (IMF) on cosmic ray anisotropy in the epoch of solar activity minimum (in 1976) is analysed by the data of the neutron super-monitors of the world network and the heliolatitudinal gradient and cosmic ray diffusion coefficient are defined.

The theoretical model. The recent investigations/1,2/ show that the neutral current sheet changes its range significantly for 11-year period of the Sun's cycle and can be one of the reasons of cosmic ray modulation. Really, the curvatures of the interplanetary magnetic field lines of forces(IMF) correspond to the waved structure of the neutral sheet that is identical with the appearance of high-value zenithal component of IMF, Hz. The experimental observations in space show that Hz component of IMF is, in the mean, a high value $\sim 2\cdot 10^{-3}$ nT /3/ and therefore, its account in solution of comic ray anisotropic diffusion equation is of necessity.

The anisotropic diffusion equation /4/ for the stationary case is used:

$$\nabla_i(\varkappa_{ik}\nabla_k n)-\nabla_i(n\cdot u_i)+\frac{1}{3R^2}\cdot\frac{\partial}{\partial R}(R^3 n)\nabla_i u_i=0 \tag{1}$$

where $\varkappa_{ik}$ -the tensor coefficients of diffusion, n and R -the density and the rigidity of the particle,and U_i -solar wind velocity. It is suggested in equation solution (1) that the radius of the modulation volume is 50 a.u., U=4.I0cm/s, the diffusion coefficient along the magnetic field has the form

$$\varkappa_{\parallel}=\varkappa_0\, EXP(R_1/R)\cdot(R_2+R)^2\cdot\varphi(\theta)\cdot\phi(r) \tag{2}$$

where $\varkappa_0$ =I0^{22}cm^2/sec, R_1 =0,05GV, R_2=3GV, $\varphi(\theta)$ is changed in the range I-5 from the helioequator to the near-polar region, and $\phi(r)=1+\alpha(r/r_0)$, where α =0,I, r_0 -modulation region radius.

The range of the waved structure of the neutral current sheet is given in the form

$$\gamma = A\gamma_0 (r/r_0) \cdot \cos(16\pi r/r_0) \qquad (3)$$

A and γ_0 are chosen so that the neutal current sheet on the Earth's orbit (r_4=I,5·IO^{13} cm) is at the heliolatitude IO° . In this case $A = 5$ and $\gamma = 10^{\circ}$.

The equation (1) is solved by the net method for the two dimensional case (r, θ) $\frac{\partial n}{\partial \varphi} = \frac{\partial^2 n}{\partial \varphi^2} = 0$ and the results are presented in Fig. 1a,b. The curve(a) shows the change of the relative density of IO Gev energy cosmic rays, when the curvature (3) is defined by the parameter A =0,5, i.e. the maximum removal of the neutral sheet from the equator of the Sun on the Earth's orbit is L=2,5 ·IO^{12} cm.The curve(b) shows the case, when $A = 0$ and $L = 0$. It is seen that, really, with the increase of neutral current sheet range, the significant cosmic ray modulation is expected, which by its value is compared with the amplitude of 11-year variation in the energy region IO-20Gev.

The experimental data on cosmic ray anisotropy.

It has been shown in our previous paper /5/ that the particle drift effect at the expense of the gradient and the curvature of the interplanetary magnetic field (IMF) is revealed singlevaluedly, especially in the epoch of solar activity minimum. It is known that the particle drift effect in distribution of cosmic ray density and anisotropy can be calculated with the antisymmetric part of the anisotropic diffusion tensor /6/, but , in our opinion, this problem is not always clear, and therefore, sometimes the incorrect interpretation is made. E.g. as it has been done in the report /7/ while reviewing paper /5/, where the epoch of solar activity minimum I965- has been considered.

Four neutron super-monitor stations: Kiel,Norikura, Lomnitsky Stif and Khafelakar have been chosen for revealing the effect of the particle drift in cosmic ray anisotropy (I976). The data of these stations were free from the trends with the periods more than 24 hours and the harmonic coefficients A_1 and B_1 for every day were defined.Then they were averaged depending on the Earth's location in "+" and "-" sectors of IMF.("+" corresponds to the direction of the magnetic lines of forces from the Sun, and "-" toward the Sun). Then, the values A_r and A_φ have been defined in cosmic space taking into account the drift into the Earth's magnetic field and the coupling coefficients /8/ and the means by all four stations were found. The results are presented in Fig.2, where the solid vectors correspond to the theoretical results, and the dashed ones- the experimental data of observation.

It can be seen that a good accord is existed there.

Having the values A_r and A_φ for "+" and "-" sectors of IMF the algebraic equations have been constituted of the form:

ORIGINAL PAGE IS
OF POOR QUALITY

$$A_r^{\pm}=\varkappa_{rr}\frac{\partial n}{\partial r}\pm\varkappa_{r\theta}\frac{\partial n}{\partial\theta}-1{,}5\,u\cdot B\ ;\qquad A_{\varphi}^{\pm}=\varkappa_{\varphi r}\frac{\partial n}{\partial r}\pm\varkappa_{\varphi\theta}\frac{\partial n}{\partial\theta}\qquad(4)$$

Solving the system of equations (4) the mean solar wind velocity is found, and the retious $\alpha=\varkappa_{\perp}/\varkappa_{\parallel}$ and $\alpha_1=\varkappa_{H}/\varkappa_{\parallel}$ are estimated. ($\varkappa_{\perp}$, $\varkappa_{H}$ and $\varkappa_{\parallel}$ -the transversal, Hall and parallel diffusion coefficients) and the heliolatitudinal gradient and the diffusion coefficient are estimated.

Discussion and conclusion

I. The degree of curvature of the IMF neutral layer influences appreciably cosmic ray modulation. The modulation depth is large during the extend of the waved neutron layer and can be compared with the amplitude of 11-year variation in the energy region 10-20 Gev.

2.The particle drift effect at the expense of the gradient and the curvature of IMF is revealed singlevaluedly in Cosmic ray anisotropy in the epoch of solar activity minimum in 1976.

3. The inverse problem is solved by the equation (4). The solar wind velocity U=455km/s (the direct observations by /9/ give U=450) and ratio α of the transverse diffusion coefficient $\varkappa_{\perp}$ to the parallel one $\varkappa_{\parallel}$ (α = 0,3) are defined.

It is of interest to note that the same value has been obtained for 1965 too.

4. The heliolatitudinal gradient and the diffusion coefficient have been estimated from (4) with the given radial gradient of cosmic rays $\nabla_r n$=(1-2) % / a.u. constituting

$$\nabla_{\theta} n=(0{,}2-0{,}4)\%/a.u.\ ,\ \varkappa_{\parallel}=(0{,}6-1{,}3)\cdot10^{23}\,cm^2/s$$

respectively.

REFERENCES

I. Hoeksema J.T., Wilcox S.M. and Scherrer P.H., SUIPR, Report №924, Stanford, California, 1982.
2. Thomas B.T. and Goldstein B.E., Solar Wind Five, NASA, p.44, 1982.
3. Slavin J.A. and Smith E.L., Solar Wind Five, NASA, p.323, 1982.
4. Dorman L.I. "Astrophizicheskie aspekti cosmicheskikh Luchei"."Nauka", M.1975.
5. Alania M.V. et al., 18th ICRC, Bangalore, India,L.P., Vol.10, pp.91, 1983.
6. Jokipii J.R., Levy E.H. and Hubbard W.B., Astr.J., 213, 864-868, 1977.
7. Jones F.C., 18th ICRC, Bangalore, India.Invited and Rapporteur Papers, Vol.12., p.379, 1983.
8. Nagashima K. et al., Coup.Coef. of Cosmic Rays,Nagoya, Japan, 1982.

9. King J.H. Interplanetary Medium Data Bock, NSSDC/WDC-A, 1977.
10. Webber W.R. and Lockwood J.A., 18th ICRC, Bangalore, India, L.p., Vol.10, p.22, 1983.

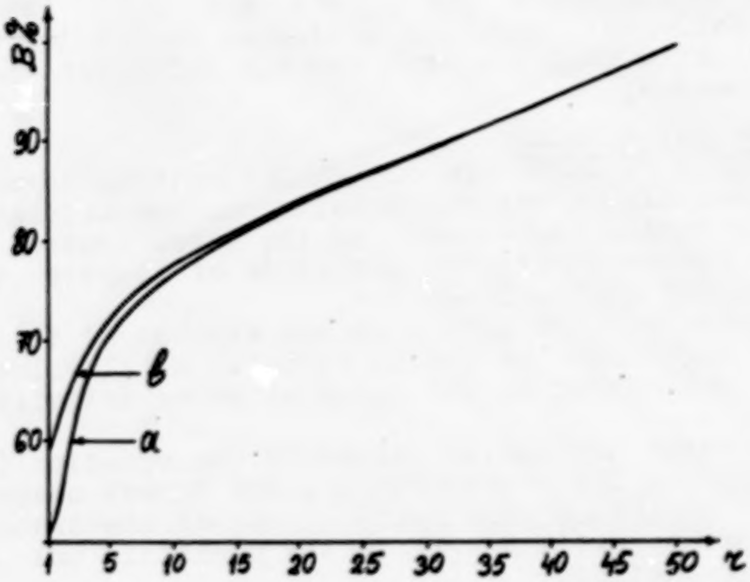

Fig. 1.

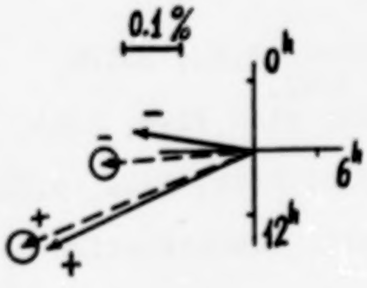

Fig. 2.

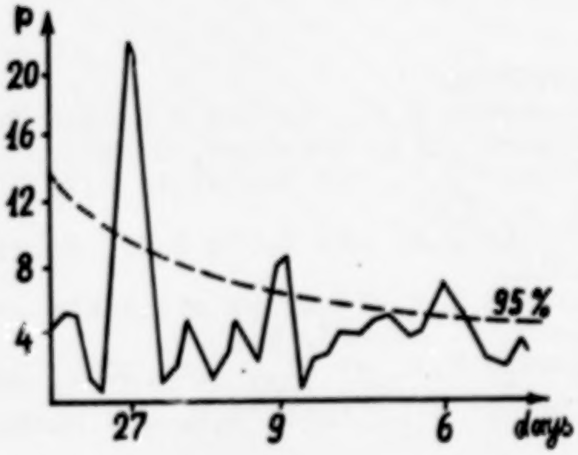

Fig. 3.

N85-34856

SH-4.2-19

ON THE INFLUENCE OF THE HELIOMAGNETOSPHERIC PERIPHERY ON THE GALACTIC COSMIC RAYS

Krainev M.B., Stozhkov Yu.I.,

P.N.Lebedev Physical Institute of the Academy
of Sciences of the USSR, Leninsky Prospect, 53,
117924, Moscow, USSR

Charakhchyan T.N.

Institute of Nuclear Physics, Moscow State
University, 119899, Moscow, USSR

ABSTRACT

The suggestion is substantiated that the periphery of the heliomagnetosphere - the region which properties depend on both solar wind and interstellar space parameters - play much more important role in the solar modulation of the galactic cosmic rays than usually believed.

1. INTRODUCTION.

As a rule the electromagnetic fields in the galactic cosmic ray modulation region are specified by the extrapolation of those known at $r \lesssim 30$ AU. Clearly the restriction imposed on the possible modulation region characteristics in this scheme also limits the range of the explicable by means of it galactic cosmic ray phenomena. Let us call the galactic cosmic ray modulation accomplished in conformity with the above scheme the "internal"modulation.

The mentioned extrapolation is valid only in the case when the whole modulation region is inside the supersound and superalfvenic solar wind which properties are controlled entirely by the Sun. In this work the suggestion is substantiated that the galactic cosmic rays should (and probably do) undergo considerable transformation in the transition region between the supersound solar wind and the undisturbed by the Sun galactic space.

2. THE THEORETICAL REASONS.

First of all note the discrepancy of the "internal" modulation scheme during the periods when the large-scale magnetic field distribution in the quiet (i.e.undisturbed from the outside) solar wind is a dipole-like one. In this case because of the space charge the potential of the inside of the modulation region boundary surface considerably depends on the heliolatitude while the exterior of the same surface conforming to the undisturbed galactic space is equipoten-

N85-34856

tial. To settle this contradiction the transition region should be included in the galactic cosmic ray modulation region/1,2/.

In /3-5/ the processes in this transition region are considered for the explanation of some galactic cosmic ray effects. It is important that for these explanations the fundumental difference of the modulation parameters from those of the Quiet solar wind is necessary: the nonradial flow of plasma /4,5/ and the large latitude component of the interplanetary magnetic field /3-5/.

At the same time the qualitative character of /3-5/ should be noted as well as the obvious insufficiency of the method suggested in /1,2/ to allow for the transition region influence on the galactic cosmic rays. This method using the Liuville theorem and the potential difference between the inside points of the quiet solar wind and the infinity (so called the "external" modulation of the galactic cosmic rays) takes into account only the charge distribution in the quiet solar wind and completely disregard the galactic space characteristics: the presence of the galactic magnetic and electric fields, the movement of the solar system through the interstellar matter and so on.

3. THE EXPERIMENTAL REASONS.

A. The most dramatic feature of the galactic cosmic rays which is evidently beyond the scope of the "internal" modulation is their behaviour in the low energy range ($E \leq 80$ MeV/n) during 1971 -1978 - the "anomalous component" (AC), /6/. The characteristics of these particles - their elemental and isotopic compositions, energy spectra - so differ fromthe expected ones that there are many advocates of the hypothesis /7/, according to which the source of the anomalous component is the interstellar neutral gas, i.e. AC does not have any bearing to the galactic cosmic rays. Yet some features in cosmic ray behaviour force us to regard the "anomalous component" as the natural part of the complex galactic cosmic ray phenomenon taking place during this period:

1) The time behaviour of the anomalous component fluxes is very simillar to that of the protons and helium nuclei of higher energy;

2) The very important fact, connecting anomalous component with the protons, is the simillar (and anomalous) behaviour of their radial gradients. With the growth of the solar activity in 1979-1980 the gradients of both anomalous component and protons of $E=29-67$ MeV sharply drop off /8/.

ORIGINAL PAGE IS
OF POOR QUALITY

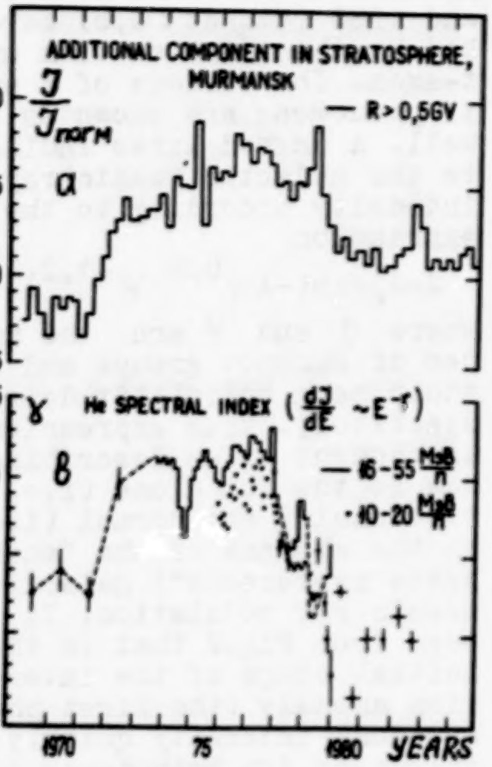

FIGURE 1

In Fig.1 the behaviour of the anomalous component (He spectral index: $dJ/dE \sim E^{-\gamma}$, /8,9/,б) is correlated with that of so called "the additional component in stratosphere",(a), which, as shown in /10/, is due to the primary H and He nuclei in the energy range 100-500 MeV/n.

The likeness of the behaviour of the anomalous component and of protons is rather difficult to understand from the viewpoint of the current hypotheses on their origin /6/. In /2/ we suggested the scheme of AC formation by the acceleration of low energy galactic cosmic rays in the process of their "external" modulation. The same process results in the considerable increase of higher energy particles.

B. The unusual from the viewpoint of the "internal" modulation the galactic cosmic ray phenomena take place during the periods of the inversion of the general magnetic field of the Sun (GMFS).

In /11-13/ we subdivided the galactic cosmic ray behaviour during GMFS inversion into two phenomena:

I - Due to the supposed attenuation of the interplanetary magnetic field strength the decrease of the galactic cosmic ray modulation so much the greater (and the more prolonged) the greater the particle energy is. This explanation of the "energetic hysteresis" is entirely in the scope of the "internal" modulation scheme.

II - The phenomenon depending on the type of GMFS inversion (characterized by the sign of the dM_z/dt, where M_z is the projection of the general magnetic field of the Sun magnetic dipole moment on the Sun rotation axis) delaying with respect to the first phenomenon by 1-2 years. We relate this delay to the location of the process responsible for the second phenomenon on the periphery of the helio-magnetosphere.

Fig.2 shows the galactic cosmic ray behaviour according to the stratospheric data (Murmansk, R_c=0.5GV) during the periods of GMFS inversions in 1969-71 ($dM_z/dt > 0$,a) and 1980 ($dM_z/dt < 0$,b) marked by the thick section on t-axes. The periods of I and II phenomena are shown as well. A dashed lines indicate the galactic cosmic ray intensity according to the expression

$$J = J_0 \exp(-A \cdot \eta^{0.8} \cdot \varphi^{-1.2}),$$

where η and φ are the number of sunspot groups and their mean heliolatitude, respectively. This expression is thought of as describing due to the Sun alone (i.e. "internal") and normal (i.e. in the absence of the "energetic hysteresis") galactic cosmic ray modulation. It is seen from Fig.2 that in the initial stage of the inversion anomaly (the first phenomenon) intensity quickly increases for both types of the inversion, this increase persisting during the second phenomenon in ($dM_z/dt > 0$)-inversion, but changing into decrease in ($dM_z/dt < 0$)-inversion.

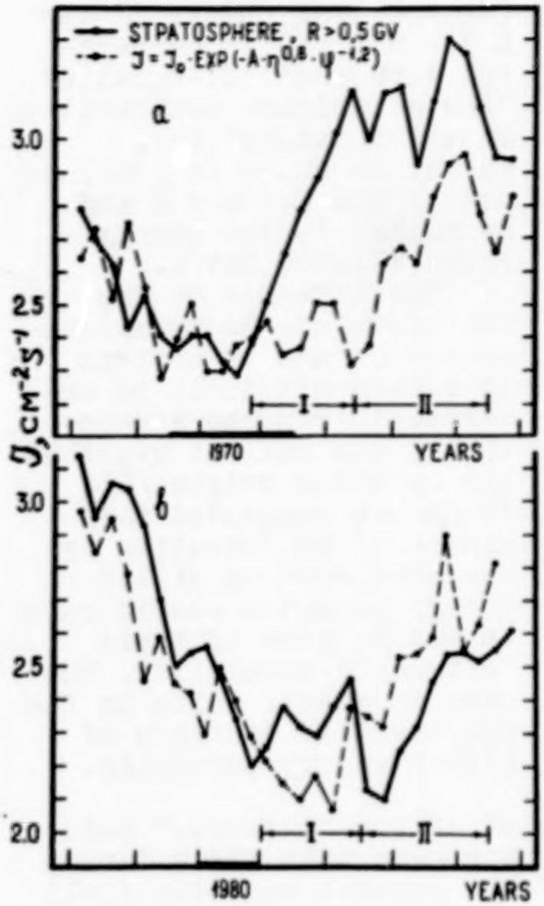

FIGURE 2.

4. THE CONCLUSION. To understand the galactic cosmic ray behaviour it is necessary to develope much more real model of the heliomagnetosphere than used now.

REFERENCES

1. Krainev M.B.(1981), Proc.17 ICRC, Paris, 3, 357
2. Krainev M.B.(1981), Proc.17 ICRC, Paris, 3, 361
3. Ahluwalia H.S.,(1979),Proc.16 ICRC, Kyoto, 12, 216
4. Krivoshapkin P.A. et al,(1981),Proc.17 ICRC,Paris,4,33
5. Kravtsov N.G. et al,(1984),Izv.Akad.nauk SSSR,ser.fiz., 43, 2129
6. Simpson J.A.,(1983),in"Compos.and Origin of Cosmic Rays"
7. Fisk L.A. et al,(1974),Astrophys.Journ.,190, L35
8. McKibben R.B.et al,(1983).Proc.18 ICRC,Bangalore,3,63
9. Garcia-Munoz M. et al,(1981),Proc.17 ICRC,Paris,3,270
10. Svirzhevskaya A.K. et al,(1985),Proc.this conf.,SH 4.4-18
11. Krainev M.B. et al,(1983),Proc.18 ICRC,Bangalore,3,23
12. Krainev M.B. et al,(1983),Proc.18 ICRC,Bangalore,3,95
13. Krainev M.B. et al,(1984),Izv.Akad.nauk,ser.fiz.,43,2100 (in russ.)

N85-34857

SH 4.2-20

SPATIAL DISTRIBUTION OF COSMIC RAYS IN MAGNETIC CYCLES OF THE SUN

M.V.Alaniya

Institute of Geophysics of the Academy of Sciences of Georgian SSR, Tbilisi, USSR

R.T.Gushchina, L.I.Dorman

Institute of Terrestrial Magnetism, Ionosphere and Radio Wave Propagation, USSR Academy of Sciences, 142092 Troitsk, Moscow Region, USSR

Space-time distribution of CR density B is determined from the solution of anisotropic diffusion equation (Dorman, 1965). The boundary problem is solved in a quasistationary (the delay of CR relative to cyclic variations of solar activity is taken into account) axisymmetric case under the following boundary conditions

$$\left.\frac{\partial B}{\partial r}\right|_{r=0}=0\,;\quad \left.B\right|_{r_0=1}=1\,;\quad \left.B\right|_{r=550\,GV}=1,$$

where r is the distance from the Sun, r_0 is the dimension of the modulation region, R is particle rigidity. The specificity of our modulation model is the use (in line with the works by Alaniya et al., 1981, 1983) of the empirical dependence of the free path of particles for scattering on the observed latitudinal distribution of solar activity. Another specific feature of the model is an account of an additional effect due to the drift of charged particles towards the helio-equator plane or backward, depending on the direction of the total magnetic field of the Sun.

The intensity of coronal radiation (λ = 5303A) and the area of solar spots were chosen as indices of helio-activity. Out of many observed manifestations of solar activity these characteristics have been chosen in the assumption that their cyclic variations are a reflection of a corresponding manifestation of poloidal and toroidal components of the magnetic field of the Sun. Such interdependence was also pointed out by Parker (1982). To confirm this assumption, the behaviour of the north-south assymetry of the chosen indices of solar activity was studied in detail in 18-21 cycles in the periods of inversion of the total magnetic field of the Sun. It has been shown (Alaniya et al., 1983) that inversion of magnetic fields in high-latitudinal regions of the Sun starts in the hemisphere where the activity is maximal, and the most convivcing proof of it is given by the intensity variation of the green coronal line. Thus, deterining the variation of the free path for particle scattering by means of the dependence which takes into account simultaneously the change in the solar spot areas and in the coronal radiation intensity (λ = 5303 A) and the delay of CR, one can associate the observed cyclically varying solar activity on the entire sphere and the spatial distribution of the diffusion tensor.

Under the above boundary conditions and under the assumptions concerning the dependence of the free path on the distance and rigidity (see Alaniya et al., 1981) the numerical solution of the CR transport equation makes it possible to estimate an additional effect induced by particle drift from poles to the equator and backwards depending on the direction of the large-scale magnetic field of the Sun. Figure I presents the latitudinal distribution of the expected modulation depth B for two different configurations of the total magnetic field of the Sun, as well as the modulation depth calculated for the case where the drift effect is disregarded.

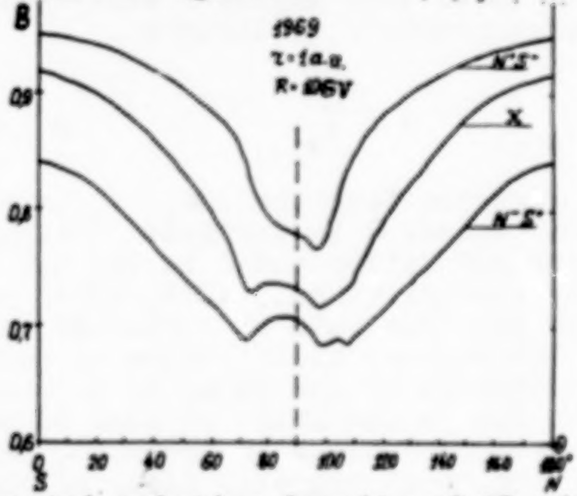

Fig. I The expected relative density of CR with a rigidity of 10 GV in 1969 at a distance r = I a.e. versus the heliolatitude with an account of drift fluxes (N^-S^- - towards the ecliptic plane, N^-S^- - backward and without an account of the drift x).

The calculations show that an account taken of this effect may increase or decrease (depending on the direction of the background magnetic field of the Sun) the modulation depth about by I/3.

According to our calculations for some periods in 19-21 cycles of solar activity, the expected amplitudes of long-term variations of CR with a rigidity of 10 GV (in the determination of which the drift of charged particles is taken into account)are in a good agreement with the ones observed on neutron monitors (which register particles with the effective rigidity of 10 GV).

From the obtained space-time distribution of the relative CR density we have determined the expected transverse gradients, which are the measure of nonsphericity of the modulation process. Increasing in the activity maxima, the latitudinal gradients whose value depends on the epoch of the solar activity cycle must show up the features of spatial distribution connected with the specificities of the CR modulation model under consideration (Fig.2).

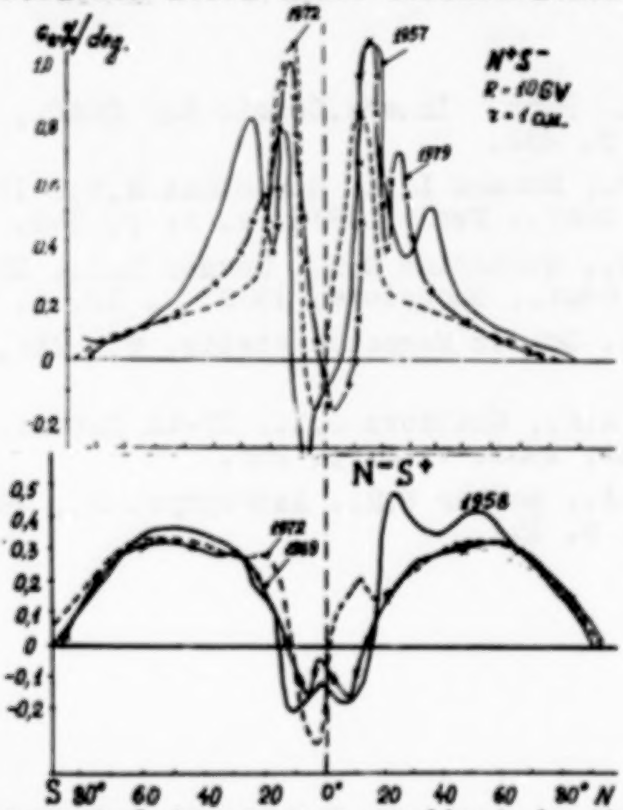

Fig. 2. The expected transverse gradient in the maxima of 19-21 cycles of solar activity for different configurations of the total magnetic field.

For the configuration of the total magnetic field of the Sun, where the magnetic field lines leave the North pole and enter the South pole (N^-S^-), the maximum of the transverse gradient must be observed at helio-latitudes $\pm(10^\circ - 15^\circ)$, and for the inverse configuration it shifts towards higher helio-latitudes ($\pm(40^\circ - 50^\circ)$). Besides, for both field configurations on the Sun, at low helio-latitudes the transverse gradient is signvariable, which confirms the results of meteorite studies (Lavrukhina, Ustinova, 1981).

Note that the agreement between the expected transverse gradients and those observed on cosmic apparates (according to Lockwood and Webber, 1984)is only of a qualitative character because one should bear in mind the difficulties in the interpretation of space measurements, which are connected with the fact that the angle of cosmic apparatus declination from the helio-equator plane is at the present time not large, and the problem of separation of radical and transverse gradients has not yet been clearly solved.

REFERENCES

I. Dorman L.I.. 9-th Intern.Cosmic Ray Conf., London, 1965, v.I, p. 292.

2. Alaniya M.V., Dorman L.I., Gushchina R.T.. 17-th Intern. Cosmic Ray Conf., Paris, 1981, v. 3, p. 349.

3. Alaniya M.V., Gushchina R.T., Dorman L.I., 18-th Intern. Cosmic Ray Conf., Bangalore, 1983, v. 10, p. 99.

4. Parker E.N.. Cosmic Magnetic Fields, M., Mir, 1982, v. 2, p. 479.

5. Lavrukhina A.K., Ustinova G.K., 17-th Intern. Cosmic Ray Conf., Paris, 1981, v. 3, p. 238.

6. Lockwood J.A., Webber W.R.. Astrophys. J., 1984, v. 279, N I, pt. I, p. 151.

N85-34858

11- AND 22-YEAR VARIATIONS OF THE COSMIC RAY DENSITY AND OF THE SOLAR WIND SPEED

N.P.Chirkov

Institute of Cosmophysical Research & Aeronomy
Lenin Ave., 31, 677891 Yakutsk, USSR

ABSTRACT

Cosmic ray density variations for 17-21 solar activity cycles and the solar wind speed for 20-21 ones are investigated. The 22-year solar wind speed recurrence was found in even and odd cycles which allows to forecast it. The 22-year variations of cosmic ray density opposite to the solar wind speed and solar activity were found. The account of solar wind speed in 11-year variations significantly decreases the modulation region of cosmic rays with E = 10-20 GeV.

1. Introduction. Many authors [1-4] to investigate the nature of 11-year variations of cosmic ray density use solar activity and obtain the large sizes of modulation region. But according to the equation of transfer the agent modulating cosmic rays should be proportional to the solar wind speed. If the latter is not proportional to the solar activity then the conclusions on large sizes of cosmic ray modulation region will be incorrect.

2. Results. To study the regularities of the solar wind speed the geomagnetic activity (aa-index) was used taking into account their close relationship [5,6] . The averaged picture of geomagnetic and solar activities is presented in Fig.1 [7] where data for 1868-1977 were used. In the left the odd solar cycles, in the right the even ones are shown. From Fig.1 it is seen that on the average in odd cycles a close correlation with solar activity is observed and in even cycles - a bad one. Both in even and odd cycles the two maxima of geomagnetic activity are observed. The first maximum coincides with the solar activity maximum, the second one delays by 1 year in odd cycles and by 4 years in even ones. The solar wind speed should have the similar regularity which in 20 and 21 solar cycles was observed [8,9] . The second maximum of geomagnetic activity has 22-year recurrence either in even or odd cycles which allows to forecast it [6,7] . The next second maxima of geomagnetic activity and solar wind speed should be observed in 1996 and 2004.
Presented in Fig.1 picture of behaviour of geomagnetic activity and solar wind speed should significantly complicate the 11-year variation of cosmic ray density as it is was observed [10] .

Here we continue the investigation of [10] for more

ORIGINAL PAGE IS
OF POOR QUALITY

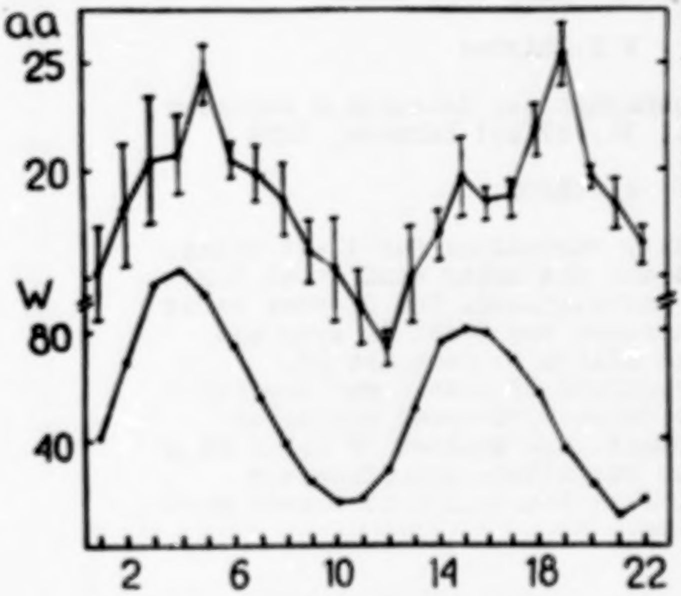

Fig. 1. 22-year averaged data of aa-index and of Wolf numbers for 1868-1977

extend energy range of the observed cosmic ray variations. The ionization chamber data for 17-21 solar cycles and the neutron and balloon data for 19-21 ones were used. Correlation and regression coefficients a, b in the equations of type

$$\Delta I = a\Delta W + b\Delta aa,$$

where ΔI, ΔW, Δaa are deviations from mean values and are presented in the Table. The values of a total correlation coefficient R and values of

$$\sigma = \sqrt{\Sigma(\Delta I_{obs} - \Delta I_{cal})^2/n}$$

are also presented. From the Table it is clear that the account of the solar wind speed significantly improves the relationship. The correlation coefficient is 0.89 - 0.96. The calculated and observed values of I are shown in Fig.2 from which their good agreement is evident. As it is seen from the Table σ for ionization chamber is 0.2 - 0.4%, for neutron monitors $\sigma = 1.3 - 2.7\%$, for balloons $\sigma = 3.7 - 5.9\%$ which is better by several times than obtained by other methods.

Table

Cycle	$r_{I,W}$	$r_{I,aa}$	$r_{W,aa}$	R	a	b	σ
			Ionization chamber, ΔI^k				
17	-0.88±0.08	-0.34±0.32	-0.03	0.95	-0.014	-0.083	0.2
18	-0.84±0.09	-0.66±0.17	0.39±0.26	0.92	-0.014	-0.098	0.4
19	-0.91±0.05	-0.93±0.04	0.85±0.08	0.96	-0.006	-0.107	0.3
20	-0.82±0.09	-0.35±0.25	-0.15±0.28	0.95	-0.012	-0.056	0.2
21	-0.79±0.14	-0.54±0.24	0.09	0.92	-0.010	-0.073	0.3
			Neutron monitor, ΔI^m				
19	-0.84±0.09	-0.91±0.05	-	0.92	-0.024	-0.865	2.7
20	-0.92±0.04	0.05	-	0.93	-0.090	-0.081	1.3
21	-0.70±0.14	-0.56±0.28	-	0.89	-0.066	-0.607	2.4
			Balloons, ΔI^c				
19	-0.95±0.04	-0.92±0.05	-	0.97	-0.096	-0.051	5.1
20	-0.91±0.05	0.06	-	0.92	-0.254	-0.249	3.7
21	-0.78±0.14	-0.45±0.28	-	0.89	-0.182	-1.222	5.9

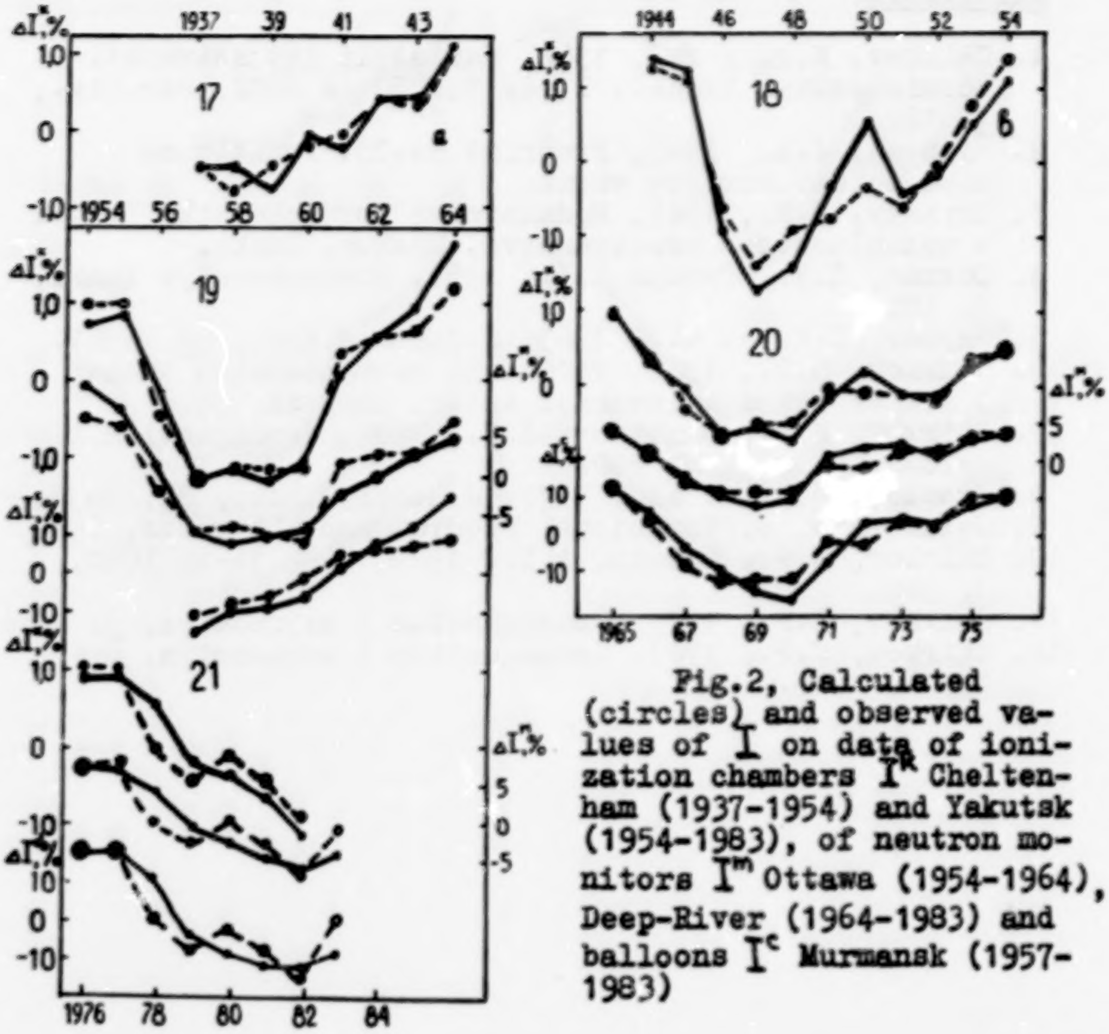

Fig.2, Calculated (circles) and observed values of I on data of ionization chambers I^{k} Cheltenham (1937-1954) and Yakutsk (1954-1983), of neutron monitors I^{m} Ottawa (1954-1964), Deep-River (1964-1983) and balloons I^{c} Murmansk (1957-1983)

The solar wind enhancement at solar activity decrease caused the delay of recovery of cosmic ray intensity by 1-2 years in 19 cycle and by 3 years in 21 cycle caused also the repeated decreases of I in 18 and 20 cycles in 4-5 years after the solar activity maximum.

A good agreement (within 6 months) of calculated and observed values ΔI allows to estimate the sizes of cosmic ray modulation region ~ 30 AU. The use of monthly values of smoothed for a year I, W and aa-index allows to decrease the sizes of modulation region up to $\leqslant$ 10 AU.

In [11] the 22-year variations of solar and geomagnetic activities were found. The even and odd cycles being closely related than odd and even ones. The similar dependence was found in [12] for cosmic ray density and it is expected in solar wind speed. The 22-year variations of cosmic ray density are opposite to 22-year variations of solar activity and of solar wind speed.

References

1. Chirkov, N.P. i dr., 1962, Variatsii intensivnosti kosmicheskikh luchei. Trudy YaF SO AN SSSR, ser.fiz., 4, 122.
2. Simpson, J.A., 1963, Preprint No.25. Poniticiae acad.scient.scripta varia.
3. Krymsky, G.F., 1969, Modulatsiya kosmicheskikh luchei v mezhplanetnom prostranstve, Moskwa, Nauka.
4. Dorman, I.V., Dorman L.I., 1967, Kosmicheskiye luchi, 8, 100.
5. Snyder, C.W. et al., 1963, J.Geophys.Res., 68, 6361.
6. Chirkov, N.P., 1980, Variatsii kosmicheskikh luchei i solnechnyi i solnechnyi veter, Yakutsk, 18.
7. Chirkov, N.P., Samsonov, I.S., 1984, Geomagnetism i aeronomiya, 24, 2, 300.
8. Crooker, N.U. et al., 1977, J.Geophys.Res., 82, 1933.
9. Solar Wind, 5, Woodstock, Program and Abstracts, 1982.
10. Chirkov, N.P., Kuzmin, A.I., 1979, Proc.16-th ICRC, 3, 360.
11. Chirkov, N.P., 1985, Geomagnetism i aeronomiya, 3.
12. Chirkov, N.P., 1983, Geomagnetism i aeronomiya, 23, 6, 1015.

N85-34859

SH 4.2-22

DIFFERENCE BETWEEN EVEN AND ODD 11-YEAR CYCLES IN COSMIC RAY INTENSITY

J.A. Otaola, R. Pérez-Enríquez and J.F. Valdés-Galicia
Instituto de Geofísica, UNAM, México 04510, D.F.

ABSTRACT

Cosmic ray data for the period 1946-1984 are used to determine the run of the cosmic ray intensity over three complete solar cycles. The analysis shows a tendency towards a regular alternation of cosmic ray intensity cycles with double and single maxima. Whereas a saddle-like shape is characteristic of even cycles, odd cycles are characterized by a peak-like shape. The importance of this behaviour is discussed in terms of different processes influencing cosmic ray transport in the heliosphere.

1. Introduction. The anomalous behaviour of the cosmic ray intensity after the 1968 solar maximum in the 20th solar cycle has been described by several authors. This was characterized by the softenning of the spectra (Evenson et al., 1983), the sudden recovery of the intensity (Kuzmin et al., 1977), a poor correlation of the cosmic ray intensity with solar activity (Akopian et al., (1981) and the sudden appearance of anomalous components in the cosmic rays (García Muñoz et al., 1981; McDonald et al., 1981).

The purpose of this study is to show that the 1946-1957 11-year cycle in cosmic ray intensity also presents this characteristic behaviour and that this seems to be the result of a similar behaviour in solar activity during even sunspot cycles. A possible physical interpretation to this phenomenon is given in terms of different contributions of drift, convection and diffusion to the whole modulation process.

2. Data. The basic data used in the present study are the monthly values of the cosmic ray intensity and the smoothed sunspot numbers over the period 1946-1984, thus covering three complete 11-yr cosmic ray intensity cycles. As the cosmic ray data are derived from the ion chamber at Huancayo (1946-1957) and the neutron monitor at Deep River (1958- 1984), and they represent two different kinds of data, we integrated them following the method described by Nagashima and Morishita (1980) which, from the point of view of long term modulation, is permissible as a first approximation.

In Figs. 1a. and 1b. the smoothed sunspot number and the integrated cosmic ray intensity over the period 1946-1984 are shown. The cosmic ray intensity is expressed in percent decrease with respect to the maximum intensity level established in May, 1965. The cosmic ray intensity, on the other hand, was smoothed using an ultra lowpass filter which essentially gives the trend of the input function and effectively removes the rapid fluctuations (Behannon and Ness, 1966). The smoothed intensity is shown as the dashed curve in Fig. 1b.

In these curves the hatched regions represent the times of reserval of the solar magnetic field and the notation $\vec{M}\uparrow\uparrow\vec{\Omega}$ and $\vec{M}\uparrow\downarrow\vec{\Omega}$ indicates the magnetic moment parallel and anti-parallel to the angular velocity axis of rotation of the Sun, respectively.

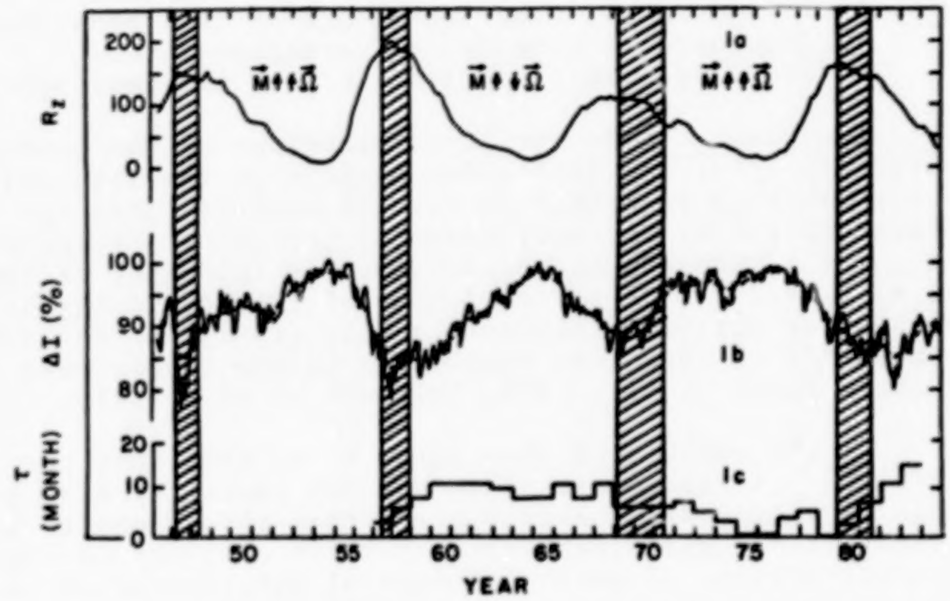

Fig. 1. a) Zurich sunspot number. b) Integrated cosmic ray intensity (solid line) and smoothed curve (dashed line). c) Time lag of intensity behind sunspot number for 11 years from t-10 years to t.

3. Results and Discussion. From the smoothed curve of cosmic ray intensity shown in Fig. 1b, one can see that the shape of the $\vec{M}\uparrow\uparrow\vec{\Omega}$ cycles differs systematically and markedly from the shape of the $\vec{M}\uparrow\downarrow\vec{\Omega}$ cycle. Whereas the shape of the $\vec{M}\uparrow\downarrow\vec{\Omega}$ cycle in characterized by a simple and relatively smooth increase to the maximum (∿ 7.5 yr), the $\vec{M}\uparrow\uparrow\vec{\Omega}$ cycles, on the average, are characterized by a two maxima structure in which the first maxima is reached relatively rapid after the previous minimum in the cosmic ray intensity (∿ 3-4 yr) and the sedond, the main and also more developed, tends to occur

at the same time in the cycle that the maximum of the $\vec{M}\uparrow\downarrow\vec{\Omega}$ cycle.

This different behaviour between $\vec{M}\uparrow\uparrow\vec{\Omega}$ and $\vec{M}\uparrow\downarrow\vec{\Omega}$ cycles is also shown in the time lag τ of cosmic ray intensity behind solar activity, as measured by the smoothed sunspot number. This 22-yr variation in the time lag, already found by Nagashima and Morishita (1980), in which τ is greater in $\vec{M}\uparrow\downarrow\vec{\Omega}$ cycles than in $\vec{M}\uparrow\uparrow\vec{\Omega}$ cycles, as can be seen in Fig. 1c, clearly shows that particles reach the Earth more easely when their access route is by the heliospheric polar regions than when they gain access along the current sheet (Kota and Jokippii, 1982). In this case as the route of access becomes longer due to the waviness of the neutral sheet the time lag τ is also longer as one would expect from theoretical considerations.

However, what this model does not explain is the two maxima structure during the $\vec{M}\uparrow\uparrow\vec{\Omega}$ cycles. This behaviour is, in fact, also present in solar (Dodson and Hedeman,1975) and in geomagnetic activity as measured by the aa-index (Halenka, 1983). According to the Dodson and Hedeman's results the solar activity during even sunspot cycles are characterized by two well defined "stillstands" in the level of activity during the declining phases of such cycles. On the other hand, Helenka shows that the aa-index during even solar cycles also presents this characteristic while the odd cycles do not.

Therefore, the results shown here clearly establish a marked distinction between even and odd solar activity cycles which in turn are reflected both in geomagnetic activity and cosmic ray intensity.

4. Conclusions. The results presented above point out towards a modulation mechanism, during even cycles,where convection plays a more important role than during odd cycles, where difussion dominates, while the effect of drifts only determines how the particles gain access to the observation point. That is, charge dependent effects are not the dominant processes in cosmic ray modulation.

References

1. Akopian, S. K. et al. (1981), 17th ICRC, París, 3, 227.
2. Behannon, K. W. and N. F. Ness (1966). Nasa T N D-3341.
3. Dodson, H. W. and E. R. Hedeman (1975). Solar Phys., 42, 121.
4. Evenson, P. et al. (1983). 18th ICRC. Bangalore, 3, 27.

5. García Muñoz, M. et al. (1981). 17th ICRC, París, 3, 270.
6. Halenka, J. (1983). Studia geoph. et geod., 27, 46.
7. Kota, J. and J. Jokipii (1982). Astrophys. J., 265, 573.
8. Kuzmin, A. I. et al. (1977). 15th ICRC, Plovdiv, 3, 150.
9. McDonald, F. B. et al. (1981). 17th ICRC, París, 3, 263.
10. Nagashima, K. and I. Morishita (1980), Planet. Space Sci., 28, 195.

N85-34860

THE DEPENDENCE OF SOLAR MODULATION ON THE SIGN OF THE COSMIC RAY PARTICLE CHARGE

M. Garcia-Munoz, P. Meyer*, K.R. Pyle and J.A. Simpson*
Enrico Fermi Institute, University of Chicago, Chicago, Illinois

and

P. Evenson
Bartol Research Foundation, University of Delaware, Newark, Delaware

ABSTRACT

We compare the solar modulation of galactic cosmic ray helium and electrons at 1 AU, within the 600-1000 MV magnetic rigidity interval, from 1965 through 1984. The time-intensity variations during the two solar maxima around 1970 and 1981 show that after 1970 the helium intensity recovers earlier than that of the electrons, whereas after 1981 the electron intensity recovers earlier than that of helium. The flux ratio of helium to electrons (He/e) undergoes a major increase during the 1969-1971 period and a major decrease during 1979-83. These experimental results can be interpreted as due to a dependence of the solar modulation of galactic cosmic rays on the sign of the particle charge, possibly as a consequence of drifts due to gradients and curvatures in the interplanetary magnetic field. However, the comparison of the shapes of the intensity-time curves of helium and electrons in the period 1970-1981 does not support a major specific prediction of the drift model.

1. __Introduction__. The perception that the interplanetary magnetic field is a distorted dipole, coherent in large scale, suggests that drifts due to field gradients and curvatures may play a significant role in solar modulation (Jokipii _et al_., 1977).

Because the drifts of particles of opposite charge move in opposite directions, the modulation effects on nuclei at a given point in the interplanetary space will be different from those on electrons.

This paper addresses the problem of the importance of drifts - trying to detect differences in the modulation of nuclear and electron cosmic rays that could be in principle attributed to the presence of drifts. We study the modulation of 70-95 MeV/n (739-866 MV) cosmic ray helium-4 and 600-1000 MeV cosmic ray electrons from 1965 through 1984 with special emphasis on the intervals around the two consecutive solar maxima in 1970 and 1981 in which the interplanetary magnetic field changed polarity.

2. __The Experimental Data__. Most of the experimental data used in this work have been obtained with the University of Chicago cosmic ray telescopes flown on balloons or aboard satellites.

Figure 1 shows the time dependence, within the 1960-1984 period of: (A) 27-day averages of the Climax neutron monitor counting rate, and; (B) 2-day averages of the 70-95 MeV/n helium-4 flux measured mostly by the U. of Chicago telescopes on IMP-3, 4, 5, 6 and 8. The open circles electrons (semifilled circles) and, finally, others using continuous satellite measurements of both helium and electrons (open circles).

---

*and Department of Physics.

The dashed vertical lines mark the times at which the individual fluxes of 70-95 MeV/n helium and 600-1000 MeV electrons reached their minimum values during the two consecutive solar maxima. Again the arrows mark the times of polarity reversal of the solar polar magnetic fields.

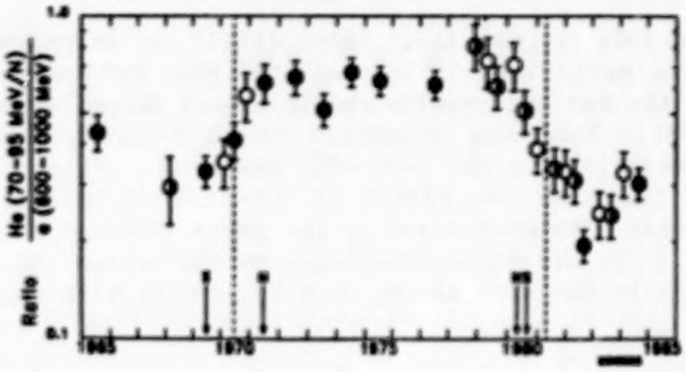

Figure 3

Figure 3 clearly shows a difference in the modulation of cosmic ray particles of opposite charge during the two solar maxima. The ratio He/e increases from 1968-69 to 1971-72, while it decreases from 1979 to 1982-83. As can be seen in Figure 2, normalizing the ISEE-3 fluxes to the 1982 balloon point would further decrease the He/e ratio after 1977, except, of course, the ratio associated with the 1984 balloon point. Thus the opposite character of the time dependence of the ratios around the two solar maxima persists, regardless of the balloon point used to normalize the ISEE-3 data.

4. Discussion and Conclusions. As can be seen in Figures 1 and 2, the periods 1971-73 and 1982-84 are similar time intervals in which the cosmic rays recover from the preceeding minimum intensity and increase towards the maximum associated with solar minimum activity. During these periods, in which the interplanetary magnetic field has opposite polarities, the ratio between the fluxes of cosmic ray helium and electrons, of nearly the same rigidity but opposite particle charge, differ by more than a factor 2. The fact that the electrons have higher velocity than the helium nuclei cannot alone explain the difference in the ratios, because any effect exclusively dependent on velocity is expected to be equally present in both compared periods.

The above facts suggest that a modulation process sensitive to the particle charge is operating in the interplanetary medium and an obvious candidate is drifts due to gradient and curvature in the interplanetary magnetic field as proposed by Jokipii et al. (1977).

However, although the results of the present work would be consistent with a significant role of drifts in solar modulation, they do not support one of the predictions of the recent drift model of solar modulation by Kota and Jokipii (1983). Their model predicts that, as a consequence of the predominant role played by drifts and the simultaneous presence of a wavy current sheet, the intensity of cosmic ray nuclei during the two halves of the 22-year magnetic cycle must have a very different time dependence, being relatively sharply peaked during the semicycle in which drifts bring positive particles from the equator to the heliospheric poles (e.g., around the 1965 solar minimum) and having a rather broad plateau during the semi-cycle in which drifts run in opposite direction (e.g., around the 1976 solar minimum). This is what is actually observed in the Climax neutron monitor counting rate for the solar minima of 1965

ORIGINAL PAGE IS
OF POOR QUALITY

and 1976 (Figure 1A). Since drifts run in opposite direction for negative particles, it is predicted that for cosmic ray electrons the shapes of the two semi-cycles should appear interchanged during the period 1959-1981. The data assembled in this work allow a check of this specific prediction for the 1970-1981 semicycle. Figure 4 shows a superposition of the time dependence of 70-95 MeV/n helium and 600-1000 MeV electron fluxes both normalized to the years 1970 and 1977. Note that from 1970 to 1980 the time dependence of the helium and electron fluxes have very closely the same shape, in disagreement with the model prediction.

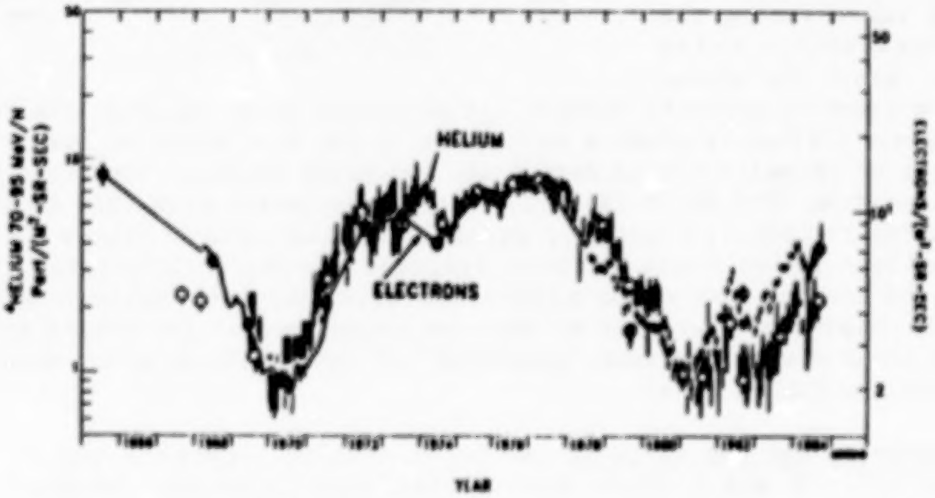

Figure 4

5. Acknowledgements. We thank Scott Marusak and Leo Krawczyk for their assistance in the preparation of the data, and Leonard Shulman and Evelyn Tuska for their assistance in the 1984 balloon flight. This research was supported in part by NASA grants NGL 14-001-005, NGL 14-001-006 and NAG 5-374, NASA Contracts NAS 5-28442 and NAS 5-28500 and NSF Grants ATM 84-12382, ATM 84-03718 and ATM 84-01427.

6. References

Burger, J.J. and Swanenburg, B.N., (1973), J. Geophys. Res., 78, 292.
Evenson, P., and Meyer, P., (1984), Phys. Rev. Letters, 17, 329.
Howard, R., (1981), Smithsonian Ap. Obs. Spec. Rep. No. 393, 155.
Jokipii, J.R., Levy, E.H. and Hubbard, W.B., (1977), Ap.J., 213, 861.
Kota, J., and Jokipii, J.R., (1983), Ap.J., 265, 573.

SH 4.2-24

N85-34861

AN UPDATE ON THE CORRELATION BETWEEN THE COSMIC RADIATION INTENSITY AND THE GEOMAGNETIC AA INDEX

M. A. Shea and D. F. Smart
Air Force Geophysics Laboratory
Hanscom AFB, Bedford, MA, 01731, U.S.A.

ABSTRACT

A statistical study between the cosmic ray intensity, as observed by a neutron monitor, and of the geomagnetic aa index, as representative of perturbations in the plasma and interplanetary magnetic field in the heliosphere, has been updated to specifically exclude time periods around the reversal of the solar magnetic field. The results of this study show a strong negative correlation for the period 1960 through 1968 with a correlation coefficient of approximately -0.86. However, there is essentially no correlation between the cosmic ray intensity and the aa index for the period 1972-1979 (i.e. correlation coefficient less than 0.16). These results would appear to support the theory of preferential particle propagation into the heliosphere via the ecliptic during the period 1960-1968 and via the solar polar regions during 1972-1979.

1. Introduction. The work of Jokipii et al. (1977) and subsequent publications has created considerable interest and discussion with their suggestion that the modulation of the galactic cosmic ray intensity should have a component controlled by the state of the interplanetary magnetic field as transported out from the sun, and hence there should be a solar cycle effect on the drift of cosmic rays in the heliosphere. In this paper we report the results of a study correlating the cosmic ray intensity at the earth with a solar and a geomagnetic parameter for periods between successive solar maxima.

2. Data Utilized. For this study the following data were utilized:

Neutron monitor data. The monthly averages of the cosmic ray intensity as measured by the Mt. Washington neutron monitor were selected primarily because of the long data base (June 1954 to the present time), the stability of the station over this long time period, and the fact that this station, located at a geomagnetic cutoff of ~ 1.3 GV, monitors the full galactic cosmic ray intensity. In addition the monthly averages of the cosmic ray intensity as measured by the Chicago neutron monitor were also utilized for the period January 1953 until the monitor closed in December 1971. These data were used primarily to allow inclusion of data as far back as 1953. The correlations reported herein were repeated using both the Mt. Washington data and the Chicago data for periods of time where the data were both available; the results were essentially the same for those time periods.

Geomagnetic data. The monthly averages of the geomagnetic aa index were selected as the parameter describing the status of the geomagnetic field and hence is a measure of turbulent plasma in the ecliptic plane. This index is computed from the K index of two antipodal observatories (invariant magnetic latitude 50°) providing a quantative characterization of the magnetic activity which is homogenous throughout the long data base (1868 to the present). A full description of this index is given by Mayaud (1973). We have utilized the aa index as being representative of the geomagnetic activity at the earth; we consider this activity to be the product of the interaction between the earth's magnetic field and the interplanetary magnetic field carried past the earth by the solar wind. Cosmic ray transport in the heliosphere would be affected by turbulence in the plasma and the interplanetary magnetic field. In contrast to the sunspot number, which may have some relationship to the three dimensional structure of the heliosphere, the geomagnetic aa index should represent disturbances only in the ecliptic plane at the position of the earth.

Solar data. The monthly averages of the Zurich relative sunspot number, Rz, were selected as a solar parameter. Although the Zurich relative sunspot number does not directly control the galactic cosmic ray intensity observed at the earth, it is an indicator of activity on the sun and is inversely correlated with the cosmic ray intensity throughout a solar cycle. This is probably because the sunspot number reflects activity over a range of heliocentric latitudes from about 45°N to about 45°S, and hence has some relationship to the three dimensional structure of the heliosphere.

3. Method. Using the method of least squares, linear correlations between the monthly averages of the cosmic ray intensity and the (a) sunspot number and (b) aa index were calculated for selected time intervals. In contrast to an earlier study (Shea and Smart, 1981), the results reported here are restricted to the following intervals:

January 1953 (Chicago data) through August 1956 (44 months);
June 1959 through December 1968 (115 months);
March 1972 through December 1979 (94 months).

The polarity at the north and south solar pole does not change at the same time. For example, the south pole changed polarity in July-August 1969; the north pole in August 1971. Since we wanted to restrict this analysis to periods when the solar polar magnetic fields were well defined, we excluded the months from September 1956 through May 1959 and January 1969 through February 1972 from this analysis.

Galactic cosmic ray particles observed at the earth have propagated through the heliosphere and are affected by the magnetic inhomogeneities encountered on their transit. Since recent results indicate that the heliosphere extends well beyond 30 AU and this distance corresponds to a solar wind transit time of four months, correlations were made between the monthly average cosmic ray intensity and averages of the aa index and the sunspot number for successively longer time periods preceding the monthly cosmic ray intensity. For each specific interval being studied the monthly average cosmic ray intensity (as recorded by neutron monitors) for month N, was first correlated against the Zurich relative sunspot number (or the aa index) for the same month. Next the same monthly average cosmic ray intensity for month N, was correlated against the two-month average sunspot number (or the aa index) for months N and N-1 and similarly for the three-month average sunspot number (or the aa index) for months N, N-1, and N-2, etc., to a maximum of 30 months.

Variations of the cosmic ray intensity, the sunspot number and the aa index for the period 1954-1979 are illustrated in Figure 1. For simplicity 3-month averages are plotted in this figure although monthly averages were utilized in this analysis.

ORIGINAL PAGE IS
OF POOR QUALITY

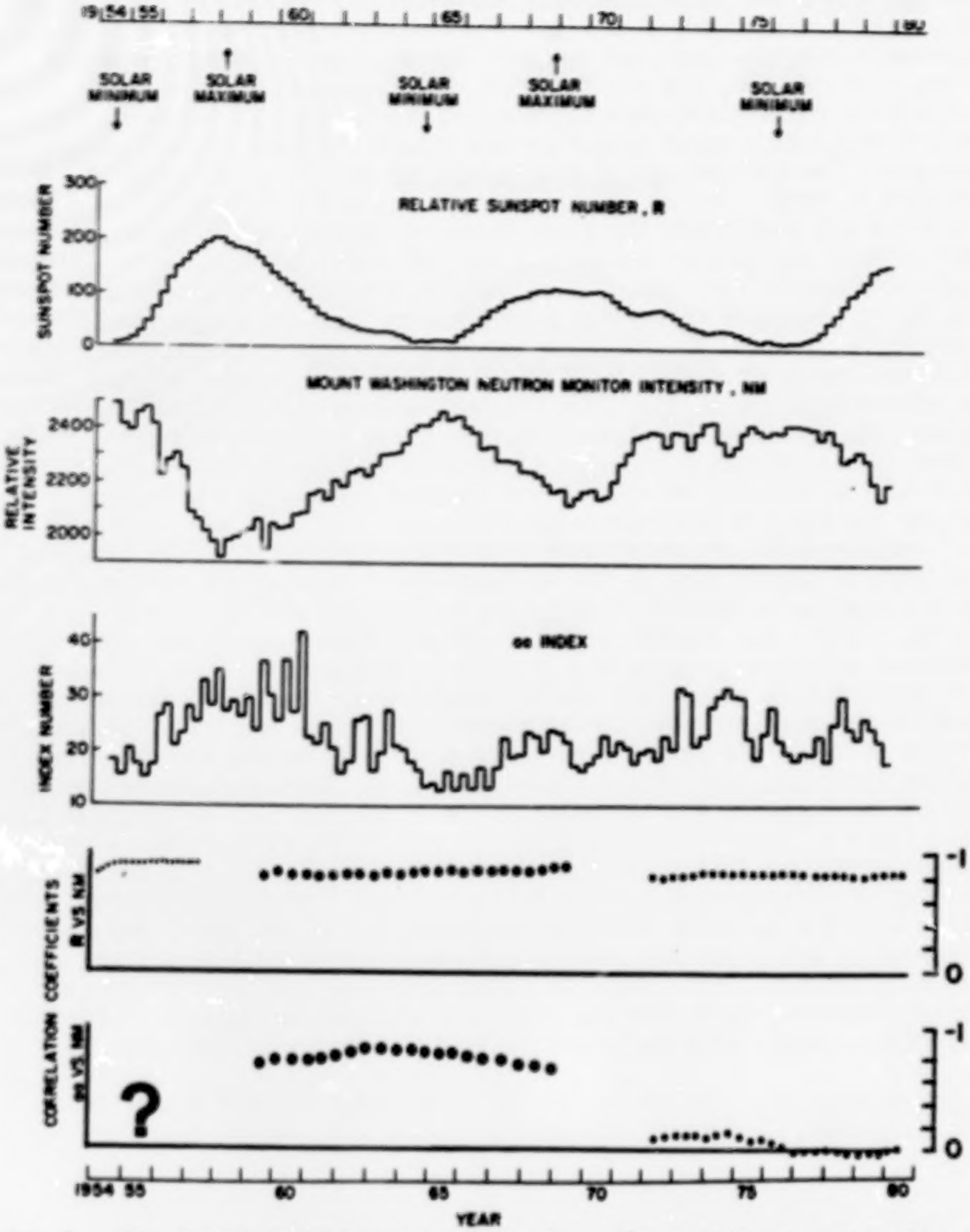

Fig. 1. The Zurich relative sunspot number, the cosmic ray intensity as measured by the Mt. Washington neutron monitor, and the aa index from 1954 through 1979. Solar minima and solar maxima are indicated at the top of the figure. The correlation coefficients are illustrated at the bottom of the figure where the individual dots represent the correlation coefficient for successively longer time lags. The question mark in the lower left indicates that it was not possible to reach any conclusion for the time period January 1953 to December 1957 because of the small time period. See text for additional description.

4. Results and Discussion. The values of the correlation coefficients for the various data sets studied are shown in the bottom section of Figure 1 where the individual dots represent the correlation coefficient for successively longer time lags. The relative position of each dot represents the time lag used for each correlation for the time period shown. For example, the first dot in each sequence represents the correlation coefficient when correlating the cosmic ray intensity for month N with the sunspot number (or aa index) for month N; the second dot represents the correlation of the cosmic ray intensity for month N with the sunspot number (or aa index) for months N and N-1 (i.e. 1-month lag), the third dot represents the correlation of the cosmic ray intensity for month N with the sunspot number (or aa index) for months N, N-1, and N-2 (i.e., two-month lag), etc. These results show that the cosmic ray intensity is inversely correlated with both the sunspot number and the geomagnetic aa index for the time interval essentially centered around the solar minimum between the 19th and 20th solar cycles. For the time period centered around the solar minimum between the 20th and 21st solar cycles, the correlation between the cosmic ray intensity and the sunspot number is approximately the same as for the earlier period; however, the value of the correlation coefficient between the cosmic ray intensity and the geomagnetic aa index reduces considerably to essentially zero.

These results are consistent with the suggestion that the sense of the drift of cosmic rays in the heliosphere is a component of the cosmic ray propagation as hypothesized by Jokipii et al. (1977), Jokipii and Kopriva (1979), and Jokipii (1981). Briefly they suggest that the drift component of cosmic rays (i.e., positively charged atomic nuclei) may have preferential entry into the heliosphere via the helio equatorial plane if the northern solar polar magnetic field is negative (i.e., direction of the field into the northern solar pole as was the case from 1959 to 1968) and that this drift component may have preferential entry into the heliosphere via the solar poles if the northern solar polar magnetic field is positive (i.e., directed out of the northern solar pole as was the case from 1972 to 1980). Thus if the cosmic ray flux has a significant drift component via the helio-equatorial plane an inverse correlation with the aa index would be expected, and if the cosmic rays have preferential entry via the solar poles, this correlation should be considerably smaller. This would be consistent with our correlation coefficients between the cosmic ray intensity and the aa index of -0.86 for June 1959-December 1968 and essentially 0 for March 1972-December 1979.

5. Acknowledgments. We would like to acknowledge helpful discussions with M. Forman, J. Feynman, C. Hatton, R. Jokipii, and M. Lee.

References

Jokipii, J.R., E.H. Levy, and W.B. Hubbard, Astrophys. J. 213, 861, 1977.

Jokipii, J.R. and D. A. Kopriva, 16th International Cosmic Ray Conference, Conference Papers 3, 7, 1979.

Jokipii, J.R., Geophys. Res. Lett., 8, 837, 1981.

Mayaud, P.N., A Hundred Year Series of Geomagnetic Data 1868-1967, IAGA Bulletin No. 33, IUGG Publications Office, Paris. 1973.

Shea, M.A., and D.F. Smart, Adv. Space Res., 1, 147, 1981.

AUTHOR INDEX

AGRAWAL, SP
392
ALANIA, MV
465,477
ALANIYA, MV
485
ALEKSEEV, NV
205
ALVAREZ, M
18,22,26
30,34,110
ANDERSON, KA
342
ARMSTRONG, TP
174,192
ARVELA, H
364
ASLAMAZASHVILI, RG
465,477
BABAYAN, VK
372
BADRUDDIN,
461
BAGDASARIAN, MB
372
BALOGH, A
178
BANDLE, J
174
BEECK, J
334
BEHANNON, KW
445
BELOV, AV
118
BIEBER, JW
335,433
BISWAS, S
221
BLOKH, YAL
118
BOBROVSKAYA, VV
205
BOCHORISHVILI, TB
477
BRAVO, S
257
BRENEMAN, HH
217,213
BRIGGS, PR
192
BURGER, RA
421
BURLAGA, LF

BURLAGA, LF
346,445
396
CANE, HV
94,66,14
CANFIELD, RC
86
CHANG, CR
86
CHARAKHCHYAN, TN
481
CHEBAKOVA, EA
356
CHIRKOV, NP
489
CHRISTON, SP
445,404
200
CHUPP, EL
126,146
CHURONOVA, LF
473
CLIVER, EW
94,14
COOPER, JF
126,146
CUMMINGS, AC
445,200
DAIBOG, EI
62
DEBRUNNER, H
351,317
126
DECKER, RB
10,166
DENEHY, BV
142
DENNIS, BR
38
DIETRICH, WF
277
DJAPIASHVILI, TV
477
DORMAN, LI
413,485
465
DOUGHERTY, WM
342
DROGE, W
2
DURAND, H
384
DURGAPRASAD, N
221

AUTHOR INDEX

DVORYANCHIKOV, YAV
289
EARL, JA
380,376
ECKES, S
192
EFIMOV, YUE
154
ELLISON, DC
6
ERDOS, G
178
EROSHENKO, EA
118
EVENSON, P
130,309
497,74,201
EVENSON, PA
335
FAN, CY
241
FEDOROV, YUI
413
FENTON, AG
339
FENTON, KB
339
FILIPPOV, AT
368
FISK, LA
241
FLUCKIGER, E
317,126
FORMAN, MA
400
FORREST, DJ
126,146
249
FRYE, GM
142
GALINDO TREJO, J
78
GALLEGOS, A
18,22,26
30,34
GALL, R
384
GALVIN, AB
241
GARCIA-MUNOZ, M
469,409
497
GARCIAMUNOZ, M
409
GLOECKLER, G
182,321
241
GOLD, RE
186,405
GOLDSTEIN, ML
396
GONCHAR, GA
457
GREEN, G
355
GRIGOROV, NL
205
GUSHCHINA, RT
485
HAMILTON, DC
321
HOVESTADT, D
281,182
241,245
285,74
HUDSON, HS
50,58
HUMBLE, JE
339,437
INOUE, A
138
IPAVICH, FM
182,241
ISHKOV, VN
118
ISKRA, K
465
ITO, K
297
IUCCI, N
134
IWERS, B
102
JAIN, AK
392
JOKIPII, JR
449,388
453,376
JONES, FC
400
KAHLER, SW
94,269,14
KANBACH, G
126
KATZ, MI
413
KEPPLER, E
158

KESSEL, RL
174
KIRSCH, E
158
KLECKER, B
182,241
285
KLEIN, KL
46
KLIMENKO, VV
313
KOCHAROV, GE
154,150
KOCHAROV, LG
293,289
KOGA, R
142
KOHNO, T
297,301
KOLOMEETS, EV
457,356
KONDRATYEVA, MMA
205
KOTA, J
449,453
KOVALTSOV, GA
106
KOZLOV, SA
122
KOZLOVSKY, B
249,253
KRAINEV, MMB
481
KRIMIGIS, SM
186,170
KROEGER, R
130
KRYAKUNOVA, ON
473
KUNOW, H
305
KURT, VG
62
KUZHEVSKY, BM
229
LANZEROTTI, LJ
186
LAVILLE, A
18,34
LIGGETT, M
269
LIN, RP
269,273
LOCKWOOD, JA
LOCKWOOD, JA
351,469
317,388
LOGACHEV, YI
62
LUHN, A
241,245
285
LUMME, M
364
LYAKHOVA, AKH
457
MACE, O
142
MACKINNON, AL
42
MACLENNAN, CG
186
MANDZHAVIDZE, NZ
150
MARSDEN, RG
322
MARTINIC, NJ
138
MASON, GM
281,321
MCDONALD, FB
346,209,98
396
MCGUIRE, RE
94,66,14
317,225
190
MEYER, JP
233
MEYER, P
130,497,74
201
MIKRYUKOVA, NA
313
MISHRA, BL
392
MOBIUS, E
285
MORAAL, H
421,421
MOROZOVA, EI
313
MOSES, D
74,201
MOUSSAS, X
162
MULLAN, DJ
237

MURPHY, RJ
249,253
NECHAEV, OYU
229
NEUBAUER, FM
162
NEUSTOCK, HH
102
NEWKIRK, G
469
NG, CK
326,330
NIEMINEN, M
364
NIKOLAEV, VS
196
NISKOVSKIKH, AS
368
NITTA, N
301,54
NOSOV, SF
413
NUBER, R
174
NYMMIK, RA
205
OHI, Y
297
OHKI, KI
50
ORISHCHENKO, AV
293
OTAOLA, JA
493
OUENBY, JJ
162
OWENS, A
142
PAKHOMOV, NI
122
PALENQUE, E
138
PARISI, M
134
PELTONEN, J
364
PEREZ-ENRIQUEZ, R
257,493
PEREZ-PERAZA, J
18,22,26
30,34,110
PETUKHOV, DI
196
PISARENKO, NF
PISARENKO, NF
313
POMERANTZ, MA
335,433
POTGIETER, MS
429,425
PYLE, KR
409,497
RAMATY, R
6,249,253
REAMES, DV
281,269
225,265
273,273
REGUERIN, A
138
REPPIN, C
126
RICHTER, K
158
RIEGER, E
146
RIVERO, F
110
ROELOF, EC
417
RYAN, JM
1,82
SAITO, T
441
SAKURAI, K
297
SANDERSON, TR
322
SARRIS, ET
170
SAVENKO, IA
229
SCHELLERT, G
305
SCHLICKEISER, R
2
SCHLUTER, W
355
SCHOLER, M
182,241
SCHWENN, R
162
SECHINOV, VP
205
SEMUKHIN, PE
106
SEVAST'YANOV, VN
356

SHAFER, YUG 313
SHAKHOV, BA 413
SHAPOVALOVA, LA 122
SHARE, GH 126,146
SHEA, MA 437,501
SHEELEY, NR 94
SHIELDS, JC 192
SHVARTSMAN, YAE 473
SIGNORINI, C 134
SIMNETT, GM 70,38,82
SIMPSON, JA 469,277 409,497
SLYUNYAEVA, NV 457
SMART, DF 501
SMITH, EJ 322
STEKOL'NIKOV, NV 457
STOKER, PH 114
STOLPOVSKY, VG 62
STONE, EC 445,217 213,404 200
STONE, RG 94,269,14 265
STORINI, M 134
STOZHKOV, YUI 481
SUDA, T 301
SWINSON, DB 437,441
TAKAHASHI, K 138
TAKENAKA, T 297
TAQUICHIRI, MA 138
THOMAS, J 142
TIMOFEEV, VE 313
TKEMALADZE, VS 477
TORSTI, JJ 364
TRAINOR, JH 209,98
TRETYAKOVA, CHA 205
TROTTET, G 42,46
TSUNETA, S 50
TURPANOV, AA 196
VAHIA, MN 221
VAINIKKA, E 364
VAKULOV, PV 205,205
VALDES-GALICIA, JF 162,493
VALTONEN, E 364
VAN HOLLEBEKE, MAI 209,98
VAUCLAIR, S 233
VENKATESAN, D 392,405
VESTRAND, WT 126,146
VILLORESI, G 134
VILMER, N 42
VLAHOS, L 10,166
VOLODICHEV, NN 229
VON ROSENVINGE, TT 281,66,14 225,190
WADA, M 138,301
WATANABE, H 54,90
WEBBER, WR

AUTHOR INDEX

WEBBER, WR
388,200
WEBB, GM
421
WENZEL, KP
322
WIBBERENZ, G
102,305
334
YADAV, RS
461
YANAGIMACHI, T
297
YANCHUKOVSKY, AL
122
YANG, GL
360
YANKE, VG
118
YOSHIMORI, M
54,90
YU, C
261
ZHANG, GL
360
ZHAN, S
261
ZHOU, R
261
ZHURAVLEV, DA
205
ZUSMANOVICH, AG
473

BIBLIOGRAPHIC DATA SHEET

1. Report No.
NASA CP-2376 Volume 4

2. Government Accession No.

3. Recipient's Catalog No.

4. Title and Subtitle
19th International Cosmic Ray Conference
Conference Papers

5. Report Date
August 1985

6. Performing Organization Code
665

7. Author(s)
Frank C. Jones, compiler

8. Performing Organization Report No.

9. Performing Organization Name and Address
Laboratory for High Energy Astrophysics
Goddard Space Flight Center
Greenbelt, MD 20771

10. Work Unit No.

11. Contract or Grant No.

12. Sponsoring Agency Name and Address
National Aeronautics and Space Administration
Washington, D. C. 20546

13. Type of Report and Period Covered
Conference Publication

14. Sponsoring Agency Code

15. Supplementary Notes

16. Abstract

These volumes contain papers submitted for presentation at the 19th International Cosmic Ray Conference, held on the campus of the University of California, San Diego in La Jolla, CA., August 11-23, 1985. The conference is held every other year. The present volume contains papers with Paper Codes SH 1.1 through SH 4.2 and deals with x-rays, electrons, protrons, and neutrons from solar flares, the propagation of solar particles in the solar corona and interplanetary space, and episodic and lo.

17. Key Words (Selected by Author(s))
solar flares, solar protons, solar neutrons, propagation, solar modulation

18. Distribution Statement
Unclassified - Unlimited
Subject Category - 93

19. Security Classif. (of this report)
Unclassified

20. Security Classif. (of this page)
Unclassified

21. No. of Pages

22. Price*

*For sale by the National Technical Information Service, Springfield, Virginia 22161

STAR 2 2 SEP 12 1985

NASA-CP-2376- Vol. 5

19TH INTERNATIONAL COSMIC RAY CONFERENCE

LA JOLLA, USA AUGUST 11-23, 1985

CONFERENCE PROGRAM SESSIONS VOL. 5

(NASA-CP-2376-Vol-5) NINTEENTH
INTERNATIONAL COSMIC RAY CONFERENCE.
SH SESSIONS, VOLUME 5 (NASA) 589 p HC as
boxed set only $200/MF A01 per volum
CSCL 03B G3/93

N85-34991
THRU
N85-35140
Unclas
20932

19TH INTERNATIONAL COSMIC RAY CONFERENCE

LA JOLLA, USA AUGUST 11-23, 1985

CONFERENCE PAPERS

SH

SESSIONS
VOL. 5

PUBLICATION COMMITTEE

F.C. Jones, Chm.
J. Adams
G.M. Mason

NASA Conference Publication 2376

Published by
Scientific and Technical Information Branch
National Aeronautics and Space Administration
Washington, D.C. 20546

August 1985

For sale by the National Technical Information Service, Springfield, VA 22151

PREFACE

The 19th International Cosmic Ray Conference, under the auspices of the Cosmic Ray Commission of the International Union of Pure and Applied Physics, is being held on the campus of the University of California, San Diego, on 11 through 23 August 1985. In keeping with the tradition begun in 1971 by the Australian organizers of the 12th ICRC, the Proceedings of this conference are appearing in two sets of volumes. The first set, consisting of volumes 1 through 8, is being distributed to all participants at the beginning of the conference. This set contains the contributed papers. The second set, distributed after the conference, contains invited, rapporteur, and highlight papers. The papers are reproduced here exactly as they were received from the authors, without refereeing.

For the 19th ICRC, the scientific program was organized according to three major divisions-- OG (cosmic rays and gamma rays of Galactic Origin), SH (Solar and Heliosphere), and HE (High Energy). Technical papers are included in each of the three divisions.

This conference depended on funds from several agencies of the United States government, including major financial support from the National Aeronautics and Space Administration and support from the National Science Foundation, the Department of Energy, and the Air Force Geophysics Laboratory. Important financial support also came from the Center for Astrophysics and Space Sciences of the University of California, San Diego, from the California Space Institute of the University of California, from the Department of Physics and Astronomy of the University of Maryland, College park, from the International Union for Pure and Applied Physics, and from several corporate sponsors who will be acknowledged by name in the post-conference volumes.

We appreciate the confidence placed in the conference organisers by the Cosmic Ray Commission, and acknowledge with thanks the role of the Commission members in setting up the rules for the conference and in advising the organisers during its planning.

We are grateful to all of the members of the various organising committees listed at the front of this volume. The three Program Committees went to great effort to organize a coherent scientific program and to schedule four parallel sessions with a minimum of conflicts. The Local Organising Committee has worked long and hard to ensure efficient and hospitable accommodations for all the participants, both in the scientific sessions and outside them. The Publications Committee not only took great pains to assemble these volumes but also maintained an orderly data base of papers and authors which was extremely helpful to the program committees. The General Organising Committee made important contributions of ideas and efforts to make the conference possible; this committee included international representation from all of North America, thus the departure from the traditional name of National Organising Committee. And the entire effort was coordinated by the dedicated members of the Steering Committee.

Martin H. Israel, Chairman
General Organizing Committee

August, 1985

LETTER FROM THE EDITORS

This conference marks a departure from previous conferences in this series in that the publication of the Conference Papers was carried out an entire continent away from the activities of Local Organising Committee. This posed some problems but, to the considerable surprise of the Publications Committee members, the one that was expected to be the most trouble turned out not to be significant. The overwhelming majority of those submitting papers and abstracts sent them to the correct address, not to La Jolla as was feared. We wish to thank our many authors for their alertness and commend them for handling a complicated situation so well.

There are eight volumes to be distributed to the conference participants in addition to the Conference Program and Author Index: three volumes for OG, two for SH and three for HE. the detailed makeup of these volumes is described in the prefaces written by the Scientific Program chairmen for their respective volumes. Out of some 1100 abstracts that were accepted by the Scientific Program Committees for inclusion in the conference some 929 papers were finally received in time for inclusion in the Conference Papers. This represents a response of approximately 84 percent, a modest improvement. Even if one excludes the 42 one page papers that should be considered as "confirming abstracts", even though there was no such formal category, the response was somewhat higher than that of recent years. We attribute this to the carrot of a later deadline than before coupled with the stick of there being no printing of post deadline contributed papers. We believe that this decision of the General Organising Committee was a wise one. Of course invited, rapporteur, and highlight talks will be printed in volumes to be distributed to the participants after the conference as usual.

The Publications Committee had much generous help in performing its duties: from Goddard Space Flight Center we had the help of B. Glasser, L. Harris, E. Schronce, N. Smith, J. Esposito and T. Smith. From the Naval Research Laboratory we were helped by T. Mazzotta, and at the University of Maryland M. L. Snidow and J. Mucha gave much needed assistance. Special thanks are due to Caryl Short, the lone staff member of the Publications Committee. She maintained the computer data base, organised the abstracts as they arrived, and kept track of the papers themselves to see that the finally arrived in the right place at the right time. Without her help the job would have been far more difficult than it was.

PUBLICATIONS COMMITTEE August, 1985

Frank C. Jones, Chm.
Jim Adams
Glen M. Mason

SH SESSIONS
VOLUME V

19th INTERNATIONAL COSMIC RAY CONFERENCE
LA JOLLA, USA
AUGUST 11–23, 1985

INTERNATIONAL UNION OF PURE AND APPLIED PHYSICS
MEMBERS OF THE COMMISSION ON COSMIC RAYS OF IUPAP

A.E. Chudakov, Chm.
F.B. McDonald
G.C. Castagnoli
P.H. Fowler
D. Hovestadt
J. Kota
T.O. Montmerle
H. Moraal
J.R. Prescot
B.V. Sreekantan
K. Suga
J. Wdowczyk

STEERING COMMITTEE

F. McDonald, Chm.
G. Burbage
M. Forman
T. Gaisser
M. Israel
F. Jones
R. Lingenfelter
R. Mewaldt
L. Peterson

GENERAL ORGANIZING COMMITTEE

M. Israel, Chm.
M. Bercovitch
P. Freier
R. Gall
R. Jokipii
L. Jones
V. Jones
S. Krimigis
J. Kurfess
J. Lockwood
P. Meyer
B. Price
R. Ramaty
F. Reines
M. Shapiro
M. Shea
J. Simpson
E. Stone
D. Venkatesan
J. Waddington
S. White

PROGRAM COMMITTEES

OG SESSIONS	SH SESSIONS	HE SESSIONS	PUBLICATIONS
R. Mewaldt, Chm.	M. Forman, Chm.	T. Gaisser, Chm.	F. Jones, Chm.
G. Cassiday	H. Hudson	K. Lande	J. Adams
C. Fichtel	G. Mason	J. Linsley	G. Mason
A. Harding	B. McKibben	E. Loh	
J. Matteson	M. Pomerantz	G. Yodh	
D. Muller			
W. Webber			

LOCAL ORGANIZING COMMITTEE

L. Peterson, Chm.
G. Burbidge
R. Lingenfelter
R. Rothschild
J. Arnold
W. Baity
A. Buffington
M. Burbidge
W. Fillius
R. Gall
R. Gould
H. Hudson
J. Linsley
K. Marti
G. Masek
J. Matteson
C. McIlwain
R. Mewaldt
O. Piccioni
M. Thiemens
W. Thompson
H. Ticho
R. White

Sponsored by
National Aeronautics and Space Administration
National Science Foundation
Department of Energy
Center for Astrophysics and Space Science, University of California, San Diego
California Space Institute, University of California
Department of Physics and Astronomy, University of Maryland, College Park

PREFACE TO THE VOLUMES 4 AND 5 (SH)

The category SH includes all papers on solar and heliospheric energetic particle phenomena. SH combines the MG (modulation of galactic) and SP (solar particles) categories used in previous conferences, with papers on particles accelerated in the solar wind. Papers about techniques and instrumentation for science in the SH category are now included in SH. Cosmogenic nuclide studies, formerly in OG (origin and galactic) are also in the new SH category. Papers on particles of strictly magnetospheric origin were not included in this conference.

The SH heading numbers are :

SH1. Particle Acceleration on the Sun and in the Heliosphere
SH2. Composition, Spectra and Anisotropy
SH3. Propagation of Solar and Interplanetary Energetic Particles
SH4. Solar-Cycle Modulation and Propagation of Galactic Particles in the Heliosphere
SH5. Transient Modulations
SH6. Geomagnetic and Atomospheric Effects and Response Functions
SH7. Cosmogenic Nuclides
SH8. Solar Neutrinos
SH9. Techniques
SH10. Others

Papers appear in this volume in a numerical sequence determined primarily by this numbering system. For example, paper number SH2.1-8 is the eighth paper in the first session formed of papers in category SH2.

We thank the SH program committee for devising this numbering system, for reading every abstract submitted and for organizing on the basis of their content coherent sessions with reasonable length for presentation. We thank them also for selecting the rapporteurs and for advice in the selection of invited and highlight speakers. The committee members are: Hugh Hudson (UCSD), Bruce McKibben (U. of Chicago), Glenn Mason (U. of Maryland), Martin Pomerantz (Bartol Res. Foundation, U. of Delaware) and alternate Walker Fillius (UCSD).

These contributed papers are reviewed in plenary session by a team of expert rapporteurs at the end of the Conference. These extremely useful reports can only be prepared during the Conference, and so their written versions will be included in a later volume. We thank the rapporteurs in advance for their willing service.

Miriam A. Forman, Chairman
Solar - Heliospheric Program Committee

This conference is the 19th in a series. Previous conferences in this series were held at:

Cracow, Poland – 1947
Como, Italy – 1949
Bagneres-de-Bigorre, France – 1953
Guanjuato, Mexico – 1955
Varenna, Italy – 1957
Moscow, USSR – 1959
Kyoto, Japan – 1961
Jaipur, India – 1963
London, UK – 1965
Calgary, Canada – 1967
Budapest, Hungary – 1969
Hobart, Australia – 1971
Denver, USA – 1973
Munchen, FRG – 1975
Plovdiv, Bulgaria – 1977
Kyoto, Japan – 1979
Paris, France – 1981
Bangalore, India – 1983

SH 4.3
GRADIENTS AND NORTH-SOUTH ANISOTROPIES

PAPER CODE PAGE

SH 4.3-7 GRADIENTS AND ANISOTROPIES OF HIGH ENERGY COSMIC RAYS IN THE OUTER HELIOSPHERE 1
F WALKER,EC ROELOF,WH IP,EJ SMITH

SH 4.3-8 ISOTROPIC INTENSITY WAVES AND FEATURES OF THEIR OCCURRENCE 5
ML DULDIG,RM JACKLYN,MA POMERANTZ

SH 4.3-9 IMF-SENSE-DEPENDENT COSMIC RAY ANISTROPY PRODUCED FROM DIFFUSIVE-CONVECTION IN HELIOSPHERE 9
K NAGASHIMA,K NUMAKATA,R TATSUOKA

SH 4.3-10 INFLUENCE OF THE NEUTRAL SHEET ON THE SWINSON'S TYPE NORTH-SOUTH ANISOTROPY OF COSMIC RAYS 13
Y MUNAKATA,S SHIBATA,K HAKAMADA

SH 4.3-12 CHARACTERISTICS OF COSMIC RAY POLE - EQUATOR ANISOTROPY DERIVED FROM SPHERICAL HARMONIC ANALYSIS OF NEUTRON MONITOR DATA 15
H TAKAHASHI,N YAHAGI,H TAKAHASHI

SH 4.3-13 FIRST ZONAL HARMONIC COMPONENT OF COSMIC RAY NEUTRON INTENSITY 19
H TAKAHASHI,N YAHAGI,T CHIBA

SH 4.3-14 COSMIC RAY INTENSITY DISTRIBUTION PERPENDICULAR TO SOLAR EQUATORIAL PLANE AT 1 AU DURING 1978-1983 23
SP PATHAK,SP AGRAWAL,PK SHRIVASTAVA
RS YADAV

VOLUME 5

SH 4.3-15 THE COROTATING VARIATION OF THE NORTH-SOUTH ANISTROPY OF COSMIC RAYS 27

S XUE,G ZHANG,S XAO

SH 4.4
SIDERIAL AND LONG TERM MODULATION

PAPER CODE PAGE

SH 4.4-2 COSMIC RAY SIDEREAL DIURNAL VARIATION OF GALACTIC ORIGIN OBSERVED BY NEUTRON MONITORS 31
Y ISHIDA, I MORISHITA, S MORI, K NAGASHIMA

SH 4.4-3 SIDEREAL ANISOTROPIES IN THE MEDIAN RIGIDITY RANGE 60-600GV IN 1978-1983 35
H UENO, Z FUJII, S MORI, S YASUE
K NAGASHIMA

SH 4.4-4 SIDEREAL VARIATIONS DEEP UNDERGROUND IN TASMANIA 39
JE HUMBLE, AG FENTON, KB FENTON

SH 4.4-5 THE EFFECT OF THE INTERPLANETARY MAGNETIC FIELD ON SIDEREAL VARIATIONS OBSERVED AT MEDIUM DEPTH UNDERGROUND DETECTORS 42
JE HUMBLE, AG FENTON

SH 4.4-6 THE SIDEREAL SEMI-DIURNAL VARIATION OBSERVED AT HIGH ZENITH ANGLES AT MAWSON, 1968-1984, AND THE POLARITY OF THE SOLAR MAIN FIELD 44
RM JACKLYN, ML DULDIG

SH 4.4-7 CORRECTED SIDEREAL ANISOTROPY FOR UNDERGROUND MUONS 48
DB SWINSON, K NAGASHIMA

SH 4.4-8 SIDEREAL ANISOTROPY OF COSMIC RAYS 52
AI KUZMIN, PA KRIVOSHAPKIN, GV SHRIPIN
GV SHAFER

SH 4.4-9 COSMIC RAY INTENSITY VARIATIONS OBSERVED AT MATSUSHIRO (220 M.W.E. IN DEPTH) 56
S YASUE, S SAGISAKA, S MORI

SH 4.4-10 LONG-TERM MODULATION OF COSMIC RAYS DURING SOLAR CYCLE 21 60
AG FENTON,KB FENTON,JE HUMBLE,AG FENTON

SH 4.4-12 ROLE OF SOLAR FLARE INDEX IN LONG TERM MODULATION OF COSMIC RAY INTENSITY 63
PK PANDEY,AK JAIN,PK SHRIVASTAVA
SP PATHAK,SP AGRAWAL

SH 4.4-14 A STUDY OF PERIODICITIES AND RECURRENCES IN SOLAR ACTIVITY AND COSMIC RAY MODULATION 67
MR ATTOLINI,S CECCHINI,M GALLI

SH 4.4-15 COSMIC RAY BIENNIAL VARIATION 71
MR ATTOLINI,S CECCHINI,GC CASTAGNOLI
M GALLI

SH 4.4-16 COSMIC RAY POWER SPECTRAL VARIATIONS: 3. SOLAR ROTATION PERIODICITIES 72
D VENKATESAN,SP AGRAWAL,LJ LANZEROTTI

SH 4.4-17 VARIATIONS OF COSMIC RAY GENERAL COMPONENT IN ANTARCTICA 75
TN CHARAKHCHYAN,AF KRASOTKIN
AI KURGUZOVA,NS SVIRZHEVSKY

SH 4.4-18 THE DIFFERENCE IN THE ENERGY SPECTRA OF GALACTIC COSMIC RAYS AT THE MINIMA OF THE 19TH AND 20TH SOLAR ACTIVITY CYCLES 79
AK SVIRZHEVSKAYA,NS SVIRZHEVSKY
YUI STOZHKOV,TN CHARAKHCHYAN

SH 4.4-19 COSMIC RAY VARIATIONS WITH THE PERIOD CLOSE TO 27 DAYS AND THEIR CONNECTION WITH SOLAR ACTIVITY LONGITUDINAL DISTRIBUTION 83
GA BAZILEVSKAYA,MI TYASTO,ES VERNOVA

SH 4.4-20 AZIMUTHAL AND MERIDIONAL ASYMETRIES OF SOLAR WIND AND QUASIPERIODIC VARIATIONS OF INTENSITY OF GALACTIC COSMIC RAYS (GCR) 87

LKH SHATASHVILI,TV DJAPIASHVILI
BG KAVLASHVILI,BD NASKIDASHVILI
OG ROGAVA,GV SHAFER

SH 4.4-21 DYNAMICS OF TWO-YEAR COSMIC RAY VARIATIONS INFERRED FROM THE DATA OF SPACECRAFT AND STRATOSPHERIC MEASUREMENTS AND FROM THE NEUTRON MONITOR DATA IN 1959-1981 90

TN CHARAKHCHYAN,EV GORCHAKOV
VP OKHLOPKOV,LS OKHLOPKOVA
MV TERNOVSKAYA

SH 4.4-22 LONG-TERM MODULATION OF GALACTIC COSMIC RAYS IN HIGH-ENERGY REGION 94

PA KRIVOSHAPKIN,AN PRIKHODKO,GV SKRIPIN
IA TRANSKY,GV SHAFER

SH 4.5
DIURNAL VARIATIONS

PAPER CODE PAGE

SH 4.5-1 THE FIRST THREE HARMONICS OF SOLAR DAILY VARIATION CAUSED BY THE DIFFUSIVE PROPAGATION OF GALACTIC COSMIC RAYS THROUGH THE HELIOSPHERE 98

K MUNAKATA,K NAGASHIMA

SH 4.5-2 FORMULATION OF COSMIC-RAY SOLAR DAILY VARIATION AND ITS SEASONAL VARIATION, PRODUCED FROM GENERALIZED STATIONARY ANISTROPY OF SOLAR ORIGIN 102

R TATSUOKA,K NAGASHIMA

SH 4.5-3 SOLAR TTRI-DIURNAL VARIATION OF COSMIC RAYS IN A WIDE RANGE OF RIGIDITY 106

S MORI,H UENO,Z FUJII,K NAGASHIMA
I MORISHITA

SH 4.5-4 UPPER CUT-OFF RIGIDITY FOR COROTATION ANISOTROPY DURING SOLAR ACTIVITY CYCLES 20 AND 21 110

HS AHLUWALIA,JF RIKER

SH 4.5-5 22-YEAR CYCLE OF THE UPPER LIMITING RIGIDITY OF DAILY WAVES 111

G ERDOS,J KOTA,E MERENYI

SH 4.5-6 SOLAR WIND VELOCITY AND DAILY VARIATION OF COSMIC RAYS 115

HS AHLUWALIA,JF RIKER

SH 4.5-7 DIURNAL ANISOTROPY DURING SOLAR ACTIVITY CYCLE TWENTY AND DIFFUSION-CONVENTION MODEL 116

HS AHLUWALIA,JF RIKER

SH 4.5-8 DIURNAL EFFECT IN COSMIC RAYS AT MIDDLE LATITUDES ACCORDING TO THE STRATOSPHERIC MEASUREMENTS 120

GA ASATRYAN,VKH BABAYAN,YUI STOZHKOV

SH 4.5-9 COMPARATIVE STUDY OF THE PHASE OF DIURNAL ANISOTROPHY ON QUIET AND DISTRUBED DAYS ON A LONG TERM BASIS UP TO RECENT PERIOD 124

S KUMAR

SH 4.5-10 STUDY OF SPECTRAL EXPONENT ON QUIET AND DISTURBED DAYS 125

S KUMAR

SH 4.5-11 DIURNAL VARIATION OF GALACTIC COSMIC RAY INTENSITY ON QUIET DAYS 126

S KUMAR,SC DATT,RS YADAV,SP AGRAWAL

SH 4.5-13 DIURNAL VARIATIONS FROM MUON DATA AT TAKEYAMA UNDERGROUND STATION 130

K TAKAHASHI,T IMAI

SH 4.5-14 LONG TERM CHANGES IN COSMIC RAY DIURNAL VARIATIONS OBSERVED BY ION CHAMBERS IN HONG KONG AND JAPAN 134

LS CHUANG,M KUSUNOSE,M WADA

SH 4.5-15 THE MODULATION FEATURES OF THE LONG-PERIOD COSMIC RAY VARIATIONS IN CONNECTION WITH THE SIGN CHANGE OF THE GENERAL MAGNETIC FIELD OF THE SUN 138

K ISKRA

SH 4.5-16 THE COSMIC RAY DIFFERENTIAL DIURNAL VARIATION DEPENDENCES ON THE ZENITH ANGLE AND THE GEOMAGNETIC DISTURBANCE 139

S KAVLAKOV,L GEORGIEV

SH 4.5-17 COSMIC RAY DENSITY GRADIENT AND ITS DEPENDENCE ON THE NORTH-SOUTH ASYMMETRY IN SOLAR ACTIVITY 143

BADRUDDIN,RS YADAV,NR YADAV

SH 4.5-18 ANOMALOUS INCREASE OF SOLAR ANISOTROPY ABOVE 150GEV IN 1981-1983 147

H UENO,Z FUJII,S MORI,I MORISHITA
K NAGASHIMA

SH 4.5-19 DIAGNOSTIC OF ELECTROMAGNETIC CONDITIONS IN SPACE USING COSMIC RAYS 151

ZS SHARVADZE,GZ SHTEMANETYAN,PV TSOMAYA

SH 4.5-20 CHANGE OF COSMIC RAY ANISTROPY WITH SOLAR ACTIVITY 155

NG KRAVTSOV,PA KRIVOSHAPKIN,AI KUZMIN
GV SKRIPIN,IA TRANSKY,GV SHAFER

SH 4.5-21 MAGNETIC FLUCTUATIONS AND COSMIC RAY DIURNAL VARIATIONS 159

JW BIEBER,MA POMERANTZ

SH 4.6
THE ANOMALOUS COMPONENT

PAPER CODE PAGE

SH 4.6-1 CHANGES IN THE ENERGY SPECTRUM OF ANOMALOUS HELIUM AND OXYGEN 1977 - 1985 163

AC CUMMINGS,EC STONE,WR WEBBER

SH 4.6-2 SOLAR CYCLE VARIATIONS OF THE ANOMALOUS COSMIC RAY COMPONENT 167

RA MEWALDT,EC STONE

SH 4.6-3 TEMPORAL VARIATIONS OF THE ANOMALOUS OXYGEN COMPONENT, 1977-1984 168

GM MASON,B KLECKER,AB GALVIN
D HOVESTADT,FM IPAVICH

SH 4.6-4 RADIAL AND LATITUDINAL GRADIENTS OF ANOMALOUS OXYGEN DURING 1977-1985 172

WR WEBBER,AC CUMMINGS,EC STONE

SH 4.6-5 OBSERVATION OF PICKUP-IONS IN THE SOLAR WIND: EVIDENCE FOR THE SOURCE OF THE ANOMALOUS COSMIC RAY COMPONENT? 176

D HOVESTADT,E MOBIUS,B KLECKER
M SCHOLER,G GLOECKLER,FM IPAVICH

SH 4.6-6 ON THE ANOMALOUS COMPONENT 180

MS POTGIETER,LA FISK,MA LEE

SH 4.6-7 POSSIBLE ORIGIN OF THE ANOMALOUS COMPONENT OF COSMIC RAYS 184

S BISWAS,N DURGAPRASAD,RK SINGH
MN VAHIA,JS YADAV

SH 4.7
INTENSITY GRADIENTS AND THE OUTER HELIOSPHERE

PAPER CODE PAGE

SH 4.7-1 THE COSMIC RAY INTERPLANETARY RADIAL GRADIENT FROM 1972 - 1985 185

WR WEBBER,JA LOCKWOOD

SH 4.7-2 TIME AND ENERGY DEPENDENCE OF THE COSMIC RAY GRADIENT IN THE OUTER HELIOSPHERE 189

W FILLIUS,I AXFORD,D WOOD

SH 4.7-3 THE LARGE SCALE DYNAMICS OF THE OUTER HELIOSPHERE AND THE LONG-TERM MODULATION OF GALACTIC COSMIC RAYS 193

FB MCDONALD,TT VON ROSENVINGE,N LAL
P SCHUSTER,JH TRAINOR,MAI VAN HOLLEBEKE

SH 4.7-4 SOLAR MODULATION AND INTERPLANETARY GRADIENTS OF THE GALACTIC ELECTRON FLUX: 1977-1984 197

SP CHRISTON,AC CUMMINGS,EC STONE
WR WEBBER

SH 4.7-5 GALACTIC COSMIC RAY RADIAL GRADIENTS AND THE ANOMALOUS HE COMPONENT NEAR MAXIMUM SOLAR MODULATION AND TO RADII BEYOND 34 AU FROM THE SUN 198

RB MCKIBBEN,KR PYLE,JA SIMPSON

SH 4.7-6 VOYAGER 1 AND 2 MEASUREMENTS OF RADIAL AND LATITUDINAL COSMIC RAY GRADIENTS IN 1981-84 202

D VENKATESAN,RB DECKER,SM KRIMIGIS

SH 4.7-7 THE RECOVERY OF THE COSMIC RAY FLUX FROM MAXIMUM SOLAR MODULATION AT IMP-8 (1AU) AND AT PIONEER 10 (R > 30 AU) 206

RB MCKIBBEN,KR PYLE,JA SIMPSON

SH 4.7-9 THE LARGE-SCALE MODULATION OF COSMIC RAYS IN MID-1982: ITS DEPENDENCE ON HELIOSPHERIC LONGITUDE AND RADIUS. 210

KR PYLE,JA SIMPSON

SH 4.7-10 NONSTATIONARY MODULATION OF GALACTIC COSMIC RAYS IN A NONLINEAR MODEL 214

VKH BABAYAN,MB BAGDASARIAN,LI DORMAN

SH 4.7-11 DIMENSIONS OF THE SOLAR WIND CAVITY AND OF THE REGION OF INTERPLANETARY COSMIC RAY MODULATION 218

IV DORMAN

SH 5.1
TRANSIENT MODULATION (FORBUSH DECREASES)

PAPER CODE		PAGE
SH 5.1-2	DRIFT AND FORBUSH DECREASES ✓ H MORAAL,MS MULDER	222
SH 5.1-3	ANOMALOUS SHORT-TERM INCREASES IN THE GALACTIC COSMIC RAY INTENSITY: ARE THEY RELATED TO INTERPLANETARY MAGNETIC CLOUD-LIKE STRUCTURES? ✓ N IUCCI,M PARISI,C SIGNORINI,M STORINI G VILLORESI	226
SH 5.1-4	THE FLARE ORIGIN OF THE FORBUSH DECREASES NOT ASSOCIATED WITH SOLAR FLARES ON THE VISBLE HEMISPHERE OF THE SUN ✓ N IUCCI,M PARISI,C SIGNORINI,M STORINI G VILLORESI	230
SH 5.1-5	LONGITUDINAL DEPENDENCE OF THE INTERPLANETARY PERTURBATION PRODUCED BY ENERGETIC TYPE IV SOLAR FLARES AND OF THE ASSOCIATED COSMIC RAY MODULATION ✓ N IUCCI,M PARISI,M STORINI,G VILLORESI S PINTER	234
SH 5.1-6	RIGIDITY SPECTRUM OF FORBUSH DECREASE ✓ S SAKAIBARA,K MUNAKATA,K NAGASHIMA	238
SH 5.1-7	SPECTRAL ANALYSIS OF THE FORBUSH DECREASE OF JULY 13, 1982 ✓ E VAINIKKA,JJ TORSTI,E VALTONEN,M LUMME M NIEMINEN,J PELTONEN,H ARVELA	242
SH 5.1-8	TRANSIENT COSMIC RAY INCREASE ASSOCIATED WITH GEOMAGNETIC STORM ✓ M KODAMA,S KUDO,M WADA	246

VOLUME 5

SH 5.1-9 GALACTIC COSMIC RAY CURRENTS AND MAGNETIC FIELD IRREGULARITY DEGREE IN HIGH-SPEED SOLAR WIND STREAMS 250

AI KUZMIN, IS SAMSONOV, ZN SAMSONOVA

SH 5.1-11 STUDY OF DOMINATING PARAMETERS OF HIGH SPEED SOLAR PLASMA STREAMS IN RELATION TO COSMIC RAY AND GEOMAGNETIC STORMS 254

BL MISHRA, SP AGRAWAL

SH 5.1-12 INFLUENCE OF MAGNETIC CLOUDS ON COSMIC RAY INTENSITY VARIATIONS 258

RS BADRUDDIN, RS YADAV, NR YADAV
SP AGRAWAL

SH 5.1-13 THE SOLAR WIND EFFECT ON COSMIC RAYS AND THE SOLAR ACTIVITY 262

K FUJIMOTO, H KOJIMA, K MURAKAMI

SH 5.1-14 A RELATION BETWEEN THE SHORT TIME VARIATIONS OF COSMIC RAYS AND GEOMAGNETIC FIELD CHANGE 266

T SAKAI, M KATO

SH 5.1-15 ANOMALOUS LOW LEVEL OF COSMIC RAY INTENSITY DECREASES OBSERVED DURING 1980 270

AK JAIN, PK PANDEY, SP AGRAWAL

SH 5.1-16 OBSERVATIONS OF COSMIC-RAY MODULATIONS IN THE FALL 1984 274

JJ TORSTI, M NIEMINEN, E VALTONEN
H ARVELA, M LUMME, J PELTONEN, E VAINIKKA

SH 5.1-17 FREQUENCY SPECTRA OF SHORT-PERIOD VARIATIONS OF COSMIC RAY 278

VP ANTONOVA, AG ZUSMANOVICH

VOLUME 5

SH 5.1-18 STUDY OF COSMIC RAY SCINTILLATIONS FROM 5-MINUTE DATA OF THE SCINTILLATOR TELESCOPE "IZMIRAN" AND WORLD-WIDE NETWORK STATIONS 281

OV GULINSKY, LI DORMAN, IYA LIBIN
RE PRILUTSKY, KF YUDAKHIN

SH 5.1-20 THE THEORETICAL AND EXPERIMENTAL INVESTIGATION OF COSMIC RAY FORBUSH-EFFECTS 285

MV ALANIA, TS BAKRADZE, TV BOCHORISHVILI
DP BOCHIKASHVILI, MA DESPOTASHVILI
NA NACHKEBIA

SH 5.1-21 PECULIARITIES OF GALACTIC COSMIC RAY (GCR) ANISOTROPY VARIATION IN CONNECTION WITH THE RECURRENT AND SPORADIC FORBUSH EFFECTS 289

BD NASKIDASHVILI, NA NACHKEBIA
GL TSERETELI, LKH SHATASHVILI

SH 5.1-22 COSMIC RAY MODULATION BY HIGH-SPEED SOLAR WIND FLUXES 293

LI DORMAN, NS KAMINER, AE KUZ'MICHEVA
NV MYMRINA

SH 5.1-23 SOLAR ACTIVITY BEYOND THE DISK AND VARIATIONS OF THE COSMIC RAY GRADIENT 296

AV BELOV, LI DORMAN, EA EROSHENKO
VN ISHKOV, VA OLENEVA

SH 6.1
GEOMAGNETIC AND ATMOSPHERIC EFFECTS AND RESPONSE FUNCTIONS

PAPER CODE		PAGE
SH 6.1-1	COUPLING FUNCTIONS FOR LEAD AND LEAD-FREE NEUTRON MONITORS FROM THE LATITUDINAL MEASUREMENTS PERFORMED IN 1982 IN THE RESEARCH STATION "ACADEMICIAN KURCHATOV" TM ALEXANYAN,LI DORMAN,VG YANKE VK KOROTKOV	300
SH 6.1-2	ON THE SOLAR CYCLE VARIATION IN THE BAROMETER COEFFICIENTS OF HIGH LATITUDE NEUTRON MONITORS M KUSUNOSE,N OGITA,S YOSHIDA	304
SH 6.1-3	ATMOSPHERIC EFFECTS ON THE UNDERGROUND MUON INTENSITY AG FENTON,KB FENTON,JE HUMBLE,GB HYLAND	308
SH 6.1-5	ALTITUDE VARIATIONS OF COSMIC-RAY SOFT AND HARD COMPONENTS OBSERVED BY AIRBORNE DETECTORS K TAKAHASHI,A INOUE,M WADA,K NISHI K MURAKAMI	309
SH 6.1-6	ADDITIONAL FLUX OF PARTICLES AND ALBEDO-ELECTRONS IN UPPER ATMOSPHERE FB AITBAEV,BM DYUISEMBAEV,EV KOLOMEETS	312
SH 6.1-7	OBSERVATION OF ENERGY SPECTRUM OF ELECTRON ALBEDO IN LOW LATITUDE REGION AT HYDERABAD, INDIA SD VERMA,SP BHATNAGAR	316
SH 6.1-8	PROTON ALBEDO SPECTRUM OBSERVED IN LOW LATITUDE REGION AT HYDERABAD, INDIA SD VERMA,SK KOTHARI	320

SH 6.1-10 THE INFLUENS OF QUIET ASYMMETRIC MAGNETOSPHERE ON THE CUTOFF RIGIDITIES OF THE MAIN CONE 324

✓ MI TYASTO,OA DANILOVA

SH 6.1-11 RE-EVALUATION OF COSMIC RAY CUTOFF TERMINOLOGY 328

✓ DJ COOKE,JE HUMBLE,MA SHEA,DF SMART
N LUND,IL RASMUSSEN,B BYRNAK,P GORET
N PETROU,DJ COOKE

SH 6.1-12 THE USE OF THE MCILWAIN L-PARAMETER TO ESTIMATE COSMIC RAY VERTICAL CUTOFF RIGIDITIES FOR DIFFERENT EPOCHS OF THE GEOMAGNETIC FIELD 332

✓ MA SHEA,DF SMART,LC GENTILE

SH 6.1-13 ESTIMATING THE CHANGE IN ASYMPTOTIC DIRECTION DUE TO SECULAR CHANGES IN THE GEOMAGNETIC FIELD 336

✓ EO FLUCKIGER,MA SHEA,DF SMART
AA BATHURST

SH 6.1-14 EMPIRICAL MODEL FOR THE EARTH'S COSMIC RAY SHADOW AT 400 KM: PROHIBITED COSMIC RAY ACCESS 340

✓ JE HUMBLE,DF SMART,MA SHEA

SH 6.1-15 PENETRATION OF SOLAR PROTONS INTO THE EARTH'S MAGNETOSPHERE ON NOVEMBER 22, 1977 344

✓ EV GORCHAKOV,KG AFANASYEV,VG AFANASYEV
PP IGNATYEV,VA IOZENAS,MV TERNOVSKAYA
GG ZENCHEV

SH 6.1-16 DYNAMICS OF THE PENETRATION BOUNDARIES OF SOLAR PROTONS DURING A STRONG MAGNETIC STORM 348

✓ GA GLUKHOV,YUP KRATENKO,YUV MINEEV

SH 6.1-18 SHORT PERTURBATIONS OF COSMIC RAY INTENSITY AND ELECTRIC FIELD IN ATMOSPHERE 352

VV ALEXEYENKO,AE CHUDAKOV,VG SBORSHIKOV
VA TIZENGAUZEN

SH 6.1-19 LONG-PERIOD COSMIC RAY VARIATIONS AND THEIR ALTITUDE DEPENDENCE 356

AV BELOV,RT GUSHCHINA,LI DORMAN
IV SIROTINA

SH 6.1-21 DIURNAL VARIATIONS OF COSMIC RAY GEOMAGNETIC CUT-OFF THRESHOLD RIGIDITIES 359

ZS SHARVADZE,GZ SHTEMANETYAN,PV TSOMAYA
OA DANILOVA,MI TYASTO

SH 6.1-22 THE INFLUENCE OF THE EARTH'S MAGNETOSPHERE ON THE HIGH-ENERGY SOLAR PROTONS 363

GA BAZILEVSKAYA,VS MAKHMUTOV
TN CHARAKHCHYAN

SH 7.1
COSMOGENIC NUCLIDES

PAPER CODE		PAGE
SH 7.1-1	COSMIC RAY **10BE BIENNIAL DATA AND THEIR RELATIONSHIP TO AURORAE AND SUNSPOTS MR ATTOLINI,S CECCHINI,M GALLI	367
SH 7.1-2	SOLAR MODULATION OF COSMIC RAY INTENSITY AND SOLAR FLARE EVENTS INFERRED FROM **14C CONTENTS IN DATED TREE RINGS CY FAN,TM CHEN,SX YUN,KM DAI	371
SH 7.1-3	COSMIC RAY SECULAR VARIATIONS IN TERRESTRIAL RECORDS AND AURORAE MR ATTOLINI,M GALLI,T NANNI GC CASTAGNOLI,G BONINO	375
SH 7.1-4	WHEN DID THE AVERAGE COSMIC RAY FLUX INCREASE? K NISHIIZUMI,SVS MURTY,K MARTI JR ARNOLD	379
SH 7.1-6	COSMOGENIC-NUCLIDE PRODUCTION BY PRIMARY COSMIC-RAY PROTONS RC REEDY	382
SH 7.1-7	COSMIC-RAY EXPOSURE RECORDS AND ORIGINS OF METEORITES RC REEDY	386
SH 7.1-8	ACCELERATOR EXPERIMENTS ON THE CONTRIBUTION OF SECONDARY PARTICLES TO THE PRODUCTION OF COSMOGENIC NUCLIDES IN METEORITES P DRAGOVITSCH,P ENGLERT	390
SH 7.1-9	DEPTH AND SIZE EFFECTS ON COSMOGENIC NUCLIDE PRODUCTION IN METEORITES P ENGLERT,P ENGLERT	394

SH 7.1-10 SPALLOGENIC ORIGIN OF NUCLEI IN METEORITES 398 ✓

B ZANDA,J AUDOUZE

SH 7.1-11 CLUSTERS AND CYCLES IN THE COSMIC RAY AGE DISTRIBUTIONS OF METEORITES 402

MF WOODARD,K MARTI

SH 7.1-12 THE 4HE/**1H RATIOS IN THE CHEMICAL COMPOSITIONS OF SOLAR FLARE PARTICLES AND THE PRIMORDIAL SOLAR NEBULA 406

K SAKURAI

SH 7.1-14 HIGH PRECISE MEASUREMENTS OF COSMOGENIC RADIOCARBON ABUNDANCE BY COMPLEX OF SCINTILLATION EQUIPMENTS 410

GE KOCHAROV,RYA METSKVARISHVILI
SL TSERETELI

SH 7.1-15 RADIOCARBON CONTENT IN THE ANNUAL TREE RINGS DURING LAST 150 YEARS AND TIME VARIATION OF COSMIC RAYS 414

GE KOCHAROV,RYA METSKVARISHVILI
SL TSERETELI,GE KOCHAROV

SH 7.1-17 COSMOGENIC MN-53 IN METEORITES 418

VA ALEXEEV,AK LAVRUKHINA

SH 8.1
SOLAR NEUTRINOS

PAPER CODE		PAGE
SH 8.1-2	RESULTS OF ULTRA-LOW-LEVEL GE**71 - COUNTING FOR APPLICATION IN THE "GALLEX"-SOLAR NEUTRINO EXPERIMENT AT THE GRAN SASSO UNDERGROUND PHYSICS LABORATORY Q HAMPEL,G HEUSSER,M HUBNER,J KIKO R SCHLOTZ	422
SH 8.1-4	CORRELATION BETWEEN SOLAR "NEUTRINO FLUX" AND OTHER SOLAR PHENOMENA L SIDDHESHWAR,A SUBRAMANIAN	426
SH 8.1-5	A POSSIBLE MECHANISM TO CAUSE THE QUASI-BIENNIAL VARIABILITY ON THE SOLAR NEUTRINO FLUX K SAKURAI,M HASEGAWA	430
SH 8.1-6	THE CONJECTURE CONCERNING TIME VARIATIONS IN THE SOLAR NEUTRINO FLUX HJ HAUBOLD,E GERTH	434
SH 8.1-7	SOLAR NEUTRINO FLUX, COSMIC RAYS AND THE 11 YEAR SOLAR CYCLE P RAYCHAUDHURI	438
SH 8.1-8	SOLAR NEUTRINOS, SOLAR FLARES, SOLAR ACTIVITY CYCLE AND THE PROTON DECAY P RAYCHAUDHURI	442
SH 8.1-9	NEUTRINO PRODUCTION FROM THE SOLAR ATMOSPHERE H INAZAWA,K KOBAYAKAWA,T KITAMURA	446
SH 8.1-10	SOLAR COSMIC RAY BURSTS AND SOLAR NEUTRINO FLUXES GA BAZILEVSKAYA,SI NIKOLSKY YUI STOZHKOV,TN CHARAKHCHYAN	450

VOLUME 5

SH 8.1-11 THREE DIMENSIONAL CALCULATION OF FLUX OF LOW ENERGY ATMOSPHERIC NEUTRINOS 454

HS LEE, SA BLUDMAN

VOLUME 5

SH 9.1
TECHNIQUES AND INSTRUMENTATION

PAPER CODE PAGE

SH 9.1-2 DETECTOR CALIBRATION OF THE INDIAN COSMIC RAY EXPERIMENT (IONS) IN SPACE-SHUTTLE SPACELAB-3 458

JS YADAV, S BISWAS, N DURGAPRASAD

SH 9.1-3 A SILICON SURFACE BARRIER TELESCOPE FOR SOLAR PARTICLES INDENTIFICATION 462

J SEQUEIROS, J MEDINA

SH 9.1-4 A BI-DIRECTIONAL CHARGED PARTICLE TELESCOPE TO OBSERVE FLUX, ENERGY SPECTRUM & ANGULAR DISTRIBUTION OF RELATIVISTIC AND NON-RELATIVISTIC PARTICLES 466

SD VERMA, SP BHATNAGAR, SK KOTHARI

SH 9.1-5 PHOTOMETRIC AND SPECTROSCOPIC GAMMA RAY OBSERVATIONS OF SOLAR TRANSIENT PHENOMENA USING LONG DURATIONS BALLOONS 470

RP LIN, WK LEVEDAHL, H PRIMBSCH
MR PELLING, KC HURLEY, RH PEHL

SH 9.1-6 MONTE CARLO CALIBRATION OF THE SMM GAMMA RAY SPECTROMETER FOR HIGH ENERGY GAMMA RAYS AND NEUTRONS 474

JF COOPER, C REPPIN, DJ FORREST, EL CHUPP
GH SHARE, RL KINZER

SH 9.1-7 COMPARISONS OF MONTHLY MEAN COSMIC RAY COUNTING RATES OBTAINED FROM WORLDWIDE NETWORK OF NEUTRON MONITORS 478

JY RYU, M WADA

SH 9.1-8 RECORDING SYSTEM FOR THE SOLAR NEUTRON MONITORING AT MT. NORIKURA 482

YS HUA, M KUSUNOSE, H SASAKI, N OHMORI
M WADA, K TAKAHASHI

SH 9.1-9 THE BURST DISTRIBUTIONS IN THE DIGITIZED DATA OF THE ION CHAMBERS AT MT. NORIKURA AND SEA LEVEL STATIONS 486

M KUSUNOSE,M WADA,S KUDO,LS CHUANG
LS CHUANG

SH 9.1-10 SENSITIVITY OF SINGLE AND MULTIPLE COSMIC RAY NEUTRONS TO THE SURROUNDING MEDIUM IN A LEAD-FREE MONITOR 490

IV DORMAN,LI DORMAN,IYA LIBIN
VK KOROTKOV

SH 9.1-11 PASTIC SCINTILLATORS IN COINCIDENCE FOR THE STUDY OF MULTI-PARTICLES PRODUCTION OF SEA LEVEL COSMIC RAYS IN DENSE MEDIUM 494

LS CHUANG,KW CHAN,MM WADA

SH 9.1-12 SONTRAC: A SOLAR NEUTRON TRACK CHAMBER DETECTOR 498

GM FRYE,TL JENKINS,A OWENS

SH 9.1-13 THE NEUTRON MODERATED DETECTOR FOR GROUNDBASED COSMIC RAY MODULATION STUDIES 502

PH STOKER,BC RAUBENHEIMER

SH 9.1-14 NEW MATSUSHIRO UNDERGROUND COSMIC RAY STATION (220 M.W.E. IN DEPTH) 506

S MORI,S YASUE,S SAGISAKA,K CHINO
S AKAHANE,T HIGUCHI,M OZAKI,M ICHINOSE

SH 9.1-15 A SUGGESTED STANDARDIZED FORMAT FOR COSMIC RAY GROUND-LEVEL EVENT DATA 510

MA SHEA,DR SMART,M WADA,A INOUE

SH 9.1-16 THE READ-OUT SYSTEM OF SPATIAL DISTRIBUTION OF THERMOLUMINESCENCE IN METEORITES 514

K NINAGAWA,I YAMAMOTO,Y TAKANO,T WADA
Y YAMASHITA,N TAKAOKA

VOLUME 5

SH 9.1-17 MEHTODS AND SOFTWARE FOR COSMIC-RAY SCINTILLATION STUDIES 518

DV GULINSKY,LI DORMAN,RE PRILUTSKY

SH 10.
OTHER TOPICS

PAPER CODE		PAGE
SH 10.1-1	THE INFLUENCES OF THE GALACTIC COSMIC RAY ON THE ATMOSPHERIC OZONE Z YE,S XUE	521
SH 10.1-2	USING THE INFORMATION OF COSMIC RAYS TO PREDICT INFLUENZA EPIDEMIC YU ZHEN-DONG	525
SH 10.1-3	STRONG EARTHQUAKES, NOVAE AND COSMIC RAY ENVIRONMENT YU ZHEN-DONG	529
SH 10.1-5	OBSERVATION OF NUCLEI WITH ENERGIES OF 8-30 MEV PER NUCLEON IN THE EARTH'S MAGNETOSPHERE AT THE ALTITUDES 350 KM VV BOBROVSKAYA,NL GRIGOROV,YUP GORDEEV DA ZHURAVLEV,RA NYMMIK,AV PODGURSKAYA LG SMOLENSKY,CHA TRETYAKOVA,IV GORDEEV VI IYAGUSHIN,AV SOLOVIEV	533
SH 10.1-6	MEASUREMENT OF LOW ENERGY COSMIC RAYS ABOARD SPACELAB-1 R BEAUJEAN,K OSCHLIES,W ENGE	536
SH 10.1-7	HEAVY COSMIC RAY MEASUREMENT ONBOARD SPACELAB-1 R BEAUJEAN,J KRAUSE,E FISCHER,W ENGE	537
SH 10.1-8	SPORADIC RADIO EMISSION CONNECTED WITH A DEFINITE MANIFESTATION OF SOLAR ACTIVTY IN THE NEAR EARTH SPACE AV DUDNIK,II ZALJUBOVSKY,VM KARTASHEV ES SHMATKO	538

SH 10.1-9 NEAR EARTH SPACE SPORADIC RADIO EMISSION BURSTS OCCURING DURING SUNRISE 542

AV DUDNIK,II ZALJUBOVSKI,VM KARTASHEV
AV LASAREV,ES SHMATKO

N85-34992

GRADIENTS AND ANISOTROPIES OF HIGH ENERGY COSMIC RAYS IN THE OUTER HELIOSPHERE

Fillius, Walker [1], E. C. Roelof [2], Edward J. Smith [3],
David Wood [1], and Wing-Huen Ip [4]

1 University of California, San Diego, La Jolla, CA 92093
2 Johns Hopkins University Applied Physics Laboratory, Laurel, MD
3 Jet Propulsion Laboratory, Pasadena, CA 91103
4 Max Planck Institut fur Aeronomie, Katlenburg-Lindau 3, Germany

Introduction Two cosmic rays which pass through the same point going in opposite directions will, in the absence of scattering and inhomogeneities in the magnetic field, trace helices about adjacent flux tubes, whose centerlines are separated by one gyrodiameter. A directional anisotropy at the point suggests a difference in the number of cosmic rays loading the two flux tubes; that is, a density gradient over the baseline of a gyrodiameter. The anisotropy produced by such a gradient can be written

$$\xi = \rho_g \hat{B} X G = P/B^2 B X G \qquad (1)$$

where ξ is the anisotropy, ρ_g the gyroradius, P the rigidity, B the field, and G the gradient. It is convenient to express ξ in %, G in %/AU, B in nT, and P in nT-AU.

Previous studies at lower energies have shown that the cosmic ray density gradients vary in space and time [1], and many authors currently are suggesting that the radial gradient associated with solar cycle modulation is supported largely by narrow barriers which encircle the sun and propagate outward with the solar wind. If so, the anisotropy is a desirable way to detect spatial gradients, because it can be associated with the local solar wind and magnetic field conditions.

With this in mind we are studying the anisotropy measurements made by the UCSD Cerenkov detectors on Pioneers 10 and 11. This is a progress report in which we show that the local anisotropy varies greatly, but that the long-term average is consistent with the global radial gradient measured between two spacecraft over a baseline of many AU.

Instrumentation Our Cerenkov detectors register cosmic rays with velocity > 3/4c, corresponding mainly to hydrogen and helium above an energy of ~500 MeV/nucleon. In this study we will consider only protons. Alpha particles are counted, in proportions exceeding their abundance, because the solid angle of the acceptance lobe is larger for multiply charged particles. However, for the same reason, the alpha particle response is less directional than the proton response, and so these particles do not have a great effect on the anisotropy measurements.

Integrating the cosmic ray proton spectra of Meyer et al [2] above our threshold, we estimate that the detector responds to protons with a mean rigidity, P, of 0.14 nT-AU at solar maximum and 0.10 at solar minimum. For a normal Parker spiral field with magnitude of 6 nT at one AU, the average gyroradius for a proton in our counter is then R*0.032

(AU) and R*0.023, respectively, and the expected north-south anisotropy, for a gradient of 2%/AU as measured over a two-spacecraft baseline, is R*0.064% and R*0.046%. Statistically we can resolve an anisotropy of 10% in 10 minutes, 1% in 18 hours, and 0.1% in 75 days, when the telemetry coverage is good. Thus it takes many days to resolve the expected effect.

As the Cerenkov detector is mounted perpendicular to the spacecraft spin axis, which points at earth, we obtain the unidirectional flux of high energy cosmic rays in a plane perpendicular to the spacecraft-earth line. When the gradient effect is dominant, a north-south anisotropy normally represents a radial gradient, and an east-west anisotropy reflects a latitude gradient.

Method The east-west and north-south components of equation (1) give usable relationships between the radial gradient and its contribution to the anisotropy.

$$\xi_{EW} = G_r{*}P{*}B_z/B^2 - [G_z{*}P{*}B_r/B^2] \quad (1a)$$
$$\xi_{NS} = -G_r{*}P{*}B_y/B^2 + [G_y{*}P{*}B_r/B^2] \quad (1b)$$

We expect the last terms to be negligible, because, as G_y is the longitudinal and G_z the latitudinal gradient, they tend to cancel themselves when averaged over a solar rotation or longer. Besides, B_r is small in the outer heliosphere, and also tends to cancel itself over a number of magnetic sector reversals.

The self-cancellation of unwanted terms becomes the basis of a powerful detection method, because, as the gradient-related anisotropy does change sign with B, we can average the data in such as way as to preserve this effect alone. Multiply equations (1a and b) by B_z and B_y.

$$B_z{*}\xi_{EW} = G_r{*}P{*}(B_z/B)^2 + \text{self-cancelling terms} \quad (2a)$$
$$-B_y{*}\xi_{NS} = G_r{*}P{*}(B_y/B)^2 + \text{self-cancelling terms} \quad (2b)$$

Adding (2a) and (2b) produces an expression relating the radial gradient, G_r, to its associated anisotropy in the scan plane.

$$B_z{*}\xi_{EW} - B_y{*}\xi_{NS} = G_r{*}P{*}(B_\perp/B)^2 + \text{self-cancelling terms} \quad (3)$$

We recognize the LHS of (3) to be $(\xi \times B)_r$. From a general expression for ξ, it can be shown [3] that $(\xi \times B)_r = (G_\perp P)_r$ + a scattering term that is proportional to the inverse of the diffusion tensor. The differences between this and equation (3) are negligible when we average over sufficiently long intervals and assume weak scattering.

Observations The scatter in the data is amply demonstrated in Figure 1, where we test for the linear relationship between ξ_{NS} and B_y/B^2 given by equation (1b). The data points are one-day accumulations, and so their accuracy is limited statistically to ± 1%. Clearly the variability of the data points exceeds this measurement limit by a large factor. We interpret this result as evidence that either the gradient is not uniform and homogeneous (it might be time dependent, or localized spatially), or the density gradient effect does not always dominate the anisotropy.

ORIGINAL PAGE IS
OF POOR QUALITY

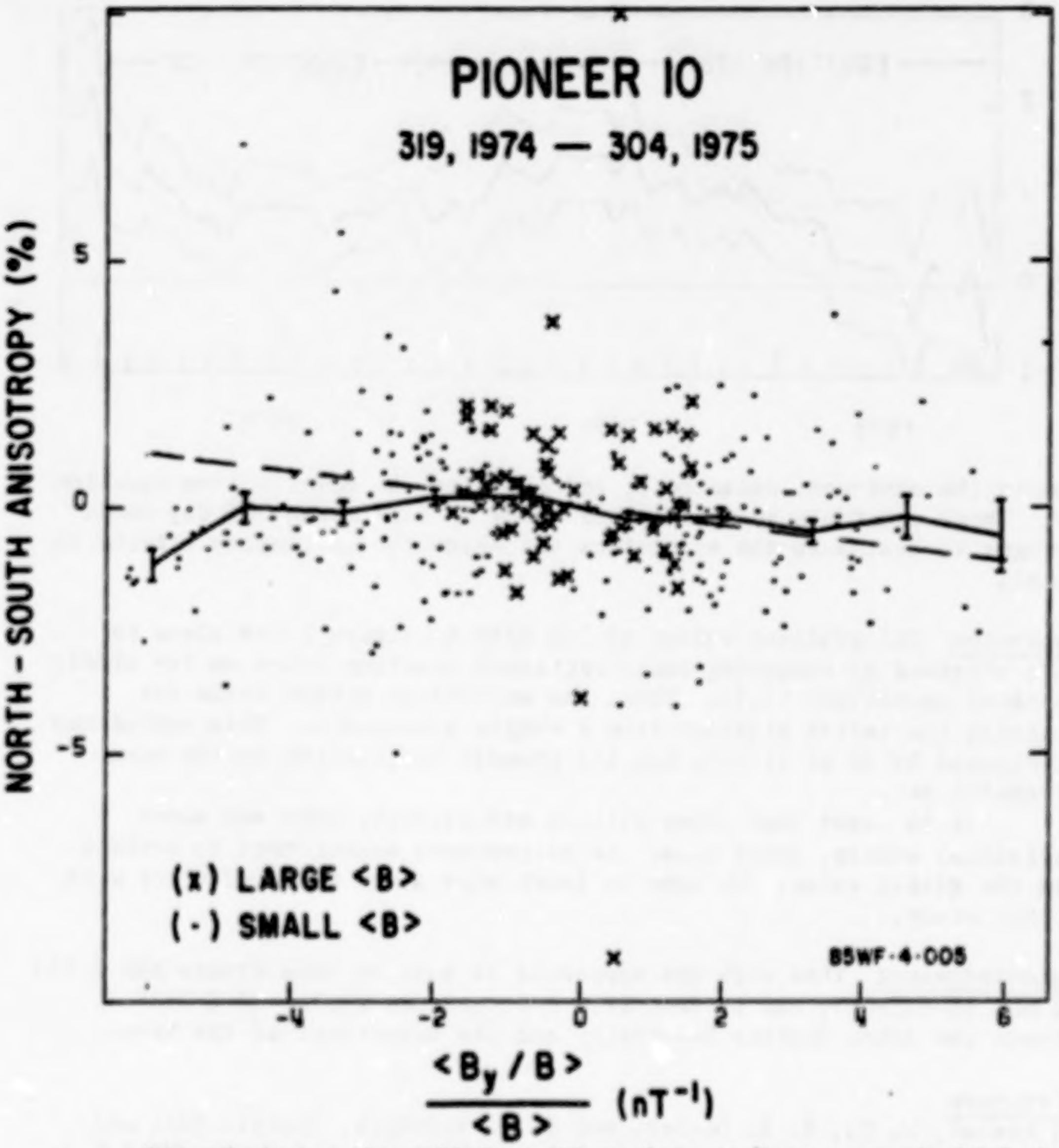

Nevertheless, the radial gradient does produce a trend which is discernible with enough data. The abscissa was divided into ten intervals, and the anisotropies averaged over each interval, as shown by the ten points with error bars. The five points at the center fall close to the expected relationship, given by the dashed line for 1.8 %/AU [4], and it is only the fringe intervals that deviate from expectations. As these intervals represent days when B is low, a possible interpretation is that the gradient is small inside rarefaction regions.

Although the gradient-related anisotropy is submerged in highly variable data, it is a robust effect. Figure 2 demonstrates how this signal persisted for 1000 days during an interval when we had adequate data coverage. Here we have solved equations (2b) and (3) for the gradient, and plotted this quantity vs time. We used equation (2b) before January, 1975 because Jovian electrons were present up to that

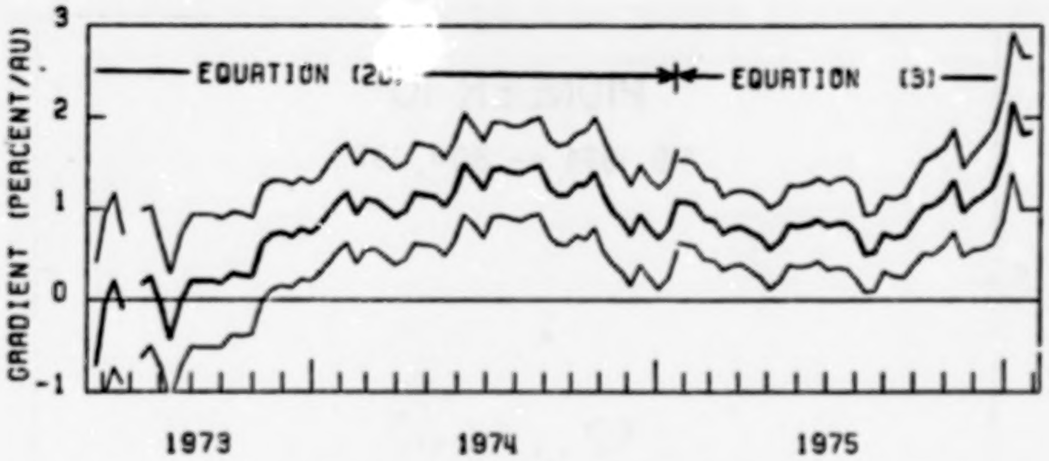

time in the east-west anisotropy, and affected the results from equation (3). These equations were evaluated every 10 days using 300 day boxcar averages to beat down the statistics and allow the extraneous effects to cancel.

Discussion The gradient values of 1-2 %/AU in Figure 2 are close to those obtained by comparing omnidirectional counting rates on two widely separated spacecraft [4,5]. Thus, the anisotropy method works for obtaining the radial gradient from a single spacecraft. This method was anticipated by Ip et al [6], but the present application is the most successful yet.

It is clear that other effects are present, over and above statistical errors, which cause the microscopic measurement to deviate from the global value. We hope to learn more about these effects with further study.

Acknowledgement This work was supported in part by NASA Grants NAS 2-153 and NGL 05-005-007, and by Task ZF10 and contract N00024-85-C-5301 between the Johns Hopkins University and the Department of the Navy.

References

[1] Roelof, E. C., R. B. Decker, and S. M. Krimigis, "Latitudinal and Field-Aligned Cosmic Ray Gradients 2-5 AU: Voyagers 1 & 2 and IMP-8," J. Geophys. Res., Vol 88, 9889, Dec. 1, 1983.
[2] Meyer, P., R. Ramaty, and W. R. Webber, "Cosmic Rays -- Astronomy With Energetic Particles," Physics Today, 23-32, October, 1974.
[3] Zwickl, R. D., and E. C. Roelof, "Interplanetary Propagation of <1 MeV Protons in Nonimpulsive Energetic Particle Events," J. Geophys. Res., Vol 86, 5449-5471, July 1, 1981.
[4] Fillius, W., B. Wake, W.-H. Ip, and I. Axford, "Cosmic Ray Gradients in the Outer Heliosphere," Proc. 18th I.C.R.C., Vol 3, p 55, 1983.
[5] Fillius, W., I. Axford, and D. Wood, "Time and Energy Dependence of the Cosmic Ray Gradient in the Outer Heliosphere," Paper SH 4.7-2, This Conference, 1985.
[6] Ip, W.-H., W. Fillius, A. Mogro-Campero, L. J. Gleeson, and W. I. Axford, "Quiet Time Interplanetary Cosmic Ray Anisotropies Observed From Pioneer 10 and 11," J. Geophys. Res., 83, 1633-1640, April 1, 1978.

N85
34993

UNCLAS

ISOTROPIC INTENSITY WAVES AND FEATURES OF THEIR OCCURRENCE.

M.L. Duldig and R.M. Jacklyn
Antarctic Division, Department of Science, Australia.
and
M.A. Pomerantz
Bartol Research Foundation, University of Delaware, U.S.A.

N85-34993

ABSTRACT

Waves of daily average cosmic ray intensity, dependent on IMF polarity, have been observed in 1982 (Jacklyn and Pomerantz, 1983) and again in 1983 and 1984. These waves at first appeared to be due to the North-South anisotropy. Further investigation has revealed that the waves comprise two components, a large isotropic and a smaller anisotropic component. The anisotropic part is attributed to the North-South anisotropy and is in phase with the larger isotropic component in the Southern hemisphere. Unlike the North-South anisotropy which is a permanent feature of cosmic ray modulation, the isotropic phenomenon appears to be episodic in character. When present it is clearly dependent on IMF polarity but does not correlate well with IMF field strength. It is conjectured that the phenomenon might indicate some difference between the intensity regimes above and below the neutral sheet.

Introduction.

Isotropic intensity waves were first observed in variations of neutron intensity which followed the cosmic ray storm of September 1978 (Pomerantz and Duggal, 1979). The spectrum of these waves was found to be similar to that for a Forbush decrease, namely p^{-1} (Duggal et al., 1981). Since that time no further examples of this phenomenon have been observed.

During the latter months of 1982, 1983 and 1984 waves of variation occurred again. On each of the three occasions the waves were similar to each other, but were different in character from the 1978 waves. They consisted of two components, one isotropic and a second smaller anisotropic component, each having a hard rigidity spectrum. The analysis of the 27-day waves observed in 1982 have been described earlier (Jacklyn and Pomerantz, 1983; Jacklyn and Duldig, 1983; Jacklyn et al., 1984a, 1984b). In this paper we reiterate the two-component structure of the 1982 intensity waves, describe the intensity waves observed in 1983 and 1984 and discuss the field dependence of the isotropic component.

The 1982 Two Component Intensity Waves.

The discovery of prominent 27-day waves of the daily average cosmic ray intensity between July and October 1982 was described at the Bangalore Conference (Jacklyn and Pomerantz, 1983). It was clear that these waves had a relatively hard spectrum and seemed to represent waves of the interplanetary North-South asymmetry. Furthermore there was a very strong linear correlation between the waves and the proven index of variation of the North-South asymmetry, namely GG Nagoya (Mori and Nagashima, 1979).

It was later realized that these waves, now referred to as A_1 waves, were far too large in relation to the GG variations to be due solely to the North-South asymmetry. By employing a constant of proportionality k_2, obtained from the CRRL tables of coupling coefficients for uni-directional anisotropies with a power index $\gamma=0.0$ and upper limiting rigidity Pu=200 GV, it was possible to remove the North-South asymmetry component through the GG variations (Jacklyn, Duldig and Pomerantz, 1984a and 1984b). The resulting residual variations, after p^{-1} isotropic and p^0 anisotropic variations had been removed, are referred to as A_2 variations and are given by

$$A_2 = A_1 - k_2 {}^{\Delta I}/_{I_0}(\mathrm{GG})$$

$$= {}^{\Delta I}/_{I_0}(\mathrm{MAW.UGN}) - k_1 {}^{\Delta I}/_{I_0}(\mathrm{McMURDO\ NM}) - k_2 {}^{\Delta I}/_{I_0}(\mathrm{GG})$$

A Chree method of superposition of epochs was employed (Figure 1) to compare the two wave components A_1 and A_2. Clearly the variation is mainly due to the A_2 component which is encompassed in the A_1 variations. Furthermore there was a strong correlation between sectorized field direction and the waves.

When underground data from the Misato multi-directional telescope system became available it appeared that, unlike the North-South asymmetry component, the A_2 variations were isotropic, being in phase worldwide. Using the appropriate coupling coefficients together with the GG data the asymmetric component was removed from 4 northern and 3 southern hemisphere asymptotic latitudes of viewing and the isotropic nature of the variations was confirmed (Figure 2).

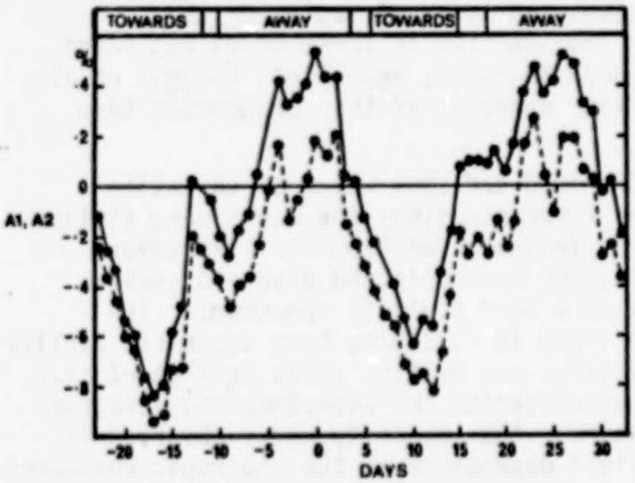

Figure 1. A 54-day Chree analysis of A_1 and A_2 using the days of maximum A_1 on 16 July and 12 August 1982 as key days. The averaged Towards and Away Periods are shown. A_1: full lines A_2: dashed lines.

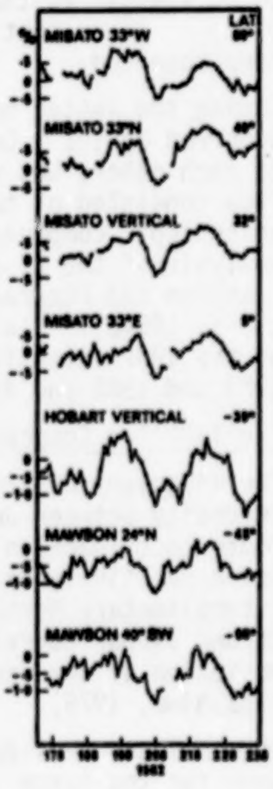

Figure 2. The A_2 intensity waves, derived from observations underground at depths of 40-60 hg cm^{-2}, July - August 1982. The asymptotic latitudes of viewing at the median rigidities of response are shown at the right of the figure.

The Intensity Waves of 1983 and 1984.

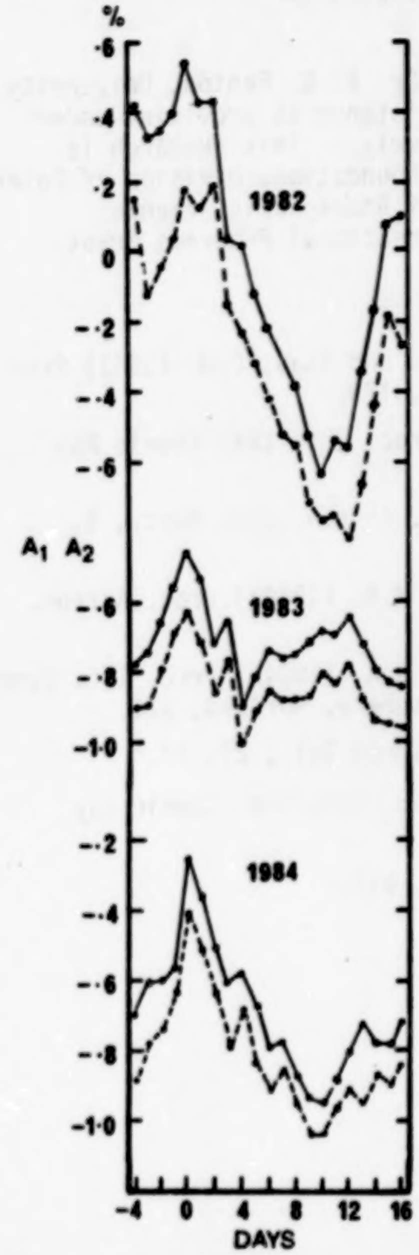

Figure 3. A 21-day Chree analysis of A_1 and A_2 in 1983 and 1984, compared with the results from 1982 (see Fig.1). Peak days in the waves of A_1 are used as key days.
A_1: full lines
A_2: dashed lines.

Figure 3 shows the 21-day Chree analysis of A_1 and A_2 waves for 1982, 1983 and 1984, on the same scale. The 1983 intensity waves were of the same intrinsic character as those of 1982 given that a 4-sector IMF structure had replaced the earlier 2-sector structure. Thus in 1983 the waves show a periodicity of 13.5 days. In 1984 a two-sector structure was again apparent. However, the A_1 and A_2 waves were significantly smaller than those of 1982.

Summary and Discussion.

Two kinds of intensity wave occuring together have been observed over the last 3 years. The first is due to the well known North-South asymmetry and can be extracted from the combined (A_1) wave. The residual waves (A_2) are much larger and are isotropic with a hard ($\gamma \gtrsim 0$) rigidity spectrum. These isotropic waves correlate well with the IMF sector direction.

Attempts to correlate the A_2 intensity waves with IMF field strength gave conflicting results. Over short time scales (single periods of waves) the correlation was good but over several periods the correlation disappeared. The delay required to optimize the correlation was different for each period. Furthermore, periods of strong IMF field strength with clearly defined sector structure early in 1983 and 1984 showed no A_2 waves in the daily average cosmic ray observations from Mawson.

A possible explanation may relate to the extent of the IMF sector structure away from the heliomagnetic equator and to an omnidirectional cosmic ray intensity that is presumed to be greater at times below the neutral sheet than above it. During periods of large amplitude of the waves in the neutral sheet, the particle radiation would tend to be confined within the wave boundary of a sector and to exhibit the intensity characteristics of either the southern or northern space of the heliosphere. When the wave amplitude of the neutral sheet is small, particle modulation should be less effective (Yasue, 1980) and confinement to a particular helio hemisphere should be less pronounced within a sector. Thus the size of the A_2 waves may give some indication of the neutral sheet amplitude.

Acknowledgements.

Professor S. Mori, Shinshu University and Dr. A. G. Fenton, University of Tasmania are thanked for their kind assistance in providing underground data for Misato and Hobart respectively. This research is supported in part by the National Science Foundation, Division of Polar Programs Grant No. DDP-8300544, Division of Atmospheric Sciences Grant No. AAM-8303758 and Division of International Programs Grant No. INT-8114863.

References.

Duggal S.P., Jacklyn, R.M., Pomerantz, M.A. and Tsao, C.H. (1981) Proc. 17th Int. Cosmic Ray Conf., Paris, 10, 179.

Jacklyn, R.M. and Pomerantz, M.A. (1983) Proc. 18th Int. Cosmic Ray Conf., Bangalore, 3, 206.

Jacklyn, R.M. and Duldig, M.L. (1983) Proc. Astron. Soc. Aust., 5, 2, 262.

Jacklyn, R.M., Duldig, M.L. and Pomerantz, M.A. (1984a) Proc. Astron. Soc. Aust., 5, 4, 581.

Jacklyn, R.M., Duldig, M.L. and Pomerantz, M.A. (1984b) Proc. Int. Symp. on Cosmic Ray Modulation in the Heliosphere, Morioka, p76.

Mori, S. and Nagashima, K. (1979) Planet. Space Sci., 27, 39.

Pomerantz, M.A. and Duggal, S.P. (1979) Proc. 16th Int. Cosmic Ray Conf., Kyoto, 3, 428.

Yasue, S. (1980) J. Geomag. Geoelectr., 32, 617.

IMF-SENSE-DEPENDENT COSMIC RAY ANISOTROPY PRODUCED FROM DIFFUSION-CONVECTION IN HELIOSPHERE

N85-34994

K. Nagashima*, K. Munakata and R. Tatsuoka

*Cosmic Ray Research Laboratory, Nagoya University
Nagoya 464, Japan
Department of Physics, Nagoya University, Nagoya 464, Japan

1. Introduction. An IMF-sense-dependent first order anisotropy of solar origin, which is produced perpendicularly to the ecliptic plane from the radial density gradient, was first pointed out by Swinson.

In addition to this anisotropy, the existence of IMF-sense-dependent higher order anisotropies has recently been suggested by Munakata and Nagashima(1), based on the simulation of cosmic ray diffusion-convection in the heliomagnetosphere.

In this paper, we discuss the characteristics of the daily variations caused by the IMF-sense-dependent 2nd order anisotropy obtained on the same condition as adopted by Munakata and Nagashima(1). A brief comparison of these variations with observations will also be made in order to demonstrate their existence.

2. Daily Variation and its Seasonal Variation. Munakata and Nagashima obtained a stationary cosmic ray anisotropy of solar origin which is expressed in the IMF-polar-coordinate system defined at any point fixed in space (cf. fig.1), as

$$\eta(\boldsymbol{r},\boldsymbol{p})=\sum_{n=1}^{\infty}\sum_{m=0}^{n}\{\eta_n^{mc}(\boldsymbol{r},\mathbf{p})\cos m\Phi'+\eta_n^{ms}(\boldsymbol{r},\mathbf{p})\sin m\Phi'\}P_n^m(\cos\Theta'), \tag{1}$$

where the angles Θ' and Φ' express the incident direction of cosmic rays with momentum $\boldsymbol{p}$ at a point $\boldsymbol{r}$, and $P_n^m(\cos\Theta')$ is the semi-normalized associate Legendre function(3).

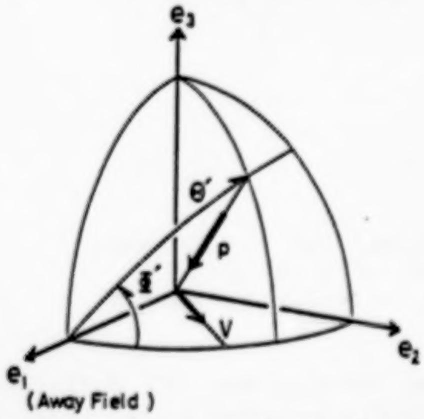

Fig. 1. The IMF-POLAR-COORDINATE SYSTEM.
p: Momentum of particle.
V: Solar wind velocity.
e_1: Unit vector in the direction of 'away' magnetic field.
e_3: Unit vector in the direction of $e_1\times V$.
$e_2=e_3\times e_1$.

The terms with coefficients η_n^{ms} in eq.(1) are called IMF-sense-dependent terms, because η_n^{ms}'s change their sign according to the sense of IMF. The IMF-sense-dependent 2nd order anisotropy is composed of two kinds of term ($\eta_2^{ms}P_2^m(\cos\Theta')\sin m\Phi'$; m=1,2) which are not symmetric for an arbitrary rotation around any axis. This anisotropy produces two kinds of daily variation at the Earth; one is a solar (SD) diurnal variation and the other is an extended sidereal ($SI_{1/2}$) semi-diurnal variation(2).

The solar diurnal variation changes the sign for a sign change of the geographic latitude($\frac{\pi}{2}-\theta$) of the viewing direction of the telescope. We call this type of variation the north-south(N-S) asymmetric type or $P_1^1(\cos\theta)$-type. For the positive and negative polarity states, fig.2(a) shows the dependence of the solar diurnal space harmonic vector(2) on the diffusion parameters(λ_0 and α_1) which are related to the scattering m.f.p (λ) as,

$$\lambda=\lambda_0(R/GV)\exp\left(\frac{r-r_e}{33\mathrm{a.u.}}\right)(1+\alpha_1\cos\theta_H). \tag{2}$$

In the equation, R is the cosmic ray rigidity, r_e=1a.u. and θ_H is the heliographic co-latitude. In fig.2, the arabic numerals express the values of α_1 and the roman numerals I and II express, respectively, the cases of λ_0=0.016a.u. and λ_0=0.032a.u.

On the other hand, the extended sidereal semi-diurnal variation is N-S symmetric or $P_2^2(\cos\theta)$-type and represents the annual variation of the solar semi-diurnal variation whose yearly average is zero. This space harmonic vector(2) is also shown in fig.2(b).

It is noteworthy that these two kinds of vector show remarkable polarity state dependences (cf. fig.2).

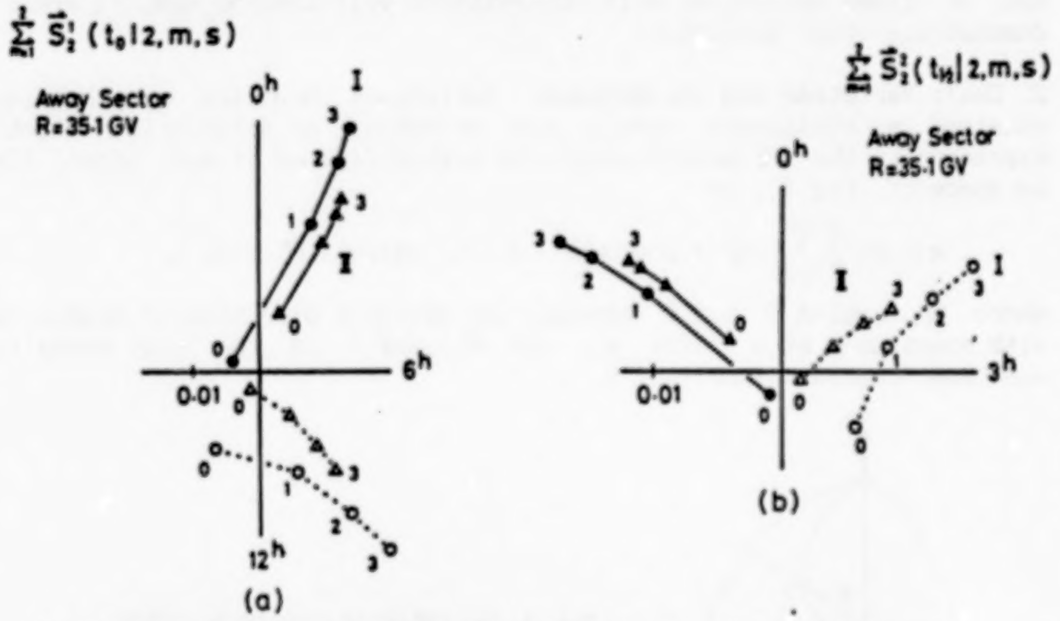

Fig. 2. PARAMETER DEPENDENCE OF THE (a) SOLAR DIURNAL AND (b) EXTENDED SIDEREAL SEMI-DIURNAL SPACE HARMONIC VECTOR IN THE AWAY SECTOR.
The solid and open symbols represent the positive and negative polarity states, respectively.

3. Comparison with Observations. Fig.3 shows the observed SD difference vectors(T-A) between the corresponding harmonic vectors in the toward(T) and away(A) sectors in the positive polarity state(1971-1979) of the multi-directional muon telescope at Nagoya. In the figure, the symbols(V,N,S,E,...) denote respectively the 17 directional component telescopes(4).

The theoretical SD vectors to be compared with the observed vectors are shown in fig.4 and are obtained by assuming that the phase of space harmonic vector is 0hr(4).

The relative configuration of the observed vectors in fig.3 bears a striking resemblance to that of $P_2^1(\cos\theta)$-type not to that of $P_1^1(\cos\theta)$-type (N-S symmetric) shown in fig.4.

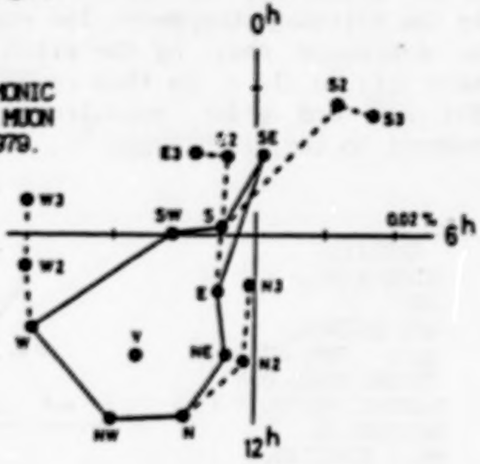

Fig. 3.
SOLAR DIURNAL "TOWARD-MINUS-AWAY" HARMONIC VECTORS (T-A) OBSERVED BY MULTI-DIRECTIONAL MUON TELESCOPE AT NAGOYA FOR THE PERIOD OF 1971-1979.

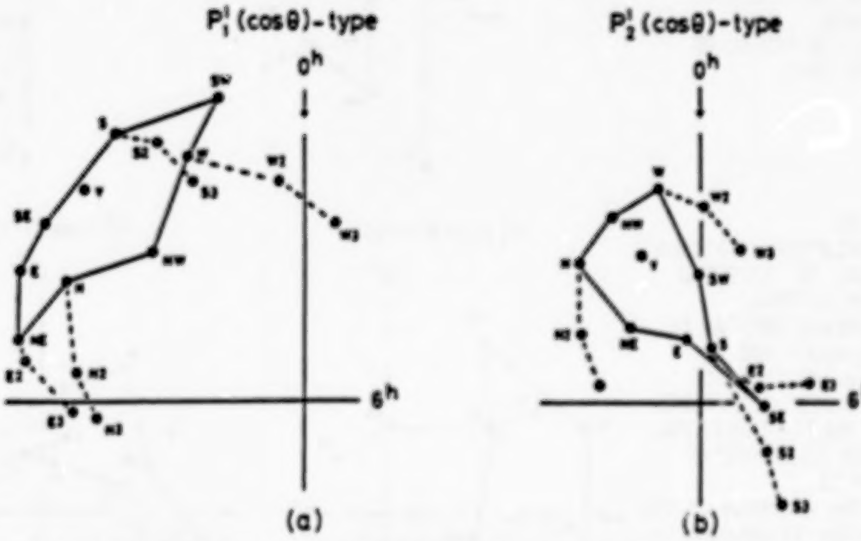

(a) (b)

Fig. 4. RELATIVE CONFIGURATION OF EXPECTED DIURNAL HARMONIC VECTORS OF $P_1^1(\cos\theta)$- AND $P_2^1(\cos\theta)$-TYPE FOR COMPONENT TELESCOPES OF MULTI-DIRECTIONAL MUON TELESCOPE AT NAGOYA.
The spectrum of the vector is assumed to be of power-type [$(R/10GV)^{0.5}$] with upper limiting rigidity (100GV).

In addition to the above solar diurnal variation, the present anisotropy produces also $SI_{1/2}$ vector. Fig.5 shows the T-A vectors in positive polarity state, and the theoretical vectors are shown in fig.6 in the same manner of fig.4. Although the observed vectors $SI_{1/2}$'s are not very significant statistically, their relative configuration is systematic and bears a resemblance to that of $P_2^2(\cos\theta)$-type in fig.6(a) not to that of $P_3^2(\cos\theta)$-type (N-S asymmetric).

In fig.5, we show also the observed $AS_{1/2}$ vectors which must be very small (~ one sixth) in comparison with $SI_{1/2}$ vectors from the theoretical point of view(2). The observed vectors $AS_{1/2}$'s are evidently small as expected.

These comparison with observations strongly suggest the existence of the 2nd order IMF-sense-dependent anisotropy. For confirmation, however, detailed analysis of the observed vectors SO and $SI_{1/2}$ is required.

4. Conclusion. It has been demonstrated that an IMF-sense-dependent 2nd order anisotropy is produced by the diffusion-convection of cosmic rays in the heliomagnetosphere. The result implies that the anisotropy cannot be expressed only by the pitch angle ($\mu=\cos\theta'$) with respect to the IMF-axis (cf. eq. (1)). In this respect, it is not suitable to discuss the 2nd and 3rd order anisotropies, based on the diffusion equation with respect to the pitch angle(5).

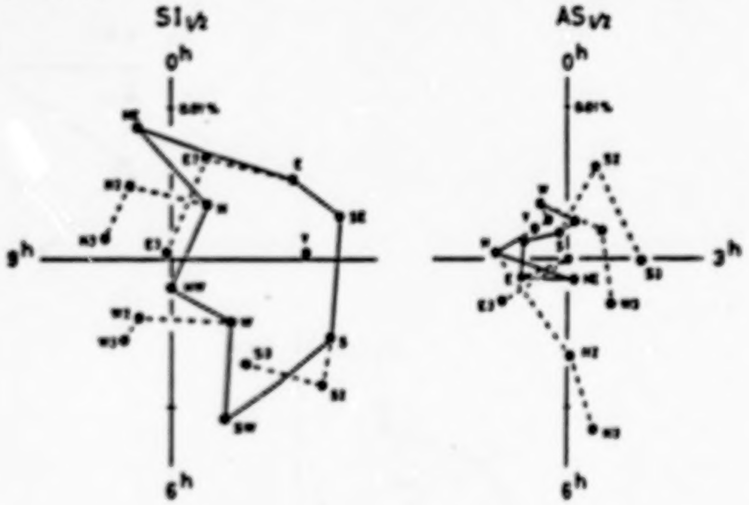

Fig. 5.
EXTENDED SIDEREAL ($SI_{1/2}$) AND ANTI-SIDEREAL ($AS_{1/2}$) SEMI-DIURNAL 'TOWARD-MINUS-AWAY' HARMONIC VECTORS(T-A) OBSERVED BY MULTI-DIRECTIONAL MUON TELESCOPE AT NAGOYA FOR THE PERIOD OF 1971-1979.

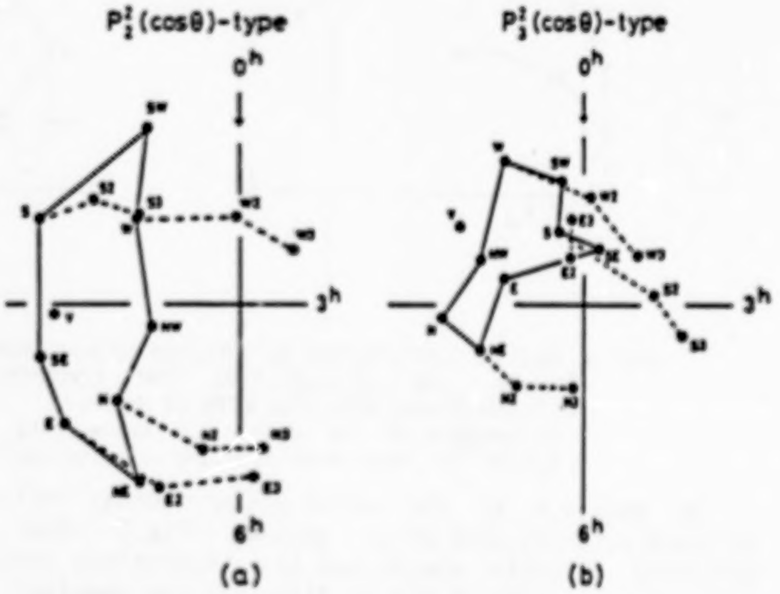

Fig. 6.
RELATIVE CONFIGURATION OF EXPECTED SEMI-DIURNAL HARMONIC VECTORS OF $P_2^2(\cos\theta)$- AND $P_3^2(\cos\theta)$-TYPE FOR COMPONENT TELESCOPES OF MULTI-DIRECTIONAL MUON TELESCOPE AT NAGOYA.
The spectrum of the vector is assumed to be of power-type [$(R/10GV)^{0.5}$] with upper limiting rigidity(100GV).

References

(1) K. Munakata and K. Nagashima: *Proc. Int. Cosmic Ray Symposium* (Morioka, Japan, 1984), p.144; This Conference SH 4.5-1.

(2) R. Tatsuoka and K. Nagashima: This Conference SH 4.5-2.

(3) S. Chapman and J. Bartels: *Geomagnetism*, Vol.2 (Oxford, 1940), p.61; K. Nagashima: *Rep. Ionos. Space Res.*, Japan, 25, 189 (1971).

(4) K. Fujimoto et al.: *Rep. of Cosmic-Ray Research Lab.*, No.9 (Nagoya Univ., 1984).

(5) J.W. Bieber and M.A. Pomerantz: *J.G.R. Lett.*, 10, 920 (1983).

Influence of the Neutral Sheet on the Swinson's Type North-South Anisotropy of Cosmic Rays

N85-34995

Y.Munakata, S.Shibata* and K.Hakamada

College of Engineering, Chubu University, Kasugai, 487,Japan
*Department of Physics, Nagoya University, Nagoya, 464,Japan

Abstract

We examine the relations between the north-south anisotropy of cosmic rays and/or nucleonic intensity variation and the latitudinal angular distance (λ) of the earth from the neutral sheet, using the data in the period from Apr. 1976 to Aug. 1977 at the solar minimum.

It is found that the nucleonic intensity variation of the cosmic rays has no correlation with sin λ in this period as shown in Figure 1; but the amplitude of the north-south anisotropy is fairly correlated with sin λ as shown in Figure 2.

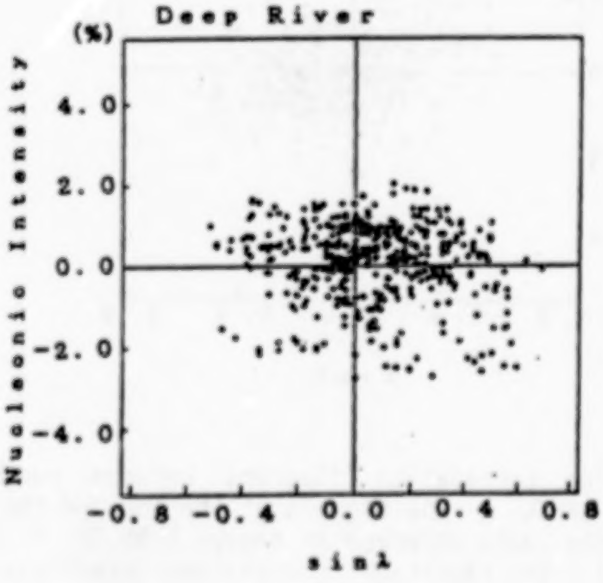

Figure 1. The correlation diagram between nucleonic intensity variation and sin λ.

ORIGINAL PAGE IS
OF POOR QUALITY

N85-34995

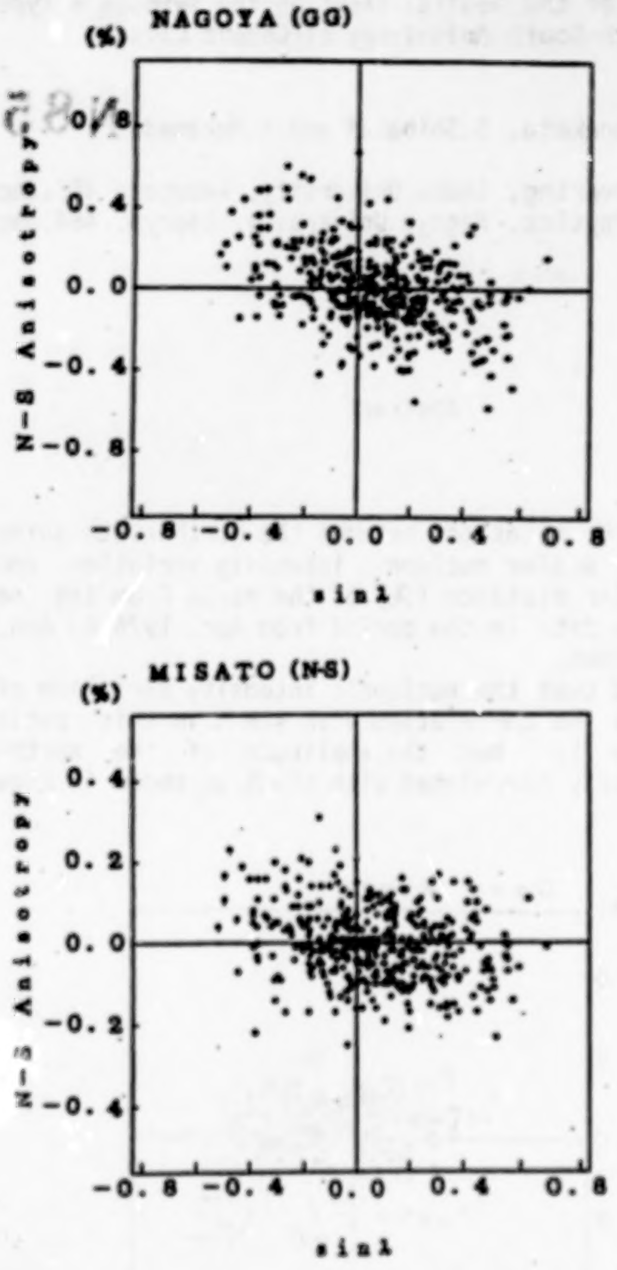

Figure 2. The correlation diagrams between north-south anisotropy and sinλ. The figures at the top and the bottom correspond to the data observed at Nagoya (85 GV) and at Misato (150 GV). The resultant correlation coefficients are -0.42 and -0.26 respectively.

CHARACTERISTICS OF COSMIC RAY POLE-EQUATOR ANISOTROPY DERIVED FROM SPHERICAL HARMONIC ANALYSIS OF NEUTRON MONITOR DATA

N85-34996

H. Takahashi and N. Yahagi
Department of Physics, Iwate University
Morioka 020, Japan

ABSTRACT

We have carried out the spherical hamonic analysis of cosmic ray neutron data from the worldwide network neutron monitor stations during the years, 1966-1969. The second zonal harmonic component obtained from the analysis corresponds to the Pole-Equator anisotropy of the cosmic ray neutron intensity. We have reported some preliminary results on such an anisotropy. In this paper, further studies on this subject are presented. The results obtained confirms our earlier results: Such an anisotropy makes a semi-annual variation. In addition to this, in this paper, it is shown that the Pole-Equator anisotropy makes a variation depending on the IMF sector polarities around the passages of the IMF sector boundary. A mechanism to interpret these results is also discussed.

1. Introduction. The method of spherical harmonic analysis of cosmic ray neutron data from the worldwide network stations is developed extensively by Nagashima (1971). The second zonal harmonic component obtainable from the analysis corresponds to the Pole-Equator anisotropy of the cosmic ray neutron intensity. We have carried out such an analysis and obtained the second zonal harmonic component, using cosmic ray neutron data in the years, 1966-1969. The preliminary results on the Pole-Equator (P-E) anisotropy obtained from the cosmic ray data in 1966 and 1967 were reported (Takahashi et al.,1974, 1975, 1977, 1981, 1984). This paper presents characteristics of time variations of the P-E anisotropy during the three years, 1966, 1967 and the additional year in this study, 1969. The relationship of the P-E anisotropy to the polarity of the IMF sector is also given and discussed.

2. Analysis. Cosmic ray neutron data in daily mean from the worldwide network cosmic ray stations (~40 stations) in 1969 in addition to 1966 and 1967 which were analysed previously are analyzed on the 27 day basis by means of the three-dimensional analysis method by Nagashima, which is given in detail in the papers (Takahashi et al., 1974, 1975, 1977).

3. Results and Discussion. Hereafter, as in our previous papers, a_2^0 means the second zonal harmonic component, i. e. the P-E anisotropy, and also a_2^0's for which the power expo-

ORIGINAL PAGE IS
OF POOR QUALITY

N85-34996

nential type spectrum having $\gamma=2.0$ and $P_0=100$ GV was best-fit in the analysis are used throughout this study.

i) Variation of P-E anisotropy, a_2^0

The results obtained are shown in Figs. 1 - 4. Fig. 1 shows the variation of the mean value, $\overline{a_2^0}$, of a_2^0's during each solar rotation interval during the year, 1969. Figs.2 -3, which have appeared in the papers (Takahashi et al., 1983) are shown again in order to compare the result obtained here with our previous results.

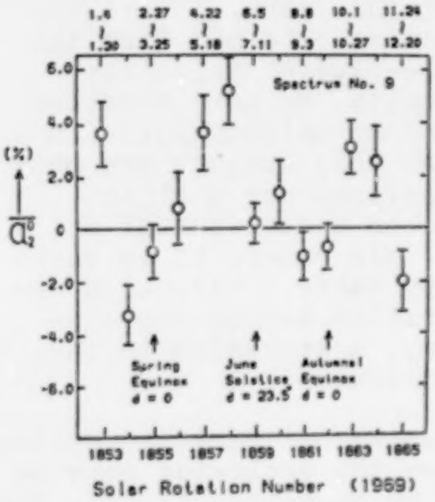

Fig.1. The variation of $\overline{a_2^0}$, which indicates the mean value of a_2^0's during each solar rotation interval in 1969.

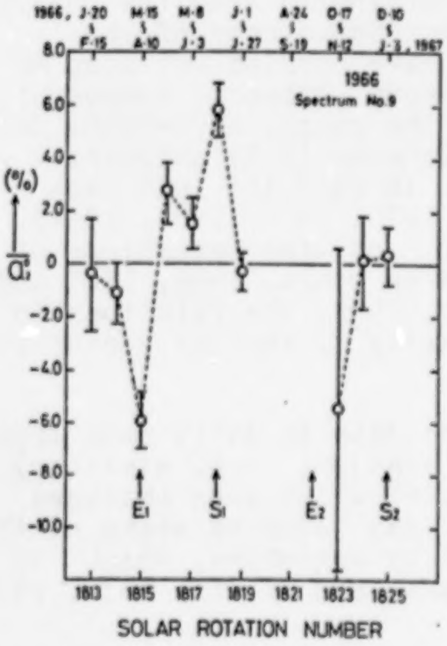

Fig.2. The variation of $\overline{a_2^0}$ in 1966 (Takahashi et al., 1983).

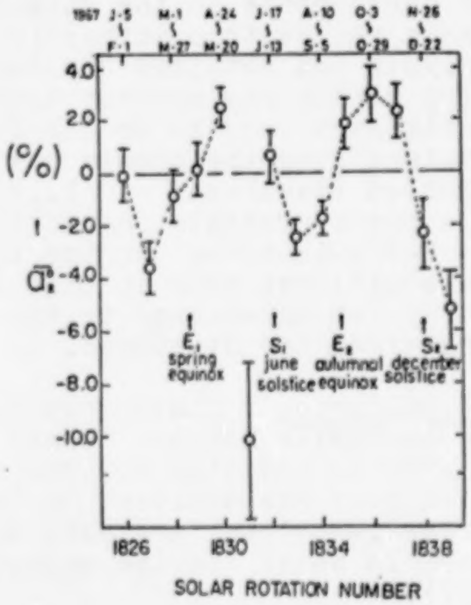

Fig.3. The variation of $\overline{a_2^0}$ in 1967 (Takahashi et al., 1967).

ORIGINAL PAGE IS
OF POOR QUALITY

It will be found that Figs.1 - 3 are similar to each other. This establishes that a_2^0 makes a semi-annual variation such as pointed out in our previous papers (Takahashi et al., 1981, 1983, 1984). The suggested mechanism in our last paper also holds good for this phenomenon.

ii) Relationship of a_2^0's to the IMF sector structure

Fig.4 shows that a_2^0 is related to the IMF sector sturcture. It should notice that the relationship of a_2^0 to the IMF sector polarity as shown in Fig.4 is reversed to the contrary to that of the N - S anisotropy, a_1^0, in other wards, the P - E anisotropy is, on an average, negative in the toward (-) sector, where-as the P - E anisotropy is positive in the away (+) sector.
Ely (1977) found the equatorial modulation, EqM, from the analysis of the cosmic ray data obtained from the measurements of galactic cosmic rays, and also has given a mechanism for the EqM, in which he predicts that the EqM would reverse its phase with respect to the sector polarity at each equinox if the mean IMF is parallel to the plane of the ecliptic. The Ely's EqM is not the same as our a_2^0. Nevertheless, such a mechanism as proposed by him may give an important hint for interpreting physically our results obtained here.

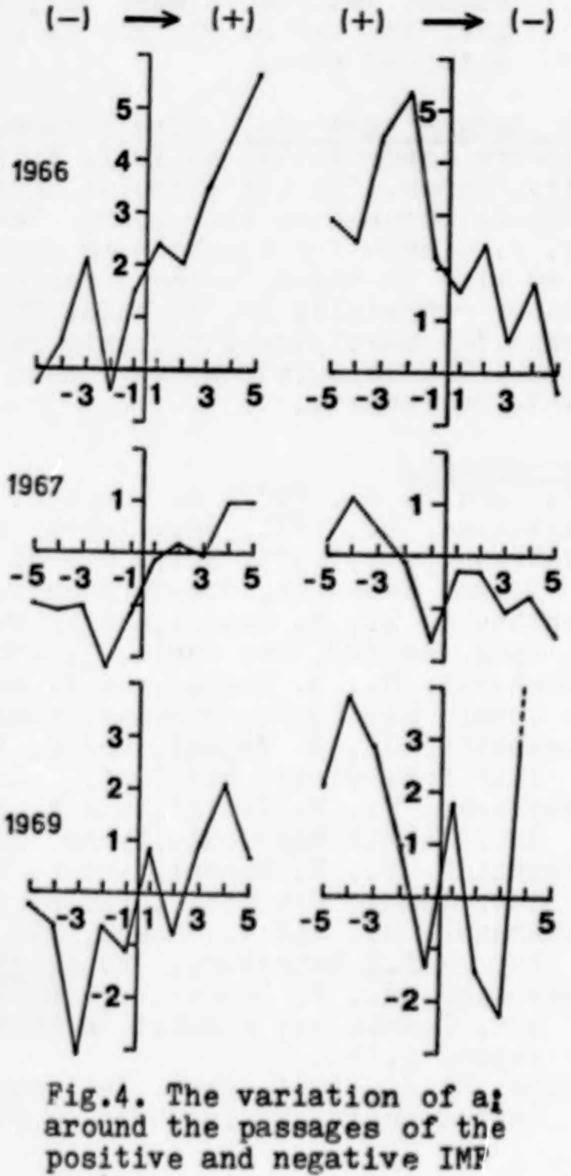

Fig.4. The variation of a_2^0 around the passages of the positive and negative IMF sectors.

4. Conclusions. The following conclusions from the results and discussion mentioned above may be drawn:

1) The P - E anisotropy makes a semi-annual variation.
2) The P - E anisotropy is related with the IMF sector structure and it is positive in the positive (away) sector, whereas it is negative in the negative (toward) sector.
3) The mechanism to interpret physically these results is not yet made clear, but, the mechanism to inter pret the EqM by Ely may be applicable for the results obtained here.

5. Acknowledgments. The authors wish to express their sincere appreciation to Prof. K. Nagashima, Nagoya University, Japan, for his stimulating suggestions and kind support throughout this study. They are also indepted to Mr. S. Oikawa for his help in preparing the data. They also wish to thank to the directors of the cosmic ray stations, espesially Dr. M. Wada, The Inst. Phys. Chem. Res. Tokyo for supplying the cosmic ray data through WDC-2 in Japan. The calculations were made at computer center of Iwate University.

References.

Ely John T. A., 1977, J. Geophys. Res., 82, 343.
Nagashima, K., 1971, Rep. Ionos. Space res. Japan, 25, 189.
Svalgaard, L., 1975, SUIPR Report No. 629, Institute for Plasma Research, Stanford University.
Takahashi, H., N. Yahagi,and K. Nagashima, 1974, Proc. Int. Symp. on STP, Sao Paulo, 1, 431.
Takahashi, H., N. Yahagi,and K. Nagashima, 1975, Proc. Int. Cosmic Ray Conf., München, West-Germany, 4, 1236.
Takahashi, H., N. Yahagi, and K. Nagashima, 1977, Proc. 15th Int. Cosmic Ray Conf., Plovdiv, Bulgaria, 3, 284.
Takahashi, H., N. Yahagi, and K. Nagashima, 1979, Proc. Int. Cosmic Ray Conf.,Kyoto, Japan, 3, 284.
Takahashi, H., N. Yahagi, and K. Nagashima, 1981, Proc. Int. Cosmic Ray Conf., Paris, France, 10, 197.
Takahashi, H., and N. Yahagi, 1983, Proc. 18th Int. Cosmic Ray Conf., Bangalore, India, 10, 148.
Takahashi, H., N. Yahagi, and K. Nagashima, 1984, Proc. Int. Cosmic Ray Modulation in the Heliosphere, Morioka, Japan, p.156.
Tolba, M. F., 1984, Proc. Int. Symp. on Cosmic Ray Modulation in the Heliosphere, Morioka,Japan, P. 69.

First Zonal Harmonic Component of Cosmic Ray Neutron Intensity

N85-34997

H. Takahashi, N. Yahagi and T. Chiba
Department of Physics, Iwate University
Morioka 020, Japan

Abstract

Cosmic Ray neutron data from the cosmic ray stations from the worldwide network in 1966, 1967 and 1969 are analysed by means of the three-dimensional analysis method by Nagashima. The variations of the north-south anisotropy, which is the first zonal harmonic component obtained from the analysis are studied. The result obtained confirms our earlier findings. Relationship of the anisotropy to the IMF sector polarity is also studied.

1. Introduction

We have carried out the analyses of the neutron monitor data in daily mean on the 27 day basis during the years 1966-1969 by means of the Nagashima's method (1971). The first zonal harmonic component of cosmic ray intensity is observed as the North-South (N-S) Asymmetry of cosmic ray intensity and interpreted as the cosmic ray flow in the direction of the earth's rotation axis (Nagashima et al., 1968). We have studied previously such a N-S anisotropy by the method and reported some results (Takahashi et al., 1974: 1979: 1981) on that matter. In this paper, further studies on the subject will be given and discussed in comparison with our earlier results (Takahashi et al., 1974: 1979: 1981). In addition to the above, in this paper, the relationship of a_1^0's to the sector polarity of IMF will be also given and discussed.

2. Method

The method of the analysis has been given previously (Takahashi et al., 1974; 1975; 1984) with particulars. In this paper, a_1^0's for which the power exponential type spectrum having γ =2.0 and P_0=100GV was best-fit in the analysis are used similarly to those in our previous papers (Takahashi et al., 1974; 1975) as a matter of convenience for comparing the results obtained with our earlier results. The data of the Interplanetary magnetic sector polarity are taken from Svalgaard's paper (Svalgaard: 1975).

3. Results and Discussion

(i) Variation of N-S anisotropy, a_1^0

The results obtained are shown in Figs. 1-4. Fig. 1

ORIGINAL PAGE IS
OF POOR QUALITY

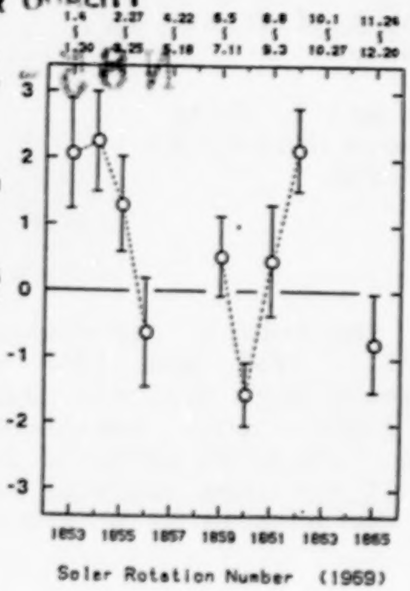

Fig. 1

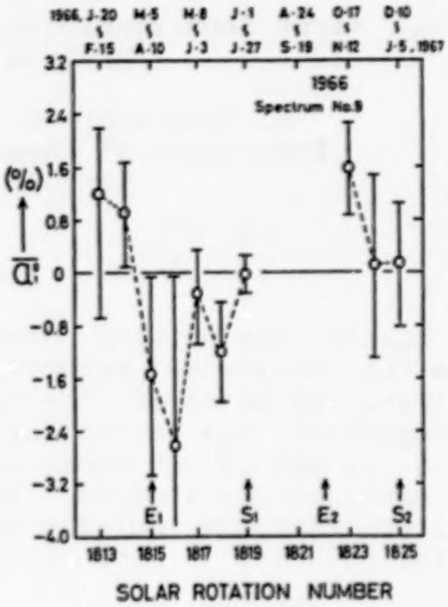

Fig. 2

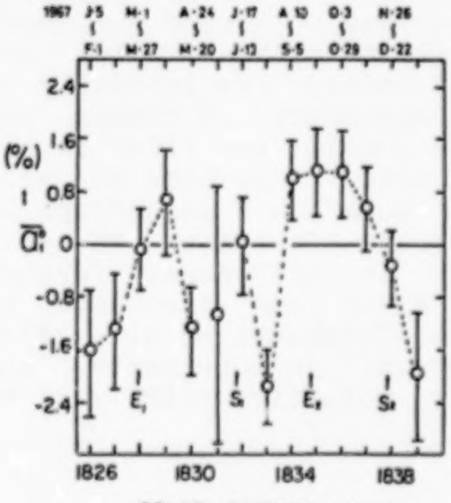

Fig. 3

Fig. 1: The Variation of $\overline{a_1^0}$. $\overline{a_1^0}$ indicates the mean value of a_1^0's during each solar rotation interval in 1969.

Fig. 2: The Variation of $\overline{a_1^0}$, which indicates the mean value of a_1^0's during each solar rotation interval in 1966 (Takahashi et al., 1981).

Fig. 3: The Variation of $\overline{a_1^0}$, which indicates the mean value of a_1^0's during each solar rotation interval in 1967 (Takahashi et al., 1981).

shows the variation of the mean value, $\overline{a_1^0}$, of a_1^0's during each solar rotation during the year 1969. Figs. 2 and 3 are given for comparison of the results obtained here with our earlier results. It will be found that the variation of $\overline{a_1^0}$ shown in Fig. 1 is very similar to that in Fig. 2, whereas there is a marked discrepancy at the period from Rot. No. 1826 to No. 1830 in Fig. 3 between the variations in 1967 and 1969, and at the period from Rot. No. 1831 to 1838, there is a close correlation between them. Although the reason of such a discrepancy is not made clear, it may be due to the difference of physical condition in Space.

(ii) Relationship of a_1^0's to the passages of the positive and negative interplanetary sectors.

Fig. 4 shows the variations of $\overline{a_1^0}$, for the two types of the passages of the interplanetary magnetic sectors, where $\overline{a_1^0}$ indicates the average value of a_1^0 during each solar rotation interval in 1966 and 1969. The figure (Fig.4) is obtained from the Chree analysis, in which the day of passage of the sector boundary is selected as zero day.

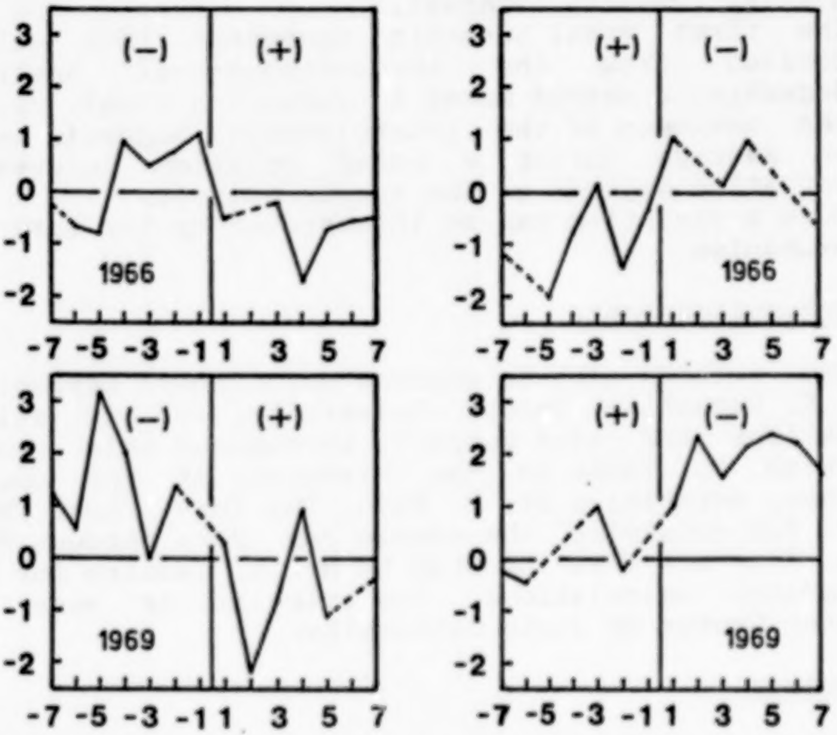

Fig. 4. The variation of $\overline{a_1^0}$ around the passages of the positive and negative interplanetary magnetic sectors where $\overline{a_1^0}$ indicates the average value of a_1^0 during each solar rotation interval in 1966 and 1969.

Yoshida et al. (1971) reported that the N-S anisotropy is related to the interplanetary magnetic sector structure. They also showed that the N-S anisotropy is, on an average, positive in the toward (-) sector (i. e. excess fluxes from the northern polar region), whereas the N-S anisotropy is negative in the away (+) sector (i. e. excess fluxes from the southern polar region (Yoshida et al., 1973). Our results (Fig. 4) are consistent with those by Yoshida et al. (1973). As for the mechanism of the N-S anisotropy, it is reported that the $B\times\nabla n$ mechanism gives a negative N-S anisotropy due to the outward direction of $B_{\parallel}$ (positive $B_{\parallel}$). Also the inward $B_{\parallel}$ produces a positive N-S anisotropy (Tolba, 1974). Pomerantz and Bieber (1984) also showed that the N-S anisotropy is prepondarantly positive, as expected if it arises from a positive radial gradient via the $B\times\nabla n$

drift mechanism. Such a mechanism is also applicable to our results obtained here.

4. Conclusions

The following conclusions from the results shown the above may be drawn:

(1) The first zonal harmonic component (N-S anisotropy) derived from the three-dimensional analysis method by Nagashima makes a yearly variation on an average during a solar rotation interval.

(2) The first zonal harmonic component (N-S anisotropy) derived from the three-dimensional analysis by Nagashima's method makes a variation closly related to the passages of the interplanetary magnetic sectors on an average during a solar rotation interval. The variation depends on the sector polarity.

(3) Such a variation may be interpreted by the $Bx\nabla n$ mechanism.

5. Acknowledgements

The authers wish to express our sincere appreciation to Prof. K. Nagashima, Nagoya University, for his stimulating suggestions and kind support throughout this study. They also wish to thank to the Directors of the cosmic ray stations, especially Dr. M. Wada, The Inst. Phys. Chem. Res. Tokyo, for supplying the cosmic ray data through WDC-2 in Japan. They are also indebted to Mr. S. Tashiro for his help in computer calculations. The calculations were made at computer Center of Iwate University.

References

Nagashima, K., S. P. Duggal, and M. A. Pomerantz, 1968, Planet. Space Sci., 16, 29.
Nagashima, K., 1971, Rep. Ionos. Space Res. Japan, 25, 189.
Pomerantz, M. A., and J. W. Bieber, 1984, Proc. Int. Symp. Cosmic Ray Modulation in the Heliosphere, Morioka, p. 39.
Svalgaard, L., 1975, SUIPR Report No. 629., Institute for Plasma Res., Stanford Univ.
Takahashi, H., N. Yahagi, and K. Nagashima, 1974, Proc. Int. Symp. on STP, São Paulo, 1, 431.
Takahashi, H., N. Yahagi, T. Chiba, and K. Nagashima, 1979, Proc. 16th Int. Cosmic Ray Conf. Kyoto, Japan, 3, 514.
Takahashi, H., N. Yahagi, T. Chiba, and K. Nagashima, 1981, Proc. 17th Int. Cosmic Ray Conf., Paris, 10, 193.
Tolba, M. F., 1984, Proc. Int. Symp. on Cosmic Ray Modulation in the Heliosphere, Morioka, Japan, p. 69.
Yoshida, S., N. Ogita, S-I. Akasofu, and L. J. Gleeson, 1973, J. Geophys. Res. 78, 6409.
Yoshida, S., S-I. Akasofu, N. Ogita, and A. Outi, 1971, J. Geophys. Res., 76, 1.

N85-34998

SH 4.3-14

COSMIC RAY INTENSITY DISTRIBUTION PERPENDICULAR TO SOLAR EQUATORIAL PLANE AT 1 A.U. DURING 1978-83.

S.P.Pathak*, S.P.Agrawal, and P.K.Shrivastava
Physics Department (Vikram Space Physics Centre)
A.P.S.University, Rewa(M.P.),486003, India.

and

R.S. Yadav
Cosmic Ray & Space Physics Group,
Aligarh Muslim University,
Aligarh (U.P.), 202001, India.

ABSTRACT

The distribution of cosmic ray intensity perpendicular to solar equatorial plane, has been investigated by using its yearly variation with respect to the helio-latitudinal position of the earth, for the two intervals 1978-80 and 1981-83. The monthly mean values of two high latitude stations along with the solar and geomagnetic indices are used to derive the cosmic ray intensity distribution free from the changes due to variation in solar activity. The correction is found to be significant only during the interval 1978-80. The results indicate a significant linear increase in cosmic ray intensity from north to south of solar equator, contrary to that observed during 1973-75. No symmetrical gradients are found during the period of study, in agreement with earlier results.

1. Introduction.

The helio-latitude of the earth changes by ± 7.25° with respect to solar equatorial plane during the period September to March each year. Any cosmic ray density gradient perpendicular to the solar equatorial plane will therefore, cause yearly variation in cosmic ray intensity. Earlier results, using high latitude neutron monitor data have failed to provide any evidence of the presence of symmetrical cosmic ray density gradients perpendicular to the solar equatorial plane, which are predicted to explain

---

* Also at, Physics Department, Govt. Science College, Rewa (M.P.), 486 001.

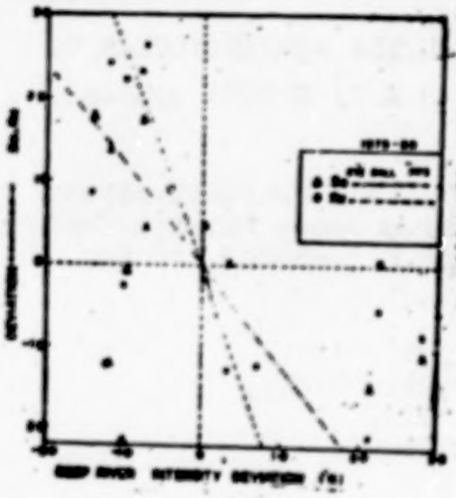

Fig.1 Cross-plot between the average percent deviation of the cosmic ray intensity, with mean deviation of sunspot number (Rz), and solar radio flux (Sa) for the interval 1978-80. Eye-ball linear fits for Sa and Rz are also drawn.

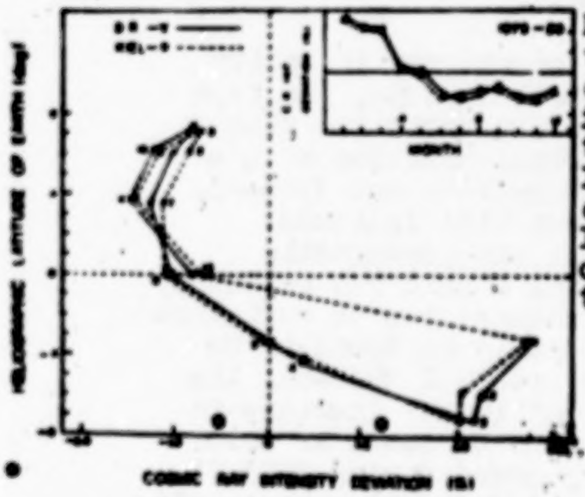

Fig.2 (a) Cross-plot between the observed average percent deviation of cosmic ray intensity for 1978-80 for two stations and helio-latitudinal position of earth. The inset shows the linear time-intensity plot of cosmic ray intensity for the 12 month period.

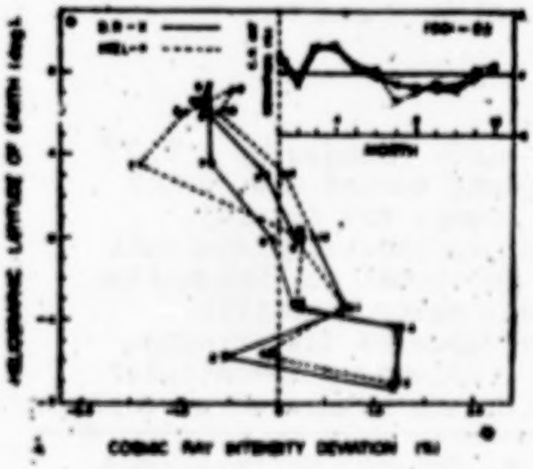

Fig.2 (b) Same as in figure 2a, for the interval 1981-83.

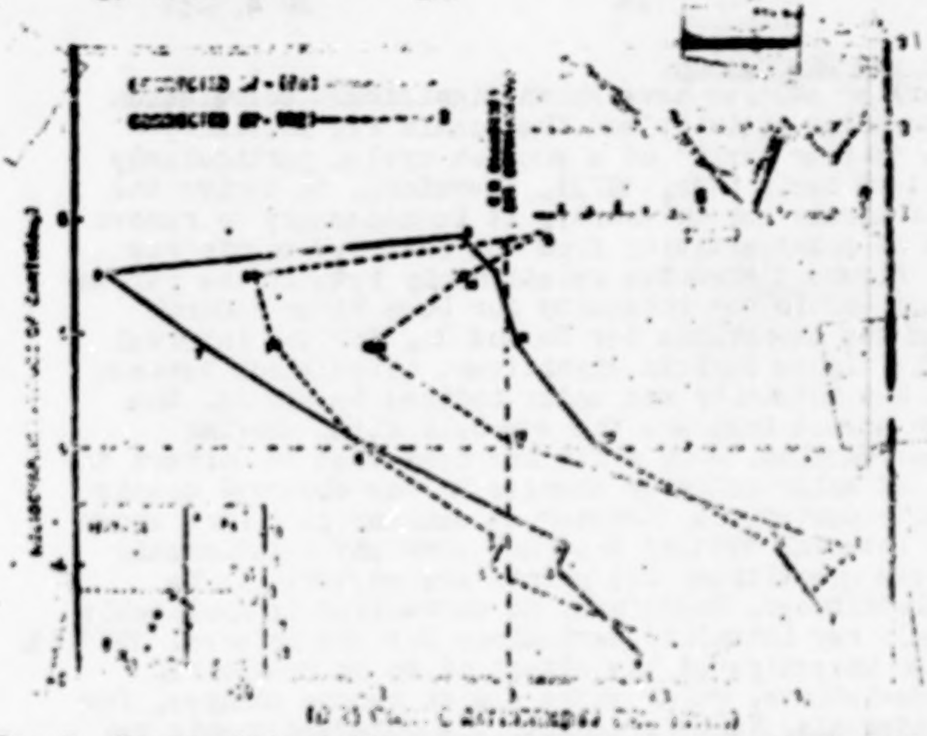

Fig.3 Cross-plot of the corrected average percent deviation of Deep River cosmic ray intensity for the interval 1978-80. The correction has been applied by using Sa & Rz separately.

the semi-diurnal anisotropy observations. In an earlier study (Pathak and Agrawal, 1982; and references there-in) for the interval 1973-75, during which the amplitude of semi-diurnal anisotropy was largest, no evidence was found for the presence of any symmetrical or linear cosmic ray gradients in the helio-latitude range ± 7.25°. Moreover, it is known that the semi-diurnal anisotropy exists during all the years of the sunspot cycle; the amplitude increases during the declining phase of the solar activity. In this paper, the analysis has been extended to include the period of maximum solar activity (1978-80) and the period of declining solar activity (1981-83), to derive the helio-latitudinal gradients by using the procedure adopted by Pathak and Agrawal (1982).

2. Method of analysis.

The corrected monthly average cosmic ray intensity values for two neutron monitor stations (Deep River and Kiel) have been used to determine the helio-latitudinal gradients, separately for the interval 1978-80 and 1981-83. Similar calculations have been performed for sunspot number (Rz), 2800 MHz solar radio flux (Sa), and for geo-magnetic field variability index (Ap), for both the intervals. The mean deviations have been obtained to derive the gradients after correcting the percent deviations of cosmicray intensity for variations in the solar indices.

ORIGINAL PAGE IS
OF POOR QUALITY

3. Results and Discussion.

Earlier studies have shown significant correlation between the solar activity and the cosmic ray intensity during the 11-year period of a sunspot cycle, particularly on a long term basis (Rao, 1972). Therefore, to derive the gradient of cosmic ray intensity, it is necessary to remove the effect of solar activity from the observed cosmic ray intensity. Figure 1 shows the relationship between the percent deviation of cosmic ray intensity for Deep River neutron monitor and the deviations for Sa and Rz, for the interval 1978-80. The figure depicts significant correlation between the cosmic ray intensity and solar indices Sa and Rz. The lines drawn across them are the eye-ball fits, showing negative correlation. Such a fit has been used to correct for the effect of solar activity changes in the observed cosmic ray intensity deviations. However, a similar plot (not shown here), for interval 1981-83 does not show any relationship between these quantities; the points are observed to be randomly distributed. Therefore, no correction is applicable in the cosmic ray intensity deviations for the interval 1981-83. We have also investigated the effect of Ap on cosmic ray intensity deviations, which shows almost random changes, for both the intervals. Next we depict, the observed cosmic ray intensity deviations for both the intervals against the heliographic latitude of the earth for each month. Figures 2(a) and 2(b) show such a cross-plot, as well as the cosmic ray intensity deviations in a linear fashion. The observations indicate a rising density gradient from north to south with a small super-position of symmetrically rising density gradients with respect to solar equatorial plane. Nevertheless, the changes observed in the northern helio-latitudes are small. Moreover, these observations are affected by the changes in solar activity (see figure 1) and hence are re-plotted in figure 3, after correcting thecosmic ray intensity deviations for the effect of solar activity changes. The bottom inset shows the relationship between Sa and Rz in which months 8 and 11 do not show concurrent variability of Sa and Rz. This has resulted in two graphs in fig.3, for the corrected intensity for the same station Deep River. It is seen that the cosmic ray intensity in both the cases, is minimum in northern hemisphere, whereas it increases linearly with a maximum in southern hemisphere; the total percent change in cosmic ray intensity is ≈ 3% during 1978-80, for the helio-graphic latitude of ± 7.25°. Similarly, the total change for the interval 1981-83 is ≈ 2%. The values of the linearly increasing gradient observed here are found to be quite significant and are much larger as compared to that reported earlier for intervals 1973-75. It is further noted that the smaller densities observed in northern hemisphere could be due to the presence of more abundant larger area solar polar coronal holes in the northern hemisphere as compared to southern hemisphere.

References.

Pathak, S.P. and Agrawal S.P., Indian J. Radio & Space Physics, Vol. 8 (1982), 140.
Rao, U.R. Space Science Rev.(Netherlands), 12 (1972) 719.

N85-34999
SH 4.3-15

THE COROTATING VARIATION OF THE NORTH-SORTH ANISOTROPY OF COSMIC RAYS

Xue Shunsheng Zhang Gongliang Xao Shaoyu
(Institute of Space physics, Academia Sinica)

Correlation analysis on the relation of the north-south (N-S) anisotropy of cosmic rays, observed by the Nagoya multi-directional meson telescope, with the IMF as well as the solar wind velocity within solar Carrington rotation for the period 1971-1976.

It is found that the N-S anisotropy of cosmic rays correlates quite well with the Bx component of the IMF. The correlation coefficient nearly equalsto 0.8.

1. Introduction. Since the cosmic ray N-S anisotropy was discovered, a number of studies about it have been published. The drift due to the radial gradient of cosmic ray density n derives the N-S anisotropy in the presence of the IMF intensity **B**, as interpreted by Swinson[1]. The correlation of the cosmic ray anisotropic index GG([4], [5]) with the daily average direction of the IMF was studied by Yasue et al.[2], and a good correlation coefficient (~0.75) was obtained. But they did not give the quantitative analysis between the GG and magnetic field intensity. Fujimoto et al.[3] pointed out that the GG value decreased, as the IMF sector boundary changes its polarity from toward to away the sun, and vice verse. Munakata et al.[4] found that N-S anisotropy correlated somewhat with the solar wind velocity, as well as the Bx component of the IMF.

We made the correlation analysis between the N-S anisotropy and solar flare, and found the flare of importance ≥ 2 with duration ≥ 1.5 hours could change significantly the anisotropy[5]. The present paper studies the relation of the corotating variation of cosmic ray N-S anisotropy with solar wind velocity, as well as the parameters of the IMF with the sun.

2. Data and Method. The cosmic ray data used are the daily average values taken from the multi-directional meson telescope at Nagoya for the period 1971-1976[6]. The cosmic ray N-S anisotropic indexes A and AA are defined below,

$$A=(N-S)/2 \qquad (1)$$

$$AA=(N-S)+(N-E) \qquad (2)$$

Another parameter I is defined as

$$I=(N+S)/2 \qquad (3)$$

Each term from formula (1) to (3) denotes a directional component of the cosmic ray intensity having its central direction of the viewing cone pointing toward the zenith angle of 30° in the north (N), the south (S), and the east (E)-directions, different from that adopted by Munakata et al.. The solar wind velocity and the IMF data are taken from

N85-34999

that compiled by King, J. H.[7].

Analysis of cosmic ray data are made by applying Chree superposed epoch method with reference to their ordinal day in a solar rotation[8]. An accurate Carrimgton rotation Period is divided into 27 round days. It avoids not only the drifting error caused by adopting Bartel's rotation, but also the difficulty produced by decimal Carrington rotation. Such a converted round day is called the "Carrington Day", with length approximately equal to 1.01 calender days. After taken the nearest whole number, the day at which the zero Carrington longitude crossing the solar central meridian is regard as the beginning day of each Carrington rotation.

In all figures of this paper the absissas represent the Carrington ordinal day from the first day to the 27th day corresponding the solar longitude from 360° to 0°. The ordinates show the parameters concerned, i.e. A, AA and I, as well as the solar wind velocity V, IMF total intensity B, its components Bx and By and its azimuthal angle φ in the ecliptic plane. In order to making the figures more clear, the values of the first three days are drawn repeatedly after the 27th day

3. Analysis and results. The distributions of cosmic ray N-S anisotropy and IMF Bx component in the Carrington rotation have been calculated. Simply shown are the results for 1973 and 1974 in Fig. 1. In Fig. 1b, two steady corotating structures of the IMF can obviously be seen. Also noted are the variations of A and AA being similar to that of Bx component. In other years, the steady corotating structures still exist, but not as clear as in 1974. Because the correlation coefficient between the A and AA is almost closed to 1, only the AA is discussed in following.

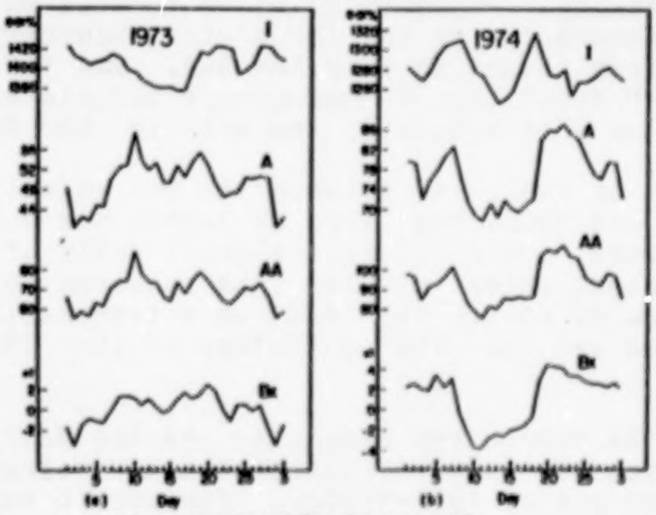

Fig. 1. Correlating variations of I, A, AA and Bx.

The single and bi-correlation between AA and Bx and By can be expressed as the following formulas,

$$AA = a_{01} + a_{1x} B_x \quad (4)$$

$$AA = a_{02} + a_{1y} B_y \quad (5)$$

$$AA = a_0 + a_{11} B_x + a_{12} B_y \quad (6)$$

Table 1 summarizes the yearly coefficients in formula (4) to (6) and respective correlation coefficients r_x, r_y and r_{xy}, as well as the I and AA. It is striking that AA correlates quite well with the Bx component with a high correlation

ORIGINAL PAGE IS
OF POOR QUALITY

coefficient r_x 0.8 The r_y is negative, its magnitude is a bit less than r_x. The bi-correlation coefficient r_{xy} is a little higher than r_x. The r_x obtained here is much higher than that by Munakata et al.. This is because the present correlation coefficients are calculated on a yearly beses, while the previous ones using five year data altogether, and the change of the AA following the solar cycle reduced the statistical accuracy. Meanwhile the superposed epoch method has filtered the short term vaviation and raised also the statistical accuracy. The coefficients a_{1x}, a_{1y}, a_{11} and a_{12} do not change very much, but a_{01}, a_{02} and a_0 increase approximately from 14 to 114 with the decreasing solar activity during 1971-1975. This fact illustrates that the variation of N-S anisotropy is due to not only $B_x v_n$, but other factor, for example, the variation solar general magnetic field.

Table 1. Values of various coefficients, as well as the I and AA during 1971-1975

year	a_{01}	a_{1x}	r_x	a_{02}	a_{1y}	r_y	a_0	a_{11}	a_{12}	r_{xy}	I	AA
1971	14	4.2	0.86	14	-4.1	-0.80	14	3.0	-1.4	0.87	1705	3
1972	38	4.2	0.71	39	-4.1	-0.63	39	3.1	-1.7	0.74	1557	38
1973	69	4.0	0.73	70	-4.3	-0.69	69	3.4	-0.8	0.73	1400	64
1974	90	3.4	0.88	92	-3.6	-0.88	91	1.8	-1.6	0.88	1294	91
1975	114	3.3	0.82	113	-3.3	-0.78	114	3.5	-0.3	0.82	1187	97

We have also calculated the distributions of cosmic ray N-S anisotropy, solar wind velocity and the IMF parameters in the Carrington rotation for this period. For simplicity only the results for 1971 and 1974 are shown in Fig. 2. Table 2 summarizes the correlation coefficients of the AA with the V, φ and B respectively. The magnitude of r_V, r_φ and r_B are much lower than those of Bx and By. Hence it is the best to study the correlation of AA with IMF component.

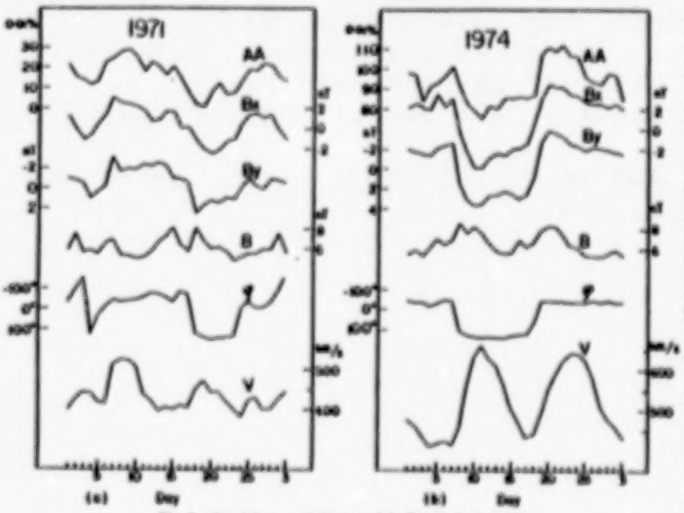

Fig 2. Corotating variations of AA, Bx, By, B, φ and V.

It is well known that the solar activity weekens from 1971-1974, the solar modulation of cosmic rays increases, and the omnidirectional intensity of cosmic rays increases

Table 2. The r_V, r_γ and r_B for 1971 and 1974

Year	r_V	r_γ	r_B
1971	-0.33	-0.61	0.29
1974	0.21	-0.75	0.02

every year. The present results show the AA follows a similar trend, however, it is unexpected that the I decreases from year to year, quite different from the variation of omnidirectional intensity.

4. Conclusion. The cosmic ray N-S anisotropy correlates quite well with the IMF components Bx and By with a correlation coefficient nearly equal to 0.8, a positive one for the Bx component and negative for the By. The bi-correlation coefficient with both Bx and By is almost closed to 0.8. The variation of the regressive coefficients illustrates that the cosmic ray N-S anisotropy, in addition to the gradient drift effect, is controlled by some kinds of long term variayion of the solar cycle.

5. Acknowledgements. The authors are grateful to Prof. K. Nagashima for providing the valuable Nagoya multi-directional meson telescope data.

References

1. Swinson, D.B., (1969), J. Geophys. Res., 74, 5591
2. Yasue, S., Mori, S. and Munakata, Y., (1981), 17th ICRC, Paris, 4, 88
3. Fujimoto, K., Kojima, H., Murakami, K. and Nagashima, K., (1981), 17th ICRC, Paris, 4, 72
4. Munakata, Y., Mori, S. and Nagashima, K., (1979), 16th ICRC, Kyoto, 4, 131
5. Xao, S., Xue, S. and Zhang, G., (1985), to be published
6. Sekido, Y. et al., Report of Cosmic-Ray Laboratory, Multi-Directional Cosmic-Ray Intensities, No. 1
   Nagashima, K. et al., Report of Cosmic-Ray Laboratory, Multi-Directional Cosmic-Ray Intensities, No. 3
7. King, J. H., Interplanetary Data Book, NSSDC/WDC-A-R & S, 77—04, 1977
8. Zhang, G., Yang, G. and Lu, C., (1985), Acta Astrophys. Sinica, Vol. 5, No. 2, 140

N85-35000

SH 4.4-2

COSMIC RAY SIDEREAL DIURNAL VARIATION OF GALACTIC ORIGIN OBSERVED BY NEUTRON MONITORS

Y. Ishida, K. Nagashima*, S. Mori** and I. Morishita***

Department of Physics, Fukushima University, Fukushima 960-12, Japan
*Cosmic-ray Research Lab., Nagoya University, Nagoya 464, Japan
**Department of Physics, Shinshu University, Matsumoto 390, Japan
***Gifu College of Dentistry, Hozumi-cho, Gifu 501-02, Japan

ABSTRACT

Cosmic ray sidereal diurnal variations observed by neutron monitors are analyzed for the period 1961-1978, by adding 134 station-years data to the previous paper (Nagashima et al., 1983). Also the dependence of the sidereal variations on Sun's polar magnetic field polarity is examined for two periods; the period of negative polarity in the northern region, 1961-1969 and the period of positive polarity, 1970-1978. It is obtained that for the former period, the amplitude $A=0.0203\pm0.0020\%$ and the phase $\phi=6.1\pm0.4$ h LST and for the latter period, $A=0.0207\pm0.0020\%$ and $\phi=8.6\pm0.4$ h LST, respectively.

1. Introduction

In the previous paper (Nagashima et al., 1983; hereafter referred to as Paper I), we presented the analyzed results of the cosmic ray sidereal diurnal variations observed by neutron monitors, by using 620 station-years data from a worldwide network for the period 1958-1979. It was shown that the sidereal variations averaged over the above period for the Northern Hemisphere are significantly different from the corresponding variations in the Southern Hemisphere. Both difference and average between two hemispheres were analyzed. The results were interpreted on a theoretical basis of the three-dimensional anisotropy and its annual modulation model (Nagashima and Ueno, 1971; Nagashima et al., 1972a, b) that the former (difference) can be identified with the spurious sidereal diurnal variation arising from annual modulation of 2nd order anisotropy in space responsible for the solar semi-diurnal variation. And the latter could be regarded as being due to uni-directional galactic anisotropy (see detail, Paper I). In the present work, we analyze the neutron monitor data by adding 134 station-years to the previous ones, in the same manner as in Paper I for the period 1961-1978.

Cini-Castagnoli et al. (1975) pointed out the association of the sidereal diurnal variations at deep underground stations in the northern hemisphere with changing Sun's polar magnetic field polarity. For the period of negative polarity in the northern region, the observed sidereal vectors were around 20 h LST, while for the period of positive polarity, the vectors were observed at ~3 h LST. Very recently, Nagashima et al. (1984) pursued this problem in detail, and demonstrated that Cini-Castagnoli et al.'s finding is not real, but virtual even for the deep underground observations (rigidity region $\lesssim$500 GV) due to modulation with the spurious sidereal diurnal variation of solar origin, based on the three-dimensional anisotropy and its annual modulation. In the present analysis, we examine the dependence of the sidereal variations on Sun's polar magnetic field polarity for two periods; for the negative period in the northern region (1961-1969) and for the positive period (1970-1978).

2.Analysis

The data used in the present analysis are those of neutron monitors from a worldwide network for the period 1961-1978. The total amount of data in the Northern and Southern Hemispheres are respectively 544 and 142 station-years by adding 134 station-years to them. The added data are mostly concentrated on 1974 to 1977.

The analysis is made in the same manner as in Paper I. The top panel of Fig. 1 show the first harmonics of the observed daily variations for Northen (N) and Southern (S) Hemispheres and are; for the (N), the amplitude A=0.0123±0.0019% and the phase ϕ=9.0±0.3 h LST and for the (S), A=0.0286±0.0037% and ϕ=6.7±0.4 h LST, respectively.

Fig. 1 shows their difference first harmonics (N-S)/2 and average (N+S)/2 for two Hemispheres; for (N-S)/2, A=0.0099±0.0014% and ϕ=17.3±0.5 h LST and for (N+S)/2 A=0.0196±0.0014% and ϕ=7.4±0.3 h LST, respectively. For comparision, the corresponding expected variations are shown for flat rigidity spectrum with an upper cut-off rigidity of 300 GV. The present results reconfirm the previous results and support the conclusion in Paper I.

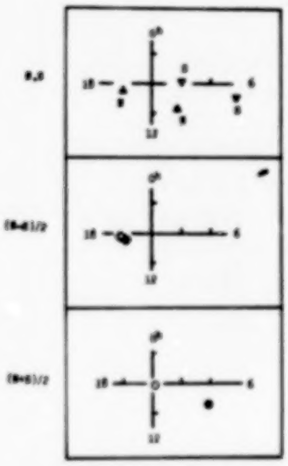

Fig. 1 The first haronic of observed sidereal daily variations for the Northern (N) and Southern (S) Hemispheres, together with their difference (N-S)/2 and their average (N+S)/2 with solid marks. The corresponding expected variations are also shown with open marks.

In order to examine the dependence of the sidereal diurnal variation on Sun's polar magnetic field polarity in neutron monitor rigidity region, we separate the variations into two groups according to Sun's polar field polarity; the negative period showing toward field polarity in the northern region (1961-1969) and the positive period showing away field polarity (1970-1978). The number of data used and their average cut-off rigidities are tabulated in Table 1. These are not necessarily balanced for both hemispheres, but we regard them almost conjugate with respect to the north-south. The sidereal diurnal variations of all the station-years for N

Table 1 Number of data and average cut-off rigidity.

	Negative period (1961-1969)		Positive period (1970-1978)	
	Station-years	Cut-off (GV)	Station-years	Cut-off (GV)
Northern Hemisphere	253	2.86	291	3.66
Southern Hemisphere	78	4.07	64	3.68

ORIGINAL PAGE IS
OF POOR QUALITY

and S for two periods are shown in Fig. 2. In the figure, the distributions of variations of N are different from those of S for both periods

Fig. 3 shows the mean vectors for N and S for these two periods, N_1 and S_1 for the negative period (1961-1969) and N_2 and S_2 for the positive period (1970-1978), respectively. The numerical values; their averages and each dispersions are tabulated in Table 2. In the vectors with a notation (N+S)/2 expresses the variation common to both hemispheres of north-south symmetric type. This could be regarded as being due to uni-directional galactic anisotropy as has been discussed in Paper I, and is shown Fig. 4. It is obtained that for the negative period, the

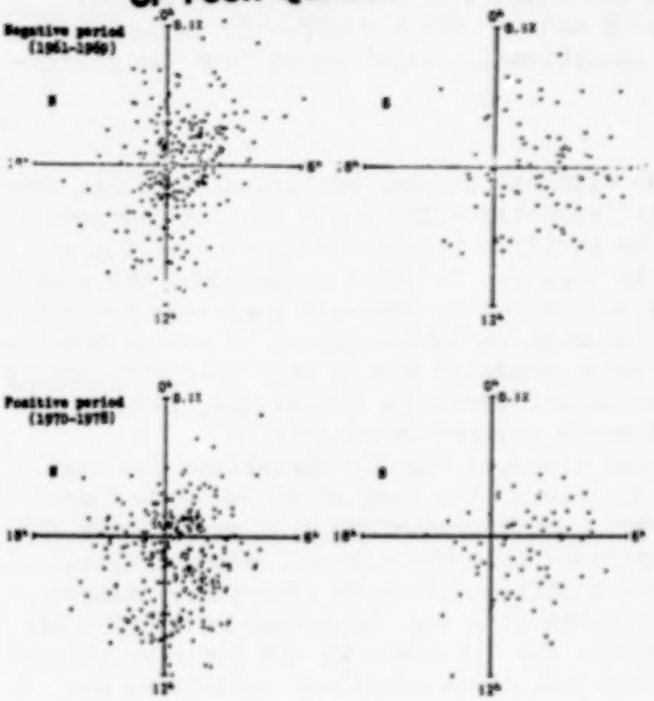

Fig. 2 Sidereal diurnal variations of all the station-years for N and S for two periods; negative (1961-1969) and positive (1970-1978) periods.

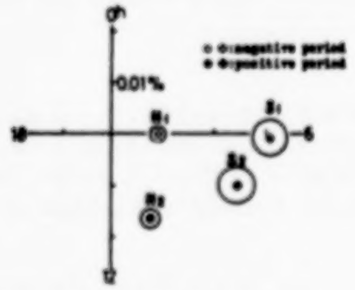

Fig. 3 Averaged sidereal diurnal variations for N and S for two periods; ○◇ with figure 1 for negative period (1961-1969) and ●◆ with figure 2 for positive period (1970-1978).

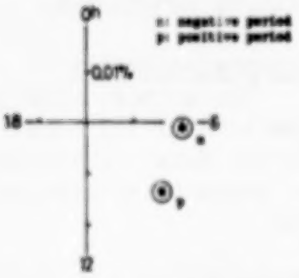

Fig. 4 Sidereal diurnal variations (N+S)/2 for two periods; negative (n) and positive (p) period.

	Negative period (1961-1969)		Positive period (1970-1978)	
	Amp.(%)×10⁻⁴	Phase(h)	Amp.(%)×10⁻⁴	Phase(h)
N	94 (16)	6.0 (0.6)	182 (19)	10.3 (0.4)
S	312 (36)	6.2 (0.4)	261 (36)	7.5 (0.5)
(N+S)/2	203 (20)	6.1 (0.4)	207 (20)	8.6 (0.4)

Table 2 Observed sidereal diurnal variations for N and S for two periods. Also (N+S)/2 is shown. Figures in the parentheses express the dispersions.

amplitude $A=0.0203\pm0.0020\%$ and the phase $\phi=6.1\pm0.4$ h LST and for the positive period, $A=0.0207\pm0.0020\%$ and $\phi=8.6\pm0.4$ h LST. It is noteworthy that the present averages are exceptionally significant from the statistical point of view.

3.Discussion and Conclusion

The present results of the sidereal diurnal variation, (N+S)/2, common to both hemispheres are statistically significant for two periods; the negative (1961-1969) and the positive (1970-1978) period of Sun's polar magnetic field as shown in Fig. 4. In these variations, the spurious sidereal variations may be eliminated by taking a long-term average. And also the spurious sidereal diurnal variation caused by annual modulation of the solar diurnal variation produced from a stationary anisotropy responsible for the solar semi-diurnal variation (Nagashima, 1984), can be eliminated due to its north-south asymmetric nature.

Also as shown in Fig. 4, the sidereal diurnal variations for these two periods are significantly different from each other (several times larger than the dispersion error). On the other hand, a recent work of Nagashima et al. (1984) demonstrated that the sidereal diurnal variations observed at deep underground stations in both hemispheres almost coincide with each other, after correcting for the annual modulation effect of the solar diurnal variation for the negative and positive period mentioned above. And they showed that these resultant variations are stationary throught the periods 1958-1983, regardless of Sun's polar magnetic field polarity reversal. The present result may somewhat contradict their conclusion, which may be due to rather larger errors in underground data.

As far as these two periods and the neutron energy regions are concerned, a clear phase difference between two periods; negative and positive periods, was obtained. A further analysis is necessary to derive a definite conclusion.

4.Acknowledgements

The authors wish to express their sincere appreciation to all the directors of the observation stations for providing invaluable neutron monitor data. These data are obtained through WDC-C2. A large part of the present calculations were made of Computer Center Fukushima University.

References

Cini-Castagnoli, G., Marocchi, D., H. Elliot, R.G. Marsden and T. Thambyahpillai, Proc. 14th Int. Cosmic Rays Conf. (Munich). 4, 1453 (1975).

Nagashima, K. and H. Ueno, Rep. Ionosph. Space Res., Japan, 25, 212 (1971).

Nagashima, K., H. Ueno, K. Fujimoto, Z. Fujii and I. Kondo, Rep. Ionosph. Space Res., Japan, 26, 1 (1972a).

Nagashima, K., H. Ueno, K. Fujimoto, Z. Fujii and I. Kondo, Ibid., 26, 31 (1972b).

Nagashima, K., S. Sakakibara, A.G. Fenton and J.E. Humble, Planet. Space Sci., (in press, 1984).

Nagashima, K., Proc. Int. Symp. Cosmic Ray Modulation Heliosph. (Morioka), 309 (1984).

N85-35001

SH 4. 4-3

Sidereal Anisotropies in the Median Rigidity Range 60-600GV in 1978-1983

H.Ueno, Z.Fujii, S.Mori*, S.Yasue* and K.Nagashima
Cosmic Ray Res. Lab., Nagoya Univ., Nagoya 464, Japan
*Depart. of Physics, Shinshu Univ., Matsumoto 390, Japan

1. Introduction

A great many observation has been made of the sidereal time variations of cosmic rays with various detectors in a wide range of rigidities from neutron monitors(effective primary rigidity 10^{10}V), surface and underground muon telescopes to small air shower arrays($10^{13} \sim 10^{14}$V), and much data have been accumlated to explore the nature of the galactic anisotropy, such as its origin and its propagation inside and outside the heliomagnetosphere.

In low rigidity region, the observed sidereal diurnal variations contain not only those of galactic origin but also those of solar and atmospheric origin. The variations of the latter origin are called the spurious sidereal variations, and almost all of them can be eliminated by taking the difference between the variations observed by two component telescopes pointing different directions (cf. Elliot and Dolbear, 1950). This elimination method, however, cannot be applied to the variation arising from the seasonal variation of solar anisotropy. A typical example for this can be seen in the spurious sidereal diurnal variation arising from the solar anisotropy of the 2nd order responsible for the solar semi-diurnal variation(Nagashima and Ueno, 1971).

In the present paper, the observed sidereal variations are corrected for the influence of this spurious variation by a method using the anti-sidereal diurnal variations produced from the same 2nd order anisotropy (Nagashima et al., 1983). It is demonstrated that the corrected variations are a resultant product of two constituents of galactic origin: one is north-south(N-S) symmetric and the other is N-S asymmetric.

2. Data Analysis and Discussions

In the present analysis, we use the data from surface(NAgoya) and underground(Misato and Sakashita) muon telescopes. Hereafter we abbreviate these stations to NAMS by picking up the top letter of the name of the stations. These data cover the rigidity range of 60 to 600GV, and the present work is concerned with 6-year averages of these data in the period of 1978-1983.

In Table 1, 6-year averages of the observed sidereal diurnal variations of NAMS are listed, together with those of the anti-sidereal diurnal variations and are shown in Fig.1 and Fig.2. Also listed in the table are some characteristics of the telescopes(Fujimoto et al., 1984). Errors of the amplitudes are derived from the dispersion of yearly vectors.

The spurious sidereal diurnal variations are produced by various noises such as the atmospheric effects and also transient cosmic ray intensity variations. In the present analysis, these noises can be eliminated statistically by taking 6-year averages and also by introducing the unknown vector common to all directional components at each station in the best fit calculation. The spurious sidereal diurnal variation is also produced from cosmic ray flow perpendicular to the solar equatorial plane. This variation is sector-structure dependent and is called Swinson-type(cf. Swinson, 1969). This variation could

N85-35001

ORIGINAL PAGE IS
OF POOR QUALITY

Table 1 6-year averages of observed sidereal diurnal variations of NAMS for 1978-1983, together with those of associated anti-sidereal diurnal variations and also corrected variations for Nagashima's component (see text). Some characteristics of the telescopes are also shown. Errors of the amplitudes are derived from the dispersion of yearly vectors.

		Zenith & Azimuth		Geographic Direction		Median Rigidity	Counting Rate	Amplitude(%) & Phase(hr) of Harmonics of 6 Years Averages 1978-1983		
STATION	TELESCOPE	Z	A	λ	φ	P_m(GV)	$\times10^4$/hr	Anti-Sidereal 1st	Sidereal 1st	Corrected Sidereal 1st
NAGOYA 0mwe	V	0°	-	35°N	137°	60	276.0	.034±.008 20.8	.011±.008 16.1	.021±.011 4.4
	N	30°	0°	65°N	-	66	125.0	.037±.008 19.3	.018±.007 14.3	.018±.010 3.3
	E	-	90°	30°N	172°	67	130.0	.026±.008 19.7	.002±.008 3.8	.026±.009 3.2
	S	-	180°	5°N	137°	66	123.0	.014±.009 21.3	.009±.008 6.2	.022±.011 6.3
	W	-	270°	30°N	102°	63	126.0	.035±.007 22.3	.016±.007 18.7	.018±.011 5.0
MISATO 34mwe	V	0°	-	36°N	138°	143	28.0	.032±.007 21.9	.028±.007 19.0	.013±.008 0.9
	N	33°	39°	57°N	177°	135	10.7	.033±.007 19.3	.030±.007 15.8	.007±.009 21.9
	E	-	129°	12°N	164°	143	14.2	.012±.007 21.7	.018±.008 21.9	.018±.008 0.3
	S	-	219°	9°N	117°	135	10.7	.025±.005 23.6	.019±.007 23.9	.022±.008 4.6
	W	-	309°	51°N	95°	136	9.8	.037±.006 23.3	.025±.006 19.3	.012±.007 3.1
SAKASHITA 80mwe	V	0°	-	36°N	138°	331	39.0	.032±.004 23.0	.017±.004 22.9	.028±.004 4.2
	N	41°	344°	73°N	194°	401	6.2	.023±.004 22.4	.008±.004 17.6	.015±.005 6.6
	E	-	76°	35°N	180°	386	7.6	.021±.004 21.2	.021±.004 22.6	.029±.005 1.5
	S	-	166°	5°N	147°	387	6.7	.018±.004 1.3	.054±.004 3.6	.054±.005 3.8
	W	-	256°	18°N	96°	444	5.6	.019±.004 2.2	.040±.005 3.6	.043±.004 3.6
	NN	60°	344°	77°N	26°	395	2.4	.062±.004 6.4	.002±.004 13.2	.074±.006 13.3
	SS	-	166°	23°S	131°	340	2.7	.013±.005 8.1	.084±.005 2.6	.072±.008 2.6

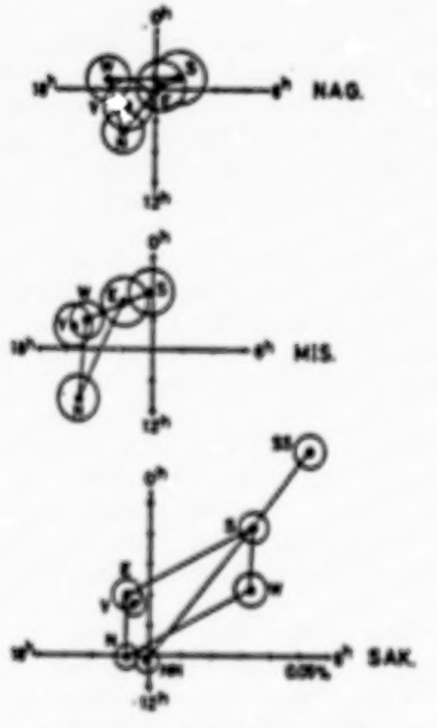

Fig.1 6-year averages of observed sidereal diurnal variations of NAMS telescopes at Nagoya (NAG), Misato (MIS) and Sakashita (SAK) for 1978-1983.

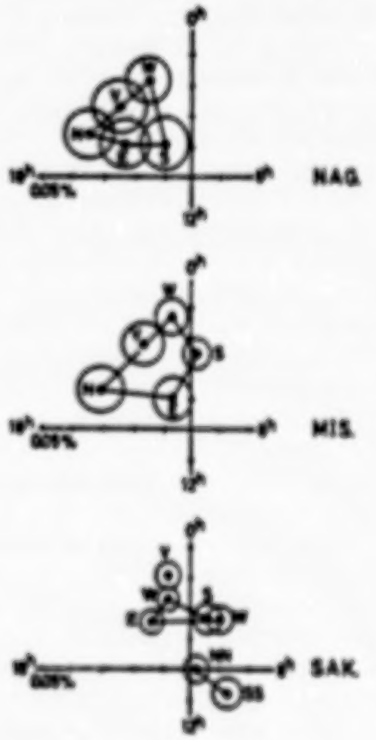

Fig.2 6-year averages of observed anti-sidereal diurnal variations of NAMS telescopes for 1978-1983.

be canceled by taking averages of the all period due to almost equal appearance of the toward and away sectors.

Spurious sidereal diurnal variation is also produced by a systematic annual variation of the solar diurnal variation arising from a solar diurnal variation caused by a stationary anisotropy responsible for the solar semi-diurnal variation(Nagashima and Ueno, 1971). According to the recent study(Nagashima et al., 1983), the spurious variation can be eliminated by multiplying the observed anti-sidereal diurnal variation by 0.947, rotating the vector counterclockwise by 68°, and subtracting it from the observed sidereal diurnal vector.

The corrected sidereal diurnal variations of NAMS are also listed in Table 1 and are shown in Fig.3. As is seen in the figure, the corrected sidereal diurnal variations at Sakashita station are statistically significant, while the variations at Misato and Nagoya stations are comparable with the corresponding dispersion errors. As the counting rates at Misato and Nagoya are large, the large errors are supposed to be caused by the scattering of year-to-year vectors mainly due to the insufficient correction for transient solar diurnal variations. On the other hand, the relative configuration of the vectors of each station seems to be reasonable from the standpoint of geometrical setting of the component telescopes. This implies that real errors may be smaller than the dispersion errors, and in this respect it is worthwhile examining the rigidity dependence of the corrected sidereal diurnal variations including those of the two stations.

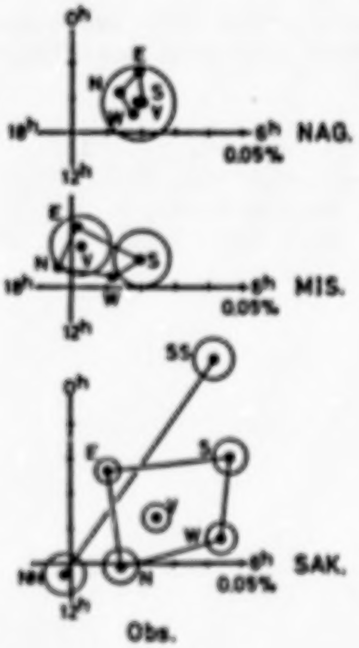

Fig.3 6-year averages of corrected sidereal diurnal variations of NAMS telescopes for 1978-1983.

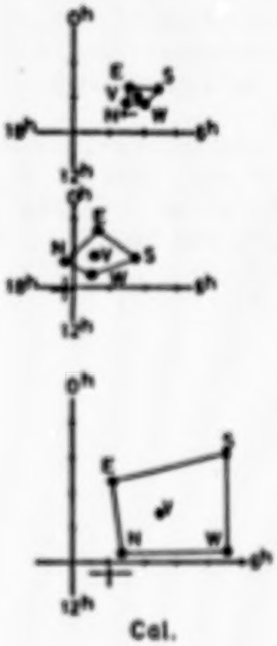

Fig.4 Best fit case of corrected sidereal diurnal variations of NAMS telescopes for 1978-1983. The cross marks are the common vector for each station calculated by the least squares method.

In order to derive the anisotropy, we assume the following in the best fit method as

1) two terms of N-S symmetric and N-S asymmetric types are assumed in the anisotropy for a better fitness between the observed and the expected variations,
2) from the observed fact that the amplitudes are larger for the deeper underground stations, we reasonably assume the low cutoff rigidity P_L in the flat rigidity spectrum, and
3) the unknown vectors are introduced to eliminate the spurious noises as mentioned above.

Tentative results using coupling coefficients given by Fujimoto et al. (1984) are obtained;

N-S symmetric term (P_1^1-type)
the amplitude 0.079±0.007%, the phase 3.5hr and P_L=200GV
N-S asymmetric term (P_2^1-type)
the amplitude 0.035±0.007%, the phase 14.9hr and P_L=200GV

In the present calculation, SS-component at Sakashita station is not included because of larger risidual error probably due to some heliospheric effect which occurs in sidereal semi-diurnal variations (Fujii et al., 1984). The calculated variations in the best fit case are shown in Fig.4.

3. Summary

1. The correction for the spurious sidereal variation using the anti-sidereal variation is indispensable to the study of sidereal anisotropy in low rigidity region.
2. Galactic sidereal anisotropy can be explained better with two terms of N-S symmetric and N-S asymmetric types than the usual uni-directional anisotropy only.

References

Elliot,H. and Dolbear,D.W.N. (1950) Proc. Phys. Soc. A, 63, 137.
Fujii,Z. et al. (1984) Proc. Int. Symp. CR Mod. Morioka, 364.
Fujimoto,K. et al. (1984) Rep. CR Res. Lab., Nagoya Univ., No.9.
Nagashima,K. and Ueno,H. (1971) Rep. Ionos. Space Res. Japan, 25, 212.
Nagashima,K. et al. (1983) Nuovo Cimento, 6C, 550.
Swinson,D.B. (1969) J. Geophys. Res., 74, 5591.

SH 4.4-4

N85-35002

SIDEREAL VARIATIONS DEEP UNDERGROUND IN TASMANIA

J.E.Humble, A.G.Fenton and K.B.Fenton
Physics Department, University of Tasmania
Box 252C, G.P.O., Hobart, Tasmania, Australia, 7001

1. Introduction. Data from the deep underground vertically directed muon telescopes at Poatina, Tasmania, have been used since 1972 for a number of investigations, including the daily intensity variations, atmospheric influences, and checking for possible effects due to the interplanetary magnetic field (1-3). These telescopes have a total sensitive area of only $3m^2$, with the result that the counting rate is low (about 1680 events per hour) and the statistical errors on the results are rather large. Consequently, it was decided several years ago to construct larger detectors for this station. The first of these telescopes has been in operation for two complete years, and the results from it are presented here.

2. Site and Equipment. The equipment is located at a vertical material depth of 139.4m underground in a hydro-electric power station. The mean density has been estimated as $2.56g\ cm^{-2}$, giving a vertical absorber of $357hg\ cm^{-2}$. This corresponds to a muon cut-off of about 100 GV and median primary rigidity $\sim$ 1200 GV. The geographic coordinates are 41.8°S, 146.9°E.

When fully operational, there will be three proportional counter telescopes each having a sensitive area of approximately $4m^2$ and semi-cubical geometry (2mx2mx1m). In each telescope there are four trays of 10cm diameter proportional counters made from thin-walled copper water pipe, with soldered brass ends and glass-metal seals. These were given a prolonged outgassing at temperatures close to 100°C before being filled with standard P-10 gas (90% argon plus 10% methane) at atmospheric pressure. Each counter was tested by pulse-height analysis of the background radiation soon after filling and again several months later as a check for leaks. During the two year period there have been no counter replacements, and no evidence for loss of detecting efficiency, a problem frequently experienced with GM counter telescopes. The four trays of counters are arranged in two crossed pairs at the top and bottom of the telescope frame so that there is a possibility of looking for narrow angle effects or grouping the data into broader directions e.g. east and west of the vertical, and for studying multiple particle events.

3. Results. The first and second harmonics for each of the years 1983 and 1984 separately, and the totals for the two-year period are shown in Table 1, analysed according to solar, sidereal and anti-sidereal time. In this Table the Poisson errors are shown; these are somewhat smaller than the standard errors obtained from the scatter in the individual values arising during analysis of a year's data.

As may be seen from the Table, the first harmonic in solar time is not convincingly different from zero; nor is there a significant anti-sidereal variation. None of the second harmonics are significantly different from zero. On the other hand, the first harmonic in sidereal time is significant during both years as well as in the total. On estimating the errors from the scatter in the values of the components of the vectors we find the amplitude of the first harmonic for the total period 1983-1984 to be (0.081±0.045)% with its maximum at 2.43±2.25 hours.

TABLE 1

	First Harmonic		Second Harmonic	
	Amplitude(%)	Max (hr)	Amplitude(%)	Max (hr)
Solar				
1983	0.053±0.035	3.14± 2.77	0.024±0.035	10.80±6.00
1984	-0.006±0.035	10.59±12.00	0.036±0.035	1.30±2.70
Total	0.026±0.025	3.63± 4.94	0.024±0.025	0.63±6.00
Sidereal				
1983	0.111±0.035	4.41± 1.23	0.022±0.035	1.40±6.00
1984	0.058±0.035	1.92± 2.46	0.005±0.035	8.11±6.00
Total	0.081±0.025	2.43± 1.20	0.009±0.025	2.37±6.00
Anti-sidereal				
1983	0.032±0.035	7.37±12.00	0.038±0.035	10.20±2.34
1984	0.026±0.035	23.41±12.00	0.023±0.035	5.77±6.00
Total	0.019±0.025	4.41±12.00	0.014±0.025	5.86±6.00

4. Discussion. Results from the new, more stable equipment at Poatina appear to confirm the existence of a first harmonic in the daily variation in sidereal time reported earlier, and are consistent with small or non-existent first harmonics in solar and anti-sidereal time. All the second harmonics appear to be small, if not zero at these energies. It will be important to establish the magnitude and phase of any of the variations (other than the 24-hour sidereal wave) which turn out to be present, since these will be crucial in testing models of the anisotropy by comparison with northern hemisphere results. Since these are evidently of very small amplitude, a long period of observation will be required using the full $12m^2$ detector system. The higher total counting rate available with the complete system should assist also in our investigation of the reasons for the observed standard errors being appreciably larger than from counting statistics alone. Systematic influence such as uncorrected atmospheric effects or year to year variations in the anisotropy itself may be responsible, apart from instrumental variability which is thought to be very small in the new designs.

5. Acknowledgements. We wish to thank the Hydro-Electric Commission of Tasmania and its staff for the excellent facilities provided at Poatina. This work is supported in part by the Australian Research Grants Scheme.

6. References.

1. Fenton A G and Fenton K B (1975). 14th Int.Cos.Ray Conf., Munich, Conference Papers 4, 1482-1484.
2. Fenton A G, Fenton K B and Humble J E (1977). 15th Int.Cos.Ray Conf. Plovdiv, Conference Papers 11, 242-244.
3. Humble J E, Fenton A G, Fenton K B and Lyons P R A (1979). 16th Int. Cos.Ray Conf., Kyoto, Conference Papers 4, 258-262.

N85-35003

SH 4.4-5

THE EFFECT OF THE INTERPLANETARY MAGNETIC FIELD ON SIDEREAL VARIATIONS OBSERVED AT MEDIUM DEPTH UNDERGROUND DETECTORS

J.E.Humble and A.G.Fenton
Physics Department, University of Tasmania
Hobart Tasmania Australia 7001

1. Introduction. It has been known for some years that the intensity variations in sidereal time observed by muon detectors at moderate underground depths are sensitive to the polarity of the interplanetary magnetic field (ipmf) near the earth (1-5). There are differences in the response to these anisotropies as observed in the northern and southern hemispheres (6, 7). When fully understood, the nature of the anisotropy seems likely to provide information on the 3-dimensional structure of the heliomagnetosphere, its time variations, and its linking with the local interstellar field - difficult to obtain by other means.

2. Data. The data were obtained from vertically-pointing wide angle (semi-cubical) G-M counter muon telescopes at the underground station near Hobart, located at a depth of 46hg cm^{-2} below the top of the atmosphere (geographic coordinates 42.9°S, 147.4°E). The inferred ipmf data used in the analysis were mainly those published in 1972 by Svalgaard (8), Wilcox et al in 1975 (9) or from Solar Geographical Data Bulletins. Unfortunately, in recent years the inferred field directions have been based only on the southern polar station at Vostok, whereas previously data from Thule were also included. This has led to a decrease in the percentage of days for which ipmf data are available.

3. Results. At the time of writing, analysis for the years 1983 and 1984 has not been completed, due to delays in acquiring the ipmf data; however, the results for the period 1958-1982 are unlikely to be altered dramatically by the addition of these two years, or by the reanalysis of data for the whole period. To date, the main results are as follows:

(i) The summation harmonic dials for the sidereal diurnal variation during 1958-1982 show that there is a strong dependence on whether the ipmf near the earth is directed outwards (away, A) from the sun or inwards (towards, T) it (see Figure 1).

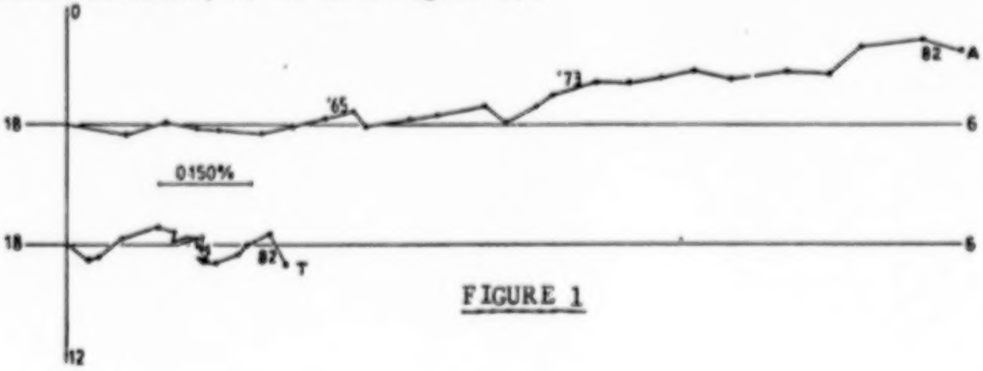

FIGURE 1

(ii) There are significant differences in the amplitude of the sidereal daily variation within the two data sets if these are divided into regimes based on the solar activity cycles (5). For example, before solar minimum in 1965 and after 1977 the amplitudes were relatively large, whereas between 1965 and 1977 the amplitudes were small.

(iii) The variation in anti-sidereal time is significant, but seems to be independent of the ipmf direction.

4. Discussion. The results for the whole period do not seem to agree with those obtained in the northern hemisphere nor are they consistent with some of the interpretations. For example, Thambyahpillai (10) concluded that the shift in position of the viewing cone on the celestial sphere accompanying solar polar field reversals accounts for the London 60 mwe observations. However, the Hobart results group better according to solar minimum years than to the times of solar magnetic field reversals. A more recent explanation of the observations in both hemispheres by Nagashima et al (11, 12) seems to be more satisfactory at the present time. The basis of this model is that the solar semi-diurnal variation undergoes an annual modulation due to the excursions in heliolatitude made by the earth; this in turn leads to a diurnal variation in anti-sidereal time which can be used to correct the observed sidereal variation. After such correction, the London and Hobart sidereal variations are more consistent. A more detailed investigation of the Hobart results is in progress.

5. Acknowledgements. The Hobart observations were assisted by grants received from the Australian Research Grants Scheme.

6. References.

1. Swinson D B (1969) J.Geophys.Res. 74, 24, 5591-98
2. Swinson D B (1971) J.Geophys.Res. 76, 19, 4217-23
3. Humble J E, Fenton A G, Speller R D, Otaola J A, Thambyahpillai T, Dutt J C, Mathews T, Miyazaki T and Peacock D S (1973), 13th Int.Cosmic Ray Conf., Denver, Conference Papers 2, 976-81
4. Humble J E and Fenton A G (1977), 15th Int.Cos.Ray Conf., Plovdiv, Conference Papers 11, 245-250
5. Humble J E and Fenton A G (1983), 18th Int.Cos.Ray Conf., Bangalore, Conference Papers 10, 214-217
6. Cini-Castagnoli G, Marocchi D, Elliot H, Marsden R G and Thambyahpillai T (1975) Paper MG10-2, 14th Int.Cosmic Ray Conf., Munich, Conference Papers 4, 1453-7
7. Humble J E and Fenton A G (1975) Paper MG10-8, 14th Int.Cosmic Ray Conf., Munich, Conference Papers 12, 4226-8
8. Svalgaard L (1972) J.Geophys.Res. 77, 4027-34
9. Wilcox J M et al (1975) J.Geophys.Res., 80, 3685-3688
10. Thambyahpillai T (1983), 18th Int.Cos.Ray Conf., Bangalore, Conference Papers 3, 383-386
11. Nagashima K et al (1984) Proc.Int.Symp.Cosmic Ray Modulation in the Heliosphere, Morioka, Japan, 337 (Abstract)
12. Nagashima K et al (1985) Planetary & Space Science, in press

44 N85-35004

SH 4.4-6

THE SIDEREAL SEMI-DIURNAL VARIATION OBSERVED AT HIGH ZENITH ANGLES AT MAWSON, 1968-1984, AND THE POLARITY OF THE SOLAR MAIN FIELD.

R.M. Jacklyn and M.L. Duldig
Antarctic Division, Department of Science, Australia.

ABSTRACT.

High zenith-angle North/South telescopes viewing equatorially and at mid-latitudes through 40 MWE of atmosphere have been operating at Mawson since early 1968. It is evident that a sidereal semi-diurnal component of galactic origin has been observed, over and above a possible spurious component proposed by Nagashima, arising from a bi-directional component of the solar anisotropy. Although a very pronounced reduction in the semi-diurnal galactic response followed the reversal of polarity of the solar main field during 1969-1971, so far the observations indicate that there has been no recurrence of a larger galactic response following the reversal of polarity around 1981. The possible role of the latitudional extent λ_o of the wavy neutral sheet is discussed.

Introduction.

There is now considerable evidence for the existance of a sidereal semi-diurnal variation of galactic origin at the low end of the high energy spectrum, from detecting systems whose median rigidities of primary response, Pm, to the omnidirectional intensity range from $\sim 10^{14}$v down to $\sim 10^{11}$v (Jacklyn, 1970; Gombosi et al., 1975; Sakakibara et al., 1976, 1979, 1984; Bergeson, 1979). From the underground vertical detectors at Hobart (Pm $\approx 10^{11}$v), for instance, the long-term average amplitude, 1958-1963, has the reported value of 0.0084 ±0.0014%, far in excess of the estimated spurious amplitude of 0.0036 ±0.0002% that is due to seasonal modulation of the solar semi-diurnal variation (Nagashima et al., 1984).

What is at issue in this paper is the role of the alternating +ve and -ve polarity states of the solar main field in affecting observations of the sidereal semi-diurnal component through associated changes in the heliomagnetic modulating regime. The extensive calculations of Nagashima et al. (1982) have shown that heliomagnetic modulation may differ considerable between the two polarity states. There are indications from his work that in the +ve polarity state (field directed away from the sun in the northern space of the heliosphere) a semi-diurnal galactic response may be relatively suppressed at the field-sensitive rigidities. It has seemed that this might explain why it was that relatively large variations characteristic of a bi-directional sidereal anisotropy were observed with detectors of the shallow-depth type, underground and at the surface, between 1958 and 1969, when the polarity state was -ve, whereas they were very much smaller in the following years of +ve polarity (Jacklyn and Duldig, 1983). More than that, in the earlier years the second harmonic observed with detectors viewing equatorially was significantly larger than that observed at mid-latitudes (Jacklyn, 1970). This suggests that heliomagnetic modulation at that time may not have seriously affected the characteristic latitude dependence of the second harmonic.

Observations now available from successive -ve, +ve and -ve polarity states are discussed here. They concern mainly the results from high zenith-angle telescopes that have been operating at Mawson since 1968.

Observations.

Equatorial and mid-latitude observations have been obtained from Geiger counter telescopes, one group located underground at Hobart (43°S) and the other at the surface at high zenith-angles at Mawson (67°S). All inclined telescopes were aligned in the geographic meridian plane. The mean absorber depth at Hobart was approximately 50 MWE. At Mawson the absorber depth of 40 MWE was entirely atmospheric. Telescope characteristics and the data periods used in the present comparison are listed in Table 1. Further details have been published elsewhere (Jacklyn, 1970; Jacklyn and Vrana, 1969).

TABLE 1.

Telescope Characteristics.

Period	Place	Site	Geometric aperture zenith	azimuth	Inc.	Asympt.* Lat.	Count rate (10^3/hr)
1958-65	Hobart	UG	126°	126°	Vert.	-39°	70
1961-62	Hobart	UG	90°	90°	30°N	-20°	17
1968-69	Mawson	Surface	20°	126°	76°N	10°	6
			20°	126°	76°S	-42°	6
1974-84	Mawson	Surface	20°	126°	76°N	-6°	40
			20°	126°	76°S	-47°	40

*Mean asymptotic latitude of viewing at median rigidity Pm.

The size of the surface telescope system at Mawson was increased from one to three crossed telescopes between 1969 and 1974 and the geometry modified to improve the counting rate and to allow the North asymtotic cone to straddle the equator more effectively. In the result there was an insignificant improvement in the coupling cinstants of response to a second harmonic. That is, the response characteristics that are of relevance here were unchanged.

In Figure 1, the results of observations of the sidereal second harmonic are shown in relation to the succession of polarity states of the heliosphere that occurred between 1958 and 1984, as shown at the foot of the Figure. Consider first the period, 1958-1968, of -ve polarity. Although the counting rate of the single high zenith-angle telescope at Mawson was very low, there was remarkable similarity between the equatorial and mid-latitude vectors at Mawson (amplitudes 0.051 ±0.015% and 0.016 ±0.015%. during 1968-69 and the more significant vectors (amplitude 0.024 ±0.010% and 0.006 ±0.002%) observed at Hobart during 1958-63. At both places the equatorial amplitudes in particular were each greatly in excess of that of the spurious component of solar origin (0.005 ±0.0008% at Hobart and 0.005 ±0.002% at Mawson).

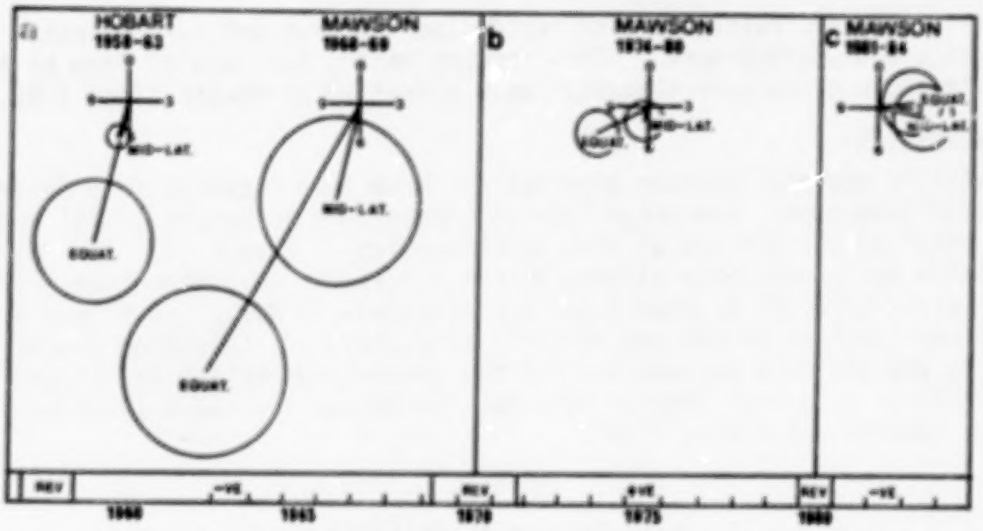

Fig. 1. Sidereal semi-diurnal vectors observed with the telescope systems at effective depths of 40-50 MWE.

(a) within the period of -ve polarity, 1958-1970, from Hobart underground vertical (mid-latitude), Hobart underground 30°N (equatorial), Mawson surface 76°S (mid-latitude) and Mawson surface 76°N (equatorial).

(b) within the period of +ve polarity, 1971-1980, from Mawson surface 76°S and 76°N.

(c) within the period of -ve polarity, 1981-1984, from Mawson surface 76°S and 76°N.

The SD circles are derived from observed fluctuations in the data.

Observations with a seven-fold increase in counting rate of the high zenith-angle equipment commenced at Mawson in 1973, after the heliomagnetic field polarity had reversed. Averaged over the following years of +ve polarity, 1974-1980, the sidereal second harmonics in the north and south directions were very small (Fig. 1b). However, the equatorial amplitude (0.010 ±0.004%) was significant and almost twice the amplitude of the estimated spurious component (0.005 ±0.0004%). The result tended to support the evidence for a latitude dependence of amplitude found in the earlier period of -ve polarity.

The most recent results, 1981-1984, relate to the present conditions of -ve polarity. There are no indications (Fig. 1c) of a return to the large equatorial amplitudes that seemed to be characteristic of the earlier period of -ve polarity. In fact, the average amplitudes to date are not greater than the estimated spurious effect.

Discussion.

Further evidence for the reality of a bi-directional galactic response at shallow depths during 1958-1970 was presented at the previous Conference from observations of the characteristic diurnal counterpart of the second harmonic (Jacklyn and Duldig, 1983). It was suggested there tha suppression of response might have occurred in the epoch of +ve polarity that followed. This was apparent not only because of the reduction of the Mawson equatorial semi-diurnal amplitude, but because there was no associated reduction of the solar semi-diurnal amplitude, thus indicating that there had been suppression not of the spurious but of a genuine galactic response.

It seems now that suppression of semi-diurnal response has continued into the present epoch of -ve polarity, at least up to the end of 1984. The possibility is in accord with the evidence given by Bercovitch that the magnitude of change in sidereal diurnal response of the Ottawa Horizontal Muon Array that was predicted to follow the latest reversal of polarity did not occur (Bercovitch, 1984). That this might have been due to increased scattering in the -ve polarity state was discounted. However, he has pointed out, on the basis of the heliomagnetic model of Nagashima et al. (1982), that if the latitudinal amplitude λ_o of the wavy neutral sheet was sufficiently large in both polarity states the expected change in the diurnal response should be small. Thus, as Nagashima et al. (1984) have noted, characteristic differences between the two polarity states tend to become lost as λ_o increases.

It seems, then, that λ_o might be the critical factor. Perhaps it was a smaller latitudinal extent of the waviness of the neutral sheet during 1958-1969 that resulted in the larger galactic semi-diurnal response evidenced during that period of -ve polarity.

Conclusion.

Although there is persistant evidence in the long term for a semi-diurnal variation of galactic origin at the shallow depths of observation, it now appears that there are groups of years when the response is suppressed and that they are not necessarily associated with a particular polarity state of the heliosphere. When large amplitudes were observed, during 1958-1969, notably in the equatorial direction, the polarity was -ve, but some other factor or factors must have favoured the increased response. It is suggested that a possible factor might have been a relatively small amplitude λ_o of the neutral sheet.

References.

Bercovitch, M. (1984) Proc Int. Symp. on Cosmic Ray Modulation in the Heliosphere, Morioka, 329.

Bergeson, H.E. et al. (1979) Proc. 14th. Int. Cosmic Ray Conf., Munich, 2, 586.

Gombosi, T., et al. (1975) Proc. 14th Int. Cosmic Ray Conf., Munich, 2,586.

Jacklyn, R.M. and Vrana, A. (1969) Proc Astron. Soc. Aust., 1, 6, 278.

Jacklyn, R.M. (1970) ANARE Sci. Rep. Series C(II), Pub. 114, Australia.

Jacklyn, R.M. and Duldig, M.L. (1983) Proc. 18th Int. Cosmic Ray Conf., Bangalore, 3, 391.

Nagashima, K. et al. (1982) Planet. Space Sci., 30, 898.

Nagashima, K., Sakakibara, S., Fenton, A.G. and Humble, J.E. (1984) Planet. Space Sci., in press.

Sakakibara, S. et al. (1976) Proc. Int. Symp. on High Energy Cosmic Ray Modulation, Tokyo, 316.

Sakakibara, S. et al. (1979) Proc 16th Int. Cosmic Ray Conf., Kyoto, 4, 216.

Sakakibara, S. et al. (1984) Proc. Int. Symp. on Cosmic Ray Modulation in the Heliosphere, Morioka, 329.

N85-35005 SH 4.4-7

CORRECTED SIDEREAL ANISOTROPY FOR UNDERGROUND MUONS

D. B. SWINSON[1] and K. Nagashima[2]

[1] Department of Physics and Astronomy, The University of New Mexico, 800 Yale N.E., Albuquerque, New Mexico 87131

[2] Cosmic Ray Research Laboratory, Faculty of Science, Nagoya University, Chikusa-Ku, Nagoya, 464 JAPAN

ABSTRACT

Data from underground muon telescopes in New Mexico and Bolivia are analyzed in sidereal time and anti-sidereal time in the rigidity range 20 GV to a few 100's of GV. Using both vertical and north- and south- pointing telescopes in both hemispheres, a latitude range of 70°N to 50°S is covered. It is shown that there is an anti-sidereal variation of the P_2^1 type, having opposite phase in the northern and southern hemispheres, and maximum amplitude at mid latitudes. The anti-sidereal data are used to correct the sidereal data, using the Nagashima method (Nagashima, 1984); the resulting corrected sidereal vectors for northern hemisphere telescopes have their sidereal maxima close to 3h sidereal time, in reasonable agreement with sidereal data at higher energies from small air showers. The Nagashima correction also eliminates effects due to the reversal of the sun's polar magnetic field which show up in the uncorrected sidereal data.

INTRODUCTION: This paper presents data from the vertical and north- and south-pointing telescopes of the underground cosmic ray muon detectors at Embudo Cave (35.2°N, threshold rigidity 19 GV, median rigidity 132 GV), Socorro (34.04°N, threshold rigidity 45 GV, median rigidity 305 GV) and Bolivia (16.31°S, threshold rigidity 16 GV, median rigidity 125 GV). The asymptotic directions of viewing for these nine telescopes are given by Regener and Swinson (1968); they cover a range in latitude from 70°N to 50°S. Data from Embudo for 1965 to 1983, Socorro for 1968 to 1983, and Boliva for 1965 to 1976 are used in this analysis. The data are analyzed both in sidereal time and in anti-sidereal time, and the nature of the anti-sidereal diurnal variation is examined; the anti-sidereal data are then used to apply the Nagashima correction to the observed sidereal data.

Nagashima et al. (1983, 1985) have shown that, owing to the Earth's orbital motion through the interplanetary magnetic field (IMF), the geographical direction of the field at the earth is subject to a systematic arrival variation; as a result, the solar diurnal and semi-diurnal cosmic ray intensity variations produced from this effect show an annual modulation which can be decomposed into sidereal and anti-

ORIGINAL PAGE IS
OF POOR QUALITY

sidereal diurnal and semi-diurnal components. The anti-sidereal diurnal variation is expected to vary with latitude according to the relation (Nagashima et al., 1983).

$$P_2^1 (\sin \lambda) = \sqrt{3}.\ \mathrm{Sin}\ \lambda.\ \mathrm{Cos}\ \lambda \qquad (1)$$

Where λ is the geographic latitude (positive in the northern hemisphere and negative in the southern hemisphere). This function has opposite signs in the two hemispheres, so the expected phases of the anti-sidereal diurnal cosmic ray variation should differ by 180° in the two hemispheres. Note that, in outer space, these phases show eigen values 23.3 h ($\lambda > 0$) and 11.3 h ($\lambda < 0$), respectively (Nagashima, 1984).

ANTI-SIDEREAL DATA: Figure 1 presents data from the nine telescopes listed earlier, displayed as harmonic dials in anti-sidereal time. Each vector represents an average for all available data (19 years for Embudo, 16 years for Socorro, and 12 years for Bolivia). The error circles are determined on the basis of the scatter of the individual daily vectors which are used to arrive at the various resultant vectors. Errors calculated on the basis of counting rate alone are appreciably smaller. The capital letters E, S and B are for Embudo, Socorro and Bolivia, respectively, and the subscripts V, N and S represent vertical, north- and south-pointing telescopes, repectively at each location. With the exception of the Bolivia north-pointing telescope, the northern latitude telescopes are clustered near 21h anti-sidereal time, and the southern latitude telescopes are clustered near 9h anti-sidereal time, thereby showing the ex-

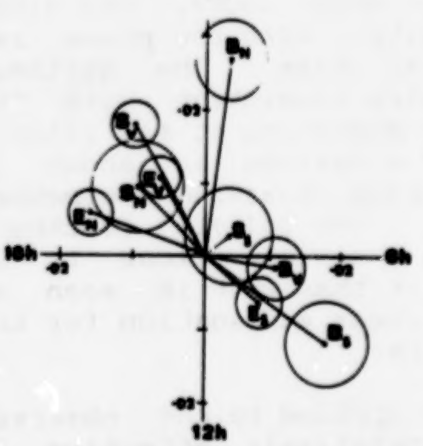

Fig. 1: Harmonic dial in anti-sidereal time for Bolivia, Embudo and Socorro North, South and Vertical Telescopes. Amplitudes are in percent.

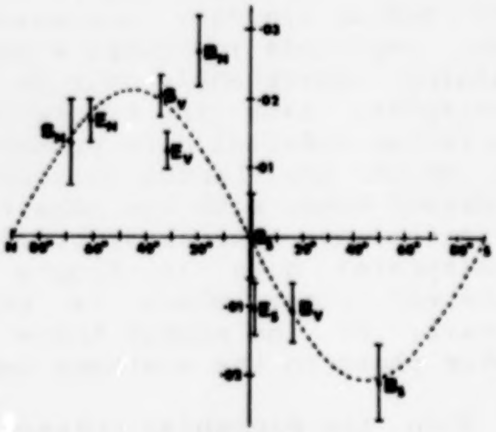

Fig. 2: Amplitude data from Fig. 1 plotted against viewing latitude λ; dashed curve is the function A sinλ Cosλ fitted to the data. Amplitudes are in percent.

ORIGINAL PAGE IS
OF POOR QUALITY

pected 180° phase difference between the two hemispheres; the deviations from the corresponding eigen values (23.3 h and 11.3 h) are consistent with the cosmic ray orbital deflection in the geomagnetic field (Fujimoto et al., 1984).

In Figure 2, the data from Figure 1 are displayed in terms of the anti-sidereal amplitude for each of the nine telescopes, plotted as a function of its asymptotic latitude. Superimposed upon the diagram is a graph of the function A $\sin\lambda.\cos\lambda$ (dashed line), with the amplitude A adjusted to provide the best fit to the experimental points. The data conform very well the theoretical expectation (equation 1).

CORRECTED SIDEREAL DATA Nagashima et al [1985] have demonstrated that the anti-sidereal data can be used to remove the related spurious sidereal diurnal variation from the observed diurnal variation in sidereal time. The correction is achieved by rotating the observed anti-sidereal vector by 4.53 hours counter-clockwise, reducing its amplitude by a factor of 0.947, and then subtracting it from the observed sidereal vector. This method has been applied to the data from the nine telescopes used here, and the resulting corrected sidereal diurnal variation vectors for each telescope, for all available data, are presented in Figure 3 as harmonic dials in sidereal time. The vectors for the northern hemisphere telescopes (Embudo and Socorro) all lie in the first quadrant, in the vicinity of 3h sidereal time. The amplitude for the Socorro telescope (median regidity 305 GV) is significantly greater than that of the Embudo telescope (median rigidity 132 GV). These results are consistent with the observations by Bercovitch [1984], using surface telescopes detecting muons arriving at large zenith angles, in which, as the median rigidity increased beyond about 100GV, the sidereal amplitude increased with rigidity, with the phase remaining consistently near 3h sidereal time. The northern hemisphere data in Figure 3 are also consistent with the corrected sidereal data presented by Nagashima et al. [1985], in which the London telescope had a maximum at about 3h sidereal time, with the Hobart telescope observing a somewhat later maximum near 6h sidereal time. The Bolivia (southern hemisphere) data in Figure 3 show a maximum close to 9h sidereal time, which is even later than what is seen at Hobart; at the moment there is no clear explanation for the later phase in the southern hemisphere.

When the Nagashima correction is applied to the observed sidereal data, the correction is relatively effective in reducing or removing phase changes which occur in uncorrected data upon the reversal of the sun's polar magnetic field in 1969-71 and 1980-81 [Swinson, 1976, 1984]. Data from the Socorro vertical telescope (where the sidereal anisotropy is greatest) are shown in Figure 4. In the uncorrected data, a clear phase change can be seen in 1971 and 1981, after the

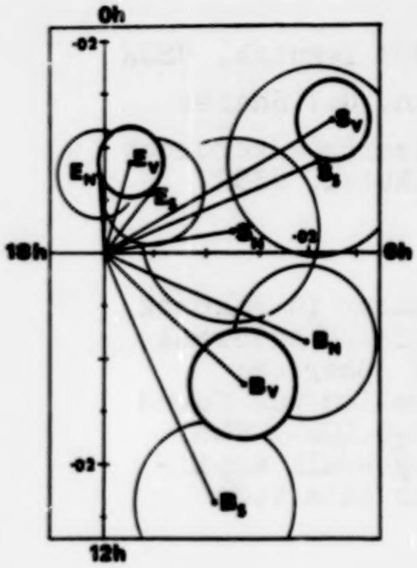

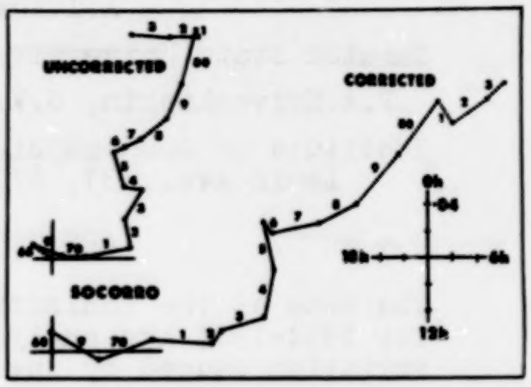

Fig. 4. Yearly harmonic dials in sidereal time for the Socorro vertical telescope, uncorrected and with the Nagashima correction.

Fig. 3. Harmonic dial in sidereal time for Bolivia, Embudo & Socorro North, South and Vertical telescopes with the Nagashima correction. Amplitude scale is in percent.

two most recent solar field reversals. The data corrected by the Nagashima method, however, show very little change, with the yearly vectors remaining relatively consistent, regardless of the magnetic configuration of the heliosphere. This gives one more confidence that the data, corrected in this fashion, are representative of a truly galactic anisotropy.

ACKNOWLEDGEMENTS: The work of one of the authors (DBS) was supported by the Atmospheric Sciences Section, National Science Foundation, under grant ATM-8305098.

REFERENCES

Bercovitch, M., Proc. Int. Symposium on Cosmic Ray Modulation in the Heliosphere, Morioka, Japan, p. 329, 1984.

Fujimoto, K., A. Inoue, K. Murakami and K. Nagashima, Rep. of Cosmic-Ray Research Laboratory, Nagoya University, No. 9, 1984.

Nagashima, K., Proc. Int. Symposium on Cosmic Ray Modulation In The Heliosphere, Morioka, Japan, p. 309, 1984.

Nagashima, K., R. Tatsuoka and S. Matsuzaki. Nuovo Cim., 6C, No. 5, p. 550, 1983.

Nagashima, K., S. Sakakibara, A. G. Fenton, and J. E. Humble, Planet. Space Sci., 1985 (in press).

Regener, V.H. and D.B. Swinson, Can. J. Phys., 46, S784, 1968.

Swinson, D.B., J. Geophys. Res., 81, 2075-2081, 1976.

Swinson, D.B., Proc. Int. Symposium on Cosmic Ray Modulation in the Heliosphere, Morioka, Japan, p. 338, 1984.

N85-35006

SH 4.4-8

SIDEREAL ANISOTROPY OF COSMIC RAYS

A.I.Kuzmin
Yakutsk State University, 677007 Yakutsk, USSR
P.A.Krivoshapkin, G.V.Skripin, G.V.Shafer
Institute of Cosmophysical Research & Aeronomy
Lenin Ave., 31, 677891 Yakutsk, USSR

ABSTRACT

The data of the ionization chamber in Yakutsk for 1954-1984 are analyzed. A false sidereal variation caused by the second spherical harmonic in cosmic ray distribution was found and it has the amplitude 0.020±0.002%. The sidereal anisotropy with a very small amplitude (not more than 0.005%) was observed to exist.

In Table 1 the characteristics of the first harmonic of the solar-diurnal, sidereal and anti-sidereal variations of cosmic rays on data of the ionization chamber in Yakutsk from 1954 to 1984 are given. The data are pressure corrected.

From Table 1 it is evident that all the three variations significantly change from year to year. The solar-diurnal variation phase in 1954 and 1955 shifted to very early time as compared with other years. This tendency manifested in 1976 which evidences the 22-year recurrence of this variation.

The sidereal variation is ∼3 times less than the solar-diurnal one. Its maximum time, on average, is 21 hr of the sidereal time varying 2-3 hours from it at various years. Sidereal variation in 1958 was somewhat anomalous with a very small amplitude (0.009%) and early maximum time (14.7 hr).

The anti-sidereal variation suffers the stronger changes from year to year either on amplitude or on phase. Its amplitude is ∼2.5 times less and the maximum time is at earlier hours (13.8 hr) in comparison with the sidereal variation.

In Table 1 data separately for two periods 1958-1968 and 1972-1981 being characterized by various polarity of the general magnetic field of the Sun are also shown. It is evident that phases of sidereal and anti-sidereal variations at these periods are almost invariable. And the phase of the solar-diurnal variation in the second period 2,4 hr to the earlier time is shifted. The amplitudes of all the variations in 1972-1981 increased by 15-30%.

In Table 2 the characteristics of all the three variations corrected to pressure, influence of atmospheric temperature and the Earth's magnetic field (J_{hTM}) are presented. Contribution of the temperature (T) was determined by the method described in [1] . Vectors T were substracted from the average observed vectors of the intensity anisotropy of of corresponding variations presented by the last three lines in Table 1. Then using receiving vectors [2] for the ionization chamber the correction to the influence of the geomagnetic field was introduced.

Table 2

Characteristics of solar, sidereal and anti-sidereal vectors of diurnal variation of ground temperature (t), of the contribution of the whole atmosphere (T) and of cosmic ray intensity corrected to atmospheric effects and to geomagnetic field (J_{hTM})

Vector	Period	Solar-diurnal		Sidereal		Anti-sidereal	
		Amp.	φ,h	Amp.	φ,h	Amp.	φ,h
t, °C	I*	3.9±0.1	15.2	1.4±0.1	8.1	1.1±0.1	21.5
T, $\%\cdot10^{-3}$	II	40 ±3	4.7	14 ±1	21.9	11 ±1	10.2
J_{hTM}, $\%\cdot10^{-3}$	I	244 ±8	16.8	24 ±2	21.7	20 ±2	20.3
t, °C	III	3.8±0.1	15.1	1.4±0.1	8.1	1.1±0.1	21.3
T, $\%\cdot10^{-3}$	III	60 ±4	4.8	22 ±1.5	21.8	17 ±1.1	11.0
J_{hTM}, $\%\,10^{-3}$	III	265 ±8	17.4	15 ±3	15.9	20 ±2.2	21.4
t, °C	IV	3.9±0.1	15.4	1.3±0.1	8.1	1.1±0.1	21.8
T, $\%\cdot10^{-3}$	IV	24 ±4	4.7	8 ±1.3	21.4	7 ±1.1	11.3
J_{hTM}, $\%\cdot10^{-3}$	IV	239 ±8	15.9	33 ±3	23.0	19 ±2.3	18.0

* I - 1954-1983, II - 1958-1979, III - 1958-1968,
IV - 1972-1981

From Table 1,2 it is evident that after the corrections J_{hTM} were made the solar diurnal variation amplitude at all the observation periods increased by ~3 times and the phase had shifted 4 hr to later time. As for above two periods the amplitude of solar diurnal variation at the first period (1958-1968) in comparison with the second period became larger and the phase difference remained almost invariable. The phases of the solar-diurnal variation vectors of ground temperature (t) and of vectors T do not change on time. However, the T vector amplitude in the second period is more than twice larger than in the first one.

The J_{hTM} vectors of sidereal and anti-sidereal variations for 30-year period are equal on the value and differ significantly on the phase. Such a behaviour of the variation can be explained as it was shown in [3] by antisymmetric diurnal variation caused by the second spherical harmonic of the cosmic ray distribution in the interplanetary magnetic field. Due to this reason a false sidereal variation with the amplitude 0.020+0.002% and phase 21.7 hr occurs. After substraction of anti-sidereal variation from

Table 1

Amplitudes and phases of solar-diurnal, sidereal and anti-sidereal variations on data of ASK-1 ionization chamber in Yakutsk

Years	Solar-diurnal		Sidereal		Anti-sidereal	
	$A\cdot10^{-3}$,%	φ,h	$A\cdot10^{-3}$,%	φ,h	$A\cdot10^{-3}$,%	φ,h
1954	55±2	5.8	70±2	22.0	29±2	4.1
1955	71	8.9	48	21.7	10	5.6
1956	107	12.2	34	20.8	16	14.3
1957	95	13.6	34	18.0	34	13.3
1958	90	13.6	9	14.7	15	14.2
1959	93	14.7	31	19.3	29	13.3
1960	95	14.9	37	19.7	14	15.3
1961	55	14.8	33	18.9	19	22.9
1962	96	14.8	27	19.4	8	13.3
1963	80	13.8	21	22.3	22	12.3
1964	72	13.3	15	21.9	9	13.8
1965	58	12.2	17	19.5	14	17.3
1966	89	13.7	15	20.5	7	15.8
1967	83	13.3	35	23.8	14	10.3
1968	87	14.3	23	23.9	3	18.2
1969	89	14.3	12	23.0	10	8.4
1970	87	13.5	15	01.4	5	9.8
1971	109	12.3	19	23.2	3	22.8
1972	91	11.4	35	22.2	6	13.0
1973	98	11.3	20	23.7	11	13.1
1974	95	12.6	24	18.5	18	17.6
1975	96	10.4	34	20.7	18	11.1
1976	84	9.9	21	23.0	10	13.2
1977	108	11.0	25	17.5	39	14.1
1978	117	11.0	18	21.7	15	18.1
1979	106	12.9	29	21.2	23	11.4
1980	91	13.1	24	22.6	22	18.2
1981	89	12.7	26	22.3	18	12.0
1982	87	14.7	26	19.4	3	13.9
1983	84	13.7	42	19.0	24	15.8
1984	105	14.7	35	21.7	15	12.5
1954-1983	78±0.3	12.8	24±0.3	21.0	9±0.3	13.8
1958-1968	80±0.5	14.0	20±0.5	20.6	10±0.5	14.3
1972-1981	93±0.5	11.6	23±0.5	21.3	13±0.5	14.2

sidereal one by means of mirrow reflection of anti-sidereal variation relative to the 21 hr direction (as in [4]) the galactic sidereal variation within the errors is not found.

Anti-sidereal variation on amplitude and phase does not change. This feature can be interpreted by the influence of the second harmonic in the cosmic ray distribution.

The sidereal variation suffers significant changes either on amplitude or on phase. Substracting anti-sidereal variation from sidereal one by the above method we obtain the galactic sidereal variation for 1958-1968 with an amplitude 0.018±0.002% and a phase 11.0±0.4 hr and for 1972-1981 - 0.015±0.002% and 22.0±0.4 hr. The vectors are equal on the value but their phases are almost opposite. It indicates the significant influence of sign change of the solar magnetic field upon galactic sidereal variation.

In conclusion it should be noted that on data of the ionization chamber in Yakutsk it was found: 1) the existence of false sidereal variation with an amplitude 0.020±0.002% and a phase 21.0+0.4 hr from contribution of the second spherical harmonic. 2) at periods of various polarities of the solar magnetic field the similar on the amplitude (0.005%) sidereal variation but with opposite phase was observed to exist.

References

1. Kuzmin, A.I. i dr.,(1971) *Geomagnetizm i aeronomiya*, *11*, 523.
2. Fujimoto, K. et al.,(1984) *Report of Cosmic Ray Research Laboratory*, No.9, Nagoya, Japan, 185.
3. Krivoshapkin P.A.,(1970) *Geomagnetizm i aeronomiya*, *6*, 761.
4. Elliot, H., et al.,(1970) *Proc.11-th ICRC*, Budapest, Acta Phys.Hung., 29, Suppl.1, 491.

SH 4.4-9

N85-35007

COSMIC RAY INTENSITY VARIATIONS OBSERVED AT MATSUSHIRO (220 M.W.E. IN DEPTH)

S. Yasue, S. Mori and S. Sagisaka
Department of Physics, Faculty of Science
Shinshu University, Matsumoto 390, JAPAN

ABSTRACT

Cosmic ray data from Matsushiro underground station have been analyzed for four years (1981-84). It is found that a marked semi-annual intensity variation has been observed in this period. Solar diurnal and semi-diurnal variations have also been observed. After correcting for the spurious sidereal diurnal variation arising from the anisotropy responsible for the solar semi-diurnal variation (Nagashima et al., 1983), it is found that the corrected siderial diurnal variation is consistent with those so far reported.

1. Introduction. Deep underground observation of the cosmic ray intensity variation provides valuable information as to the nature of modulation in the heliosphere. Matsushiro underground cosmic ray station has been in operation since Aug. 1980 at the depth of 220 m.w.e. (Yasue et al., 1981a). The median primary rigidity of the vertical telescope is about 700 GV (Fujimoto et al., 1984), and its counting rate is 2.1×10^4/h. The analyses of the observed intensity variations of the vertical telescope for four complete years (1981-84) are presented.

2. Semi-annual intensity variation. At the Paris Conference, we have reported that the most part of the unexpectedly large barometric coefficient (~-0.05%/mb) observed at deep underground stations (Humble et al., 1979; Yasue et al., 1981b) can be attributed to the atmospheric temperature effect (Yasue et al, 1981b). In this report, we present another phenomenon which also seems to be caused by the atmospheric temperature effect. Fig. 1 shows the monthly averaged intensity varia

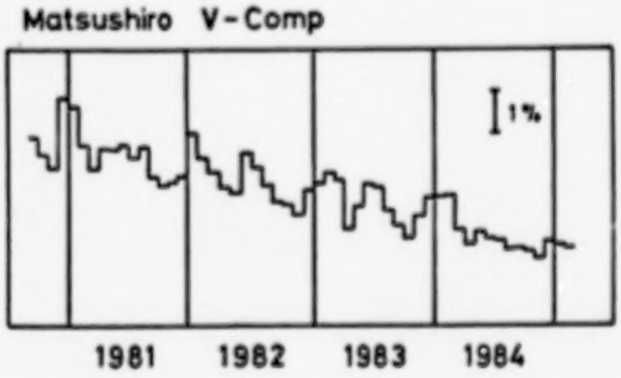

Fig.1 Monthly averaged intensity variation.

tion of the vertical telescope (abbreviated as V-Comp) observed at Matsushiro. In the figure, we can notice a marked semi-annual intensity variation superposed on a gradual intensity decrease. The intensity decrease (about 1 % per year) may be due to the decrease in detector efficiency of the scintillation counters (Ueno, private communication). The semi-annual intensity variation takes the maximum value both in summer and in winter. Such a variation has not been observed at the shallower underground stations than Matsushiro (Ueno et al., 1979). The most part of this variation can be explained quantitatively in terms of the variation of the upper atmospheric temperature (Sagisaka, 1984).

3. Observed daily variations. Fig. 2 shows the daily variations of V-Comp (top) and atmospheric pressure (bottom) averaged over four years (1981-84) for solar (SO), sidereal (SI) and anti-sidereal (AS) time. Cosmic ray data are not corrected for pressure. In the figure, V-Comp shows not only significant SI daily variation but also SO and AS daily variations. It is noted, however, that the atmospheric temperature effect described in the previous section may contaminate also the daily variations.

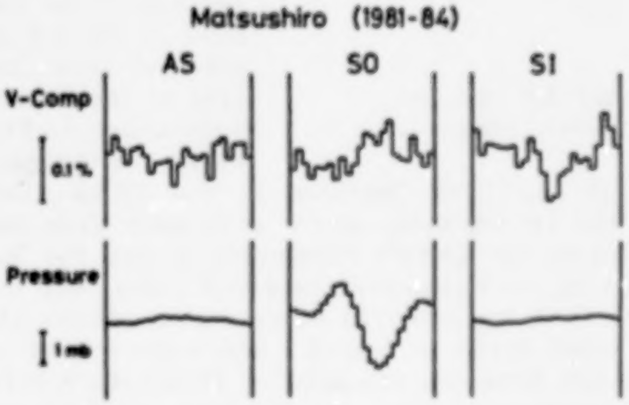

Fig.2 Averaged daily variation of V-Comp and atmospheric pressure for solar(SO), sidereal(SI) and anti-sidereal(AS) time.

We can find in Fig. 2 that the daily variations of pressure in SI and AS time are negligibly small (about one-tenth) compared with that in SO time. This fact implys that we may reasonably assume that the influence of the atmospheric effects becomes serious only in SO time and can be neglected in SI and AS time.

4. Solar daily variation. The heavy solid lines in Fig. 3 show the 1st and 2nd harmonic vectors of the daily variation (SO) of V-Comp shown in Fig. 2. The error circles are the standard error of each mean vector estimated from the dispersion of yearly vectors. In the following, we try to estimate SO harmonic vectors caused by the temperature effect. By analyzing observed data from multi-directional

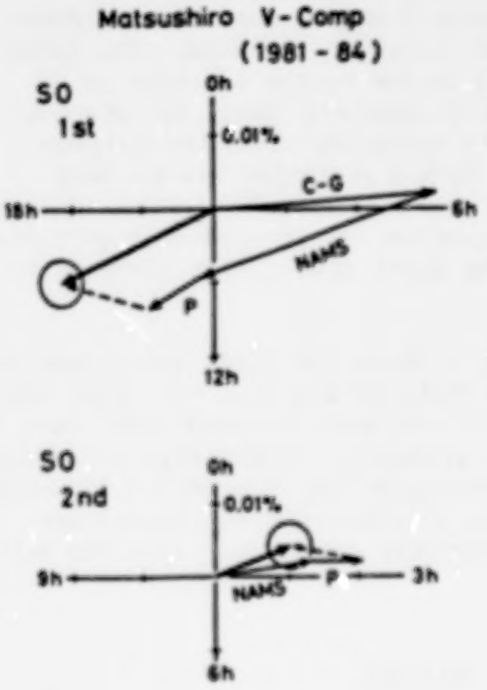

Fig. 3 Solar 1st and 2nd harmonic vectors.

muon telescopes at Nagoya and underground telescopes at Misato and Sakashita (NAMS) in the period of 1978-83, Ueno et al. (1984) and Morishita et al. (1984) determined, respectively, the characteristics of the anisotropies responsible for the solar diurnal and semi-diurnal variations. Assuming those anisotropies obtained by them, and using the coupling coefficients (Fujimoto et al, 1984), we can estimate the expected solar diurnal and semi-diurnal variations at Matsushiro in this period. The obtained vectors are shown in Fig. 3 with the vectors 'NAMS'. These vectors are free from the atmospheric effects. The vectors 'P' in the same figure show SO 1st and 2nd harmonics produced from the daily variation of the atmospheric pressure shown in Fig. 2. Here, we assume the genuine barometric coefficient of -0.01%/mb (Sagisaka et al., 1979). The vector 'C-G' in Fig. 3 shows the 1st harmonic vector originated from the Compton-Getting effect due to the Earth's revolution around the Sun. Composing the above vectors on the respective harmonic dials, and comparing the resultant vectors with the observed ones, we can obtain the residual vectors (dashed line) shown in Fig. 3. One might expect that these vectors are produced from the atmospheric temperature effect. (It is noted that other unknown vectors, one of which may be originated from the galactic anisotropy (Nagashima et al., 1982), might also be included in these vectors.)

5. SI and AS daily variations. It is emphasized that the solar daily variation is observed even at this depth (220 m.w.e.) in this period. As has been described by Nagashima et al. (1983, 1985), the second order solar anisotropy responsible for the observed semi-diurnal variation produces the AS 1st harmonic vector with the phase of 0h, due to the tilt of the spin axis of the Earth to the ecliptic plane. The present observation seems to support his expectation. Namely, the observed AS vector in Fig. 4 seems to be interpreted as the side-band vector produced from the 2nd order anisotropy at 3h-21h. In this case, another side-band vector (spurious sidereal vector) should be observed according to his theory. This vector can be derived from the observed AS vector (Nagashima et al., 1983), and is shown by the dashed line (amplitude and phase of the vector is 0.014% and 19.4h, respectively) on the SI harmonic dial (see Fig. 4). If we subtract this spurious S

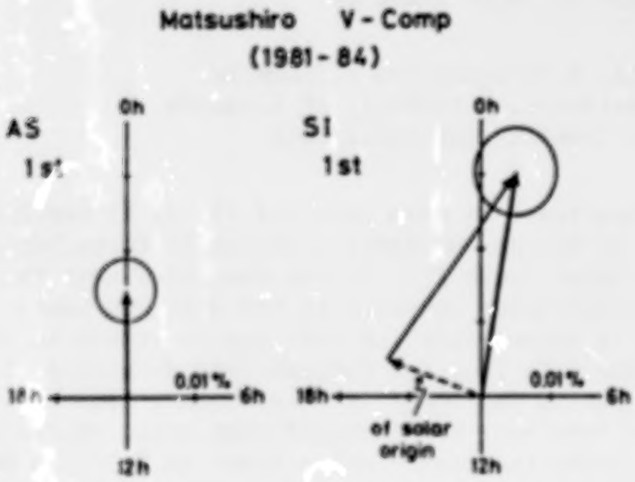

Fig.4 Sidereal and anti-sidereal harmonic vectors.

vector from the observed SI vector, we can obtain the true SI vector of galactic origin. The resultant vector has the amplitude of 0.031% and the phase of 2.3h. The present result seems to be consistent with those so far reported (Nagashima et al., 1985).

Acknowledgements. The authors express harty thanks to Prof. K. Nagashima for his encouragement and discussions with them. Thanks are also due to Mr. K. Chino for his help in data processing.

References

Fujimoto, K. et al. (1984), Rep. of C. R. Res. Lab. Nagoya Univ. No.9.
Humble, J.E. et al. (1979), Proc. 16th ICRC (Kyoto) 4, 258.
Morishita,I. et al. (1984), Proc. Int. Symp. C.R. Mod. (Morioka), p130.
Nagashima, K. et al. (1982), Planet. Space Sci. 30, 879.
Nagashima, K. et al (1983), Nuovo Cimento 6C, 550.
Nagashima, K. et al. (1985), Planet. Space Sci. (in press).
Sagisaka,S. et al. (1979), Proc. 16th ICRC (Kyoto) 4, 235.
Sagisaka, S. (1984), Proc. Int. Symp. C. R. Mod. (Morioka), p360.
Ueno, H. et al. (1979), Proc. 16th ICRC (Kyoto) 12, 228.
Ueno, H. et al. (1984), Proc. Int. Symp. C. R. Mod. (Morioka), p109.
Yasue, S. et al. (1981a), Proc. 17th ICRC (Paris) 4, 304.
Yasue, S. et al. (1981b), Proc. 17th ICRC (Paris) 4, 308.

60 N85-35008

SH 4.4-10

LONG-TERM MODULATION OF COSMIC RAYS DURING SOLAR CYCLE 21

A.G.Fenton, K.B.Fenton and J.E.Humble
Physics Department, University of Tasmania
Hobart Tasmania Australia 7001

1. Introduction. In recent years we have reported (1, 2, 3) results from the Australian chain of neutron monitors relating to Forbush-type decreases observed during Solar Cycle 21. It was concluded that the rigidity dependence of the decreases observed in the southern hemisphere during this period is essentially the same now as it was in the previous cycle. Fitting the data from ten Forbush-type decreases of amplitude ≥ 4% during the period September 1977 to January 1983 to a modulation function of the form $\exp(-K/P^{\gamma})$ showed that these events were consistent with $0.5<\gamma<0.9$, with the mean γ-value close to 0.7. In this paper we report a preliminary result concerning the rigidity dependence of the longer-term solar cycle modulation.

2. Neutron Monitors, Data and Methods. The neutron monitors chiefly referred to in this paper are 9NM64-type, located near sea level at Hobart (42.9°S, 147.3°E, vertical cut-off 1.89 GV), Brisbane (27.4°S, 153.1°E, 7.24 GV) and Darwin (12.4°S, 130.9°E, 14.07 GV). The neutron monitor at The Springs at an altitude of 725m on the slopes of Mt.Wellington, overlooking Hobart, is currently a 6NM64, but before 1967 there was a 12-counter IGY-type monitor at this site. By careful normalisation of data from different neutron monitors operated in the Hobart area it has been possible to obtain a continuous record of intensity back to July 1956. Other monitors operated by the Hobart group include a 12-counter IGY-type at Mawson, Antarctica (67.6°S, 62.9°E, 0.22 GV) and IGY-type monitors operated at Lae, New Guinea (6.7°S, 147.0°E, 15.52 GV) for some years beginning with the IGY period, and at Brisbane from 1960 until the 9NM64 was installed. It is hoped that it will be possible in the near future to coordinate the results from these stations to determine the solar cycle modulation during Solar Cycle 20, as observed by these southern recorders.

The 11-year solar cycle modulation was assumed to be of the exponential form with exponent $-K/P^{\gamma}$, as discussed in earlier papers (1, 2, 3). An attempt was made to find a best-fit γ, using monthly mean data selected to be relatively free from Forbush-type decreases. Figures 1 and 2 show respectively the long term changes observed at Mt.Wellington, and daily mean intensities over the 4-months period including the major transient event of July, 1982.

3. Results. The long-term modulation, using monthly mean intensities selected as above, and referred to November 1977 as a normalising level, appear to be in accordance with the exponent $\gamma = 1$, provided only Brisbane and Hobart data are used. Darwin data do not conform to this pattern except perhaps during the early years of the cycle until about the end of 1980, since when the Darwin long-term intensity has been largely steady, apart from Forbush-type decreases and as yet unidentified

ORIGINAL PAGE IS
OF POOR QUALITY

small changes of the order of 1%. Thus these results must be regarded as preliminary.

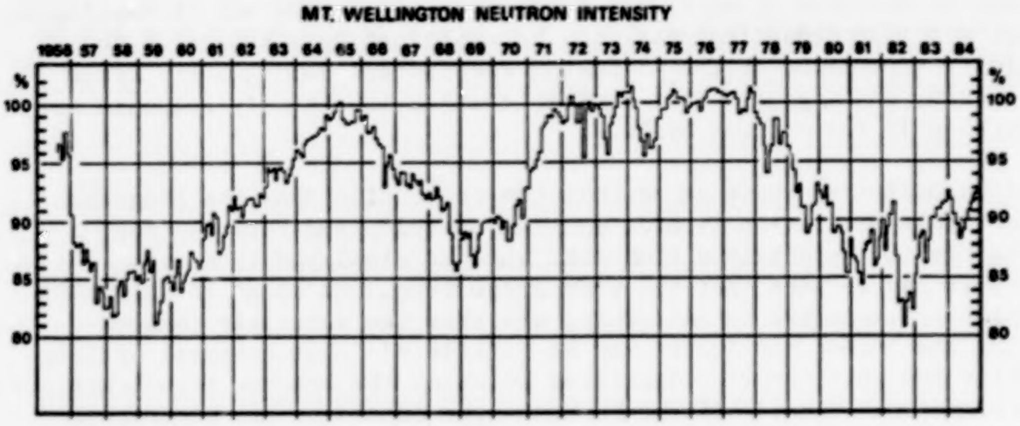

FIGURE 1

Monthly mean neutron intensities relative to May, 1965.

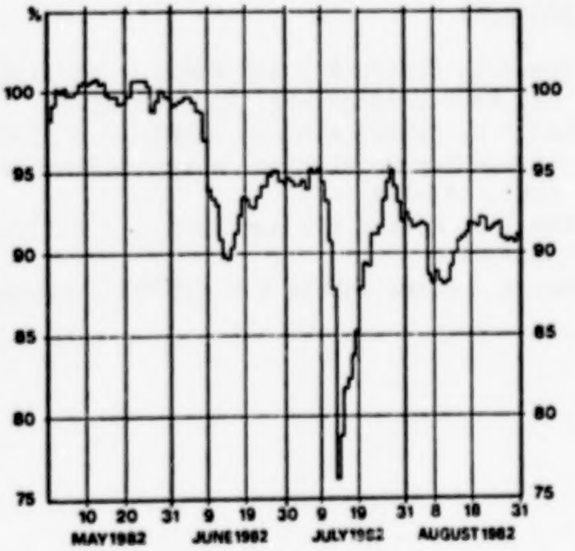

FIGURE 2

Daily mean pressure-corrected Mt.Wellington neutron intensities for May-August 1982, expressed as percent of mean level for May.

4. Discussion. The results seem to confirm the conclusion reached earlier that the Forbush-type modulation and the 11-year cyclic changes have a different rigidity response, and thus is probably caused by different mechanisms under solar influence; however, from our preliminary analysis it may be that the long-term changes have been limited to rigidities below about 10 GV since solar maximum, which occurred in December 1979. This observation would agree with a report by Lockwood and Webber (4) that the observed hysteresis effect between the integral intensity measured by satellite cosmic ray telescopes and Mt.Washington neutron monitor counting rates can be explained by a change in the rigidity dependence of the diffusion coefficient during Solar Cycle 20, 1965-1976, and suggests that similar changes in rigidity response are occurring in the current cycle.

Semi-quantitative evidence against the contention that the long-term solar cycle modulation is made up from superimposed Forbush-type decreases may be obtained from data such as displayed in Figure 2. Here, it may be seen that the very large transient event in July 1982 completely recovered by late July, and that the intensity changes during the period May-August may be considered to be composed of long-lasting possibly stepwise decreases on which the shorter transients are superimposed. Indeed, if the Forbush-type decreases are considered separately, the total 'count' removed by them is only about half the total removed by the longer-term effect.

5. Acknowledgements. We wish to thank the staff of the Bureau of Meteorology stations at Brisbane and Darwin airports for their valuable assistance in the operation of these neutron monitors. The neutron monitor programme at Hobart, Brisbane and Darwin has been supported in part by grants from the Australian Research Grants Scheme.

6. References.

1. Fenton A G, Fenton K B and Humble J E (1983). Proc.18th Int.Cosmic Ray Conf., Bangalore, 10, 164-167
2. Fenton A G, Fenton K B and Humble J E (1984). Proc.Int.Symposium on Cosmic Ray Modulation in the Heliosphere, Morioka, Japan, 1984, 191-196
3. Fenton A G, Fenton K B and Humble J E (1984). Proc.ASA 5 (4), 590-593
4. Lockwood J A and Webber W R (1979) J.Geophys.Res. 84, 197-202

ORIGINAL PAGE IS
OF POOR QUALITY

N85-35009

ROLE OF SOLAR FLARE INDEX IN LONG TERM MODULATION OF COSMIC RAY INTENSITY

P.K.Pandey*, A.K.Jain, P.K.Shrivastava, S.P.Pathak**
and S.P.Agrawal
Physics Department(Vikram Space Physics Centre)
A.P.S.University, Rewa(M.P.)486003, India.

ABSTRACT

Recently, the importance of the occurrence of solar flares in the long-term modulation of cosmic ray intensity has been re-emphasized. For this purpose, the data of solar flares have been used from various publications, such as Solar Geophysical Data books, U.A.G. reports and Quarterly Bulletin Of Solar Activity. Our investigation, very clearly reveals that even the periodic changes in the solar flare observations, obtained from the four different data sources, for the same interval, differ significantly from one another; this is evident even on an average basis. Hence, in any study using solar flares, the importance of selecting a single compilation of the solar-flare data for the entire period of investigation is stressed.

1. Introduction. The study of the long term records of cosmic ray measurements, extending to energies beyond 100 Gev., have confirmed the eleven year solar cycle variation of cosmic ray intensity. Recent results (Hatton, 1980; Hatton and Bowe, 1981; Hatton and Bowe, 1983) using the number of solar flares, of importance ≥ 1, and the cosmic ray intensity deviations, have provided an empirical relation with better correlations for a time lag of ≈ 10 months. Such a time lag corresponds to a value of ≈ 70 A.U. for the solar modulating boundary. The goodness of fit has been shown to be quite satisfactory. The use of solar flares for such a correlation studies, often assumes that the total number and importance of solar flares would be the same, irrespective of the source of data of the solar flares. In this paper, we define a more realistic index for using the solar flare data, and then derive the monthly solar flare indices (SFI) for an extended period of time, from 1957-84, to compare it with the monthly averages of the cosmic ray intensity. During the course of investigation, we have found very significant difference in the solar flare indices, when derived from the tabulation of solar flares published in different data sources. These differences are quite large, hence need to be emphasized.

---

* Also at - Govt.Girls Degree College,Rewa(MP.)486001.
** Also at - Govt.Science College, Rewa (MP.) 486001.

ORIGINAL PAGE IS
OF POOR QUALITY

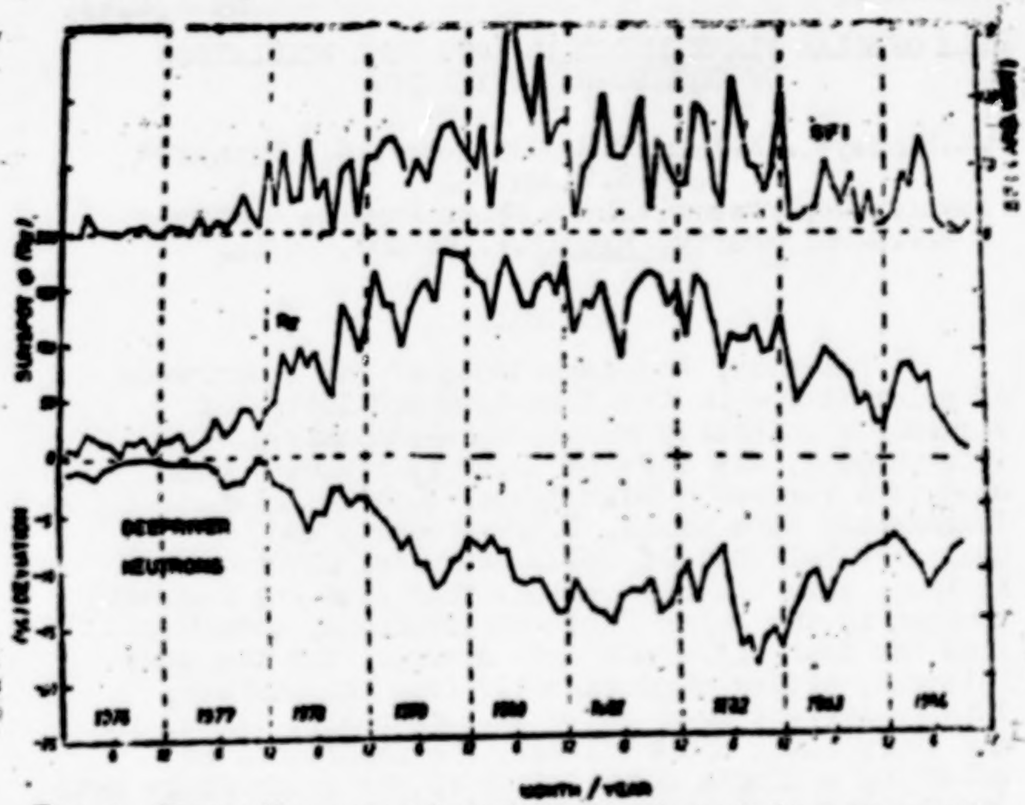

Fig.1 Shows the percent deviation of monthly mean cosmic ray intensity observed by Deep River Neutron monitoring station. The 100% level is taken as the average for the month, Sept.-Nov. 1976. The monthly values of sunspot number (Rz) and solar flare index (SFI; see text for details for computing SFI) are also plotted for the year 1976-84.

2. Solar flare index. The occurrence of the solar flares are routinely published in solar Geophysical Data, both in the prompt reports as well as in the comprehensive reports. The solar flares are also listed in the quarterly Bulletin of solar Activity as well as in a slightly modified form in the UAG reports of World Data Centre-A. From these listing, various investigators have used the information of the occurrence of solar flares for comparison, with other observations. Usually, for most of the studies the solar flares of importance $\geqslant 1$ are selected (as was done by Hatton, 1980; for Cosmic ray investigations). In these studies the number of solar flares were added without giving any weight either to the importance of the flares or to their brightness. The solar flare brightness is usually represented by B, N and F, whereas the flare-importance is represented by numerical numbers 1, 2, 3 and rarely also 4. We have therefore, generated a

ORIGINAL PAGE IS OF POOR QUALITY

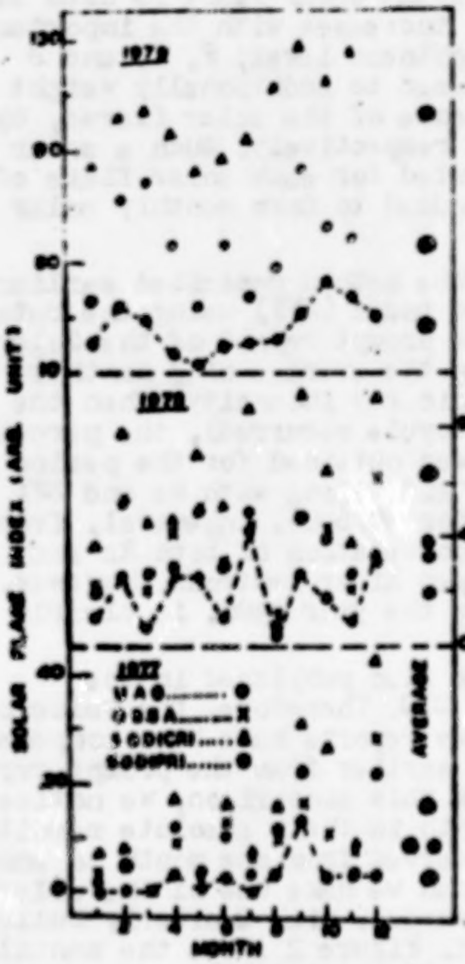

Fig.2 Shows the solar flare index for each month for the three years of high solar activity period 1977,78,79,for four different data sources, which are routinely published. The month to month changes are distinguished by joining the line for the solar flare computed from UAG report. The averages are shown in the right most part of the figure.

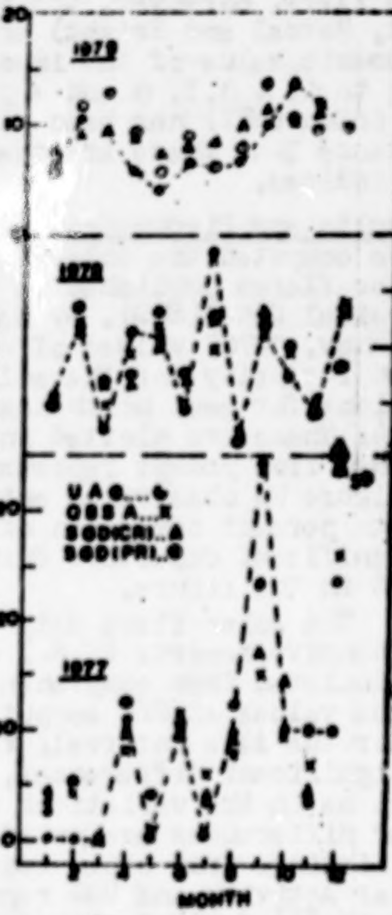

Fig.3 Shows the normalised values of solar flare index for all the monthly data sets and the time interval shown in figure 2. In each case the yearly sums are normalised to 100, to derive the percent solar flare index for each month.

Solar Flare Index (SFI) for each flare, for the interval for which the solar flare data from various sources (mentioned earlier) are available. In generating the new flare index (SFI) the reported importance of the solar flare is used as a numerical weight i.e. the SFI increases with the importance of the flare. Moreover, the brightness level, F, N, and B (Faint, Normal and Bright) are used to additionally weight the numeric value of the importance of the solar flares, by adding to it - 0.3, 0 and + 0.3 respectively. Such a solar flare index (SFI) has been computed for each solar flare of importance ≥ 1. These are then added to form monthly solar flare indices.

3. Results and Discussion. By the method described earlier, we have computed the solar flare index (SFI) using the data of solar flares published in the prompt report of the Solar Geophysical Data (SGD). By using the average of 3 monthly (Sept.-Nov., 1976) values of cosmic ray intensity (when the maximum intensity for the solar cycle occurred), the percent deviations for each month has been obtained for the period 1976-84. These are plotted in fig. 1, along with Rz and SFI (obtained from prompt reports) for 1976-84. In general, from this figure we observe an anti-correlation of both Rz and SFI with percent deviation of Deep River neutrons. However, the significant departure during the year 1980, is clearly evident in the figure.

The solar flare data are also published in the comprehensive reports (C.R.) of SGD. Therefore, the value of SFI calculated from comprehensive reports have been compared with the values of SFI computed earlier from the prompt reports (PR) for the same interval. From this comparison, we notice very significant differences, both in their absolute magnitude as well as in the variations observed from one month to another. Similar differences are noted when we make use of the solar flare listings from other two sources, viz. Quarterly Bulletin of solar Activity and UAG report. Figure 2 shows the monthly values of SFI derived from four different data sources. The annual averages are also marked, to show the difference in their absolute values. It is apparent from the figure that the changes from one month to another are not always similar. As mentioned earlier, if one uses different data sources to compute SFI for different periods, it is necessary to normalise the indices. This has been done for each year by using the yearly sums which are each normalised to 100. The percent solar flare index for each month, has been computed and plotted in figure 3, by using the absolute values plotted in figure 2. From this figure, the large differences in % SFI, from one month to another, comes out in a very significant manner. We conclude therefore, that the solar flare indices generated by either giving weight or otherwise, one should use only one type of data source.

4. References.

Agrawal, S.P.; 1983. Space Science Rev. 34 p. 127.
Hatton, C.J.; 1980 Solar Physics, 66 p. 159.
Hatton, C.J. and Bowe, G.A.; 1981. Proc. 17th ICRC Paris 3 p. 255.
Hatton, C.J. and Bowe, G.A. 1983. Proc. 18th ICRC Bangalore 3, p. 68.

A STUDY OF PERIODICITIES AND RECURRENCES IN SOLAR ACTIVITY AND COSMIC RAY MODULATION

N85-35010

Attolini M. R., Cecchini S.
Istituto TE.S.R.E -C.N.R., Bologna, Italy

Galli M.
Dipartimento di Fisica dell'Università,Bologna, Italy

1. Introduction. Time variability on a wide range of time scales is the main characteristic of cosmic rays observed inside the solar cavity. As the intensity of galactic cosmic rays is assumed to be essentially constant outside the heliosphere, the temporal changes observed must be due to the interaction of CR particles with the IMF which is carried by the solar wind.

The question is then to find out the pattern of the IMF and its flow, to determine the time and spatial evolution of their configurations and to relate them to CR variations.

Unfortunately the direct measurements of the IMF and of the solar wind plasma are insufficient because they are limited to a region close to the ecliptic plane as compared to the vast 3-dimensional extension of the heliosphere. On the other hand CR particles provide an indirect measurement of the global structure of IMF since they sample a large volume of the solar cavity in their travel from its boundary to the Earth.

Yet one can tentatively try to derive important parameters of the interplanetary medium by means of the observations of the source itself, the Sun.

Solar output during the 11yr activity cycle has many different aspects such as the sunspot area and number, the development of polar coronal holes, the solar flares and the solar wind.

Furthermore among the cyclic variations of the various kinds of solar activity one has to distinguish the ones having same period but differing in phase, amplitude and pattern.

It is common practice to use the sunspot number variation as the standard of the solar cycle and to compare to it all the other relevant parameters, even though this approach has not a good physical ground. The same is true for CR intensity since Forbush (1954) discovered an inverse correlation between this latter and the sunspot number. On the other hand the changes in the solar wind characteristics are related to the temperature variations of the corona, which in turn depend on different solar features such as sunspots, flares, polar coronal holes, plages etc. It is then extremely interesting to investigate the possible relationship between these phenomena and the CR intensity.

The spectral and cross-spectral power analysis is the tool that can be used to consider over a wide range of frequencies in a global way correlations on the same time scale between two time series.

We have already analyzed CR variation of ergodic nature (Attolini et al., 1984) but we cannot exclude variations corresponding to spectral lines.

From the operational point of view the best way to study line spectrum is to obtain estimates of the power trough the periodograms and average them on a band as narrow as possible.

This has been done by averaging each periodogram to its consecutive and then repeating this operation six time. in that way we obtain a binomial smoothing which preserve the frequency information over 7 periodograms corresponding to the average of 4.43 independent data equivalent. Since before performing the FFT operation the number of data has been increased to 1024 via zero padding, each coherency value correrponds to 2.13 independent data equivalent. The coherency figure (Y12) is the one defined by Jenkins and Watts (1968). The 95% significance level has been found using simulations on random data series with the same number of data.

In our analysis we have used the monthly data series of the following relevant parameters: *sunspot number* (Rz) from 1944 to 1984 (Solar Geophys. Data); *CR intensity* (RC) from 1944 to 1984 (Huancayo-Climax pressure crrected counting rates); *aa indexes* (aa) from 1944 to 1984 (Mayaud,1973,1975); *major flares* from 1955 to 1979 (Dodson et al.,report UAG N.14,19,52,80).

2. Computations and Results.

a) RC vs Rz

The first thing to note in the comparison of the coherency spectra in Figure 1a-c computed for three different time intervals, is that we can identify two regions,the first one with frequencies higher than 1c/yr, the other one with frequencies lower than 1c/yr. The first one contains few peaks that exceed the 95% confidence level, which do not shift in frequency when increasing the length of the series and whose amplitudes remain the or at least increase with the increase of the number of data. In the other range the peaks slightly wander in frequency and in amplitude; the long wave of 22yr appears only in the longer data set and with low significant level. All the peaks in this region correspond to nearly all possible harmonicsup to 10th order of the 11yr cycle in all the series as it can be better seen in the computation with zero padding of the data up to 2048. The other significant peaks of the second region are at periodicities 10.4m, 156.5d, 70.9d.
The correlation is negative (⊖) in the first two and positive (⊕) in the last case. The 156.5 days may be related to the flare occurrence.

b) RC vs aa

Since solar wind plasma drives geomagnetic activity the aa index has been used to investigate CR intensity variations caused by solar wind changes. Following the study by Feynman(1982) we have considered the aa and the aa_T (i.e. aa corrected for Rz) monthly indexes. The results are shown in Figure 2. One can see that the coherencies between CR and either aa or aa_T do not differ very much. The only difference between the two is the 11yr cycle periodicity. The significant peaks are, however, different from the RC vs Rz and the correlation is always negative. More meaningful is to compare the CR intensity deduced after the subtraction of the sunspot correlation computed according to Nagashima and Morishita (1980). In that case the coherency (Figure 3) is significant in a greater number of frequencies. These periodicities are linked to the polarity of the IMF and possibly some of them represent the aliased peaks of more fundamental periodicities such as 28.2,27.15 and 26.85 days typical either of sector structure as described by Svalgaard and Wilcox (1975) or of the recurrent decreases in CR intensity in correspondence to aa_T increases. This last fact can be consistent with the description of high speed stream effects on CR (Iucci et al.,1979). In fact the analysis by Feynman (1982) has put in evidence that the property

ORIGINAL PAGE IS OF POOR QUALITY

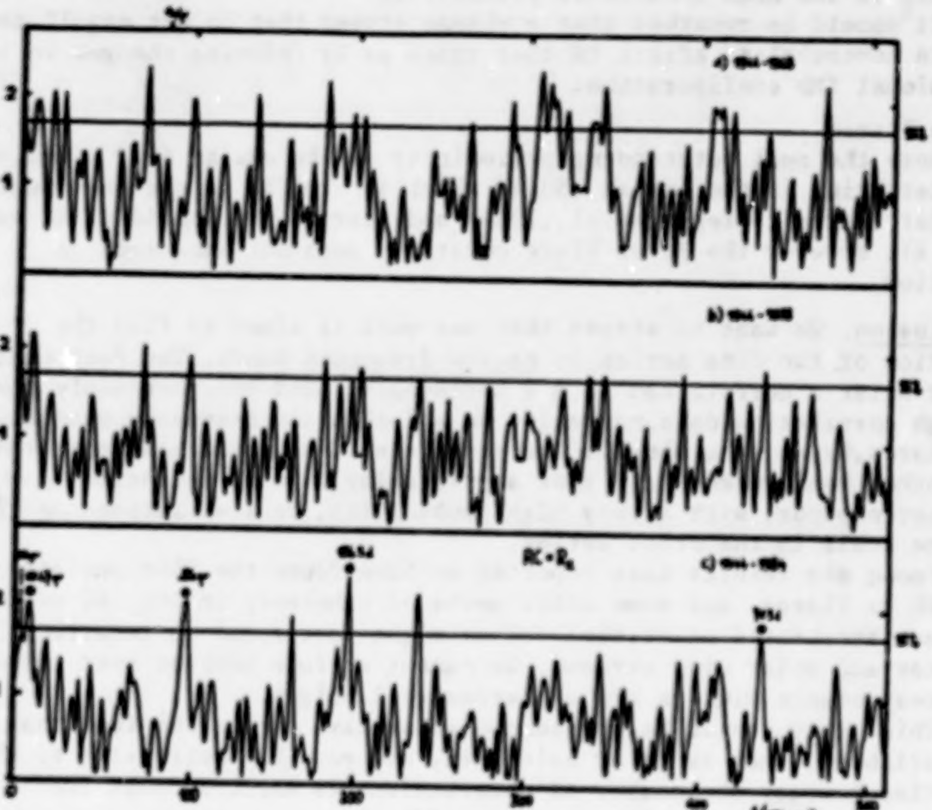

Fig.1

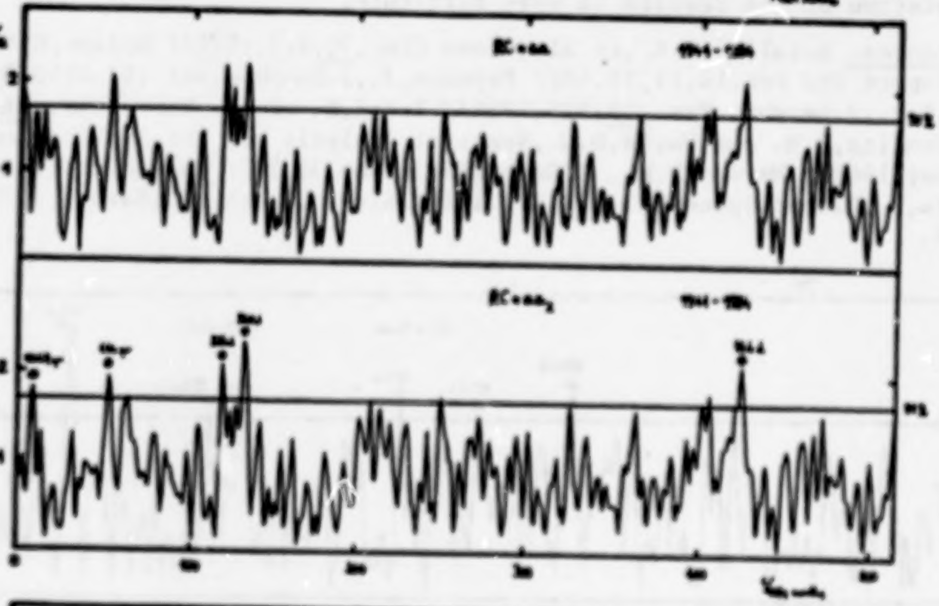

Fig.2

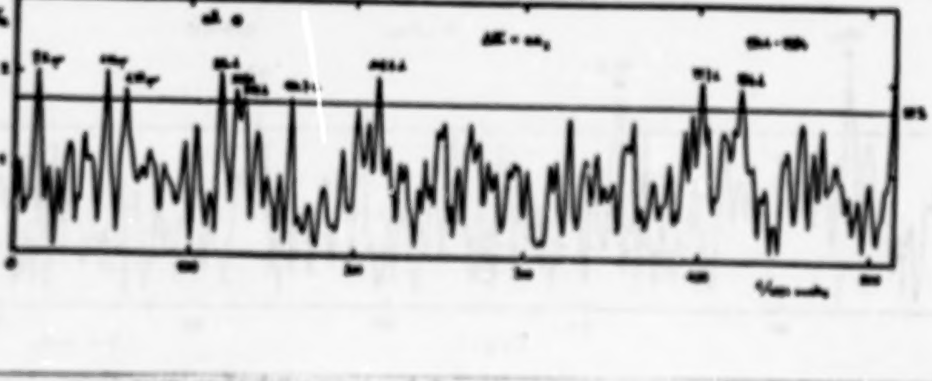

Fig.3

of the aa_I is the high recurrence probability.

It should be remarked that a plasma stream that do not engulf the Earth can nevertheless affect CR that reach us by inducing changes in the 3-dimensional IMF configuration.

c) RC vs Flares

Here the most outstanding periodicity is the one at 66.2 d and the most interesting is the one at 153.4d which is similar to the one found in hard solar flares (Rieger at al.,1984) and near to the 156.4d of RC vs Rz (Figure 4). However the Rz vs Flare coherency does not show such a correlation.

3. Conclusion. We want to stress that our work is aimed to find the correlation of two data series in narrow frequency bands. The fact that does not exist a correlation on a 2 periodogram band does not imply that a very high correlation does not exist on a much wider frequency band (e.g. CR vs Flares,Rz,aa as a whole). The existence of a narrow band correlation, on the other hand, means only that a particular type of variation in a series corresponds, with a very high probability, to a variations on the same time scale in the other series.

Among the results here reported we have found the 154d periodicity in the RC vs Flares, and some other peaks of coherency in the RC vs aa_I that when interpreted as aliased values might correspond to recurring IMF structures and solar wind streams. We cannot exclude however that some of the correspondence with aa are of terrestrial origin.

This study cannot be considered exhaustive due to the fact that other solar variables, such as polar hole size, are possibly correlated to CR intensities,however the number of observations is small so that the interpretation of the results is very difficult.

4. References. Attolini,M.R.,et al.,Nuovo Cim.,7C,413,1984// Dodson,H.W. et al.,Report UAG Nos.14,19,52,80// Feynman,J.,J.Geophys.Res.,87,6153,1982// Forbush,S.E.,J.Geophys.Res.,59,525,1954// Iucci,N. et al.,Nuovo Cim.,26,421, 1979// Jenkins,G.M. and Watts,D.G.,Spectral Analysis and Its Applications, Holden-Day,1968// Mayaud,P.N., IAGA Bulletin Nos.33,39// Nagashima,K.,and Morishita,L.,Planet.Space Sci.,28,177,1980//Rieger,E.,et al.,Nature,312, 623,1984.

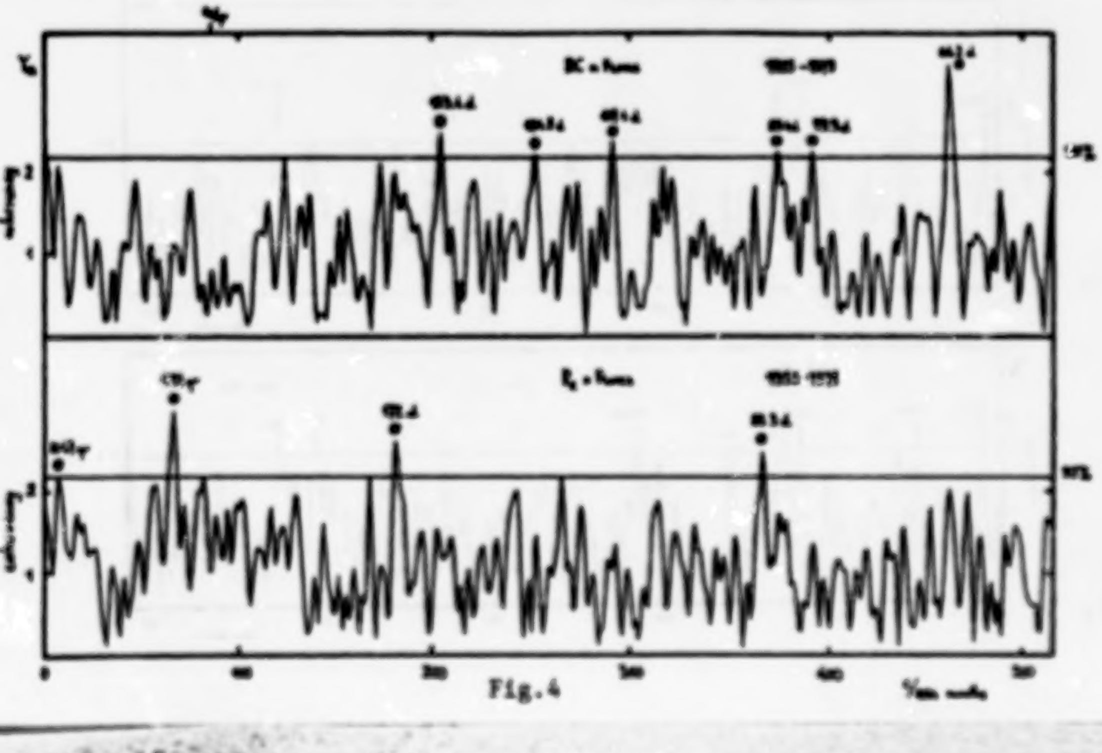

Fig.4

SH 4.4-15

N85-35011

COSMIC RAY BIANNUAL VARIATION

Attolini, M.R., Cecchini, S.
Istituto TE.S.R.E.- C.N.R.,Bologna, Italy

Cini Castagnoli, G.
Istituto di Cosmogeofisica - C.N.R.,Torino, Italy
Istituto di Fisica Generale dell'Università,Torino, Italy

Galli, M.
Dipartimento di Fisica dell'Università, Bologna, Italy

ABSTRACT

The study of the CR power spectrum (Attolini et al., 18th ICRC, Conf.Papers, 10,174,Bangalore 1983) has revealed a significant variation with a period around 2 yr that cannot be explained as a high order harmonic of the 11 yr solar cycle. Comparative study of the correlation on different time scales between CR intensity and Rz, aa, high speed streams and polar hole size (SH 4.4-14, this conference) has put in evidence that a high degree of coherency exists between each couple of variables at 1.58-1.64 yr, except between CR and Rz. On the other hand cyclic variation on a short time scale, around 26 months, has been claimed (Sakurai, 18th ICRC,Conf. Papers, 4,210,Bangalore 1983) to be present in the neutrino flux (Davis et al.,AIP Conf. Proceedings,No.96, 1983). Critical tests of this hypothesis are considered and a preliminary result seems to indicate that the hypothesis of the existence of a 1.6 yr periodicity in the neutrino data during the measurement time interval, has a significance $\geqslant$ 99.9 %.

The possible origin of this variation as due to a contribution either of CR interactions in the upper atmosphere or to the solar dynamics,will be discussed.

SH4.4-16

N85-35012

COSMIC RAY POWER SPECTRAL VARIATIONS:
3. SOLAR ROTATION PERIODICITIES

S. P. Agrawal
Department of Physics (Vikram Space Physics Centre)
A.P.S. University, Rewa (M.P.) 486003, India

ABSTRACT

Earlier studies of the periodic changes in cosmic ray intensity by power spectral analysis provided some understanding of the daily variation in terms of ambient power. The solar rotation periodicities are investigated here using daily means of Calgary neutron monitor data during 1965-76. Significant peaks with periods of 27 and 13.5 days with varying magnitudes are observed.

1. Introduction. It is generally accepted that the galactic cosmic radiation is modulated by the continuously varying solar plasma and fields of the modulating region within the heliosphere. Most cosmic ray variational studies (1-1000 Gev), have used 4 decades of ground-based measurements. These include ~ eleven-year solar cycle variation, Forbush decreases, 27-day variation and the various harmonics of the daily variation.

The 27-day variation has direct bearing on the solar features, on or above the solar surface and remain stable for more than one solar rotation of average period 27 days. The solar modulation is a continuous process and any variations in solar output will affect the interplanetary plasma and field, and in turn upon the flow of cosmic rays. Thus a study of the 27-day recurrence in cosmic ray intensity can provide us with information on solar output and its propagation in the interplanetary medium. Here we derive the 27-day rotation periodicities by power spectral analysis during the interval 1965-76, using the procedure adopted by Lanzerotti et al., (1981).

2. Spectral analysis of cosmic ray data. Daily mean values of Calgary neutron monitor data have been used over the interval 1965-76, for power spectral analysis, to investigate the 27-day periodicies and its harmonics. The Calgary neutron monitor is an 18-NM-64 type detector with statistical fluctuations of 0.02% in daily means. Initially the computations were carried out using one year's data at a time; however the peaks under investigation, were not very clear. Hence we combined 2 3 years of data for deriving the power spectra. The choice of 2 years of data at a time was found optimum to look for individual peaks and to compare their variations during the solar cycle.

3. Results and Discussion. The results of the power spectral analysis are shown in Figure 1. Over a sunspot cycle, the cosmic ray intensity changes (at median energies ~ 10-15 Gev) by about 15-20%, and any two successive years combined here generally correspond to similar solar conditions, with very small changes in cosmic ray intensity. However, large changes in cosmic ray intensity, which occur over periods of days (Forbush type decreases), do affect to some extent the overall spectral

shape, but are not effective in modulating the peaks observed. The vertical dashed lines indicate frequencies corresponding to peaks at 27 and 13.5 days. Note that the main peaks occur for the 27-days period and is quite significant for all the years, except for 1973-74. However, the 13-14 day peak is not very significant for a number of years, such as 1965-66, 1967-68 and 1975-76. These results were essentially confirmed by Sulphur Mountain Cosmic ray data. The power associated with the 27-day peak in 1973-74 is quite low and indicates the possibility that even the stable periodic features of the solar surface were not effective in producing any significant changes in the cosmic ray intensity. Solar coronal holes are quite abundant during 1973-74 and also in 1975-76, and thus an absence of any solar rotation periodicity in 1973-74 perhaps indicated that some other solar feature may be responsible. Venkatesan et al., (1982) have shown that only small changes occur in cosmic rays due to coronal holes. The Chree type of analysis involving some specific solar features, in future, may provide the answer for the observations reported here. It is likely that the solar flares/solar active centres could be the source for the solar rotation periodicity observed. The reason for this is not obvious at present.

4. Acknowledgement. The assistance of Messrs. Arun Tiwari and Vishwarnath Khare in data reduction, etc. is acknowledged. I also wish to acknowledge the Calgary data kindly provided by D. Venkatesan and T. Mathews.

5. References.

Lanzerotti, L. J., Maclennan, C. J., Agrawal, S. P. and Venkatesan, D., (1981), J. Geophys. Res., 86, 6951.

Venkatesan, D., Shukla, A. K., and Agrawal, S. P., (1982), Solar Physics, 81, 375.

ORIGINAL PAGE IS OF POOR QUALITY

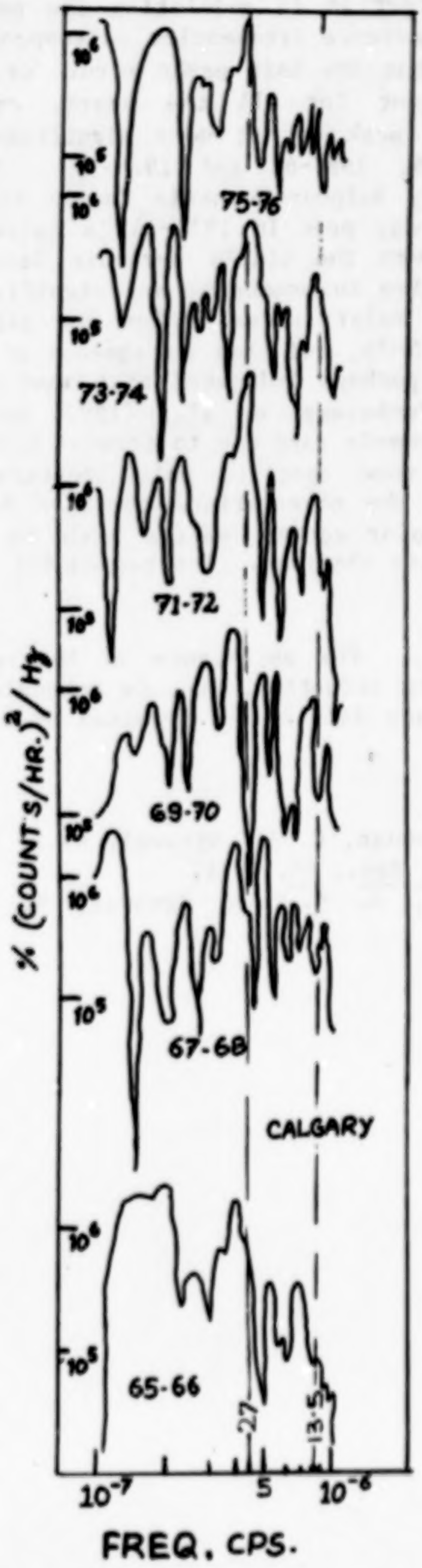

Figure 1. Power spectra for the Calgary neutron monitor for the interval 1965-76. Vertical dashed lines indicate the 27 and 13.5 day period.

N85-35013

VARIATIONS OF THE COSMIC RAY GENERAL COMPONENT IN ANTARCTICA

T.N. Charakhchyan, A.F. Krasotkin, A.I. Kurguzova
Institute of Nuclear Physics, Moscow State
University, Moscow 119899, USSR

N.S. Svirzhevsky
P.N.Lebedev Physical Institute of the Academy of
Sciences of the USSR, Moscow, USSR

ABSTRACT

The report treats the cosmic ray variations connected with the changes of atmospheric temperature and solar activity level and the variations which are probably due to zonal cosmic ray modulation.

A new type of cosmic ray variations, so called zonal cosmic ray modulation, was found in the lower atmosphere from the sonde measurement results /1/. The new variations give rise to anomalies in the latitude distributions of the cosmic ray charged component and the anomalous north-south asymmetry. To find the nature of the variations, we began measuring the cosmic ray general component with the same detectors as in the sonde measurements (the STS-6) gas-discharge counters and the counter telescopes with 7-mm Al filters detecting the electrons of energy above 200 keV and 5 MeV).

In this report the measurement data obtained in Antarctica (Mirny) in the years 1978-1983 are presented and discussed.

Measurement results. Two B-1 instruments described in /2/ are in operation at Mirny. The measurements are taken daily for two hours (0800-1000 UT). The data on the time dependence of the cosmic ray global component are obtained using six independent units (the unit consists of ten STS-6 counters with a 16 cm^2 geometric factor each). The monthly means of charged-particle number per minute corrected for barometric effect (-0.16%/mb) are shown in Fig. 1 (curve C). The data on time dependence of the cosmic ray vertical component are obtained using three independent units. These data corrected for barometric effect (-0.24%/mb) are shown in Fig. 1 (curve T).

Considering that radioactive background is in practice absent at Mirny /3/(the charged particle flux is

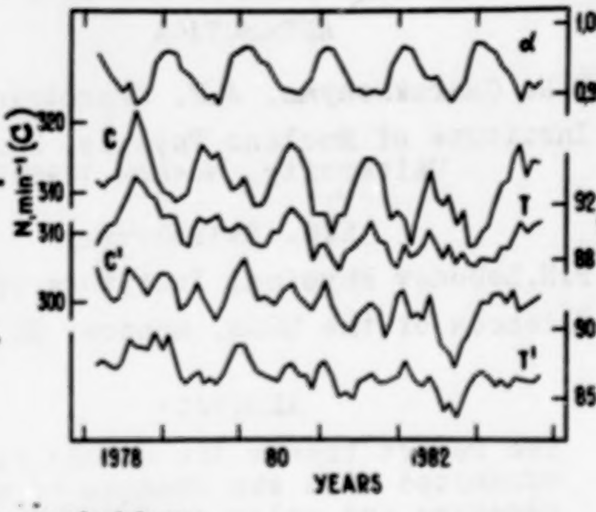

Fig.1. Time dependences at Mirny ($x=1030$ g/cm^2). C and T- cosmic ray global and vertical components correlated for barometric effect; α -correction coefficient for temperature; C' and T'-cosmic ray global and vertical components corrected for barometric and temperature effects.

about 300 m^{-2}s^{-1}), the observed variations are mainly due to cosmic ray variations.

Seasonal cosmic ray variations. As it should be expected, the main variations of the measured particle number on the Earth's surface in Antarctica are due to the seasonal temperature variations. The seasonal variation amplitude (3-4%) is in a good agreement with the calculated values because of the muon component intensity variations /4/. Curve α in Fig. 1 presents the values of the correction factors calculated allowing for the atmospheric temperature distribution inferred from meteorological sounding data and of the partial temperature coefficients for the cosmic ray general component at sea level. The correction factor $\alpha = 1/(1+K\Delta t)$, where K is a partial temperature coefficient, Δt is the difference between the temperature measured at a given isobaric level and the temperature of the standard atmosphere at the same level; $\langle K\Delta t\rangle$ is the mean of the 10 isobaric levels in the 10-1000 g/cm^2 interval. Curves C' and T' in Fig. 1 show the data corrected for the temperature effect. It is seen that, apart from the temperature-induced variations, the general component suffers other types of variations.

The variations due to changes of solar activity level. From 1978 to 1982, the mean level of the charged-particle number at Mirny has changed by ~3%. The same change of the particle number was inferred from the data of the vertical telescope with the 7-mm Al filter at Murmansk. The changes are in a good agreement with the nucleon component variations inferred from the data of high-latitude neutron monitors (see Fig. 2).

During the above mentioned period the sunspot number increased markedly, so the observed cosmic ray intensity decrease was mainly due to the rise of solar activity level. From Fig. 2 it may be seen that the amplitude of these variations in the nucleon component (NM) is 4 times greater than the amplitude in the general component (T) of cosmic rays at sea

ORIGINAL PAGE IS
OF POOR QUALITY

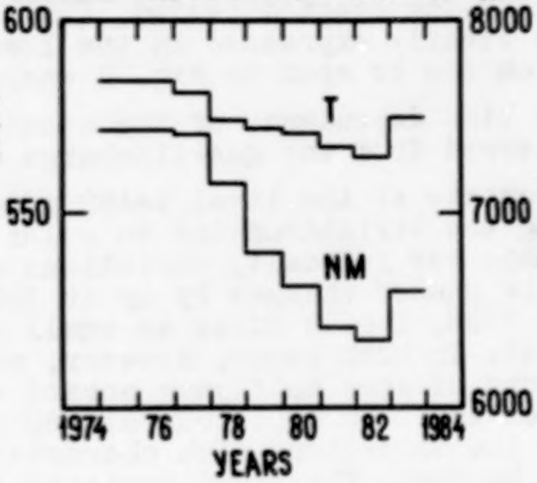

Fig. 2. The yearly means of the detected particle number at sea level. T-charged component (7-mm Al filter); NM-nucleon component (the data of the Apatity neutron monitor).

level. Once the continuous series of the nucleon component data from Apatity are available, the cosmic ray variations due to solar activity changes may be excluded from the data shown in Fig. 1 C' and T'. The time dependences of cosmic rays at Mirny after excluding the temperature variations and the variations due to solar activity are shown in Fig. 3 (Curves C'' and T''). The residual variations may be thought to be due mainly to the measurement errors and to the errors in introducing the corrections for the barometric and temperature effects. It should be noted, however, that the found variations resemble the variations in the lower atmosphere inferred from the sonde measurements of cosmic rays.

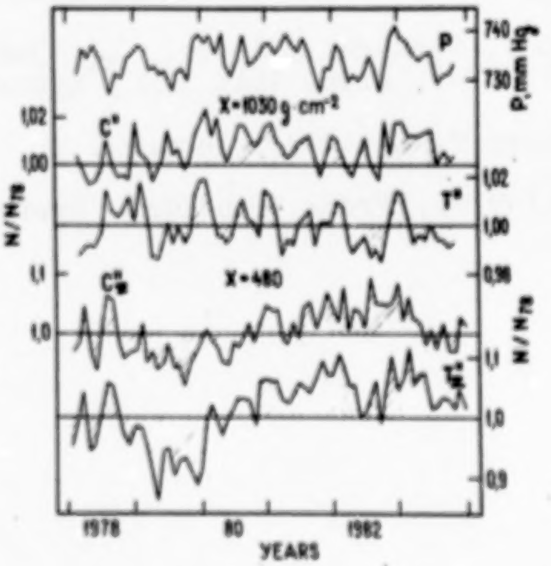

Fig. 3. The corrected time dependences of the cosmic ray charged component at Mirny. C'' and T'' - at sea level; C''_z and T''_z - at the level $x=480$ g/cm^2; P - atmospheric pressure at Mirny.

The variations due to the zonal cosmic ray modulation. During the studied period, the zonal cosmic ray modulation was clearly expressed in the lower atmosphere over Mirny, which can be seen in Fig. 3 where curves C''_Z and T''_z show the time dependence of the cosmic ray charged component inferred from the gas-discharge counter and telescope measurements at the level $x=480$ g/cm^2 over Mirny after excluding the variations due to solar activity changes. Here the cosmic ray intensity variations are significant. The particle number changes by up to 10%. The changes at sea level are 1-2%, i.e. 5 times as small as the changes at 500 g/cm^2 level. In both cases, however, we can clearly see the variations of some half-year period with 1-1.5% amplitude at sea level and 2-5% amplitude at 480 g/cm^2 level. At the same time, the variations with characteristic times of 2-3 years can be seen. The found variations can hardly be accounted for by incorrect inclusion of the barometric and temperature effects because such variations are absent both in pressure (curve P in Fig. 3) and temperature (curve α in Fig. 1). In this case the annual variations would have been most probably found because they show the largest amplitudes in both pressure and temperature.

Thus, the measurements of the cosmic ray charged component at Mirny have shown that the zonal cosmic ray modulation seems to exist also at sea level, but its amplitude is about an order as low as at ~ 500 g/cm^2 level. The same conclusion can essentially be drawn from the analysis of the neutron monitor data made in /5/ for the solar minimum of 1964-1965.

References

1. Charakhchyan A.N., et al.(1979), Proc. 16th ICRC, Kyoto, v. 3, p. 277.
2. Altukhov A.M. et al. (1984), Geomagn. i Aeron., 24, 386.
3. Charakhchyan A.N. et al. (1979), Proc. 16th ICRC, Kyoto, v. 4, p. 253.
4. Kurguzova A.I., Charakhchyan T.N. (1983), Geomagn. i Aeron., 23, 715.
5. Charakhchyan A.N. et al. (1979), Proc. 16th ICRC, Kyoto, v. 3, p. 271.

SH 4.4-18

THE DIFFERENCE IN THE ENERGY SPECTRA OF GALACTIC COSMIC RAYS AT THE MINIMA OF THE 19TH AND 20TH SOLAR ACTIVITY CYCLES

N85-35014

A.K. SVIRZHEVSKAYA, N.S. SVIRZHEVSKY, YU.I. STOZHKOV,

P.N.LEBEDEV Physical Institute of the Academy
of Sciences of the USSR, Leninsky Prospect, 53,
117924, Moscow, USSR

T.N. CHARAKHCHYAN

Institute of Nuclear Physics, Moscow State
University, 119899, Moscow, USSR

ABSTRACT

The absorption curves of the cosmic ray charged component for solar minima in 1965 and 1975-1977 are analysed on the basis of daily stratospheric measurements in Murmansk, Moscow, Alma-Ata and Mirny (Antarctic).

Two distinct features in the energy spectra of galactic cosmic rays are revealed during these periods.

1. At the 20th solar activity minimum there was the additional short range component of cosmic rays. Additional fluxes in the stratosphere at high latitudes (Murmansk, Mirny) caused by this component are probably protons and He nuclei with the energy 100-500 MeV/n. The fluxes are estimated as $\sim 300\ m^{-2}s^{-1}sr^{-1}$.

2. At the minimum in 1975-1977 the proton intensity in the energy range 1-15 GeV is 10-15% lower than that in the 1965 solar activity minimum.

Numerous experimental evidences are indicative of a significant role of the solar general magnetic field in the cosmic ray modulation effects /1,2/. The magnetic field direction in the polar regions of the Sun proves to be of importance for the formation of the energy spectra of galactic cosmic rays in the Earth's vicinity.

The differences in the primary cosmic ray energy spectra in the consecutive solar minima are pointed out in particular by the short range component detected in the stratosphere /3,4/. Although the nature of the particles of this component is not clear yet at middle latitudes (Moscow, Alma-Ata), at the same time the data obtained in /5/ suggest that the short range component at high latitudes (Murmansk, Mirny) should be associated probably with the protons and helium nuclei of energies below 500 MeV/n.

Information on the variations of the primary cosmic ray energy spectrum may be derived from the altitude dependence of the relative variations of the cosmic ray intensity $\Delta N/N$ in the stratosphere. In the case of the 11-year cosmic ray modulation the variation amplitude decreases with increasing the primary particle energy, and then the value of $\Delta N/N$ decreases with rising the atmospheric pressure X. Over Murmansk, for example, $\Delta N/N$ at $X=10$ g/cm^2 is two times as high as that at $X=150$ g/cm^2 . However the shape of the dependence $\Delta N/N(X)$ in the years near the 20 solar activity minimum proved to be quite different.

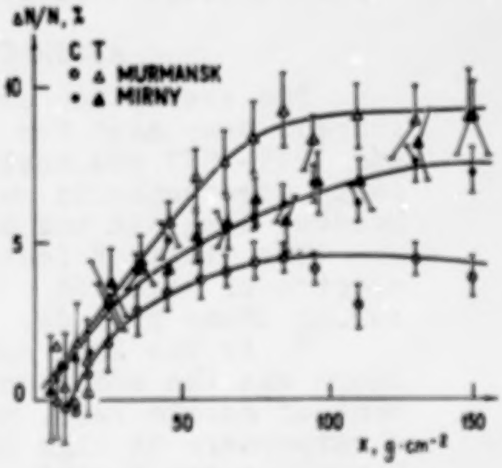

Fig.1. $\Delta N/N$ versus the atmospheric pressure in 1976 for a Geiger counter (C) and counter telescope (T) at Murmansk and Mirny.

Fig.1 shows the variations of the cosmic ray intensity $N_{76}(X)$ in 1976 relative to the intensity in 1965, $\Delta N/N=(N_{65}-N_{76})/N_{65}$, over Murmansk and Mirny. In a broad interval of pressures the cosmic ray intensity in the stratosphere and hence the primary particle intensity in 1976 was lower than that in 1965. The character of the dependence $\Delta N/N$ at $X > 70$ g/cm^2 indicates that the primary spectrum variation in a certain energy range is independent of the particle energy. The decrease of $\Delta N/N$ at $X < 70$ g/cm^2 may be explained by the existence of the cosmic ray short range component in 1976. The same situation took place also in 1975 and 1977.

The data presented in Fig.1 were used to obtain the absorption curves for the additional short range component of cosmic rays (see Fig.2). The absorption curves are actually identical at high latitudes in the nothern and southern hemispheres. The energy spectrum of the additional proton flux, which is also shown in Fig.2, was determined assuming that the additional component consists of protons. The value of the additional 100-400 MeV proton flux is ~ 300 m^{-2}s^{-1}sr^{-1}. Taking into account the fact that He nuclei make a definite contribution to the particles detected in the stratosphere, the flux obtained proves to be in a good agreement with the additional flux of protons and He nuclei in 1977 (compared with 1965) according to /5/. The short range particles at high latitudes in the stratosphere appeared in 1972 and disappeared practically after 1979 /4/, that is they existed during about the same period as the anomalous He component of cosmic rays detected by space probes /6/.

Another important conclusion can be drawn from the data presented in Fig.1, namely, the 1-12 GV rigidity cosmic ray fluxes were much lower in 1976 than in 1965. The same conclusion may be drawn from the analysis of the data of latitude stratospheric measurements in the years 1965, 1969 and 1975 /7/. Fig.3 shows the energy spectra of the variations of primary cosmic rays in 1969 and 1976 relative to 1965 inferred from the latitude measurements. From Fig.3 it seen that the primary cosmic ray intensity in the 4-12 GV was 10-15% lower in 1976 than that in 1965. In the examined energy range the cosmic ray intensity in 1976 was essentially the same as during the solar activity maximum of 1969. The dashed line in Fig.3 presents the spectrum of the variations ΔI/I(R)

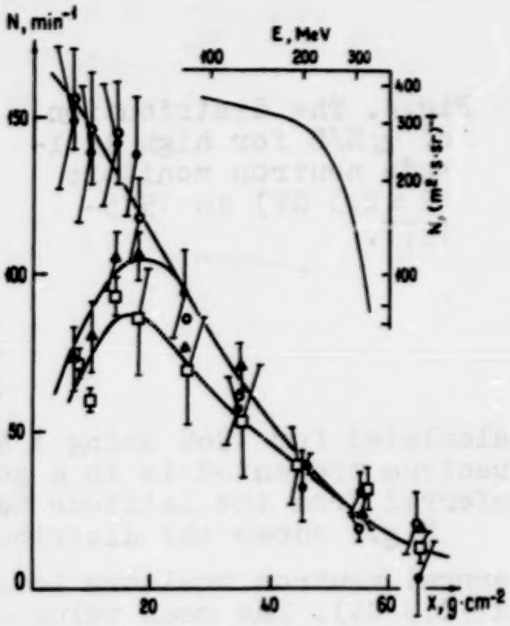

Fig.2. Additional fluxes of the cosmic ray short range component in the stratosphere over Murmansk (○), Mirny (●), Moscow (▲) and Alma-Ata (□). At the top right-hand corner the energy spectrum of the additional proton flux is shown.

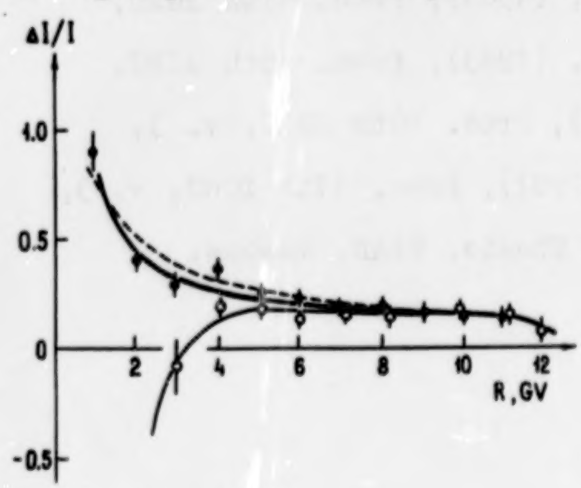

Fig.3. The spectra of the primary cosmic ray variations $\Delta I/I=(I_{65}-I_i)/I_{65}$ in 1969 and 1976 (the dark and light dots respectively). The dashed line shows the variation spectrum in 1969 calculated using the values of ΔN/N at high latitudes.

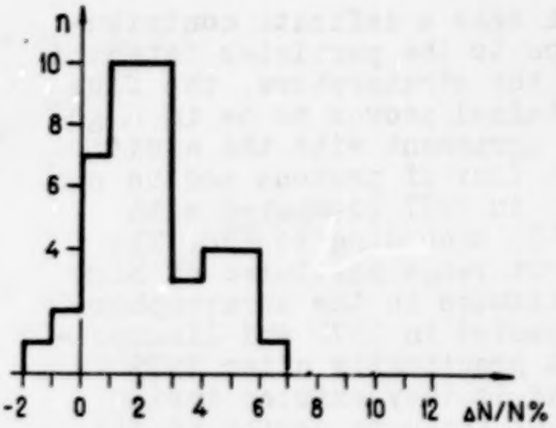

Fig.4. The distribution of ΔN/N for high latitude neutron monitors ($R \leq 2.3$ GV) in 1975-1977.

calculated for 1969 using ΔN/N at Murmansk and Mirny. The spectrum presented is in a good agreement with the spectrum inferred from the latitude measurements.

Fig.4 shows the distribution of $\Delta N/N=(N_{65}-N_1)/N_{65}$ for several neutron monitors located at high latitudes ($R \leq 2.3$ GV). The mean value of ΔN/N for neutron monitors is 2.3 ± 0.3 per cent, but ΔN/N appears to be 5-7 % for some of them (for example, Mt. Washington, Durham). The conclusion that the cosmic ray intensity was lower in 1976 than in 1965 is generally confirmed by the neutron monitor data. The broad distribution of ΔN/N inferred from the neutron monitor data and the difference in ΔN/N over Murmansk and Mirny together with the difference in ΔN/N from the data of a Geiger counter and counter telescope (Fig.1) seems to indicate that the modulation mechanism in the solar activity minima is different from the mechanism of the 11-year cosmic ray modulation.

References

1. Charakhchyan A.N. et al., (1973), Izv. Akad. Nauk SSSR, ser.fiz., v. 37, p. 1258.
2. Nagashima K. et al., (1977), Proc. 15th ICRC, v. 10, p.380.
3. Svirzhevskaya A.K. et al., (1981), Proc. 17th ICRC, v. 3, p. 187.
4. Svirzhevskaya A.K. et al., (1983), Proc. 18th ICRC, v. 3, p. 43.
5. Webber W.R. et al., (1983), Proc. 18th ICRC, v. 3, p. 35.
6. Garcia-Munoz M. et al., (1981), Proc. 17th ICRC, v. 3, p. 270.
7. Svirzhevsky N.S., (1983), Thesis, FIAN, Moscow.

COSMIC RAY VARIATIONS WITH THE PERIOD CLOSE TO 27 DAYS AND THEIR CONNECTION WITH SOLAR ACTIVITY LONGITUDINAL DISTRIBUTION

N85-35015

G.A.Bazilevskaya
P.N.Lebedev Physical Institute of the Academy of Sciences of the USSR, Moscow, USSR
M.I.Tyasto, E.S.Vernova
Leningrad Branch of IZMIRAN, Leningrad, USSR

ABSTRACT

The amplitude and phase changes of the 27 day cosmic ray variation from 1958 to 1975 were studied. The comparison between cosmic ray intensity characteristics and longitudinal distribution of solar activity ones for different stages of the solar cycle were made.

1. Introduction

In some cases the longitudinal redistribution of the solar activity (SA) leads to the changes in 27 day cosmic ray (CR) variations connected with the solar rotation period / 1 /. The purpose of this paper is to analyse in detail the amplitude and the phase evolution of CR 27 day variations along with the longitudinal redistribution of SA. The neutron monitor data I of Thule and the sunspot group area Sp from 1958 to 1975 (except for 1964) were processed.

2. Method

As a result of the sunspot group area treatment for each solar rotation, the polar vector with the amplitude ρ_{SA} and the phase λ_{SA} was obtained, which characterized the non-uniformity of the sunspot longitudinal distribution / 2 /. Indeed, the existence of a longitudinal interval with increased activity means the increased value of ρ_{SA}, and the movement of this interval on the solar surface causes the changes of λ_{SA} from one rotation to another. The amplitude ρ_{CR} and the phase λ_{CR} of the first harmonic of the 27 day CR variation was used for comparison with ρ_{SA} and λ_{SA} of SA / 1 /. The 11-year CR variation, which plays a part of the trend for the present analysis was firstly withdrawn from the primary CR data.

3. Results

Fig. 1 shows the correlation coefficient values R (λ_{SA} , λ_{CR}) between time series of the phases of 27 day SA variations and CR ones with the zero shift between these two series. The horizontal bars correspond to the time intervals, for which these correlation coefficients were obtained. Fig. 1 shows R(λ_{SA}, λ_{CR}) keep the high values during the long time intervals; but for two time intervals from 1970 to 1973 correlation coefficient sharply fell. For these two time intervals (III 1970 - IX 1971, II 1972 - VIII 1973) R(λ_{SA} , λ_{CR}) were computed with the time shift between time series of the phases of 27 day SA variations and CR ones.

Fig. 2 shows the dependence of the R(λ_{SA} , λ_{CR}) on the time shift. It can be seen in Fig. 2 the R(λ_{SA}, λ_{CR}) reached the maximum value R $\approx$ 0.86 for the time shift equal to about three months CR variations being prior to the SA ones. It should be noted that not far from 1970-1973 the polarity reversal of the Sun's general magnetic field took place / 3 /, thus we may expect the redistribution of solar magnetic fields among these the SA longitudinal redistribution. The corresponding changes of interplanetary magnetic fields and 27 day CR variations may be expected. To check this assumption we consider the 27 day variation cyclogram of sunspot group areas shown in Fig.3 / 4 /. As could be expected the SA amplitude of variations decreased and the phase became unstable (region A in the cyclogram). When SA is high the phase of variations is more stable, except for time intervals B and C which concerned with the polarity reversal of the Sun's general magnetic field. This result is confirmed by Table 1 where the parameter of the phase conservation is presented which is the relation $|\Sigma \vec{p}_i| / \Sigma |\vec{p}_i|$ in percent / 5 /. This parameter was more than 58% during the years of high SA except for XI 1959 - VIII 1960 and II 1970 - III 1972, when it fell abruptly.

Table 1

Year	$\lvert\Sigma \vec{p}_i\rvert / \Sigma\lvert\vec{p}_i\rvert$, %	Year	$\lvert\Sigma \vec{p}_i\rvert / \Sigma\lvert\vec{p}_i\rvert$, %
II-V 1958	85	VIII 1961 - IV 1962	89
VI-X 1958	95	VII 1966-V 1967	87
XI 1958-X 1959	65	VI 1967-II 1968	60
XI 1959-VIII 1960	58	III 1968-I 1970	58
IX 1960-VII 1961	76	II 1970-III 1972	5

4. Conclusion

The strong variability of the longitudinal distribution of SA took place near the polarity reversal of the Sun's general magnetic field. The disturbance of 27 day CR variations may be expected in turn.

Nevertheless from the point of view of current ideas about the solar modulation of CR intensities it is difficult to explain a high value of R(λ_{SA} , λ_{CR}) between the time series of the phases of 27 day SA variations and CR ones for 1970-1973 with CR variations being prior to the

Fig. 1. Correlation coefficients between the 27 day variation phases of CR intensity and sunspot area with zero shift between time series.

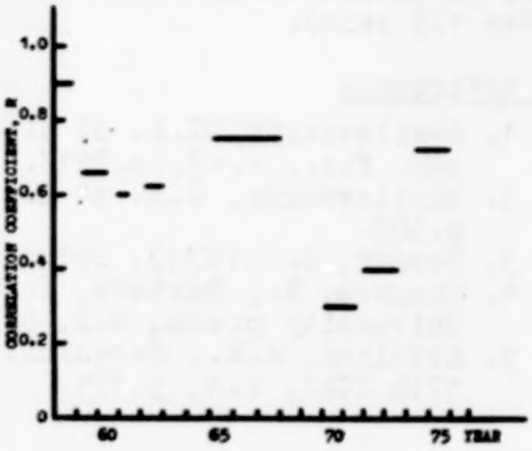

Fig. 2. Correlation coefficient R(λ_{SA} , λ_{CR}) versus the time shift between the series.

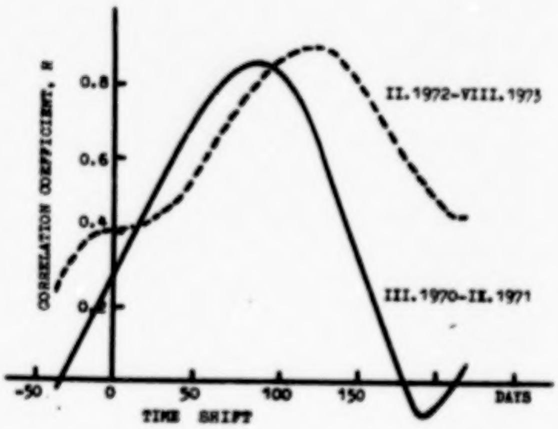

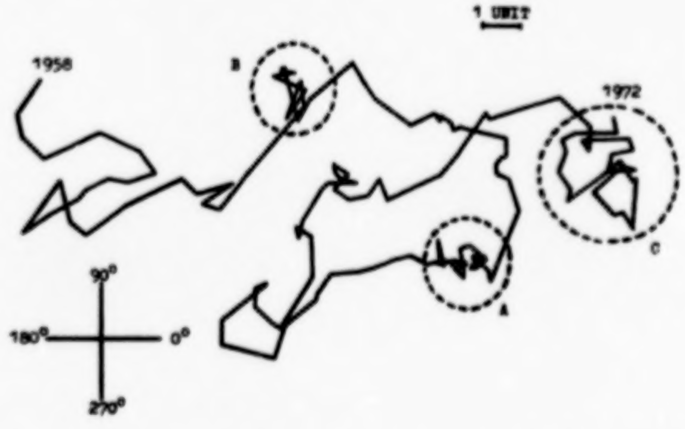

Fig. 3. The cyclogram of sunspot area for 1958-1972 (1 unit is equal to 20 000millionths of the solar hemisphere).

SA. At the same time it is unlikely to obtain such a high value of R(λ_{SA} , λ_{cR}) by chance because of rather long time intervals under consideration (each of them being of order 1.5 year).

5. References

1. Bazilevskaya, G.A. et al., (1984), Izv. Akad. Nauk, ser. fiz., v.49, p.2117.
2. Bazilevskaya, G.A. et al., (1979), 16th ICRC, v.3, p.385.
3. Howard, R. (1974), Solar Phys., v.38. p.283.
4. Chapman, S., Bartets, Y. (1951), Geomagnetism, Oxford University press, v.2, p.569.
5. Attolini, M.R., Cecchini, S., Galli, M., (1981), 17th ICRC, v.4, p.171.

N85-35016

AZIMUTHAL AND MERIDIONAL ASYMMETRIES OF THE SOLAR WIND AND QUASIPERIODIC VARIATIONS OF INTENSITY OF GALACTIC COSMIC RAYS (GCR)

L.Kh.Shatashvili, T.V.Djapiashvili, B.G.Kavlashvili,
B.D.Naskidashvili, O.G.Rogava, G.V.Shafer

The Institute of Geophysics, Georgian Academy of
Sciences, Z.Rukhadze str. I, 380093, Tbilisi,USSR

ABSTRACT

The results of analysis of 27-day, annual and quasi-two-year variation of GCR are presented. The dependence of the periods of 27-day GCR variation on the energy of initial radiation is discovered, according to the data during 1980 of the World network of station in sufficiently wide range of the observed threshold energy. The dependence of the annual variation of GCR is established, according to the data of the Huancayo station in conformity with the change of the polarity of the General Magnetic Field of the Sun (GMFS).

I. 27-day variation of GCR intensity

In paper /1/, the supposition, that the duration τ of 27-day oscillation of GCR ought not depend on the stage of development of the 11-year cycleness was expressed and in average τ =9÷10 Sun's rotation time was addmited. However, observations on the wider intervals of time show that these confirmations are true not for all cycles of Solar activity, in particular, it appeared, that for the period of 1962-1964 τ = 22 Sun's rotation time. At present we have the data for 20-21 cycles of Solar activity, which show that τ is changing in a quite wide range of time.

We have made complex analysis of Solar activity data; gemagnetic activity(Solar Geophysical data) of neutron component of GCR Kiel(FRG), Tokyo(Japan), Sanae(antarctica) South Africa, the vertical direction of GCR rigid component of supertelescopes on ground station at Nagoya and the underground station at Sakashita (80 m.w.e. underground) Not so often we meet the case, when the duration of 27-day variations of GCR intensity is very long. Particular interest has been attached to the epoch 1980 when τ was quite big and at the same time it was possible to correlate the GCR data with the change of Solar wind characteristics, made directly in cosmic space. The results of calculation by the method of superposition analysis for several stations of CR are presented in Fig.I. The stations are chosen so that the difference in the cut-off of initial radiation could be noticable. The attention must be paid to the extremly interesting observed phenomena- the dependence of the period of the reccurent change of GCR intensity on the cut-off energy. The period, determined in first rotations of the Sun according to the data with less cutoff of CR is essentialy longer than according to the data with the big cutoff. It is difficult to ascribe the above mentioned dependence to the not considered temperature effects in the rigid component data at Nagoya and Sakashita stations, as the analogic phenomenon is observed in the neutron data at Tokyo station, where the temperature effect is obviously small, at the cutoff energy is essentialy more than at Kiel station.

In a number of papers the change of periods of 27-day GCR variation was investigated. In paper/4/ it is established that the average period of 27-day GCR variation depends on the polarity of GMPS. In the present paper the dependence of period of 27-day GCR variation on the cycle phase of Solar activity (SA) is investigated. The investigation was made by the method of Fourier transform /5/ using the Han windows, on the basis of hour data of neutron monitor at Kiel station.

The period of 27-day variation- T_{27} of GCR intensity is defined by 2-year data with the subsequent drifts of number of datum for a year. The value of the period T_{27} was determined by Fourier spectrum function $F(T)$ so that T_{27} -corresponded to the maximum of function $F(T)$ in the interval of period $T = 25 \div 32$ days.

In Fig. 2 the change of the period T_{27} in time is presented. It is possible, to notice that the period T_{27} 27-day GCR variation in the maximum epoch of SA reaches the synodic period of the Sun's rotation, but in minimum of SA T_{27} is maximum.

2. Annual variation

In paper /6/ the annual variation of GCR intensity was investigated, according to the data of CR neutron component in connection with the polarity of GMPS. We've made the analogical analysis, using the data of ionic chamber (IC) at stations, Iakytsk and Huancayo for the other epochs. The averaging of vectors of the annual variation was made in conformity with the direction of GMPS (1946-1955 and 1960-1968). The results of harmonic analysis of the average monthly data of these stations, show that the IC data at Iakytsk contains the influence of the seasonal temperature change. It is due to expect that so far as the Huancayo station is equatorial, the seasonal change is not essential. Indeed the results of harmonic analysis according to the data of Huancayo station, show that supposed in /6/ the effect observed in the neutron component of highlatitudinal station, connected with the change of GMPS polarity is as well clearly expressed in the data of IC equatorial station at Huancayo /Fig.3/.

3. GCR quasi-two-year variations

In paper /7/ it was noticed, that the observed quasi-two-year variations of neutron and μ -meson components of CR are caused not only by the cycle changes of parameters of solar modulation of CR, but at the expense of two-year variations of meteorological parameters of the Earth atmosphere.

For the present moment we've widened our analysis. For the more assurance we used the Forbush data too /2/.

Then we obtained that the quasi-two-year variations of intensity of rigid μ -meson component of CR, corrected on the temperature and barometric effects of IC-I(Iakytsk) for the period I954-I976 are synchronous with the quasi-two-year variations of SA. Quasi-two-year variations corrected on the meteorological effects, are apparently caused /7/ rather by the quasi-two-year variations of the meridional asymmetry of Solar wind velocity /8/.

REFERENCES

I. Dorman L.I., Shatashvili L.Ch., sb. "Cosmicheskie luchi" I965, Izd-vo "Nauka", № 7, Str.I6I.
2. Forbush S.E., Cosmic Ray Results. vol.XX I957.
3. Bazilevskaya G.A., Okhlopkov B.P., Charakchyan T.N. Tr. FIAN, I976, 88, 94.
4. Bazilevskaya G.A., Vernova E.S., Grigoryan M.S., Sladkova A.I., Tiasto M.N., Charakchyan T.V., Geomagnetizm i aeronomia" № 4, I984.
5. Bendat J., Pyrsol A., Primenenie correlatsionnogo i spectralnogo analyza. "Mir", I983.
6. Krimsky G.F., Krivoshaphin P.A., Mamrukova V.P., Skripin G.V., Geomagnetizm i aeronomia, 2I, 823, I98I.
7. Djapiashvili T.V., Rogava O.G., Shatashvili L.Kh., I8th ICRC, v. IO, p.235, I983.
8. Djapiashvili T.V. , Rogava O.G., Shatashvili L.Kh. Shafer G.V., Geomagnetizm i aeronomia, 24 , c. 680.

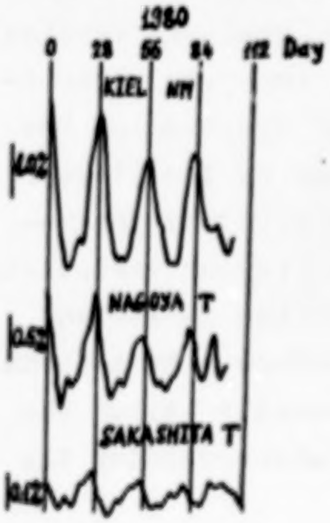

Fig. 1

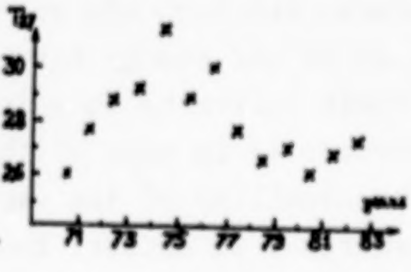

Fig. 2

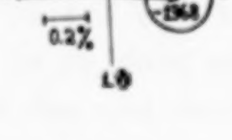

Fig.3

DYNAMICS OF TWO-YEAR COSMIC RAY VARIATIONS INFERRED FROM THE DATA OF SPACECRAFT AND STRATOSPHERIC MEASUREMENTS AND FROM THE NEUTRON MONITOR DATA IN 1959-1981

N85-35017

T.N. Charakhchyan, E.V. Gorchakov, V.P. Okhlopkov,
L.S. Okhlopkova, M.V. Ternovskaya
Institute of Nuclear Physics, Moscow State University,
Moscow 119899, U S S R

ABSTRACT

The two-year cosmic ray variations are studied using the spacecraft measurements of 1967-1976, the sonde measurements at high latitudes in the stratosphere (Murmansk, Mirny), and the neutron monitor data of 1959-1981. The two-year variations are most pronounced from 1967 to 1975. An anticorrelation is observed between the two-year variations in cosmic rays and in geomagnetic activity.

In work /1/ the two-year cosmic ray variations were singled out from the stratospheric sounding data and were shown to be of isotropic character. The variation amplitude and phase are the same in the southern and northern hemispheres, they are also the same for the global and vertical fluxes of cosmic rays. The nature of the two-year variations is still obscure. Although the energy spectrum of the variations is close to the energy spectrum of the 11-year variations, but their relevance to solar activity parameters is not so obvious as in case of the 11-year variations. The problem of the stability of the variation period and phase has not been resolved either. Therefore, the information derivable from the satellite measurements beyond the Earth's magnetosphere gets essential in understanding the nature of the variations.

In the present work, the two-year variation was sought in the low-energy cosmic ray intensity beyond the Earth's magnetosphere. We processed the $\geqslant$60 MeV proton detection data (the Explorer satellites data in May,1967- May 1973/2/ and, the Soviet space probes data in June 1973-March,1976/3/).

The method of mathematical selective filter used in/1,4/ can hardly be used to discriminate the two-year variations in such a comparatively small series of experimental data because the information for two years is lost at the ends of the series, so but a single period of the two-year variation may be singled out from the satellite data. Therefore, the peculiar method based on the difference in the approximation of the data by the Fourier series was developed /5/ for small data series. If the Fourier series with different numbers of harmonics are used, they will have different cut frequencies and the difference of transforms will discriminate a narrow frequency band. Such a transform is a selective filter. The method was used to process the spaccoraft data. Fig. 1 shows the results of the processing.

Fig. 1 shows also the two-year cosmic ray variations inferred from the data of stratospheric sounding at a 20 g/ /cm^2 layer at Murmansk and Mirny (Antarctica) and the neutron component data at Deep River and Climax discriminated using the numerical selective filter /4/.

It is seen that the two-year cosmic ray intensity variation was in practice absent in 1959-1965 and was pronounced in 1966-1976 when its amplitude was 4-7% on spacecraft,2-4% in the stratosphere, and 1-1.4% in the neutron component. All the cosmic ray data show a good coincidence of the variation phases. The fact that the two-year variation appeared in the spacecraft data is worth noting because it demonstrates that the variation is actually due to the two-year variation of the interplanetary medium parameters rather than to some geophysical effect.

A change should be noted in the variation period which was 24-25 months in 1966-1972 and 19-20 months in

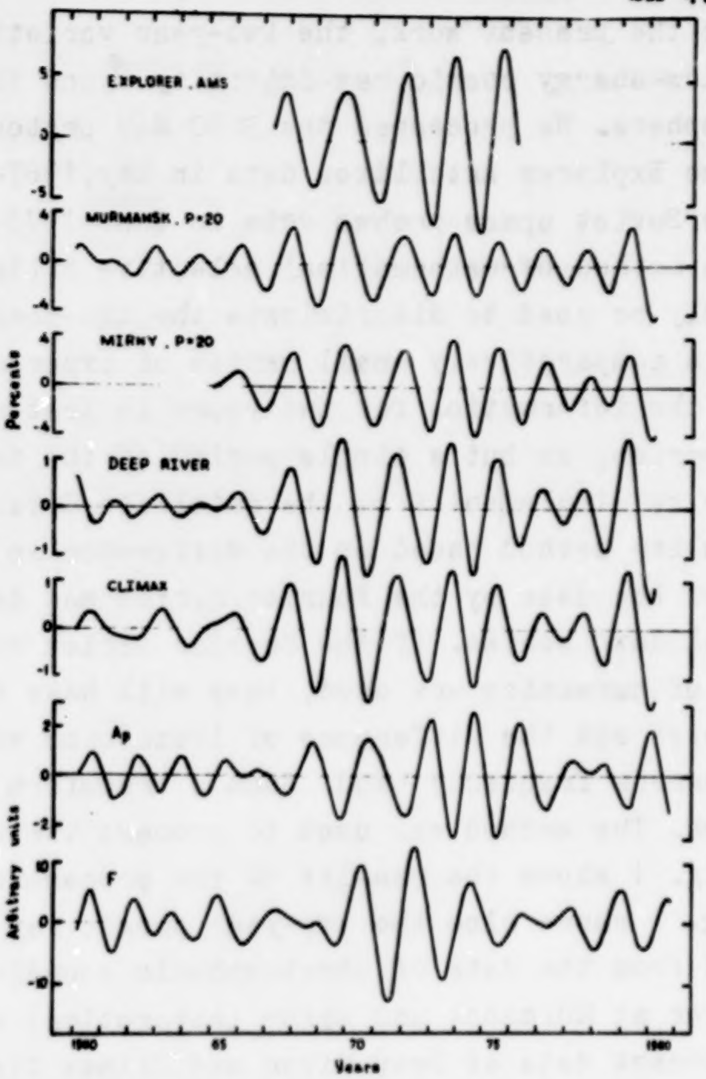

Fig. 1.

The twoyear variations obtained using the selective filter. The upper curve shows the data from the Explorer satellite and from the Soviet space probes. The stratospheric data at 20 g/cm^2 level over Murmansk and Mirny. The neutron component at Deep River and Climax. The Ap-index. F is the 10.7 cm radio emission from the Sun.

1973-1977. Since the change is seen in all the data,it is not accidental and reflects the real changes of the character of the variations in the interplanetary medium parameters. Fig. 1 also shows the two-year variations inferred from the solar 10.7 cm radio emission (F) and from the Ap-index. Although the two-year variation was felt in solar activity, its dynamics differs much from the two-year cosmic ray variation. The two-year wave in solar stivity was in practice absent in 1966-1969. Considering that the variations in solar activity and cosmic rays must be of opposite phase,the phase shift between solar activity and cosmic rays was about half-year in 1970-1975.This fact should have meant that a large modulation region is responsible for the cosmic ray variation,but such a conclusion is at variance with the data on the two-year geomagnetic activity variations.

From Fig. 1 it is seen that the pronounced two-year variation was observed simultaneously in the Ap-index and in cosmic rays. It is woth noting that the waves in the Ap--index and in cosmic rays are clearly of opposite phase. Both the Ap-index and cosmic rays exhibit the trend in the variation period to change from 24-25 months to 19-20 months. All the above means most probably that the two-year cosmic ray variation is due to the changes in the properties of the near region of interplanetary space and is contingent upon the variations of the same parameters which give rise to the geomagnetic activity variations (solar wind velocity and density,interplanetary magnetic field).

The preliminary processing of the data obtained before 1984 has shown that the amplitude of the two-year cosmic ray variation increased markedly after 1979,so in 1980-1983 it was closer to the variation amplitude in 1968-1974.

Thus, the two-year variation dynamics is characterized by significant changes in the amplitude,phase,and period of the variation. Since the significant decreases of the variation amplitude occur during the periods close to the solar minima (1964-1965,1975-1977)and in the periods close to the solar maximum (1959-1982),the dynamics of the two--year variations does not seem to depend on the phase of the 11-year solar activity cycle,but is most probably determined by the state of the heliosphere,the approach adopted, for example, in /6/.

References

1.Charakhchyan T.N.et al.(1979),Proc. 16th ICRC,Kyoto,v.3, p.297.
2.Solar Geophysical Data,Boulder,USA,1967-1973.
3.Ignatiev P.P.,Shvidkovskaya T.E.(1980).In:Cosmic Rays, No. 27,p. 57.
4. Charakhchyan T.N.et al.(1979).Proc.16th ICRC,Kyoto,v.3, p.308.
5.Okhlopkov V.P.VINITI AN USSR,No.7382-85 DEP.
6. Dorman L.I.,Ptuskin V.S. (1981).Astrophys. and Space Sci. v. 179,p.397.

LONG-TERM MODULATION OF GALACTIC COSMIC RAYS IN HIGH-ENERGY REGION

P.A.Krivoshapkin, A.N.Prikhodko, G.V.Skripin,
I.A.Transky, G.V.Shafer

Institute of Cosmophysical Research & Aeronomy
Lenin Ave., 31, 677891 Yakutsk, USSR

ABSTRACT

The results of continious registration of the cosmic ray muon intensity on the ground and underground at 7, 20 and 60 m w.e. depths in Yakutsk for 1957-1983 are presented. In years of the solar activity maximum in cosmic ray density were found two minima or two-stepped decrease. The second intensity minimum appears to be not the result of the inversion of the general magnetic field of the Sun but caused by the increase of the solar wind speed.

In [1] it was shown that the galactic cosmic ray intensity in even cycles of the solar activity is associated mainly with the number of sunspots and in odd ones - with the solar wind speed.

In [2] to describe the galactic cosmic ray density the index is suggested which is as a function of the number of sunspot groups and of their average heliolatitude. In [2] it was found as well that correlation of the galactic cosmic ray intensity with the above index is violated during the periods of the inversion of the general magnetic field of the Sun. The violation of the close correlation between the temporal behaviour of high- and low-energy galactic cosmic rays at this period has been explained by the decrease of the regular interplanetary magnetic field intensity.

In [3] it is obtained that on the 11-year galactic cosmic ray intensity variation the effect of interaction of the general magnetic field of the Sun and of the galactic magnetic field is superimposed. The dependence of the galactic cosmic ray intensity on the solar activity in even and odd cycles forms a narrow and a wide loops of hysteresis, respectively.

The cosmic ray muon intensity by telescopes at 0, 7, 20 and 60 m w.e. depths in Yakutsk beginning from 1957 is continuously registered. The median values of energy for coupling coefficients at the above levels are 40, 78, 123 and 260 GeV, respectively. The average monthly statistical accuracy for vertical telescopes at these levels was 0.014, 0.017, 0.017 and 0.025%, respectively. In 1963-1964 the pit was reconstructed, i.e. the area at all the three underground levels was significantly enlarged. Because of this reason the telescopes at 7 and 20 m w.e. operated with breaks. Beginning from 1970 to 1982 at all the depths two and more telescopes were in operation. At present the statistical accuracy increased by ~ 2 times as compared with 1957. Beginning from June 1953 to present the ionization chamber of a large volume (the mean monthly statistical accuracy is 0.003%) is continiously operating [4] .

In the Figure the geomagnetic activity (A_p-index), sunspot numbers R_z, the galactic cosmic ray density smoothed in an annual interval on measurements by the muon vertical telescopes at 0, 7, 20, 60 m w.e. and by the ionization chamber in Yakutsk for the recent three solar cycles are presented.

During the 19-th solar activity cycle three peaks in geomagnetic activity were observed. The first increase of A_p was early in 1958 and it coincides with the maximum of R_z. The second peak is when the R_z started to decrease, the third one - near the minimum of the solar activity. The increases of A_p coincided with decreases of the galactic cosmic ray intensity at all the depths up to 60 m w.e. (in the Figure a scale for 60 m w.e. is twice larger in comparison with other levels).

In the 20-th cycle the two peaks in A_p were observed. The first peak coincides with the solar activity maximum, the second one was caused by the occurence of high-speed stationary solar wind streams with regular magnetic field in 1973-

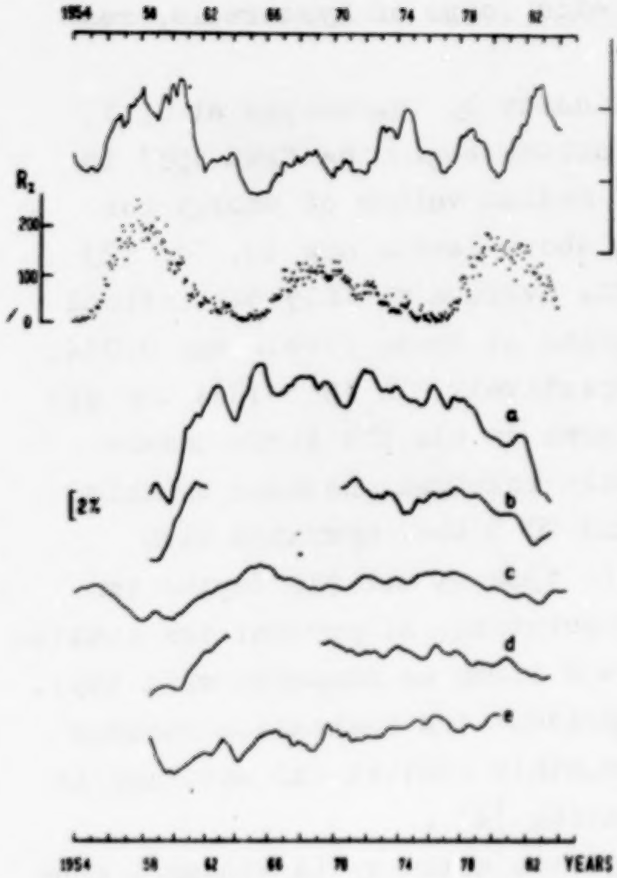

Geomagnetic activity (A_p-index), sunspot number R_z and the galactic cosmic ray intensity smoothed in annual interval on Yakutsk measurements by the muon telescopes (vertical) at 0, 7, 20 and 60 m w.e. depths (a,b,d,e, respectively) and by ionization chamber (c)

1974. In the galactic cosmic ray density the two minima are observed. The first (deep) minimum was in 1970, the second one (less deep) - was in 1974.

In the 21-st cycle also two peaks in A_p were observed. The first peak coincides with the phase of the solar activity increase, the second one was at the R_z decrease. A_p minimum coincided with the R_z maximum. In the galactic cosmic ray density the two-stepped decrease is revealed. The first decrease appears to be caused by the solar activity maximum, the second one - by the A_p increase in 1982.

The moments of the galactic cosmic ray density maxima delay by 9-12 months with respect to the solar activity minima. The geomagnetic activity minima in the 19-20-th cycles coincide with the galactic cosmic ray density maxima. In the years of the solar activity maxima in the high-energy galactic cosmic ray density the two minima or two-stepped decrease were observed. The second minimum in the galactic cosmic ray intensity appear to be not the result of the inversion of the general magnetic field of the Sun. This fact confirms the results of [1] . The enrgy spectrum of 11-year variation in the galactic cosmic ray density obtained based on underground data is of the form $\sim E^{-1.0}$.

References

1. Chirkov, N.P. Solnechnyi veter i variatsii plotnosti kosmicheskikh luchei. - V kn.: Variatsii kosmicheskikh luchei i solnechnyi veter, (1980), Yakutsk, 25.
2. Krainev, M.V., Stozhkov, Yu.I., Charakhchyan, T.N., (1983), Proc. 18-th ICRC, Bangalore, 3, 23.
3. Nagashima, K. and Morishita, I. Twenty-Two Modulation of Cosmic Rays Associated with Polarity Reversal of Polar Magnetic Field of the Sun, (1979), Nagoya, Japan, 24.
4. Shafer, G.V., Shafer, Yu.G. Pretsizionnye nablyudeniya kosmicheskikh luchei v Yakutske, (1984), Novosibirsk, Nauka. 734 p.

N85-35019

THE FIRST THREE HARMONICS OF SOLAR DAILY VARIATION CAUSED BY THE DIFFUSIVE PROPAGATION OF GALACTIC COSMIC RAYS THROUGH THE HELIOSPHERE

K. Munakata and K. Nagashima*

Department of Physics, Faculty of Science,
Nagoya University, Nagoya 464, JAPAN

*Cosmic Ray Research Laboratory, Faculty of Science,
Nagoya University, Nagoya 464, JAPAN

Introduction

Forming a complement to our preceeding paper(1), we present some results for the first three harmonics derived from the simulation of diffusion-convection of galactic cosmic rays. We present also some dependences of the results to the modulation parameters. The results are discussed in comparison with observations and with the former studies of higher order anisotropy.

In addition to this, we suggest the existence of the IMF-sense-dependent anisotropy of higher order which is discussed in detail in a separate paper(2).

Theory and Model

The cosmic ray anisotropy $\eta(r, p)$ can be expressed as

$$\eta(r,p) \sim 1+\sum_{n=1}^{3}\sum_{m=0}^{n}[\eta_n^{mc}(r,p)\cos(m\phi')+\eta_n^{ms}(r,p)\sin(m\phi')]P_n^m(\cos\theta'). \quad (1)$$

where θ' and ϕ' express the incident direction of cosmic rays, defined as(cf. Fig.1)

$$\theta'=\pi-\theta, \quad \phi'=\pi+\phi,$$

and

$$\eta_n^{mc}(r,p)=(-1)^n F_n^{mc}(r,p)/F_0^{0c}(r,p),$$

$$\eta_n^{ms}(r,p)=(-1)^n F_n^{ms}(r,p)/F_0^{0c}(r,p).$$

As shown in our preceeding paper(1), F_n^{mc} and F_n^{ms} in Eq.(1) are given by the cosmic ray denrity U, stream S_i, stress tensor T_{ij} and heat flow tensor H_{ijk} which are governed by the following equations.

$$\nabla\cdot(CUV-\underline{\kappa}^{(1)}\cdot\nabla U)=-\frac{\partial}{\partial p}\left(\frac{1}{3}pV\cdot\nabla U\right), \quad (2)$$

$$S=CUV-\underline{\kappa}^{(1)}\cdot\nabla U, \quad (3)$$

$$T_{ij}=-\kappa^{(2)}{}_{ijl\alpha}(\overline{\nabla S})_{l\alpha}, \quad (4)$$

$$H_{ijk}=-\kappa^{(3)}{}_{ijkl\alpha\beta}(\overline{\nabla \underline{T}})_{l\alpha\beta}. \quad (5)$$

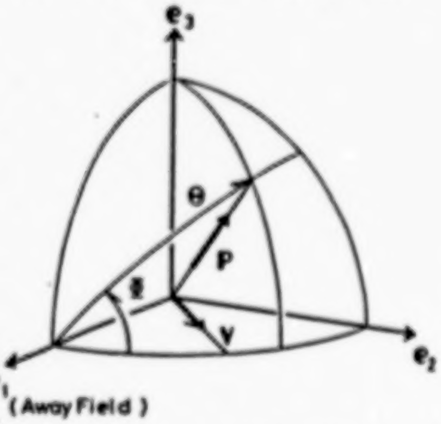

Fig.1 IMF-COORDINATE SYSTEM

p ; Particle's momentum.
V ; Solar wind velocity.
e_1; Unit vector in the direction of B in the 'away' sector.
$e_3 = e_1 \times V/|e_1 \times V|$.
$e_2 = e_3 \times e_1$.

where

$$(\dot{\overline{\nabla S}})_{lq}=\frac{1}{2}\left[\frac{\partial S_l}{\partial x_q}+\frac{\partial S_q}{\partial x_l}+S_s(Z_{slq}+Z_{sql})\right]-\frac{1}{3}(\nabla\cdot S)\delta_{lq}, \qquad (\nabla\cdot S)=\frac{\partial S_q}{\partial x_q}+S_q Z_{qrr},$$

and

$$Z_{ijk}=\frac{\partial e_i}{\partial x_j}\cdot e_k=-Z_{kji}. \qquad (6)$$

Note that, in the IMF-coordinate system, Z_{ijk}'s in Eq.(6) represent the IMF-curvature and focusing. We first solve Eq.(2) in the model heliosphere and, starting from the solution for U, we can calculate successively S_i, T_{ij} and H_{ijk} by Eqs.(3)-(5). In these calculations, the following scattering m.f.p. is assumed.

$$\lambda=\lambda_0(R/GV)\exp\left(\frac{r-r_e}{33\mathrm{a.u.}}\right)(1+a_\lambda\cos\theta_H), \qquad (7)$$

where λ_0 and a_λ are the parameters, R is the rigidity and θ_H is the polar angle in the heliocentric polar coordinate system. The calculations were carried out for various values of λ_0 and a_λ and, in this paper, the results in the following two cases will be presented.

case I .... λ_0 = 0.016 a.u. and $0\leq a_\lambda \leq 3$,

case II .... λ_0 = 0.032 a.u. and $0\leq a_\lambda \leq 3$.

It is noteworthy that, in Eqs.(3)-(5), S_i, T_{ij}, H_{ijk} having subscript '3' odd times are IMF-sense-dependent and their associated anisotropies symbolized by η_n^{ms} with mark '*s*' change their signs according to the alteration of the 'away' and 'toward' sectors whereas η_n^{mc} with mark '*c*' do not. In this paper, we restrict ourselves only to η_n^{mc}, and the natures of η_n^{ms} mentioned above will be discussed in a separate paper(2).

Results and Discussions

The anisotropies η_n^{mc}'s in space can be expressed by the surface harmonics in the equatorial coordinate system and can be observed as solar daily variations at the Earth(3).

The resultant first space harmonic vectors for cases I and II are shown in Fig.2, with black characters in the positive state and white characters in the negative state. It can be clearly seen that the harmonic vector in the positive state changes its phase toward earlier hours from that of 18h in the negative state, in accordance with the observed 22-year variation of the diurnal variation(4,5,6).

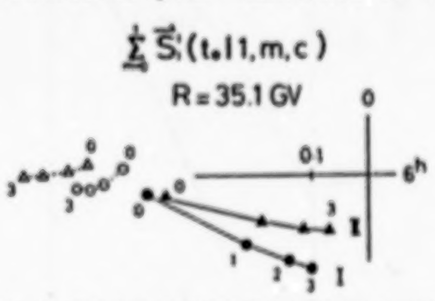

Fig.2 FIRST SPACE HARMONIC VECTORS

Arabic numerals represent the value of a_λ in Eq.(7). The black and white characters represent the positive and negative polarity states, respectively.

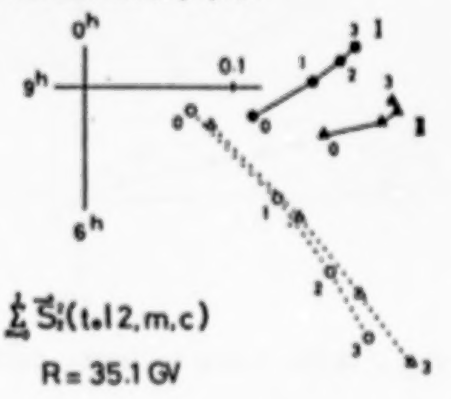

Fig.3 SECOND SPACE HARMONIC VECTORS

The resultant second space harmonic vectors are shown in Fig.3. These vectors in both polarity states are mainly due to the η_2^{0c}-type anisotropy which is independent of ϕ (cf. Eq.(1)). The magnitude η_2^{0c} of the anisotropy includes three terms expressing, respectively, the spatial derivatives of S_i, the IMF-curvature effect and the IMF-focusing effect. On the basis of simulations, it is found that all these terms have significant contribution to the anisotropy and the IMF-focusing effect is not always most predominant. A similar ϕ- independent anisotropy was obtained also by Bieber and Pomerantz(7), on the basis of the following diffusion equation with respect to the pitch angle cosine ($\mu=\cos\theta$).

$$\frac{\partial f(\mu,x_1,t)}{\partial t}+\mu v\frac{\partial f(\mu,x_1,t)}{\partial x_1}-\frac{\partial}{\partial\mu}D_{\mu\mu}\frac{\partial f(\mu,x_1,t)}{\partial\mu}+\frac{v}{2L}(1-\mu^2)\frac{\partial f(\mu,x_1,t)}{\partial\mu}=0, \qquad (8)$$

where $D_{\mu\mu}$ is the Fokker-Planck coefficient for pitch angle scattering and L is the focusing length of IMF(8). They concluded that the anisotropy is principally a result of the focusing effect of IMF represented by the last term in Eq.(8). This anisotropy can be regarded as a special case which is applicable only for one dimensional diffusion along the IMF with infinite radius of curvature in the equatorial plane. In other words, this special anisotropy lacks the term expressing the IMF-curvature effect which has a dominant influence on the anisotropy as pointed out previously.

Turning to the third order anisotropy, we obtained two dominant terms η_3^{0c} and η_3^{1c}. The eigen phases of the tri-diurnal variation arising from these two terms are almost orthogonal to each other, that is, (1h,5h) from η_3^{0c} and (3h,7h) from η_3^{1c}. It is noteworthy that one of the eigen phases(3h,7h) arising from η_3^{1c} coincides with the observed phase around 7h in local time(9,10). Since the η_3^{1c}-type distribution is not symmetrical with respect to the field, this implies that the angular

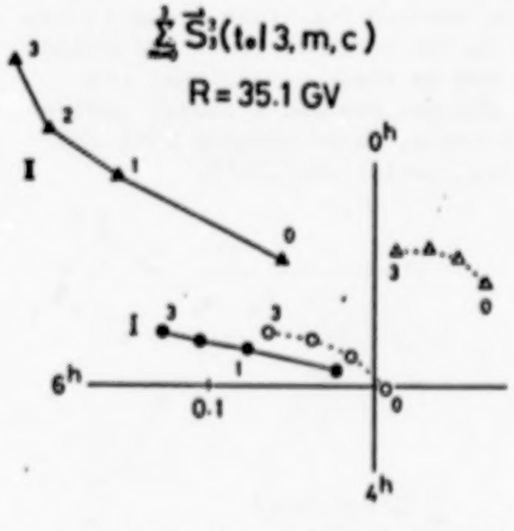

Fig.4 THIRD SPACE HARMONIC VECTORS

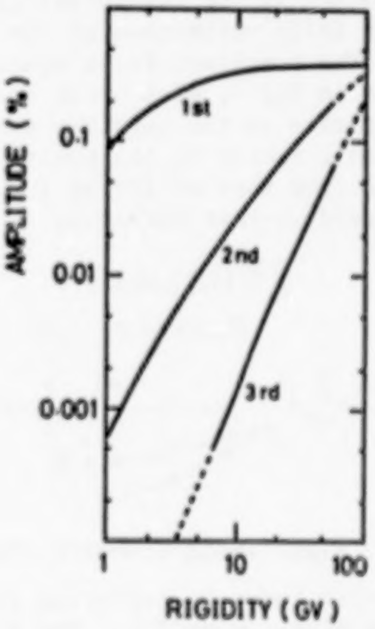

Fig.5 RIGIDITY SPECTRA OF THE FIRST THREE HARMONICS

distribution of the third order anisotropy can not expressed generally in terms of only the pitch angle cosine μ. In this respect, it is not suitable to discuss the third order anisotropy on the basis of the diffusion equation of Eq.(8). Fig.4 shows the resultant tri-diurnal variations which are mainly composed of the above mentioned two types of distribution, i.e., η_3^{0c} and η_3^{1c}. It is noted that the tri-diurnal variations obtained show polarity dependence. This dependence, however, is sensitive to the modulation parameters and, for instance, in case I we can get almost a polarity independent variation with increasing a_λ.

Lastly, Fig.5 shows the rigidity spectra of the first three harmonics obtained in case I for $a_\lambda = 0$. The spectrum of the higher harmonic rises more steeply than that of the lower harmonic, and in the high rigidity region, the spectra of the second and third harmonic are almost proportional, respectively, to R and R^2. This is due to λ linearly increasing with rigidity R(cf. Eq.(7)). Such a rigidity dependence is consistent with the observations(10,11).

References

1. Munakata,K. and Nagashima,K.(1984)
   Proc. Int. Sympo. on Cosmic Ray Modulation(Morioka), p144.
2. Nagashima,K. et al.(1985)
   paper code SH 4.3-9, in this conference.
3. Tatsuoka,R. and Nagashima,K.(1985)
   paper code SH 4.5-2, in this conference.
4. Thambyahpillai,T. and Elliot,H.(1953)
   Nature,171, p918.
5. Forbush,S.E.(1969)
   J. Geophys. Res., 74, p3451.
6. Mori,S. et al.(1979)
   Proc. 16th Int. Cosmic Ray Conf.(Kyoto), 4, p64.
7. Bieber,J.W. and Pomerantz,M.A.(1983)
   J. Geophys. Res. Lett., 10, p920.
8. Earl,J.A.(1976)
   Astrophys. J., 205, p900.
9. Nagashima,K. et al.(1977)
   Proc. 15th Int. Cosmic Ray Conf.(Plovdiv), 4, p72.
10. Mori,S. et al.(1984)
    Proc. Int. Sympo. on Cosmic Ray Modulation(Morioka), p138.
11. Morishita,I. et al.(1984)
    Proc. Int. Sympo. on Cosmic Ray Modulation(Morioka), p130.

N85-35020

FORMULATION OF COSMIC-RAY SOLAR DAILY VARIATION AND ITS SEASONAL VARIATION, PRODUCED FROM GENERALIZED STATIONARY ANISOTROPY OF SOLAR ORIGIN

R. Tatsuoka and K. Nagashima*

Department of Physics, Nagoya University, Nagoya 464, Japan
*Cosmic Ray Research Laboratory, Nagoya University
Nagoya 464, Japan

1. **Introduction.** In the previous papers(1-3), we presented a formulation of cosmic-ray daily variations produced from solar anisotropies stationary through a year and also of their annual (or seasonal) modulation caused by the annual variation of the rotation axis of the Earth relative to that of the Sun. These anisotropies are symmetric for an arbitrary rotation around an axis. On the other hand, from observations of the tri-diurnal variation(5), it has been suggested that solar anisotropies also contain some axis-asymmetric term of the third order with respect to the IMF-axis. This suggestion has recently found support in a theoretical study by Munakata and Nagashima(4). According to their results, the terms of axis-asymmetry with respect to IMF-axis appear also in the 2nd order anisotropy, together with some different kinds of axis-symmetric terms.

The contribution of these anisotropies to the daily variation is different from that of those discussed previously. In the present paper, we extend the above mentioned formulation to a case of a generalized anisotropy.

2. **Formulation.** Following after the formulation by Munakata and Nagashima(4), we express the stationary anisotropy $\eta(\mathbf{r},p)$ through a year in the IMF-polar-coordinate system defined in fig. 1, as

$$\eta(\mathbf{r},p)=\sum_{n=1}^{\infty}\sum_{m=0}^{n}\{\eta_n^{mc}(\mathbf{r},p)\cos m\Phi'+\eta_n^{ms}(\mathbf{r},p)\sin m\Phi'\}P_n^m(\cos\theta'), \tag{1}$$

where $\eta_n^{mc}(\mathbf{r},p)$ and $\eta_n^{ms}(\mathbf{r},p)$ are coefficients, and the angles θ' and Φ' express the incident direction of cosmic rays with momentum p at a point $\mathbf{r}$. $P_n^m(\cos\theta')$ in the equation is the semi-normalized associate Legendre function(6). It is noted that the terms with coefficients $\eta_n^{0c}(\mathbf{r},p)$'s have a symmetry with respect to the IMF-axis, and have been discussed in the previous papers(1-3). In eq. (1), each term with the coefficient η_n^{mc} or η_n^{ms} can be expressed in the equatorial coordinate system, as

$$\begin{cases}\eta_n^{mc}(\mathbf{r},p)P_n^m(\cos\theta')\cos m\Phi'=\sum_{k=0}^{n}P_n^k(\cos\theta)S_n^k(\alpha|n,m,c)\\[2ex] \eta_n^{ms}(\mathbf{r},p)P_n^m(\cos\theta')\sin m\Phi'=\sum_{k=0}^{n}P_n^k(\cos\theta)S_n^k(\alpha|n,m,s),\end{cases} \tag{2}$$

where

$$S_n^k(\alpha|n,m,\sigma)=\eta_n^{m\sigma}\{a_n^k(\alpha_S|n,m,\sigma)\cos k(\alpha-\alpha_S+\pi)+b_n^k(\alpha_S|n,m,\sigma)\sin k(\alpha-\alpha_S+\pi)\}, \tag{3}$$

in which the angles α and θ are, respectively, the right-ascension and the co-declination $(\theta=\pi-\delta)$ of the particle's incident direction. α_S in eq. (3) is the right-ascension of the Sun, and $\alpha-\alpha_S+\pi$ is related to solar local time t as $\alpha-\alpha_S+\pi=2\pi(t/24\mathrm{hr})$. Using this relation, the incident direction can be expressed in terms of θ and t instead of θ and α. The coefficients a_n^k and b_n^k in eq. (3) vary with α_S, owing to the seasonal variation of the relative configuration between the equatorial- and IMF-coordinate systems arising from the Earth's revolution around the Sun. Applying the frequency modulation method(²), S_n^k of eq. (3) can be transformed as

$$S_n^k(\alpha|n,m,\sigma)=\sum_{l=-\infty}^{\infty} S_n^k(t_{l/k}|n,m,\sigma) \quad \text{for } \sigma{=}c \text{ or } s, \text{ and } k\neq 0, \tag{4}$$

where

$$S_n^k(t_{l/k}|n,m,\sigma)=x_n^k(l|n,m,\sigma)\cos(2k\pi t_{l/k}/24\mathrm{hr}) + y_n^k(l|n,m,\sigma)\sin(2k\pi t_{l/k}/24\mathrm{hr}), \tag{5}$$

where

$$\begin{cases} x_n^k(l|n,m,\sigma)=\mathrm{T}_x(k,l|n,m,\sigma)\eta_n^{m\sigma} \\ y_n^k(l|n,m,\sigma)=\mathrm{T}_y(k,l|n,m,\sigma)\eta_n^{m\sigma}, \end{cases} \tag{6}$$

in which T_x and T_y are called the transformation coefficients. In eqs. (4) and (5), $t_{l/k}$ is the time in hours (0~24hr) in a day defined by 1year/(365+l/k) and therefore $P_n^k(\cos\theta)S_n^k(t_{l/k}|n,m,\sigma)$ expresses the k-th harmonic of the daily variation in the time frame of $t_{l/k}$ observed by a vertical telescope pointing toward the θ-direction in the outer space of the Earth.

The terms with $l=0$ are the yearly averaged solar k-th harmonic variations and are expressed by the symbol "*SO*", while those for $l\neq 0$ are called the extended sidereal ($l>0$) and anti-sidereal ($l<0$) daily variations(²) and are expressed by the symbol "$SI_{l/k}$" for $l>0$ and "$AS_{|l|/k}$" for $l<0$.

Assuming that the anisotropy is stationary through a year, all the transformation coefficients $\mathrm{T}_x(k,l|n,m,\sigma)$ and $\mathrm{T}_y(k,l|n,m,\sigma)$ in eq. (6) are obtained for $n\leq 3$ and $|l|\leq 3$ and are shown in Tables I, II and III. In the calculations, $\boldsymbol{B}$, assumed to have Parker's Archimedian spiral structure, is expressed in the heliographic polar co-ordinate system (r, θ_h, φ_h) as

$$\begin{aligned} B_r&=B_0(1\mathrm{a.u.}/r)^2, \\ B_{\theta_h}&=0, \\ B_{\varphi_h}&=-B_0(1\mathrm{a.u.}/r)\sin\theta_h, \end{aligned} \tag{7}$$

where B_0 is positive(negative) for the away (toward) sector. The inclination of the solar equatorial plane with respect to the ecliptic plane is also taken into account in the calculations(³).

3. Discussion and Conclusion. The terms with a mark "c" in tables express the IMF-sense-*independent* terms, as the corresponding coefficients η_n^{mc}'s in eq. (2) are independent of IMF-sense(⁴). On the contrary, the terms with a mark "s" express the IMF-sense-*dependent* terms, as η_n^{ms}'s change their sign with the change of IMF-sense.

The No.1 and No.2 terms in Table I produce the solar diurnal variation of north-south symmetric type, whereas the No.3 term produces the IMF-sense-dependent sidereal diurnal variation of Swinson type(⁷).

The most important term in Table Ⅱ is that of No.1. It is noteworthy that the No.4 and No.5 terms are IMF-sense-dependent and will be discussed in detail in a separate paper(8).

The importance of the No.1 term in Table Ⅱ has been well acknowledged for the explanation of the solar tri-diurnal variation from the theoretical point of view, whereas the existence of the No.2 term has recently been pointed out by Munakata and Nagashima(4).

In conclusion, it is emphasized that the transformation coefficients(T_x and T_y) in these tables enable us to connect solar anisotropies produced from the diffusion-convection process with the observed cosmic-ray solar daily variation and its seasonal variation and, as the result, enable us to obtain the information of electromagnetic state in interplanetary space from the observation of solar daily variation of cosmic rays.

References

(1) K. Nagashima: *Rep. Ionos. Space Res.*, Japan, **25**, 189 (1971).
(2) K. Nagashima and H. Ueno: *Rep. Ionos. Space Res*, Japan, **25**, 212 (1971).
(3) K. Nagashima, R. Tatsuoka and S. Matsuzaki: *Nuovo Cim.*, **6C**, 550 (1983).
(4) K. Munakata and K. Nagashima: *Proc. Int. Cosmic Ray Symposium* (Morioka, Japan, 1984), p.144; This Conference SH 4.5-1.
(5) K. Nagashima et al.: *Proc. Int. Conf. Cosmic Rays*, Vol.4 (Plovdiv, 1977), p.72; S. Mori et al.: *Proc. Int. Cosmic Ray Symposium* (Morioka, Japan, 1984), p.138.
(6) S. Chapman and J. Bartels: *Geomagnetism*, Vol.2 (Oxford, 1940), p.611.
(7) D.B. Swinson: *J. Geophys. Res.*, **76**, 4217 (1971).
(8) K. Nagashima, K. Munakata and R. Tatsuoka: This Conference SH 4.3-9.

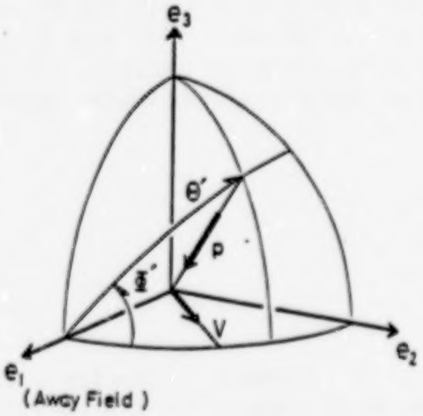

Fig. 1. The IMF-POLAR-COORDINATE SYSTEM.
p: Momentum of particle.
V: Solar wind velocity.
e_1: Unit vector in the direction of 'away' magnetic field.
e_3: Unit vector in the direction of $e_1 \times V$.
$e_2 = e_3 \times e_1$.

Table Ⅰ The transformation coefficients $T_x(k,l|n,m,\sigma)$ and $T_y(k,l|n,m,\sigma)$ in eq.(6) for n=1, in units of 10^{-3}.

No.	$nm\sigma$	k	l = 3		l = 2		l = 1		l = 0		l = -1		l = -2		l = -3	
			T_x	T_y	T_x	T_y	T_x	T_y	T_x	T_y	T_x	T_y	T_x	T_y	T_x	T_y
1	10c	1			-3,	47			696.	-668			16.	-15		
2	11c	1			32.	-46			660.	671			13.	16		
3	11s	1	-4.	9			62.	-410			-57.	-25			-1,	0

Table Ⅰ . The transformation coefficients $T_x(k,l|n,m,\sigma)$ and $T_y(k,l|n,m,\sigma)$ in eq.(6) for n=2, in units of 10^{-3}.

No.	nmσ	k	$l = 3$ T_x T_y	$l = 2$ T_x T_y	$l = 1$ T_x T_y	$l = 0$ T_x T_y	$l = -1$ T_x T_y	$l = -2$ T_x T_y	$l = -3$ T_x T_y
1	20c	1	-8, -12		-55, 285		-300, 59		-7, 1
		2		51, 60		34, -804		2, -36	
2	21c	1	-9, 16		57, 1		-15, -395		0, -9
		2		-41, -25		907, 25		40, 4	
3	22c	1	23, -8		-80, 579		268.		6, 1
		2		134, 17		8, 421		-3 17	
4	21s	1		22, 102		591, -553		28, 6	
		2	22, 13		-230, -330		-61, 13		-2, 1
5	22s	1		121, -100		531, 522		-12, 28	
		2	-25, -13		313, -227		-13, -59		-1, -2

Table Ⅱ . The transformation coefficients $T_x(k,l|n,m,\sigma)$ and $T_y(k,l|n,m,\sigma)$ in eq.(6) for n=3, in units of 10^{-3}.

No.	nmσ	k	$l = 3$ T_x T_y	$l = 2$ T_x T_y	$l = 1$ T_x T_y	$l = 0$ T_x T_y	$l = -1$ T_x T_y	$l = -2$ T_x T_y	$l = -3$ T_x T_y
1	30c	1		-35, -110		-291, 274		82, 46	
		2	-30, -7		167, 247		-186, 276		-9, 12
		3		103, 10		-466, -532		-31, -36	
2	31c	1		-61, 40		-127, -101		-70, 122	
		2	10, 15		-60, 46		-343, -267		-14, -13
		3		-47, 51		627, -568		44, -36	
3	32c	1		-42, -132		-342, 293		-117, -75	
		2	-38, -15		268, 390		238, -228		12, -9
		3		104, -96		353, 350		19, 25	
4	33c	1		-223, 161		-342, -314		59, -74	
		2	52, 53		-410, 306		102, 139		3, 7
		3		84, 128		-113, 140		-9, 5	
5	31s	1	-19, -26		-83, 449		-373, 75		-9, -7
		2		137, 85		42, -563		28, -22	
		3	39, -15		-368, -77		-41, 46		-1, 3
6	32s	1	-25, 47		75, 11		-60, -537		12, -12
		2		-30, -57		655, 14		23, 38	
		3	-21, 28		84, -451		-57, -49		-4, -2
7	33s	1	63, 0		-83, 639		389, -8		8, 11
		2		256, 48		27, 345		-25, 9	
		3	2, -51		261, 38		27, -34		1, -2

ORIGINAL PAGE IS
OF POOR QUALITY

N85-35021
SH 4.5-3

SOLAR TRI-DIURNAL VARIATION OF COSMIC RAYS IN A WIDE RANGE OF RIGIDITY

Mori, S., H. Ueno*, Z. Fujii*, I. Morishita** and K. Nagashima*

Department of Physics, Shinshu University, Matsumoto 390, Japan
*Cosmic-Ray Research Lab., Nagoya University, Nagoya 464, Japan
**Department of Physics, Asahi University, Hozumi-cho, Gifu 501-02, Japan

ABSTRACT

Solar tri-diurnal variations of cosmic rays have been analyzed in a wide range of rigidity, using data from neutron monitors, and the surface and underground muon telescopes for the period 1978-1983. The rigidity spectrum of the anisotropy in space is assumed to be of power-exponential type as $(P/\gamma P_0)^{\gamma}\exp(\gamma-P/P_0)$. By means of the best-fit method between the observed and the expected variations, it is obtained that the spectrum has a peak at $P\ (=\gamma P_0) \cong 90$ GV, where $\gamma \cong 3.0$ and $P_0 \cong 30$ GV. The phase in space of the tri-diurnal variation is also obtained as 7.0 hr (15 hr and 23 hr LT), which is quite different from that of $\sim$1 hr, arising from the axis-symmetric distribution of cosmic rays with respect to the IMF.

1. Introduction

Studies of higher harmonics in the daily variation of cosmic rays provide valuable infromations as to the nature of the cosmic ray modulation in the heliosphere. So far a great many investigation has been performed of the solar tri-diurnal variation, and some of its characteristic natures have been revealed; its extra-terrestrial origin and also its rising spectrum with rigidity (e.g., Bieber et al., 1983; Mori et al., 1984; hereafter referred to as Paper I).

These results, however, have not yet been firmly founded because of the statistical uncertainty of the data used which is largely due to limited rigidity range. In particular, there is a wide divergence of opinion as to the direction of the anisotropy; some analyses reported $\sim$1 hr direction, while some obtained $\sim$7 hr direction. This discrepancy is crucial for determining the modulation mechanism; 1 hr direction is in favor of the 'loss-cone' model (Fujii, 1971) or the model of Bieber et al. (1983), whereas 7 hr direction requires other kind of model such as the one presented by Munakata and Nagashima (1985, in this issue).

In the present analysis, we try to obtain a definite form of the anisotropy responsible for the averaged tri-diurnal variations over 6 years (1978-1985), using data in a wide range of rigidity from neutron monitors to underground muon telescopes, which respond to the effective rigidity of 10 to 600 GV.

2. Analysis of Data

The present experimental data include 2 to 6-year averages of neutron monitor data in a worldwide network (36 stations from the polar to the equatorial regions) and 6-year averages of the surface (NAGOYA) and underground (MISATO and SAKASHITA) muon telescopes for the period 1978-1983.

Fig. 1 illustrates the summation harmonic dial, showing clearly the persistency of year-to-year changes of the observed tri-diurnal variations of three muon telescopes at NAGOYA (surface) for 1971-1983, at MISATO (34 m.w.e. in depth underground) for 1974-1983 and at SAKASHITA (80 m.w.e. in depth underground) for 1978-1983. In the present analysis, 6-year averages over 1978-1983 were used; of 13 directional components at NAGOYA, 9 components at MISATO and 10 components at SAKASHITA, and these are listed in Paper I.

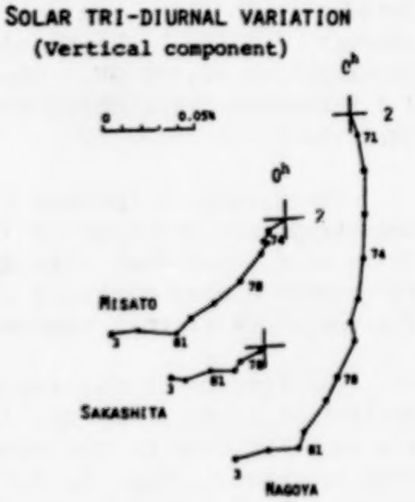

Fig. 1 Observed solar tri-diurnal variations of V-component at NAGOYA, MISATO and SAKASHITA in summation dial.

In order to derive the 3rd order anisotropy, the tri-diurnal variation produced by the anisotropy with a certain form of the rigidity spectrum G(P), will be compared with the observed results. In the anaysis, G(P) is assumed to be of power-exponential type as

$$G(P)=(P/\gamma P_0)^{\gamma}\exp(\gamma-P/P_0) \quad (1)$$

Evidently, G(P) becomes maximum at $P=\gamma P_0$ for $\gamma>0$, and is normalized to unity.

The expected 3rd harmonic components (A_{ij}, B_{ij}) for j-th components telescopes of i-th station including neutron monitor station, are related to the space harmonic components (X, Y) by the following equations with coupling coefficients c_{ij} and s_{ij} as

$$A_{ij} = (c_{ij}X + s_{ij}Y), \qquad B_{ij} = (-s_{ij}X + c_{ij}Y) \quad (2)$$

The coefficients c_{ij} and s_{ij} were derived from the differential coupling coefficients dc_{ij} and ds_{ij} given by Fujimoto et al. (1984). The best-fit parameters satisfying the following equation are determined.

$$\sum_{ij} w_{ij}\{ (A_{ij} - a_{ij})^2 + (B_{ij} - b_{ij})^2 \}= \text{minimum} = \delta^2 \quad (3)$$

In Eq. (3), the weight w_{ij} is given for the observed a_{ij} and b_{ij} so as to balance the difference in the number of the data used in the rigidity interval; 6 divisions in all the ranges of 10 to 600 GV to have equal weight. Also each vector in all the muon components was subtracted from the reference component to eliminate the atmospheric temperatute effect; in this analysis, V-component for NAGOYA and MISATO and SE-component for SAKASHITA were taken as the reference.

3. Results and Discussions

The contour map of equal δ^2's obtained from the residual sum of the observed vectors and the expected vectors computed by Eq. (2), is shown against γ and P_0 in Fig. 2. As is seen in the figure, minimal δ^2 region locates in relatively narrow regions of γ and P_0-value. It is noted that in these regions the product of γ and P_0 keeps almost invariant as $\gamma P_0 \cong 90$ GV. The best-fit parameters were obtained as that $\gamma \cong 3.0$ and $P_0 \cong 30$ GV.

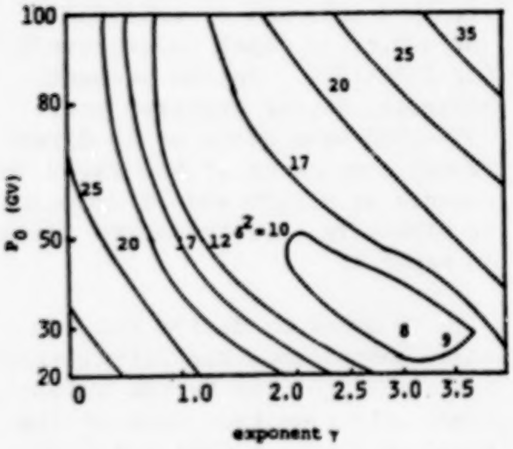

Fig. 2 Contour map of equal δ^2 plotted against γ and P , showing minimal δ^2 ($\cong$8) for $\gamma \cong 3.0$ and $P_0 \cong 30$ GV.

The direction (phase) of the anisotropy was obatined as 7.0 hr. It is also noted that this direction shows almost constant value for the above minimal region.

The fitness of the reproduced variations computed by Eq. (2) in the best-fit case to the observed ones is shown in Fig. 3; (a) for NAGOYA, (b) for MISATO and (c) for SAKASHITA, respectively. The observed vectors are shown with the solid circles (●) and the reproduced ones with the open circles (○). Also the reference component mentioned above is shown by the symbol (⊙) and the origin of the diagram in the best-fit case is given by the cross (✖). A fairly good agreement can be seen between two patterns drawn by connecting each observed point (solid line) and each reproduced point (dotted line) for each station.

The present anaysis can obtain a definite parameter set as; $\gamma \cong 3.0$ and $P_0 \cong 30$ GV. As shown in Paper I, where only muon data at the above three stations (NAGOYA, MISATO and SAKASHITA) were used, parameter set (γ,P_0) rather spereads as; γ=2∿12 and P_0=50∿8 GV. The present form can be derived by adding neutron monitor data to Paper I. Note that the observed vectors of neutron monitors from 36 stations are so divergent even if in the best-fit case, which may be largely due to inaccurate barometric correction in the data.

On the other hand, the direction (phase) of the anisotropy in space was obtained as ∿7 hr (∿15 hr and ∿23 hr LT). So far there has been a wide divergence of opinion as to the direction; ∿1 hr direction was reported by the analyses of neutron monitor data alone, while ∿7 hr direction was reported by using muon data. The former is in favor of the 'loss-cone' model (Fujii, 1971) or the model of Bieber et al. (1983), arising from the axis-symmetric distribution of cosmic rays with respect to the IMF. On the other hand, the latter requires other kind of model such as the one preseneted by Munakata and Nagashima (1985, in this issue). The present result provides a firm basis for the latter model.

A further analysis would be necessary to derive the detailed form and its year-to-year variation.

ORIGINAL PAGE IS
OF POOR QUALITY

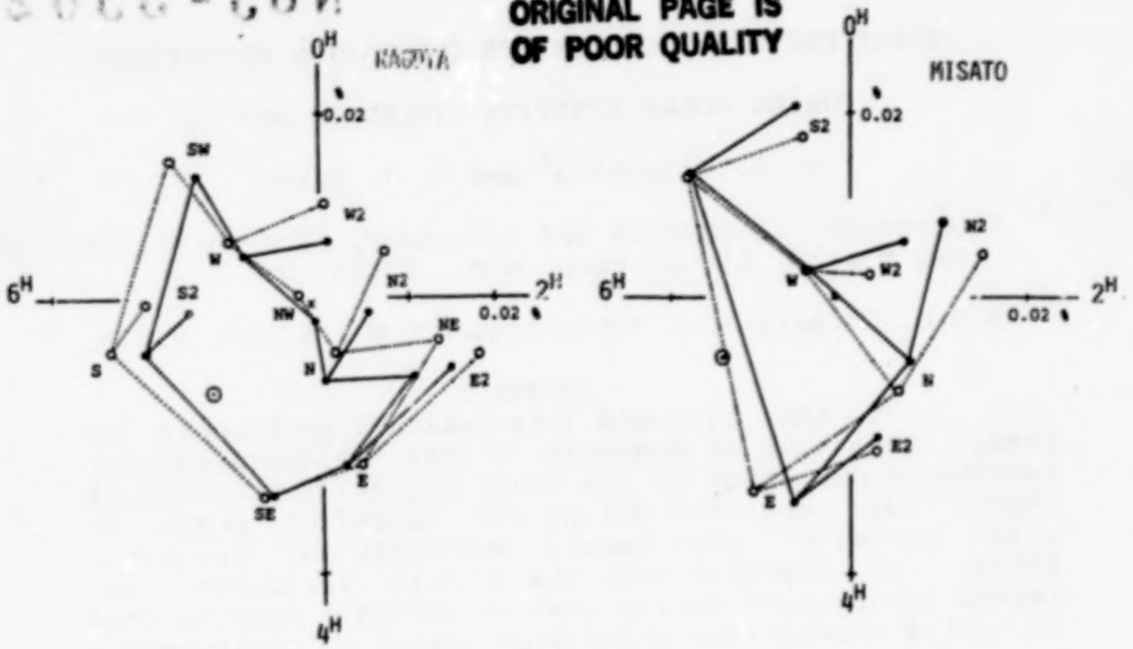

(a) for NAGOYA (b) for MISATO

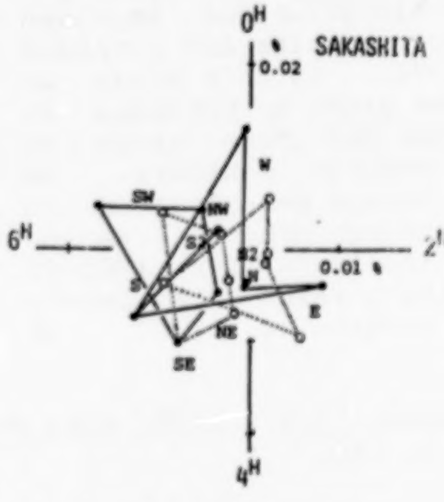

(c) for SAKASHITA

Fig. 3 Fitness between the observed (●) and the reproduced (○) variations; (a) for NAGOYA, (b) for MISATO and (c) fro SAKASHITA for the period 1978-1983.

4. Acknowledgements

The authors express their appreciation to Messrs. K. Chino and S. Nakamura for their computational help. Neutron monitor data were obtained through WDC-C2, whom we acknowledge much.

References

Bieber, J.W. et al., (1983), 18th ICRC (Bangalore), 3, 289.
Fujii, Z., (1971), Rep. Ionos. Space Res., Japan, 25, 242.
Fujimoto, K. et al., (1984), Rep. of CR-Lab,, Nagoya Univ., No. 9.
Mori, S. et al., (1984), Int. CR-Symp. (Morioka), p138.
Munakata, K. and K. Nagashima, (1985), in this issue (SH 4.5-1).

N85-35022

UPPER CUT-OFF RIGIDITY FOR COROTATION ANISOTROPY DURING SOLAR ACTIVITY CYCLES 20 AND 21

H. S. Ahluwalia[1] and J. F. Riker[2]

[1] Department of Physics and Astronomy, The University of New Mexico, Albuquerque, N.M. 87131, U.S.A.

[2] B.D.M. Corporation, Albuquerque, N.M., 87106, U.S.A.

ABSTRACT

At the Eleventh International Conference on Cosmic Rays held at Budapest in 1969, we discussed the results of our study of the solar diurnal variations of cosmic rays observed during the ascending phase of solar activity cycle twenty (Ahluwalia and Ericksen, 1970). We reported that the diurnal variation, observed underground during 1965-68 period, results from an extra-terrestrial anisotropy having a continuously increasing upper cut-off rigidity R_c. However, the coupling functions applicable to underground telescopes were controversial then. This situation has improved now. So we have re-examined those results and extended them to cover the period 1965-78. In this study we have used the coupling functions given by Murakami et al. (1979) for underground muons and those given by Lockwood and Weber (1967) for neutron monitors. We show that a great deal of care should be exercised in calculating the value of R_c. Although numerical values of R_c are a little different, the trend for 1965-68 period remains unchanged. Highest value of R_c occurs in 1970 and the lowest value occurs in 1976. Our results are discussed.

Ahluwalia, H.S., and Ericksen, J.H., 1970, Acta Phys. Acad. Scient. Hung., 29, Suppl. 2, 139.

Murakami, K., Nagashima, K., Sagisaka, K., Mishima, Y., and Inoue, A., 1979, Nuovo Com., 2C, 635.

Lockwood, J.A., and Weber, W. R., 1967, J. Geophys. Res., 72, 3395.

SH 4.5-5

N85-35023

22-YEAR CYCLE OF THE UPPER LIMITING RIGIDITY OF DALY WAVES

G. Erdős, J. Kóta and E. Merényi

Central Research Institute for Physics, Budapest, Hungary

Abstract. The method of calculating energy losses along regular particle trajectories is applied to obtain the predicted cosmic ray anisotropies from 200 to 500 GV. The tilt angle of the interplanetary neutral sheet varies to simulate a 22-year cycle magnetic cycle. The calculated values of solar diurnal and semidiurnal, and siderial diurnal intensity waves are compared with observations.

1. Introduction. Earlier we suggested (Erdős and Kóta 1979, 1980) that the cosmic ray anisotropies observed at underground energies can be interpreted in terms of regular particle motion in the Interplanetary Magnetic Field (IMF) incorporating a wavy neutral sheet. At high rigidities, the effects of small-scale irregularities should be negligible and, being the dominant large-scale feature of the IMF, the wavy neutral sheet plays the decisive role.

In this paper we investigate how cosmic ray anisotropies change during a 22-year magnetic cycle. We consider the 200 - 500 GV range which represents the high rigidity tail of the modulation spectrum. The state of the heliosphere changes in a complex way during a solar cycle. From this complexity, the only feature we consider here is the variation of the inclination of the tilted heliospheric neutral sheet. The tilt angle is minimal around solar minimum and increases with increasing solar activity (Thomas and Smith 1981). As a crude approximation, we simulate the 22-year cycle by simply changing the tilt angle.

2. The Model. The IMF model and the method of calculation are described in detail elsewhere (Erdős and Kóta 1979, 1980, 1981). Briefly, a conventional Parker spiral field is applied with a 5 gamma field strength at the earth. The wavy neutral sheet dividing the opposite polarities is given by

$$\sin\theta = \sin\alpha \cdot \cos(\varphi + r) \qquad (1)$$

where θ and φ are heliographic latitude and longitude, respectively, r is heliocentric distance in units of AU. The tilt angle, α, gives the maximum latitudinal excursion of the neutral sheet. The configuration of away polarity above the sheet and toward polarity below the sheet will be referred to as $A > 0$.

We note that equation (1) does not exactly correspond to a tilted plane at the sun. Calculations were also carried out for a tilted plane of 90° inclination. This case of indefinite A, where the two configurations merge, will be labelled with 90^{*}.

The theoretical results to be presented always give the full free-space anisotropy that would be observed by an equatorial observer in the absence of geomagnetic deflection. Calculations do not include the Compton-Getting effect due to the orbital motion of the earth.

3. Results. In this paragraph we briefly report on the daily intensity waves predicted for 200, 300 and 500 GV at various values of the tilt angle, α.

The harmonic dial of the solar daily variation calculated for 200 GV is shown in Figure 1. For comparision, Figure 2 (taken from Benkő et. al., 1984) shows the year-to-year daily vectors observed by the Budapest underground telescopes (median energy: 180 GeV) in the period of 1976 (A>0, low solar activity) to 1983 (A<0). We find a remarkable agreement if correction is made to the 1.5 hr geomagnetic deflection, the Compton-Getting effect due to the earth's orbital motion, and the cos 47° ≃ 0.68 attenuation factor due to the 47° N geografical latitude of the station.

The amplitudes of the solar daily waves calculated for 200, 300 and 500 GV are shown in Figure 3.

The predicted harmonic dial of the semidiurnal variation of 200 GV cosmic rays is shown in Figure 4, while the calculated amplitudes are given in Figure 5. A charge asymmetry can clearly be seen: for A > 0, an earlier phase and a smaller amplitude is to be expected. These findings are in general agreement with numerous observations (see, for example, Morishita et. al., 1984).

As expected, the phase of the sidereal daily wave was always found to be close to either 6 hr or 8 hr, depending on the polarity of the magnetic sector. Figure 6 gives the calculated sidereal amplitudes. Our theoretical results suggest a hard energy spectrum; the spectrum of the sidereal variation turns out markedly harder than the solar diurnal and semidiurnal spectra. This finding also suggests that a sidereal variation of solar origin may still be present at rigidities where solar diurnal and semidiurnal waves already diminish. Thus, in searching for a genuine galactic anisotropy of cosmic rays one should be cautious in establishing the upper rigidity limit of the heliospheric effects.

References:

Benkő, G., Kecskeméty, K., Kóta, J., Somogyi, A., Varga, A., 1984: Proc. Int. Symp. on CR Modulation, Morioka, p104

Erdős, G. and Kóta, J., 1979: Proc. 16th ICRC, Kyoto, 4, 45

Erdős, G. and Kóta, J., 1980: Astrophys. Space Sci., 67, 45

Erdős, G. and Kóta, J., 1981: Proc. 17th ICRC, Paris, 10, 105

Morishita, I., Ueno, H., Fujii, Z., Mori, S. and Nagashima, K., 1984: Proc. Int. Symp. on CR Modulation, Morioka, Japan, p130.

Thomas, B. T. and Smith, E. J., 1981: J. Geophys. Res., 86, 11105

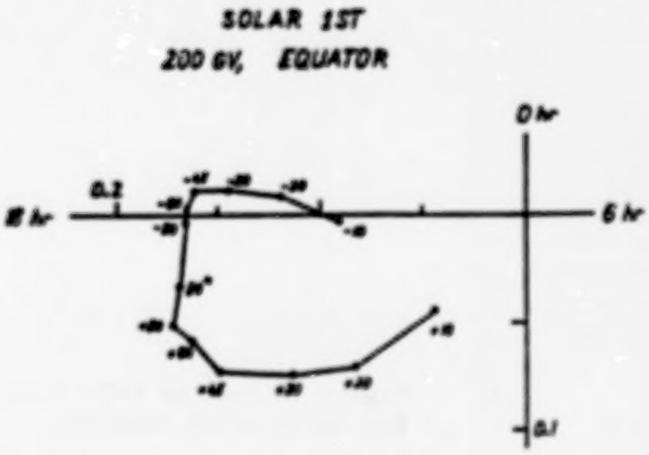

Figure 1. Calculated harmonic dial of the solar daily waves of 200 GV cosmic rays. Numbers stand for the tilt angle, α, in degrees (negative values refer to A < 0).

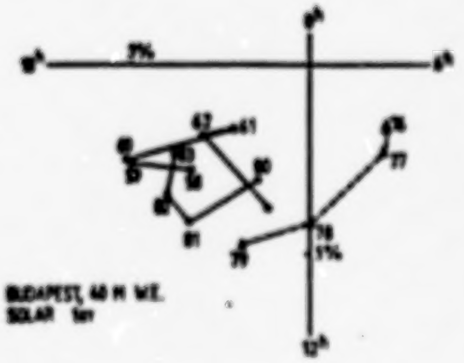

Figure 2. The Budapest solar daily vectors without geomagnetic correction. Numbers stand for the year of observation. Results are grouped according to the polarity state (triangles and dashed lines refer to A > 0).

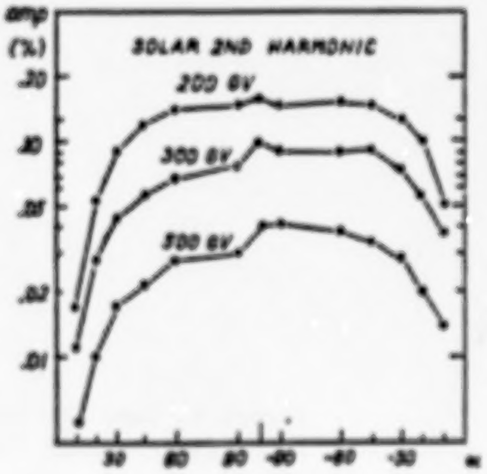

Figure 3. Calculated amplitudes of the solar daily vectors of 200, 300 and 500 GV cosmic rays vs the tilt angle, α, in degrees. (Negative values of α refer to A < 0.)

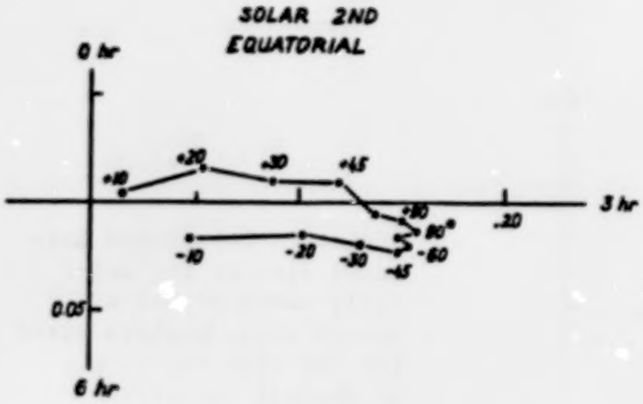

Figure 4. Same as Fig. 1., for semidiurnal vectors.

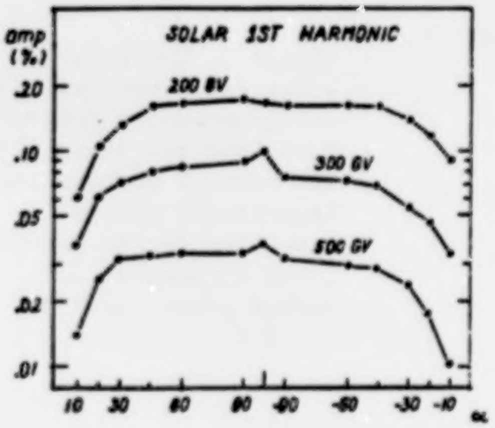

Figure 5. Same as Fig. 3., for semidiurnal vectors.

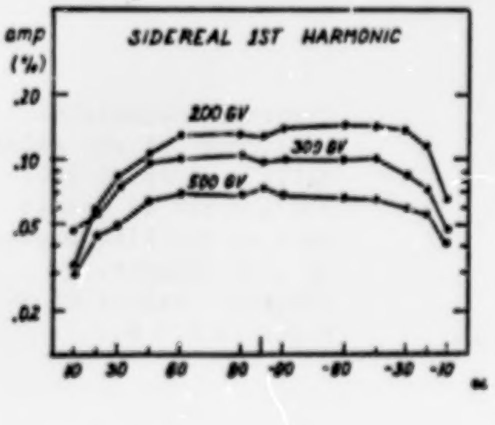

Figure 6. Same as Fig. 3., for sidereal daily vectors.

SH 4.5-6

N85-35024

SOLAR WIND VELOCITY AND DAILY VARIATION OF COSMIC RAYS

H. S. Ahluwalia[1] and J. F. Riker[2]

[1] Department of Physics and Astronomy, The University of New Mexico, Albuquerque, N.M., 87131, U.S.A.

[2] B. D. M. Corporation, Albuquerque, N.M. 87106, U.S.A.

ABSTRACT

Recently parameters applicable to the solar wind and the interplanetary magnetic field (IMF) have become much better defined (King, 1981). Superior quality of data bases that are now available, particularly for post-1971 period, make it possible to believe the long-term trends in the data. These data are correlated with the secular changes observed in the diurnal variation parameters obtained from neutron monitor data at Deep River and underground muon telescope data at Embudo (30 MWE) and Socorro (82 MWE). The annual mean amplitudes appear to have large values during the epochs of high speed solar wind streams. Our results are discussed.

King, J. H., 1981. J. Geophys. Res., 86, 4828.

N85-35025

DIURNAL ANISOTROPY DURING SOLAR ACTIVITY CYCLE TWENTY AND DIFFUSION-CONVECTION MODEL

H. S. Ahluwalia and J. F. Riker

Department of Physics and Astronomy, The University of New Mexico, Albuquerque, N.M., 87131, U.S.A.

ABSTRACT

Underground muon telescope data obtained at Embudo and Neutron monitor data obtained at Deep River are divided into two sets; one covers the ascending phase of the cycle (1965-70) and the other covers the descending phase (1971-76). The amplitude of diurnal anisotropy calculated from the data does not agree with the value predicted by the simplified version of the Diffusion-Convection Model (DCM); the discrepancy is worse for neutron data.

INTRODUCTION. We report here an extension of our earlier study (Ahluwalia and Ericksen, 1970, 1971). Coupling functions (W) given by Murakami et al. (1979) and those given by Lockwood and Weber (1967) are used to calculate the amplitude of diurnal anisotropy. Median rigidity of response (R_m) ~ 16 GV for Deep River neutrons and ~ 134 GV for Embudo muons. Unlike Subramanian (1971) we are not able to reconcile our calculations with the predictions of the simplified version of Diffusion-Convection Model (Forman and Gleeson, 1975).

DATA. Figure 1 summarizes the available data on the annual mean amplitudes of the diurnal variation observed at Embudo (open circles) for the period 1965-79 and at Deep River (solid dots) for the period 1962-79. The flags indicate the standard deviation, computed from the observed scatter in the data for a given year. Zurich sunspot numbers (R_z) indicate the level of solar activity. Epoch of solar polar field reversal is also shown; after 1970 the solar polar field is directed out of the sun in the northern hemisphere. In

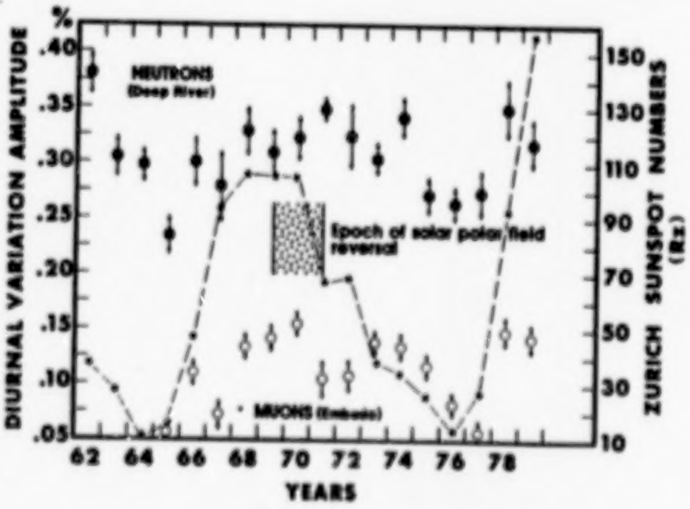

Fig 1

general the amplitudes have the lowest values during activity minima and large values during activity maximum. In particular, we wish to point out that the amplitudes at Embudo have large values for the years 1973, 1974 and 1975 during which the mean level of the solar activity is only about one third of the maximum value in 1968. Bulk velocity (V) of solar wind is high during these years.

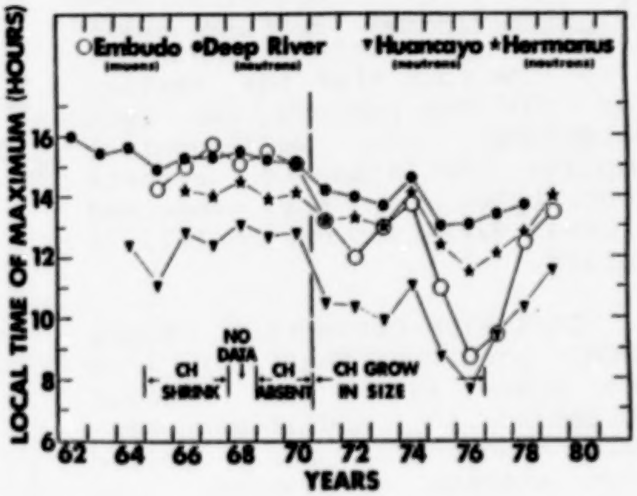

FIG 2

Another important feature of the dependence of the diurnal variation on the solar activity is shown in Figure 2. It gives the annual mean time of maximum of the diurnal variation observed at Embudo, Deep River, Hermanus ($R_m=20$ GV) and Huancayo ($R_m=30$ GV). The data exhibit a remarkable, worldwide, systematic, rigidity-dependent shift of the time of maximum of diurnal variation to early hours, during the period 1971-76. The data for Huancayo and Hermanus are staggered in time, with respect to Deep River, to minimize an overlap. The rigidity dependent nature of this effect was emphasized by us elsewhere (Ahluwalia, 1976). Note that prior to 1971 the observed time of maximum at Embudo is nearly steady at about 15 hours (LT) but in 1976 the time of maximum is at 8.7 hours (LT). The diurnal times of maximum return to pre-1971 values by about 1979, at all stations. Agrawal (1983) has reported similar behavior for neutron and surface-level muon detectors at sites in Canada. Also summarized in Figure 2 is the information about the size of the coronal holes during solar activity cycle (SAC) 20.

ANALYSIS. We subdivide the data into two sets; one set covers the period 1965-70 and the other set covers the period 1971-76. The reader is reminded that the observed diurnal variation is rather steady, on a year to year basis, during the first period and undergoes a remarkable systematic change during the second period. The characteristics of the annual mean diurnal variation observed at Embudo and at Deep River for the two periods are displayed in Fig. 3 on the harmonic dial. The error circles are for 2σ. One can see that the amplitudes for the two periods remain the same for both Embudo muons and Deep River neutrons. However, the time of maximum is significantly early for both detectors, for the second period (1971-76). The fact that the amplitudes are the same for muons as well as neutrons, implies that upper cut-off rigidity R_c has the same average value for both periods; in fact $R_c \sim 70$ GV. Also the fact that the vectors for the two periods, for both detectors, are well-resolved implies that some new effects contribute to the observed diurnal variation during 1971-76 period.

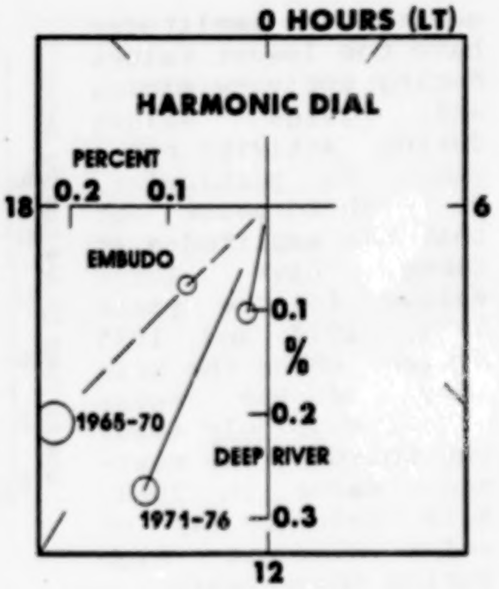

Fig 3

Diffusion-Convection Model (DCM) predicts that if $K_\perp = 0$ and there is no net radial streaming (S_r) and if perpendicular gradient is zero, cosmic rays undergo corotation. In this case the anisotropy (δ) recorded by a detector with a mean asymptotic latitude λ of viewing is given by

$$\delta = 0.6 \text{ Cos } \lambda, \%$$

So we expect that δ should be independent of solar wind bulk velocity (V). An obvious limitation of the model is that it does not contain the concept of R_c. Somehow the diffusion coefficients $K_{\parallel}$, $K_\perp$ must depend upon primary rigidity (R) in such a way as to lend some physical significance to the concept of R_c. The theory in its present state is obscure on this point. Let us assume that,

$$\delta_{\text{theo}} = \begin{cases} 0.6 \cos \lambda \text{ \%}, & \text{if } R<R_c \\ 0.0, & \text{if } R>R_c \end{cases}$$

This form of variational spectrum is consistent with the results obtained in our analyses earlier, for the first period (1965-70). Table 1 gives a summary of results for the two detectors, for the three periods, assuming $R_c = 70$ GV. The direction of anisotropy in free space is calculated after applying corrections for the "orbital-effect" and for the "geomagnetic bending" of the primaries. These corrections are model independent.

RESULTS. (1) Diurnal Anisotropy in free-space is in the direction of 18 hours (LT) for the first (1965-70) and third periods (1965-76), but the direction is significantly earlier for the second period (1971-76).

(2) Within errors of observations the amplitudes of diurnal variations for the two detectors, for the three periods, are the same. The amplitude of the anisotropy, calculated from the data for the two detectors, is tabulated in the last column of Table 1. The calculated value is about 33% less for neutrons and about 8% less for muons when compared to the theoretical value. So our results do not

TABLE 1

Station	λ deg	$\int_{R_o}^{R_c} WdR$ %	Free Space Direction of Diurnal Anisotropy hours (LT) 1965-70	 1971-76	 1965-76	δcalc %
Deep River	11.8	0.78	18.21 ± 0.12	16.87 ± 0.12	17.54 ± 0.12	0.43 ± 0.01
Embudo	19.1	0.28	17.83 ± 0.11	16.87 ± 0.11	17.74 ± 0.11	0.55 ± 0.02

agree with the predictions of the simplified DCM, for SAC 20. However in practice we may not have $K_\perp = 0$. Also $K_\perp$ may be inversely proportional to the square of the particle rigidity (Jokipii, 1971). If we follow Jokipii's suggestion and take $(K_\perp/K_{||}) = 0.15$ and further note that median primary rigidity of response for muons is about a factor of *eight* larger than for neutrons, the calculated values agree much better with the theoretical value. *But this does not explain why the direction of anisotropy is significantly earlier in the second period* (1971-76). Also it is hard to believe that the ratio $K_\perp/K_{||}$ is invariant in time.

(3) In recent years Jokipii has emphasized very strongly that drifts should play an important role in the modulation of cosmic rays (Kota and Jokipii, 1983 and references therein). It would be interesting to see if one obtains a better agreement between theory and observations by invoking charged particle drifts.

REFERENCES.

Agrawal, S. P., 1983. Space Sci. Rev., 34, 127.

Ahluwalia, H. S. and Ericksen, J. H., 1970. Acta. Phys. Acad. Scient. Hung., 29, Suppl. 2, 139.

Ahluwalia, H. S., and Ericksen, J. H., 1971. J. Geophys. Res., 76, 6613.

Ahluwalia, H. S., 1976. Proc. Intern. Cosmic Ray Symp. on High Energy Cosmic Ray Modulation, Tokyo, p. 260.

Forman, M. A., and Gleeson, L. J., 1975. Astrophys. Space Sci., 32, 77.

Jokipii, J. R., 1971. Rev. Geophys. Space Phys., 9, 27.

Kota, J., and Jokipii, J. R., 1983. Astrophys. J., 265, 573.

Lockwood, J. A., and Weber, W. R., 1967. J. Geophys. Res., 72, 3395.

Murakami, K., Nagashima, K., Sagisaka, K., Mishima, Y., and Inoue, A., 1979, Nuova Cim. 2C(5), 635.

Subramanian, G., 1971. J. Geophys. Res., 76, 1093.

SH 4.5-8

DIURNAL EFFECT IN COSMIC RAYS AT MIDDLE LATITUDES ACCORDING TO STRATOSPHERIC MEASUREMENTS

N85-35026

Asatryan G.A., Babayan V.Kh.
Yerevan Physics Institute, Markarian st.2
375036, Yerevan, Armenia, USSR

Stozhkov Yu.I.
P.N. Lebedev Physical Institute of the Academy of Sciences of the USSR, Leninsky prospect,53, 117924, Moscow, USSR

ABSTRACT

Results of measurements of the diurnal wave of the cosmic ray (CR) intensity in stratosphere at the latitude with the geomagnetic cutoff rigidity $R_c = 7.6$ GV are presented.

Measurements of diurnal variation of the CR intensity were carried by means of radiosondes - by a detector composed of a gas-discharge counter CTC-6 and a telescope containing two counters with a 7 mm aluminium filter between them. Radiosondes were launched in Yerevan daily during a month (May 23 to June 23, 1984) at the following hours: 2,5,8,11,14,17,20,23 LT. The period of time during which the measurements were carried out is characterized by a quiet situation: the average three-hourly value $K_p < 3$ [1]. The CR intensity fluctuations in the absorption curve maximum in stratosphere did not exceed ~2.5%

at high altitudes ($R_c = 0.5$ GV) and ~ 1% at the latitude with $R_c = 2.5$ GV.

Experimental data allowed to obtain the altitude dependence of the CR intensity on the atmospheric depth, N(x), for eight different times of LT. To reveal the diurnal wave of the CR intensity in stratosphere, we have used the following method of processing of altitude dependences for a vertical CR flux. Three pressure intervals $X = 8 \div 50$, $50 \div 100$ and $100 \div 150$ g/cm^2 were analyzed, each of which was in its turn divided into several subintervals. Then the mean for the daily CR intensity for each interval, $\bar{N}(x)$, was found. After that the value $\delta = \frac{N_i(x) - \bar{N}(x)}{\bar{N}(x)}$, %, was defined, where i is the time of measurements. To improve the accuracy, values of δ were averaged for each interval. Mean values of $\bar{\delta}$ are presented in figs. 1a,b,c for the above three pressure intervals. A diurnal wave is observed with the amplitude which decreases from ~ 4% to ~ 2% with the increase in the atmosphere pressure from ~ 30 g/cm^2 to ~ 130 g/cm^2. The time of maximum is $11^h \div 14^h$ LT. These results agree with measurements of the diurnal wave in stratosphere carried out in 1981 [2]. The daily wave of the CR intensity on the neutron monitor in Tbilisi ($R_c = 7.4$ GV) is presented in fig.1d for the same period of the time (23 May ÷ 23 June 1984).

The dependence of the diurnal wave amplitude on the atmospheric depth X is shown in fig.2. A substantial decrease in the value of $\bar{\delta}$ is observed with the increase in the atmospheric depth.

Certain difficulties arise in trying to give a correct explanation of a large amplitude of the CR intensity diurnal amplitude in stratosphere (~ 4%) and of the early time of maximum ($11^h \div 14^h$ LT). The presence of such a large anisotropy of CR in stratosphere may be connected to the anisotropic pitch-angular distribution of particles in the interplanetary space and possible to the large contribution of nuclei of galactic cosmic rays in the diurnal wave. It is difficult to explain the obtained results by the temperature effect in cosmic rays or by the drift radiosondes during the flight and appropriate variations of the value of R_c.

References:

1. Solar Geophysical Data.(1984), № 479, part 1, p.91, № 480, part 1, p.86, Boulder, USA.
2. G.A. Asatryan, Yu.I. Stozhkov, (1983), 18-th ICRC, Bangalore, India, v.3, p.299.

ORIGINAL PAGE IS OF POOR QUALITY

SH 4.5-8

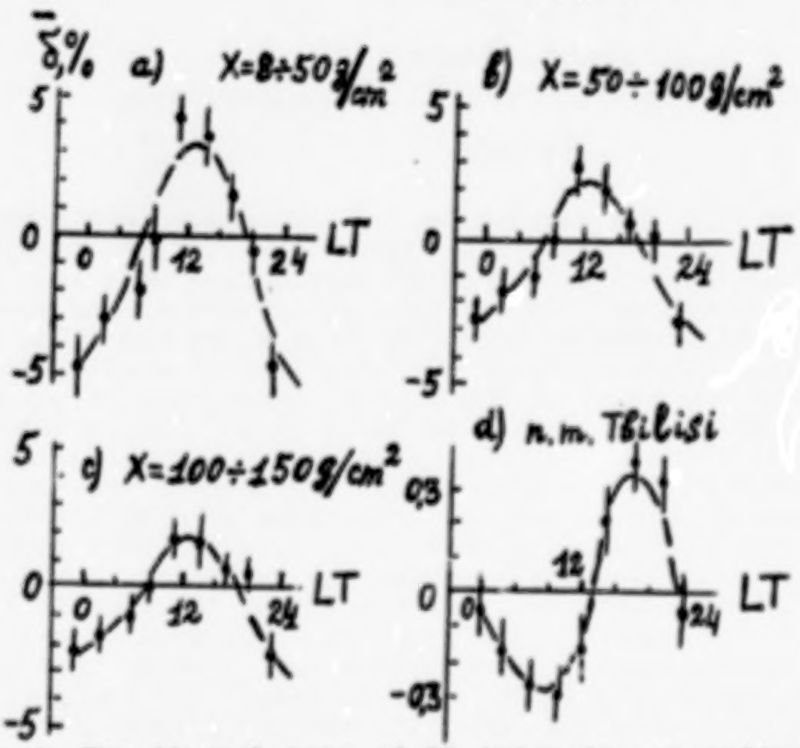

Fig.1. The diurnal wave of CR intensity according to the measurements in 23 May ÷ 23 June 1984 in the stratosphere (Yerevan, R_c=7,6 Gv) at the atmospheric pressure X=8÷50 g/cm (a), X=50÷100 g/cm (b), X=100÷150 g/cm (c) and on the neutron monitor Tbilisi, R_k=7,4 GV (d).

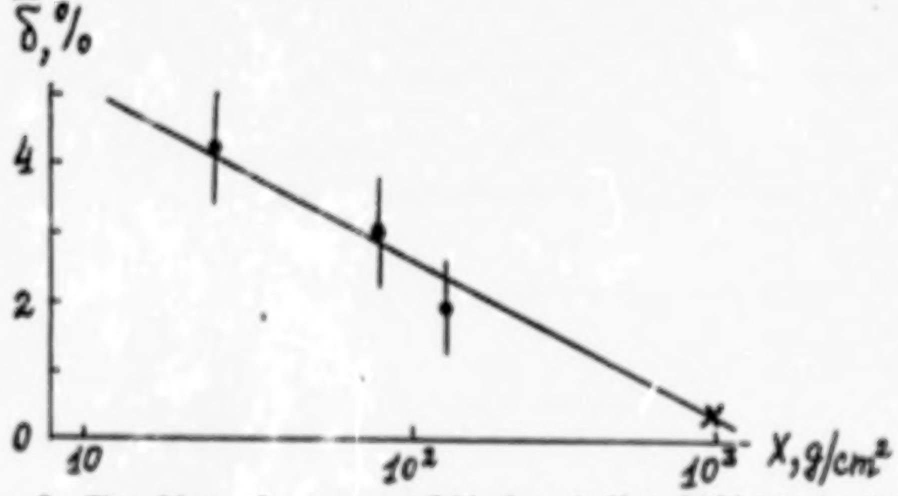

Fig.2. The diurnal wave amplitude at the different atmospheric data; X - neutron monitor Tbilisi, • - stratospheric data.

ORIGINAL PAGE IS
OF POOR QUALITY

sidereal diurnal and semi-diurnal components. The anti-sidereal diurnal variation is expected to vary with latitude according to the relation (Nagashima et al., 1983).

$$P_2^1(\sin\lambda) = \sqrt{3}.\ \mathrm{Sin}\ \lambda.\ \mathrm{Cos}\ \lambda \qquad (1)$$

Where λ is the geographic latitude (positive in the northern hemisphere and negative in the southern hemisphere). This function has opposite signs in the two hemispheres, so the expected phases of the anti-sidereal diurnal cosmic ray variation should differ by 180° in the two hemispheres. Note that, in outer space, these phases show eigen values 23.3 h ($\lambda>0$) and 11.3 h ($\lambda<0$), respectively (Nagashima, 1984).

ANTI-SIDEREAL DATA: Figure 1 presents data from the nine telescopes listed earlier, displayed as harmonic dials in anti-sidereal time. Each vector represents an average for all available data (19 years for Embudo, 16 years for Socorro, and 12 years for Bolivia). The error circles are determined on the basis of the scatter of the individual daily vectors which are used to arrive at the various resultant vectors. Errors calculated on the basis of counting rate alone are appreciably smaller. The capital letters E, S and B are for Embudo, Socorro and Bolivia, respectively, and the subscripts V, N and S represent vertical, north- and south-pointing telescopes, repectively at each location. With the exception of the Bolivia north-pointing telescope, the northern latitude telescopes are clustered near 21h anti-sidereal time, and the southern latitude telescopes are clustered near 9h anti-sidereal time, thereby showing the ex-

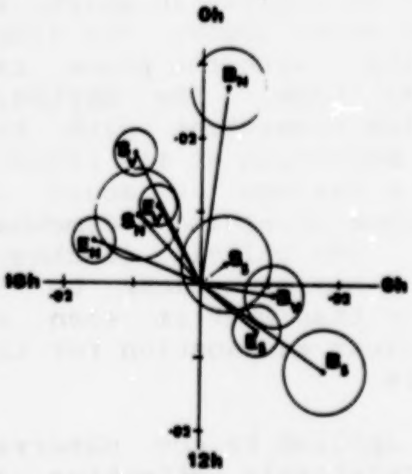

Fig. 1: Harmonic dial in anti-sidereal time for Bolivia, Embudo and Socorro North, South and Vertical Telescopes. Amplitudes are in percent.

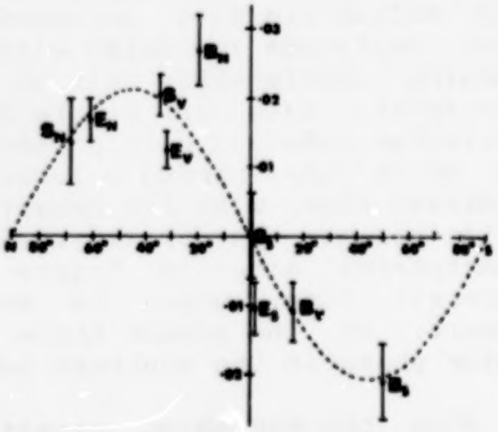

Fig. 2: Amplitude data from Fig. 1 plotted against viewing latitude λ; dashed curve is the function A sinλ Cosλ fitted to the data. Amplitudes are in percent.

C-2

pected 180° phase difference between the two hemispheres; the deviations from the corresponding eigen values (23.3 h and 11.3 h) are consistent with the cosmic ray orbital deflection in the geomagnetic field (Fujimoto et al., 1984).

In Figure 2, the data from Figure 1 are displayed in terms of the anti-sidereal amplitude for each of the nine telescopes, plotted as a function of its asymptotic latitude. Superimposed upon the diagram is a graph of the function A $\sin\lambda.\cos\lambda$ (dashed line), with the amplitude A adjusted to provide the best fit to the experimental points. The data conform very well the theoretical expectation (equation 1).

CORRECTED SIDEREAL DATA Nagashima et al [1985] have demonstrated that the anti-sidereal data can be used to remove the related spurious sidereal diurnal variation from the observed diurnal variation in sidereal time. The correction is achieved by rotating the observed anti-sidereal vector by 4.53 hours counter-clockwise, reducing its amplitude by a factor of 0.947, and then subtracting it from the observed sidereal vector. This method has been applied to the data from the nine telescopes used here, and the resulting corrected sidereal diurnal variation vectors for each telescope, for all available data, are presented in Figure 3 as harmonic dials in sidereal time. The vectors for the northern hemisphere telescopes (Embudo and Socorro) all lie in the first quadrant, in the vicinity of 3h sidereal time. The amplitude for the Socorro telescope (median regidity 305 GV) is significantly greater than that of the Embudo telescope (median rigidity 132 GV). These results are consistent with the observations by Bercovitch [1984], using surface telescopes detecting muons arriving at large zenith angles, in which, as the median rigidity increased beyond about 100GV, the sidereal amplitude increased with rigidity, with the phase remaining consistently near 3h sidereal time. The northern hemisphere data in Figure 3 are also consistent with the corrected sidereal data presented by Nagashima et al. [1985], in which the London telescope had a maximum at about 3h sidereal time, with the Hobart telescope observing a somewhat later maximum near 6h sidereal time. The Bolivia (southern hemisphere) data in Figure 3 show a maximum close to 9h sidereal time, which is even later than what is seen at Hobart; at the moment there is no clear explanation for the later phase in the southern hemisphere.

When the Nagashima correction is applied to the observed sidereal data, the correction is relatively effective in reducing or removing phase changes which occur in uncorrected data upon the reversal of the sun's polar magnetic field in 1969-71 and 1980-81 [Swinson, 1976, 1984]. Data from the Socorro vertical telescope (where the sidereal anisotropy is greatest) are shown in Figure 4. In the uncorrected data, a clear phase change can be seen in 1971 and 1981, after the

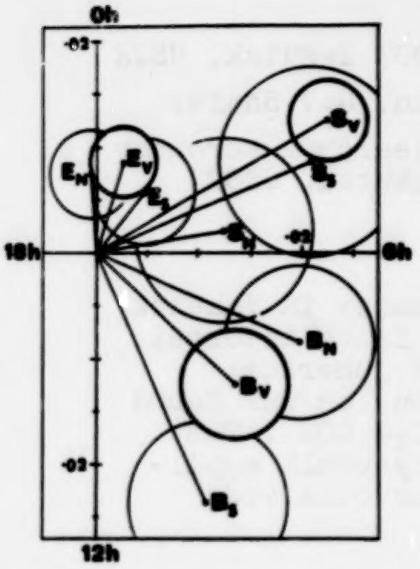

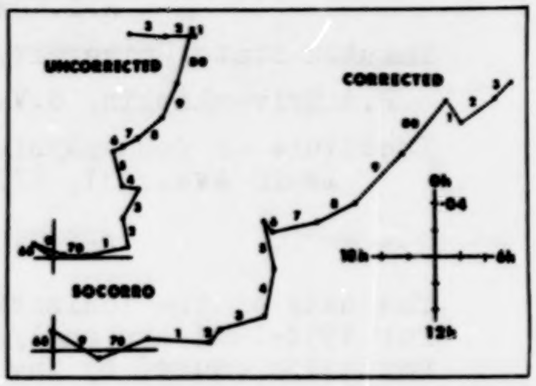

Fig. 4. Yearly harmonic dials in sidereal time for the Socorro vertical telescope, uncorrected and with the Nagashima correction.

Fig. 3. Harmonic dial in sidereal time for Bolivia, Embudo & Socorro North, South and Vertical telescopes with the Nagashima correction. Amplitude scale is in percent.

two most recent solar field reversals. The data corrected by the Nagashima method, however, show very little change, with the yearly vectors remaining relatively consistent, regardless of the magnetic configuration of the heliosphere. This gives one more confidence that the data, corrected in this fashion, are representative of a truly galactic anisotropy.

ACKNOWLEDGEMENTS: The work of one of the authors (DBS) was supported by the Atmospheric Sciences Section, National Science Foundation, under grant ATM-8305098.

REFERENCES

Bercovitch, M., Proc. Int. Symposium on Cosmic Ray Modulation in the Heliosphere, Morioka, Japan, p. 329, 1984.

Fujimoto, K., A. Inoue, K. Murakami and K. Nagashima, Rep. of Cosmic-Ray Research Laboratory, Nagoya University, No. 9, 1984.

Nagashima, K., Proc. Int. Symposium on Cosmic Ray Modulation In The Heliosphere, Morioka, Japan, p. 309, 1984.

Nagashima, K., R. Tatsuoka and S. Matsuzaki. Nuovo Cim., 6C, No. 5, p. 550, 1983.

Nagashima, K., S. Sakakibara, A. G. Fenton, and J. E. Humble, Planet. Space Sci., 1985 (in press).

Regener, V.H. and D.B. Swinson, Can. J. Phys., 46, S784, 1968.

Swinson, D.B., J. Geophys. Res., 81, 2075-2081, 1976.

Swinson, D.B., Proc. Int. Symposium on Cosmic Ray Modulation in the Heliosphere, Morioka, Japan, p. 338, 1984.

SIDEREAL ANISOTROPY OF COSMIC RAYS

A.I.Kuzmin
Yakutsk State University, 677007 Yakutsk, USSR
P.A.Krivoshapkin, G.V.Skripin, G.V.Shafer
Institute of Cosmophysical Research & Aeronomy
Lenin Ave., 31, 677891 Yakutsk, USSR

ABSTRACT

The data of the ionization chamber in Yakutsk for 1954-1984 are analyzed. A false sidereal variation caused by the second spherical harmonic in cosmic ray distribution was found and it has the amplitude 0.020±0.002%. The sidereal anisotropy with a very small amplitude (not more than 0.005%) was observed to exist.

In Table 1 the characteristics of the first harmonic of the solar-diurnal, sidereal and anti-sidereal variations of cosmic rays on data of the ionization chamber in Yakutsk from 1954 to 1984 are given. The data are pressure corrected.

From Table 1 it is evident that all the three variations significantly change from year to year. The solar-diurnal variation phase in 1954 and 1955 shifted to very early time as compared with other years. This tendency manifested in 1976 which evidences the 22-year recurrence of this variation.

The sidereal variation is ~3 times less than the solar-diurnal one. Its maximum time, on average, is 21 hr of the sidereal time varying 2-3 hours from it at various years. Sidereal variation in 1958 was somewhat anomalous with a very small amplitude (0.009%) and early maximum time (14.7 hr).

The anti-sidereal variation suffers the stronger changes from year to year either on amplitude or on phase. Its amplitude is ~2.5 times less and the maximum time is at earlier hours (13.8 hr) in comparison with the sidereal variation.

In Table 1 data separately for two periods 1958-1968 and 1972-1981 being characterized by various polarity of the general magnetic field of the Sun are also shown. It is evident that phases of sidereal and anti-sidereal variations at these periods are almost invariable. And the phase of the solar-diurnal variation in the second period 2,4 hr to the earlier time is shifted. The amplitudes of all the variations in 1972-1981 increased by 15-30%.

In Table 2 the characteristics of all the three variations corrected to pressure, influence of atmospheric temperature and the Earth's magnetic field (J_{hTM}) are presented. Contribution of the temperature (T) was determined by the method described in [1] . Vectors T were substracted from the average observed vectors of the intensity anisotropy of of corresponding variations presented by the last three lines in Table 1. Then using receiving vectors [2] for the ionization chamber the correction to the influence of the geomagnetic field was introduced.

Table 2

Characteristics of solar, sidereal and anti-sidereal vectors of diurnal variation of ground temperature (t), of the contribution of the whole atmosphere (T) and of cosmic ray intensity corrected to atmospheric effects and to geomagnetic field (J_{hTM})

Vector	Period	Solar-diurnal		Sidereal		Anti-sidereal	
		Amp.	φ,h	Amp.	φ,h	Amp.	φ,h
t, °C	I*	3.9 ± 0.1	15.2	1.4 ± 0.1	8.1	1.1 ± 0.1	21.5
T, $\% \cdot 10^{-3}$	II	40 ± 3	4.7	14 ± 1	21.9	11 ± 1	10.2
J_{hTM}, $\% \cdot 10^{-3}$	I	244 ± 8	16.8	24 ± 2	21.7	20 ± 2	20.3
t, °C	III	3.8 ± 0.1	15.1	1.4 ± 0.1	8.1	1.1 ± 0.1	21.3
T, $\% \cdot 10^{-3}$	III	60 ± 4	4.8	22 ± 1.5	21.8	17 ± 1.1	11.0
J_{hTM}, $\% \cdot 10^{-3}$	III	265 ± 8	17.4	15 ± 3	15.9	20 ± 2.2	21.4
t, °C	IV	3.9 ± 0.1	15.4	1.3 ± 0.1	8.1	1.1 ± 0.1	21.8
T, $\% \cdot 10^{-3}$	IV	24 ± 4	4.7	8 ± 1.3	21.4	7 ± 1.1	11.3
J_{hTM}, $\% \cdot 10^{-3}$	IV	239 ± 8	15.9	33 ± 3	23.0	19 ± 2.3	18.0

* I - 1954-1983, II - 1958-1979, III - 1958-1968, IV - 1972-1981

From Table 1,2 it is evident that after the corrections J_{hTM} were made the solar diurnal variation amplitude at all the observation periods increased by ~3 times and the phase had shifted 4 hr to later time. As for above two periods the amplitude of solar diurnal variation at the first period (1958-1968) in comparison with the second period became larger and the phase difference remained almost invariable. The phases of the solar-diurnal variation vectors of ground temperature (t) and of vectors T do not change on time. However, the T vector amplitude in the second period is more than twice larger than in the first one.

The J_{hTM} vectors of sidereal and anti-sidereal variations for 30-year period are equal on the value and differ significantly on the phase. Such a behaviour of the variation can be explained as it was shown in [3] by antisymmetric diurnal variation caused by the second spherical harmonic of the cosmic ray distribution in the interplanetary magnetic field. Due to this reason a false sidereal variation with the amplitude $0.020 \pm 0.002\%$ and phase 21.7 hr occurs. After substraction of anti-sidereal variation from

Table 1

Amplitudes and phases of solar-diurnal, sidereal and anti-sidereal variations on data of ASK-1 ionization chamber in Yakutsk

Years	Solar-diurnal		Sidereal		Anti-sidereal	
	$A\cdot10^{-3}$,%	φ,h	$A\cdot10^{-3}$,%	φ,h	$A\cdot10^{-3}$,%	φ,h
1954	55±2	5.8	70±2	22.0	29±2	4.1
1955	71	8.9	48	21.7	10	5.6
1956	107	12.2	34	20.8	16	14.3
1957	95	13.6	34	18.0	34	13.3
1958	90	13.6	9	14.7	15	14.2
1959	93	14.7	31	19.3	29	13.3
1960	95	14.9	37	19.7	14	15.3
1961	55	14.8	33	18.9	19	22.9
1962	96	14.8	27	19.4	8	13.3
1963	80	13.8	21	22.3	22	12.3
1964	72	13.3	15	21.9	9	13.8
1965	58	12.2	17	19.5	14	17.3
1966	89	13.7	15	20.5	7	15.8
1967	83	13.3	35	23.8	14	10.3
1968	87	14.3	23	23.9	3	18.2
1969	89	14.3	12	23.0	10	8.4
1970	87	13.5	15	01.4	5	9.8
1971	109	12.3	19	23.2	3	22.8
1972	91	11.4	35	22.2	6	13.0
1973	98	11.3	20	23.7	11	13.1
1974	95	12.6	24	18.5	18	17.6
1975	96	10.4	34	20.7	18	11.1
1976	84	9.9	21	23.0	10	13.2
1977	108	11.0	25	17.5	39	14.1
1978	117	11.0	18	21.7	15	18.1
1979	106	12.9	29	21.2	23	11.4
1980	91	13.1	24	22.6	22	18.2
1981	89	12.7	26	22.3	18	12.0
1982	87	14.7	26	19.4	3	13.9
1983	84	13.7	42	19.0	24	15.8
1984	105	14.7	35	21.7	15	12.5
1954-1983	78±0.3	12.8	24±0.3	21.0	9±0.3	13.8
1958-1968	80±0.5	14.0	20±0.5	20.6	10±0.5	14.3
1972-1981	93±0.5	11.6	23±0.5	21.3	13±0.5	14.2

sidereal one by means of mirrow reflection of anti-sidereal variation relative to the 21 hr direction (as in [4]) the galactic sidereal variation within the errors is not found.

Anti-sidereal variation on amplitude and phase does not change. This feature can be interpreted by the influence of the second harmonic in the cosmic ray distribution.

The sidereal variation suffers significant changes either on amplitude or on phase. Substracting anti-sidereal variation from sidereal one by the above method we obtain the galactic sidereal variation for 1958-1968 with an amplitude 0.018±0.002% and a phase 11.0±0.4 hr and for 1972-1981 - 0.015±0.002% and 22.0±0.4 hr. The vectors are equal on the value but their phases are almost opposite. It indicates the significant influence of sign change of the solar magnetic field upon galactic sidereal variation.

In conclusion it should be noted that on data of the ionization chamber in Yakutsk it was found: 1) the existence of false sidereal variation with an amplitude 0.020±0.002% and a phase 21.0+0.4 hr from contribution of the second spherical harmonic. 2) at periods of various polarities of the solar magnetic field the similar on the amplitude (0.005%) sidereal variation but with opposite phase was observed to exist.

References

1. Kuzmin, A.I. i dr.,(1971) Geomagnetizm i aeronomiya, 11, 523.
2. Fujimoto, K. et al.,(1984) Report of Cosmic Ray Research Laboratory, No.9, Nagoya, Japan, 185.
3. Krivoshapkin P.A.,(1970) Geomagnetizm i aeronomiya, 6, 761.
4. Elliot, H., et al.,(1970) Proc.11-th ICRC, Budapest, Acta Phys.Hung., 29, Suppl.1, 491.

N85-35007

COSMIC RAY INTENSITY VARIATIONS OBSERVED AT MATSUSHIRO
(220 M.W.E. IN DEPTH)

S. Yasue, S. Mori and S. Sagisaka
Department of Physics, Faculty of Science
Shinshu University, Matsumoto 390, JAPAN

ABSTRACT

Cosmic ray data from Matsushiro underground station have been analyzed for four years (1981-84). It is found that a marked semi-annual intensity variation has been observed in this period. Solar diurnal and semi-diurnal variations have also been observed. After correcting for the spurious sidereal diurnal variation arising from the anisotropy responsible for the solar semi-diurnal variation (Nagashima et al., 1983), it is found that the corrected siderial diurnal variation is consistent with those so far reported.

1. Introduction. Deep underground observation of the cosmic ray intensity variation provides valuable information as to the nature of modulation in the heliosphere. Matsushiro underground cosmic ray station has been in operation since Aug. 1980 at the depth of 220 m.w.e. (Yasue et al., 1981a). The median primary rigidity of the vertical telescope is about 700 GV (Fujimoto et al., 1984), and its counting rate is 2.1×10^4/h. The analyses of the observed intensity variations of the vertical telescope for four complete years (1981-84) are presented.

2. Semi-annual intensity variation. At the Paris Conference, we have reported that the most part of the unexpectedly large barometric coefficient (∼-0.05%/mb) observed at deep underground stations (Humble et al., 1979; Yasue et al., 1981b) can be attributed to the atmospheric temperature effect (Yasue et al, 1981b). In this report, we present another phenomenon which also seems to be caused by the atmospheric temperature effect. Fig. 1 shows the monthly averaged intensity varia

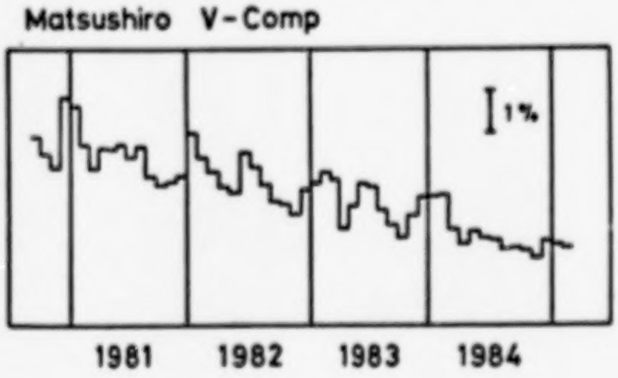

Fig.1 Monthly averaged intensity variation.

tion of the vertical telescope (abbreviated as V-Comp) observed at Matsushiro. In the figure, we can notice a marked semi-annual intensity variation superposed on a gradual intensity decrease. The intensity decrease (about 1 % per year) may be due to the decrease in detector efficiency of the scintillation counters (Ueno, private communication). The semi-annual intensity variation takes the maximum value both in summer and in winter. Such a variation has not been observed at the shallower underground stations than Matsushiro (Ueno et al., 1979). The most part of this variation can be explained quantitatively in terms of the variation of the upper atmospheric temperature (Sagisaka, 1984).

3. Observed daily variations. Fig. 2 shows the daily variations of V-Comp (top) and atmospheric pressure (bottom) averaged over four years (1981-84) for solar (SO), sidereal (SI) and anti-sidereal (AS) time. Cosmic ray data are not corrected for pressure. In the figure, V-Comp shows not only significant SI daily variation but also SO and AS daily variations. It is noted, however, that the atmospheric temperature effect described in the previous section may contaminate also the daily variations.

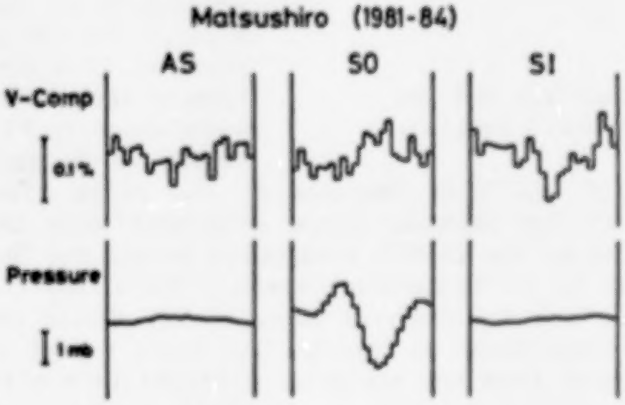

Fig.2 Averaged daily variation of V-Comp and atmospheric pressure for solar(SO), sidereal(SI) and anti-sidereal(AS) time.

We can find in Fig. 2 that the daily variations of pressure in SI and AS time are negligibly small (about one-tenth) compared with that in SO time. This fact implys that we may reasonably assume that the influence of the atmospheric effects becomes serious only in SO time and can be neglected in SI and AS time.

4. Solar daily variation. The heavy solid lines in Fig. 3 show the 1st and 2nd harmonic vectors of the daily variation (SO) of V-Comp shown in Fig. 2. The error circles are the standard error of each mean vector estimated from the dispersion of yearly vectors. In the following, we try to estimate SO harmonic vectors caused by the temperature effect. By analyzing observed data from multi-directional

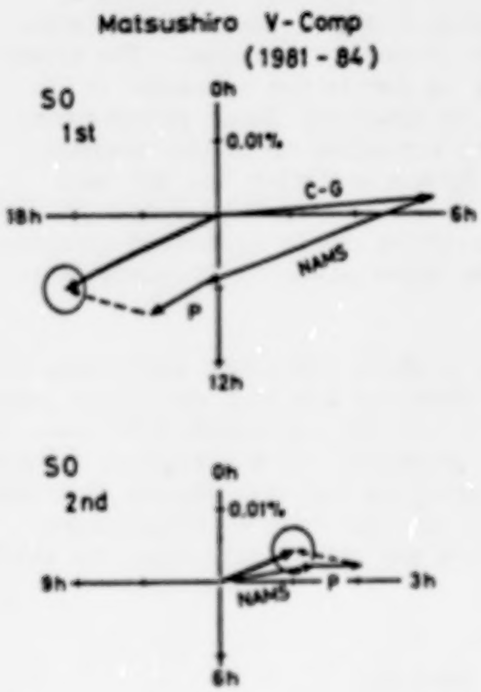

Fig. 3 Solar 1st and 2nd harmonic vectors.

muon telescopes at Nagoya and underground telescopes at Misato and Sakashita (NAMS) in the period of 1978-83, Ueno et al. (1984) and Morishita et al. (1984) determined, respectively, the characteristics of the anisotropies responsible for the solar diurnal and semi-diurnal variations. Assuming those anisotropies obtained by them, and using the coupling coefficients (Fujimoto et al, 1984), we can estimate the expected solar diurnal and semi-diurnal variations at Matsushiro in this period. The obtained vectors are shown in Fig. 3 with the vectors 'NAMS'. These vectors are free from the atmospheric effects. The vectors 'P' in the same figure show SO 1st and 2nd harmonics produced from the daily variation of the atmospheric pressure shown in Fig. 2. Here, we assume the genuine barometric coefficient of -0.01%/mb (Sagisaka et al., 1979). The vector 'C-G' in Fig. 3 shows the 1st harmonic vector originated from the Compton-Getting effect due to the Earth's revolution around the Sun. Composing the above vectors on the respective harmonic dials, and comparing the resultant vectors with the observed ones, we can obtain the residual vectors (dashed line) shown in Fig. 3. One might expect that these vectors are produced from the atmospheric temperature effect. (It is noted that other unknown vectors, one of which may be originated from the galactic anisotropy (Nagashima et al., 1982), might also be included in these vectors.)

5. SI and AS daily variations. It is emphasized that the solar daily variation is observed even at this depth (220 m.w.e.) in this period. As has been described by Nagashima et al. (1983, 1985), the second order solar anisotropy responsible for the observed semi-diurnal variation produces the AS 1st harmonic vector with the phase of 0h, due to the tilt of the spin axis of the Earth to the ecliptic plane. The present observation seems to support his expectation. Namely, the observed AS vector in Fig. 4 seems to be interpreted as the side-band vector produced from the 2nd order anisotropy at 3h-21h. In this case, another side-band vector (spurious sidereal vector) should be observed according to his theory. This vector can be derived from the observed AS vector (Nagashima et al., 1983), and is shown by the dashed line (amplitude and phase of the vector is 0.014% and 19.4h, respectively) on the SI harmonic dial (see Fig. 4). If we subtract this spurious SI

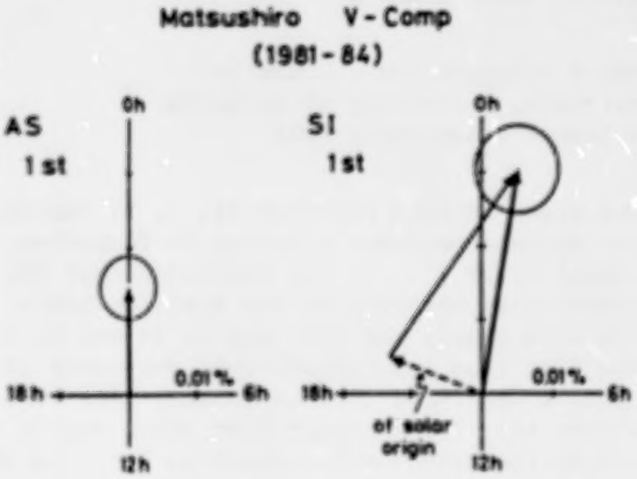

Fig.4 Sidereal and anti-sidereal harmonic vectors.

vector from the observed SI vector, we can obtain the true SI vector of galactic origin. The resultant vector has the amplitude of 0.031% and the phase of 2.3h. The present result seems to be consistent with those so far reported (Nagashima et al., 1985).

Acknowledgements. The authors express harty thanks to Prof. K. Nagashima for his encouragement and discussions with them. Thanks are also due to Mr. K. Chino for his help in data processing.

References

Fujimoto, K. et al. (1984), Rep. of C. R. Res. Lab. Nagoya Univ. No.9.
Humble, J.E. et al. (1979), Proc. 16th ICRC (Kyoto) 4, 258.
Morishita,I. et al. (1984), Proc. Int. Symp. C.R. Mod. (Morioka), p130.
Nagashima, K. et al. (1982), Planet. Space Sci. 30, 879.
Nagashima, K. et al (1983), Nuovo Cimento 6C, 550.
Nagashima, K. et al. (1985), Planet. Space Sci. (in press).
Sagisaka,S. et al. (1979), Proc. 16th ICRC (Kyoto) 4, 235.
Sagisaka, S.(1984), Proc. Int. Symp. C. R. Mod. (Morioka), p360.
Ueno, H. et al. (1979), Proc. 16th ICRC (Kyoto) 12, 228.
Ueno, H. et al. (1984), Proc. Int. Symp. C. R. Mod. (Morioka), p109.
Yasue, S. et al. (1981a), Proc. 17th ICRC (Paris) 4, 304.
Yasue, S. et al. (1981b), Proc. 17th ICRC (Paris) 4, 308.

60 N85-35008

SH 4.4-10

LONG-TERM MODULATION OF COSMIC RAYS DURING SOLAR CYCLE 21

A.G.Fenton, K.B.Fenton and J.E.Humble
Physics Department, University of Tasmania
Hobart Tasmania Australia 7001

1. Introduction. In recent years we have reported (1, 2, 3) results from the Australian chain of neutron monitors relating to Forbush-type decreases observed during Solar Cycle 21. It was concluded that the rigidity dependence of the decreases observed in the southern hemisphere during this period is essentially the same now as it was in the previous cycle. Fitting the data from ten Forbush-type decreases of amplitude $\geq 4\%$ during the period September 1977 to January 1983 to a modulation function of the form $\exp(-K/P^{\gamma})$ showed that these events were consistent with $0.5<\gamma<0.9$, with the mean γ-value close to 0.7. In this paper we report a preliminary result concerning the rigidity dependence of the longer-term solar cycle modulation.

2. Neutron Monitors, Data and Methods. The neutron monitors chiefly referred to in this paper are 9NM64-type, located near sea level at Hobart (42.9°S, 147.3°E, vertical cut-off 1.89 GV), Brisbane (27.4°S, 153.1°E, 7.24 GV) and Darwin (12.4°S, 130.9°E, 14.07 GV). The neutron monitor at The Springs at an altitude of 725m on the slopes of Mt.Wellington, overlooking Hobart, is currently a 6NM64, but before 1967 there was a 12-counter IGY-type monitor at this site. By careful normalisation of data from different neutron monitors operated in the Hobart area it has been possible to obtain a continuous record of intensity back to July 1956. Other monitors operated by the Hobart group include a 12-counter IGY-type at Mawson, Antarctica (67.6°S, 62.9°E, 0.22 GV) and IGY-type monitors operated at Lae, New Guinea (6.7°S, 147.0°E, 15.52 GV) for some years beginning with the IGY period, and at Brisbane from 1960 until the 9NM64 was installed. It is hoped that it will be possible in the near future to coordinate the results from these stations to determine the solar cycle modulation during Solar Cycle 20, as observed by these southern recorders.

The 11-year solar cycle modulation was assumed to be of the exponential form with exponent $-K/P^{\gamma}$, as discussed in earlier papers (1, 2, 3). An attempt was made to find a best-fit γ, using monthly mean data selected to be relatively free from Forbush-type decreases. Figures 1 and 2 show respectively the long term changes observed at Mt.Wellington, and daily mean intensities over the 4-months period including the major transient event of July, 1982.

3. Results. The long-term modulation, using monthly mean intensities selected as above, and referred to November 1977 as a normalising level, appear to be in accordance with the exponent $\gamma = 1$, provided only Brisbane and Hobart data are used. Darwin data do not conform to this pattern except perhaps during the early years of the cycle until about the end of 1980, since when the Darwin long-term intensity has been largely steady, apart from Forbush-type decreases and as yet unidentified small changes of the order of 1%. Thus these results must be regarded as preliminary.

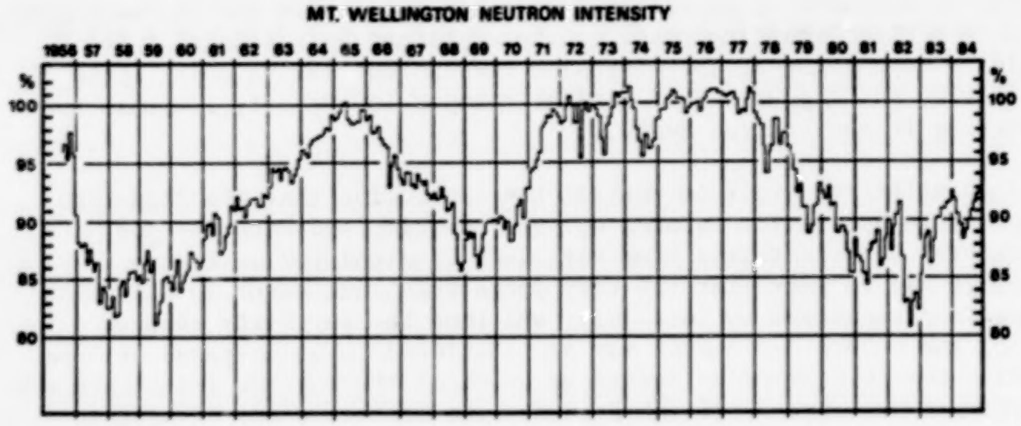

FIGURE 1

Monthly mean neutron intensities relative to May, 1965.

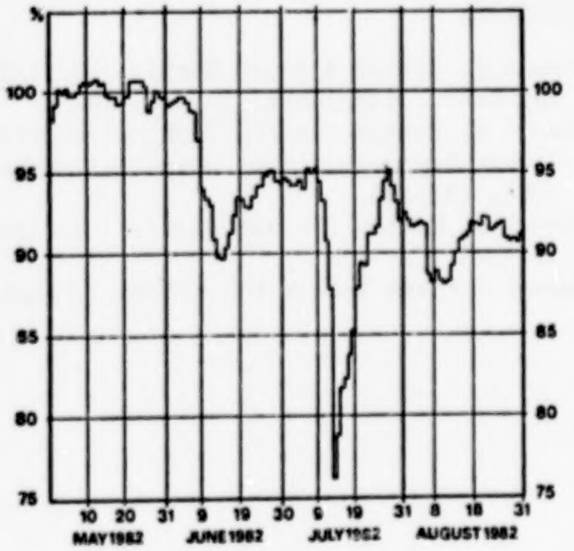

FIGURE 2

Daily mean pressure-corrected Mt.Wellington neutron intensities for May-August 1982, expressed as percent of mean level for May.

4. Discussion. The results seem to confirm the conclusion reached earlier that the Forbush-type modulation and the 11-year cyclic changes have a different rigidity response, and thus is probably caused by different mechanisms under solar influence; however, from our preliminary analysis it may be that the long-term changes have been limited to rigidities below about 10 GV since solar maximum, which occurred in December 1979. This observation would agree with a report by Lockwood and Webber (4) that the observed hysteresis effect between the integral intensity measured by satellite cosmic ray telescopes and Mt.Washington neutron monitor counting rates can be explained by a change in the rigidity dependence of the diffusion coefficient during Solar Cycle 20, 1965-1976, and suggests that similar changes in rigidity response are occurring in the current cycle.

Semi-quantitative evidence against the contention that the long-term solar cycle modulation is made up from superimposed Forbush-type decreases may be obtained from data such as displayed in Figure 2. Here, it may be seen that the very large transient event in July 1982 completely recovered by late July, and that the intensity changes during the period May-August may be considered to be composed of long-lasting possibly stepwise decreases on which the shorter transients are superimposed. Indeed, if the Forbush-type decreases are considered separately, the total 'count' removed by them is only about half the total removed by the longer-term effect.

5. Acknowledgements. We wish to thank the staff of the Bureau of Meteorology stations at Brisbane and Darwin airports for their valuable assistance in the operation of these neutron monitors. The neutron monitor programme at Hobart, Brisbane and Darwin has been supported in part by grants from the Australian Research Grants Scheme.

6. References.

1. Fenton A G, Fenton K B and Humble J E (1983). Proc.18th Int.Cosmic Ray Conf., Bangalore, 10, 164-167
2. Fenton A G, Fenton K B and Humble J E (1984). Proc.Int.Symposium on Cosmic Ray Modulation in the Heliosphere, Morioka, Japan, 1984, 191-196
3. Fenton A G, Fenton K B and Humble J E (1984). Proc.ASA 5 (4), 590-593
4. Lockwood J A and Webber W R (1979) J.Geophys.Res. 84, 197-202

ORIGINAL PAGE IS
OF POOR QUALITY

N85-35009

SH 4.4-12

ROLE OF SOLAR FLARE INDEX IN LONG TERM MODULATION OF COSMIC RAY INTENSITY

P.K.Pandey*, A.K.Jain, P.K.Shrivastava, S.P.Pathak**
and S.P.Agrawal
Physics Department(Vikram Space Physics Centre)
A.P.S.University, Rewa(M.P.)486003, India.

ABSTRACT

Recently, the importance of the occurrence of solar flares in the long-term modulation of cosmic ray intensity has been re-emphasized. For this purpose, the data of solar flares have been used from various publications, such as Solar Geophysical Data books, U.A.G. reports and Quarterly Bulletin Of Solar Activity. Our investigation, very clearly reveals that even the periodic changes in the solar flare observations, obtained from the four different data sources, for the same interval, differ significantly from one another; this is evident even on an average basis. Hence, in any study using solar flares, the importance of selecting a single compilation of the solar-flare data for the entire period of investigation is stressed.

1. Introduction. The study of the long term records of cosmic ray measurements, extending to energies beyond 100 Gev., have confirmed the eleven year solar cycle variation of cosmic ray intensity. Recent results (Hatton, 1980; Hatton and Bowe, 1981; Hatton and Bowe, 1983) using the number of solar flares, of importance $\geqslant 1$, and the cosmic ray intensity deviations, have provided an empirical relation with better correlations for a time lag of ≈ 10 months. Such a time lag corresponds to a value of ≈ 70 A.U. for the solar modulating boundary. The goodness of fit has been shown to be quite satisfactory. The use of solar flares for such a correlation studies, often assumes that the total number and importance of solar flares would be the same, irrespective of the source of data of the solar flares. In this paper, we define a more realistic index for using the solar flare data, and then derive the monthly solar flare indices (SFI) for an extended period of time, from 1957-84, to compare it with the monthly averages of the cosmic ray intensity. During the course of investigation, we have found very significant difference in the solar flare indices, when derived from the tabulation of solar flares published in different data sources. These differences are quite large, hence need to be emphasized.

---

* Also at - Govt.Girls Degree College, Rewa(MP.) 486001.
** Also at - Govt.Science College, Rewa (MP.) 486001.

ORIGINAL PAGE IS
OF POOR QUALITY

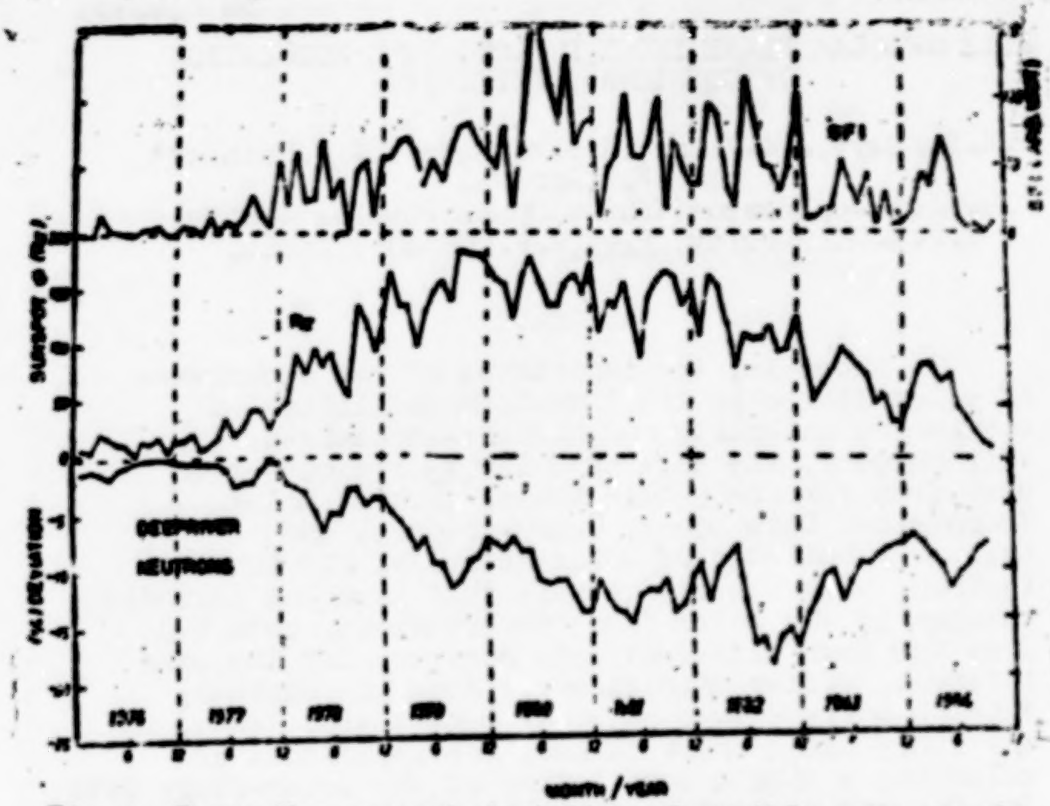

Fig. 1 Shows the percent deviation of monthly mean cosmic ray intensity observed by Deep River Neutron monitoring station. The 100% level is taken as the average for the month, Sept.-Nov. 1976. The monthly values of sunspot number (Rz) and solar flare index (SFI; see text for details for computing SFI) are also plotted for the year 1976-84.

2. Solar flare index. The occurrence of the solar flares are routinely published in solar Geophysical Data, both in the prompt reports as well as in the comprehensive reports. The solar flares are also listed in the quarterly Bulletin of solar Activity as well as in a slightly modified form in the UAG reports of World Data Centre-A. From these listing, various investigators have used the information of the occurrence of solar flares for comparison, with other observations. Usually, for most of the studies the solar flares of importance ≥ 1 are selected (as was done by Hatton, 1980; for Cosmic ray investigations). In these studies the number of solar flares were added without giving any weight either to the importance of the flares or to their brightness. The solar flare brightness is usually represented by B, N and F, whereas the flare-importance is represented by numerical numbers 1, 2, 3 and rarely also 4. We have therefore, generated a

ORIGINAL PAGE IS
OF POOR QUALITY

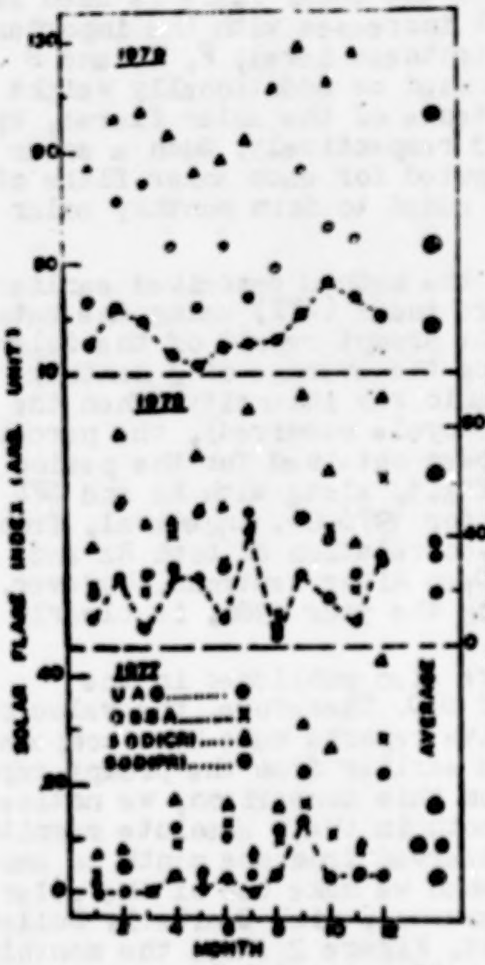

Fig.2 Shows the solar flare index for each month for the three years of high solar activity period 1977,78,79,for four different data sources, which are routinely published. The month to month changes are distinguished by joining the line for the solar flare computed from UAG report. The averages are shown in the right most part of the figure.

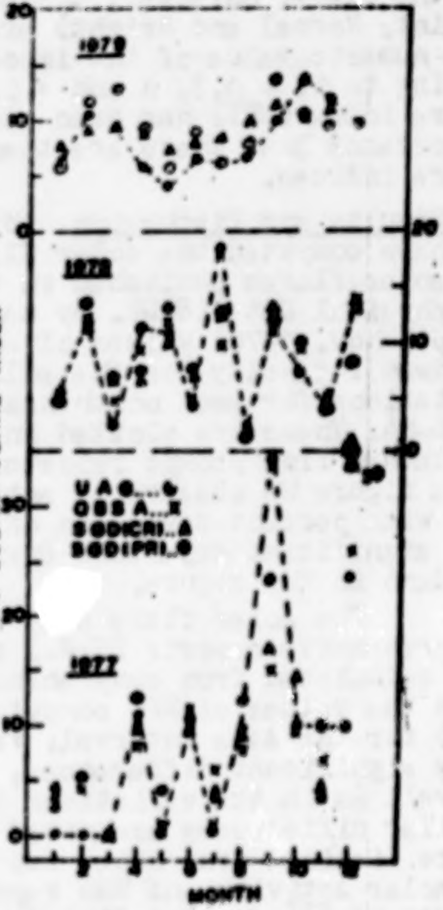

Fig.3 Shows the normalised values of solar flare index for all the monthly data sets and the time interval shown in figure 2. In each case the yearly sums are normalised to 100, to derive the percent solar flare index for each month.

Solar Flare Index (SFI) for each flare, for the interval for which the solar flare data from various sources (mentioned earlier) are available. In generating the new flare index (SFI) the reported importance of the solar flare is used as a numerical weight i.e. the SFI increases with the importance of the flare. Moreover, the brightness level, F, N, and B (Faint, Normal and Bright) are used to additionally weight the numeric value of the importance of the solar flares, by adding to it - 0.3, 0 and + 0.3 respectively. Such a solar flare index (SFI) has been computed for each solar flare of importance ≥ 1. These are then added to form monthly solar flare indices.

3. Results and Discussion. By the method described earlier, we have computed the solar flare index (SFI) using the data of solar flares published in the prompt report of the Solar Geophysical Data (SGD). By using the average of 3 monthly (Sept.-Nov., 1976) values of cosmic ray intensity (when the maximum intensity for the solar cycle occurred), the percent deviations for each month has been obtained for the period 1976-84. These are plotted in fig. 1, along with Rz and SFI (obtained from prompt reports) for 1976-84. In general, from this figure we observe an anti-correlation of both Rz and SFI with percent deviation of Deep River neutrons. However, the significant departure during the year 1980, is clearly evident in the figure.

The solar flare data are also published in the comprehensive reports (C.R.) of SGD. Therefore, the value of SFI calculated from comprehensive reports have been compared with the values of SFI computed earlier from the prompt reports (PR) for the same interval. From this comparison, we notice very significant differences, both in their absolute magnitude as well as in the variations observed from one month to another. Similar differences are noted when we make use of the solar flare listings from other two sources, viz. Quarterly Bulletin of solar Activity and UAG report. Figure 2 shows the monthly values of SFI derived from four different data sources. The annual averages are also marked, to show the difference in their absolute values. It is apparent from the figure that the changes from one month to another are not always similar. As mentioned earlier, if one uses different data sources to compute SFI for different periods, it is necessary to normalise the indices. This has been done for each year by using the yearly sums which are each normalised to 100. The percent solar flare index for each month, has been computed and plotted in figure 3, by using the absolute values plotted in figure 2. From this figure, the large differences in % SFI, from one month to another, comes out in a very significant manner. We conclude therefore, that the solar flare indices generated by either giving weight or otherwise, one should use only one type of data source.

4. References.

Agrawal, S.P.; 1983. Space Science Rev. 34 p. 127.
Hatton, C.J.; 1980 Solar Physics, 66 p. 159.
Hatton, C.J. and Bowe, G.A.; 1981. Proc. 17th ICRC Paris 3 p. 255.
Hatton, C.J. and Bowe, G.A. 1983. Proc. 18th ICRC Bangalore 3, p. 68.

A STUDY OF PERIODICITIES AND RECURRENCES IN SOLAR ACTIVITY AND COSMIC RAY MODULATION

N85-35010

Attolini M. R., Cecchini S.
Istituto TE.S.R.E -C.N.R., Bologna, Italy

Galli M.
Dipartimento di Fisica dell'Università,Bologna, Italy

1. Introduction. Time variability on a wide range of time scales is the main characteristic of cosmic rays observed inside the solar cavity. As the intensity of galactic cosmic rays is assumed to be essentially constant outside the heliosphere, the temporal changes observed must be due to the interaction of CR particles with the IMF which is carried by the solar wind.

The question is then to find out the pattern of the IMF and its flow, to determine the time and spatial evolution of their configurations and to relate them to CR variations.

Unfortunately the direct measurements of the IMF and of the solar wind plasma are insufficient because they are limited to a region close to the ecliptic plane as compared to the vast 3-dimensional extension of the heliosphere. On the other hand CR particles provide an indirect measurement of the global structure of IMF since they sample a large volume of the solar cavity in their travel from its boundary to the Earth.

Yet one can tentatively try to derive important parameters of the interplanetary medium by means of the observations of the source itself, the Sun.

Solar output during the 11yr activity cycle has many different aspects such as the sunspot area and number, the development of polar coronal holes, the solar flares and the solar wind.

Furthermore among the cyclic variations of the various kinds of solar activity one has to distinguish the ones having same period but differing in phase, amplitude and pattern.

It is common practice to use the sunspot number variation as the standard of the solar cycle and to compare to it all the other relevant parameters, even though this approach has not a good physical ground. The same is true for CR intensity since Forbush (1954) discovered an inverse correlation between this latter and the sunspot number. On the other hand the changes in the solar wind characteristics are related to the temperature variations of the corona, which in turn depend on different solar features such as sunspots, flares, polar coronal holes, plages etc. It is then extremely interesting to investigate the possible relationship between these phenomena and the CR intensity.

The spectral and cross-spectral power analysis is the tool that can be used to consider over a wide range of frequencies in a global way correlations on the same time scale between two time series.

We have already analyzed CR variation of ergodic nature (Attolini et al., 1984) but we cannot exclude variations corresponding to spectral lines.

From the operational point of view the best way to study line spectrum is to obtain estimates of the power trough the periodograms and average them on a band as narrow as possible.

This has been done by averaging each periodogram to its consecutive and then repeating this operation six time. in that way we obtain a binomial smoothing which preserve the frequency information over 7 periodograms corresponding to the average of 4.43 independent data equivalent. Since before performing the FFT operation the number of data has been increased to 1024 via zero padding, each coherency value corresponds to 2.13 independent data equivalent. The coherency figure (Y12) is the one defined by Jenkins and Watts (1968). The 95% significance level has been found using simulations on random data series with the same number of data.

In our analysis we have used the monthly data series of the following relevant parameters: *sunspot number* (Rz) from 1944 to 1984 (Solar Geophys. Data); *CR intensity* (RC) from 1944 to 1984 (Huancayo-Climax pressure crrected counting rates); *aa indexes* (aa) from 1944 to 1984 (Mayaud,1973,1975); *major flares* from 1955 to 1979 (Dodson et al.,report UAG N.14,19,52,80).

2. Computations and Results.

a) RC vs Rz

The first thing to note in the comparison of the coherency spectra in Figure 1a-c computed for three different time intervals, is that we can identify two regions,the first one with frequencies higher than 1c/yr, the other one with frequencies lower than 1c/yr. The first one contains few peaks that exceed the 95% confidence level, which do not shift in frequency when increasing the length of the series and whose amplitudes remain the or at least increase with the increase of the number of data. In the other range the peaks slightly wander in frequency and in amplitude; the long wave of 22yr appears only in the longer data set and with low significant level. All the peaks in this region correspond to nearly all possible harmonics up to 10th order of the 11yr cycle in all the series as it can be better seen in the computation with zero padding of the data up to 2048. The other significant peaks of the second region are at periodicities 10.4m, 156.5d, 70.9d.
The correlation is negative (⊖) in the first two and positive (⊕) in the last case. The 156.5 days may be related to the flare occurrence.

b) RC vs aa

Since solar wind plasma drives geomagnetic activity the aa index has been used to investigate CR intensity variations caused by solar wind changes. Following the study by Feynman(1982) we have considered the aa and the aa_T (i.e. aa corrected for Rz) monthly indexes. The results are shown in Figure 2. One can see that the coherencies between CR and either aa or aa_T do not differ very much. The only difference between the two is the 11yr cycle periodicity. The significant peaks are, however, different from the RC vs Rz and the correlation is always negative. More meaningful is to compare the CR intensity deduced after the subtraction of the sunspot correlation computed according to Nagashima and Morishita (1980). In that case the coherency (Figure 3) is significant in a greater number of frequencies. These periodicities are linked to the polarity of the IMF and possibly some of them represent the aliased peaks of more fundamental periodicities such as 28.2,27.15 and 26.85 days typical either of sector structure as described by Svalgaard and Wilcox (1975) or of the recurrent decreases in CR intensity in correspondence to aa_T increases. This last fact can be consistent with the description of high speed stream effects on CR (Iucci et al.,1979). In fact the analysis by Feynman (1982) has put in evidence that the property

ORIGINAL PAGE IS
OF POOR QUALITY

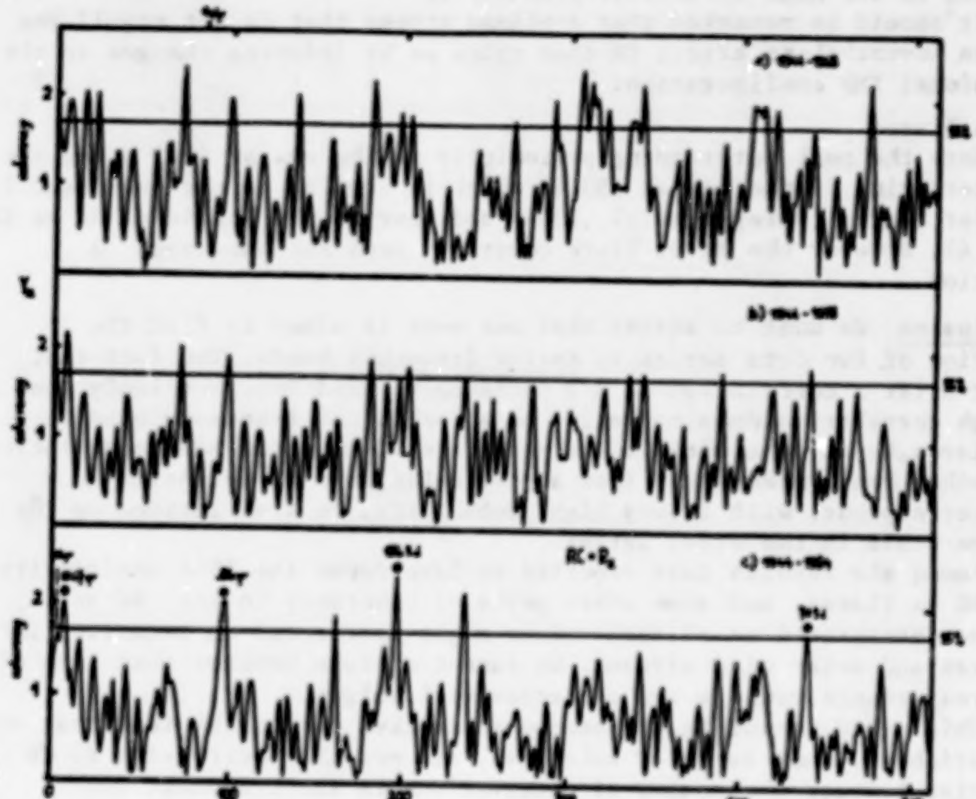

Fig.1

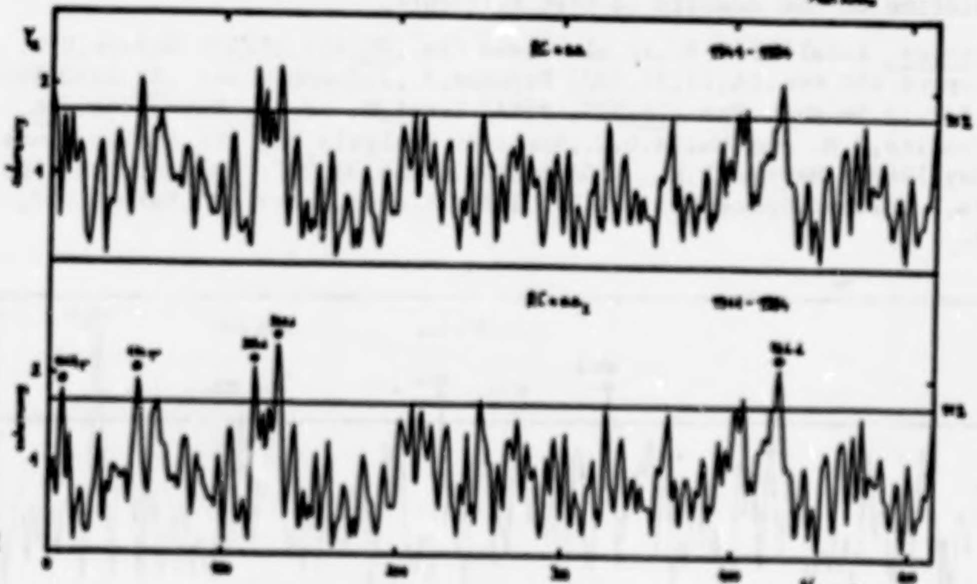

Fig.2

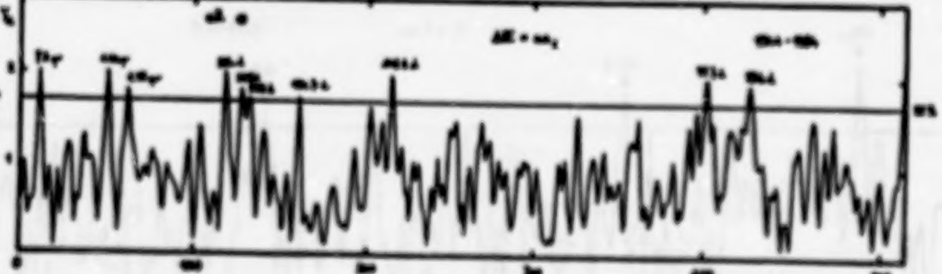

Fig.3

ORIGINAL PAGE IS OF POOR QUALITY

of the aa_I is the high recurrence probability.

It should be remarked that a plasma stream that do not engulf the Earth can nevertheless affect CR that reach us by inducing changes in the 3-dimensional IMF configuration.

c) RC vs Flares

Here the most outstanding periodicity is the one at 66.2 d and the most interesting is the one at 153.4d which is similar to the one found in hard solar flares (Rieger at al.,1984) and near to the 156.4d of RC vs Rz (Figure 4). However the Rz vs Flare coherency does not show such a correlation.

3. Conclusion. We want to stress that our work is aimed to find the correlation of two data series in narrow frequency bands. The fact that does not exist a correlation on a 2 periodogram band does not imply that a very high correlation does not exist on a much wider frequency band (e.g. CR vs Flares,Rz,aa as a whole). The existence of a narrow band correlation, on the other hand, means only that a particular type of variation in a series corresponds, with a very high probability, to a variations on the same time scale in the other series.

Among the results here reported we have found the 154d periodicity in the RC vs Flares, and some other peaks of coherency in the RC vs aa_I that when interpreted as aliased values might correspond to recurring IMF structures and solar wind streams. We cannot exclude however that some of the correspondence with aa are of terrestrial origin.

This study cannot be considered exhaustive due to the fact that other solar variables, such as polar hole size, are possibly correlated to CR intensities,however the number of observations is small so that the interpretation of the results is very difficult.

4. References. Attolini,M.R.,et al.,Nuovo Cim.,7C,413,1984// Dodson,H.W. et al.,Report UAG Nos.14,19,52,80// Feynman,J.,J.Geophys.Res.,87,6153,1982// Forbush,S.E.,J.Geophys.Res.,59,525,1954// Iucci,N. et al.,Nuovo Cim.,26,421, 1979// Jenkins,G.M. and Watts,D.G.,Spectral Analysis and Its Applications, Holden-Day,1968// Mayaud,P.N., IAGA Bulletin Nos.33,39// Nagashima,K.,and Morishita,L.,Planet.Space Sci.,28,177,1980//Rieger,E.,et al.,Nature,312, 623,1984.

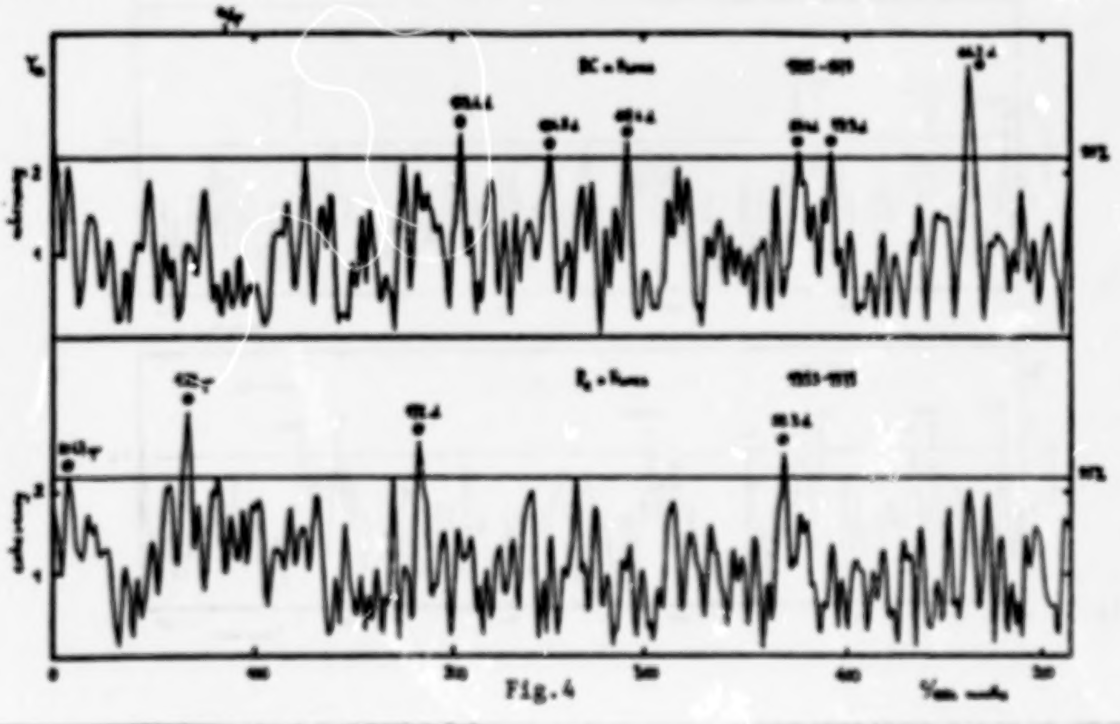

Fig.4

SH 4.4-15

N85-35011

COSMIC RAY BIANNUAL VARIATION

Attolini, M.R., Cecchini, S.
Istituto TE.S.R.E.- C.N.R.,Bologna, Italy

Cini Castagnoli, G.
Istituto di Cosmogeofisica - C.N.R.,Torino, Italy
Istituto di Fisica Generale dell'Università,Torino, Italy

Galli, M.
Dipartimento di Fisica dell'Università, Bologna, Italy

ABSTRACT

The study of the CR power spectrum (Attolini et al., 18th ICRC, Conf.Papers, 10,174,Bangalore 1983) has revealed a significant variation with a period around 2 yr that cannot be explained as a high order harmonic of the 11 yr solar cycle. Comparative study of the correlation on different time scales between CR intensity and Rz, aa, high speed streams and polar hole size (SH 4.4-14, this conference) has put in evidence that a high degree of coherency exists between each couple of variables at 1.58-1.64 yr, except between CR and Rz. On the other hand cyclic variation on a short time scale, around 26 months, has been claimed (Sakurai, 18th ICRC,Conf. Papers, 4,210,Bangalore 1983) to be present in the neutrino flux (Davis et al.,AIP Conf. Proceedings,No.96, 1983). Critical tests of this hypothesis are considered and a preliminary result seems to indicate that the hypothesis of the existence of a 1.6 yr periodicity in the neutrino data during the measurement time interval, has a significance $\geqslant$ 99.9 %.

The posssible origin of this variation as due to a contribution either of CR interactions in the upper atmosphere or to the solar dynamics,will be discussed.

N85-35012

COSMIC RAY POWER SPECTRAL VARIATIONS:
3. SOLAR ROTATION PERIODICITIES

S. P. Agrawal
Department of Physics (Vikram Space Physics Centre)
A.P.S. University, Rewa (M.P.) 486003, India

ABSTRACT

Earlier studies of the periodic changes in cosmic ray intensity by power spectral analysis provided some understanding of the daily variation in terms of ambient power. The solar rotation periodicities are investigated here using daily means of Calgary neutron monitor data during 1965-76. Significant peaks with periods of 27 and 13.5 days with varying magnitudes are observed.

1. Introduction. It is generally accepted that the galactic cosmic radiation is modulated by the continuously varying solar plasma and fields of the modulating region within the heliosphere. Most cosmic ray variational studies (1-1000 Gev), have used 4 decades of ground-based measurements. These include ~ eleven-year solar cycle variation, Forbush decreases, 27-day variation and the various harmonics of the daily variation.

The 27-day variation has direct bearing on the solar features, on or above the solar surface and remain stable for more than one solar rotation of average period 27 days. The solar modulation is a continuous process and any variations in solar output will affect the interplanetary plasma and field, and in turn upon the flow of cosmic rays. Thus a study of the 27-day recurrence in cosmic ray intensity can provide us with information on solar output and its propagation in the interplanetary medium. Here we derive the 27-day rotation periodicities by power spectral analysis during the interval 1965-76, using the procedure adopted by Lanzerotti et al., (1981).

2. Spectral analysis of cosmic ray data. Daily mean values of Calgary neutron monitor data have been used over the interval 1965-76, for power spectral analysis, to investigate the 27-day periodicies and its harmonics. The Calgary neutron monitor is an 18-NM-64 type detector with statistical fluctuations of 0.02% in daily means. Initially the computations were carried out using one year's data at a time; however the peaks under investigation, were not very clear. Hence we combined 2 3 years of data for deriving the power spectra. The choice of 2 years of data at a time was found optimum to look for individual peaks and to compare their variations during the solar cycle.

3. Results and Discussion. The results of the power spectral analysis are shown in Figure 1. Over a sunspot cycle, the cosmic ray intensity changes (at median energies ~ 10-15 Gev) by about 15-20%, and any two successive years combined here generally correspond to similar solar conditions, with very small changes in cosmic ray intensity. However, large changes in cosmic ray intensity, which occur over periods of days (Forbush type decreases), do affect to some extent the overall spectral

shape, but are not effective in modulating the peaks observed. The vertical dashed lines indicate frequencies corresponding to peaks at 27 and 13.5 days. Note that the main peaks occur for the 27-days period and is quite significant for all the years, except for 1973-74. However, the 13-14 day peak is not very significant for a number of years, such as 1965-66, 1967-68 and 1975-76. These results were essentially confirmed by Sulphur Mountain Cosmic ray data. The power associated with the 27-day peak in 1973-74 is quite low and indicates the possibility that even the stable periodic features of the solar surface were not effective in producing any significant changes in the cosmic ray intensity. Solar coronal holes are quite abundant during 1973-74 and also in 1975-76, and thus an absence of any solar rotation periodicity in 1973-74 perhaps indicated that some other solar feature may be responsible. Venkatesan et al., (1982) have shown that only small changes occur in cosmic rays due to coronal holes. The Chree type of analysis involving some specific solar features, in future, may provide the answer for the observations reported here. It is likely that the solar flares/solar active centres could be the source for the solar rotation periodicity observed. The reason for this is not obvious at present.

4. Acknowledgement. The assistance of Messrs. Arun Tiwari and Vishwarnath Khare in data reduction, etc. is acknowledged. I also wish to acknowledge the Calgary data kindly provided by D. Venkatesan and T. Mathews.

5. References.

Lanzerotti, L. J., Maclennan, C. J., Agrawal, S. P. and Venkatesan, D., (1981), *J. Geophys. Res.*, *86*, 6951.

Venkatesan, D., Shukla, A. K., and Agrawal, S. P., (1982), *Solar Physics*, *81*, 375.

ORIGINAL PAGE IS
OF POOR QUALITY

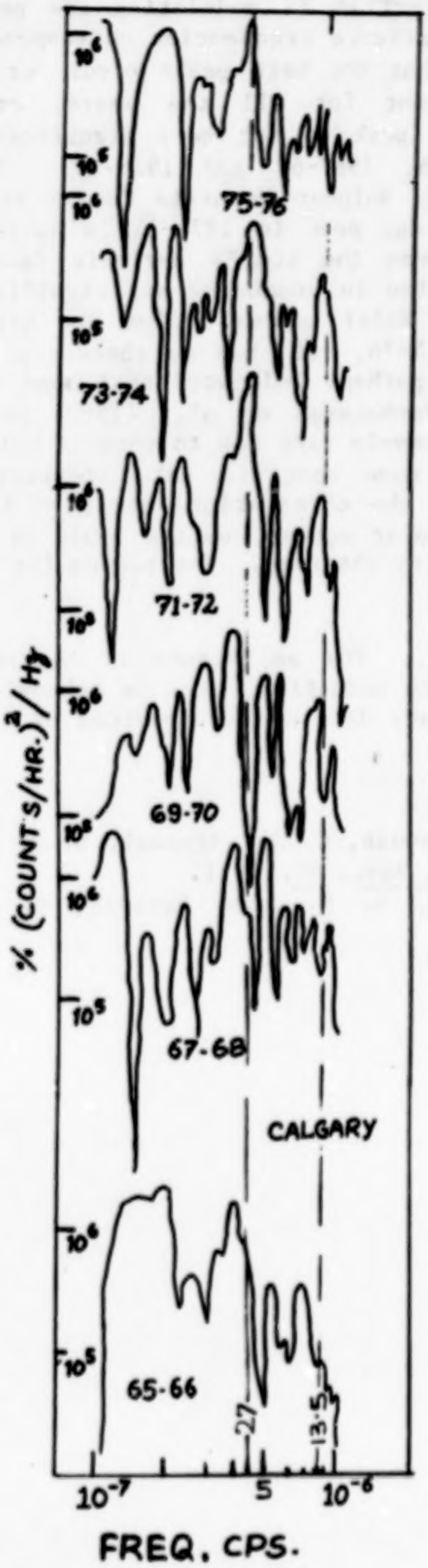

Figure 1. Power spectra for the Calgary neutron monitor for the interval 1965-76. Vertical dashed lines indicate the 27 and 13.5 day period.

N85-35013
SH 4.4-17

VARIATIONS OF THE COSMIC RAY GENERAL COMPONENT IN ANTARCTICA

T.N. Charakhchyan, A.F. Krasotkin, A.I. Kurguzova
Institute of Nuclear Physics, Moscow State University, Moscow 119899, USSR

N.S. Svirzhevsky
P.N.Lebedev Physical Institute of the Academy of Sciences of the USSR, Moscow, USSR

ABSTRACT

The report treats the cosmic ray variations connected with the changes of atmospheric temperature and solar activity level and the variations which are probably due to zonal cosmic ray modulation.

A new type of cosmic ray variations, so called zonal cosmic ray modulation, was found in the lower atmosphere from the sonde measurement results /1/. The new variations give rise to anomalies in the latitude distributions of the cosmic ray charged component and the anomalous north-south asymmetry. To find the nature of the variations, we began measuring the cosmic ray general component with the same detectors as in the sonde measurements (the STS-6) gas-discharge counters and the counter telescopes with 7-mm Al filters detecting the electrons of energy above 200 keV and 5 MeV).

In this report the measurement data obtained in Antarctica (Mirny) in the years 1978-1983 are presented and discussed.

Measurement results. Two B-1 instruments described in /2/ are in operation at Mirny. The measurements are taken daily for two hours (0800-1000 UT). The data on the time dependence of the cosmic ray global component are obtained using six independent units (the unit consists of ten STS-6 counters with a 16 cm^2 geometric factor each). The monthly means of charged-particle number per minute corrected for barometric effect (-0.16%/mb) are shown in Fig. 1 (curve C). The data on time dependence of the cosmic ray vertical component are obtained using three independent units. These data corrected for barometric effect (-0.24%/mb) are shown in Fig. 1 (curve T).

Considering that radioactive background is in practice absent at Mirny /3/(the charged particle flux is

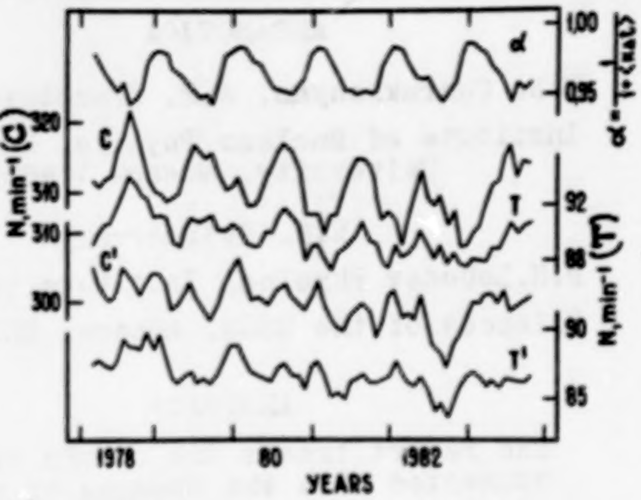

Fig.1. Time dependences at Mirny ($x=1030$ g/cm^2). C and T- cosmic ray global and vertical components correlated for barometric effect; α -correction coefficient for tempereture; C' and T'-cosmic ray global and vertical components corrected for barometric and temperature effects.

about 300 $m^{-2}s^{-1}$), the observed variations are mainly due to cosmic ray variations.

Seasonal cosmic ray variations. As it should be expected, the main variations of the measured particle number on the Earth's surface in Antarctica are due to the seasonal temperature variations. The seasonal variation amplitude (3-4%) is in a good agreement with the calculated values because of the muon component intensity variations /4/. Curve α in Fig. 1 presents the values of the correction factors calculated allowing for the atmospheric temperature distribution inferred from meteorological sounding data and of the partial temperature coefficients for the cosmic ray general component at sea level. The correction factor $\alpha = 1/(1+K\Delta t)$, where K is a partial temperature coefficient, Δt is the difference between the temperature measured at a given isobaric level and the temperature of the standard atmosphere at the same level; $\langle K\Delta t\rangle$ is the mean of the 10 isobaric levels in the 10-1000 g/cm^2 interval. Curves C' and T' in Fig. 1 show the data corrected for the temperature effect. It is seen that, apart from the temperature-induced variations, the general component suffers other types of variations.

The variations due to changes of solar activity level. From 1978 to 1982, the mean level of the charged-particle number at Mirny has changed by ~3%. The same change of the particle number was inferred from the data of the vertical telescope with the 7-mm Al filter at Murmansk. The changes are in a good agreement with the nucleon component variations inferred from the data of high-latitude neutron monitors (see Fig. 2).

During the above mentioned period the sunspot number increased markedly, so the observed cosmic ray intensity decrease was mainly due to the rise of solar activity level. From Fig. 2 it may be seen that the amplitude of these variations in the nucleon component (NM) is 4 times greater than the amplitude in the general component (T) of cosmic rays at sea

ORIGINAL PAGE IS
OF POOR QUALITY

Fig. 2. The yearly means of the detected particle number at sea level. T-charged component (7-mm Al filter); NM-nucleon component (the data of the Apatity neutron monitor).

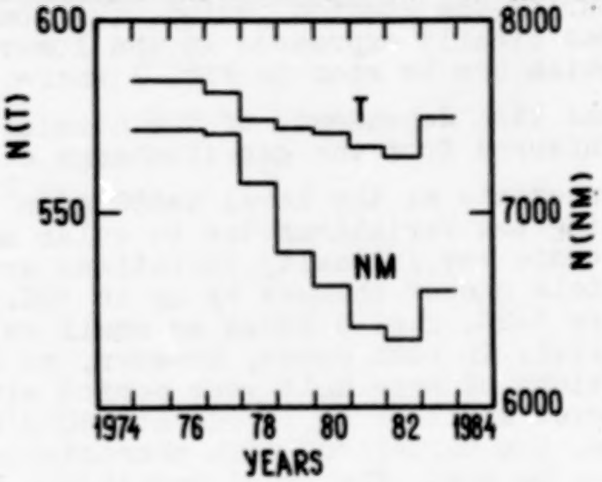

level. Once the continuous series of the nucleon component data from Apatity are available, the cosmic ray variations due to solar activity changes may be excluded from the data shown in Fig. 1 C' and T'. The time dependences of cosmic rays at Mirny after excluding the temperature variations and the variations due to solar activity are shown in Fig. 3 (Curves C'' and T''). The residual variations may be thought to be due mainly to the measurement errors and to the errors in introducing the corrections for the barometric and temperature effects. It should be noted, however, that the found variations resemble the variations in the lower atmosphere inferred from the sonde measurements of cosmic rays.

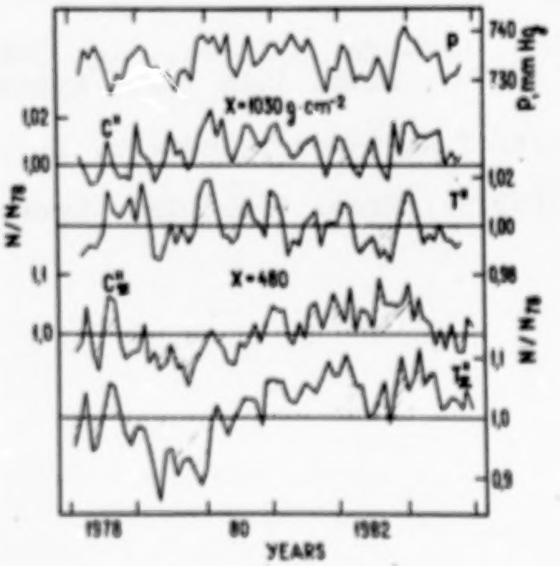

Fig. 3. The corrected time dependences of the cosmic ray charged component at Mirny. C'' and T'' - at sea level; C''_z and T''_z - at the level x=480 g/cm^2; P - atmospheric pressure at Mirny.

The variations due to the zonal cosmic ray modulation. During the studied period, the zonal cosmic ray modulation was clearly expressed in the lower atmosphere over Mirny, which can be seen in Fig. 3 where curves C''_Z and T''_z show the time dependence of the cosmic ray charged component inferred from the gas-discharge counter and telescope measurements at the level $x=480$ g/cm^2 over Mirny after excluding the variations due to solar activity changes. Here the cosmic ray intensity variations are significant. The particle number changes by up to 10%. The changes at sea level are 1-2%, i.e. 5 times as small as the changes at 500 g/cm^2 level. In both cases, however, we can clearly see the variations of some half-year period with 1-1.5% amplitude at sea level and 2-5% amplitude at 480 g/cm^2 level. At the same time, the variations with characteristic times of 2-3 years can be seen. The found variations can hardly be accounted for by incorrect inclusion of the barometric and temperature effects because such variations are absent both in pressure (curve P in Fig. 3) and temperature (curve α in Fig. 1). In this case the annual variations would have been most probably found because they show the largest amplitudes in both pressure and temperature.

Thus, the measurements of the cosmic ray charged component at Mirny have shown that the zonal cosmic ray modulation seems to exist also at sea level, but its amplitude is about an order as low as at ~ 500 g/cm^2 level. The same conclusion can essentially be drawn from the analysis of the neutron monitor data made in /5/ for the solar minimum of 1964-1965.

References

1. Charakhchyan A.N., et al.(1979), Proc. 16th ICRC, Kyoto, v. 3, p. 277.
2. Altukhov A.M. et al. (1984), Geomagn. i Aeron., 24, 386.
3. Charakhchyan A.N. et al. (1979), Proc. 16th ICRC, Kyoto, v. 4, p. 253.
4. Kurguzova A.I., Charakhchyan T.N. (1983), Geomagn. i Aeron., 23, 715.
5. Charakhchyan A.N. et al. (1979), Proc. 16th ICRC, Kyoto, v. 3, p. 271.

SH 4.4-18

THE DIFFERENCE IN THE ENERGY SPECTRA OF GALACTIC COSMIC RAYS AT THE MINIMA OF THE 19TH AND 20TH SOLAR ACTIVITY CYCLES

N85-35014

A.K. SVIRZHEVSKAYA, N.S. SVIRZHEVSKY, YU.I. STOZHKOV,

P.N.LEBEDEV Physical Institute of the Academy of Sciences of the USSR, Leninsky Prospect, 53, 117924, Moscow, USSR

T.N. CHARAKHCHYAN

Institute of Nuclear Physics, Moscow State University, 119899, Moscow, USSR

ABSTRACT

The absorption curves of the cosmic ray charged component for solar minima in 1965 and 1975-1977 are analysed on the basis of daily stratospheric measurements in Murmansk, Moscow, Alma-Ata and Mirny (Antarctic).

Two distinct features in the energy spectra of galactic cosmic rays are revealed during these periods.

1. At the 20th solar activity minimum there was the additional short range component of cosmic rays. Additional fluxes in the stratosphere at high latitudes (Murmansk, Mirny) caused by this component are probably protons and He nuclei with the energy 100-500 MeV/n. The fluxes are estimated as $\sim 300\ m^{-2}s^{-1}sr^{-1}$.
2. At the minimum in 1975-1977 the proton intensity in the energy range 1-15 GeV is 10-15% lower than that in the 1965 solar activity minimum.

Numerous experimental evidences are indicative of a significant role of the solar general magnetic field in the cosmic ray modulation effects /1,2/. The magnetic field direction in the polar regions of the Sun proves to be of importance for the formation of the energy spectra of galactic cosmic rays in the Earth's vicinity.

The differences in the primary cosmic ray energy spectra in the consecutive solar minima are pointed out in particular by the short range component detected in the stratosphere /3,4/. Although the nature of the particles of this component is not clear yet at middle latitudes (Moscow, Alma-Ata), at the same time the data obtained in /5/ suggest that the short range component at high latitudes (Murmansk, Mirny) should be associated probably with the protons and helium nuclei of energies below 500 MeV/n.

Information on the variations of the primary cosmic ray energy spectrum may be derived from the altitude dependence of the relative variations of the cosmic ray intensity $\Delta N/N$ in the stratosphere. In the case of the 11-year cosmic ray modulation the variation amplitude decreases with increasing the primary particle energy, and then the value of $\Delta N/N$ decreases with rising the atmospheric pressure X. Over Murmansk, for example, $\Delta N/N$ at $X=10$ g/cm^2 is two times as high as that at $X=150$ g/cm^2 . However the shape of the dependence $\Delta N/N(X)$ in the years near the 20 solar activity minimum proved to be quite different.

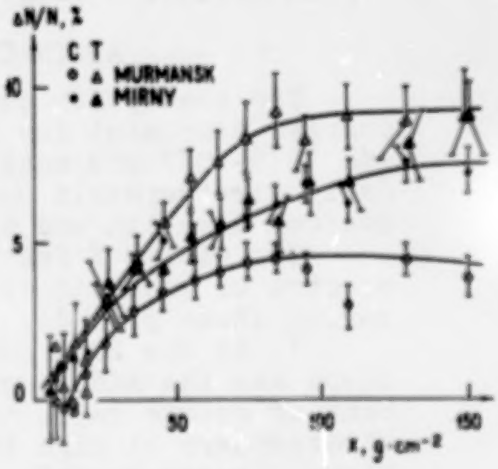

Fig.1. $\Delta N/N$ versus the atmospheric pressure in 1976 for a Geiger counter (C) and counter telescope (T) at Murmansk and Mirny.

Fig.1 shows the variations of the cosmic ray intensity $N_{76}(X)$ in 1976 relative to the intensity in 1965, $\Delta N/N=(N_{65}-N_{76})/N_{65}$, over Murmansk and Mirny. In a broad interval of pressures the cosmic ray intensity in the stratosphere and hence the primary particle intensity in 1976 was lower than that in 1965. The character of the dependence $\Delta N/N$ at $X > 70$ g/cm^2 indicates that the primary spectrum variation in a certain energy range is independent of the particle energy. The decrease of $\Delta N/N$ at $X < 70$ g/cm^2 may be explained by the existence of the cosmic ray short range component in 1976. The same situation took place also in 1975 and 1977.

The data presented in Fig.1 were used to obtain the absorption curves for the additional short range component of cosmic rays (see Fig.2). The absorption curves are actually identical at high latitudes in the nothern and southern hemispheres. The energy spectrum of the additional proton flux, which is also shown in Fig.2, was determined assuming that the additional component consists of protons. The value of the additional 100-400 MeV proton flux is ~ 300 m^{-2}s^{-1}sr^{-1}. Taking into account the fact that He nuc-

ORIGINAL PAGE IS
OF POOR QUALITY

lei make a definite contribution to the particles detected in the stratosphere, the flux obtained proves to be in a good agreement with the additional flux of protons and He nuclei in 1977 (compared with 1965) according to /5/. The short range particles at high latitudes in the stratosphere appeared in 1972 and disappeared practically after 1979 /4/, that is they existed during about the same period as the anomalous He component of cosmic rays detected by space probes /6/.

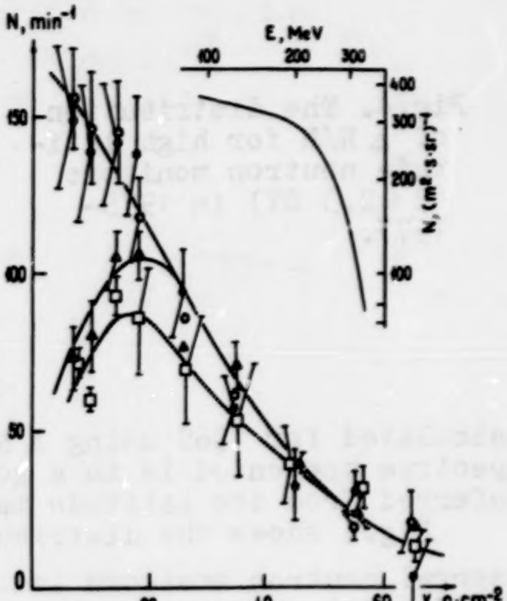

Fig.2. Additional fluxes of the cosmic ray short range component in the stratosphere over Murmansk (○), Mirny (●), Moscow (▲) and Alma-Ata (□). At the top right-hand corner the energy spectrum of the additional proton flux is shown.

Another important conclusion can be drawn from the data presented in Fig.1, namely, the 1-12 GV rigidity cosmic ray fluxes were much lower in 1976 than in 1965. The same conclusion may be drawn from the analysis of the data of latitude stratospheric measurements in the years 1965, 1969 and 1975 /7/. Fig.3 shows the energy spectra of the variations of primary cosmic rays in 1969 and 1976 relative to 1965 inferred from the latitude measurements. From Fig.3 it seen that the primary cosmic ray intensity in the 4-12 GV was 10-15% lower in 1976 than that in 1965. In the examined energy range the cosmic ray intensity in 1976 was essentially the same as during the solar activity maximum of 1969. The dashed line in Fig.3 presents the spectrum of the variations $\Delta I/I(R)$

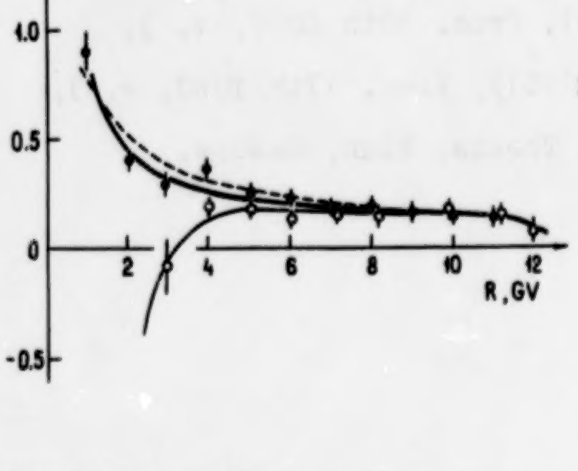

Fig.3. The spectra of the primary cosmic ray variations $\Delta I/I=(I_{65}-I_i)/I_{65}$ in 1969 and 1976 (the dark and light dots respectively). The dashed line shows the variation spectrum in 1969 calculated using the values of $\Delta N/N$ at high latitudes.

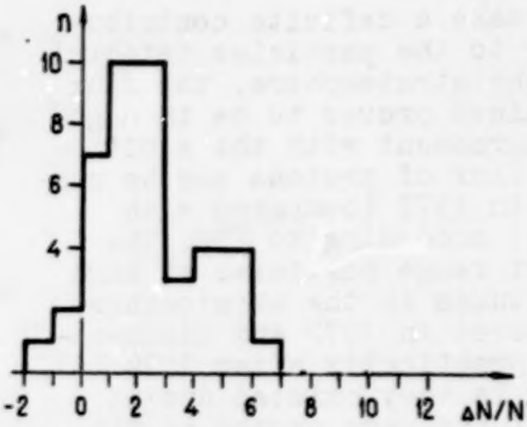

Fig.4. The distribution of Δ N/N for high latitude neutron monitors ($R \leq 2.3$ GV) in 1975-1977.

calculated for 1969 using Δ N/N at Murmansk and Mirny. The spectrum presented is in a good agreement with the spectrum inferred from the latitude measurements.

Fig.4 shows the distribution of $\Delta N/N=(N_{65}-N_i)/N_{65}$ for several neutron monitors located at high latitudes ($R \leq 2.3$ GV). The mean value of Δ N/N for neutron monitors is 2.3 ± 0.3 per cent, but Δ N/N appears to be 5-7 % for some of them (for example, Mt. Washington, Durham). The conclusion that the cosmic ray intensity was lower in 1976 than in 1965 is generally confirmed by the neutron monitor data. The broad distribution of Δ N/N inferred from the neutron monitor data and the difference in Δ N/N over Murmansk and Mirny together with the difference in Δ N/N from the data of a Geiger counter and counter telescope (Fig.1) seems to indicate that the modulation mechanism in the solar activity minima is different from the mechanism of the 11-year cosmic ray modulation.

References

1. Charakhchyan A.N. et al., (1973), Izv. Akad. Nauk SSSR, ser.fiz., v. 37, p. 1258.
2. Nagashima K. et al., (1977), Proc. 15th ICRC, v. 10, p.380.
3. Svirzhevskaya A.K. et al., (1981), Proc. 17th ICRC, v. 3, p. 187.
4. Svirzhevskaya A.K. et al., (1983), Proc. 18th ICRC, v. 3, p. 43.
5. Webber W.R. et al., (1983), Proc. 18th ICRC, v. 3, p. 35.
6. Garcia-Munoz M. et al., (1981), Proc. 17th ICRC, v. 3, p. 270.
7. Svirzhevsky N.S., (1983), Thesis, FIAN, Moscow.

COSMIC RAY VARIATIONS WITH THE PERIOD CLOSE TO 27 DAYS AND THEIR CONNECTION WITH SOLAR ACTIVITY LONGITUDINAL DISTRIBUTION

N85-35015

G.A.Bazilevskaya

P.N.Lebedev Physical Institute of the Academy of Sciences of the USSR, Moscow, USSR

M.I.Tyasto, E.S.Vernova

Leningrad Branch of IZMIRAN, Leningrad, USSR

ABSTRACT

The amplitude and phase changes of the 27 day cosmic ray variation from 1958 to 1975 were studied. The comparison between cosmic ray intensity characteristics and longitudinal distribution of solar activity ones for different stages of the solar cycle were made.

1. Introduction

In some cases the longitudinal redistribution of the solar activity (SA) leads to the changes in 27 day cosmic ray (CR) variations connected with the solar rotation period / 1 /. The purpose of this paper is to analyse in detail the amplitude and the phase evolution of CR 27 day variations along with the longitudinal redistribution of SA. The neutron monitor data I of Thule and the sunspot group area Sp from 1958 to 1975 (except for 1964) were processed.

2. Method

As a result of the sunspot group area treatment for each solar rotation, the polar vector with the amplitude ρ_{SA} and the phase λ_{SA} was obtained, which characterized the non-uniformity of the sunspot longitudinal distribution / 2 /. Indeed, the existence of a longitudinal interval with increased activity means the increased value of ρ_{SA}, and the movement of this interval on the solar surface causes the changes of λ_{SA} from one rotation to another. The amplitude ρ_{CR} and the phase λ_{CR} of the first harmonic of the 27 day CR variation was used for comparison with ρ_{SA} and λ_{SA} of SA / 1 /. The 11-year CR variation, which plays a part of the trend for the present analysis was firstly withdrawn from the primary CR data.

3. Results

Fig. 1 shows the correlation coefficient values R (λ_{SA} , λ_{CR}) between time series of the phases of 27 day SA variations and CR ones with the zero shift between these two series. The horizontal bars correspond to the time intervals, for which these correlation coefficients were obtained. Fig. 1 shows R(λ_{SA}, λ_{CR}) keep the high values during the long time intervals; but for two time intervals from 1970 to 1973 correlation coefficient sharply fell. For these two time intervals (III 1970 - IX 1971, II 1972 - VIII 1973) R(λ_{SA} , λ_{CR}) were computed with the time shift between time series of the phases of 27 day SA variations and CR ones.

Fig. 2 shows the dependence of the R(λ_{SA} , λ_{CR}) on the time shift. It can be seen in Fig. 2 the R(λ_{SA}, λ_{CR}) reached the maximum value $R \approx 0.86$ for the time shift equal to about three months CR variations being prior to the SA ones. It should be noted that not far from 1970-1973 the polarity reversal of the Sun's general magnetic field took place / 3 /, thus we may expect the redistribution of solar magnetic fields among these the SA longitudinal redistribution. The corresponding changes of interplanetary magnetic fields and 27 day CR variations may be expected. To check this assumption we consider the 27 day variation cyclogram of sunspot group areas shown in Fig.3 / 4 /. As could be expected the SA amplitude of variations decreased and the phase became unstable (region A in the cyclogram). When SA is high the phase of variations is more stable, except for time intervals B and C which concerned with the polarity reversal of the Sun's general magnetic field. This result is confirmed by Table 1 where the parameter of the phase conservation is presented which is the relation $|\Sigma \vec{\rho}_i| / \Sigma |\vec{\rho}_i|$ in percent / 5 /. This parameter was more than 58% during the years of high SA except for XI 1959 - VIII 1960 and II 1970 - III 1972, when it fell abruptly.

Table 1

Year	$\lvert\Sigma \vec{\rho}_i\rvert / \Sigma\lvert\vec{\rho}_i\rvert$, %	Year	$\lvert\Sigma \vec{\rho}_i\rvert / \Sigma\lvert\vec{\rho}_i\rvert$, %
II-V 1958	85	VIII 1961 - IV 1962	89
VI-X 1958	95	VII 1966-V 1967	87
XI 1958-X 1959	65	VI 1967-II 1968	60
XI 1959-VIII 1960	58	III 1968-I 1970	58
IX 1960-VII 1961	76	II 1970-III 1972	5

4. Conclusion

The strong variability of the longitudinal distribution of SA took place near the polarity reversal of the Sun's general magnetic field. The disturbance of 27 day CR variations may be expected in turn.

Nevertheless from the point of view of current ideas about the solar modulation of CR intensities it is difficult to explain a high value of R(λ_{SA}, λ_{CR}) between the time series of the phases of 27 day SA variations and CR ones for 1970-1973 with CR variations being prior to the

Fig. 1. Correlation coefficients between the 27 day variation phases of CR intensity and sunspot area with zero shift between time series.

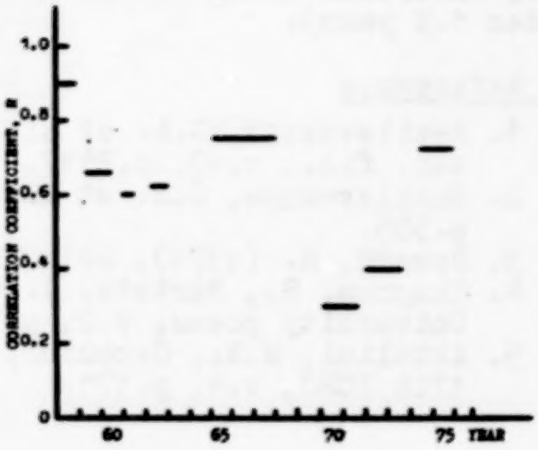

Fig. 2. Correlation coefficient R(λ_{SA} , λ_{CR}) versus the time shift between the series.

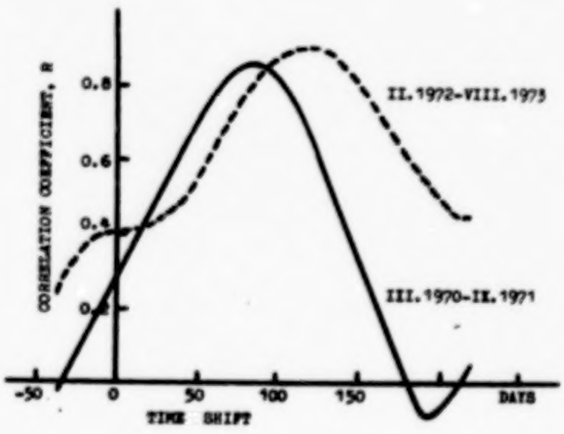

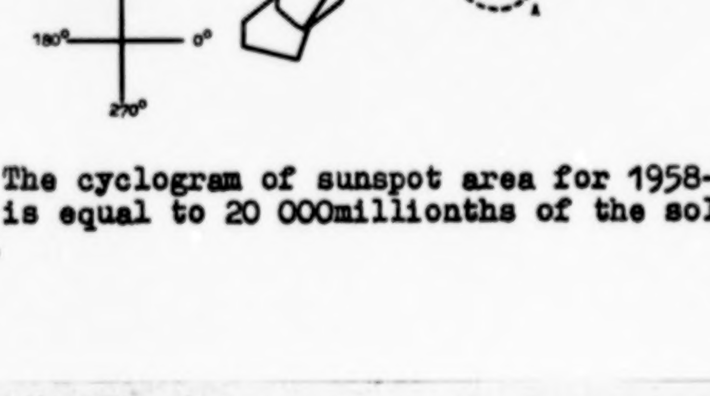

Fig. 3. The cyclogram of sunspot area for 1958-1972 (1 unit is equal to 20 000millionths of the solar hemisphere).

SA. At the same time it is unlikely to obtain such a high value of R(λ_{SA} , λ_{cr}) by chance because of rather long time intervals under consideration (each of them being of order 1.5 year).

5. References

1. Bazilevskaya, G.A. et al., (1984), Izv. Akad. Nauk, ser. fiz., v.49, p.2117.
2. Bazilevskaya, G.A. et al., (1979), 16th ICRC, v.3, p.385.
3. Howard, R. (1974), Solar Phys., v.38. p.283.
4. Chapman, S., Bartets, Y. (1951), Geomagnetism, Oxford University press, v.2, p.569.
5. Attolini, M.R., Cecchini, S., Galli, M., (1981), 17th ICRC, v.4, p.171.

N85-35016

AZIMUTHAL AND MERIDIONAL ASYMMETRIES OF THE SOLAR WIND AND QUASIPERIODIC VARIATIONS OF INTENSITY OF GALACTIC COSMIC RAYS (GCR)

L.Kh.Shatashvili, T.V.Djapiashvili, B.G.Kavlashvili,
B.D.Naskidashvili, O.G.Rogava, G.V.Shafer

The Institute of Geophysics, Georgian Academy of
Sciences, Z.Rukhadze str. 1, 380093, Tbilisi,USSR

ABSTRACT

The results of analysis of 27-day, annual and quasi-two-year variation of GCR are presented. The dependence of the periods of 27-day GCR variation on the energy of initial radiation is discovered, according to the data during 1980 of the World network of station in sufficiently wide range of the observed threshold energy. The dependence of the annual variation of GCR is established, according to the data of the Huancayo station in conformity with the change of the polarity of the General Magnetic Field of the Sun (GMFS).

I. 27-day variation of GCR intensity

In paper /1/, the supposition, that the duration τ of 27-day oscillation of GCR ought not depend on the stage of development of the 11-year cycleness was expressed and in average τ =9+10 Sun's rotation time was addmited. However, observations on the wider intervals of time show that these confirmations are true not for all cycles of Solar activity, in particular, it appeared, that for the period of 1962-1964 $\tau \approx 22$ Sun's rotation time. At present we have the data for 20-21 cycles of Solar activity, which show that τ is changing in a quite wide range of time.

We have made complex analysis of Solar activity data; gemagnetic activity(Solar Geophysical data) of neutron component of GCR Kiel(FRG), Tokyo(Japan), Sanae(antarctica) South Africa, the vertical direction of GCR rigid component of supertelescopes on ground station at Nagoya and the underground station at Sakashita (80 m.w.e. underground) Not so often we meet the case, when the duration of 27-day variations of GCR intensity is very long. Particular interest has been attached to the epoch 1980 when τ was quite big and at the same time it was possible to correlate the GCR data with the change of Solar wind characteristics, made directly in cosmic space. The results of calculation by the method of superposition analysis for several stations of CR are presented in Fig.I. The stations are chosen so that the difference in the cut-off of initial radiation could be noticable. The attention must be paid to the extremly interesting observed phenomena- the dependence of the period of the reccurent change of GCR intensity on the cut-off energy. The period, determined in first rotations of the Sun according to the data with less cutoff of CR is essentialy longer than according to the data with the big cutoff. It is difficult to ascribe the above mentioned dependence to the not considered temperature effects in the rigid component data at Nagoya and Sakashita stations, as the analogic phenomenon is observed in the neutron data at Tokyo station, where the temperature effect is obviously small, at the cutoff energy is essentialy more than at Kiel station.

In a number of papers the change of periods of 27-day GCR variation was investigated. In paper /4/ it is established that the average period of 27-day GCR variation depends on the polarity of GMPS. In the present paper the dependence of period of 27-day GCR variation on the cycle phase of Solar activity (SA) is investigated. The investigation was made by the method of Fourier transform /5/ using the Han windows, on the basis of hour data of neutron monitor at Kiel station.

The period of 27-day variation- T_{27} of GCR intensity is defined by 2-year data with the subsequent drifts of number of datum for a year. The value of the period T_{27} was determined by Fourier spectrum function $F(T)$ so that T_{27} -corresponded to the maximum of function $F(T)$ in the interval of period $T = 25 \div 32$ days.

In Fig. 2 the change of the period T_{27} in time is presented. It is possible, to notice that the period T_{27} 27-day GCR variation in the maximum epoch of SA reaches the synodic period of the Sun's rotation, but in minimum of SA T_{27} is maximum.

2. Annual variation

In paper /6/ the annual variation of GCR intensity was investigated, according to the data of CR neutron component in connection with the polarity of GMPS. We've made the analogical analysis, using the data of ionic chamber (IC) at stations, Iakytsk and Huancayo for the other epochs. The averaging of vectors of the annual variation was made in conformity with the direction of GMPS (1946-1955 and 1960-1968). The results of harmonic analysis of the average monthly data of these stations, show that the IC data at Iakytsk contains the influence of the seasonal temperature change. It is due to expect that so far as the Huancayo station is equatorial, the seasonal change is not essential. Indeed the results of harmonic analysis according to the data of Huancayo station, show that supposed in /6/ the effect observed in the neutron component of highlatitudinal station, connected with the change of GMPS polarity is as well clearly expressed in the data of IC equatorial station at Huancayo /Fig.3/.

3. GCR quasi-two-year variations

In paper /7/ it was noticed, that the observed quasi-two-year variations of neutron and μ -meson components of CR are caused not only by the cycle changes of parameters of solar modulation of CR, but at the expense of two-year variations of meteorological parameters of the Earth atmosphere.

For the present moment we've widened our analysis. For the more assurance we used the Forbush data too /2/.

Then we obtained that the quasi-two-year variations of intensity of rigid μ -meson component of CR, corrected on the temperature and barometric effects of IC-I(Iakytsk) for the period I954-I976 are synchronous with the quasi-two-year variations of SA. Quasi-two-year variations corrected on the meteorological effects, are apparently caused /7/ rather by the quasi-two-year variations of the meridional asymmetry of Solar wind velocity /8/.

REFERENCES

I. Dorman L.I., Shatashvili L.Ch., sb. "Cosmicheskie luchi" I965, Izd-vo "Nauka", № 7, Str.I6I.
2. Forbush S.E., Cosmic Ray Results. vol.XX I957.
3. Bazilevskaya G.A., Okhlopkov B.P., Charakchyan T.N. Tr. FIAN, I976, 88, 94.
4. Bazilevskaya G.A., Vernova E.S., Grigoryan M.S., Sladkova A.I., Tiasto M.N., Charakchyan T.V., Geomagnetizm i aeronomia" № 4, I984.
5. Bendat J., Pyrsol A., Primenenie correlatsionnogo i spectralnogo analyza. "Mir", I983.
6. Krimsky G.F., Krivoshaphin P.A., Mamrukova V.P., Skripin G.V., Geomagnetizm i aeronomia, 2I, 823, I98I.
7. Djapiashvili T.V., Rogava O.G., Shatashvili L.Kh., I8th ICRC, v. IO, p.235, I983.
8. Djapiashvili T.V. , Rogava O.G., Shatashvili L.Kh. Shafer G.V., Geomagnetizm i aeronomia, 24 , c. 680.

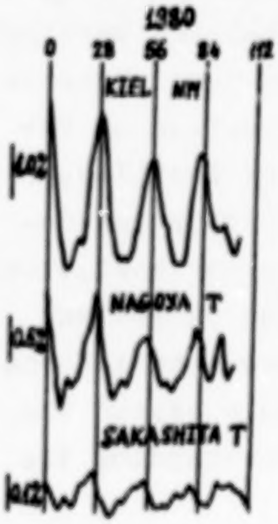

Fig. 1

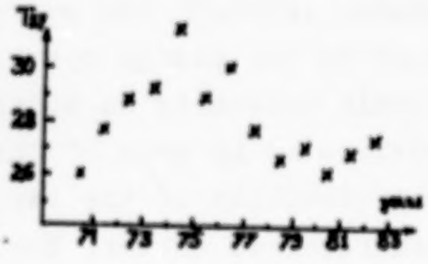

Fig. 2

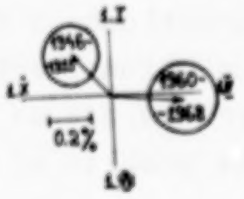

Fig.3

DYNAMICS OF TWO-YEAR COSMIC RAY VARIATIONS INFERRED FROM THE DATA OF SPACECRAFT AND STRATOSPHERIC MEASUREMENTS AND FROM THE NEUTRON MONITOR DATA IN 1959-1981

N85-35017

T.N. Charakhchyan, E.V. Gorchakov, V.P. Okhlopkov,
L.S. Okhlopkova, M.V. Ternovskaya
Institute of Nuclear Physics, Moscow State University,
Moscow 119899, U S S R

ABSTRACT

The two-year cosmic ray variations are studied using the spacecraft measurements of 1967-1976, the sonde measurements at high latitudes in the stratosphere (Murmansk, Mirny), and the neutron monitor data of 1959-1981. The two-year variations are most pronounced from 1967 to 1975. An anticorrelation is observed between the two-year variations in cosmic rays and in geomagnetic activity.

In work /1/ the two-year cosmic ray variations were singled out from the stratospheric sounding data and were shown to be of isotropic character. The variation amplitude and phase are the same in the southern and northern hemispheres, they are also the same for the global and vertical fluxes of cosmic rays. The nature of the two-year variations is still obscure. Although the energy spectrum of the variations is close to the energy spectrum of the 11-year variations, but their relevance to solar activity parameters is not so obvious as in case of the 11-year variations. The problem of the stability of the variation period and phase has not been resolved either. Therefore, the information derivable from the satellite measurements beyond the Earth's magnetosphere gets essential in understanding the nature of the variations.

In the present work, the two-year variation was sought in the low-energy cosmic ray intensity beyond the Earth's magnetosphere. We processed the $\geqslant$60 MeV proton detection data (the Explorer satellites data in May,1967- May 1973/2/ and, the Soviet space probes data in June 1973-March,1976/3/).

The method of mathematical selective filter used in/1,4/ can hardly be used to discriminate the two-year variations in such a comparatively small series of experimental data because the information for two years is lost at the ends of the series, so but a single period of the two-year variation may be singled out from the satellite data. Therefore, the peculiar method based on the difference in the approximation of the data by the Fourier series was developed /5/ for small data series. If the Fourier series with different numbers of harmonics are used, they will have different cut frequencies and the difference of transforms will discriminate a narrow frequency band. Such a transform is a selective filter. The method was used to process the spacecraft data. Fig. 1 shows the results of the processing.

Fig. 1 shows also the two-year cosmic ray variations inferred from the data of stratospheric sounding at a 20 g/cm^2 layer at Murmansk and Mirny (Antarctica) and the neutron component data at Deep River and Climax discriminated using the numerical selective filter /4/.

It is seen that the two-year cosmic ray intensity variation was in practice absent in 1959-1965 and was pronounced in 1966-1976 when its amplitude was 4-7% on spacecraft,2-4% in the stratosphere, and 1-1.4% in the neutron component. All the cosmic ray data show a good coincidence of the variation phases. The fact that the two-year variation appeared in the spacecraft data is worth noting because it demonstrates that the variation is actually due to the two-year variation of the interplanetary medium parameters rather than to some geophysical effect.

A change should be noted in the variation period which was 24-25 months in 1966-1972 and 19-20 months in

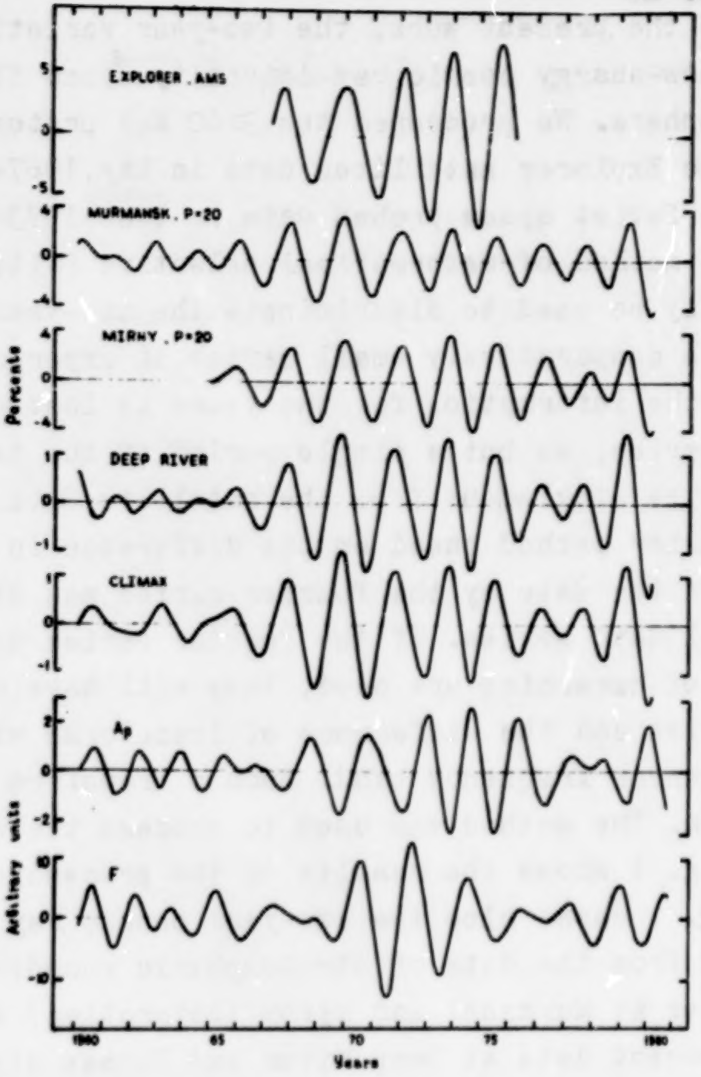

Fig. 1.

The twoyear variations obtained using the selective filter. The upper curve shows the data from the Explorer satellite and from the Soviet space probes. The stratospheric data at 20 g/cm^2 level over Murmansk and Mirny. The neutron component at Deep River and Climax. The Ap-index. F is the 10.7 cm radio emission from the Sun.

1973-1977. Since the change is seen in all the data,it is not accidental and reflects the real changes of the character of the variations in the interplanetary medium parameters.Fig. 1 also shows the two-year variations inferred from the solar 10.7 cm radio emission (F) and from the Ap-index. Although the two-year variation was felt in solar activity, its dynamics differs much from the two-year cosmic ray variation. The two-year wave in solar stivity was in practice absent in 1966-1969. Considering that the variations in solar activity and cosmic rays must be of opposite phase,the phase shift between solar activity and cosmic rays was about half-year in 1970-1975.This fact should have meant that a large modulation region is responsible for the cosmic ray variation,but such a conclusion is at variance with the data on the two-year geomagnetic activity variations.

From Fig. 1 it is seen that the pronounced two-year variation was observed simultaneously in the Ap-index and in cosmic rays. It is woth noting that the waves in the Ap--index and in cosmic rays are clearly of opposite phase. Both the Ap-index and cosmic rays exhibit the trend in the variation period to change from 24-25 months to 19-20 months. All the above means most probably that the two-year cosmic ray variation is due to the changes in the properties of the near region of interplanetary space and is contingent upon the variations of the same parameters which give rise to the geomagnetic activity variations (solar wind velocity and density,interplanetary magnetic field).

The preliminary processing of the data obtained before 1984 has shown that the amplitude of the two-year cosmic ray variation increased markedly after 1979,so in 1980-1983 it was closer to the variation amplitude in 1968-1974.

Thus, the two-year variation dynamics is characterized by significant changes in the amplitude,phase,and period of the variation. Since the significant decreases of the variation amplitude occur during the periods close to the solar minima (1964-1965,1975-1977)and in the periods close to the solar maximum (1959-1982),the dynamics of the two--year variations does not seem to depend on the phase of the 11-year solar activity cycle,but is most probably determined by the state of the heliosphere,the approach adopted, for example, in /6/.

References

1.Charakhchyan T.N.et al.(1979),Proc. 16th ICRC,Kyoto,v.3,
2.Solar Geophysical Data,Boulder,USA,1967-1973. p.297.
3.Ignatiev P.P.,Shvidkovskaya T.E.(1980).In:Cosmic Rays,
No. 27,p. 57.
4. Charakhchyan T.N.et al.(1979).Proc.16th ICRC,Kyoto,v.3,
5.Okhlopkov V.P.VINITI AN USSR,No.7382-85 DEP. p.308.
6. Dorman L.I.,Ptuskin V.S. (1981).Astrophys. and Space Sci.
v. 179,p.397.

94 N85-35018

LONG-TERM MODULATION OF GALACTIC COSMIC RAYS IN HIGH-ENERGY REGION

P.A.Krivoshapkin, A.N.Prikhodko, G.V.Skripin,
I.A.Transky, G.V.Shafer

Institute of Cosmophysical Research & Aeronomy
Lenin Ave., 31, 677891 Yakutsk, USSR

ABSTRACT

The results of continious registration of the cosmic ray muon intensity on the ground and underground at 7, 20 and 60 m w.e. depths in Yakutsk for 1957-1983 are presented. In years of the solar activity maximum in cosmic ray density were found two minima or two-stepped decrease. The second intensity minimum appears to be not the result of the inversion of the general magnetic field of the Sun but caused by the increase of the solar wind speed.

In [1] it was shown that the galactic cosmic ray intensity in even cycles of the solar activity is associated mainly with the number of sunspots and in odd ones - with the solar wind speed.

In [2] to describe the galactic cosmic ray density the index is suggested which is as a function of the number of sunspot groups and of their average heliolatitude. In [2] it was found as well that correlation of the galactic cosmic ray intensity with the above index is violated during the periods of the inversion of the general magnetic field of the Sun. The violation of the close correlation between the temporal behaviour of high- and low-energy galactic cosmic rays at this period has been explained by the decrease of the regular interplanetary magnetic field intensity.

In [3] it is obtained that on the 11-year galactic cosmic ray intensity variation the effect of interaction of the general magnetic field of the Sun and of the galactic magnetic field is superimposed. The dependence of the galactic cosmic ray intensity on the solar activity in even and odd cycles forms a narrow and a wide loops of hysteresis, respectively.

The cosmic ray muon intensity by telescopes at 0, 7, 20 and 60 m w.e. depths in Yakutsk beginning from 1957 is continuously registered. The median values of energy for coupling coefficients at the above levels are 40, 78, 123 and 260 GeV, respectively. The average monthly statistical accuracy for vertical telescopes at these levels was 0.014, 0.017, 0.017 and 0.025%, respectively. In 1963-1964 the pit was reconstructed, i.e. the area at all the three underground levels was significantly enlarged. Because of this reason the telescopes at 7 and 20 m w.e. operated with breaks. Beginning from 1970 to 1982 at all the depths two and more telescopes were in operation. At present the statistical accuracy increased by ~ 2 times as compared with 1957. Beginning from June 1953 to present the ionization chamber of a large volume (the mean monthly statistical accuracy is 0.003%) is continiously operating [4] .

In the Figure the geomagnetic activity (A_p-index), sunspot numbers R_z, the galactic cosmic ray density smoothed in an annual interval on measurements by the muon vertical telescopes at 0, 7, 20, 60 m w.e. and by the ionization chamber in Yakutsk for the recent three solar cycles are presented.

During the 19-th solar activity cycle three peaks in geomagnetic activity were observed. The first increase of A_p was early in 1958 and it coincides with the maximum of R_z. The second peak is when the R_z started to decrease, the third one - near the minimum of the solar activity. The increases of A_p coincided with decreases of the galactic cosmic ray intensity at all the depths up to 60 m w.e. (in the Figure a scale for 60 m w.e. is twice larger in comparison with other levels).

In the 20-th cycle the two peaks in A_p were observed. The first peak coincides with the solar activity maximum, the second one was caused by the occurence of high-speed stationary solar wind streams with regular magnetic field in 1973-

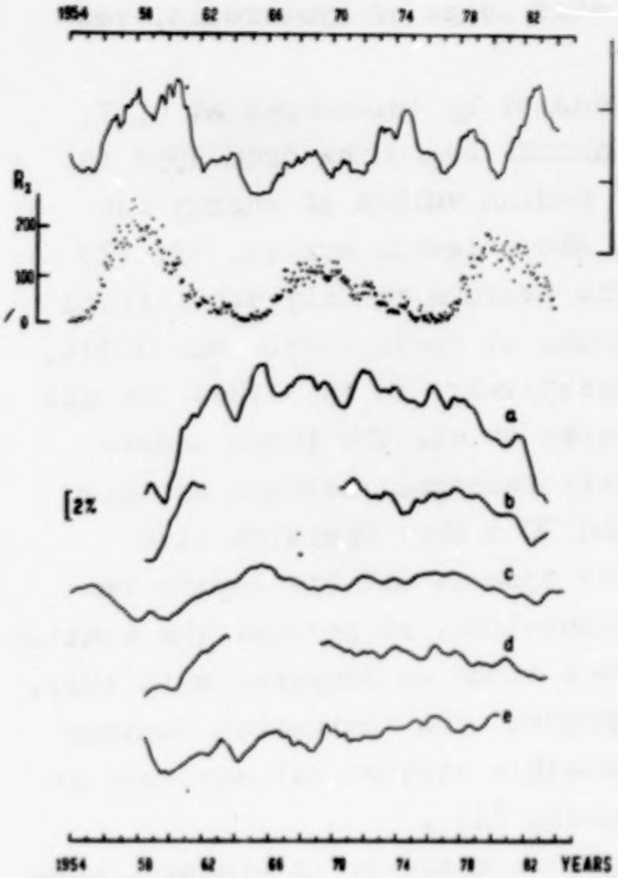

Geomagnetic activity (A_p-index), sunspot number R_z and the galactic cosmic ray intensity smoothed in annual interval on Yakutsk measurements by the muon telescopes (vertical) at 0, 7, 20 and 60 m w.e. depths (a,b,d,e, respectively) and by ionization chamber (c)

1974. In the galactic cosmic ray density the two minima are observed. The first (deep) minimum was in 1970, the second one (less deep) - was in 1974.

In the 21-st cycle also two peaks in A_p were observed. The first peak coincides with the phase of the solar activity increase, the second one was at the R_z decrease. A_p minimum coincided with the R_z maximum. In the galactic cosmic ray density the two-stepped decrease is revealed. The first decrease appears to be caused by the solar activity maximum, the second one - by the A_p increase in 1982.

The moments of the galactic cosmic ray density maxima delay by 9-12 months with respect to the solar activity minima. The geomagnetic activity minima in the 19-20-th cycles coincide with the galactic cosmic ray density maxima. In the years of the solar activity maxima in the high-energy galactic cosmic ray density the two minima or two-stepped decrease were observed. The second minimum in the galactic cosmic ray intensity appear to be not the result of the inversion of the general magnetic field of the Sun. This fact confirms the results of [1] . The enrgy spectrum of 11-year variation in the galactic cosmic ray density obtained based on underground data is of the form $\sim E^{-1.0}$.

References

1. Chirkov, N.P. Solnechnyi veter i variatsii plotnosti kosmicheskikh luchei. - V kn.: *Variatsii kosmicheskikh luchei i solnechnyi veter*, (1980), Yakutsk, 25.

2. Krainev, M.V., Stozhkov, Yu.I., Charakhchyan, T.N., (1983), *Proc. 18-th ICRC*, Bangalore, *3*, 23.

3. Nagashima, K. and Morishita, I. *Twenty-Two Modulation of Cosmic Rays Associated with Polarity Reversal of Polar Magnetic Field of the Sun*, (1979), Nagoya, Japan, 24.

4. Shafer, G.V., Shafer, Yu.G. *Pretsizionnye nablyudeniya kosmicheskikh luchei v Yakutske*, (1984), Novosibirsk, Nauka. 734 p.

N85-35019

THE FIRST THREE HARMONICS OF SOLAR DAILY VARIATION CAUSED BY THE DIFFUSIVE PROPAGATION OF GALACTIC COSMIC RAYS THROUGH THE HELIOSPHERE

K. Munakata and K. Nagashima*

Department of Physics, Faculty of Science,
Nagoya University, Nagoya 464, JAPAN

*Cosmic Ray Research Laboratory, Faculty of Science,
Nagoya University, Nagoya 464, JAPAN

Introduction

Forming a complement to our preceeding paper(1), we present some results for the first three harmonics derived from the simulation of diffusion-convection of galactic cosmic rays. We present also some dependences of the results to the modulation parameters. The results are discussed in comparison with observations and with the former studies of higher order anisotropy.

In addition to this, we suggest the existence of the IMF-sense-dependent anisotropy of higher order which is discussed in detail in a separate paper(2).

Theory and Model

The cosmic ray anisotropy $\eta(r, p)$ can be expressed as

$$\eta(r,p) \sim 1+\sum_{n=1}^{3}\sum_{m=0}^{n}[\eta_n^{mc}(r,p)\cos(m\Phi')+\eta_n^{ms}(r,p)\sin(m\Phi')]P_n^m(\cos\Theta'). \quad (1)$$

where Θ' and Φ' express the incident direction of cosmic rays, defined as(cf. Fig.1)

$$\Theta'=\pi-\Theta, \quad \Phi'=\pi+\Phi,$$

and

$$\eta_n^{mc}(r,p)=(-1)^n F_n^{mc}(r,p)/F_0^0(r,p),$$

$$\eta_n^{ms}(r,p)=(-1)^n F_n^{ms}(r,p)/F_0^0(r,p).$$

As shown in our preceeding paper(1), F_n^{mc} and F_n^{ms} in Eq.(1) are given by the cosmic ray denrity U, stream S_i, stress tensor T_{ij} and heat flow tensor H_{ijk} which are governed by the following equations.

$$\nabla\cdot(CUV-\underline{\kappa}^{(1)}\cdot\nabla U)=-\frac{\partial}{\partial p}\left(\frac{1}{3}pV\cdot\nabla U\right), \quad (2)$$

$$S=CUV-\underline{\kappa}^{(1)}\cdot\nabla U, \quad (3)$$

$$T_{ij}=-\kappa^{(2)}{}_{ijlm}(\dot{\overline{\nabla S}})_{lm}, \quad (4)$$

$$H_{ijk}=-\kappa^{(3)}{}_{ijklmn}(\dot{\overline{\nabla \underline{T}}})_{lmn}. \quad (5)$$

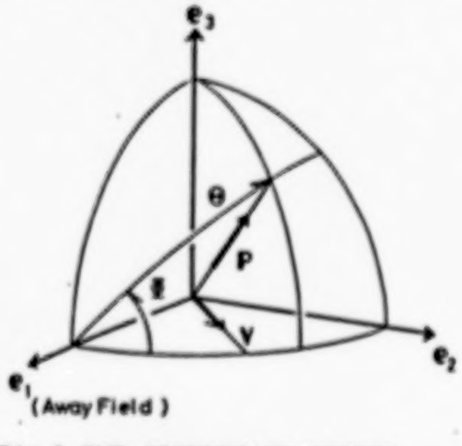

Fig.1 IMF-COORDINATE SYSTEM

p ; Particle's momentum.
V ; Solar wind velocity.
e_1; Unit vector in the direction of B in the 'away' sector.
$e_3 = e_1 \times V/|e_1 \times V|$.
$e_2 = e_3 \times e_1$.

where

$$\overset{\bullet}{\overline{(\nabla S)}}_{jq}=\frac{1}{2}\left[\frac{\partial S_j}{\partial x_q}+\frac{\partial S_q}{\partial x_j}+S_s(Z_{sjq}+Z_{sqj})\right]-\frac{1}{3}(\nabla\cdot S)\delta_{jq},\qquad (\nabla\cdot S)=\frac{\partial S_s}{\partial x_s}+S_s Z_{sqq},$$

and

$$Z_{ijk}=\frac{\partial e_i}{\partial x_j}\cdot e_k=-Z_{kji}. \qquad (6)$$

Note that, in the IMF-coordinate system, Z_{ijk}'s in Eq.(6) represent the IMF-curvature and focusing. We first solve Eq.(2) in the model heliosphere and, starting from the solution for U, we can calculate successively S_i, T_{ij} and H_{ijk} by Eqs.(3)-(5). In these calculations, the following scattering m.f.p. is assumed.

$$\lambda=\lambda_0(R/GV)\exp\left(\frac{r-r_e}{33\text{a.u.}}\right)(1+a_\lambda\cos\theta_H), \qquad (7)$$

where λ_0 and a_λ are the parameters, R is the rigidity and θ_H is the polar angle in the heliocentric polar coordinate system. The calculations were carried out for various values of λ_0 and a_λ and, in this paper, the results in the following two cases will be presented.

case I .... λ_0 = 0.016 a.u. and $0\leq a_\lambda\leq 3$,

case II .... λ_0 = 0.032 a.u. and $0\leq a_\lambda\leq 3$.

It is noteworthy that, in Eqs.(3)-(5), S_i, T_{ij}, H_{ijk} having subscript '3' odd times are IMF-sense-dependent and their associated anisotropies symbolized by η_n^{ms} with mark 's' change their signs according to the alteration of the 'away' and 'toward' sectors whereas η_n^{mc} with mark 'c' do not. In this paper, we restrict ourselves only to η_n^{mc}, and the natures of η_n^{ms} mentioned above will be discussed in a separate paper(2).

Results and Discussions

The anisotropies η_n^{mc}'s in space can be expressed by the surface harmonics in the equatorial coordinate system and can be observed as solar daily variations at the Earth(3).

The resultant first space harmonic vectors for cases I and II are shown in Fig.2, with black characters in the positive state and white characters in the negative state. It can be clearly seen that the harmonic vector in the positive state changes its phase toward earlier hours from that of 18h in the negative state, in accordance with the observed 22-year variation of the diurnal variation(4,5,6).

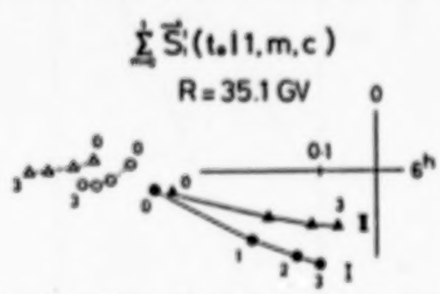

Fig.2 FIRST SPACE HARMONIC VECTORS

Arabic numerals represent the value of a_λ in Eq.(7). The black and white characters represent the positive and negative polarity states, respectively.

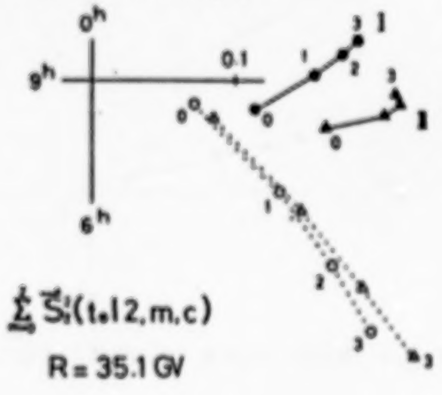

Fig.3 SECOND SPACE HARMONIC VECTORS

The resultant second space harmonic vectors are shown in Fig.3. These vectors in both polarity states are mainly due to the η_2^{0c}-type anisotropy which is independent of Φ (cf. Eq.(1)). The magnitude η_2^{0c} of the anisotropy includes three terms expressing, respectively, the spatial derivatives of S_i, the IMF-curvature effect and the IMF-focusing effect. On the basis of simulations, it is found that all these terms have significant contribution to the anisotropy and the IMF-focusing effect is not always most predominant. A similar Φ- independent anisotropy was obtained also by Bieber and Pomerantz(7), on the basis of the following diffusion equation with respect to the pitch angle cosine ($\mu=\cos\theta$).

$$\frac{\partial f(\mu,x_1,t)}{\partial t}+\mu v\frac{\partial f(\mu,x_1,t)}{\partial x_1}-\frac{\partial}{\partial \mu}D_{\mu\mu}\frac{\partial f(\mu,x_1,t)}{\partial \mu}+\frac{v}{2L}(1-\mu^2)\frac{\partial f(\mu,x_1,t)}{\partial \mu}=0, \qquad (8)$$

where $D_{\mu\mu}$ is the Fokker-Planck coefficient for pitch angle scattering and L is the focusing length of IMF(8). They concluded that the anisotropy is principally a result of the focusing effect of IMF represented by the last term in Eq.(8). This anisotropy can be regarded as a special case which is applicable only for one dimensional diffusion along the IMF with infinite radius of curvature in the equatorial plane. In other words, this special anisotropy lacks the term expressing the IMF-curvature effect which has a dominant influence on the anisotropy as pointed out previously.

Turning to the third order anisotropy, we obtained two dominant terms η_3^{0c} and η_3^{1c}. The eigen phases of the tri-diurnal variation arising from these two terms are almost orthogonal to each other, that is, (1h,5h) from η_3^{0c} and (3h,7h) from η_3^{1c}. It is noteworthy that one of the eigen phases(3h,7h) arising from η_3^{1c} coincides with the observed phase around 7h in local time(9,10). Since the η_3^{1c}-type distribution is not symmetrical with respect to the field, this implies that the angular

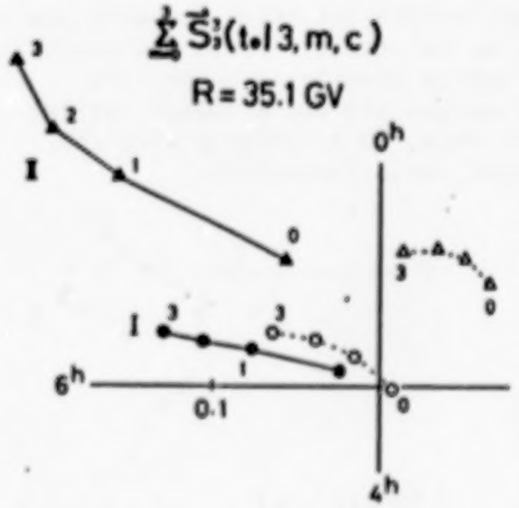

Fig.4 THIRD SPACE HARMONIC VECTORS

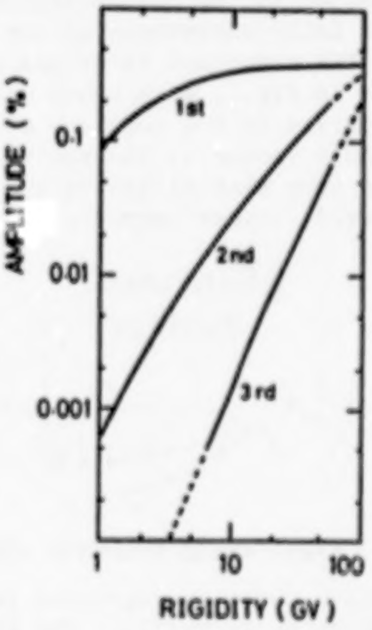

Fig.5 RIGIDITY SPECTRA OF THE FIRST THREE HARMONICS

distribution of the third order anisotropy can not expressed generally in terms of only the pitch angle cosine μ. In this respect, it is not suitable to discuss the third order anisotropy on the basis of the diffusion equation of Eq.(8). Fig.4 shows the resultant tri-diurnal variations which are mainly composed of the above mentioned two types of distribution, i.e., η_3^{0c} and η_3^{1c}. It is noted that the tri-diurnal variations obtained show polarity dependence. This dependence, however, is sensitive to the modulation parameters and, for instance, in case I we can get almost a polarity independent variation with increasing a_λ.

Lastly, Fig.5 shows the rigidity spectra of the first three harmonics obtained in case I for $a_\lambda = 0$. The spectrum of the higher harmonic rises more steeply than that of the lower harmonic, and in the high rigidity region, the spectra of the second and third harmonic are almost proportional, respectively, to R and R^2. This is due to λ linearly increasing with rigidity R(cf. Eq.(7)). Such a rigidity dependence is consistent with the observations(*10*,*11*).

References

1. Munakata,K. and Nagashima,K.(1984)
   Proc. Int. Sympo. on Cosmic Ray Modulation(Morioka), p144.
2. Nagashima,K. et al.(1985)
   paper code SH 4.3-9, in this conference.
3. Tatsuoka,R. and Nagashima,K.(1985)
   paper code SH 4.5-2, in this conference.
4. Thambyahpillai,T. and Elliot,H.(1953)
   Nature,171, p918.
5. Forbush,S.E.(1969)
   J. Geophys. Res., 74, p3451.
6. Mori,S. et al.(1979)
   Proc. 16th Int. Cosmic Ray Conf.(Kyoto), 4, p64.
7. Bieber,J.W. and Pomerantz,M.A.(1983)
   J. Geophys. Res. Lett., 10, p920.
8. Earl,J.A.(1976)
   Astrophys. J., 205, p900.
9. Nagashima,K. et al.(1977)
   Proc. 15th Int. Cosmic Ray Conf.(Plovdiv), 4, p72.
10. Mori,S. et al.(1984)
    Proc. Int. Sympo. on Cosmic Ray Modulation(Morioka), p138.
11. Morishita,I. et al.(1984)
    Proc. Int. Sympo. on Cosmic Ray Modulation(Morioka), p130.

N85-35020
SH 4.5-2

FORMULATION OF COSMIC-RAY SOLAR DAILY VARIATION AND ITS SEASONAL VARIATION, PRODUCED FROM GENERALIZED STATIONARY ANISOTROPY OF SOLAR ORIGIN

R. Tatsuoka and K. Nagashima*

Department of Physics, Nagoya University, Nagoya 464, Japan
*Cosmic Ray Research Laboratory, Nagoya University
Nagoya 464, Japan

1. Introduction. In the previous papers(1-3), we presented a formulation of cosmic-ray daily variations produced from solar anisotropies stationary through a year and also of their annual (or seasonal) modulation caused by the annual variation of the rotation axis of the Earth relative to that of the Sun. These anisotropies are symmetric for an arbitrary rotation around an axis. On the other hand, from observations of the tri-diurnal variation(5), it has been suggested that solar anisotropies also contain some axis-asymmetric term of the third order with respect to the IMF-axis. This suggestion has recently found support in a theoretical study by Munakata and Nagashima(4). According to their results, the terms of axis-asymmetry with respect to IMF-axis appear also in the 2nd order anisotropy, together with some different kinds of axis-symmetric terms.

The contribution of these anisotropies to the daily variation is different from that of those discussed previously. In the present paper, we extend the above mentioned formulation to a case of a generalized anisotropy.

2. Formulation. Following after the formulation by Munakata and Nagashima(4), we express the stationary anisotropy $\eta(r,p)$ through a year in the IMF-polar-coordinate system defined in fig. 1, as

$$\eta(r,p)=\sum_{n=1}^{\infty}\sum_{m=0}^{n}\{\eta_n^{mc}(r,p)\cos m\Phi'+\eta_n^{ms}(r,p)\sin m\Phi'\}P_n^m(\cos\theta'), \tag{1}$$

where $\eta_n^{mc}(r,p)$ and $\eta_n^{ms}(r,p)$ are coefficients, and the angles θ' and Φ' express the incident direction of cosmic rays with momentum p at a point r. $P_n^m(\cos\theta')$ in the equation is the semi-normalized associate Legendre function(6). It is noted that the terms with coefficients $\eta_n^{0c}(r,p)$'s have a symmetry with respect to the IMF-axis, and have been discussed in the previous papers(1-3). In eq.(1), each term with the coefficient η_n^{mc} or η_n^{ms} can be expressed in the equatorial coordinate system, as

$$\begin{cases}\eta_n^{mc}(r,p)P_n^m(\cos\theta')\cos m\Phi'=\sum_{k=0}^{n}P_n^k(\cos\theta)S_n^k(\alpha|n,m,c)\\ \eta_n^{ms}(r,p)P_n^m(\cos\theta')\sin m\Phi'=\sum_{k=0}^{n}P_n^k(\cos\theta)S_n^k(\alpha|n,m,s),\end{cases} \tag{2}$$

where

$$S_n^k(\alpha|n,m,\sigma)=\eta_n^{m\sigma}\{a_n^k(\alpha_S|n,m,\sigma)\cos k(\alpha-\alpha_S+\pi)+b_n^k(\alpha_S|n,m,\sigma)\sin k(\alpha-\alpha_S+\pi)\}, \tag{3}$$

in which the angles α and θ are, respectively, the right-ascension and the co-declination $(\theta=\pi-\delta)$ of the particle's incident direction. α_S in eq.(3) is the right-ascension of the Sun, and $\alpha-\alpha_S+\pi$ is related to solar local time t as $\alpha-\alpha_S+\pi=2\pi(t/24\text{hr})$. Using this relation, the incident direction can be expressed in terms of θ and t instead of θ and α. The coefficients a_n^k and b_n^k in eq.(3) vary with α_S, owing to the seasonal variation of the relative configuration between the equatorial- and IMF-coordinate systems arising from the Earth's revolution around the Sun. Applying the frequency modulation method(2), S_n^k of eq.(3) can be transformed as

$$S_n^k(\alpha|n,m,\sigma)=\sum_{l=-\infty}^{\infty} S_n^k(t_{l/k}|n,m,\sigma) \quad \text{for } \sigma=c \text{ or } s, \text{ and } k\neq 0, \tag{4}$$

where

$$S_n^k(t_{l/k}|n,m,\sigma)=x_n^k(l|n,m,\sigma)\cos(2k\pi t_{l/k}/24\text{hr}) + y_n^k(l|n,m,\sigma)\sin(2k\pi t_{l/k}/24\text{hr}), \tag{5}$$

where

$$\begin{cases} x_n^k(l|n,m,\sigma)=\mathrm{T}_x(k,l|n,m,\sigma)\eta_n^{m\sigma} \\ y_n^k(l|n,m,\sigma)=\mathrm{T}_y(k,l|n,m,\sigma)\eta_n^{m\sigma}, \end{cases} \tag{6}$$

in which T_x and T_y are called the transformation coefficients. In eqs.(4) and (5), $t_{l/k}$ is the time in hours (0~24hr) in a day defined by 1year/$(365+l/k)$ and therefore $P_n^k(\cos\theta)S_n^k(t_{l/k}|n,m,\sigma)$ expresses the k-th harmonic of the daily variation in the time frame of $t_{l/k}$ observed by a vertical telescope pointing toward the θ-direction in the outer space of the Earth.

The terms with $l=0$ are the yearly averaged solar k-th harmonic variations and are expressed by the symbol 'SO', while those for $l\neq 0$ are called the extended sidereal ($l>0$) and anti-sidereal ($l<0$) daily variations(2) and are expressed by the symbol '$SI_{l/k}$' for $l>0$ and '$AS_{|l|/k}$' for $l<0$.

Assuming that the anisotropy is stationary through a year, all the transformation coefficients $\mathrm{T}_x(k,l|n,m,\sigma)$ and $\mathrm{T}_y(k,l|n,m,\sigma)$ in eq.(6) are obtained for $n\leq 3$ and $|l|\leq 3$ and are shown in Tables I, II and III. In the calculations, B, assumed to have Parker's Archimedian spiral structure, is expressed in the heliographic polar co-ordinate system (r, θ_h, φ_h) as

$$\begin{aligned} B_r&=B_0(1\text{a.u.}/r)^2, \\ B_{\theta_h}&=0, \\ B_{\varphi_h}&=-B_0(1\text{a.u.}/r)\sin\theta_h, \end{aligned} \tag{7}$$

where B_0 is positive(negative) for the away (toward) sector. The inclination of the solar equatorial plane with respect to the ecliptic plane is also taken into account in the calculations(3).

3. Discussion and Conclusion. The terms with a mark 'c' in tables express the IMF-sense-*independent* terms, as the corresponding coefficients η_n^{mc}'s in eq.(2) are independent of IMF-sense(4). On the contrary, the terms with a mark 's' express the IMF-sense-*dependent* terms, as η_n^{ms}'s change their sign with the change of IMF-sense.

The No.1 and No.2 terms in Table I produce the solar diurnal variation of north-south symmetric type, whereas the No.3 term produces the IMF-sense-dependent sidereal diurnal variation of Swinson type(7).

The most important term in Table II is that of No.1. It is noteworthy that the No.4 and No.5 terms are IMF-sense-dependent and will be discussed in detail in a separate paper(8).

The importance of the No.1 term in Table II has been well acknowledged for the explanation of the solar tri-diurnal variation from the theoretical point of view, whereas the existence of the No.2 term has recently been pointed out by Munakata and Nagashima(4).

In conclusion, it is emphasized that the transformation coefficients(T_x and T_y) in these tables enable us to connect solar anisotropies produced from the diffusion-convection process with the observed cosmic-ray solar daily variation and its seasonal variation and, as the result, enable us to obtain the information of electromagnetic state in interplanetary space from the observation of solar daily variation of cosmic rays.

References

(1) K. Nagashima: *Rep. Ionos. Space Res.*, Japan, 25, 189 (1971).

(2) K. Nagashima and H. Ueno: *Rep. Ionos. Space Res* , Japan, 25, 212 (1971).

(3) K. Nagashima, R. Tatsuoka and S. Matsuzaki: *Nuovo Cim.*, 6C, 550 (1983).

(4) K. Munakata and K. Nagashima: *Proc. Int. Cosmic Ray Symposium* (Morioka, Japan, 1984), p.144; This Conference SH 4.5-1.

(5) K. Nagashima et al.: *Proc. Int. Conf. Cosmic Rays*, Vol.4 (Plovdiv, 1977), p.72; S. Mori et al.: *Proc. Int. Cosmic Ray Symposium* (Morioka, Japan, 1984), p.138.

(6) S. Chapman and J. Bartels: *Geomagnetism*, Vol.2 (Oxford, 1940), p.611.

(7) D.B. Swinson: *J. Geophys. Res.*, 76, 4217 (1971).

(8) K. Nagashima, K. Munakata and R. Tatsuoka: This Conference SH 4.3-9.

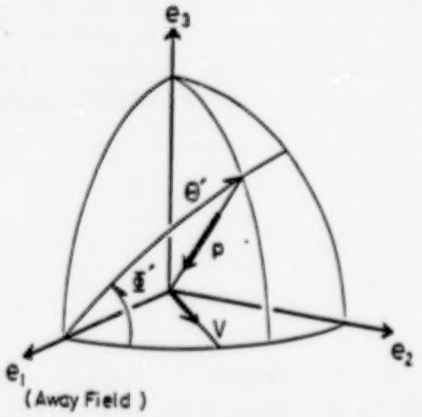

Fig. 1. The IMF-POLAR-COORDINATE SYSTEM.
$\mathbf{p}$: Momentum of particle.
$\mathbf{V}$: Solar wind velocity.
$\mathbf{e}_l$: Unit vector in the direction of 'away' magnetic field.
$\mathbf{e}_3$: Unit vector in the direction of $\mathbf{e}_l \times \mathbf{V}$.
$\mathbf{e}_2 = \mathbf{e}_3 \times \mathbf{e}_l$.

Table I . The transformation coefficients $T_x(k,l|n,m,\sigma)$ and $T_y(k,l|n,m,\sigma)$ in eq.(6) for n=1, in units of 10^{-3}.

No.	$nm\sigma$	k	$l=3$		$l=2$		$l=1$		$l=0$		$l=-1$		$l=-2$		$l=-3$	
			T_x	T_y	T_x	T_y	T_x	T_y	T_x	T_y	T_x	T_y	T_x	T_y	T_x	T_y
1	10c	1			-3,	47			696,	-668			16,	-15		
2	11c	1			32,	-46			660,	671			13,	16		
3	11s	1	-4,	9			62,	-410			-57,	-25			-1,	0

Table I . The transformation coefficients $T_x(k,l|n,m,\sigma)$ and $T_y(k,l|n,m,\sigma)$ in eq.(6) for n=2, in units of 10^{-3}.

No.	nmσ	k	$l = 3$ T_x T_y	$l = 2$ T_x T_y	$l = 1$ T_x T_y	$l = 0$ T_x T_y	$l = -1$ T_x T_y	$l = -2$ T_x T_y	$l = -3$ T_x T_y
1	20c	1	-8, -12		-55, 265		-300, 59		-7, 1
		2		51, 60		34, -804		2, -36	
2	21c	1	-9, 16		57, 1		-15, -395		0, -9
		2		-41, -25		907, 25		40, 4	
3	22c	1	23, -8		-80, 579		266.		6, 1
		2		134, 17		8, 421		-3 17	
4	21s	1		22, 102		591, -553		29, 6	
		2	22, 13		-230, -330		-61, 13		-2, 1
5	22s	1		121, -100		531, 522		-12, 28	
		2	-25, -13		313, -227		-13, -59		-1, -2

Table II . The transformation coefficients $T_x(k,l|n,m,\sigma)$ and $T_y(k,l|n,m,\sigma)$ in eq.(6) for n=3, in units of 10^{-3}.

No.	nmσ	k	$l = 3$ T_x T_y	$l = 2$ T_x T_y	$l = 1$ T_x T_y	$l = 0$ T_x T_y	$l = -1$ T_x T_y	$l = -2$ T_x T_y	$l = -3$ T_x T_y
1	30c	1		-35, -110		-291, 274		82, 46	
		2	-30, -7		167, 247		-186, 276		-9, 12
		3		103, 10		-466, -532		-31, -36	
2	31c	1		-61, 40		-127, -101		-70, 122	
		2	10, 15		-60, 46		-343, -267		-14, -13
		3		-47, 51		627, -568		44, -36	
3	32c	1		-42, -132		-342, 293		-117, -75	
		2	-38, -15		268, 390		238, -228		12, -9
		3		104, -96		353, 350		19, 25	
4	33c	1		-223, 161		-342, -314		59, -74	
		2	52, 53		-410, 306		102, 139		3, 7
		3		84, 128		-113, 140		-9, 5	
5	31s	1	-19, -28		-83, 449		-373, 75		-9, -7
		2		137, 85		42, -563		28, -22	
		3	39, -15		-368, -77		-41, 46		-1, 3
6	32s	1	-25, 47		75, 11		-60, -537		12, -12
		2		-30, -57		655, 14		23, 38	
		3	-21, 28		84, -451		-57, -49		-4, -2
7	33s	1	63, 0		-83, 639		389, -8		8, 11
		2		258, 48		27, 345		-25, 9	
		3	2, -51		261, 38		27, -34		1, -2

N85-35021

SH 4.5-3

SOLAR TRI-DIURNAL VARIATION OF COSMIC RAYS IN A WIDE RANGE OF RIGIDITY

Mori, S., H. Ueno*, Z. Fujii*, I. Morishita** and K. Nagashima*

Department of Physics, Shinshu University, Matsumoto 390, Japan
*Cosmic-Ray Research Lab., Nagoya University, Nagoya 464, Japan
**Department of Physics, Asahi University, Hozumi-cho, Gifu 501-02, Japan

ABSTRACT

Solar tri-diurnal variations of cosmic rays have been analyzed in a wide range of rigidity, using data from neutron monitors, and the surface and underground muon telescopes for the period 1978-1983. The rigidity spectrum of the anisotropy in space is assumed to be of power-exponential type as $(P/\gamma P_0)^{\gamma}\exp(\gamma-P/P_0)$. By means of the best-fit method between the observed and the expected variations, it is obtained that the spectrum has a peak at $P\ (=\gamma P_0)\cong 90$ GV, where $\gamma\cong 3.0$ and $P_0\cong 30$ GV. The phase in space of the tri-diurnal variation is also obtained as 7.0 hr (15 hr and 23 hr LT), which is quite different from that of ∿1 hr, arising from the axis-symmetric distribution of cosmic rays with respect to the IMF.

1. Introduction

Studies of higher harmonics in the daily variation of cosmic rays provide valuable infromations as to the nature of the cosmic ray modulation in the heliosphere. So far a great many investigation has been performed of the solar tri-diurnal variation, and some of its characteristic natures have been revealed; its extra-terrestrial origin and also its rising spectrum with rigidity (e.g., Bieber et al., 1983; Mori et al., 1984; hereafter referred to as Paper I).

These results, however, have not yet been firmly founded because of the statistical uncertainty of the data used which is largely due to limited rigidity range. In particular, there is a wide divergence of opinion as to the direction of the anisotropy; some analyses reported ∿1 hr direction, while some obtained ∿7 hr direction. This discrepancy is crucial for determining the modulation mechanism; 1 hr direction is in favor of the 'loss-cone' model (Fujii, 1971) or the model of Bieber et al. (1983), whereas 7 hr direction requires other kind of model such as the one presented by Munakata and Nagashima (1985, in this issue).

In the present analysis, we try to obtain a definite form of the anisotropy responsible for the averaged tri-diurnal variations over 6 years (1978-1985), using data in a wide range of rigidity from neutron monitors to underground muon telescopes, which respond to the effective rigidity of 10 to 600 GV.

2. Analysis of Data

The present experimental data include 2 to 6-year averages of neutron monitor data in a worldwide network (36 stations from the polar to the equatorial regions) and 6-year averages of the surface (NAGOYA) and underground (MISATO and SAKASHITA) muon telescopes for the period 1978-1983.

Fig. 1 illustrates the summation harmonic dial, showing clearly the persistency of year-to-year changes of the observed tri-diurnal variations of three muon telescopes at NAGOYA (surface) for 1971-1983, at MISATO (34 m.w.e. in depth underground) for 1974-1983 and at SAKASHITA (80 m.w.e. in depth underground) for 1978-1983. In the present analysis, 6-year averages over 1978-1983 were used; of 13 directional components at NAGOYA, 9 components at MISATO and 10 components at SAKASHITA, and these are listed in Paper I.

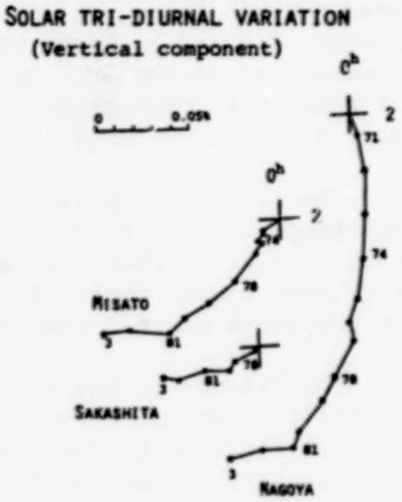

Fig. 1 Observed solar tri-diurnal variations of V-component at NAGOYA, MISATO and SAKASHITA in summation dial.

In order to derive the 3rd order anisotropy, the tri-diurnal variation produced by the anisotropy with a certain form of the rigidity spectrum G(P), will be compared with the observed results. In the anaysis, G(P) is assumed to be of power-exponential type as

$$G(P)=(P/\gamma P_0)^{\gamma}\exp(\gamma-P/P_0) \quad (1)$$

Evidently, G(P) becomes maximum at $P=\gamma P_0$ for $\gamma>0$, and is normalized to unity.

The expected 3rd harmonic components (A_{ij}, B_{ij}) for j-th components telescopes of i-th station including neutron monitor station, are related to the space harmonic components (X, Y) by the following equations with coupling coefficients c_{ij} and s_{ij} as

$$A_{ij} = (c_{ij}X + s_{ij}Y), \qquad B_{ij} = (-s_{ij}X + c_{ij}Y) \quad (2)$$

The coefficients c_{ij} and s_{ij} were derived from the differential coupling coefficients dc_{ij} and ds_{ij} given by Fujimoto et al. (1984). The best-fit parameters satisfying the following equation are determined.

$$\sum_{ij} w_{ij}\{ (A_{ij} - a_{ij})^2 + (B_{ij} - b_{ij})^2 \}= \text{minimum} = \delta^2 \quad (3)$$

In Eq. (3), the weight w_{ij} is given for the observed a_{ij} and b_{ij} so as to balance the difference in the number of the data used in the rigidity interval; 6 divisions in all the ranges of 10 to 600 GV to have equal weight. Also each vector in all the muon components was subtracted from the reference component to eliminate the atmospheric temperatute effect; in this analysis, V-component for NAGOYA and MISATO and SE-component for SAKASHITA were taken as the reference.

3. Results and Discussions

The contour map of equal δ^2's obtained from the residual sum of the observed vectors and the expected vectors computed by Eq. (2), is shown against γ and P_0 in Fig. 2. As is seen in the figure, minimal δ^2 region locates in relatively narrow regions of γ and P_0-value. It is noted that in these regions the product of γ and P_0 keeps almost invariant as $\gamma P_0 \cong 90$ GV. The best-fit parameters were obtained as that $\gamma \cong 3.0$ and $P_0 \cong 30$ GV.

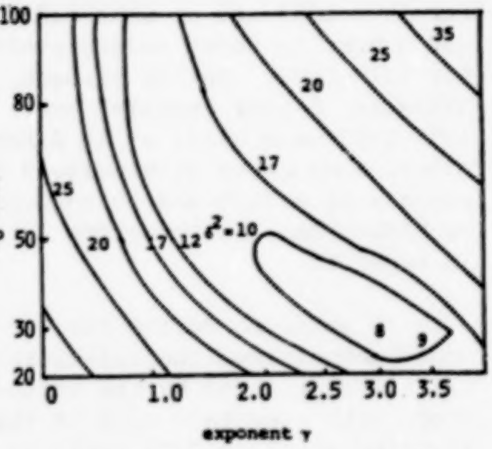

Fig. 2 Contour map of equal δ^2 plotted against $\gamma_2$and P , showing minimal δ^2 ($\cong$8) for $\gamma \cong 3.0$ and $P_0 \cong 30$ GV.

The direction (phase) of the anisotropy was obatined as 7.0 hr. It is also noted that this direction shows almost constant value for the above minimal region.

The fitness of the reproduced variations computed by Eq. (2) in the best-fit case to the observed ones is shown in Fig. 3; (a) for NAGOYA, (b) for MISATO and (c) for SAKASHITA, respectively. The observed vectors are shown with the solid circles (●) and the reproduced ones with the open circles (○). Also the reference component mentioned above is shown by the symbol (⊙) and the origin of the diagram in the best-fit case is given by the cross (✖). A fairly good agreement can be seen between two patterns drawn by connecting each observed point (solid line) and each reproduced point (dotted line) for each station.

The present anaysis can obtain a definite parameter set as; $\gamma \cong 3.0$ and $P_0 \cong 30$ GV. As shown in Paper I, where only muon data at the above three stations (NAGOYA, MISATO and SAKASHITA) were used, parameter set (γ,P_0) rather spereads as; γ=2∿12 and P_0=50∿8 GV. The present form can be derived by adding neutron monitor data to Paper I. Note that the observed vectors of neutron monitors from 36 stations are so divergent even if in the best-fit case, which may be largely due to inaccurate barometric correction in the data.

On the other hand, the direction (phase) of the anisotropy in space was obtained as ∿7 hr (∿15 hr and ∿23 hr LT). So far there has been a wide divergence of opinion as to the direction; ∿1 hr direction was reported by the analyses of neutron monitor data alone, while ∿7 hr direction was reported by using muon data. The former is in favor of the 'loss-cone' model (Fujii, 1971) or the model of Bieber et al. (1983), arising from the axis-symmetric distribution of cosmic rays with respect to the IMF. On the other hand, the latter requires other kind of model such as the one preseneted by Munakata and Nagashima (1985, in this issue). The present result provides a firm basis for the latter model.

A further analysis would be necessary to derive the detailed form and its year-to-year variation.

N85-35022

ORIGINAL PAGE IS
OF POOR QUALITY

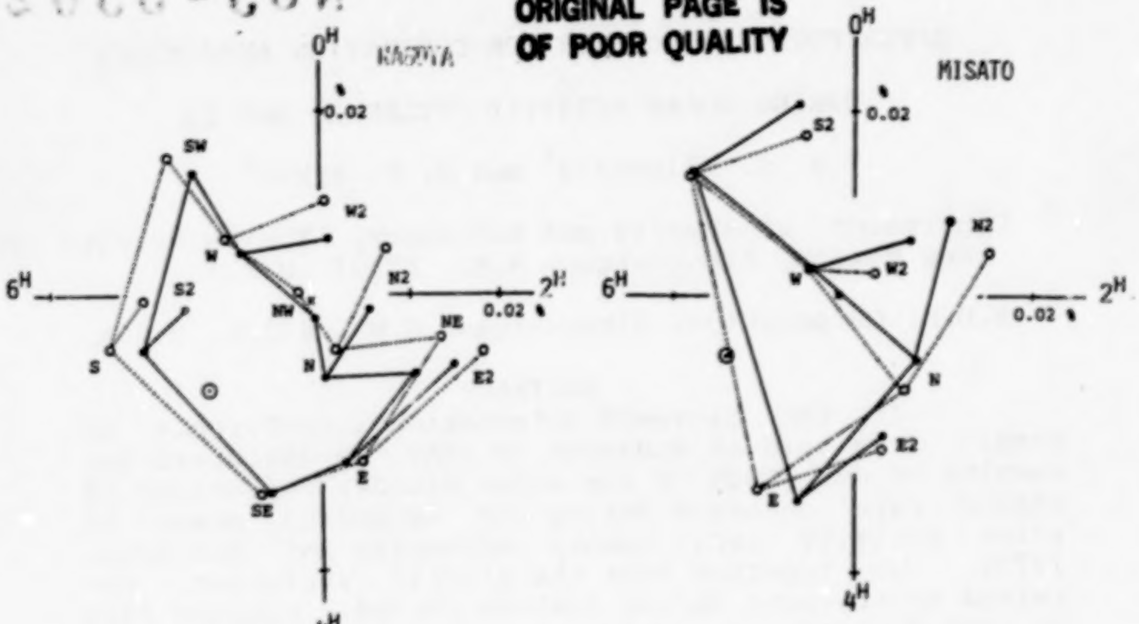

(a) for NAGOYA

(b) for MISATO

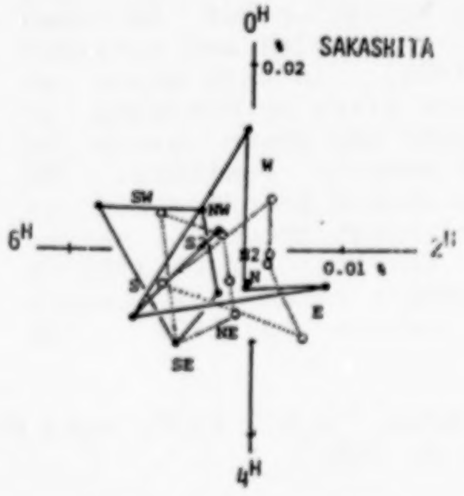

(c) for SAKASHITA

Fig. 3 Fitness between the observed (●) and the reproduced (○) variations; (a) for NAGOYA, (b) for MISATO and (c) fro SAKASHITA for the period 1978-1983.

4. Acknowledgements

The authors express their appreciation to Messrs. K. Chino and S. Nakamura for their computational help. Neutron monitor data were obtained through WDC-C2, whom we acknowledge much.

References

Bieber, J.W. et al., (1983), 18th ICRC (Bangalore), 3, 289.
Fujii, Z., (1971), Rep. Ionos. Space Res., Japan, 25, 242.
Fujimoto, K. et al., (1984), Rep. of CR-Lab,, Nagoya Univ., No. 9.
Mori, S. et al., (1984), Int. CR-Symp. (Morioka), p138.
Munakata, K. and K. Nagashima, (1985), in this issue (SH 4.5-1).

N85-35022

UPPER CUT-OFF RIGIDITY FOR COROTATION ANISOTROPY DURING SOLAR ACTIVITY CYCLES 20 AND 21

H. S. Ahluwalia[1] and J. F. Riker[2]

[1] Department of Physics and Astronomy, The University of New Mexico, Albuquerque, N.M. 87131, U.S.A.

[2] B.D.M. Corporation, Albuquerque, N.M., 87106, U.S.A.

ABSTRACT

At the Eleventh International Conference on Cosmic Rays held at Budapest in 1969, we discussed the results of our study of the solar diurnal variations of cosmic rays observed during the ascending phase of solar activity cycle twenty (Ahluwalia and Ericksen, 1970). We reported that the diurnal variation, observed underground during 1965-68 period, results from an extra-terrestrial anisotropy having a continuously increasing upper cut-off rigidity R_c. However, the coupling functions applicable to underground telescopes were controversial then. This situation has improved now. So we have re-examined those results and extended them to cover the period 1965-78. In this study we have used the coupling functions given by Murakami et al. (1979) for underground muons and those given by Lockwood and Weber (1967) for neutron monitors. We show that a great deal of care should be exercised in calculating the value of R_c. Although numerical values of R_c are a little different, the trend for 1965-68 period remains unchanged. Highest value of R_c occurs in 1970 and the lowest value occurs in 1976. Our results are discussed.

Ahluwalia, H.S., and Ericksen, J.H., 1970, Acta Phys. Acad. Scient. Hung., 29, Suppl. 2, 139.

Murakami, K., Nagashima, K., Sagisaka, K., Mishima, Y., and Inoue, A., 1979, Nuovo Com., 2C,635.

Lockwood, J.A., and Weber, W. R., 1967, J. Geophys. Res., 72, 3395.

N85-35023

22-YEAR CYCLE OF THE UPPER LIMITING RIGIDITY OF DALY WAVES

G. Erdős, J. Kóta and E. Merényi

Central Research Institute for Physics, Budapest, Hungary

Abstract. The method of calculating energy losses along regular particle trajectories is applied to obtain the predicted cosmic ray anisotropies from 200 to 500 GV. The tilt angle of the interplanetary neutral sheet varies to simulate a 22-year cycle magnetic cycle. The calculated values of solar diurnal and semidiurnal, and siderial diurnal intensity waves are compared with observations.

1. Introduction. Earlier we suggested (Erdős and Kóta 1979, 1980) that the cosmic ray anisotropies observed at underground energies can be interpreted in terms of regular particle motion in the Interplanetary Magnetic Field (IMF) incorporating a wavy neutral sheet. At high rigidities, the effects of small-scale irregularities should be negligible and, being the dominant large-scale feature of the IMF, the wavy neutral sheet plays the decisive role.

In this paper we investigate how cosmic ray anisotropies change during a 22-year magnetic cycle. We consider the 200 - 500 GV range which represents the high rigidity tail of the modulation spectrum. The state of the heliosphere changes in a complex way during a solar cycle. From this complexity, the only feature we consider here is the variation of the inclination of the tilted heliospheric neutral sheet. The tilt angle is minimal around solar minimum and increases with increasing solar activity (Thomas and Smith 1981). As a crude approximation, we simulate the 22-year cycle by simply changing the tilt angle.

2. The Model. The IMF model and the method of calculation are described in detail elsewhere (Erdős and Kóta 1979, 1980, 1981). Briefly, a conventional Parker spiral field is applied with a 5 gamma field strength at the earth. The wavy neutral sheet dividing the opposite polarities is given by

$$\sin\theta = \sin\alpha \cdot \cos(\varphi + r) \qquad (1)$$

where θ and φ are heliographic latitude and longitude, respectively, r is heliocentric distance in units of AU. The tilt angle, α, gives the maximum latitudinal excursion of the neutral sheet. The configuration of away polarity above the sheet and toward polarity below the sheet will be referred to as $A > 0$.

We note that equation (1) does not exactly correspond to a tilted plane at the sun. Calculations were also carried out for a tilted plane of 90° inclination. This case of indefinite A, where the two configurations merge, will be labelled with 90^*.

The theoretical results to be presented always give the full free-space anisotropy that would be observed by an equatorial observer in the absence of geomagnetic deflection. Calculations do not include the Compton-Getting effect due to the orbital motion of the earth.

3. Results. In this paragraph we briefly report on the daily intensity waves predicted for 200, 300 and 500 GV at various values of the tilt angle, α.

The harmonic dial of the *solar daily* variation calculated for 200 GV is shown in Figure 1. For comparision, Figure 2 (taken from Benkő et. al., 1984) shows the year-to-year daily vectors observed by the Budapest underground telescopes (median energy: 180 GeV) in the period of 1976 ($A>0$, low solar activity) to 1983 ($A<0$). We find a remarkable agreement if correction is made to the 1.5 hr geomagnetic deflection, the Compton-Getting effect due to the earth's orbital motion, and the $\cos 47° \approx 0.68$ attenuation factor due to the 47° N geografical latitude of the station.

The amplitudes of the solar daily waves calculated for 200, 300 and 500 GV are shown in Figure 3.

The predicted harmonic dial of the *semidiurnal* variation of 200 GV cosmic rays is shown in Figure 4, while the calculated amplitudes are given in Figure 5. A charge asymmetry can clearly be seen: for $A > 0$, an earlier phase and a smaller amplitude is to be expected. These findings are in general agreement with numerous observations (see. for example, Morishita et. al., 1984).

As expected, the phase of the *sidereal daily wave* was always found to be close to either 6 hr or 8 hr, depending on the polarity of the magnetic sector. Figure 6 gives the calculated sidereal amplitudes. Our theoretical results suggest a hard energy spectrum; the spectrum of the sidereal variation turns out markedly harder than the solar diurnal and semidiurnal spectra. This finding also suggests that a sidereal variation of solar origin may still be present at rigidities where solar diurnal and semidiurnal waves already diminish. Thus, in searching for a genuine galactic anisotropy of cosmic rays one should be cautious in establishing the upper rigidity limit of the heliospheric effects.

References:

Benkő, G., Kecskeméty, K., Kóta. J., Somogyi, A., Varga, A., 1984: Proc. Int. Symp. on CR Modulation, Morioka, p104

Erdős, G. and Kóta. J., 1979: Proc. 16th ICRC, Kyoto. 4, 45

Erdős, G. and Kóta, J., 1980: Astrophys. Space Sci., 67, 45

Erdős, G. and Kóta. J., 1981: Proc. 17th ICRC, Paris, 10, 105

Morishita, I., Ueno, H., Fujii, Z., Mori, S. and Nagashima, K., 1984: Proc. Int. Symp. on CR Modulation, Morioka, Japan, p130.

Thomas, B. T. and Smith, E. J., 1981: J. Geophys. Res., 86, 11105

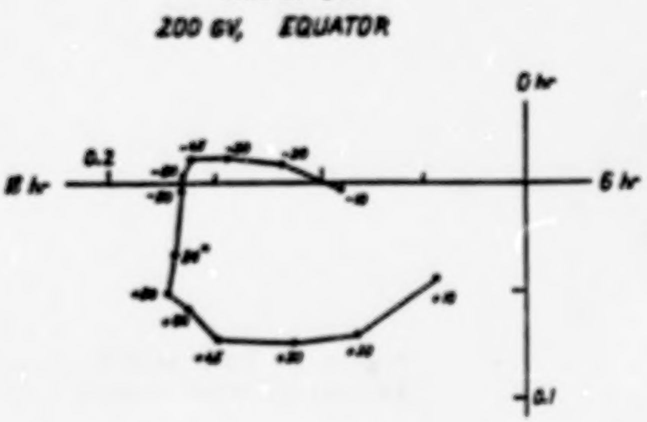

Figure 1. Calculated harmonic dial of the solar daily waves of 200 GV cosmic rays. Numbers stand for the tilt angle, α, in degrees (negative values refer to A < 0).

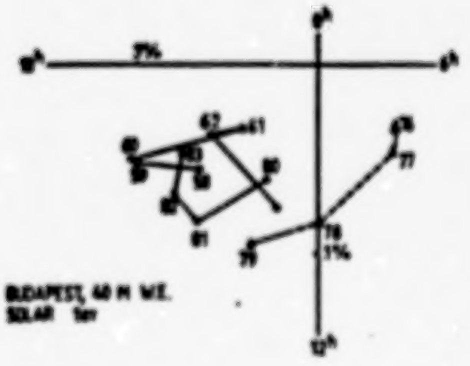

Figure 2. The Budapest solar daily vectors without geomagnetic correction. Numbers stand for the year of observation. Results are grouped according to the polarity state (triangles and dashed lines refer to A > 0).

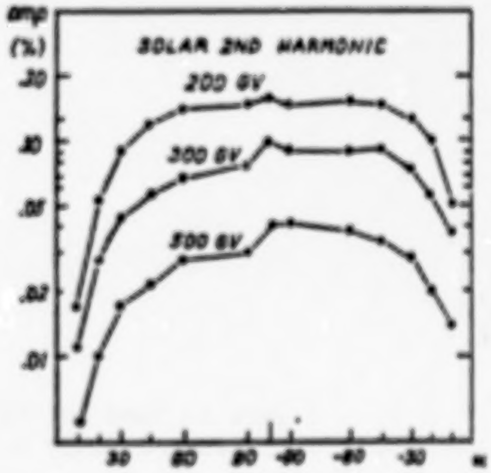

Figure 3. Calculated amplitudes of the solar daily vectors of 200, 300 and 500 GV cosmic rays vs the tilt angle, α, in degrees. (Negative values of α refer to A < 0.)

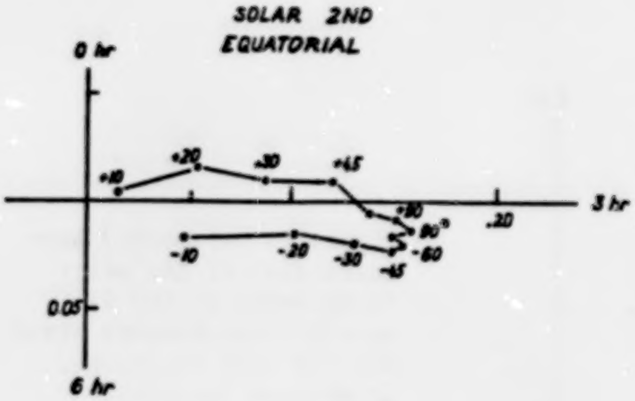

Figure 4. Same as Fig. 1., for semidiurnal vectors.

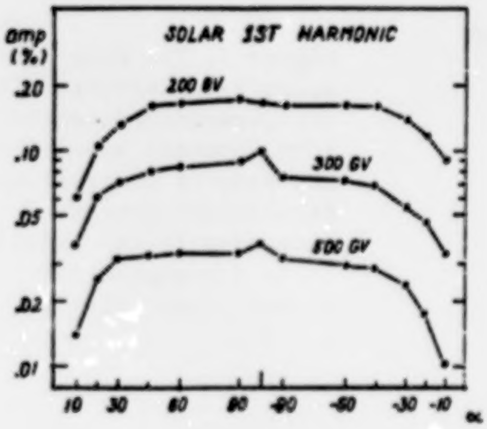

Figure 5. Same as Fig. 3., for semidiurnal vectors.

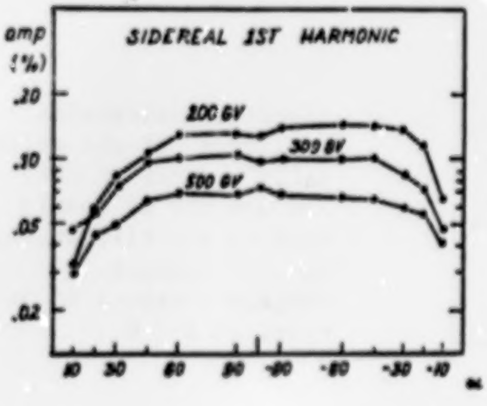

Figure 6. Same as Fig. 3., for sidereal daily vectors.

SH 4.5-6

N85-35024

SOLAR WIND VELOCITY AND DAILY VARIATION OF COSMIC RAYS

H. S. Ahluwalia[1] and J. F. Riker[2]

[1] Department of Physics and Astronomy, The University of New Mexico, Albuquerque, N.M., 87131, U.S.A.

[2] B. D. M. Corporation, Albuquerque, N.M. 87106, U.S.A.

ABSTRACT

Recently parameters applicable to the solar wind and the interplanetary magnetic field (IMF) have become much better defined (King, 1981). Superior quality of data bases that are now available, particularly for post-1971 period, make it possible to believe the long-term trends in the data. These data are correlated with the secular changes observed in the diurnal variation parameters obtained from neutron monitor data at Deep River and underground muon telescope data at Embudo (30 MWE) and Socorro (82 MWE). The annual mean amplitudes appear to have large values during the epochs of high speed solar wind streams. Our results are discussed.

King, J. H., 1981. J. Geophys. Res., 86, 4828.

DIURNAL ANISOTROPY DURING SOLAR ACTIVITY CYCLE TWENTY AND DIFFUSION-CONVECTION MODEL

H. S. Ahluwalia and J. F. Riker

Department of Physics and Astronomy, The University of New Mexico, Albuquerque, N.M., 87131, U.S.A.

ABSTRACT

Underground muon telescope data obtained at Embudo and Neutron monitor data obtained at Deep River are divided into two sets; one covers the ascending phase of the cycle (1965-70) and the other covers the descending phase (1971-76). The amplitude of diurnal anisotropy calculated from the data does not agree with the value predicted by the simplified version of the Diffusion-Convection Model (DCM); the discrepancy is worse for neutron data.

INTRODUCTION. We report here an extension of our earlier study (Ahluwalia and Ericksen, 1970, 1971). Coupling functions (W) given by Murakami et al. (1979) and those given by Lockwood and Weber (1967) are used to calculate the amplitude of diurnal anisotropy. Median rigidity of response (R_m) ~ 16 GV for Deep River neutrons and ~ 134 GV for Embudo muons. Unlike Subramanian (1971) we are not able to reconcile our calculations with the predictions of the simplified version of Diffusion-Convection Model (Forman and Gleeson, 1975).

DATA. Figure 1 summarizes the available data on the annual mean amplitudes of the diurnal variation observed at Embudo (open circles) for the period 1965-79 and at Deep River (solid dots) for the period 1962-79. The flags indicate the standard deviation, computed from the observed scatter in the data for a given year. Zurich sunspot numbers (R_z) indicate the level of solar activity. Epoch of solar polar field reversal is also shown; after 1970 the solar polar field is directed out of the sun in the northern hemisphere. In

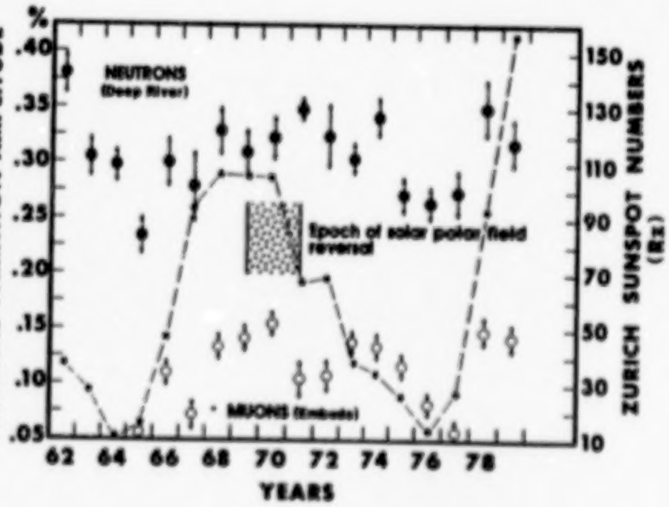

Fig 1

general the amplitudes have the lowest values during activity minima and large values during activity maximum. In particular, we wish to point out that the amplitudes at Embudo have large values for the years 1973, 1974 and 1975 during which the mean level of the solar activity is only about one third of the maximum value in 1968. Bulk velocity (V) of solar wind is high during these years.

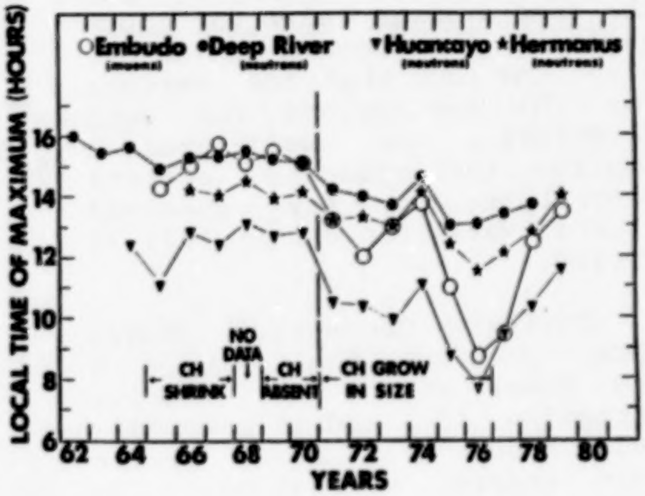

FIG 2

Another important feature of the dependence of the diurnal variation on the solar activity is shown in Figure 2. It gives the annual mean time of maximum of the diurnal variation observed at Embudo, Deep River, Hermanus (R_m=20 GV) and Huancayo (R_m=30 GV). The data exhibit a remarkable, worldwide, systematic, rigidity-dependent shift of the time of maximum of diurnal variation to early hours, during the period 1971-76. The data for Huancayo and Hermanus are staggered in time, with respect to Deep River, to minimize an overlap. The rigidity dependent nature of this effect was emphasized by us elsewhere (Ahluwalia, 1976). Note that prior to 1971 the observed time of maximum at Embudo is nearly steady at about 15 hours (LT) but in 1976 the time of maximum is at 8.7 hours (LT). The diurnal times of maximum return to pre-1971 values by about 1979, at all stations. Agrawal (1983) has reported similar behavior for neutron and surface-level muon detectors at sites in Canada. Also summarized in Figure 2 is the information about the size of the coronal holes during solar activity cycle (SAC) 20.

ANALYSIS. We subdivide the data into two sets; one set covers the period 1965-70 and the other set covers the period 1971-76. The reader is reminded that the observed diurnal variation is rather steady, on a year to year basis, during the first period and undergoes a remarkable systemmatic change during the second period. The characteristics of the annual mean diurnal variation observed at Embudo and at Deep River for the two periods are displayed in Fig. 3 on the harmonic dial. The error circles are for 2σ. One can see that the amplitudes for the two periods remain the same for both Embudo muons and Deep River neutrons. However, the time of maximum is significantly early for both detectors, for the second period (1971-76). The fact that the amplitudes are the same for muons as well as neutrons, implies that upper cut-off rigidity R_c has the same average value for both periods; in fact $R_c \sim 70$ GV. Also the fact that the vectors for the two periods, for both detectors, are well-resolved implies that some new effects contribute to the observed diurnal variation during 1971-76 period.

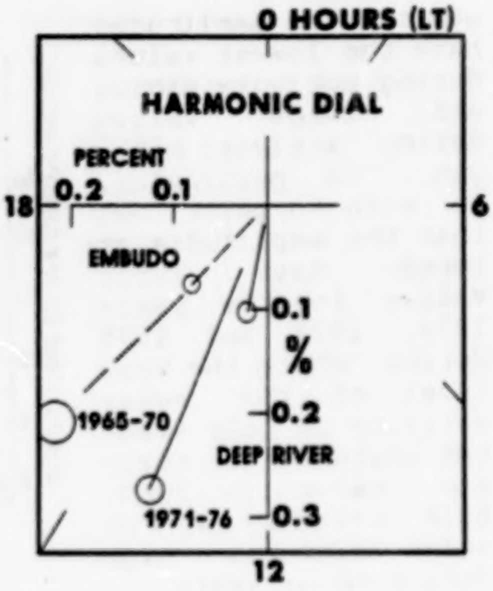

Fig 3

Diffusion-Convection Model (DCM) predicts that if $K_\perp = 0$ and there is no net radial streaming (S_r) and if perpendicular gradient is zero, cosmic rays undergo corotation. In this case the anisotropy (δ) recorded by a detector with a mean asymptotic latitude λ of viewing is given by

$$\delta = 0.6 \text{ Cos } \lambda, \%$$

So we expect that δ should be independent of solar wind bulk velocity (V). An obvious limitation of the model is that it does not contain the concept of R_c. Somehow the diffusion coefficients $K_{||}$, $K_\perp$ must depend upon primary rigidity (R) in such a way as to lend some physical significance to the concept of R_c. The theory in its present state is obscure on this point. Let us assume that,

$$\delta_{theo} = \begin{cases} 0.6 \cos \lambda \ \%, & \text{if } R<R_c \\ 0.0, & \text{if } R>R_c \end{cases}$$

This form of variational spectrum is consistent with the results obtained in our analyses earlier, for the first period (1965-70). Table 1 gives a summary of results for the two detectors, for the three periods, assuming R_c=70 GV. The direction of anisotropy in free space is calculated after applying corrections for the "orbital-effect" and for the "geomagnetic bending" of the primaries. These corrections are model independent.

RESULTS. (1) Diurnal Anisotropy in free-space is in the direction of 18 hours (LT) for the first (1965-70) and third periods (1965-76), but the direction is significantly earlier for the second period (1971-76).

(2) Within errors of observations the amplitudes of diurnal variations for the two detectors, for the three periods, are the same. The amplitude of the anisotropy, calculated from the data for the two detectors, is tabulated in the last column of Table 1. The calculated value is about 33% less for neutrons and about 8% less for muons when compared to the theoretical value. So our results do not

TABLE 1

Station	λ	$\int_{R_o}^{R_c} W dR$	Free Space Direction of Diurnal Anisotropy			δ calc
	deg	%	hours (LT) 1965-70	1971-76	1965-76	%
Deep River	11.8	0.78	18.21 ± 0.12	16.87 ± 0.12	17.54 ± 0.12	0.43 ± 0.01
Embudo	19.1	0.28	17.83 ± 0.11	16.87 ± 0.11	17.74 ± 0.11	0.55 ± 0.02

agree with the predictions of the simplified DCM, for SAC 20. However in practice we may not have $K_\perp = 0$. Also $K_\perp$ may be inversely proportional to the square of the particle rigidity (Jokipii, 1971). If we follow Jokipii's suggestion and take $(K_\perp/K_{||}) \approx 0.15$ and further note that median primary rigidity of response for muons is about a factor of eight larger than for neutrons, the calculated values agree much better with the theoretical value. But this does not explain why the direction of anisotropy is significantly earlier in the second period (1971-76). Also it is hard to believe that the ratio $K_\perp/K_{||}$ is invariant in time.

(3) In recent years Jokipii has emphasized very strongly that drifts should play an important role in the modulation of cosmic rays (Kota and Jokipii, 1983 and references therein). It would be interesting to see if one obtains a better agreement between theory and observations by invoking charged particle drifts.

REFERENCES.

Agrawal, S. P., 1983. Space Sci. Rev., 34, 127.
Ahluwalia, H. S. and Ericksen, J. H., 1970. Acta. Phys. Acad. Scient. Hung., 29, Suppl. 2, 139.
Ahluwalia, H. S., and Ericksen, J. H., 1971. J. Geophys. Res., 76, 6613.
Ahluwalia, H. S., 1976. Proc. Intern. Cosmic Ray Symp. on High Energy Cosmic Ray Modulation, Tokyo, p. 260.
Forman, M. A., and Gleeson, L. J., 1975. Astrophys. Space Sci., 32, 77.
Jokipii, J. R., 1971. Rev. Geophys. Space Phys., 9, 27.
Kota, J., and Jokipii, J. R., 1983. Astrophys. J., 265, 573.
Lockwood, J. A., and Weber, W. R., 1967. J. Geophys. Res., 72, 3395.
Murakami, K., Nagashima, K., Sagisaka, K., Mishima, Y., and Inoue, A., 1979, Nuova Cim. 2C(5), 635.
Subramanian, G., 1971. J. Geophys. Res., 76, 1093.

SH 4.5-8

DIURNAL EFFECT IN COSMIC RAYS AT MIDDLE LATITUDES ACCORDING TO STRATOSPHERIC MEASUREMENTS

N85-35026

Asatryan G.A., Babayan V.Kh.
Yerevan Physics Institute, Markarian st.2
375036, Yerevan, Armenia, USSR

Stozhkov Yu.I.
P.N. Lebedev Physical Institute of the Academy
of Sciences of the USSR, Leninsky prospect,53,
117924, Moscow, USSR

ABSTRACT

Results of measurements of the diurnal wave of the cosmic ray (CR) intensity in stratosphere at the latitude with the geomagnetic cutoff rigidity $R_c = 7.6$ GV are presented.

Measurements of diurnal variation of the CR intensity were carried by means of radiosondes - by a detector composed of a gas-discharge counter CTC-6 and a telescope containing two counters with a 7 mm aluminium filter between them. Radiosondes were launched in Yerevan daily during a month (May 23 to June 23, 1984) at the following hours: 2,5,8,11,14,17,20,23 LT. The period of time during which the measurements were carried out is characterized by a quiet situation: the average three-hourly value $K_p < 3$ [1]. The CR intensity fluctuations in the absorption curve maximum in stratosphere did not exceed ~2.5%

at high altitudes ($R_c = 0.5$ GV) and $\sim 1\%$ at the latitude with $R_c = 2.5$ GV.

Experimental data allowed to obtain the altitude dependence of the CR intensity on the atmospheric depth, $N(x)$, for eight different times of LT. To reveal the diurnal wave of the CR intensity in stratosphere, we have used the following method of processing of altitude dependences for a vertical CR flux. Three pressure intervals $X = 8 \div 50$, $50 \div 100$ and $100 \div 150$ g/cm^2 were analyzed, each of which was in its turn divided into several subintervals. Then the mean for the daily CR intensity for each interval, $\overline{N}(x)$, was found. After that the value $\delta = \frac{N_i(x) - \overline{N}(x)}{\overline{N}(x)}$, %, was defined, where i is the time of measurements. To improve the accuracy, values of δ were averaged for each interval. Mean values of $\overline{\delta}$ are presented in figs. 1a,b,c for the above three pressure intervals. A diurnal wave is observed with the amplitude which decreases from $\sim 4\%$ to $\sim 2\%$ with the increase in the atmosphere pressure from ~ 30 g/cm^2 to ~ 130 g/cm^2. The time of maximum is $11^h \div 14^h$ LT. These results agree with measurements of the diurnal wave in stratosphere carried out in 1981 [2]. The daily wave of the CR intensity on the neutron monitor in Tbilisi ($R_c = 7.4$ GV) is presented in fig. 1d for the same period of the time (23 May ÷ 23 June 1984).

The dependence of the diurnal wave amplitude on the atmospheric depth X is shown in fig.2. A substantial decrease in the value of $\overline{\delta}$ is observed with the increase in the atmospheric depth.

Certain difficulties arise in trying to give a correct explanation of a large amplitude of the CR intensity diurnal amplitude in stratosphere (~ 4%) and of the early time of maximum ($11^{h} \div 14^{h}$ LT). The presence of such a large anisotropy of CR in stratosphere may be connected to the anisotropic pitch-angular distribution of particles in the interplanetary space and possible to the large contribution of nuclei of galactic cosmic rays in the diurnal wave. It is difficult to explain the obtained results by the temperature effect in cosmic rays or by the drift radiosondes during the flight and appropriate variations of the value of R_c.

References:

1. Solar Geophysical Data.(1984), № 479, part 1, p.91, № 480, part 1, p.86, Boulder, USA.
2. G.A. Asatryan, Yu.I. Stozhkov, (1983), 18-th ICRC, Bangalore, India, v.3, p.299.

ORIGINAL PAGE IS
OF POOR QUALITY

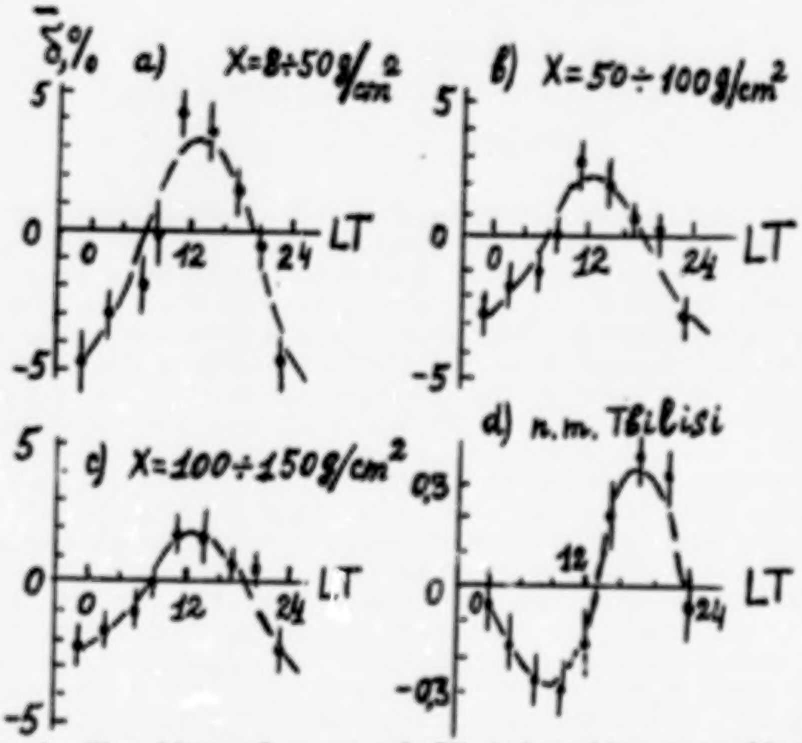

Fig.1. The diurnal wave of CR intensity according to the measurements in 23 May ÷ 23 June 1984 in the stratosphere (Yerevan, R_c=7,6 GV) at the atmospheric pressure X=8÷50 g/cm (a), X=50÷100 g/cm (b), X=100÷150 g/cm (c) and on the neutron monitor Tbilisi, R_k=7,4 GV (d).

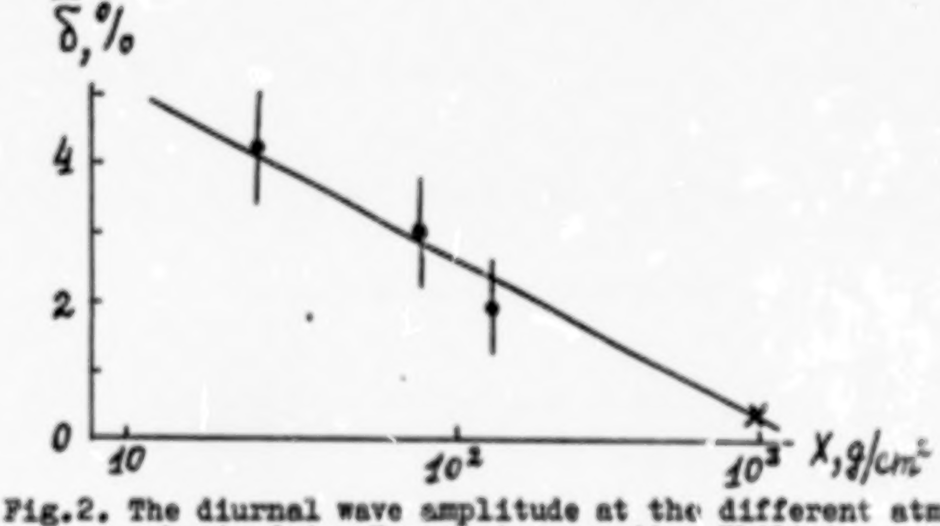

Fig.2. The diurnal wave amplitude at the different atmospheric data; X - neutron monitor Tbilisi,
• - stratospheric data.

N85-35027
SH 4.5-9

COMPARATIVE STUDY OF THE PHASE OF DIURNAL ANISOTROPY ON QUIET AND DISTURBED DAYS ON A LONG TERM BASIS UPTO RECENT PERIOD

Santosh Kumar
Rani Durgavati University,Jabalpur.India.

ABSTRACT

The data from the world-wide grid of neutron monitoring stations have been analysed for a comparative study of the phase of diurnal anisotropy on quiet and disturbed days on a long term basis upto recent period. It has been observed that the phase of the diurnal anisotropy on disturbed days where the value of the Ap-index is higher, is found to shift towards earlier hours in comparison to the phase of the diurnal anisotropy on quiet days where the value of Ap-index is lower on all the stations from 1965 to 71. Such a trend is not observable for the later period. This affect is found to be more pronounced on equatorial stations, in particular, in comparison to high latitude stations. It has been derived from these observational facts that the relationship between Ap-index and the phase of the diurnal anisotropy is not invariant throughout the period of consideration. Furthermore, the exact cause of such a drastic change is not known, but it demonstrates very clearly that the interplanetary conditions which are responsible for both, diurnal anisotropy of cosmic ray intensity and the geomagnetic Ap-index variation, have drastically changed during the period 1971 and onwards.

Key words: Ap-index, latitude, phase

☐ Theoretical ☐ Observational ☒ Both

Paper to be presented by : Dr.Santosh Kumar

Name and address for scientific correspondence :

Dr.Santosh Kumar
Department of Post Graduate Studies and
Research in Physics,
Rani Durgavati University,
Jabalpur (M.P.)- 482001 (INDIA)

C-3

SH 4.5-10

N85-35028

STUDY OF SPECTRAL EXPONENT ON QUIET AND DISTURBED DAYS

Santosh Kumar
Rani Durgavati University, Jabalpur.India.

ABSTRACT

The spectral exponents of the diurnal and semi-diurnal anisotropies are studied on quiet and disturbed days for a period from 1964 to 75. It has been observed for the diurnal anisotropy that the spectral exponent for quiet days is 0.0 from 1964 to 70, however during 1971 and onwards its value is found different from zero and is -0.4; for disturbed days the spectral exponent is observed to be 0.0 from 1964 to 75 with an exception of the year 1966. Further, it has been observed for the semi-diurnal anisotropy that the best value for the spectral exponent on quiet days being + 0.6 from 1964 to 74; however on disturbed days the value of spectral exponent is sometimes negative or positive but different from zero. It has been derived from the present investigation that superimposed on the corotational anisotropy, expected from a balance between outward radial convection and inward field alligned diffusion, there is an additional component operating during the period under consideration.

Key words: Spectral exponent, quiet days, diurnal, semi-diurnal

☐ Theoretical ☐ Observational ☒ Both

Paper to be presented by : Dr. Santosh Kumar

Name and address for scientific correspondence :

Dr.Santosh Kumar
Department of Post Graduate Studies and Research in Physics,
Rani Durgavati University,
Jabalpur (M.P.) - 482001 (INDIA)

N85-35029

SH 4.5-11

DIURNAL VARIATION OF GALACTIC COSMIC RAY INTENSITY ON QUIET DAYS

Santosh Kumar, S.C.Datt
Department of P.G.Studies & Research in Physics,
Rani Durgavati University, Jabalpur. India.

R.S.Yadav
Department of Physics, A.M.U., Aligarh. India.

S.P.Agrawal
Vikram Space Physics Centre, A.P.S. University, Rewa. India.

ABSTRACT

A detailed study of the diurnal variation on long term basis has been performed on geomagnetically quiet days using the experimental data of the cosmic ray intensity from the world-wide neutron monitoring stations. During the period when the polarity of the solar magnetic field in the northern hemisphere of the sun is negative the phase and amplitude of the diurnal anisotropy on quiet days has been observed to remain almost constant. When the polarity of solar magnetic field in northern hemisphere changes from negative to positive, a shift in the phase of the diurnal anisotropy on quiet days towards earlier hours is observed and the shift is found to be maximum during minimum solar activity periods 1953-54 and 1975-76. Further, when the polarity of solar magnetic field changes from positive to negative in the northern hemisphere of the sun the phase of the diurnal anisotropy on quiet days recovers to its usual direction of corotational anisotropy and is observed to remain almost constant till the polarity of the solar magnetic field does not change. Furthermore, during the period when the polarity of solar magnetic field in the northern hemisphere of the sun is negative the amplitude of the diurnal anisotropy on quiet days is observed to remain almost constant. And when the polarity of the solar magnetic field in the northern hemisphere of the sun changes from negative to positive the amplitude of the diurnal anisotropy on quiet days is observed to decrease quite significantly. The decrease in the amplitude of the diurnal anisotropy on quiet days is maximum during 1976. Further, when the polarity of the solar magnetic field changes from positive to negative the amplitude of the diurnal anisotropy on quiet days recovers to its usual value and is observed to remain almost constant.

1. Introduction. It has been shown (Kumar et al., 1981, and references therein) that daily geomagnetic index A_p correlates

well with both the diffusive as well as the convective components of the convection-diffusion theory. Also, this is a parameter which is least affected on quiet days in particular, evenwhen the days with abrupt fluctuations in IMF are quite frequent. This has led for the study of the diurnal variation of galactic cosmic ray intensity on quiet days on a long as well as short term basis.

2. Experimental Data and Analysis. The data of the neutron monitors for the stations, shown in figure-1, are used in the analysis. The data has been corrected for meteorological effects. The long term effects have been removed by the method of trend correction. Thus obtained magnetically most quiet days cosmic ray intensity data is subjected for the harmonic analysis and the average values of the amplitude,the phase of the first harmonic component of neutron intensity for different stations are obtained. Essentially, whole of the period has been divided into four parts- (i) before 1956 including 1953-54; (ii) after 1971 and earlier than 1978; (iii) after 1960 upto 1968 and (iv) 1981 and onwards. During the periods (i) and (ii) the polarity of the solar magnetic field in the northern hemisphere is positive, where as during the periods (iii) and (iv) the polarity of the solar magnetic field in the northern hemisphere is negative.

3. Results and Discussion. The long term plots of yearly average values of the geomagnetic disturbance index-A_p for the interval 1957-81 for all the days as well as for sixty most geomagnetic quiet days and sixty most geomagnetic disturbed days are represented in figure-2. It is apparent from the figure-2 that there is a marked variation in the plots for all days and disturbed days from year to year, particularly, for years of high sunspot activity. However, we noticed a very smooth and small variations for the quiet days which proves the importance of selecting most quiet days and in deriving the daily variations for these days only, to represent the long term or short term behaviour.

The interstation dispersion for the yearly average values for the magnetically most quiet days have already been plotted and shown (Kumar et al.,1981). It has been noted that the dispersion is small as compared to changes fron one year to another. This is found to be true even for the most recent period for which we have limited amount of data.

In this presentation we have used the data for Deep River neutron monitoring station for which the pressure corrected hourly cosmic ray intensity is available for an extended period of time. The average values derived for each year for the neutron monitoring station Deep River have been shown in figure-3 without making any correction for the effect of the geomagnetic field. Earlier[1] the vectors derived for different stations were corrected to derive the space vectors to facilitate comparison between different stations. The interstation agreement can not be judged by comparing the observed

ORIGINAL PAGE IS
OF POOR QUALITY

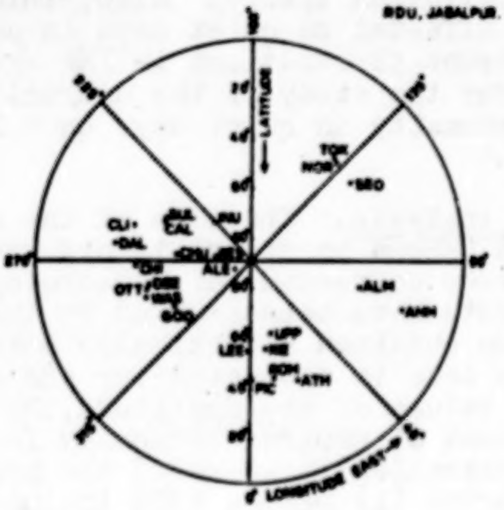

FIG. 1. ILLUSTRATES THE GEOGRAPHICAL LATITUDES AND LONGITUDES OF THE NEUTRON MONITORING STATIONS USED IN THE ANALYSIS.

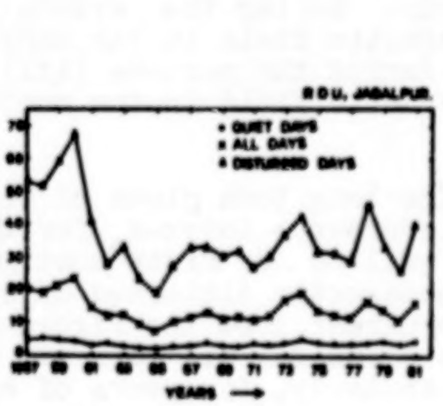

FIG. 2. VARIATION OF Ap-INDEX DURING THE PERIOD 1957-81 ON QUIET DAYS, ALL DAYS AND DISTURBED DAYS.

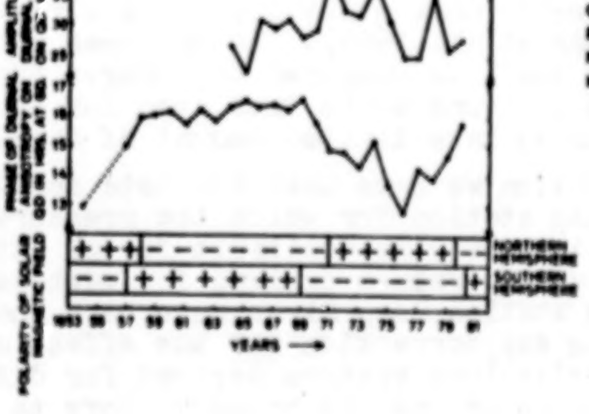

FIG. 3. VARIATION OF THE AMPLITUDE AND PHASE OF DIURNAL ANISOTROPY ON QUIET DAYS AT GROUND AND POLARITY OF SOLAR MAGNETIC FIELD IN NORTHERN AND SOUTHERN HEMISPHERES DURING DIFFERENT YEARS.

amplitude and phase in space because the geomagnetic corrections are different for different stations. So far, it is not clear that β and R_{max} are constant during period of 11-year or more, and hence the constant geomagnetic corrections generally applied on a long term basis is not very effective.

It is quite apparent from the figure-3 that during the period when the polarity of the solar magnetic field in the northern hemisphere of the sun is negative the phase and amplitude of the diurnal anisotropy on quiet days are almost constant. When the polarity of solar magnetic field in northern hemisphere changes from negative to positive, a shift in the phase of the diurnal anisotropy on quiet days towards earlier hours is observed and the shift is found to be maximum during minimum solar activity periods 1953-54 and 1975-76. Further, when the polarity of solar magnetic field changes from positive to negative in the northern hemisphere of the sun the phase of the diurnal anisotropy on quiet days recovers to its usual direction of corotational anisotropy and is observed to remain almost constant till the polarity of the solar magnetic field does not change.

Earlier results (Yadav and Badruddin, 1983) have indicated that on an average the two solar cycles when the northern hemisphere of the sun is dominated with negative polarity and when the northern hemisphere of the sun is dominated with the positive polarity, show different behaviour of diurnal anisotropy. This was done by considering all the 365 days in the year. We have considered the average of only magnetically most quiet days for the same interval (1964-68) and (1972-76) as well as for (1960-68) and (1972-78) to compare the effect of polarity reversal on diurnal anisotropy during magnetically most quiet days. Here again the vectors are drawn for the diurnal amplitude and phase observed at the station Deep River.

The results show that, in general, magnetically most quiet days are slightly more effective by the polarity reversal as compared to all days. The significance of magnetically most quiet days comes from the fact that these are least affected days due to disturbances in the interplanetary medium and hence are best suited for understanding the anisotropy on long as well as short term basis. It has been visualised further that if the similar trend exists, one should observe a steady variation in the diurnal amplitude and phase on magnetically most quiet days during 1981 and onwards till the polarity of the solar magnetic field in the northern hemisphere remains negative.

References

1. Kumar, S. et al., 1981, Proc. 17th Int.Conf.Cosmic Rays., France (Paris). pp.226-229.
2. Yadav, R.S. and Badruddin, 1983, Proc. 18th Int.Conf. Cosmic Rays, Bangalore (India) pp.366-369.

DIURNAL VARIATIONS FROM MUON DATA AT TAKEYAMA UNDERGROUND STATION

N85-35030

K.Takahashi, K.Imai, T.Imai, S.Kudo, and M.Wada
The Institute of Physical and Chemical Research
7-13 Kaga-1, Itabashi, Tokyo 173, Japan

ABSTRACT

An underground station, Takeyama, is introduced, and some results of the solar diurnal and semi-diurnal variations for the period between 1967 and 1984 are presented. There are clear tendency of double and single solar cycle variations in the daily variations which are in good accord with those detected by other underground and neutron monitor observations.

1. Introduction.

Takeyama is the first Japanese underground station for the study of the time variations of cosmic ray intensity. The depth is 54 mwe which is equivalent to the median rigidity of primary cosmic rays around 200 GV. The geographic latitude and longitude are 35.22° N and 139.62° E, respectively. The continuous observation was started in September 1967. The operation was stopped in September 1981. It was restarted in June 1982. The area of detector has been increased from 9 m^2 to 16 m^2. The detector consists of 2 layers of 16 plastic scintillators, 1 m^2 each.

Since the station is situated a few tens km apart from the main laboratory, the memorized data are communicated through public telephone lines. The recording and communication modes are controled through the terminal computers set at both sites. The computer at the observation site can memorize one week data. The data are read out at the laboratory by the command. Generally the coincidence counts per hour of 256 combinations (16 × 16) are communicated. They are rearranged in the laboratory to get the counts of directional components, i.e., vertical and four azimuthal directions inclined around 30° from zenith. The observed counting rates are corrected for the pressure effect with the coefficient, -0.035 %/mb.

2. Daily variations.

The yearly average solar diurnal and semi-diurnal variations are presented here. Figs.1a and 1b show the summation diagrams of the diurnal vectors of the vertical component, without and with the correction for Compton-Getting effect, respectively, for the earth's revolution around the sun. The correction values have been given by Prof. H.Ueno of Nagoya University. He has calculated them using the listed coupling coefficients (Fujimoto et al. 1984) for the variation spectrum which is flat upto essentially infinite rigidity. They are listed in Table 1.

It is clearly seen from the figures that the phases are earlier during the period from 1969 to 1980 compared with those after 1982. This tendency has already been pointed out by Swinson (1983) from his underground observations. There is a period, 1975-77, when virtually no diurnal variation is seen if Compton-Getting effect is concerned as Fig.1b. The phases of diurnal variations detected by neutron monitors are also relatively earlier in this period as seen in Fig.2. The level of cosmic ray intensity is highest and the variations are calm in the same period when the sunspot numbers are minimum.

Figs.3a and 3b show the vector diagrams of directional components for three year periods, 1978-80 and 1981-83, respectively. It is clear that the phases are later for the latter case as expected from those illustrated in Fig.1. Those results can be added on Ueno and others' "NAMS" analysis (1984) which utilizes the muon data from Nagoya, Misato, and Sakashita, and may become "NAMTS".

Fig.4 shows the summation diagram of solar semi-diurnal variation. The phases are nearly at 1.5 hour. There again some tendency of advancing the phases during the years in 1970's comparing with the periods before and after that.

Table 1. Correction values for Compton-Getting effect in percent. (after H.Ueno)

Axis	Vert.	North	East	South	West
0 hr	0.0073	0.0088	0.0227	0.0053	-0.0093
6 hr	0.0351	0.0232	0.0316	0.0422	0.0335

3. Summary. The underground observation at Takeyama is presented, with some information of the restart of observation with somewhat larger area than before. The solar diurnal and semi-diurnal variations are analyzed. The double solar cycle variation in the diurnal variation is seen. The diurnal variations in 1975-77 indicate the character of single solar cycle variation, for the period corresponds to the sunspot minimum years. Those double and single solar cycle variations are in good accord with those detected by the muon and neutron monitors.

The multi-component or multi-station analysis will give more information about the anisotropy in space. Further observation, at least until the next solar minimum with better quality, will result much complete conclusion of the analysis given above.

4. Acknowledgment. The earlier observation was performed by Prof. K.Murakami and others in the laboratory and the technical team in the Institute. The revised observation has been operated under the same members of the laboratory and of the technical workshop, specially K.Nishi and H.Kato. Prof. H.Ueno has provided us Compton-Getting values of Takeyama. We are grateful to them all.

References

Fujimoto,K., A.Inoue, K.Murakami, and K.Nagashima, (1984), *Coupling Coefficients of Cosmic Ray Daily Variations for Meson Telescopes*, Rep.Cosmic-Ray Res.Lab., CRRL., Nagoya Univ., Nagoya, Japan.

Swinson,D.B., (1983), *Long Term Change in the Solar Diurnal Variation of Cosmic Rays and Cosmic Ray Density Gradients at High Rigidities*, 18th ICRC, Bangalore, 10, 55-58.

Ueno,H., Z.Fujii, S.Mori, I.Morishita, and K.Nagashima, (1984), *Solar Diurnal Variations Observed at Nagoya, Misato, and Sakashita Stations (NAMS)*, Proc.Int.Symp.Cosmic Ray Mod.Heliosphere, Morioka, Iwate Univ. Japan, 109-113; and will be given in this conference.

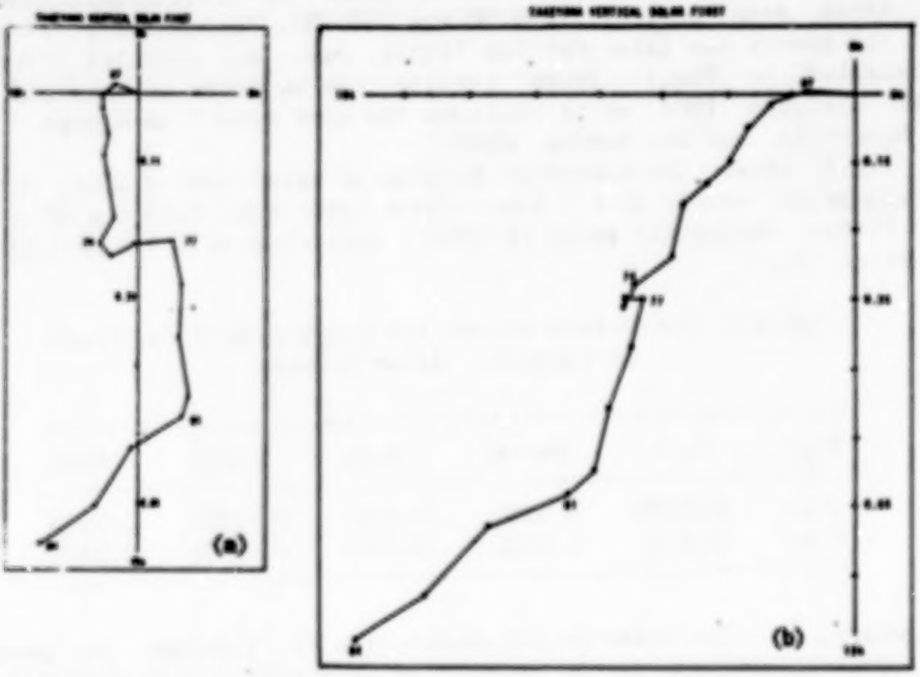

Fig.1. Summation diagrams of yearly solar diurnal variation, vertical component observed at Takeyama underground station from 1957 to 1984: (a): without, and (b): with the correction for Compton-Getting effect, respectively.

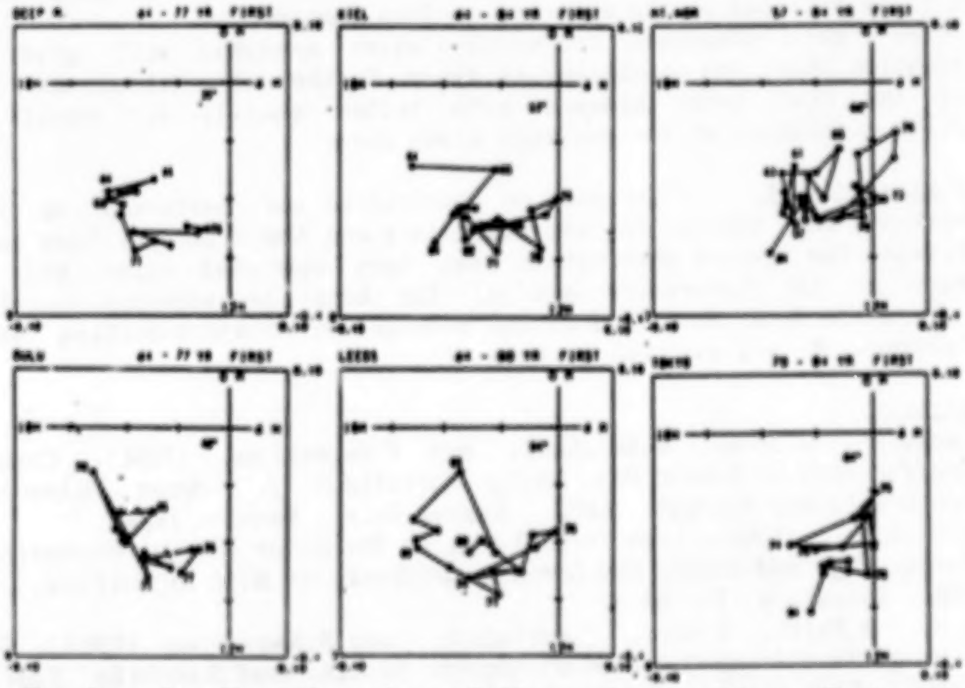

Fig.2. Yearly solar diurnal vectors of the neutron monitors. Each vector is drawn from the origin, and the lines connect the vectors to show the year to year changes. Notice the vector of 1976 which is at the upper right corner of the evolution in each graph.

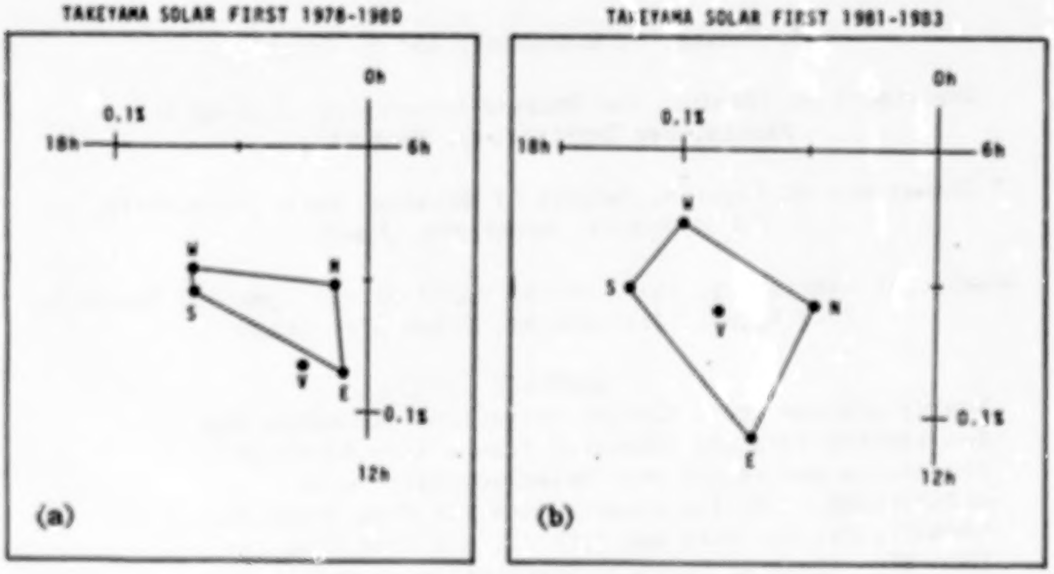

Fig.3. Solar diurnal vectors of directional components at Takeyama for the periods: (a): 1978-80, and (b): 1981-83, respectively.

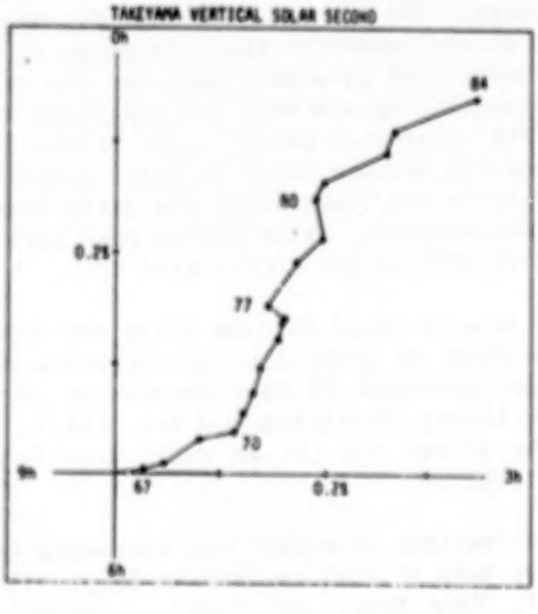

Fig.4. Summation diagrams of yearly solar semi-diurnal variation, vertical component at Takeyama for 1967-84.

N85-35031

SH 4.5-14

LONG TERM CHANGES IN COSMIC RAY DIURNAL VARIATIONS OBSERVED BY ION CHAMBERS IN HONG KONG AND JAPAN

L.S. Chuang, M. Kusunose*, and M. Wada**

Department of Physics, the Chinese University of Hong Kong,
Shatin, New Territories, Hong Kong

* Department of Physics, Faculty of Science, Kochi University,
5-1 Akebono-2, Kochi 780, Japan

** Cosmic Ray Laboratory, Institute of Physical and Chemical Research,
7-13 Kaga-1, Itabashi-ku, Tokyo 173, Japan

ABSTRACT

Yearly average solar diurnal variations of cosmic ray ion chamber data are inspected from a view point of the eleven and the 22 year solar activity cycle modulations. The ion chamber data are from Tokyo for 1948-77, Mt. Norikura for 1958-77, and Hong Kong for 1970-83. Those of Carnegie Institution of Washington are also used. The neutron data from various stations are further added. From an inspection of observed data, we propose a simplest approximation that the 11 year and the 22 year variations of the solar diurnal variation are along 18-hour and 12-hour axes, respectively. The 18-hour component of diurnal variation in the 11 year cycle increases toward the solar active years. The 12-hour component is enhanced when the solar general magnetic field is parallel to the rotation vector, and is almost zero for the other state. The transition occurs when the amplitude of the 18-hour component is greater owing to the transition of the field during the maximum phase of solar activity. The 22 year shift is consistent with the drift modulation model in heliosphere. While the 11 year variation along the 18-hour axis is not interpreted yet.

1. Introduction. The present paper follows after the discovery of the 22 year variation in the phase of solar diurnal variation by Thambyahpillai and Elliot (1953), the invariant 18-hour anisotropy which is agreeable with the Axford-Parker theory (McCracken and Rao, 1965), and the two component analysis of the eleven and the 22 year variation in the diurnal variation by Forbush (1969).

Continuous observations of cosmic ray intensity by means of identical ion chambers have been started in 1948 at Tokyo, then Mt. Norikura, Sapporo (now stopped), Hong Kong, and Kochi. Though the observation accuracy is not so high as current muon telescopes and the neutron monitors, the data can be used as tools to inspect the diurnal variations in yearly basis for long time period.

If the deflection of the cosmic ray particles through the geomagnetic field, and the background diurnal variation due to, say, the temperature effect are taken into account, the observed diurnal variation can be converted to the anisotropy detectable in space. The greatests of all the yearly average diurnal variations are the eleven year solar cycle variation and that related to the reversal of the solar general magnetic field at nearly the years of maximum activity which makes the 22 year variation.

Though there are fluctuations, from an inspection of the vector diagrams of diurnal variation, the eleven year and the 22 year variation can be separated into the amplitude variations along 18-hour and 12-hour axes, respectively. Such an approximation is given from a very rough idea, but the shift along 12-hour axis accords with the drift model of heliospheric modulation.

2. Display of the diurnal variations. Fig. 1 shows the vector diagram of the solar diurnal variation observed at Tokyo. Hong Kong data are added to extend the years. The data have only been corrected for the barometer effect. The broken lines indicate expected observations if the direction of anisotropy in space is 18 hour. The variation spectrum is assumed to be flat upto rigidity given in the figure. The values with % in the figure is the amplitude observable in space. If the diurnal variation due to the temperature effect is concerned, the origin of the observed vectors must be shifted, though the amount of shift can not reasonably be given, for the temperature diurnal variation is not known accurately. It can be allowed, however, the origin can be shifted so that the pattern becomes similar to those observed by the neutron monitors. The diagrams for other stations including those of the Carnegie Institution (Forbush, 1969) and of some neutron monitors are seen in the following Figs. 2-5.

3. Discussion. The hand writing drawing in Fig. 6 indicates our idea to interpret approximately the variations during 11 and 22 year periods. It can be shifted and rotated to fit the observed diagram of the anisotropy. There are appreciable scatter around the proposed simple variation, but one can see this kind of interpretation is possible. It is seen that the transition from different 12-hour states occur at around years of the reversal of the solar general magnetic field. This situation is understandable if the drift effect of modulation in heliosphere is concerned (Jokipii and Kopriva, 1979).

Kadokura and Nishida (1984) have simulated the anisotropy of cosmic rays in heliosphere putting the effect of drift as well as the diffusion through the interplanetary magnetic field (IMF) and Compton-Getting effect in the system of solar wind. They compared the results for different states of the solar general magnetic field which is parallel or anti-parallel to the rotation vector. The difference appears in the term of diffusion if restricted the position at the earth orbit. The anisotropy due to the diffusion is enhanced during the anti-parallel state. Since the diffusion is along IMF, the anisotropy is along 21-hour axis. That makes the 18-hour component greater than that of the other state. On the other hand, because of the enhancement of 0-hour component, the overall effect of the 12-hour component is almost canceled out, while that in the parallel state remains to be significant. It appears as the enhancement of the 12-hour component during the parallel state compared with that of the anti-parallel state.

ORIGINAL PAGE IS
OF POOR QUALITY

As for the eleven year variation of the diurnal variation, though the observed variation is clearly seen, the model for that has not been fixed yet. One point which should be examined further is the distribution of the diurnal vectors in daily basis. While the average amplitude changes, at least two patterns can exist. The one is that the total distribution shifts without change in shape. The other is that the shape of distribution is distorted; for example, the frequencies at greater amplitudes increase compared with those at lower amplitudes. If the latter is a real case, there are various origins which enhance the amplitude during the solar active years. For example, the frequencies of occurrence of solar flares, Forbush decreases and so on are greater during the active years. Still, why the enhancement occurs along the 18-hour direction during the active years is an open question. We leave this problem for further studies

Fig.1. Observed yearly average diurnal vectors for ion chambers in Tokyo and Hong Kong. The broken lines indicate expected observations if the direction of anisotropy is 18 hour in space The spectrum is flat upto GV written inside. The % values correspond to the amplitude in space.

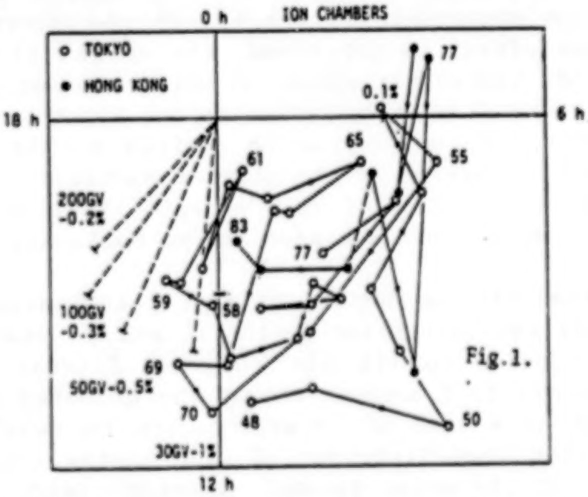

Figs.2-5. The same as Fig.1, but for ion chambers at Mt.Norikura, Huancayo, and Cheltenham (Forbush, 1989), and neutron monitor at Mt.Norikura (Kawasaki et al. 1983), respectively.

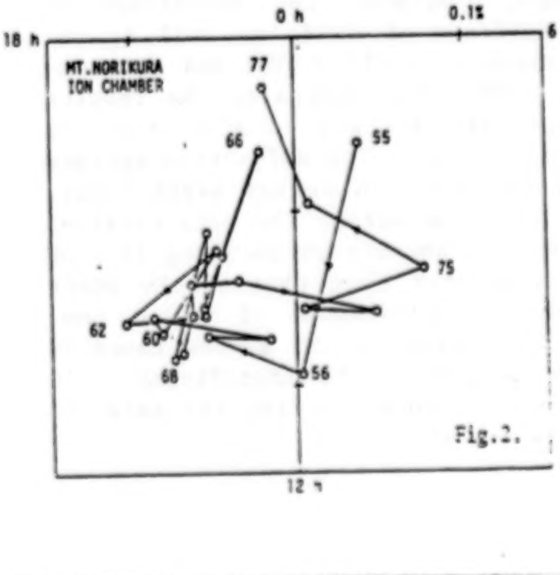

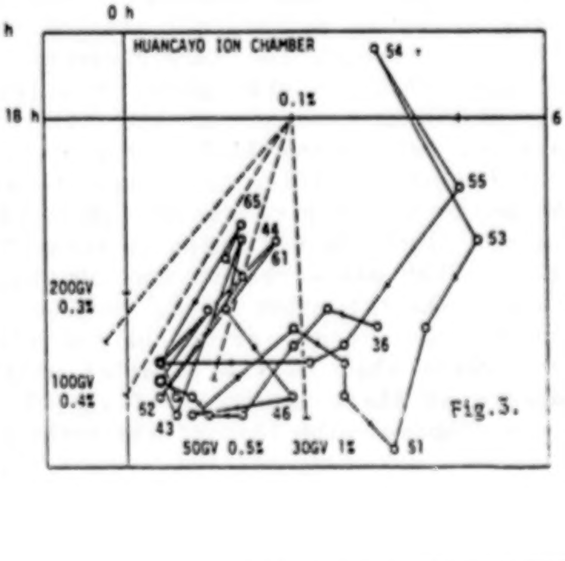

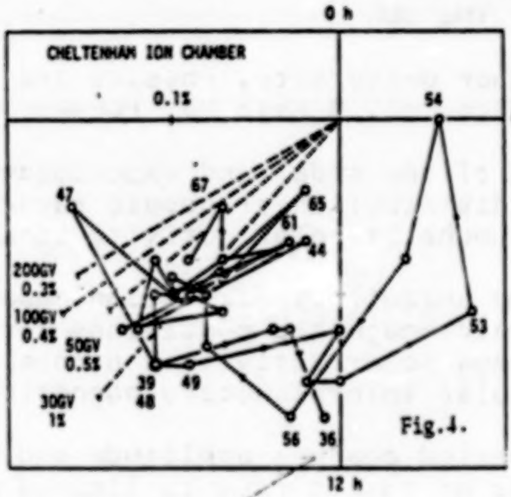

Fig.4.

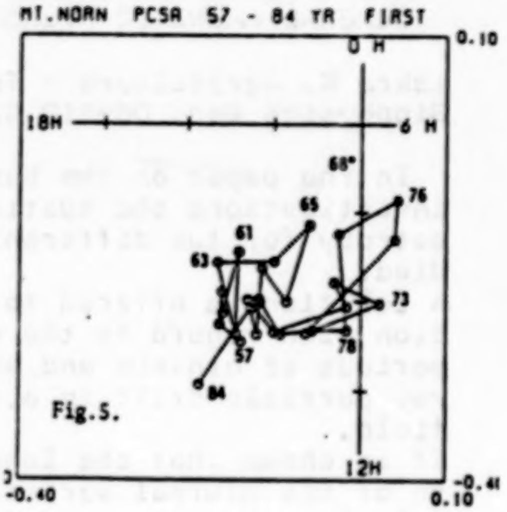

Fig.5.

Fig.6. Simplest and approximate aspect of the 11 and the 22 year variations of the solar diurnal variation. See text.

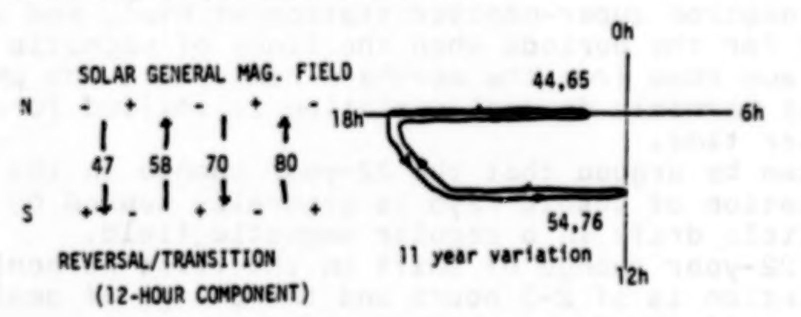

4. Acknowledgements. We are grateful to all the investigators who continued to operate and to process data for such long periods as shown here.

References

Forbush, S.E., (1969), Variation with a Period of Two Solar Cycles in the Cosmic-Ray Diurnal Anisotropy and the Superposed Variations Correlated with Magnetic Activity, J. Geophys. Res. 74, 3451-3468.

Jokipii, J.R. and Kopriva, D.A., (1979), Effects of Drift on the Transport of Cosmic Rays, III. Numerical Models of Galactic Cosmic-Ray Modulation, Astrophys. J. 234, 384-392.

Kadokura, A. and Nishida, A., (1984), private communication.

Kawasaki, S., Imai, K. and Wada, M., (1983), Cosmic-Ray Data at Mt. Norikura, Neutron Monitor 1968.9-1980.12, ICR-Report 109-83-03, Inst. Cosmic Ray Res. Univ. Tokyo.

McCracken, K.G. and Rao, U.R., (1965), A Survey of the Diurnal Anisotropy, Proc. Int. Conf. Cosmic Rays, London, 1, 213-218.

Thambyahpillai, T. and Elliot, H., (1953), World-Wide Change in the Phase of the Cosmic-Ray Solar Daily Variation, Nature, 171, 918-920.

ORIGINAL PAGE IS
OF POOR QUALITY

N85-35032
SH 4.5-15

THE MODULATION FEATURES OF THE LONG - PERIOD COSMIC RAY VARIATIONS IN CONNECTION WITH THE SING CHANGE OF THE GENERAL MAGNETIC FIELD OF THE SUN

Iskra K. Agriculture - Teacher University, Physics and Biophysics Dep. 08-110 Siedlce, ul. 3 Maja 54 POLAND

In the paper on the basis of the model and experimental investigations the spatial distribution of cosmic ray anisotropy for the different epochs of solar activity is studied.

A solution is offered to the anizotropic diffusion equation with regard to the electro-magnetic conditions for the periods of minimum and maximum solar activity and cosmic ray particle drift in a regular interplanetary magnetic field.

It is shown that the long-period changes amplitude and phase of the diurnal variations of cosmic rays is limited not only by convection and diffusion of particles but also by the drift effect before and after the sing change of the general magnetic field of the sun.

The calculated model is compared with the results obtained on the basis of an analysis of the experimental data from the neutron super-monitor station at Kiel, and it is shown that for the periods when the lines of magnetic force of the sun come from the northern hemisphere the phase of the first harmonic diurnal variation is shifted forwards to an earler time.

It can be argued that the 22-year change in the diurnal variation of cosmic rays is generally caused by cosmic-ray particle drift in a regular magnetic field.

The 22-year change of shift in the first harmonic diurnal variation is of 2-3 hours and the change of amplitude between twenty and thirty percent.

SH 4.5 - 16

N85-35033

THE COSMIC RAY DIFFERENTIAL DIURNAL VARIATION DEPENDENCES ON THE ZENITH ANGLE AND THE GEOMAGNETIC DISTURBANCE

S. Kavlakov and L. Georgiev

INSTITUTE FOR NUCLEAR RESEARCH AND NUCLEAR ENERGY.
BULGARIAN ACADEMY OF SCIENCES. SOFIA 1784. BULGARIA.

1. INTRODUCTION.

Simultaneous and continuous muon measurements in two opposite azimuthal directions under equal zenith angles I1I demonstrated the importance of this method for cosmic ray diurnal variation investigations. Lately these measurements were extended by means of improved telescopes I2,3I. The obtained cosmic ray diurnal variations were presented as intensity differential curves.

Theoretical investigations I4I connected the properties of these curves with some interplanetary space parameters. The harmonics of these curves were interpreted I5I physically. Second order difference curves were introduced I6I.

In our earlier works I7,8,9I some dependences between the parameters charachterizing the first and the second harmonics of the differential intensity curves and the geomagnetic activity were found. Then all measurements were carried out under only one zenith angle.

Here we presented the results of investigations of similar dependences using data of simultaneous measurements under three different zenith angles.

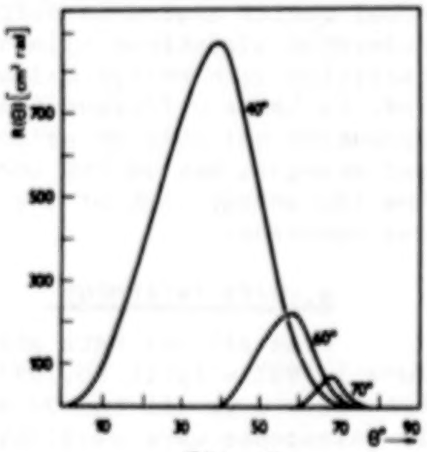

Fig. 1.

2. EXPERIMENT.

The measurements were carried out on p. Musala ($\varphi = 42^{0}11'N; \lambda = 23^{0}35'E;$ $H = 2925$ m.a.s.l.) by means of a multidirectional counter telescope I10I. After the connection of a supplementary electronic circuit it became possible to measure simultaneously in the four cardinal azimuthal directions (East(E), West(W), North(N), South(S)) under three different zenith angles (40°; 60°; 70°) I11I.

On fig. 1. are shown the zenith angle sensitivities for the telescopes inclined under 40°; 60°; 70°.

On fig. 2. are plotted in polar coordinates the azimuth angle sensitivities for all our 12 telescopes measuring simultaneously.

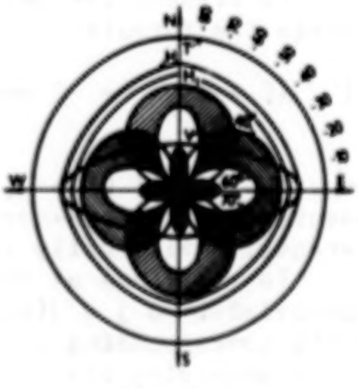

Fig. 2.

ORIGINAL PAGE IS
OF POOR QUALITY

3. ASYMPTOTIC DIRECTIONS.

If the energy is sufficiently grate the particle's primery direction does not change when it moves through the earth megnetosphere. On fig. 3. the small circles present the asymptotic directions ($\varphi_{E=\infty}, \lambda_{E=\infty}$) calculated following I12I for our telescopes and projected on the extended map of the Globe surface. There p. Musala is shown with a triangle.

The asymptotic directions for the same telescopes computed I13I for different lower energies are shown on the same figure as separate points. The points are connected with suitable curves for every one of the telescopes.

Because of the considerable width of the distributions of $R(\theta)$ and $P(\alpha)$ for the real telescopes, the points corresponding to all asymptotic direction projections for a certain energy cover a considerable area on the Globe surface. Then the curves plotted on fig. 3. form large strips.

It could be accepted that the differences of intensity data obtained simultaneously from two inclined telescopes, detecting under equal zenith angles in different azimuthal directions eliminate particles with energy below 18 - 20 GeV. So these differences are independent not only on meteorological changes, but on the changes in the low energy part of the cosmic ray spectrum.

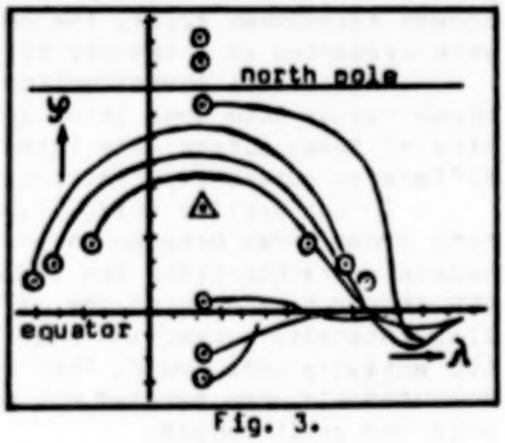

Fig. 3.

4. DATA TREATMENT.

From all the data obtained on p. Musala in the period June 1,1981 - April 30,1983 only "complete" data days were used. For these days all the 24 separate hourly measurements for all the 12 telescopes were available. From the measured hourly intensities for every separate day, for every separate zenith angle the following 8 differences were formed

I ordre: E - W; E - N; E - S; W - N; W - S; N - S;
II ordre: G = (N - S) - (E - N); K = (N - S) - (W - N).

To present the deviations in percentage arround a zero average the formula

$$(1) \quad (E - W)_{ij} = 2 \, \frac{E_{ij} - W_{ij} - (\overline{E}_j - \overline{W}_j)}{\overline{E}_j + \overline{W}_j} \, 100\,\%$$

was used. Here i (i = 1,2...24) was the index of the i-hour measurement in the j-day. $\overline{E}_j$ and $\overline{W}_j$ are the corresponding dayly averages. Analogically all other differences were formed.

To every one of the chosen days the indexes m and n were appropriate. So j = j(m,n). The index m charachterized the degree of the corresponding day magnetic activity. The values of m were chosen according I14I. The index n specified the continuity of the days arround the beginning of the magnetic storm.

The combinations between m and n are classified on table 1.

Table 1.

	quiet m = 0	weak m = 1	moderate m = 2	intense m = 3	strong m = 4	All for the row
PRECEDING n = -1	—	1,-1	2,-1	3,-1	4,-1	N =-1
BEGINNING n = 0	—	1, 0	2, 0	3, 0	4, 0	N = 0
FOLLOWING n = 1	—	1, 1	2, 1	3, 1	4, 1	N = 1
For the column	—	M = 1	M = 2	M = 3	M = 4	MN

For every one of the three zenith angles (40°;60°;70°), for every one of the 21 index combinations (table 1.) the average diurnal variation of every one of the 8 differences was investigated. Fourier analysis was applied for every one of these 3 x 21 x 8 = 504 cases to compute the amplitudes A1; A2; A3 (in percents) and the phases t1; t2; t3 (in hours Local Solar Time (LST)) of the first (I), the second (II), and the third (III) harmonics.

5. RESULTS.

The first (I) and the second (II) harmonics for some of the computed differences for magnetically quiet days (m = 0), for the zenith angles 40°,60°,70° are presented on fig. 4. as vector-hourly diagrams. The phases of the first harmonics remain grouped arround 6 h.LST and the phases of the second harmonics - arround 9 h.LST. That is valid for all the three zenith angles and practically for all other differences (not shown on the figure).

If these vectors are compared with those obtained 10 years ago on the same place, with the same apparatus (measureing then only under zenith angle of 60°) it could be assumed that they are rather stable in time

The amplitudes A1 and A2 increase with the zenith angle. As an example that is shown for G on fig. 5.

The first harmonic amplitude dependences on the magnetic disturbance degree are shown for K on fig. 6. for the three zenith angles. This amplitude, as well as the amplitudes of the other differences (not shown on the figure) increases with m. The increase is rather faster for greater zenith angles.

An interesting phenomena - the first harmonic amplitude increase in the days preceding the beginning of the magnetic storm observed in our earlier investigation I9I for zenith angle 60°,now is clearly expressed for all the three zenith angles (40°,60°,70°). On fig. 7. are presented the changes of the first harmonic amplitude of the difference K in the days arround the beginning of the magnetic storm compared with its value during magnetically quiet days. If the statistical accuracy of the separate diurnal measurement is sufficient then after a sudden jump in the amplitude's value, some short time forcast for a forthcomming magnetic disturbance could be done. This dependence is not well expressed for the second amplitudes.

In our case the third harmonics are generally small and their changes are practically in the limits of the statistical accuracy.

ORIGINAL PAGE IS
OF POOR QUALITY

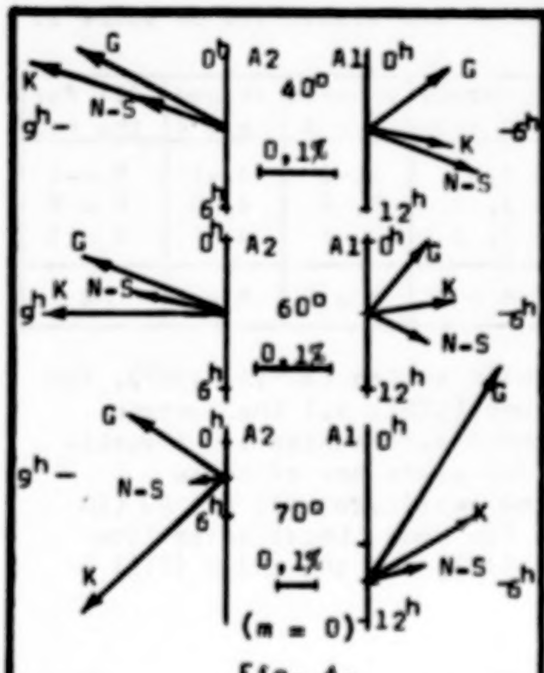
0^h
A2
40°
A1
0^h
G
K
N-S
g^h
6^h
0,1%
K
N-S
6^h
12^h
G
A2
K
N-S
60°
A1
0^h
G
K
N-S
0,1%
6^h
12^h
G
A2
A1
0^h
N-S
70°
K
0,1%
K
N-S
(m = 0)
12^h

Fig. 4.

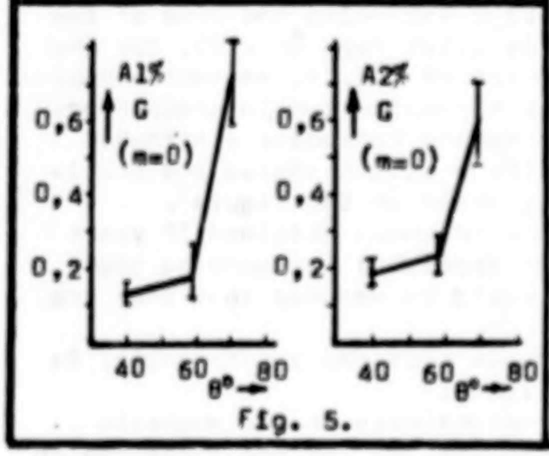

Fig. 5.

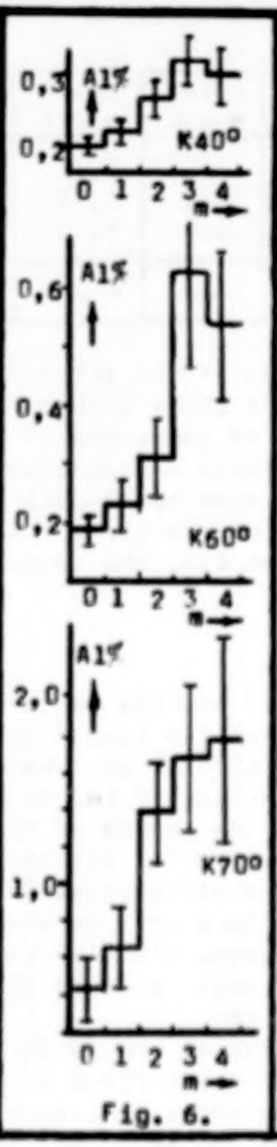

Fig. 6.

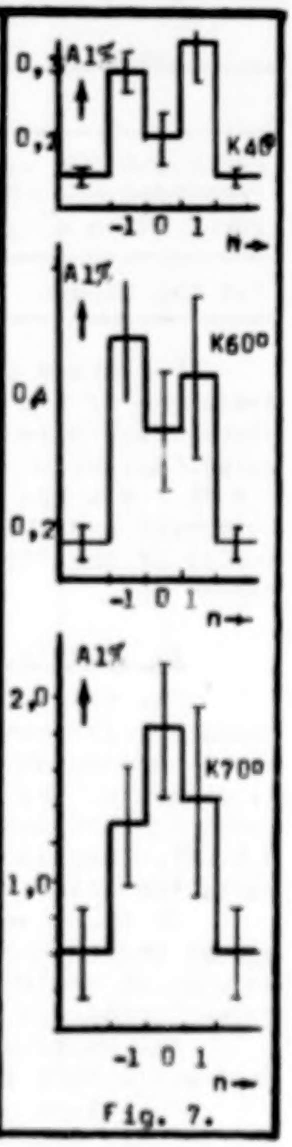

Fig. 7.

REFERENCES.

1. Kohlhörster W., Phys. Zs., 42 55 1941.
2. Elliot H., D. Dolbear, Proc. Phys. Soc., 63A 137 1950.
3. Sekido Y. et all. Multidirectional C.R.Intensity, Nagoya, 1975.
4. Nagashima K., Rep. Ionos. Space Res. Japan, 25/3 189 1971.
5. Nagashima K. et all.,Rep. Ionos. Space Res. Japan, 26/1 1 1972.
6. Kondo I. et all., Proc. 14 ICRC München, 4 1182 1975.
7. Kavlakov S., Izv. Acad. Nauk USSR (Physics), 40/3 607 1976.
8. Kavlakov S., Proc. ICR Symp., Tokyo, 285 1976.
9. Kavlakov S., Proc. 15 ICRC, Plovdiv, 4 82 1977.
10. Kavlakov S., Compt. Rend. Acad. Bulg. Sci. 18/8 731 1965.
11. Kavlakov S., Thesis, Sofia, 1977.
12. Kavlakov S. et all. Proc. 17 ICRC, Paris, 4 237 1981.
13. Shea M. A. and D. F. Smart, Tables, Private communication.
14. Cosmic Data (in rushan) Moscau, 1981, 1982, 1983.

N85-35034
SH 4.5- I7

COSMIC RAY DENSITY GRADIENT AND ITS DEPENDENCE ON THE NORTH-SOUTH ASYMMETRY IN SOLAR ACTIVITY

Badruddin,R.S.Yadav and N.R.Yadav
Space Science Group,Dept. of Phys.,A.M.U.,Aligarh (India).

ABSTRACT

An analysis of the diurnal anisotropy on geomanetically quiet days has been performed using neutron monitor data at Deep River($R_c \sim 1.02$GV),Leeds($R_c \sim 2.20$GV),Rome($R_c \sim 6.32$GV)and Tokyo ($R_c \sim$II.6IGV),well distributed in latitude and longitude for the period I964-79.The days have been separated according to the polarity of IMF on that day.A significant difference in the amplitude and phase has been found on towards and away polarity days particularly during the years of high solar activity and large north-south asymmetry.These results (particularly time of maximum) on geomanetically quiet days show some better relationship to the expected results as compared to the results obtained using all the days in a year.

I.Introduction. The existence of perpendicular gradient has been studied by separating the cosmic ray diurnal vectors into groups corresponding to the direction of IMF.This method has been recently applied(Kananen et al.I98I;Swinson and Kananen,I982)by using the neutron and meson monitor data for the period I965-75.These authors have found that the amplitude of the diurnal anisotropy on away polarity days exceeds those of towards polarity days during year I965-68 and that the reverse is generally the case after the reversal of sun's polar magnetic field in I969-7I.These data points to a cosmic ray gradient,perpendicular to the ecliptic plane,pointing southward prior to I969 and there was some evidence about northward pointing gradient after the reversal of sun's polar magnetic field in I969-7I except in I974.However, the phase does not show the effect expected from the amplitude behaviour. They found no significant difference,in the amplitude and phase both,of the away and towards polarity days in I969-7I, at neutron monitor energies.

We found in our paper that on day-to -day basis the coherence for the cosmic ray anisotropy is better for days of low to average solar wind speed,which also is related to geomagnetically quiet days,and it would be more meaningful to use only these days for determining the annual average of the cosmic ray daily variation particularly for sunspot maximum activity period,during which one observed large number of cases of time varying isotropic changes in cosmic ray intensity.In this paper we have analysed the neutron monitor data for I964-79 period for the stations mentioned above on magnetically most quiet days and determined the amplitude and phase for away and towards polarity days separately.On the basis of these results the perpendicular density gradient are discussed.Some indirect information about the three dimensional structure of the heliosphere especially current sheet has been inferred from these results.

2. Result. Fig.I shows that the amplitude on away polarity days is ,in general, higher than on towards polarity days during I964-68.But the phase on towards polarity days is higher than the away polarity days during this period.The difference in amplitude and phase on away & towards polarity days are more pronounced during the higher solar activity period I967 and I968.These results are in agreement with the results of the earlier workers(Hashimand Bercovitch,I972; Kananen et al.,I98I;Swinson &Kananen,I982).However the results of Kananen et al.(I98I) for the time of maximum does not show the right type of effect as expected.We found using the data from three neutron monitors, for geomanetically quiet days that the results for the time of maximum are also generally in agreement to that expected from the amplitude behaviour during I964-68,especially in I967 and I968.To give a better representation,we have plotted the average vectors for the period I964-68,separately on away and towards polarity days (Fig.2).

Kananen et al.(I98I) and Swinson & Kananen(I982) do not found any significant difference in the amplitude and phase on away and towards polarity days during I969-7I.Their results imply no density gradient (pointing northward or southward)during this period of reversal of sun's polar magnetic field.The solar activity was high and north-south asymmetry was also quite large(and positve)throughout the period I966-70(Badruddin et al.,I983).We see from Fig.I that the amplitude at Deep River and Leeds,which was higher for away polarity days than for towards polarity days during the year I964-68,changed to higher value for towards polarity days than away polarity days in I969 though at Rome similar change has been observed in I970.However,as far as phase is concerned,it has changed to later hours for towards polarity days than the away polarity days in I969 at all the three stations Deep River,Leeds,& Rome.In I970,the amplitude was much higher for towards polarity days than away polarity days and the time of maximum was quite significantly changed towards later hours for away polarity days than towards polarity days.These results are also shown on the vector diagram in Fig.2.In many earlier studies it has been assumed that the IMF in northern and southern hemispheres have reverse configurations in I964-68 and I969-79.The north-south asymmetry in solar activity in I969-70 was of the same sign(positive) as it was in I967-68.Thus if the current sheet was displaced downward due to positive north-south asymmetry in I967-68,it will be the same case in I969-70.But since the IMF polarity may be different in northern and southern hemispheres in I967-68 and I969-70,the reverse behaviour of diurnal amplitude and phase on away and towards polarity days in I967-68 and I969-70 may be due this reason. However,in I97I,when solar activity was lower as compared to I969 and I970 and north-south asymmetry was also small in this year,no significant difference in amplitude and time of maximum for towards and away polarity days is observed at all the four stations(only the amplitude at Deep River shows some diffrence).Similar difference at Deep River was also reported by Swinson and Kananen (I982).

During the period I97I,I972 and I973 there is some [illegible] difference in the amplitude at towards and away polarity days only at Deep River.The average vectors for the period I97I-I973 have also been shown in Fig.2 for all the four stations.During these periods there was no marked north-south asymmetry as evidenced form solar flares.Swinson and Kananen (I982)did not found a consistent northward gradient at meson monitor energies during I97I-73,though their results point to a northward gradient in I972 and in I973 for Deep River and Oulu neutron monitors.

In I974 the amplitude on away polarity days is higher than the towards polarity days.Various arguments have been advanced to explain the observed amplitude and phase behaviour in I974(Swinson &Kananen,I982;Ahluwalia & Riker,I98I).It is to be mentioned here that the north-south asymmetry in solar activity was some-what negative as evidenced from solar flares and moreover in I973-75 the monster type solar wind streams were prominently observed.

In the solar activity minimum period I975-76, there is no appreciable difference in the amplitude and phase values for towards and away polarity days.The north-south asymmetry was also very small during these years.However, in I977,there is some evidence for a northward pointing gradient as seen from amplitude at Deep River and the amplitude and phase at Tokyo for towards and away polarity days.The solar activity in I977 was not high and north-south asymmetry was also small.However there was an accelerated increase in solar activity after mid-I977.

In I978 & I979 the solar activity was very high.However, the north-south asymmetry was small.We see from results for amplitude and phase on away and towards polarity days that there is no appreciable difference in amplitude and phase for the two types of days both at Deep River and Tokyo.

3.Conclusion. From the above results we see that there is an appreciable difference in the amplitude and/or phase on towards and away plarity days during years of high solar activity and large north-south asymmetry.During the years of lower solar activity and/or small north-south asymmetry this difference is not appreciable.These results support the view that at least during the period of high solar activity and appreciable north-south asymmetry,either the density gradient pointing away from the solar equatorial plane is not symmetric or the current sheet might have been displaced from the ecliptic plane.Thus it seems right to suggest(Swinson,I983) that in order to detect any $\vec{B} \times \vec{\nabla} N$ anisotropy the position of the current sheet(on average)would have to be displaced from the ecliptic plane due to asymmetric activity on the sun.

References

Ahluwalia,H.S.and Riker,J.F.,(I98I),I7th ICRC,I0,230.
Badruddin,Yadav,R.S.and Yadav,N.R.(I983),Ind.J.Radio Space,

Phys.,I2,I24.
Hashim,A.and Bercovitch,M.(I972),Planet.Space Sci.,20,79I.
Kananen,H.,Komari,H.,Tamskanen,P.and Oksman,J.,(I98I), I7th ICRC,IO, I90 .
Swinson,D.B.and Kananen,H.,(I982),J.Geophys.Res.,87,I685.
Swinson,D.B.,(I983),I8th ICRC, IO, 55 .

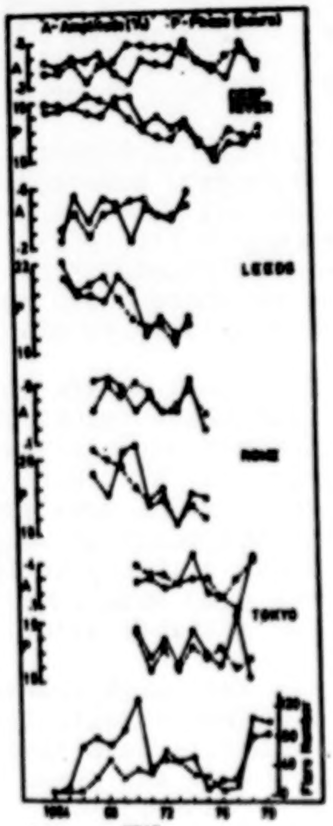

Fig.1

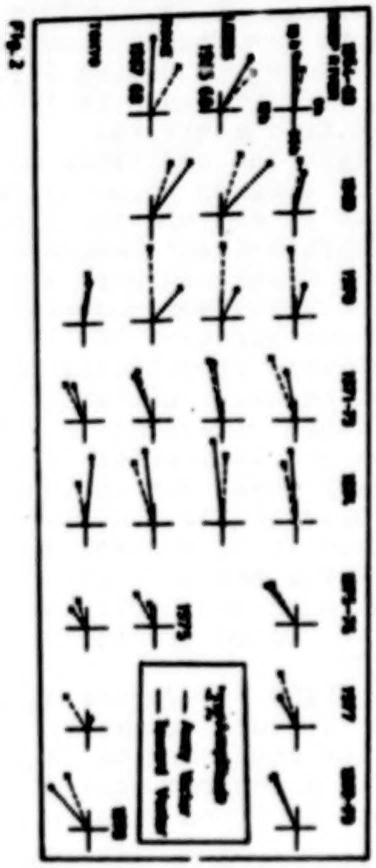

Fig.I shows average amplitude(A) and phase(P) of away polarity days(solid line) and towards polarity days(broken line)from I964-79.The diagram in the bottom shows the major solar flares numbers in respective years in northern(circle) and southern(crosses) hemispheres.
Fig.2 shows the average diurnal vectors on away polarity days(solid line)and towards polarity days(broken line) for the years and stations indicated.

N85-35035

Anomalous Increase of Solar Anisotropy above 150GV in 1981-1983

H.Ueno, Z.Fujii, S.Mori*, I.Morishita** and K.Nagashima
Cosmic Ray Res. Lab., Nagoya Univ., Nagoya 464, Japan
*Department of Physics, Shinshu Univ., Matsumoto 390, Japan
**Gifu College of Dentistry, Gifu 501-02, Japan

Abstract

An analysis was carried out of the observed data with Nagoya(surface), Misato(34mwe) and Sakashita(80mwe) multi-directional muon telescopes, for the solar activity maximum period of 1978-1983. These data respond to primaries extending over the median rigidity range 60GV to 600GV.

The observed amplitude at Sakashita station in 1981-1983 increased, especilly in 1982; the amplitude is twice as large as that in 1978-1980, when those at Nagoya and Misato stations are nearly the same as those in 1978-1980.

Uni-directional anisotropy is derived by the best fit method by assuming the flat rigidity spectrum with the upper cutoff rigidity Pu. The value of Pu obtained is 270GV in 1981-1983 and 150GV in 1978-1980.

1. Introduction

Earlier analyses (e.g., Rao et al.; 1963, Jacklyn et al.; 1970) have shown that the steady-state solar diurnal anisotropy of cosmic rays is rigidity independent up to the upper cutoff rigidity Pu which varies from 50GV to 100GV according to the characters of solar-controlled electromagnetic conditions in the heliomagnetosphere. So far, the obtained values of Pu were dependent on the rigidity range of the data used. To investigate the year-to-year changes of Pu, an analysis over a wide range of rigidities is most necessary during various levels of solar activity.

Since 1978, Sakashita underground multi-directional muon telescope has been in routine operation at the depth of 80mwe and 6-year data have been accumulated. The following observed fact is obtained that the amplitude increases for the period of 1981-1983, especially in 1982. This shows a very remarkable contrast to rather invariant variations at Nagoya and Misato for these years. On the other hand, the observed phases are gradually recover to the 18 hr direction from 1978 due to systematic changes by 22-year modulation.

In the present report, we try to derive the solar diurnal anisotropy responsible for the observed variations showing the above mentioned characteristics.

2. Data and Analysis

In the present analysis, the observed data from Nagoya, Misato and Sakashita stations are exclusively used, then these data are hereafter abbreviated as NAMS by picking up the top letter of these NAgoya, Misato and Sakashita stations. The observed variations are corrected for the Compton-Getting effect due to Earth's orbital motion (.046%,6hr in space), and the corrected variations are used as the basic data in the present analysis.

In Table 1, 3 year averages of the observed solar diurnal variations of NAMS are shown, together with some characteristics of the component

ORIGINAL PAGE IS
OF POOR QUALITY

Table 1 NAMS solar diurnal variations corrected for Compton-Getting effect due to earth's orbital motion and the characteristics of NAMS telescopes. Errors in the amplitudes are determined by the dispersion of yearly vectors.

		Zenith & Azimuth		Geographic Direction		Median Rigidity	Counting Rate	3 Years Averages of Amplitude(%) & Phase(hr) of Solar 1st Harmonics	
STATION	TELESCOPE	Z	A	λ	φ	P_{ME}(GV)	$\times 10^4$/hr	'78-'80	'81-'83
NAGOYA 0mwe	V	0°	-	35°N	137°	60	276.0	.218±.035 12.0	.207±.014 13.3
	N	30°	0°	65°N	"	66	125.0	.204±.063 10.8	.189±.031 12.0
	E	"	90°	30°N	172°	67	120.0	.225±.072 10.6	.221±.034 11.9
	S	"	180°	5°N	137°	64	123.0	.214±.024 12.7	.212±.028 14.1
	W	"	270°	30°N	102°	63	126.0	.182±.016 13.3	.170±.030 14.8
MISATO 34mwe	V	0°	-	36°N	138°	145	28.0	.136±.015 13.4	.145±.024 14.9
	N	33°	39°	57°N	177°	155	10.7	.131±.042 11.4	.152±.018 12.8
	E	"	129°	12°N	164°	143	14.2	.151±.032 12.3	.175±.018 13.9
	S	"	219°	9°N	117°	155	10.7	.124±.025 15.3	.157±.048 16.9
	W	"	309°	51°N	95°	156	9.8	.090±.010 14.5	.091±.012 15.9
SAKASHITA 80mwe	V	0°	-	36°N	138°	331	39.0	.066±.015 14.2	.091±.013 15.8
	N	41°	346°	73°N	104°	401	6.2	.030±.026 12.8	.037±.015 15.6
	E	"	76°	35°N	188°	384	7.6	.064±.027 12.3	.086±.014 13.5
	S	"	166°	5°S	147°	387	6.7	.061±.014 14.8	.097±.015 15.7
	W	"	256°	18°N	96°	444	5.6	.046±.013 16.4	.068±.008 19.2
	NN	60°	346°	77°N	26°	595	2.4	.017±.028 12.4	.002±.031 6.9
	SS	"	166°	23°S	151°	540	2.7	.028±.011 14.0	.065±.029 16.1

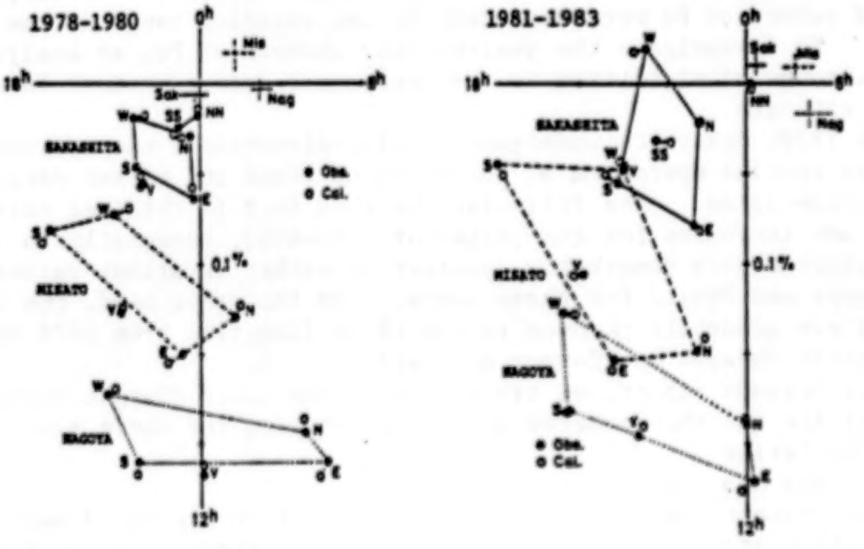

Fig.1(a)

Fig.1(b)

Fig.1 Solar diurnal variation of NAMS in the period of 1978-1980 (Fig.1 a) and of 1981-1983(Fig.1 b).
Solid circles represent the vectors observed, and open circles are those reproduced from the best fit anisotropies. The three kind of cross are respectively the common vectors of each station calculated by the least squares method.

telescopes used and are plotted in Fig.1(a) for 1978-1980 and in 1(b) for 1981-1983 with dotted circles(•).

The solar diurnal anisotropy responsible for the observed variations was determined. Space harmonic vector(X,Y) responsible for the diurnal variation is related to the observed harmonic vector(a_{ij}, b_{ij}) of the j-th component telescope at the i-th station by the following equation with coupling coefficients c_{ij} and s_{ij}.

$$a_{ij} = (c_{ij}X + s_{ij}Y) + a_{ci}, \quad b_{ij} = (-s_{ij}X + c_{ij}Y) + b_{ci} \qquad (1)$$

where (a_{ci}, b_{ci}) represents the unknown vector common to all the components for i-th station. By the least squares method with equal weight for each component, the unknown quantities(X,Y) and (a_{ci}, b_{ci}) were determined for the flat rigidity spectrum with the upper cut-off rigidity Pu, which is taken every 10GV from 50GV to 200GV and so on. The coupling coefficients were referred to the table presented by Fujimoto et al. (1984).

Table 2 Best-fit quantities of anisotropy

	1978-1980	1981-1983
Amplitude in space	0.377 ± 0.016 %	0.320 ± 0.010 %
Direction of anisotropy	15.8 ± 0.2 hr	17.0 ± 0.1 hr
Upper cut-off rigidity	150 ± 10 GV	$270 \pm ^{35}_{20}$ GV

The best-fit parameters are obtained for two periods; 1978-1980 and 1981-1983 and these are shown in Table 2. Also in Figs. 1(a) and 1(b), the reproduced vectors for each component in the best fit case computed by eq.(1) are shown with open circles(○), where the cross marks (┼, ┼, ┼) represent the common vector (a_{ci}, b_{ci}) for each station. As is shown in Figs. 1(a) and 1(b), a good agreement between the observed and the reproduced vectors is clearly seen, suggesting uni-directional anisotropy having the characteristics given in Table 2, is well consistent with the present observations.

Year-to-year basis calculation was also performed by the same method. Best-fit quantities

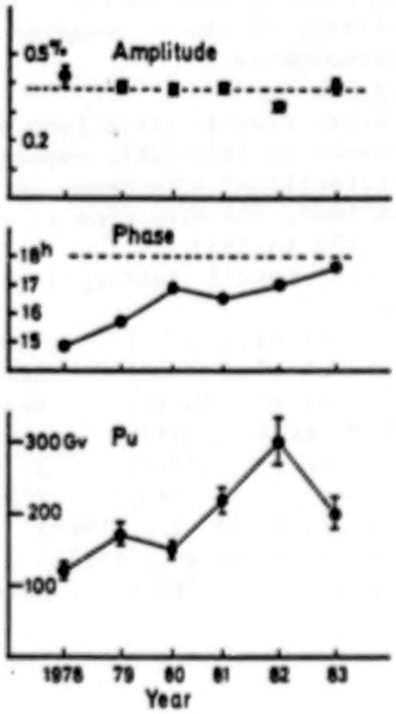

Fig.2 Year-to-year variations of the obtained amplitude, the phase and the upper cutoff rigidity of the solar diurnal anisotropy. Errors in P_U are replaced from the errors of the amplitudes of the anisotropy obtained by the least squares method.

of the anisotropy are shown in Fig.2 as a function of time from 1978 to 1983. As seen in the figure, the amplitude of the anisotropy remains invariant with time for these 6 years. The direction of the anisotropy gradually recovers to 18 hr level. The upper cutoff rigidity varies with time from 100GV to 300GV, particularly Pu in 1982 is extremely higher than those so far reported (Davies et al., 1977, Fenton et al., 1983).

3. Discussions

The increase of solar diurnal variation around 1982 has been observed at London(Thambyahpillai; 1983), Socorro(Swinson; 1983) and Takeyama (Wada et al.; 1985), by the underground muon telescopes at the depth deeper than 60mwe, where the amplitudes are nearly twice as large as in 1978-1980 similar to that at Sakashita station. The origin of the increase of Pu from 150GV to 300GV is yet unknown, but it may be considered to be due to some effect of strong solar activity or the influence of the field reversal resulted in the transition of the heliomagnetosphere from positive state to the negative.

Solar activity of the cycle 21 reaches its first maximum at the end of 1979 and increases again with the second maximum at about Sep. 1981. The cosmic ray intensity minima observed by neutron monitors which correspond to the solar activity maxima are in the middle of 1980 and much lower in July of 1982. In 22-years ago after the period of the maximum solar activity since the start of the cosmic ray observation and at the same phase of the field reversal as in 1981-1983, the cosmic ray neutron intensity had the double minima in Apr. 1958 and in July 1959. At that time, the solar diurnal variations did not increase at London(60mwe, Thambyahpillai et al.; 1965). These facts are very important for the interpretation of the increase of Pu and also for the study of the heliomagnetosphere.

4. Summary

1. The solar diurnal variations observed at Sakashita station remarkably increased in 1981-1983, especially 1982.
2. Uni-directional anisotropy is well consistent with the observed variations, the direction of which gradually recovers to 18 hr level from 1978 to 1983.
3. The upper cutoff rigidity is obtained as 300GV in 1982.

References

Davies S.T. et al., (1977) ICRC(Plovdiv), 4, 7.
Fenton A.G. et al., (1983) ICRC(Bangalore), 10, 186.
Fujimoto K. et al., (1984) Rep. CRRL, Nagoya Univ., No.9.
Jacklyn R.M. et al., (1970) Acta Physica Hungaricae, 39 Suppl. 2, 47.
Rao U.R. et al., (1963) J. Geophys. Res., 68, 345.
Swinson D.B., (1983) ICRC(Bangalore), 10, 55.
Thambyahpillai T. et al., (1965) ICRC(London), 1, 138.
Thambyahpillai T. et al., (1983) ICRC(Bangalore), 3, 383.
Wada M. et al., (1985) Private Communication.

N85-35036

DIAGNOSTIC OF ELECTROMAGNETIC CONDITIONS IN SPACE USING COSMIC RAYS

V.M.Dvornikov, V.E.Sdobnov, A.V.Sergeev

Siberian Institute of Terrestrial Magnetism, Ionosphere and Radio Wave Propagation, USSR Academy of Sciences, Irkutsk 33, P.O.Box 4, USSR

Abstract. The method of spectrographic global survey was used to study the time variations in parameters of cosmic ray (CR) pitch-angle anisotropy and their relationship with the variations of some solar wind characteristics under different electromagnetic conditions in interplanetary space. A classification is made of the conditions that are accompanied by the increase in CR anisotropy.

According to the new ideas, under development now, of the physics of modulational effects of cosmic rays (CR) in the heliosphere /1, 2/, the crucial influence upon the CR distribution function in interplanetary space is exerted by effects that are accumulated during a multiple rotation of particles in a Larmor circumference: drift motions, variations in pitch-angle due to an approximate conservation of the transverse adiabatic invariant and particle energy variations in regular fields of solar wind (SW).

The development of these ideas has been stimulated by the obtained phenomena of strong pitch-angle anisotropy of CR during Forbush-effects /3/ whose explanation in terms of a convection-diffusion model /4/ renders itself impossible.

In the context of the model under development, strong pitch-angle CR anisotropy is a reflection of structural features of large-scale fields in interplanetary space due to dynamical processes in the heliosphere, i.e. it is some kind of an indicator of these processes.

The aim of the present work is to study the time variations in parameters of CR pitch-angle anisotropy and their relationships with the variations in some SW characteristics under different electromagnetic conditions in interplanetary space. The analysis has been carried out using the method of spectrographic global survey (SGS) that has been devised using the physics, under development now, of CR modulational effects in the heliosphere, according to which the variations in particle flux density in interplanetary space can be described by a function of the form

$$\frac{\delta J}{J}(R,\psi,\lambda) = \sum_{n=0}^{N}\Big(\sum_{k=1}^{m_n} a_{nk} R^{-k}\Big) P_n(\mu) =$$

$$= \sum_{n=0}^{N}\Big(\sum_{k=1}^{m_n} a_{nk} R^{-k}\Big)\Big[P_n(\sin\lambda)\, P_n(\sin\lambda_0) +$$

$$+ 2\sum_{m=1}^{n}\frac{(n-m)!}{(n+m)!}\, P_n^m(\sin\lambda)\, P_n^m(\sin\lambda_0)\cos m(\psi-\psi_0)$$

Here $\mu = \cos\theta$, θ is the pitch-angle of a particle in

ORIGINAL PAGE IS
OF POOR QUALITY

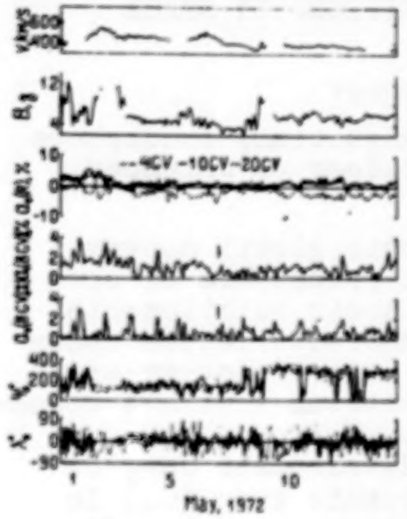

Fig. 1

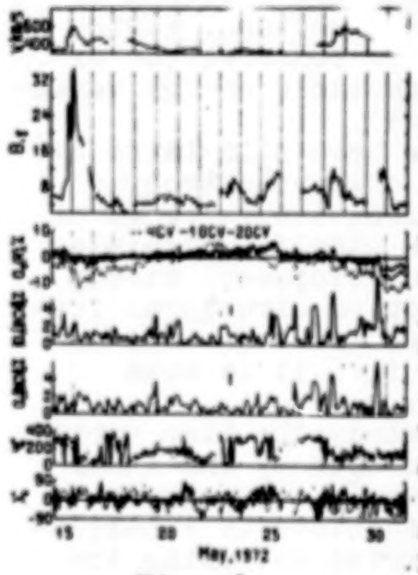

Fig. 2

the IMF, R is the magnetic rigidity of the particles, $P_n(\mu)$ and $P_n^m(\sin\lambda)$ are polynomials and associated Legendre polynomials, ψ and λ are asymptotic angles that determine the direction of the particles outside the magnetosphere in some selected system of coordinates, ψ_0 and λ_0 are the angles that characterize the direction of the IMF vector in this same system, and a_{nk} are the parameters characterizing the amplitudes and rigidity dependences of the isotropic component, and of the first and second harmonics of CR pitch-angle anisotropy. The SGS method makes it possible to determine using ground-based CR observations from the world-wide network of stations, the parameters a_{nk}, ψ_0, and λ_0 (accurate to within π) as well as the variations of the planetary system of geomagnetic cut-off rigidities for each hour of the observations.

The SGS method was used to analyze the variations of the CR distribution function for the periods 1 May through 30 June and 1 through 15 August 1972. The analysis results as well as direct measurements of SW characteristics are presented in Figs 1-5 in the following order (from top to bottom): V - SW velocity, B - IMF modulus; $a_0(R)$-amplitudes of the isotropic component of CR intensity variations for particles of different rigidity; a_1(8GV) and a_2(8GV) are respectively the amplitudes of the first and second harmonics of CR pitch-angle distribution (for R = 8 GV); and ψ_0, λ_0-angles characterising the IMF direction (heavy lines - direct measurements /5/, thin lines - CR data); in addition, Fig. 4 shows the variations in geomagnetic cut-off rigidity ΔR_c at Irkutsk, determined from CR variations, and D_{st} - index).

The comparison between the variations in CR pitch-angle anisotropy and SW characteristics has led to the following classification of the events accompanied by the increase in CR anisotropy of the type considered:

1. Anisotropy increases during powerful SW disturbances (see Figs 2, 4, and 5). During the growth phase of the IMF modulus, the amplitude of the first harmonic ($a_1 \gtrsim 3\%$) increases while during the declining phase, the amplitude of the second harmonic does ($a_2 \gtrsim 3\%$). A minimum flux density of

---

ORIGINAL PAGE IS
OF POOR QUALITY

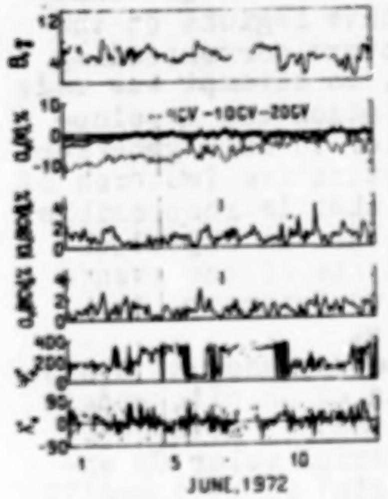

Fig. 3

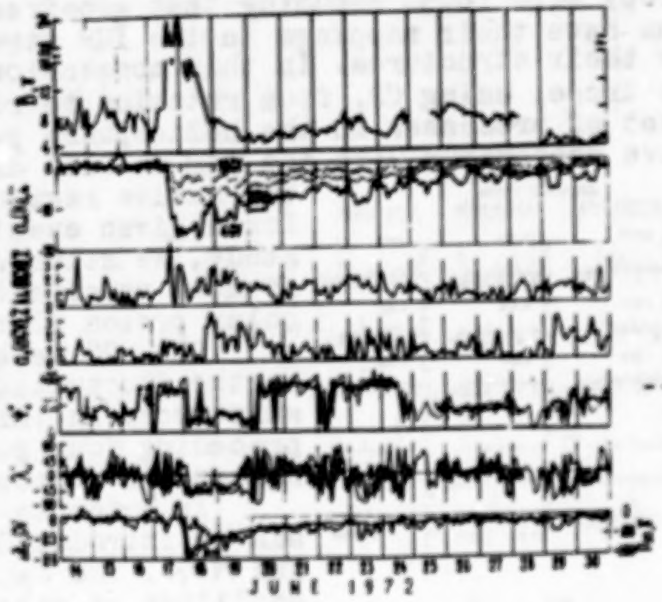

Fig. 4

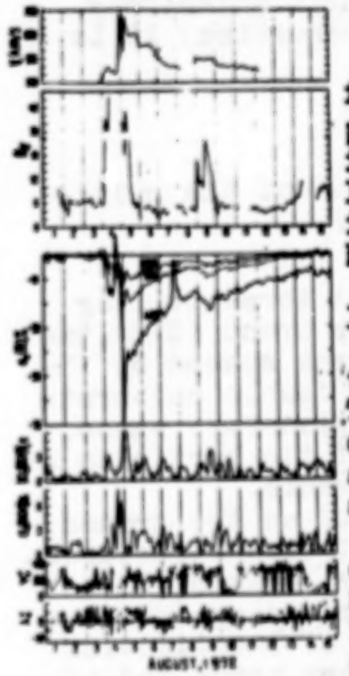

Fig. 5

flow is observed for particles with large pitch-angles. A likely reason might be the influence upon the CR angle distribution of large-scale magnetic traps that form in interplanetary space at propagation of high-speed solar wind streams.

II. Anisotropy increases at places of local decreases in IMF strength (a_1 and $a_2 \sim 2\%$). The character of pitch-angle distribution is the same as for type I events. The likely reason might be trapping and deceleration of particles with large pitch-angles in the traps between the maxima of a random field.

III. Anisotropy increases at places of local increases in IMF strength accompanied by an increase in flux density by 5-15% from some selected direction. In the opposite direction, throughout the entire hemisphere the intensity remains unaltered and is almost independent of the CR direction. This type of anisotropy was observed during 25 to 30 May 1972 (see Fig. 2), with a maximum of the flux density from directions 120-150° westward of the Earth-Sun line and 50-70° southward of the helioequatorial plane. A likely cause of the observed anisotropy may be IMF structures arising as the azimuthal and meridional components of the magnetic field are carried away from the corona. In this case, arrival of CR along the IMF flux tubes is possible from interplanetary space regions (for example, from middle heliolatitudes) where the CR density exceeds significantly the observed density in the helioequatorial region.

IV. Recurrent double enhancements of pitch-angle anisotropy were found assuming that geoeffective regions on the Sun have their mappings in the IMP structure corresponding to their structures. In this connection, an attempt was made to trace, using CR, from rotation to rotation the development of processes in the heliosphere prior to some geoeffective phenomenon with the aim to find distinctive features of the active region that is responsible for a given event. As the object of study, we selected one of the events of most geoeffective interest, the solar proton flares.

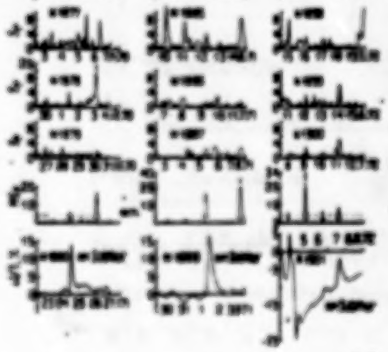

Fig. 6

The SGS method was used to analyze the fluctuations of CR pitch-angle anisotropy in three solar rotations preceding four powerful solar CR enhancements (outbursts) in 1971 and '72.

In order to simplify the analysis we introduced two indices, S_μ and MS_μ. The S_μ-index defines the amplitude of pitch-angle anisotropy at time t_i of the observation; it is calculated in the following way

$$S_\mu(t_i) = \int_R \int_\mu \left\{ \frac{\partial}{\partial \mu} \left[\frac{\delta J}{J}(t_i, R, \mu) \right] \right\}^2 dR\, d\mu$$

We used as the indicator of the recurrent event the multiplicative index $MS_\mu(t_i) = \prod_{k=0} S_\mu(t_i + k\tau)$, where τ is the period of solar rotation.

The analysis (see Fig. 6) revealed that three or four rotations before the onset of a solar proton event (SPE), two comparatively narrow recurrent IMP structures spaced by 15-30° in heliolongitude and causing recurrent double outbursts of CR pitch-angle anisotropy, form in interplanetary space. The character of pitch-angle distribution of the particles at these moments is the same as for type III events.

The four SCR outbursts were all observed on the ground at moments of passage through one of the detected structures. The fact that these structures are identifiable using CR pitch-angle anisotropy in solar rotations preceding SPE can be used for long-term prediction of regions of localization of radiation-dangerous zones in interplanetary space and of times when the Earth enters these zones.

REFERENCES

1. V.M.Dvornikov, Yu.G.Matyukhin, 1976, Izv.AN SSSR, ser.fiz. 40, 624.
2. V.M.Dvornikov, Yu.G.Matyukhin, Izv.AN SSSR, ser.fiz. 43, 2573.
3. V.M.Dvornikov, V.P.Karpov, A.V.Sergeev, 1978, Izv.AN SSSR, ser.fiz., 42, 1043.
4. E.N.Parker. "Dynamical Processes in the Interplanetary Medium", Moscow, Mir, 1965, 216.
5. J.H.King, 1977, Interplanetary Medium Data Book, NSSD C/H--C4.

CHANGE OF COSMIC RAY ANISOTROPY WITH SOLAR ACTIVITY

N.G.Kravtsov, P.A.Krivoshapkin, A.I.Kuzmin,
G.V.Skripin, I.A.Transky, G.V.Shafer

Institute of Cosmophysical Research & Aeronomy
Lenin Ave., 31, 677891 Yakutsk, USSR

ABSTRACT

Muon telescope data at various depths underground in Yakutsk within energy range 10-300 GeV for 1957-1984 are analyzed. 22-year variation of the interplanetary magnetic field aligned component is found. The variation is caused by interaction of heliomagnetosphere with the local galactic field and interstellar wind.

In [1,2] was convincingly shown the existence of 22-year variation of cosmic ray anisotropy aligned with the interplanetary magnetic field. Unfortunately, there are no reliable results on data of ground and underground registration during the end of the 20-th and the beginning of the 21-st solar activity cycle which confirm the result of [1,2].

Here we investigate the long-term variations of cosmic ray anisotropy for 1937-1984 and define the energy range at which the variation is observed. For the analysis were used the Fourier components of mean annual diurnal variation of muon intensity on data of ionization chambers at Cheltenham, Huancayo (1937-1972) and at Yakutsk (1954-1983) and muon telescopes of the Yakutsk underground complex at depths 0, 7, 20 and 60 m w.e. (1958-1984). Data are pressure corrected. To estimate the contribution of the atmospheric temperature into the observed diurnal variation on data of ionization chambers we used the indirect methods. Firstly, we supposed the mean-annual total vector of diurnal temperature fluctuations on the whole depth of atmosphere is practically invariable, at least, for 22 years. In this case the difference vector of the cosmic ray diurnal variation $\Delta\vec{r}_i = \vec{r}_i - \vec{r}_{aver}$ ($\vec{r}_i$ is the observed vector of the diurnal variation for i-year, $\vec{r}_{aver}$ is the average vector for 22 years) is of extra-atmospheric origin.

The observed vector for 1951-1972 at Huancayo and Cheltenham and for 1954-1975 at Yakutsk as $\vec{r}_{aver}$ was taken. We calculated the receiving vectors of the diurnal variation for various mechanism of formation of the cosmic ray anisotropy. In the given case the receiving vectors were used: for Huancayo $z = 0.80e^{-i\cdot 51°}$, for Cheltenham $z = 0.82\ e^{-i\cdot 31°}$; for Yakutsk $z = 0.72\ e^{-i\cdot 31°}$. Secondary, one of the reliable methods of exclusion of the temperature effect is the crossed telescope method which allows to obtain the absolute anisotropy value. In the Table are presented the amplitude and the maximum time of primary anisotropy for 1958-1980 obtained on difference of telescope readings directed southward and northward at an angle 30° relative to vertical at depths 0, 7, 20 and 60 m w.e.

m w.e.	0	7	20	60
Amp., %	0.194±0.008	0.149±0.006	0.118±0.005	0.050±0.009
t_{max}, h	16.0±0.1	15.4±0.2	16.1±0.2	14.8±0.7

It is clear from the Table that at all the levels the maximum time differs significantly from 18^h.

Then we consider the problem on the separation of 11- and 22-year variations of the cosmic ray anisotropy. Two versions of decomposition of the primary anisotropy vector into two components on clock-dial were considered: the first version - into components along $9\text{-}21^h$ and $6\text{-}18^h$ lines (in Figures 1 and 2 the open circles), the second version - along $9\text{-}21^h$ line and the line of anisotropy maximum time for 22 years (the Table and closed circles in Figures 1,2).

In Fig.1 and 2 the ionization chamber data for 1937-1953 are for Huancayo and Cheltenham stations and for 1954-1983 are for ASK-1 Yakutsk. The statistical accuracy of determination of anisotropy components for the first period is ±0.01%, for the second one is ±0.004%.

In Fig.1 the 22-year cosmic ray anisotropy variation is shown. As seen from the Fig.1 it is observed at all the registration levels except 60 m w.e. At the 20 m w.e. depth where the effective energy of registered patricles is ~ 70 GeV, its amplitude is 0.05%.

Note that in the case of the first version of decomposition the point scattering increases. More pronounced variation is observed at a longer set of data of ionization chambers. The magnetic field of the northern solar hemisphere (a dashed line in Fig.1) which was estimated on a number of polar faculaes [3] evidences the negative correlation with 22-year anisotropy variation along the $9\text{-}21^h$ line. When the interplanetary magnetic field being in the north part of the ecliptic is directed from the Sun the cosmic ray anisotropy is field-aligned to the Sun. If in the same region the field sign changes to opposite then the anisotropy will be directed field-aligned from the Sun. At the moment of sign-change of general magnetic field of the Sun the 22-year wave in Fig.1 crosses the zero line. It is clear from Fig.2 that the 11-year cosmic ray anisotropy variation is observed as well at all the depths which is probably caused by the decrease of regularity degree of the interplanetary magnetic field at solar activity minima. From the Table it follows that the maximum time of anisotropy caused by convective-diffusive process for 23 observation years is $15\text{-}16^h$. It means that the inhomogeneous solar wind is of a flattened form.

The obtained temporal change of the galactic cosmic ray anisotropy can be caused by the peculiarities of interaction of the heliomagnetosphere with the local interstellar magnetic field. It is known that the local galactic magnetic field (Orion's arm field) is oriented in the direction of solar apex ($\alpha = 20°$, $\delta = 35°$) and the speed vector of the interstellar wind ($\sim$ 20 km/s) lies in the plane of the ecliptic at the angle 53° with respect to the direction of the field (see references in [4]).

In [5,6] a model of opened and closed configurations of the heliosphere was proposed. The opened heliosphere is formed if the solar magnetic field in the northern hemisphere is derected outward, the closed one - at the opposite field orientation. In the first case the galactic cosmic rays penetrate into the heliosphere along force lines in polar regions, in the second case the penetration occurs by a diffusion way.

In the given here model it is not taken into account that the solar wind speed increases while moving away from the solar equator [7] and the magnetic field in heliosphere polar regions forms a structure of magnetic cork type. Therefore even in the case of the "opened" heliosphere the galactic cosmic rays penetrate mainly by a diffusive way. Besides, particle transfer within the inner part of the heliosphere from high latitudes to low ones is rather slow due to a small ratio of perpendicular diffusion coefficient to the parallel one ($D_\perp/D_\parallel \ll 1$). On the whole the approach to be solution of considered problem can be retained if to assume that at the opened configuration the local galactic field and the heliosphere field under interaction dissipate in a restricted narrow layer enveloping the part of the heliosphere where the interstellar wind blows. The energy of magnetic fields passes to the plasma of the interaction region and spreads along force lines [8] .

Thus in the case of the opened heliosphere an additional diffusion outflow of particles from the heliosphere in the plane of ecliptic can be formed which compensates the wind speed increase at high latitudes. Due to the condition $D_\perp/D_\parallel \ll 1$ the additional current for particles, at least, at 20 m w.e. will be directed along force lines, mainly. At the opposite orientation of the magnetic field

ORIGINAL PAGE IS
OF POOR QUALITY

of the heliosphere the supersonic interstellar wind causes the field increase (beyond the region of a possible heliomagnetosphere "tail") and therefore some excess of cosmic rays. It leads, in its turn, to the increase of the diffusive stream of cosmic rays directed inside the heliosphere.

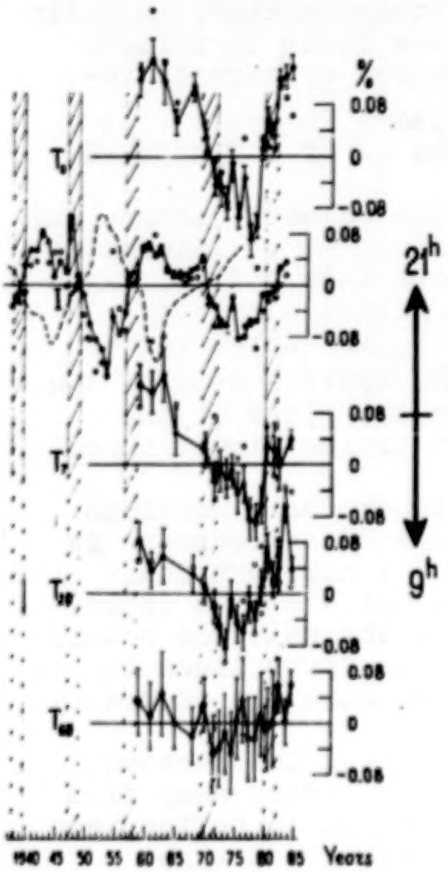

Fig.1. 22-year variation of cosmic ray anisotropy. T_o, T_7, T_{20}, T_{60} are muon telescope data at the 0, 7, 20 and 60 m w.e., I is ionization chamber data. Dashed line - magneric field of northern hemisphere of the Sun

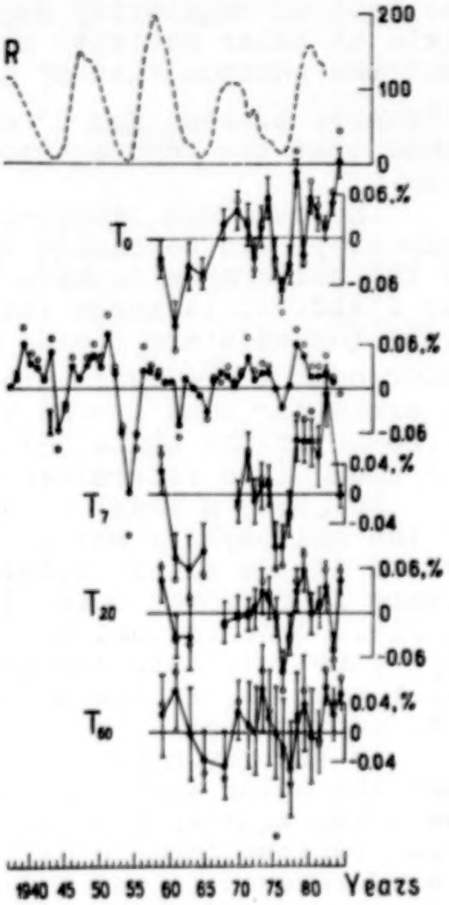

Fig.2. 11-year variation of cosmic ray anisotropy. R is solar activity (sunspot numbers). I, T_o, T_7, T_{20}, T_{60} the same as in Fig.1

References

1. Forbush,S.E.,(1969) J.Geophys.Res., 74, 3451.
2. Forbush, S.E.,(1972) J.Geophys.Res., 78, 7933.
3. Sheeley, N.R.,Jr.,(1976) J.Geophys.Res., 81, 3462.
4. Baranov, V.B., Lebedev M.G. et al.,(1979) Astrophys.Space Sci., 66,429.
5. Shatten, K.H., Wilcox J.,(1969) J.Geophys.Res., 74, 4157.
6. Ahluwalia, H.S.,(1979) Proc.16-th ICRC, Kyoto, 12, 216.
7. Efimov,A.I., Lotova,N.A.,(1975) Kosmich.issled.,13,603.
8. Parker, E.N. Kosmicheskiye magn.polya,I,(1982)M.:Mir.

N85-35038

MAGNETIC FLUCTUATIONS AND COSMIC RAY DIURNAL VARIATIONS

J. W. Bieber and M. A. Pomerantz
Bartol Research Foundation of The Franklin Institute
University of Delaware, Newark, Delaware 19716

ABSTRACT

A unified theory of cosmic ray diurnal variations has been proposed in which the first 3 harmonics of the cosmic ray daily variation all result from a single anisotropy produced by the combined effects of adiabatic focusing and anisotropic pitch angle scattering. The purpose of the present report is twofold: (1) to simplify and improve the theoretical description of steady-state cosmic ray anisotropies, and (2) to present and discuss, in light of the theory, preliminary results of a study of correlations between cosmic ray diurnal variations and the fluctuation characteristics of the interplanetary magnetic field.

1. Theory. Several theoretical investigations of energetic particle anisotropies (Roelof, 1969; Kunstmann, 1979; Earl, 1981) suggest that observed anisotropies may appropriately be cast in the form of a simple analytic solution of the steady-state Boltzmann equation, which, according to Earl (1981), is given by

$$f = c_0 + c_1 \, B \exp\left\{ \frac{(4-q)\lambda}{3\,L} \, \mu \, |\mu|^{1-q} \right\} . \qquad (1)$$

Here, f is the phase space density, c_0 and c_1 are constants, B is the magnetic field magnitude, q is a parameter characterizing the anisotropy of pitch angle scattering, λ is the scattering mean free path, L is the focusing length (~ 0.94 AU for the nominal Parker field at Earth), and μ is the cosine of the particle pitch angle. The property of (1) relevant to the present work is that it has a non-sinusoidal form, and hence will naturally contribute higher order harmonics to the cosmic ray daily variation observed by ground-based instrumentation.

For reasons connected with geomagnetic correction of neutron monitor observations (Yasue et al., 1982), it is convenient to express the free space anisotropy as a Legendre series. Figure 1 shows the relationship between the parameters λ/L and q and the coefficients a_l of the Legendre expansion of (1). Note that a measurement of the 3 coefficients a_1, a_2, and a_3 serves to determine uniquely the values of both λ/L and q. Figure 1 thus allows values of interplanetary scattering parameters to be inferred from measurements of cosmic ray diurnal variations.

ORIGINAL PAGE IS
OF POOR QUALITY

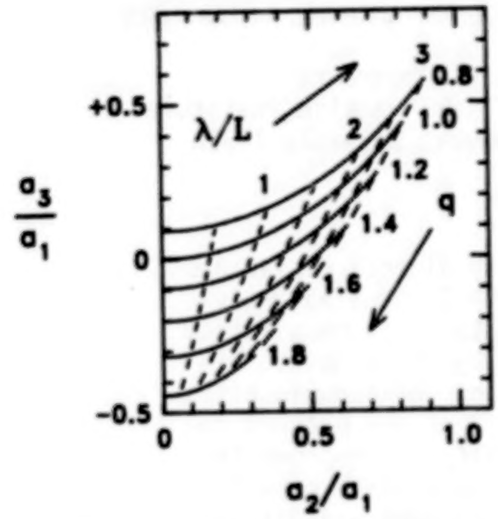

Fig. 1. Lines of constant λ/L (dashed) and constant q (solid) are plotted in a coordinate system representing ratios of the coefficients a_i of a Legendre series expansion of the exponential anisotropy (1). The coefficients a_1, a_2, and a_3 are closely related to the first, second, and third harmonics, respectively, of the cosmic ray diurnal variation.

Bieber and Pomerantz (1983) used essentially this procedure to infer values for λ and q from an analysis of 12 years of neutron monitor data. However, that earlier analysis expressed the anisotropy as a first-order focusing eigenfunction, which is closely related to the exponential (1), but which differs somewhat in the quantitative prediction of harmonic amplitudes. Because the exponential anisotropy is derived from the steady-state Boltzmann equation which includes the effect of a field-aligned density gradient, as well as the effects of focusing and scattering, it should be the more accurate approximation to actual cosmic ray anisotropies in most circumstances. If the observational results of Bieber and Pomerantz are re-interpreted in terms of the exponential anisotropy, then the long-term average of the scattering mean free path at 10 GV changes from 0.5 to 0.3 AU, while the long-term average of q remains unchanged at 1.1.

2. Magnetic Fluctuations and Diurnal Variations. In light of the theory described above, it might be expected that cosmic ray diurnal variations would be correlated with the fluctuation characteristics of the interplanetary magnetic field. In particular, one might expect the amplitude of the second harmonic relative to the first to decrease as the fluctuation level increases, since an increase in fluctuations should correspond to a decrease in λ and, according to Figure 1, a decrease in a_2/a_1.

A thorough investigation of this effect would require that the scattering mean free path be calculated from the observed power spectrum of the magnetic field (e.g., Jokipii, 1971). However, for this preliminary study a simpler procedure was chosen in which the fluctuation level is characterized by the relative variance of the magnetic field. Relative variance was calculated on a daily basis by taking the vector variance of observed hourly field vectors and dividing this by the mean-square field. For days in which both toward and away field polarities occurred, the direction of toward vectors was reversed before the variance was taken. Days with fewer than 12 hours of data were excluded from the analysis. The remaining days were then divided into 7 groups according to relative variance, and the first 3 harmonics of the cosmic ray daily variation observed at Swarthmore over the period 1965-1978 were averaged separately for each group.

Results of the analysis appear in Figure 2, where the amplitudes and phases of the first 3 harmonics of the diurnal variation are displayed as a function of relative variance. The only quantity to exhibit a strong dependence upon magnetic fluctuation level is the amplitude of the second harmonic, which decreases significantly at the higher fluctuation levels.

After correction for geomagnetic effects and for the Compton-Getting anisotropy (Bieber and Pomerantz, 1983), the data of Figure 2 may be used to infer values of the interplanetary scattering parameters λ/L and q, as described above. For relative variances in the range 0-0.5, λ/L remains nearly constant at a value ~ 0.35, while for ranges 0.5-0.7 and 0.7-1.0 λ/L decreases to 0.27 and 0.19, respectively. For all values of relative variance the q parameter remains near a value of 1.1.

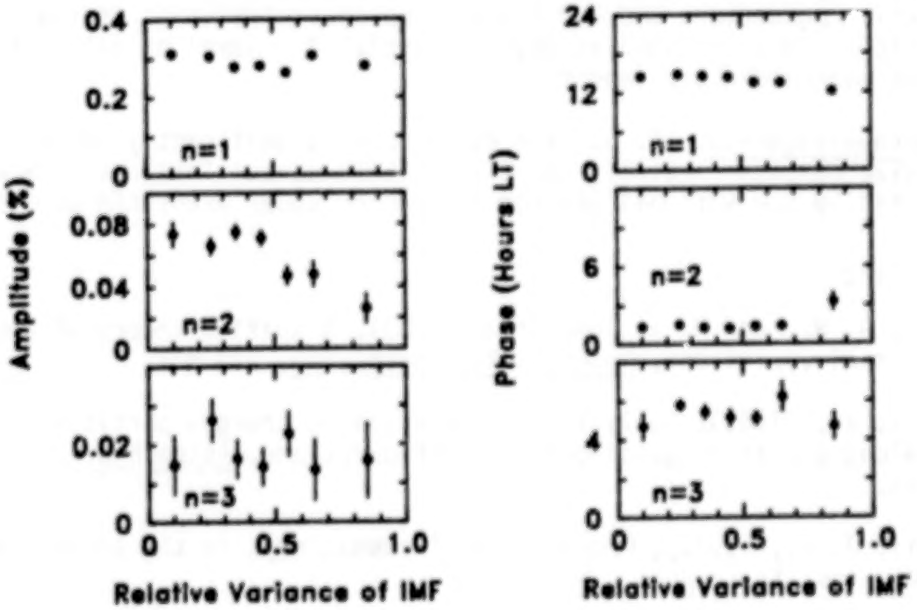

Fig. 2. The amplitudes and phases of the first (top panels), second (middle panels), and third (bottom panels) harmonics of the cosmic ray daily variation observed at Swarthmore are plotted as a function of the relative variance of the interplanetary magnetic field. Data are not corrected for geomagnetic effects or for the Compton-Getting anisotropy. Error bars are ± 1σ.

3. Discussion. The daily variance calculated from hourly-averaged magnetic field vectors will naturally be most influenced by fluctuations with time scales in the range of 1 to 24 hours. This, it turns out, is a very suitable range insofar as the scattering of cosmic rays of neutron monitor energies is concerned, as a cosmic ray of 10 GV rigidity is resonant with waves that have periods ~ 24 hours in the spacecraft frame. Thus, it is reasonable to suppose that the relative variance provides a rough measure of the scattering rate that would be calculated from the actual power spectrum of fluctuations.

Under this hypothesis, the results described above show general agreement with theoretical expectation, in that the mean free path inferred from particle anisotropies decreases at the higher fluctuation levels. There is also a hint of a possible discrepancy, however, in that the inferred mean free path seems to be independent of fluctuation level for relative variances < 0.5.

Further analysis is required to see whether any significance can be attached to this puzzling result. In particular, the characterization of fluctuation level by daily relative variance should be replaced by a careful evaluation of observed magnetic power spectra. This will allow the relationship between interplanetary scattering parameters and the fluctuation characteristics of the magnetic field to be studied quantitatively at a level of detail that has not heretofore been possible.

4. Acknowledgments. C. H. Tsao contributed significantly to the extensive computer analysis involved in this work. This research was supported by the National Science Foundation under grant ATM-8303758.

References

Bieber, J. W., and M. A. Pomerantz, (1983), A unified theory of cosmic ray diurnal variations, *Geophys. Res. Lett.*, *10*, 920-923.

Earl, J. A., (1981), Analytical description of charged particle transport along arbitrary guiding field configurations, *Astrophys. J.*, *251*, 739-755.

Jokipii, J. R., (1971), Propagation of cosmic rays in the solar wind, *Rev. Geophys. Space Phys.*, *9*, 27-87.

Kunstmann, J. E., (1979), A new transport mode for energetic charged particles in magnetic field fluctuations superposed on a diverging mean field, *Astrophys. J.*, *229*, 812-820.

Roelof, E. C., (1969), Propagation of solar cosmic rays in the interplanetary magnetic field, *Lectures in High-Energy Astrophysics*, *NASA Spec. Publ. 199*, edited by *H. Ogelman and J. R. Wayland*, *National Aeronautics* and Space Administration, Washington, D.C.

Yasue, S., S. Mori, S. Sakakibara, and K. Nagashima, (1982), Coupling coefficients of cosmic ray daily variations for neutron monitor stations, *Report of Cosmic-Ray Research Lab*, *No. 7*, Nagoya, Japan.

N85-35039

Changes in the Energy Spectrum of Anomalous Oxygen and Helium During 1977-1985

A. C. Cummings and E. C. Stone

California Institute of Technology, Pasadena, CA 91125 USA

W. R. Webber

University of New Hampshire, Durham, NH 03824 USA

We have used data from the cosmic-ray experiment on the Voyager spacecraft to measure the energy spectrum of anomalous O and He during the period 1977 to 1985. We find that these spectra change dramatically after the middle of 1980, with the peak or plateau region of the differential spectrum shifting to a higher energy. This change appears to be related to the reversal of the solar magnetic field and could imply that particle drifts are important to the acceleration or propagation of these particles.

1. Introduction. The study of the anomalous component of cosmic rays over the solar cycle may prove to be key to the understanding of the role of drifts in cosmic-ray modulation. *Pesses et al.* [1981] have suggested that the acceleration site of the anomalous component is most likely in the polar regions of the solar wind termination shock. In their model the particles drift latitudinally toward the neutral sheet from the polar regions during the last solar cycle, but drift radially inward along the neutral sheet during the current solar cycle. Consequently, they predict a strong dependence of the intensity of the anomalous component near the solar equator on solar magnetic field polarity. In this analysis we make use of measurements of the spectra of O and He from the Cosmic Ray Subsystem (CRS) [*Stone et al.*, 1977] on the Voyager 1 (V1) and 2 (V2) spacecraft to address whether or not these spectra exhibit changes associated with the polarity of the solar magnetic field.

2. Observations. The general features of the 11-year cosmic-ray modulation cycle are evident in the counting rate of the particles which penetrate the high energy telescope on V1, shown in Fig. 1 for 1977-1985. In order to minimize the contamination by solar and interplanetary energetic particles, quiet times were selected by setting limits to the maximum low-energy He flux, in a manner similar to that described in *Cummings et al.* [1984]. The six quiet-time periods that were selected for analysis for V1 are shown as horizontal bars in Fig. 1 and are labeled A through F. Also shown are the approximate times of the reversal of the solar polar magnetic fields [*Webb et al.*, 1984]. Note that the field reversal occurs approximately between periods C and D.

The anomalous O spectrum for the Voyager measurements is derived from the observed total O spectrum for a particular time interval by subtracting a low-energy solar or interplanetary component and the high-energy galactic cosmic-ray component. This subtraction procedure is illustrated in Fig. 2 for two extreme examples. The low-energy component is scaled and extrapolated from a power-law fit to the observed He spectrum in the energy range 3-6.1 MeV/nuc using a ratio He/O = 100 ± 50 (see *Gloeckler et al.* [1979]). The galactic cosmic-ray O component is estimated by normalizing the observed carbon spectrum to the O intensity in the 66-125 MeV/nuc energy interval.

Figure 3 shows the spectra of anomalous O for the six quiet-time intervals A through F derived from the V2 observations in the manner just described. The a and b panels show the spectra for the three intervals before and after the solar magnetic field reversal in 1980, respectively. The spectra for intervals A, B, and C are essentially monotonic with a tendency to flatten into a peak or plateau at less than ~6 MeV/nuc. It is clear from Fig. 3b that the energy dependence of the spectra for the intervals after the field reversal (D, E, and F) is significantly different, having a peak or plateau at ~10-20 MeV/nuc.

A similar change in the energy spectrum is also apparent in the V1 data. In Fig. 4a we show the V1 observed O spectra for intervals B and F. The galactic cosmic-ray intensity is dom-

ORIGINAL PAGE IS
OF POOR QUALITY

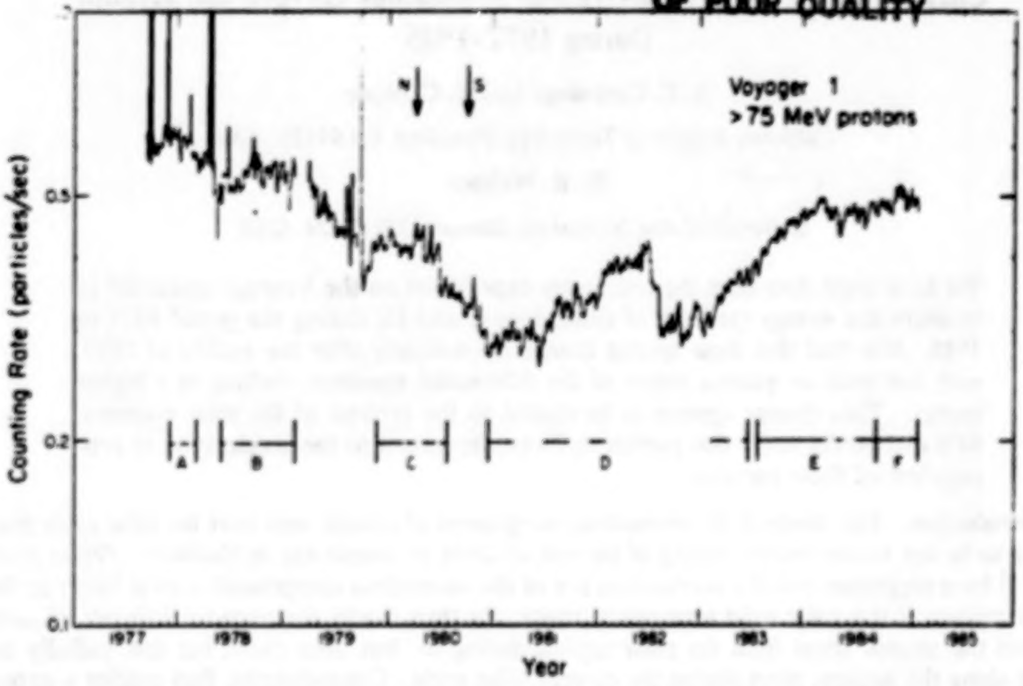

Fig. 1. Three-day average counting rate of penetrating particles in the HET 1 (High-Energy Telescope number 1) of the V1 CRS instrument from 1977 to 1986. The rate is dominated by protons with energy > 75MeV. The bars and arrows are described in the text.

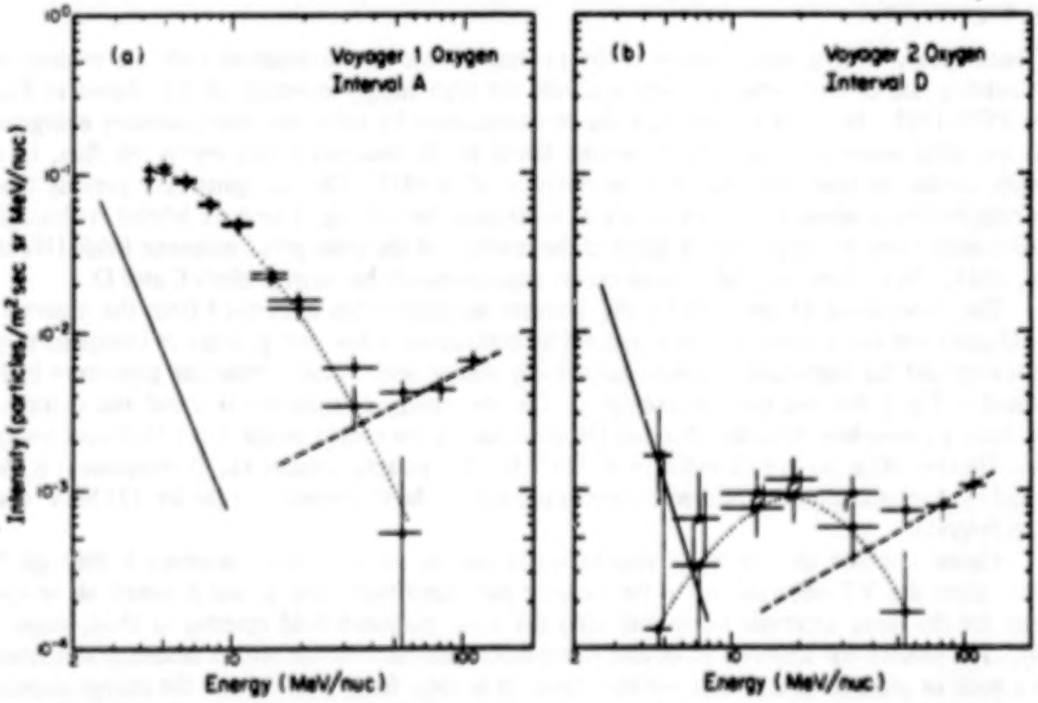

Fig. 2. Quiet-time energy spectra of O from Voyager data for two sample time intervals. The observed spectra are shown as the solid circles. Estimated spectra of interplanetary and galactic components are shown as solid and dashed lines, respectively. The spectra of anomalous O are indicated by the open squares which are joined by the dotted lines.

ORIGINAL PAGE IS
OF POOR QUALITY

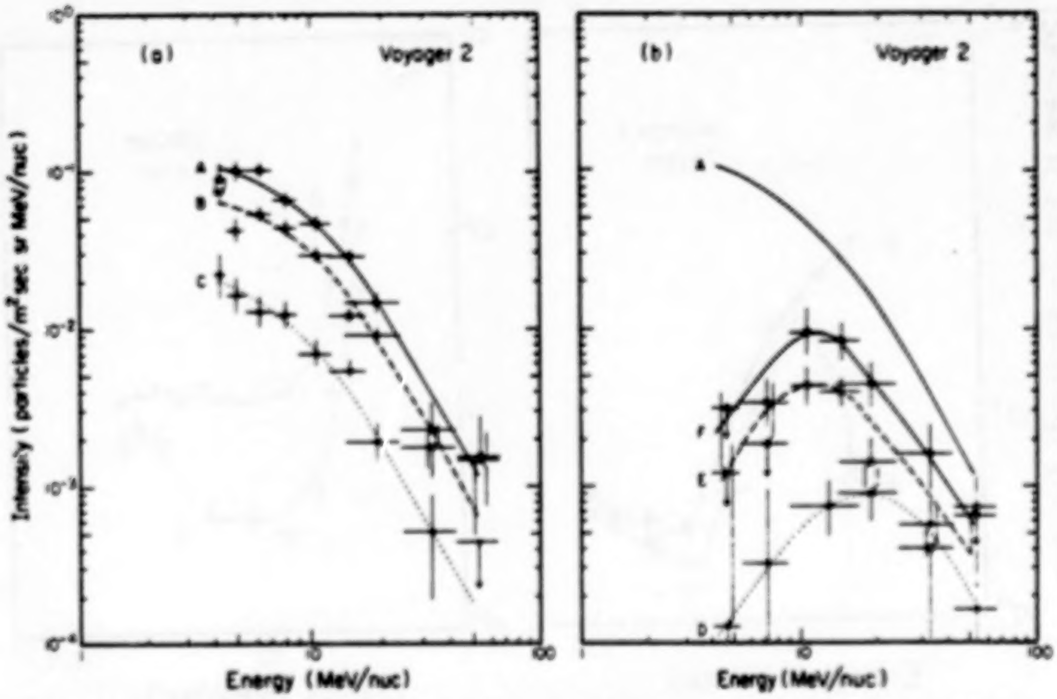

Fig. 3. Spectra of anomalous O from V2 for the six quiet-time intervals. Panels a and b show the spectra for periods before and after the solar magnetic field reversal, respectively. The smooth curves are drawn to aide the eye and are not functional fits to the data. The dashed line labeled "A" in panel b is copied from panel a to facilitate comparison. Note the higher energy of the peak (or plateau) intensity of the spectra in panel b when compared to those of panel a.

inant in the 50-125MeV/nuc energy range for both time intervals. The intensity in this energy range is only ~20% higner for interval B than for interval F, indicating that a similar level of modulation has been reached. Similarly, the anomalous O intensity in the 10-30MeV/nuc energy range is approximately the same for the two time intervals. However, below 10MeV/nuc there is a factor of 10 difference in intensity producing a striking difference in the spectrum.

This change in the energy spectrum is also evident in the He data. We show in Fig. 4b the observed He spectrum for the same two intervals as for Fig. 4a. Below ~8MeV/nuc a low-energy solar or interplanetary component is dominant and causes a sharp upturn in the spectrum. For interval B the flat region of the spectrum from ~8to50MeV/nuc indicates that anomalous He is the primary component, dominating the flux of solar and galactic cosmic rays. The period F spectrum has a much lower intensity than the period B spectrum below ~30MeV/nuc suggesting that the anomalous He spectrum has shifted to higher energies. If the particles are singly ionized, the energy dependence of the He spectrum is expected to be obtained by shifting the anomalous O spectrum by a factor of ~4 in energy [*Cummings et al.*, 1984], so that the absence of anomalous He below 30MeV/nuc is consistent with the reduced intensity of anomalous O below 8MeV/nuc.

3. Discussion. If the changes in the energy spectra of the anomalous component are to be explained by "conventional" modulation theory, in which the effects of diffusion, convection, and adiabatic deceleration are considered, and the effects of drifts ignored (see *Fisk* [1980], for a review of solar modulation theory), then it would require either a very prolonged "hysteresis" effect or a significant change in the rigidity dependence of the diffusion coefficient between halves of the solar cycle. A hysteresis effect (phase-lag between intensity variations of low-rigidity and high-rigidity particles) has been reported for the anomalous O component by *Klecker et. al* [1980] for the 1974-1975 period. They found a phase lag of 72 days between the intensity of

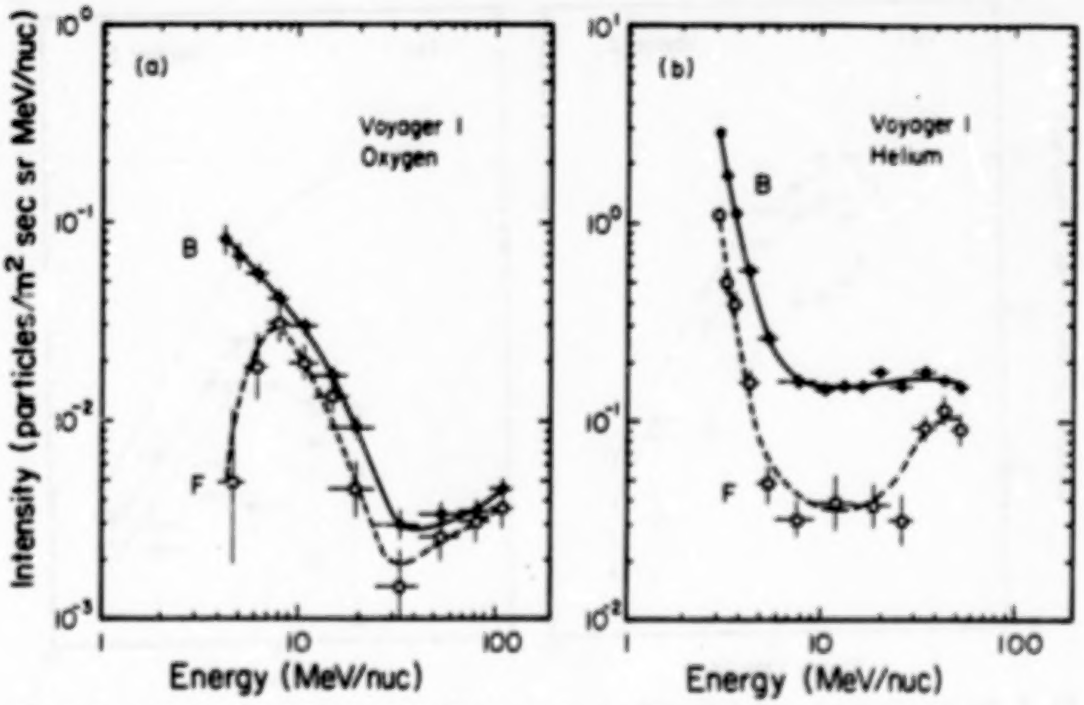

Fig. 4. Spectra of observed O (a) and He (b) for time intervals B and F from V1.

anomalous O with 7.6-24 MeV/nuc and the intensity of galactic cosmic rays with energy > 10GeV. If the energy spectrum changes in our study are to be ascribed to hysteresis, then a phase lag of ~4 years would be required between particles with only modestly different rigidities and velocities. If changes in the diffusion coefficient between halves of the solar cycle are to account for our observations then the spectra of other cosmic-ray species would show pronounced effects at the corresponding rigidities.

It appears more likely, therefore, that the observed time variation of the energy spectra of anomalous O and He may be related to changes in the acceleration of particles at the termination shock due to the change in the polarity of the solar magnetic field. Recently, *Jokipii* [1985] has used a model of the anomalous component which includes acceleration at the termination shock and particle drifts and has calculated spectra of anomalous O and He in the two halves of the solar cycle with different field polarity that resemble the observations reported here.

4. Acknowledgments. We are grateful to R. E. Vogt and other CRS team members at the California Institute of Technology, the Goddard Space Flight Center, the University of Arizona, and the University of New Hampshire. This work was supported in part by NASA under contract NAS 7-918 and grant NGR 05-002-160.

5. References.

Cummings, A. C., E. C. Stone, and W. R. Webber, *Ap. J. (Letters), 287*, L99, 1984.
Fisk, L. A., *Proc. Conf. Ancient Sun*, edited by R. O. Pepin, J. A. Eddy, and R. B. Merrill, (Pergamon Press : New York), 103, 1980.
Gloeckler, G., D. Hovestadt, and L. A. Fisk, *Ap. J. (Letters), 230*, L191, 1979.
Jokipii, J. R., submitted to *J. Geophys. Res.*, 1985.
Klecker, B., D. Hovestadt, G. Gloeckler, and C. Y. Fan, *Geophys. Res. Letters, 7*, 1033, 1980.
Pesses, M. E., J. R. Jokipii, and D. Eichler, *Ap. J. (Letters), 246*, L85, 1981.
Stone, E. C., R. E. Vogt, F. B. McDonald, B. J. Teegarden, J. H. Trainor, J. R. Jokipii, and W. R. Webber, *Space Sci. Rev., 21*, 355, 1977.
Webb, D. F., J. M. Davis, and P. S. McIntosh, *Solar Phys., 92*, 109, 1984.

ORIGINAL PAGE IS
OF POOR QUALITY

N85-35040

SOLAR CYCLE VARIATIONS OF THE ANOMALOUS COSMIC RAY COMPONENT

R. A. Mewaldt and E. C. Stone

California Institute of Technology
Pasadena, California 91125 USA

The intensity of the "anomalous" cosmic ray component, consisting of He, N, O, and Ne, has long been known to be especially sensitive to the effects of solar modulation. Following its discovery in 1972, this component dominated the quiet-time flux of cosmic ray nuclei below ~30 MeV/nucleon during the 1972-1978 solar minimum, but then became essentially unobservable at 1 AU with the approach of solar maximum conditions. One recent theoretical model predicts substantial differences in the intensity of the anomalous fluxes from one solar minimum period to the next because of the reversal of the solar magnetic field. Using data from the Caltech experiments on IMP-8 and ICE (ISEE-3), we report on the intensity of anomalous O and He at 1 AU during the years 1972 to 1985. In particular, we hope to determine whether the anomalous fluxes will return to their 1972-1978 levels, as predicted by spherically symmetric modulation models, or whether they will fail to return to 1 AU, as suggested by modulation models in which gradient and curvature drifts dominate.

Our preliminary analysis of data from 1984 shows that the intensity of 8 to 27 MeV/nucleon O is still more than an order of magnitude below its 1972 to 1978 levels, while the intensity of 25 to 43 MeV/nucleon He is a factor of ~8 below its maximum level in 1977. Data from 1985 is now being analyzed.

This work was supported in part by NASA under grant NGR 05-002-160 and contracts NAS5-28441 and NAS5-28449.

N85-35041

TEMPORAL VARIATIONS OF THE ANOMALOUS OXYGEN COMPONENT, 1977 - 1984

G.M. Mason[1], B. Klecker[2], A.B. Galvin[1], D. Hovestadt[2], and F.M. Ipavich[1]

[1]Dept. of Physics & Astronomy, Univ. of MD, College Park, MD 20742 USA
[2]MPI fur Extraterrestrische Physik, 8046 Garching, FRG

ABSTRACT

We present a survey of the long term temporal variations of 6.6-12 MeV/nucleon anomalous oxygen at 1 AU covering the period 1977-1984. This time interval included the recent solar maximum, with the recovery at neutron monitor energies beginning in 1982. During this time interval, 6.6-12 MeV/nucleon O fluxes decreased by at least a factor of 50, and indeed remained below our instrumental detection threshold after 1979. By late 1984, neutron monitors had recovered to roughly 1979 levels from the 1982 solar maximum, and anomalous O still remained below our detection threshold.

1. Introduction. The 1972 discovery of the anomalous components of He (4), N, O and Ne (1,5,8) added a new particle population to the set available to probe acceleration and transport processes in the heliosphere. Observed over the energy range from a few to a few 10s of MeV/nucleon during the 1972-77 solar minimum, these components display an unusual composition resembling neither galactic cosmic rays nor solar energetic particles. Of the many models suggested to explain the anomalous components, perhaps the most attractive is that by Fisk, Kozlovsky and Ramaty (3), who proposed that the particles begin as interstellar neutrals which are ionized and accelerated in the heliosphere, yielding a particle population in which high ionization potential elements are favored.

A key prediction of this model (3) is that the particles are singly ionized. However, a direct test of this prediction remains beyond the capabilities of any instruments flown to date. Temporal variations, however, may offer clues pertinent to this question. For example, a special temporal behavior has been predicted by Pesses, Jokipii and Eichler (10) in a model where the anomalous component is accelerated at the solar wind termination shock over the solar poles, and the particles subsequently flow down to the ecliptic plane. In this case, particle drifts yield a 22-year modulation cycle, and thus the component would not be expected to re-appear during the upcoming solar minimum. In order to probe these questions we present measurements of ~10 MeV/nucleon oxygen over the period 1977-1984, thus updating our previous report for the years 1974-79 (7).

2. Instrumentation. The measurements presented here were carried out in interplanetary space with the Ultra Low Energy Wide Angle Telescope (ULEWAT), which is part of the MPI/UMD experiments on the ISEE-1 and ISEE-3 spacecrafts. Figure 1 shows a cross sectional view of the ULEWAT, which identifies particle type and energy by the dE/dx versus residual energy method. For the particles discussed in this paper, the flow-through proportional counters P1 and P2 serve as dE/dx elements, and the silicon detector D1 is the residual energy detector. The

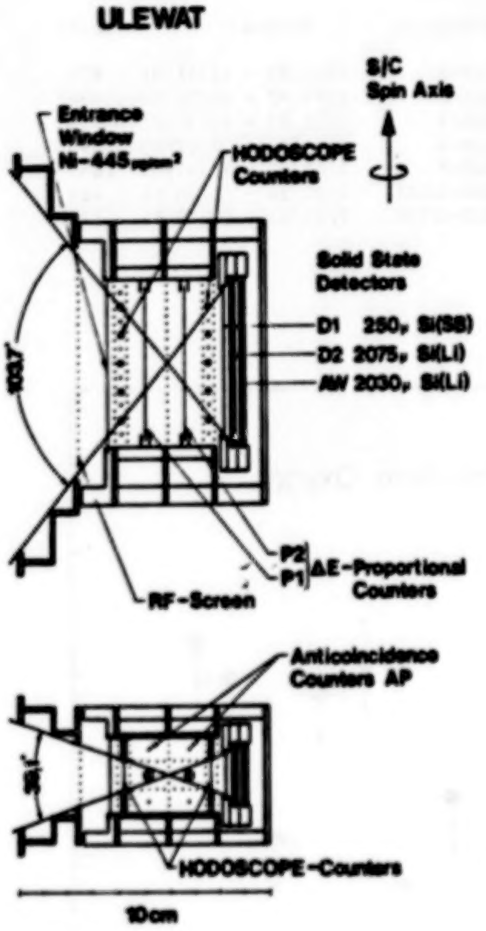
ULEWAT
S/C
Spin Axis
Entrance
Window
Ni-445 μg/cm²
HODOSCOPE
Counters
Solid State
Detectors
D1 250μ Si(SB)
D2 2075μ Si(Li)
AW 2030μ Si(Li)
103.7°
P2
P1
ΔE-Proportional
Counters
RF-Screen
Anticoincidence
Counters AP
38.1°
HODOSCOPE-Counters
10cm

Figure 1

hodoscope detectors shown in the Figure permit correction of the ΔE signals for particles entering the telescope at different angles, thus allowing a wide opening angle while preserving instrument resolution. For the present study, particles with incident angles up to ~25° were accepted, resulting in a geometrical factor of ~1.3 cm^2 sr. A complete instrument description has been published elsewhere (6).

In order to remove the possibility of contamination by, e.g., solar flare particles, a strict criterion was adopted wherein observation times were used only if the counting rate channel for $Z \geq 6$ particles above 300 keV/nucleon counted less than 30 particles in 24 hours of observing time. Assuming E^{-3} spectra, this criterion extrapolates roughly to a level of 10^{-4} particles/sec-m^2-sr-MeV/nuc at 10 MeV/nucleon, a factor of ~500 below anomalous O flux levels during solar minimum. Table 1 lists the observing time periods and number of hours observing time for each point. High levels of solar activity decreased the number of hours of quiet time in some intervals, and, after ISEE-3 was targeted for comet encounter, spacecraft tracking coverage was an important factor.

3. Observations. Figure 2 shows the fluxes and upper limits of 6.6-12 MeV/nucleon quiet time O during the survey period. Note that after the end of 1978, only upper limits are shown. In the figure, upper limit data points plotted with positive standard deviation bars indicate finite O measurements where the spectral information was not sufficient to conclusively identify the particles as part of the anomalous component. Points that are shown as upper limits only are 1-count upper limits. For comparison with the solar modulation at high energies, the lower panel shows 3-month averages of the Deep River neutron monitor as compiled from Solar-Geophysical Data. While the neutron monitor has been increasing since its 1982 minimum, by late 1984 it has not surpassed 1979 levels, and thus it is not surprising that even in 1984 anomalous O remained below our detection threshold.

ORIGINAL PAGE IS
OF POOR QUALITY

Table 1

OBSERVATION PERIODS AND COLLECTION TIMES

Spacecraft	Period	Hours	Spacecraft	Period	Hours
ISEE-1	10/26/77 - 12/30/77	343	ISEE-3	7/01/81 - 12/31/81	635
ISEE-1	01/01/78 - 08/08/78	368	ISEE-3	1/01/82 - 06/30/82	734
ISEE-3	08/14/78 - 12/30/78	784	ISEE-3	7/01/82 - 12/31/82	758
ISEE-3	01/01/79 - 06/30/79	709	ISEE-3	1/01/83 - 07/01/83	1299
ISEE-3	07/01/79 - 12/31/79	684	ISEE-3	7/01/83 - 12/31/83	2058
ISEE-3	01/01/80 - 06/30/80	1148	ISEE-3/ICE	1/01/84 - 06/30/84	418
ISEE-3	07/01/80 - 12/31/80	686	ISEE-3/ICE	7/01/84 - 09/28/84	172
ISEE-3	01/01/81 - 07/01/81	586			

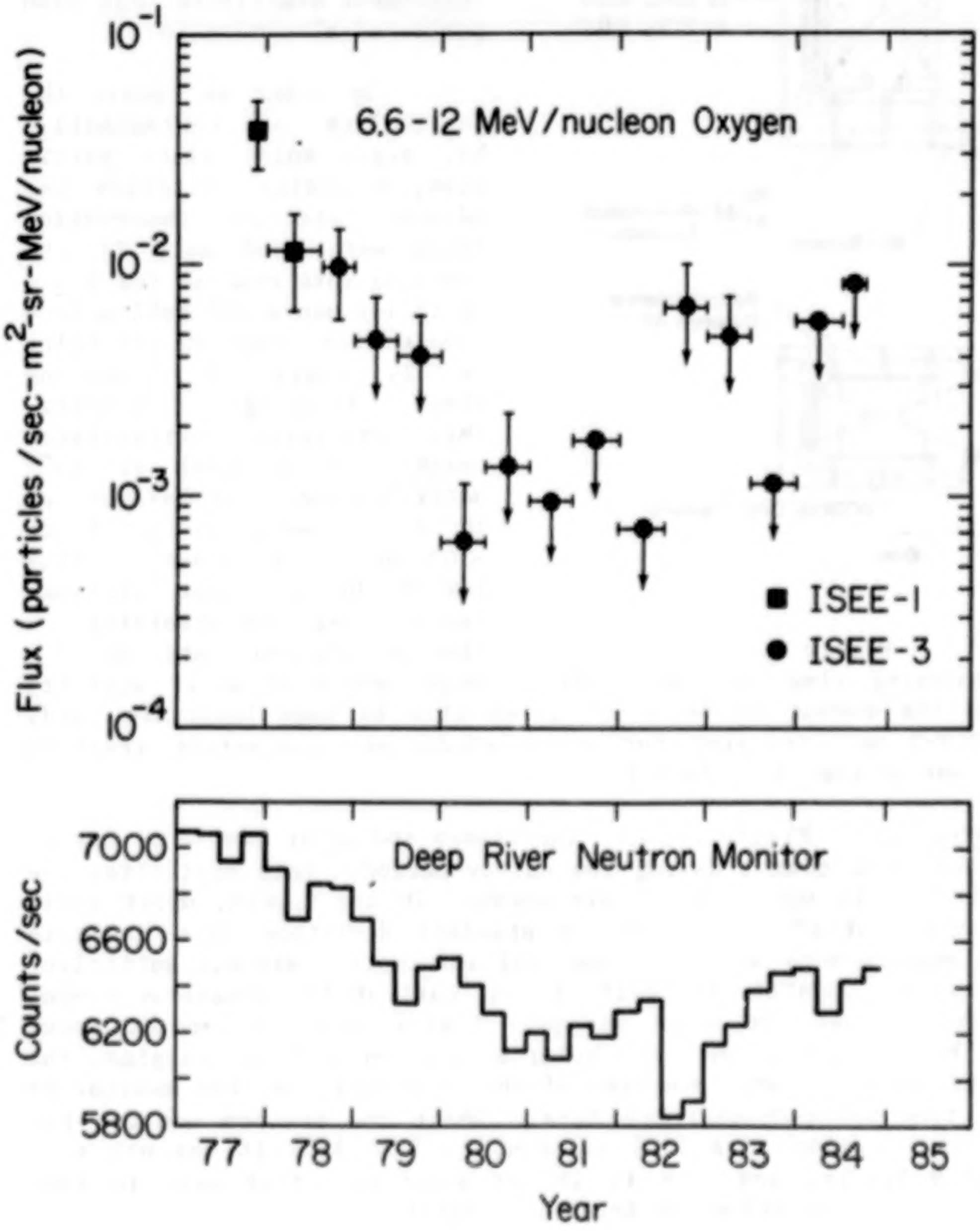

Figure 2

4. Discussion. From Figure 2 it is clear that at 1 AU anomalous O decreased by at least a factor of 50 between 1977 and solar maximum levels in 1981-82. This is much larger than the factor of ~10 observed for cosmic ray protons near 100 MeV (13), but is comparable to the factor of ~30 decrease in 10-20 MeV/nucleon anomalous He between 1977 and 1981 (9). The fact that the anomalous components show greater sensitivity to the solar cycle than galactic cosmic rays may be due to a combination of source (acceleration) and modulation effects; however, the unique spectral shapes of the anomalous components may also play an important role (11).

During the 1977-81 time period the ~10 MeV/nucleon O flux observed on the Voyager spacecrafts decreased also by a factor of ~50 (12), almost the same as the upper limits shown in Figure 2. However, since the Voyagers were at ~10 AU in 1981, the measurements cannot be directly compared with the results presented here. Indeed, since the anomalous He component has typically shown rather large positive radial gradients, the Voyager results could imply an anomalous O flux level at 1 AU a factor of 2 or more below our upper limits--yielding an overall modulation factor of >100 between 1977 and 1981.

Since the neutron monitors have not returned to levels at which our instrumental sensitivity would allow us to see anomalous O based on an 11-year cycle, we are not yet able to address the predictions of a 22-year cycle as in the model in reference (10). Recently, the anomalous O fluxes have been increasing at large distances from the sun (2), so it may be soon possible to address this question with measurements at 1 AU.

5. Acknowledgements. We are grateful to the MPI and UMD individuals responsible for the success of the ISEE instruments. This work was supported by NASA under contract NAS5-28704, grants NGR 21-002-224/316 and NAGW-101, by the NSF under grant ATM-84-07546, and by the Bundesministerium fur Forschung und Technologie, contract RV 14-B8/74.

References

1. Chan, J.H. and Price, P.B. 1974, Ap.J. (Letters), 190, L39.
2. Cummings, A.C. et al. 1984, EOS, 65, 1035.
3. Fisk, L.A. et al. 1974, Ap.J. (Letters), 190, L35.
4. Garcia-Munoz, M. et al. 1973, Ap.J. (Letters), 182, L81.
5. Hovestadt, D. et al. 1973, Phys. Rev. Letters, 31, 650.
6. Hovestadt, D. et al. 1978, IEEE Trans. Geo. El., GE-16, 166.
7. Hovestadt, D. et al. 1979, 16th ICRC, Kyoto, 3, 255.
8. McDonald, F.B. et al. 1974, Ap.J. (Letters), 187, L105.
9. McKibben, R.B. et al. 1982, Ap.J. (Letters), 257, L41.
10. Pesses, M.E. et al. 1981, Ap.J. (Letters), 246, L85.
11. von Rosenvinge, T.T. and Paizis, C. 1981, 17th ICRC, Paris, 10, 69.
12. Webber, W.R. and Cummings, A.C. 1983, Solar Wind V, NASA CP-2280, 435.
13. Webber, W.R. et al. 1983, 18th ICRC, Bangalore, 3, 35.

N85-35042

Radial and Latitudinal Gradients of Anomalous Oxygen During 1977-1985

W. R. Webber

University of New Hampshire, Durham, NH 03824 USA

A. C. Cummings and E. C. Stone

California Institute of Technology, Pasadena, CA 91125 USA

We find that the radial gradient of anomalous O remains constant during 1977-85 at ~10-15%/AU although the intensity changes by more than a factor of 100. These results can be used to deduce that most of the modulation of the intensities of these particles is occurring beyond 27 AU. We also find evidence for a latitudinal gradient of ~+3%/degree at low energies (7.1-10.6 MeV/nuc).

1. Introduction. In this analysis we make use of measurements of the spectrum of O nuclei from the Cosmic Ray Subsystem (CRS) on the Voyager 1 (V1) and 2 (V2) spacecraft [*Stone et al.*, 1977] and from the Goddard-University of New Hampshire experiment on Pioneer 10 [*McDonald et al.*, 1977] to study the radial and latitudinal gradients and temporal variations of anomalous O. Quiet-time data from 1977 to 1985 are utilized.

2. Observations. The general features of the 11-year cosmic-ray modulation cycle may be examined by using the counting rate of particles which penetrate the high-energy telescope on V1 as shown in Fig. 1 (curve "P", mainly protons > 75 MeV). A change in this rate by a factor ~2 is observed between 1977 and the minimum in 1981-82. This change is mainly due to solar modulation; however, some gradient effects are present in the data as well since V1 is moving outward from 1 to ~22 AU during this time period. Figure 1 also shows a similar plot for 40-106 MeV/nuc C+O nuclei for 24 quiet-time intervals between 1977-85 (curve "C+O"). Here the change in intensity between 1977 and the minimum in 1981 is a factor ~5. Finally, in Fig. 1 the temporal variations for 5.6-17.2 MeV/nuc anomalous O are shown for the same 24 quiet-time intervals (curve "O"). All three components show a similar pattern of variations but for the anomalous O the overall intensity variation is larger than the others, approaching a factor ~100.

In order to minimize contamination by solar and interplanetary particles and to help separate temporal and radial variations, six quiet-time intervals labeled A-F in Fig. 1 were selected by setting limits to the maximum low-energy helium flux, in a manner similar to that described in *Cummings et al.* [1984]. The anomalous O spectrum is derived from the observed total O spectrum for a particular time interval by subtracting both a low-energy solar or interplanetary component and the high-energy galactic cosmic-ray component [*Cummings et al.*, 1985].

In Fig. 2a, b, c we show the differential intensities of anomalous O nuclei in three separate energy intervals for each of the six quiet-time intervals at each of the spacecraft as they moved outward from the sun. The solid lines are least-squares fits to the data points, except for the lowest energy interval for periods E and F when V1 is at ~24 degrees north heliographic latitude. (V1 left the ecliptic plane after encounter with Saturn in 1980.) In these two cases the V1 points, connected by the dashed lines, are significantly above the straight lines (representing a constant radial gradient) connecting the V2 and P10 points. We attribute the deviation to a latitude gradient at low energies having a weighted average value of 3.0 ± 1.0%/degree for the combined two periods E and F.

In Fig. 3 we show the calculated radial gradient (slope of solid lines in Fig. 2) for each of the three energy intervals. In the lowest energy interval (7.1-10.6 MeV/nuc) the spectrum of anomalous O is changing with time [*Cummings et al.*, 1985], which may contribute to the observed variation in the radial gradient. Above 10.6 MeV/nuc no such energy spectral changes are found and the resulting gradient is remarkably constant. In the 10.6-17.1 MeV/nuc interval the average value of the gradient is 10.7 ± 0.6%/AU, somewhat lower than the 15 ± 3%/AU found by

ORIGINAL PAGE IS
OF POOR QUALITY

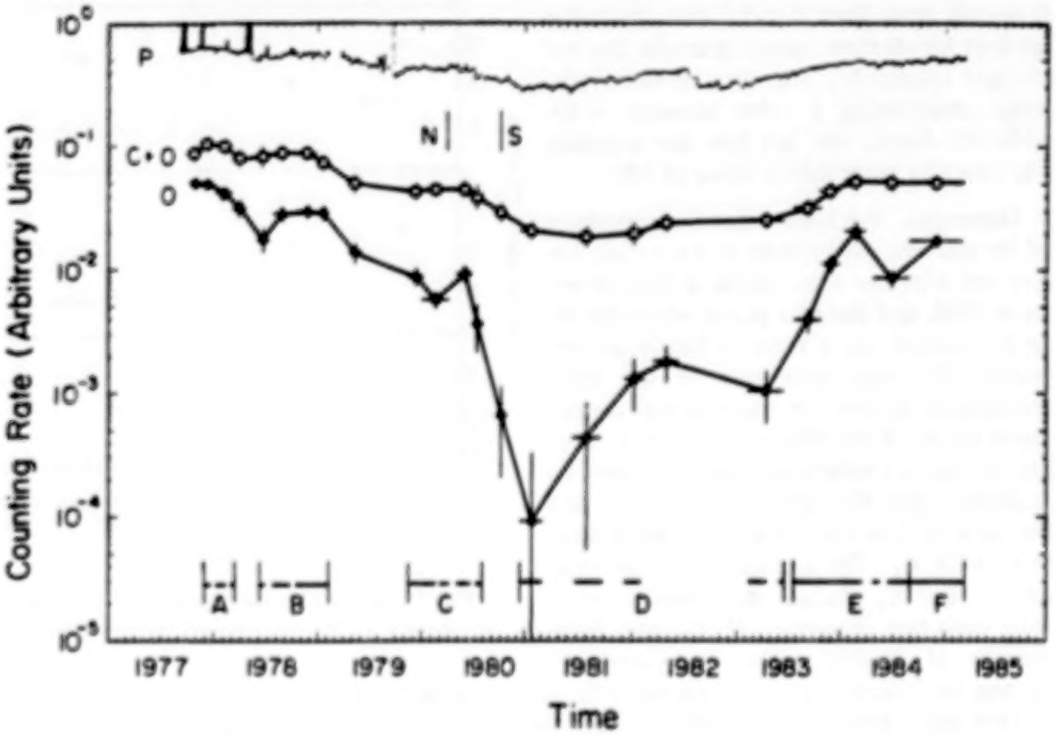

Fig. 1. Counting rates of three particle types from Voyager 1 telescopes. P labels the penetrating rate from the high-energy telescope (mainly protons > 75 MeV), C+O labels the rate of 40-106 C+O, and O labels the rate of 5.6-17.2 MeV/nuc anomalous oxygen. The approximate times of the solar magnetic field reversal in the northern (N) and southern (S) polar regions are indicated by the vertical bars [*Webb et al.*, 1984]. The horizontal bars represent quiet-time intervals as discussed in the text.

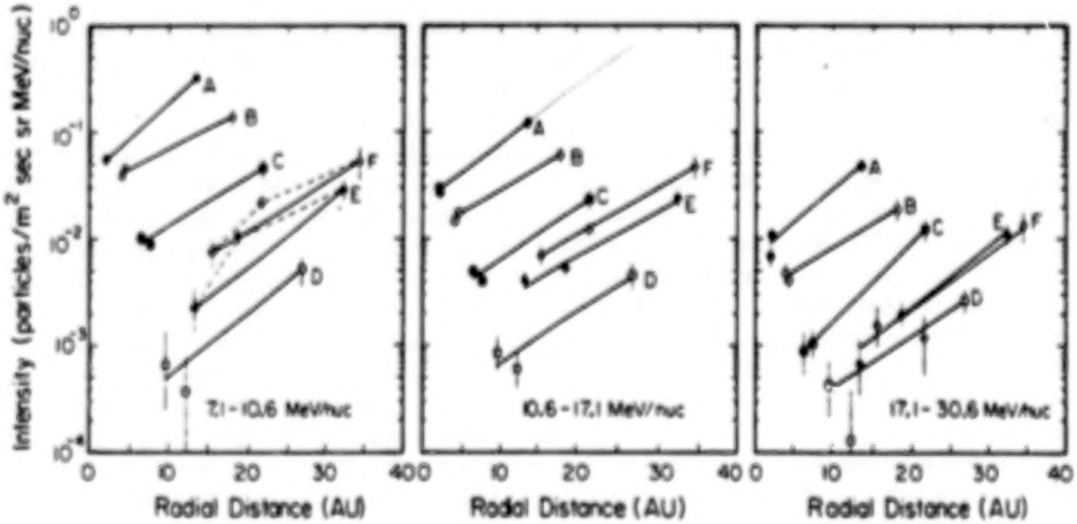

Fig. 2. Intensity of anomalous O versus heliocentric radial distance in three energy intervals from the V1, V2, and P10 cosmic-ray instruments. The labels A-F refer to the six quiet-time intervals chosen for analysis. The lines are described in the text.

Webber et al. [1981] for the period 1972-79. It is clear from Figs. 2 and 3 that the radial gradient for all three energy intervals has not changed appreciably with time or radial distance, maintaining a value between ~10-15%/AU despite the fact that the intensity has varied by more than a factor of 100.

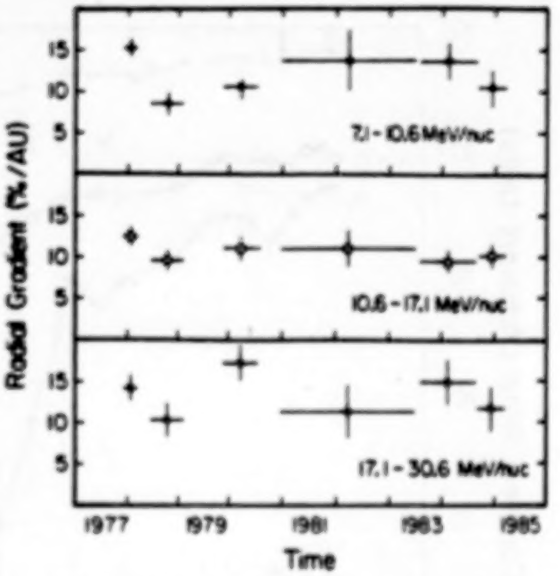

Fig. 3. Measured radial gradients of anomalous O versus time for the three energy intervals of Fig. 2.

3. Discussion. We believe that the constancy of the gradient with respect to time both before and after the solar magnetic field reversal in 1980, and during a period when the intensity change was a factor ~100 is an important clue and constraint on the solar modulation process. In conventional modulation theory, if the effects of particle streaming in the interplanetary medium can be neglected, then the radial gradient, G_r, and the radial diffusion coefficient, κ_r, are related by $G_r = CV/\kappa_r$. The average solar wind velocity, V, and κ_r change only slightly over a solar cycle (see *Hedgecock* [1974] and *Feldman et al.* [1979]). Also the Compton-Getting coefficient C, which is related to the spectral shape, does not change appreciably since the spectral shape remains similar above ~10 MeV/nuc. Thus, if the gradient can be described by these local parameters, it would be expected to be constant as observed.

In this simple conventional modulation model in which κ_r is independent of radial distance r, the particle intensity j at r is given by $j = j_b \exp[CV(r-r_b)/\kappa_r]$, where j_b is the intensity at the modulation boundary. Since C, V, and κ_r are not changing appreciably with time, and assuming j_b is constant, the large modulation at a given position would require a time variation in the boundary location r_b. The magnitude of the required change in the boundary distance can be estimated from Fig. 2b. The dotted line is an extrapolation of the intensity in the 10.6-17.1 MeV/nuc energy range during the time of solar minimum to the position of P10 (27AU) during the solar maximum period of interval D. The implied intensity change from period A to D at 27AU is a factor of 136 ± 52, indicating that most of the modulation during period D is occurring beyond 27AU. Using the average radial gradient for this energy interval we find that the required change in the boundary distance r_b is 46 ± 4AU. A similar boundary shift has been suggested by *Evenson et al.* [1979] to explain electron observations.

Such a boundary shift would also produce changes in the intensity of other particle species. For example, the penetrating particle rate (P) in Fig. 1 shows a variation from solar minimum to solar maximum of a factor ~2. The median rigidity of the particles dominating this rate is ~1.8GV, the same rigidity as 7MeV/nuc anomalous O if O is singly charged (as expected if they are freshly-ionized neutrals [*Fisk et al.*, 1974]). The spectral shapes of the anomalous O (above 10MeV/nuc) and high-energy protons are similar (spectral index ~-2) implying they have similar values of C. Since $\kappa_r \propto \beta f(R)$, where β is the particle velocity and R is the rigidity, the expected gradient for the P rate can be scaled from the gradient of anomalous O by $G_r(P) = G_r(O)(\beta_O/\beta_P) \sim 10(.12/.89) = 1.5$%/AU, a value in approximate agreement with observations by others (see *McKibben et al.* [1982] and *Lockwood and Webber* [1984]). The intensities at two different times are related by $j_1/j_2 = \exp(G_r(\delta r_b))$ Therefore, a boundary change of 46AU and a radial gradient of 1.5-3%/AU would result in $j_1/j_2 = 2$-4 for the penetrating particles, similar to what we observe.

An alternative way to accomplish the same modulation without changing the boundary distance is to decrease κ_r, and thus increase the gradient, in a localized shell of turbulence in the outer heliosphere, as suggested by *Burlaga et al.* [1984]. The observed change in modulation would require, for example, an increase in the anomalous O gradient from 11%/AU to 44%/AU in a shell 15 AU thick.

It is also possible that variations in the source of the anomalous O may contribute to the observed solar cycle variation. We note that *Jokipii* [1985], using a model of the anomalous component in which the particles are accelerated at the polar termination shock and drift to the solar equatorial regions, has calculated spectra of anomalous O that depend on the polarity of the magnetic field and which are in reasonable agreement with observations of changes in the spectra associated with the magnetic field reversal (see *Cummings et al.* [1985]). However, we find no evidence of a change in the gradient of the anomalous O at the time of the solar magnetic field reversal as would presumably be expected from such a model.

4. Acknowledgments. We are grateful to R. E. Vogt and other CRS team members consisting of scientists and engineers at the California Institute of Technology, the Goddard Space Flight Center, the University of Arizona, and the University of New Hampshire. This work was supported in part by NASA under contract NAS 7-918 and grant NGR 05-002-160.

5. References.

Burlaga, L. F., F. B. McDonald, N. F. Ness, R. Schwenn, A. J. Lazarus, and F. Mariani, *J. Geophys. Res.*, *89*, 6579, 1984.

Cummings, A. C., E. C. Stone, and W. R. Webber, *Ap. J. (Letters)*, *287*, L99, 1984.

Cummings, A. C., E. C. Stone, and W. R. Webber, *19th Internat. Cosmic-Ray Conf., La Jolla*, paper SH4.6-1, 1985.

Evenson, P., J. Caldwell, S. Jordan, and P. Meyer, *J. Geophys. Res.*, *84*, 5361, 1979.

Feldman, W. C., J. R. Asbridge, S. J. Bame, and J. T. Gosling, *J. Geophys. Res.*, *84*, 7371, 1979.

Fisk, L. A., B. Kozlovsky, and R. Ramaty, *Ap. J. (Letters)*, *190*, L35, 1974.

Hedgecock, P. C., *J. Geophys. Res.*, *79*, 4775, 1974.

Jokipii, J. R., submitted to *J. Geophys. Res.*, 1985.

Lockwood, J. A., and W. R. Webber, *Ap. J.*, *279*, 151, 1984.

McKibben, R. B., K. R. Pyle, and J. A. Simpson, *Ap. J. (Letters)*, *254*, L23, 1982.

McDonald, F. B., N. Lal, J. H. Trainor, M. A. I. Van Hollebeke, and W. R. Webber, *Ap. J.*, *216*, 930, 1977.

Stone, E. C., R. E. Vogt, F. B. McDonald, B. J. Teegarden, J. H. Trainor, J. R. Jokipii, and W. R. Webber, *Space Sci. Rev.*, *21*, 355, 1977.

Webb, D. F., J. M. Davis, and P. S. McIntosh, *Solar Phys.*, *92*, 109, 1984.

Webber, W. R., F. B. McDonald, T. T. Von Rosenvinge, and R. A. Mewaldt, *17th Internat. Cosmic-Ray Conf., Paris*, *10*, 92, 1981.

SH 4. 6 - 5

176 N85-35043

OBSERVATION OF PICK-UP IONS IN THE SOLAR WIND: EVIDENCE FOR THE SOURCE OF THE ANOMALOUS COSMIC RAY COMPONENT?

D. HOVESTADT, E. MÖBIUS, B. KLECKER, M. SCHOLER,
Max-Planck-Institut für extraterrestrische Physik, 8046 GARCHING, Germany
G. GLOECKLER and F.M. IPAVICH
Dept. of Physics and Astronomy, University of Maryland, COLLEGE PARK, MD 20742, USA

ABSTRACT. Singly ionized energetic helium has been observed in the solar wind by using the time-of-flight spectrometer SULEICA on the AMPTE/IRM satellite between September and December, 1984. The energy-density spectrum shows a sharp cut-off which is strongly correlated with the four-fold solar wind bulk energy. The absolute flux of the He^+ ions of about 10^4 ions/cm^2-s is present independent of the IPL magnetic field orientation. The most likely source is the neutral helium of the interstellar wind which is ionized by solar UV-radiation. It is suggested that thes particles represent the source of the anomalous cosmic ray component.

1. Introduction. In 1972 anomalous features in the low energy quiet time cosmic ray energy spectrum have been detected for helium, oxygen, nitrogen, and neon by GARCIA-MUNOZ et al.(1972), HOVESTADT et al.(1973), and Mc DONALD et al.(1974). These four elements are known to have a high first ionization potential compared to other elements like carbon, magnesium, silicon and iron (e.g ALLEN (1973)). This fact lead FISK et al.(1974) to suggest that the source of the particles is the interstellar neutral wind which becomes ionized in the inner heliosphere by interaction of the atoms with solar ultra-violett radiation and/or solar wind ions. The newly created ions then are picked-up by the interplanetary magnetic field. With their gyro-motion in the solar wind frame they represent a distinguished population which is subsequently convected into the outer heliosphere while being accelerated within the turbulent magnetic fields of the heliosphere (e.g. FISK 1976a,b) or at the terminating shock (PESSES et al. (1981)). The resulting energy spectrum is then reshaped to the observed spectrum by modulation and propagation effects in interplanetary space. This paper presents first direct observations of the distribution function of freshly ionized helium in the solar wind which likely has its origin in the neutral interstellar wind and probably represent the source of the anomalous helium component in cosmic rays.

2. **The Pick-Up Process.** Freshly ionized helium atoms are locally subjected to the combined forces of the interplanetary $V_{SW} \times B$ field of the solar wind and the Lorentz-force in the magnetic field, B, where V_{SW} is the solar wind velocity; i.e. in the *inertial-system* (which nearly coincides with the spacecraft-system) the particles undergo initially a cycloidal motion in a plane perpendicular to the local magnetic field, B, with a minimum velocity which is equal to the velocity of the neutral wind (assumed to be < 20 km/s and therefore being neglected in the following). The maximum velocity which these ions can obtain in the pick-up process is determined by the solar wind velocity and the angle α between its flow direction and the direction of the local magnetic field:

$$v(\max,\mathrm{loc}) = 2 \cdot V_{SW} \cdot \sin\alpha \qquad (1)$$

This leads to an energy of

$$E(\max,\mathrm{loc}) = 4 \cdot M/2 \cdot V_{SW}^2 \cdot \sin^2\alpha \qquad (2)$$

In the *solar wind* frame the motion initially leads to a conical pitch-angle distribution with the pitch angle α. The velocities parallel and perpendicular to the local magnetic field are given by

$$v(par) = V_{SW} \cdot \cos\alpha \quad (3) \quad \text{and}$$

$$v(perp) = V_{SW} \cdot \sin\alpha \quad (4) .$$

Therefore the total ion velocity in the solar wind frame is given by

$$v = (v_{par}{}^2 + v_{perp}{}^2)^{1/2} = |V_{SW}| \qquad (5)$$

If the interplanetary medium were homogenious with parallel magnetic field lines and if there were no scattering imposed by intrinsic or self-generated waves, the distribution function would remain gyrotropic and ring-shaped in the three-dimensional velocity space.

In the real world ,however, the motion of the particles is subjected to effects generated by temporal and spatial magnetic irregularities in the expanding interplanetary medium. While energy-changing wave-particle interactions can be neglected, pitch-angle scattering and adiabatic deceleration can greatly influence the particle distribution. Within a scattering mean free path-length λ the initially ring-type velocity distribution is expected to be reshaped by pitch-angle diffusion into a spherical-shell type distribution which is fully convected with the solar wind . The orbital velocity $|v| = |V_{SW}|$ remains constant in the solar wind frame as long as adiabatic deceleration does not play a significant role. In the inertial system the expected velocities range from zero to $2 \cdot V_{SW}$ with corresponding observable energies between zero and four times the solar wind bulk energy ($0 < E_{pick-up} < 4 \cdot M/2 \cdot V_{SW}{}^2$).The energy spectrum should show a clean cut-off at that energy value . The spectrum below cut-off should reflect the effect of adiabatic deceleration in the expanding interplanetary medium upstream of the observer.

3. INSTRUMENTATION and SATELLITE. The data presented here are obtained with the suprathermal particle spectrometer SULEICA of the Max-Planck-Institute/ University of Maryland onboard the IRM spacecraft of the Active-Magnetospheric-Particle-Tracer Explorer project (AMPTE), launched on 11. August 1984 into a highly elliptical orbit with an apogee of 18.9 earthradii. During the time period from launch until December 1984 the S/C spent a large fraction of each orbit in the solar wind upstream of the bow-shock of the earth. The SULEICA spectrometer is based on the techniques of electrostatic deflection followed by a time-of-flight and residual energy measurement(for details see MÖBIUS et al.1985). The electrostatic deflection analyser, represented by two concentric segments of a sphere, selects incoming ions according to their energy per charge in 24 logarithmically spaced voltage steps corresponding to an energy range from 5 to 226 keV/charge. After passing through the analyser the ions enter the time-of-flight section where the velocity of the ions is measured. The ions are stopped in a Silicon surface barrier detector where the residual energy is determined. The geometrical factor of the instrument is $4.3 \cdot 10^{-2}$ cm ^{2}sr and the energy resolution is $\Delta E/E \approx 0.097$.
For the investigation presented here the energy of the pick-up ions is too low to create a sufficiently high energy signal in the solid-state detectors. Therefore we identify the ion-species only by combining the electrostatic deflection (E/Q)and the time of flight signal (TOF). For a given E/Q step the TOF histogram as shown in figure 1 therefore represents a mass-per-charge histogram which is taken in the direction of the solar wind.

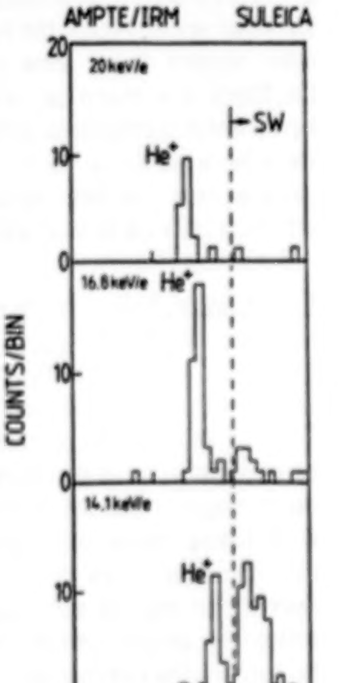

Figure1: Typical TOF-histograms at three different energy steps, takenin the solar sector.Data are obtained on Nov.11,1984 at ≈ 18 R_E in front of the bow- shock

4. OBSERVATIONS. A limited number(ten) of observational periods were chosen in the solar wind between launch of the S/C and December,15, 1984. During all periods we observed a peak in the TOF-histograms at M/Q = 4 at E/Q steps which are significantly higher then we would expect for genuine solar wind particles. Depending on the E/Q step and the solar wind velocity, we also observe in addition a broad and variable peak at TOF values which correspond to the solar wind velocity. These ions with M/Q values above 5 correspond to solar wind heavy ions. Figure 1 shows a typical example of TOF histograms for three different E/Q steps obtained on November 11, 1984. It should be noted, that the He$^+$ peak is visible at all orientations of the interplanetary magnetic field no matter wether bow-shock accelerated ions are present or not.

Figure 2 shows the energy-density spectrum of the M/Q = 4 peak as measured during a sample period of 40 minute duration on Novenber 11,1984, when there are no bow-shock accelerated particles present. The spectra are taken from the directional sector which also contains the solar wind. Except the two neighbouring sectors all other sectors do not show any counts in the M/Q = 4 bin.There is a sharp cut-off at an energy of about 23 keV/e which corresponds to four time the bulk-energy of the solar wind. Below the cut-off energy we observe a more or less flat distribution which ends at a sharp rise of the spectrum at about 8 keV/e. We attribute the rise to solar wind particles of M/Q = 4 which will be not discussed in this paper.

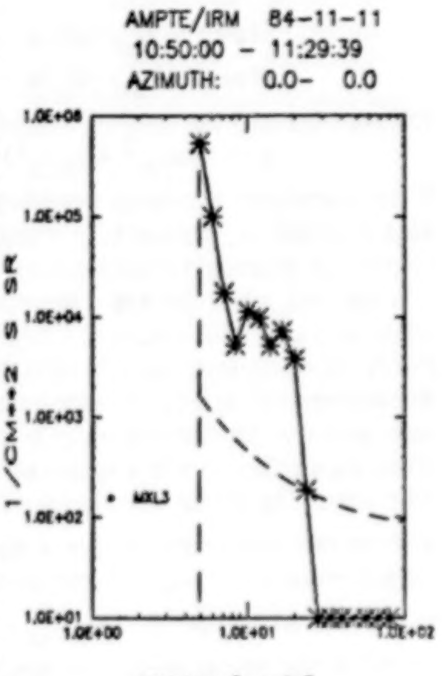

Figure 2:Example of an energy-density spectrum of the M/Q=4 ion channel accu- mulated over 40 minutes. Dashed curved line represents the 1 count/step level.

5. Discussion. Following the arguments in section 2 we tried to correlate the experimental cut-off energies, firstly (figure 3) with the full four-fold solar wind bulk-energy for mass M = 4 (Helium), and secondly (figure 4) with the four-fold component perpendicular to the local interplanetary magnetic field (eq. (2)).

There is an excellent correlation with the full energy (correlation coefficient = 0.98) while the correlation with the perpendicular component is rather poor (correlation coefficient = 0.26). This result suggests that the originally injected ions have lost their directional information in the solar wind frame due to pitch angle scattering, while maintaining their injection energy. The poor correlation with the perpendicular component shows that the ions have lost their directional information and therefore suggests that the source region of the ions extends beyond one mean free scattering length upstream of the observer. The magnetic rigidity of suprathermal singly ionized helium of a few keV/nucleon is in the order of 5 to 10 MV. The mean free path is known to be of the order of 0.05 AU during quiet interplanetary conditions (e.g.compilation in MASON et al.(1983)). The apparently large extent of the source region excludes a terrestrial origin of the ions.

The effect of adiabatic deceleration is expected to be high due to strong coupling of the particles to the solar wind. This sets an upper limit for the distance between point of origin and observer. Ions originating too far upstream (or too close to the sun) loose so much energy that they become indistinguishable from the solar wind itself.

To get a rough estimate of the source strength of the pick-up ions we use the energy spectrum (figure 2) and argue that the energy channels below the cutoff energy are populated via adiabatic deceleration, the rate of which is assumed to very as 1/r with heliocentric distance. The measured quantity $E \cdot dj/dE \cdot d\Omega$ in each energy channel in figure 3 is related to the relevant source- quantities as: $E \cdot dj/dE\, d\Omega \approx E \cdot S(r) \cdot \Delta r \cdot 4 \cdot \Delta\Omega_{SULEICA}/(4\pi \cdot \Delta E \cdot \Delta\Omega) = S(R) \cdot \Delta r/\pi \cdot (E/\Delta E)$

where $S(r) = N_{He} \cdot \nu_{ion}$ is the source strength of singly ionized helium. For a relative energy width of the instrument of $\Delta E/E = 0.1$ the length of the source column upstream of the S/C translates into $\Delta r = 0.2$ AU $= 3 \cdot 10^{12}$cm. Using an average value of $7 \cdot 10^3$ for the energy density of the pick-up ions(from figure 2) we obtain a source strength $S(r=1\ \text{AU}) \approx 8 \cdot 10^{-10}$ /cm^{3}s. For an ionization rate of $8 \cdot 10^{-8}$/s (e.g.Holzer 1977) we arrive at a neutral interstellar helium density $N_0 = 10^{-2}$ /cm^3, a value which is fully compatible with results from optical EUV measurements of He II resonantly scattered EUV-lines (WELLER and MEIER 1974; DALAUDIER et al.1984) in the heliosphere. These measurements represent the first direct observation of energetic helium ions picked-up by the solar wind from the interstellar neutral wind thereby filling one more gap in the hypotheses to explain the anomalous cosmic ray component.

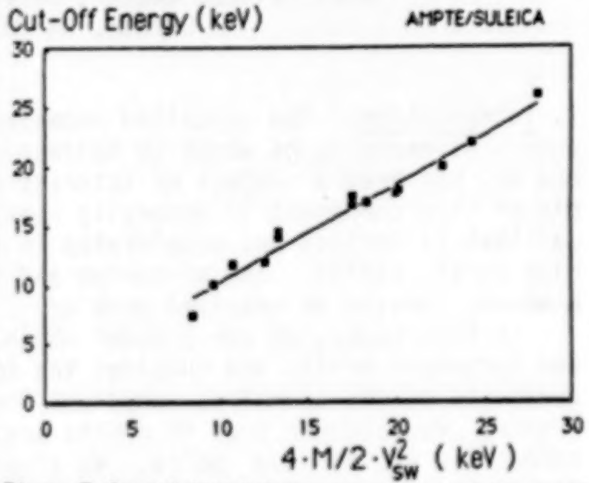

Figure 3: Correlation between experimenmtal cut-off energies and the four-fold solar wind bulk-energy (Correlation coefficient = 0.98).

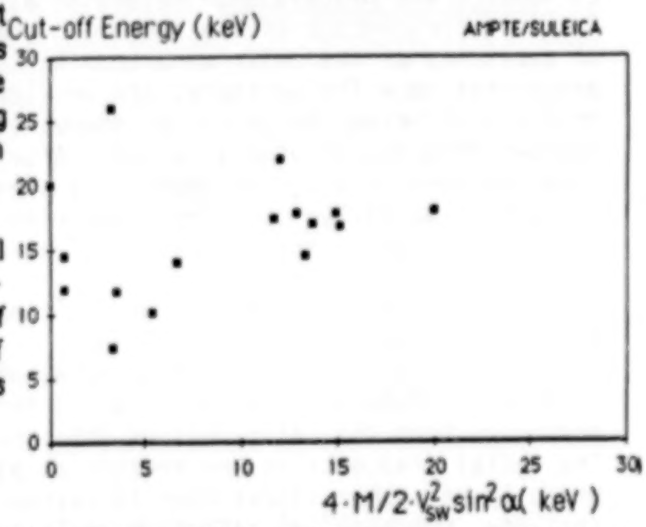

Figure 4: Same as figure 3, but abscissa is vertical-to-B component of the SW bulk-energy(Corr.coeff.=0.26).

Acknowledgement The authors are grateful to the many individuals at the Max-Planck-Institut and the University of Maryland who contributed to the success of the experiment and to the AMPTE project as a whole.

REFERENCES

Allen 1973, ASTROPHYSICAL QUANTITIES, The Athlone Press, London
Dalaudieretal.1984, Astron. Astrophys.,**14**, 171
Fisk et al.1974, Ap. J. Letters **190**, L35
FiskL.A.1976a, Ap.J. **206**, 333; 1976b, J.Geophys.Res.**81**, 4633,
Garcia-Munoz et al.1973, Ap.J.Letters **182**, L81
Holzer 1977, Rev.Geophys. Space Phys.,**15**,467
Hovestadt et.al. 1973, Phys.Rev.Letters, **3**, 650
Mason et al. 1983,Ap.J. **267**, 844
Mc Donald et al.1974, Ap.J. Letters **187**, L105
Möbius et al. 1985, IEEE Transactions on Remote Sensing, issue May 1985
Pesses et al.1981, Ap.J.Letters, **246**, L85
Weller and Meier 1974, Ap.J. **193**, 471

N85-35044

ON THE ANOMALOUS COMPONENT

M. S. Potgieter, L. A. Fisk and M. A. Lee
Space Science Center, University of New Hampshire
Durham, NH 03824, USA

1. Introduction. The so-called anomalous cosmic ray component, which occurs at energies of about 10 MeV/nucleon and consists only of He, N, O, and Ne, has been a subject of interest for more than a decade. The origin of this component is generally considered to be interstellar neutral gas that is ionized and accelerated in the solar wind, as was proposed by Fisk et al. (1974). The mechanism and the location for the acceleration, however, remains an unsolved problem.

In this paper, we use a model which includes the effects of gradient and curvature drifts and consider the implications of observed spatial gradients of the anomalous component for the location of the acceleration region. We conclude that if drifts are important the acceleration region cannot lie at the solar poles. We also conclude that there is no single region for the acceleration which can account for both the observed intensities and gradients in models which include drift effects.

2. Results and Discussion. Pesses et al. (1981) proposed a mechanism for the acceleration of the anomalous component based on the acceleration of particles at the solar wind termination shock over the poles. They argue that once the particles are accelerated, gradient and curvature drifts will bring the particles downward from the heliospheric polar regions onto the equatorial plane. After a polarity reversal of the solar magnetic field, the oppositely directed drifts will restrict the passage of particles onto the equatorial plane. They therefore predict a dramatic change in the intensity of the anomalous component from cycle to cycle.

A complicating factor for drift models, however, is the small radial gradients these models predict for periods when the interplanetary magnetic field (IMF) is directed outwards in the northern heliosphere, as in 1970-80 (Potgieter, 1985). During this period the downward drifts of particles from the polar regions onto the equatorial plane tend to make the radial gradients in the equatorial plane small. The gradients also prove to be rather insensitive to changes in modulation parameters, for instance, the parallel diffusion coefficient. The question therefore arises whether a polar source for the anomalous component and strong drift effects can be compatible with the observed radial gradients of 10%-15%/AU for the anomalous component (Webber et al., 1981, 1985).

In this preliminary study we assumed a source spectrum for the anomalous oxygen which yields approximately the observed 1976-77 energy spectrum at Earth using a drift model for the modulation of cosmic rays (Potgieter and Moraal, 1985). To obtain a source which can be placed at various Θ-(polar angle) values at a radial distance of 50 AU, we used Gaussian spectra of the form

$$j_T^* = j_T \exp\{-0.028(\Theta - \Theta_o)^2\} \quad ,$$

with a half-width of 10° about Θ_o and j_T the assumed Θ-independent anomalous oxygen spectrum. We then solved the cosmic-ray transport equation,

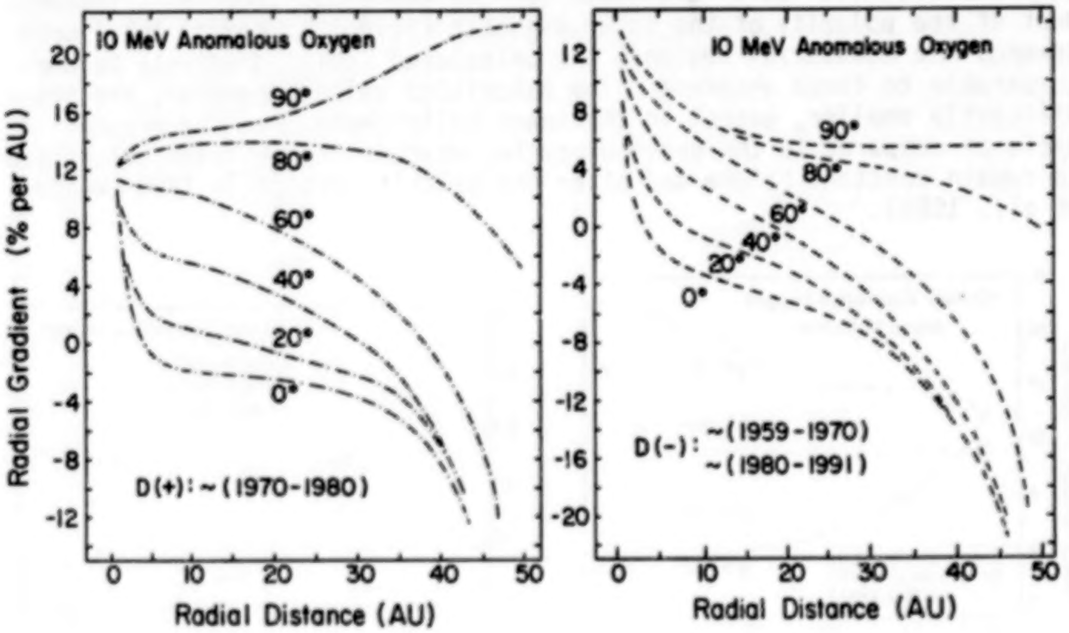

(a) (b)

Fig. 1: Calculated radial gradients in the equatorial plane as a function of radial distance with a source at 50 AU and various polar angles; (a) for a D(+) cycle with drifts downward onto the equatorial plane at Θ = 90°, and (b) for a D(-) cycle that is with the polarity of the IMF reversed.

assuming a steady-state and azimuthal symmetry, shifted the source in 10° intervals from the pole to the equator at $\Theta = 90°$, and calculated the radial gradients in the equatorial plane for each location of the source. We repeated the calculations with the IMF polarity reversed, but otherwise unchanged modulation parameters. The diffusion coefficients used correspond to solar-minimum conditions (Potgieter and Moraal, 1985).

To distinguish between the two configurations of the IMF, we use the notation D(+) for ∿1970-80 and D(-) for the 11 years before and after this period. Starting with a D(+) period, that is with drifts directed downward onto the equatorial plane, we show in Fig. 1a the radial gradients in the equatorial plane for 10 MeV anomalous oxygen as a function of radial distance with the source at 50 AU and various polar angles. The striking feature of this figure is the dramatic decrease of the radial gradient with increasing radial distance, from ∿10%/AU at Earth to a negative gradient, with the source placed at 50 AU over the pole. With the source at the equatorial plane, the radial gradient steadily increases from 12%/AU at Earth to about 22%/AU at 50 AU. Fig. 1b shows the situation with the polarity of the IMF reversed, that is with drifts directed from the equatorial plane toward the polar regions. The radial gradients, with the source at the pole, again rapidly decrease with increasing radial distance. With the source at the equator, the radial gradients compared to Fig. 1a are smaller for most of the heliosphere out to 50 AU.

The results of Fig. 1 indicate the following. The radial gradients in the equatorial plane, with a source at the pole, are inconsistent with the observed radial gradients for the anomalous component, independent of the polarity of the solar magnetic field. By moving the source towards the equatorial regions, the calculated radial gradients become comparable to those observed. The calculated values, however, are significantly smaller, except in the inner heliosphere, for the present cycle as compared to the previous cycle, whereas the observed values seem to remain constant before and after the polarity change in 1980 (Webber et al., 1985).

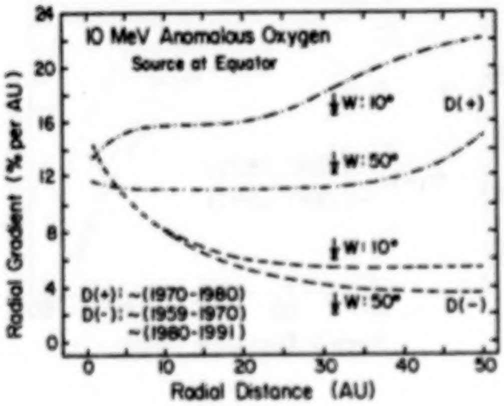

Fig. 2: The effect of increasing the half-width (W) of the source spectrum, from 10° to 50°, on the radial gradients in the equatorial plane with a source at the equator at 50 AU.

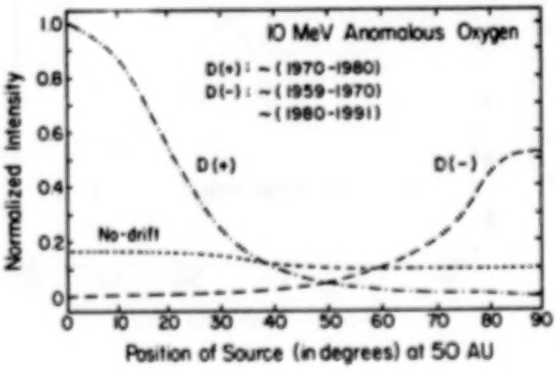

Fig. 3: The normalized intensity at Earth of 10 MeV anomalous oxygen as a function of various polar angle positions of the source at 50 AU for periods before and after a polarity reversal.

We also investigated the effect of increasing the half-width of the source spectra from 10°, in steps of 10°, to 50° to simulate an extended, less localized source. For both the D(+) and D(-) cycle of the magnetic field the radial gradients in the equatorial plane change insignificantly with the extended source over the polar regions. The effect of an extended source placed at the equator is shown in Fig. 2. For the D(+) period the radial gradients now seem compatible with those observed.

The intensity for the anomalous oxygen at Earth with a source at various latitudes should also be taken into consideration. The intensity of the 10 MeV anomalous oxygen at Earth, normalized to the intensity during a D(+) period with a source at the pole, is given in Fig. 3 as a function of the position of the source at 50 AU at various polar angles. For the D(+) period (downward drifts) the intensity at Earth decreases rapidly as the source is shifted from the pole to the equator. Comparing the intensity for the two periods, with the source at the pole, the D(-) intensity is substantially lower (a factor of 200) as was suggested by Pesses et al. (1981). For the D(-) cycle the intensity increases as the source is shifted toward the equator. It is interesting to compare this behavior, dependent on the polarity of the IMF, to the no-drift case shown in Fig. 3.

Our calculations show that, although the intensity of the anomalous oxygen, with a source at the pole, dramatically decreases after a change in the IMF polarity, the radial gradients in the equatorial plane are inconsistent to those observed. Furthermore, although the radial gradients for a D(-) cycle (the present cycle) with a source at 50 AU at the equator seem comparable to observations, the calculated intensity during this cycle exceeds the intensity during a D(+) cycle (the previous cycle), which is again contrary to what is observed.

3. Concluding Remarks. It should be noted that no attempt has been made in this preliminary study to include acceleration at the termination shock in a self-consistent manner. As has been pointed out recently by Jokipii (1985), drifts along the shock front and in the IMF can affect the spectrum and the spatial distribution of particles at the termination shock. When drifts are downward from the poles, they are poleward along the shock front. Both effects tend to limit the shock acceleration of particles that are injected near the poles. Conversely, when the drifts are towards the poles in the IMF, as they are in the current cycle, the drifts are downward from the poles along the shock front. These effects will increase the number of times particles interact with the shock, thereby increasing the energy they can gain, and will spread particles injected over the poles towards the equatorial region.

The complication of an accelerated spectrum which evolves with changing field polarity does not affect our conclusion that the injection and acceleration cannot occur primarily over the solar poles in models in which drift effects are important. During the last cycle, when drifts were downward from the poles, drifts along the termination shock front would concentrate the acceleration at the poles. However, as we demonstrated above, in this case the radial gradient seen in the equatorial plane is inconsistent with observations. An evolving spectrum at the termination shock could, however, affect the intensity seen at Earth.

In conclusion, we argued in this paper that the source for the acceleration of the anomalous component cannot lie at the solar poles in models that include gradient and curvature drifts. Such models will not yield the observed spatial gradients in the equatorial plane. We argued also that a source near the equatorial plane can yield the correct gradients, but in drift models will not yield the observed behavior in the intensity from cycle to cycle.

It would appear, therefore, that drift models may have significant difficulty in accounting for the observed features of the anomalous component.

References

Fisk, L. A., Kozlovsky, B., and Ramaty, R., 1974, Ap.J., 190, L35.
Jokipii, J. R., 1985, submitted to J. Geophys. Res.
Pesses, M. E., Jokipii, J. R., and Eichler, D., 1981, Ap. J., 246, L85.
Potgieter, M. S., 1985, Paper SH4.2-5, this conference.
Potgieter, M. S., and Moraal, H., 1985, Ap. J., in press.
Webber, W. R., McDonald, F. B., Von Rosenvinge, T. T., and Mewaldt, R.A., 1981, Proc. 17th ICRC (Paris), 10, 92.
Webber, W. R., Cummings, A. C., and Stone, E. C., 1985, this conference.

N85-35045

SH 4.6-7

POSSIBLE ORIGIN OF THE ANOMALOUS COMPONENT OF COSMIC RAYS

Biswas, S., Durgaprasad, N., Singh, R.K.,
Vahia, M.N., and Yadav, J.S.
Tata Institute of Fundamental Research
Bombay 400 005, India

ABSTRACT

In this work we have studied the possible origin of the anomolous cosmic rays (ACR) in terms of stellar wind injection from O-type stars and their acceleration in shock fronts of SNR's. This is in continuation of our earlier work (Biswas, Durgaprasad, and Trevedi, Proc. Ind. Acad. Sci. 1981) in which we estimated that heavy ions of He^{+2}, O^{+4}, etc. of energy 10-100 KeV/N from the stellar wind will travel a distance of the order of (1-5) x 10^2 pc in a hot and thin ISM. We assume that a fraction of these will encounter interstellar shock fronts of SNR's and these are accelerated to about 5-100 MeV/N and give rise to ACR's. Typically these ions would travel a distance of the order of a few 10^3 pc. Therefore we estimate that O-type stars in a volume of radius of a few Kpc around the solar system are contributing to the intensity of ACR in the local ISM. From observational data, the intensity of ACR in the local ISM is estimated. It is suggested that these ACR ions enter the solar system along the solar dipole field lines connected to the interplanetary magnetic field lines.

THE COSMIC RAY INTERPLANETARY RADIAL GRADIENT FROM 1972 - 1985

N85-35046

Webber, W. R. and J. A. Lockwood
Space Science Center, University of New Hampshire
Durham, New Hampshire 03824 USA

1. Introduction It is now established that the solar modulation of the cosmic-rays is produced by turbulent magnetic fields propagated outward by the solar wind. Observations show that the modulation effects themselves propagate outward from the sun with speeds of the order of the solar wind speed [1, 2, 3, 4]. Therefore, changes in the cosmic-ray intensity are not simultaneous throughout the modulation region, thus requiring time-dependent theories for the cosmic-ray modulation [e.g., 5] . Fundamental to an overall understanding of this observed time-dependent cosmic-ray modulation is the behavior of the radial intensity gradient with time and heliocentric distance over the course of a solar modulation cycle.

We have focussed our attention primarily on the period from 1977 to 1985 when data are available from the cosmic-ray telescopes on Pioneer (P) 10, Voyager (V) 1 and 2, and IMP 8 spacecraft. Additional data from P10 and other IMP satellites for 1972 to 1977 can be used to determine the gradient (G_R) at the minimum in the solar modulation cycle and as a function of heliocentric distance R. All of these telescopes have thresholds for protons and helium nuclei of $E \gtrsim 60$ MeV/nucleon.

2. Observations In order to compare the cosmic-ray intensity at different heliocentric distances over a long time period we have calculated the 26-day average counting rates of the IMP 8, V1, V2 and P10 cosmic-ray telescopes. The normalized rates of these telescopes are shown in Fig. 1 along with the heliocentric distances of V1 and P10. There are several striking features about these normalized rates. First, the progressive separation of rates is a clear measure of a radial gradient. Second, time lags in specific decreases at the different spacecraft beginning about 1977 indicate an outward radial propagation speed for the solar modulation comparable to the solar wind speed [1,2]. Third, there is also an apparent time lag during the recovery phase seen in specific increases starting in early 1983. Fourth, the fractional decrease from late 1977 to the end of 1982 at earth and at P10 (~ 30 AU) are comparable in magnitude.

We can use the data shown in Fig. 1 to obtain the heliocentric radial gradient, keeping in mind that the gradient must be computed including the time delay noted above.

The differential radial gradient g_R is defined by:

$$g_R = 1/N\ (\partial N/\partial R) \qquad (1),$$

where N, the cosmic-ray intensity, is taken to be a separable function of R and t. Hence, N can be written:

$$N(R,t) = n_o f(R) h(t) \qquad (2),$$

where h(t) accounts for this delay time and f (R) represents the radial dependence of the quasi-stationary intensity.

Thus,

$$q_R = \frac{1}{f(R)} \frac{df}{dR} \qquad (3),$$

In general, we use spacecraft at different R to determine the gradient, with one spacecraft remaining near earth (R = 1 AU). Then,

$$\int_{R_1}^{R_2} q_R dR = \int_{f_1}^{f_2} \frac{df}{f} = \ln \frac{N(R_2)}{N(R_1)} = G_R(R_2 - R_1) \qquad (4),$$

where G_R is an integral gradient and $N(R_2)$ is taken at the time $t + (R_2-R_1)/V_{sw}$.

In Fig. 2 we have plotted G_R for P10/IMP as a function of R. There are several interesting features in this plot. First, G_R reaches a maximum around 5 AU, which is seen in all three panels of Fig. 2. Second, G_R is nearly constant as a function of both R (beyond ∿ 5 AU) and t between 1976-1982. During this period the cosmic-ray intensity at earth decreased in 1982 to 32% of the intensity in 1976 and the solar magnetic field reversed in 1980 with no apparent change in the gradient. Third, the decrease in G_R seen after 1982 indicates a different state in the cosmic-ray modulation in the heliospheric cavity.

3. Discussion There are several significant implications in the data shown in Figs. 1 and 2. We shall discuss two of them here.

a) The constancy of G_R over extended periods of time and radius as observed between 1976 and 1982 can be related to limits on the interstellar cosmic-ray intensity. Between 1976 and 1982 the normalized counting rate at earth decreased from 1.0 to 0.32, with a comparable decrease at P10 so that G_R remained essentially constant throughout this period. This behavior is indicated in Fig. 3 for six time periods of relatively constant intensity (no large transient variations propagating outward) between 1976 and 1984 as indicated by shaded areas in Fig. 1. We can use Fig. 3 to determine the fraction of total modulation beyond a given R. First, we need to estimate the residual modulation at earth at sunspot minimum [6]. We assume that the interstellar proton spectrum can be parameterized by the form $dJ/dT = \text{constant} \cdot T^{0.3} (T + T_o)^{-3.0}$, where T = kinetic energy and T_o is a variable parameter between 0.3 - 0.5 GeV/nuc. This corresponds to a residual modulation parameter $\phi = 450 \pm 100$ MV at sunspot minimum [7]. We have integrated interstellar spectra for this range of T_o to determine the expected rate for $T > 60$ MeV/nuc as indicated on Fig. 3. Thus, for 1976 the reduction in the intensity between the heliospheric boundary and earth is calculated to be a factor of 4.3 if $T_o = 0.4$ GeV/nuc. In 1977 when P10 is at ∿ 15 AU about 60% of the modulation must occur beyond this distance. During 1981-82 about 85% of the modulation must occur beyond 30 AU. Thus, at solar minimum, and even more so at solar maximum, most of the modulation is occurring in the outer heliospere beyond 15-30 AU!

b) It appears from Fig. 2 that the conditions in the heliospheric cavity were different after 1982 since G_R in the inner heliosphere decreased from ∿ 2.8%/AU to ∿ 1.8%/AU. This is shown more clearly in Fig. 3 where it is evident that this is a temporal effect and the

ORIGINAL PAGE IS
OF POOR QUALITY

gradient remains relatively constant as a function of radius.

From a study of the heliocentric radial dependence of the characteristic recovery time t_o of 19 transient Forbush-type decreases occurring from 1980 to 1984 we found that t_o is about 20 times longer at 30 AU [8]. We would then expect that at $R \sim 30$ AU a typical transient would take ∿ 100 days to recover to 1/e whereas near earth it is only ∿ 5 days. In a simple model then the intensity will recover first at earth as the transient decreases pass outward beyond earth and become less frequent. This more rapid recovery at earth produces a lower G_R. We would expect this situation of a smaller G_R to persist until the number and magnitude of the transient decreases are insignificant. At that time (∿ 1988) one might expect the gradient to return to its sunspot minimum value of ∿3%/AU. In 1988 when P10 will be at ∿ 45 AU we would estimate that the normalized intensity at 1 AU would be unity. If at that time $G_R \sim 3\%$/AU, the normalized intensity at P10 relative to earth would be ∿ 3.5, so P10 would then possibly be sampling the interstellar spectrum. However, if the gradient remains ∿ 2%/AU, P10 at 45 AU would still be well within the modulation region. An important clue as to the origin of the modulation in the distant heliosphere will be obtained from observations of this gradient between now and 1988.

4. Acknowledgements The authors thank Frank McDonald for making available the data from the Pioneer and Voyager spacecraft and Tycho vonRosenvinge for providing the IMP data. This study was supported by the NSF (ATM-8304486) and GSFC (NAS-24354).

5. References

1. McDonald, F.B., et al., (1981), Ap. J., 249, L71.
2. Webber, W.R. and J.A. Lockwood, (1981), J. Geophys. Res. 86, 11458.
3. McKibben, R.B., et al., (1982), Ap. J., 254, L23.
4. Lockwood, J.A., and W.R. Webber, (1984), J. Geophys. Res., 87, 17.
5. Perko, J. and L. Fisk, (1983), J. Geophys. Res., 88, 9033.
6. Webber, W.R., and J.A. Lockwood, (1983), 18th ICRC, 3, 59.
7. Webber, W.R., and S.M. Yusak, (1983), Ap. J., 275, 391.
8. Webber, W.R., et al., (1985), J. Geophys. Res., to be published.

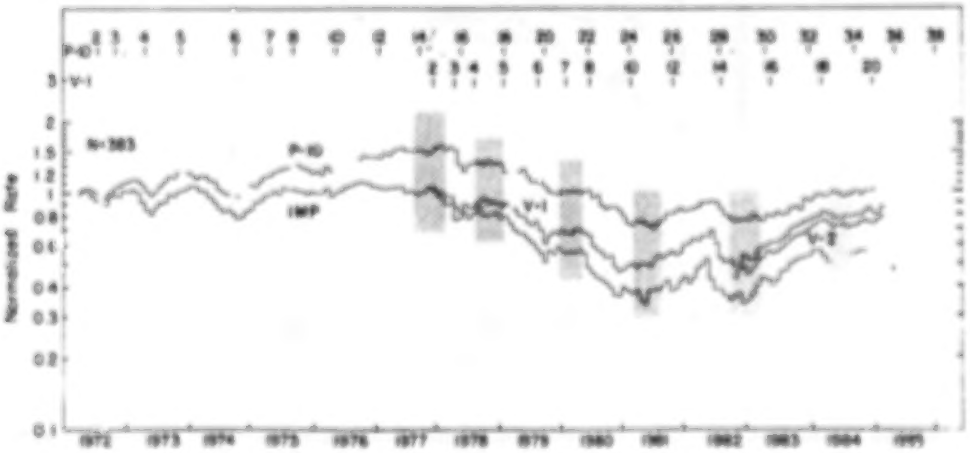

Fig 1: Normalized rates of > 60 MeV particles from IMP8, V1, V2 and P10. Heliocentric distances for V1 and P10 are shown.

ORIGINAL PAGE IS
OF POOR QUALITY

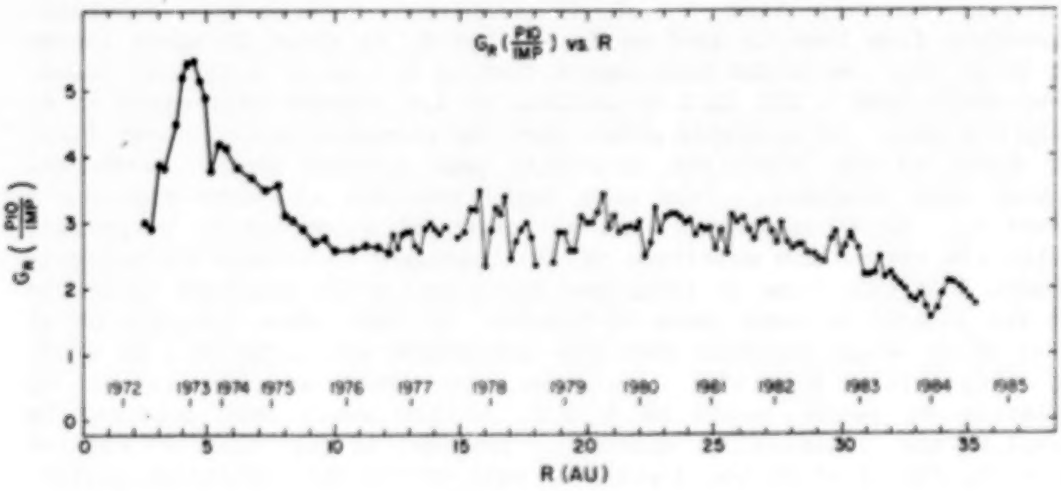

Fig. 2 G_R(%/AU) for P10/IMP8

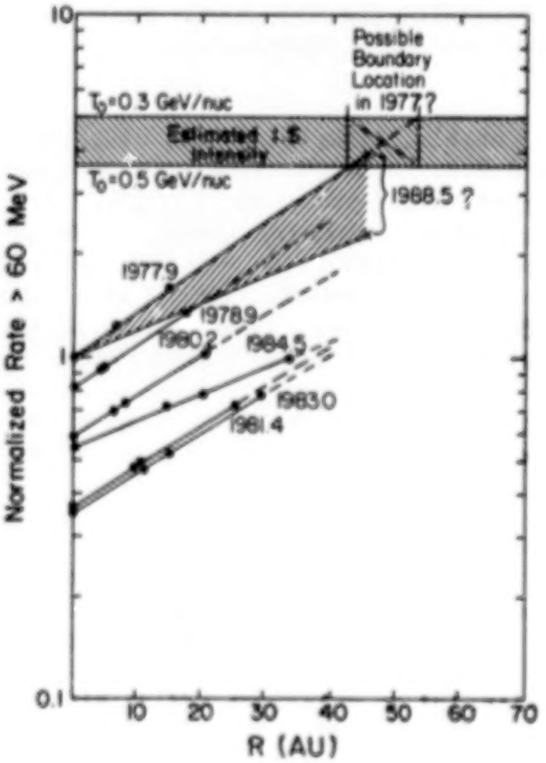

Fig 3: Radial variation of >60 MeV rate at various 26-day periods (see Fig. 1) from P10, V1, V2 and IMP8 data. Estimated interstellar rates are shown as described in text.

N85-35047

TIME AND ENERGY DEPENDENCE OF THE COSMIC RAY GRADIENT IN THE OUTER HELIOSPHERE

Fillius, Walker
University of California, San Diego, La Jolla, CA 92093

Axford, Ian
Victoria University of Wellington, New Zealand

Wood, David
University of California, San Diego, La Jolla, CA 92093

ABSTRACT

Pioneers 10 and 11, now 35 and 18 AU from the sun, continue to extend our knowledge of the spatial dependence of cosmic ray intensities in the heliosphere. We report radial gradients measured from these spacecraft by UCSD detectors which have integral energy responses above thresholds of 80 and 500 MeV/nucleon. An average gradient of ~ 2 %/AU typifies the data set as a whole, but there are time and energy dependences that deviate from this value.. With operating lifetimes of 13 and 12 years, respectively, for the two spacecraft, we have followed the time dependence for over a solar cycle.. The higher energy channel shows less modulation on all time scales.. At the start of the present cycle, the gradient is lower than the average value during the last solar cycle.

INSTRUMENTATION

Table I outlines the characteristics of the four UCSD data channels used in this report..

Table I

CHARACTERISTICS OF FOUR UCSD DATA CHANNELS

	Z = 1 Energy Range	Relative Response (Ratio)	Z > 1 Energy Range
M3	80<E<300 MeV	50 : 50	>80 MeV/nucl
M1	>80 MeV	90 : 10	>80 MeV/nucl
C1	>500 MeV	80 : 20	>500 MeV/nucl
C3	>500 MeV	30 : 70	>500 MeV/nucl

OBSERVATIONS

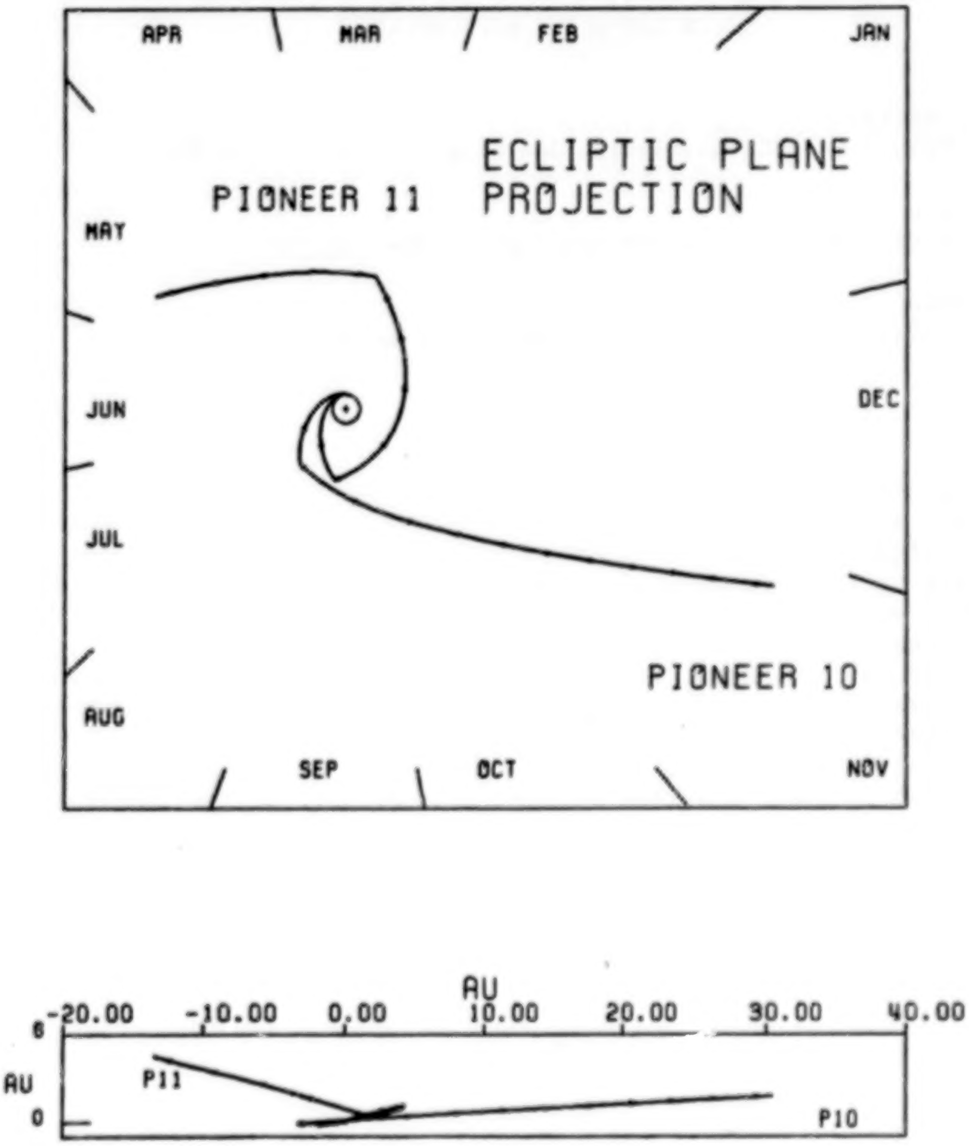

Figure 1 shows the positions of the two Pioneer spacecraft up to mid-1985..

ORIGINAL PAGE IS
OF POOR QUALITY

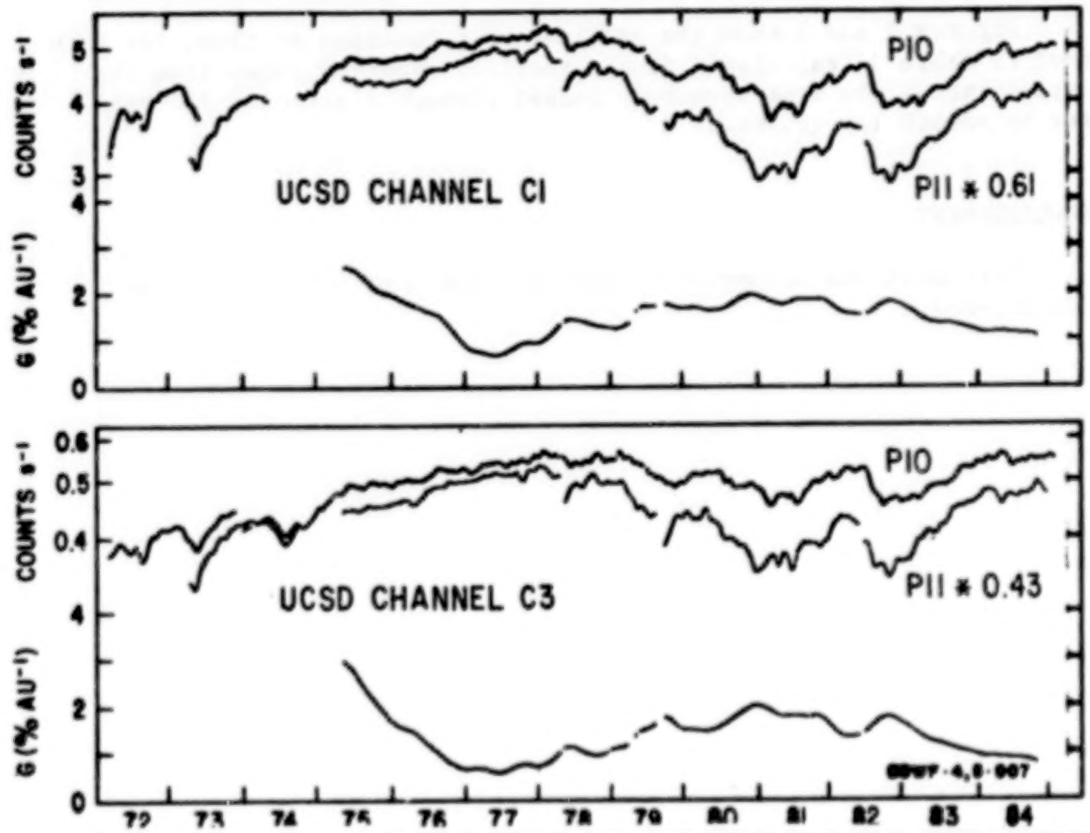

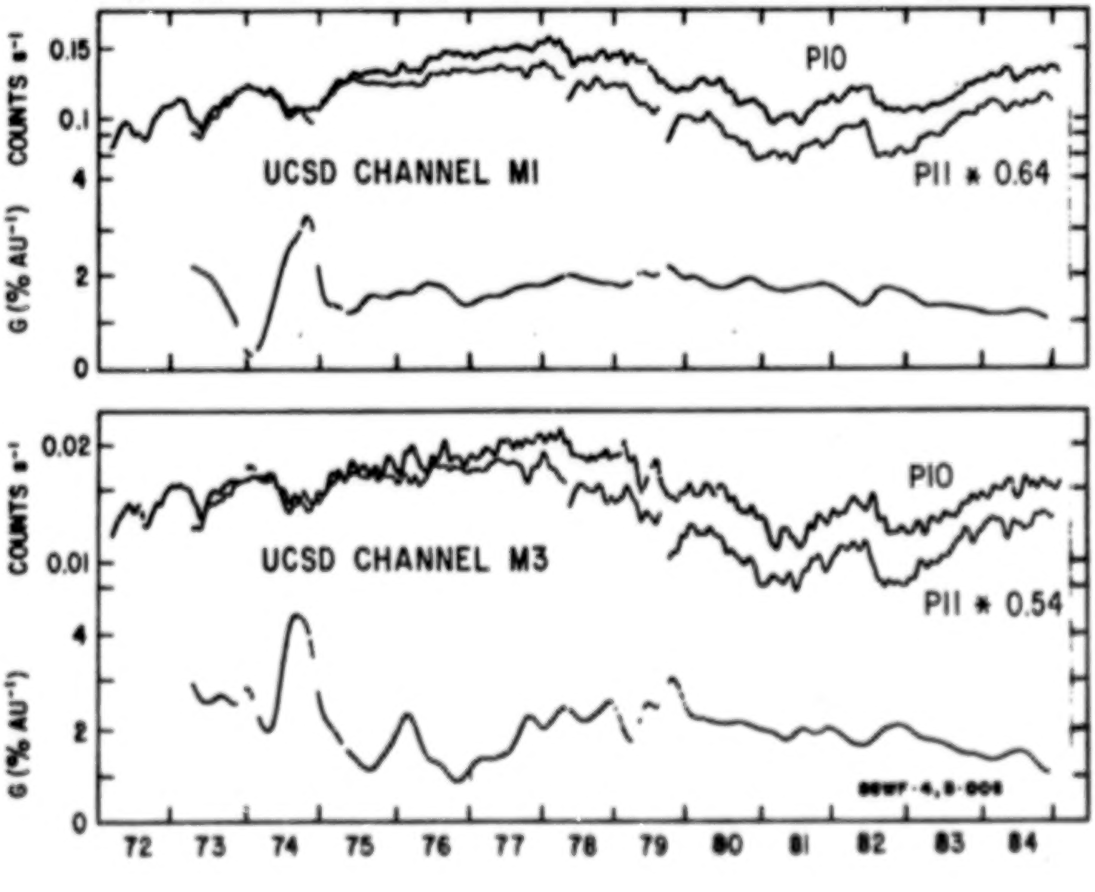

Figures 2 and 3 show the gradient as a function of time. for each channel in Table I, calculated from normalized counting rates from the two spacecraft.. The data have been passed through a gaussian low-pass filter to smooth the graphs..

ACKNOWLEDGEMENT

This work was supported in part by NASA Grants NAS 2-153 and NGL 05-005-007..

THE LARGE SCALE DYNAMICS OF THE OUTER HELIOSPHERE AND THE LONG-TERM MODULATION OF GALACTIC COSMIC RAYS

Frank B. McDonald, NASA Headquarters/Code P, Washington, DC 20546
T.T. von Rosenvinge, N. Lal, P. Schuster, J. H. Trainor,
NASA/GSFC, Greenbelt, MD 20770
M.A.I. Van Hollebeke, Musee National des Sciences, Technique et Industrie
PARC de La Villette, Paris, France

ABSTRACT

The network of cosmic-ray observatories reaching across the heliosphere has given new insight into the process of solar modulation, establishing that the decreases occur principally in the outer heliosphere and are produced by interplanetary flow systems; that the hysteresis effects appear to be produced by changes in the rigidity dependence of the diffusion coefficient and that the predicted effects on the cosmic ray gradients associated with the reversal of the solar magnetic field polarity are not observed.

1. Introduction. The study of cosmic ray modulation has traditionally been of importance in determining the local interstellar spectra of galactic cosmic rays and their transport in the heliosphere. The presence of a network of cosmic ray detectors at various heliocentric distances not only offers new insight into these areas but also offers a means of studying the dynamics of the interplanetary medium in the outer heliosphere. Pioneer 10 cosmic ray measurements now cover the period from 1972 to the present and extend to heliocentric distances beyond 32 AU (Fig. 1). Voyagers 1 and 2, launched in 1977, provide observations at intermediate heliocentric distances while Helios 1 and ISEE-3 provide "baseline" measurements at 1 AU. The data from the Goddard cosmic ray experiments (done in collaboration with the California Institute of Technology and the University of New Hampshire on Voyagers 1 and 2 and with the University of New Hampshire on Pioneers 10 and 11) on these missions give detailed differential energy spectra for galactic cosmic ray helium nuclei from 3-500 MeV/nuc and for hydroden nuclei from 3-250 MeV. The detector systems used on these various missions are similar in their method of operation but differ in detail and in their relative geometric factors. In this paper a summary overview is given of these observations along with differential measurements of the cosmic ray gradient over the last solar cycle.

2. Observations. Intensities of the higher energy He ($\sim$185-450 MeV/nuc) and H ($\sim$130-240 MeV) along with the integral measurements >70 MeV are shown in Fig. 2 in the form of 26 day averages. Lower energy data for 30-56 MeV/nuc H and He and the 10-21 MeV/nuc anomalous He interval are shown in Fig. 3 for Pioneer 10 and Voyager. The 1 AU data has not been included in this later plot because of the difficulty in removing the solar energetic particle contribution at low energies.

As noted previously (McDonald et al., 1981; Lockwood and Webber, 1984; McKibben et al.,1982; Van Allen and Randall, 1985) the long term decrease occurs in a series of three distinct steps between April 1978 and January 1981. These decreases propagate radially outward with a velocity of 400-500 km/sec. There is a recovery period starting in early 1981 which is interrupted by the onset of increased solar activity in 1982 which results in a fourth step decrease. In early 1981 at ~24 AU and in late 1982 at 28 AU the galactic cosmic ray intensities at energies less than 500 MeV/nuc were distinctly lower than their 1 AU solar minimum values - suggesting that the bulk of the modulation must occur in the distant heliosphere.

The recovery is more complex and will have to be examined over a larger period of time to establish a pattern. One distinctive feature is a hysteresis effect as seen from the lag in the recovery of 10-21 MeV/nuc He and 30-56 MeV H (Fig. 3) as compared to the substantial recovery of the 185-450 MeV/nuc He (Fig. 2). If a clear rigidity

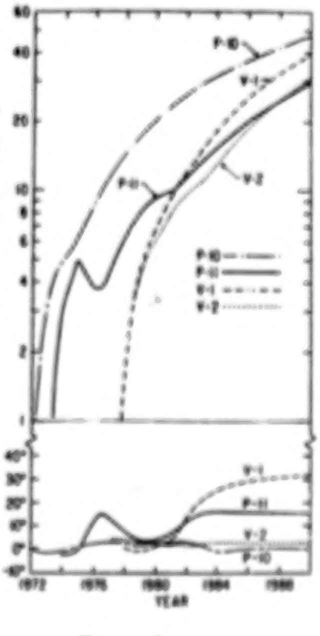

Fig. 1

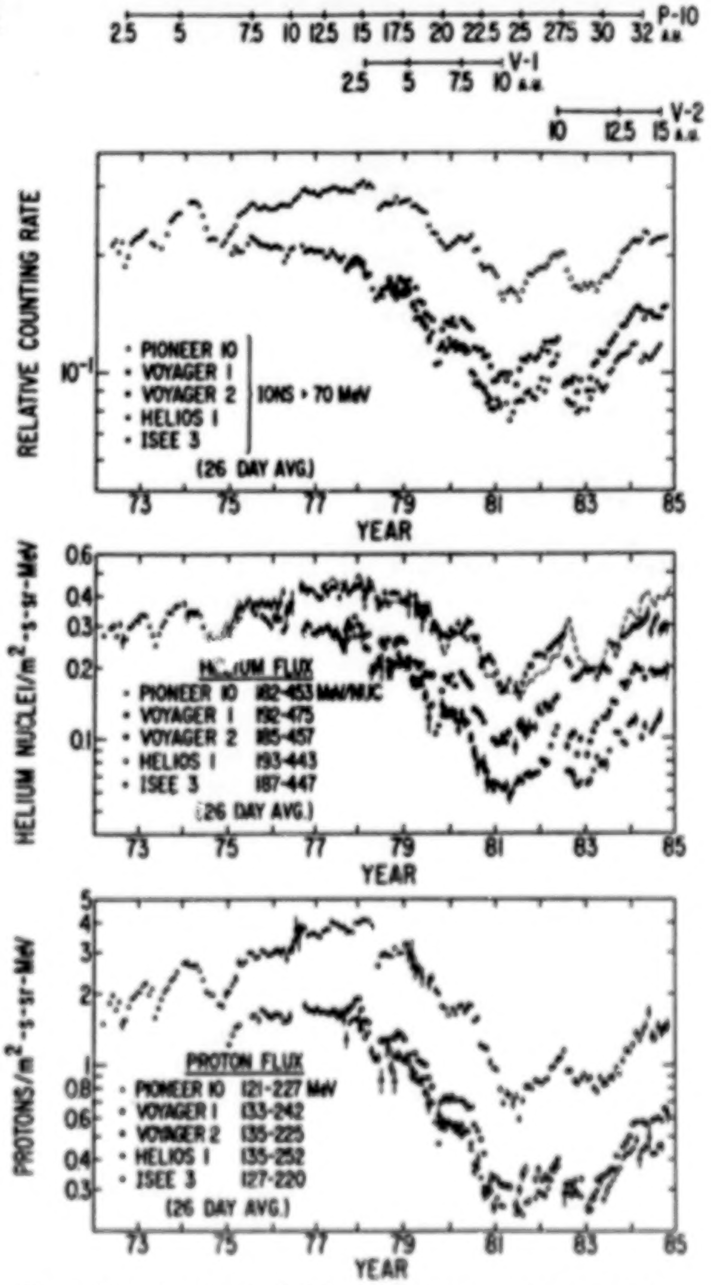

Fig. 2. The dashed line in the center panel is the extrapolation of the Helios/ISEE-3 data to the orbit of Pioneer 10 assuming a constant 4% AU gradient and a solar wind velocity of 550 km/sec.

ORIGINAL PAGE IS
OF POOR QUALITY

dependence can be established for this effect it may offer a method of determining the charge state of the anomalous component (McKibben, 1973; Paizis and von Rosenvinge, 1981). It is also seen that the decreases propagate rapidly outward for the first three steps, this concept breaks down after ∿ 1982. This breakdown probably reflects large heliolongitude asymmetries resulting from a few very strong shocks.

Measurements of the differential gradient are shown for the solar minimum period (3/77, 12/77) and the plateau regions between the step decreases(Fig4). At solar minimum (3/77) the gradients in the inner solar system are substantially higher than those in the outer heliosphere. With the onset of increased solar activity, they show a complex change. For the high energy He (150-380 MeV/nuc), the gradient approaches a value of ∿4%/AU for both sets of measurements. A similar pattern is observed for 30-56 MeV/nuc H and He and in the outer heliosphere for the high energy protons. However this latter component has a very small gradient in the inner solar system after the onset of the first recovery period in early 1981. The anomalous He interval approaches a value of ∿10%/AU until this same recovery period and then also shows a sharp decrease in the outer heliosphere - in agreement with the observations of McKibben, et al., 1985.

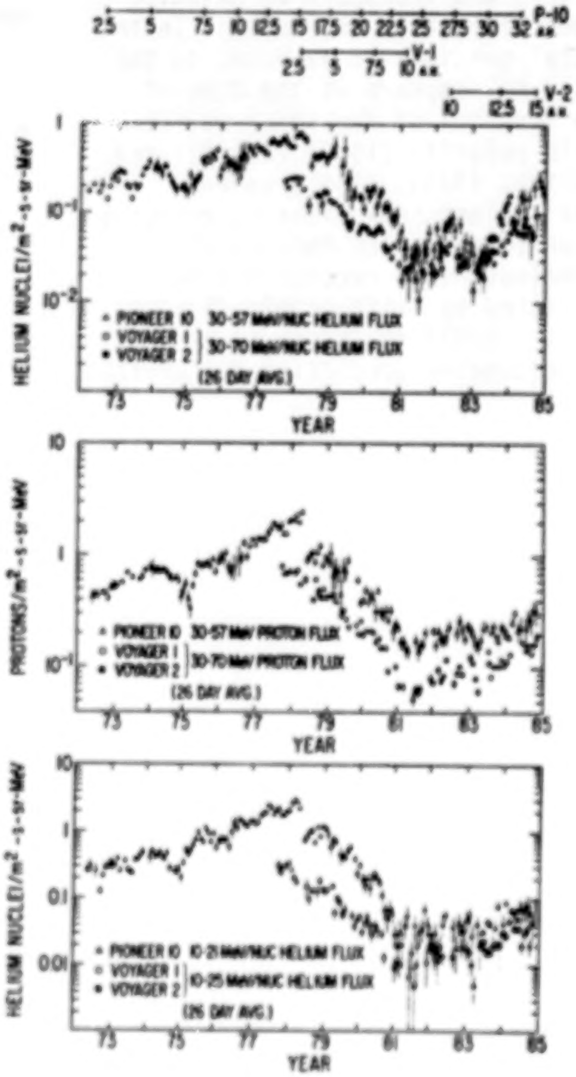

Fig. 3

3. Discussion. The step decreases have been explained in broad outline by Burlaga, et al., 1984, in terms of interplanetary flow systems containing a number of transient shocks and post shock flows. These systems of transient flows should evolve into expanding pressure waves such that the systems would merge and the outer heliosphere would be a region of enhanced turbulance. With such a system there would not be corresponding "step-increases" and the hysteresis effect would be explained by changes in the rigidity dependence of the diffussion coefficient in the outer region. If particle drifts play a major

role in the transport of galactic cosmic rays then an increase in the radial gradient is expected in the inner heliosphere at the time of the reversal of the solar magnetic field polarity (1980) (Jokipii and Kopriva, 1979). The gradient observations show either a decrease or no change. The failure of the anomalous He to recover has been predicted by drift models (Pesses et al., 1981) but there is no corresponding prediction for protons.

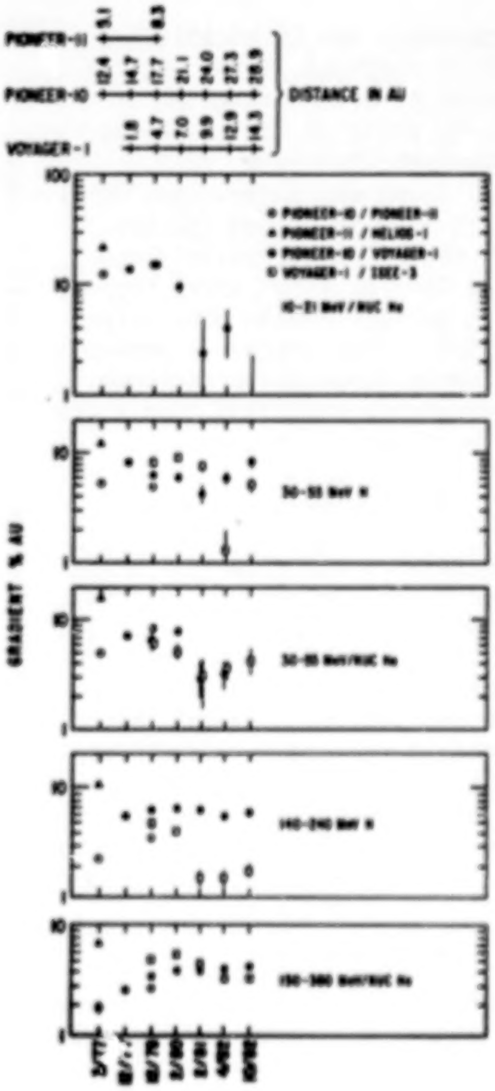

Fig. 4

References
1. Jokipii, J.R. and Kopriva, D.A., (1979), Ap.J., 234, 384.
2. Lockwood, J.A. and Webber, W.R., (1984), J. Geophys. Res., 89, 17.
3. McDonald, F.B., Lal, N., Trainor, J.H., Van Hollebeke, M.A.I., and Webber, W.R., (1981), Astrophys. J., 249, L71.
4. McKibben, R.B., Pyle, K.R., and Simpson, J.A., (1982), Astrophys. J., 254, L23.
5. McKibben, R.B., Pyle, K.R., and Simpson, J.A., (1985), Astrophys. J., 289, L35.
6. McKibben, R.B., (1977), Astrophys. J., 217, L113.
7. Paizis, C., and von Rosenvinge, T.T., (1981), Proc. 17th ICRC, 10, 73.
8. Pesses, M.E., Jokipii, J.R., and Eichler, D., (1981), Astrophy. J., 246, L85.
9. Van Allen, J.A. and Randall, B.A., (1985), J. Geophys. Res., 90, 1399.

SH4.7-4

N85-35049

Solar Modulation and Interplanetary Gradients of the Galactic Electron Flux 1977-1984

S. P. Christon, A. C. Cummings, and E. C. Stone

California Institute of Technology, Pasadena, CA 91125 USA

W. R. Webber

University of New Hampshire, Durham, NH 03824 USA

Previously, only one measurement of electrons at a location remote from earth has been reported [*Eraker*, 1982]. That measurement was made with a cosmic ray instrument on board the Pioneer 10 spacecraft during the period from 1972 - 1980, when Pioneer proceeded outward from 1 to 21.5 AU. Electrons of 1.75 - 25 MeV were observed. This energy range appears to be dominated by Jovian electrons, and no significant temporal or radial effects due to galactic electrons were observed.

In this paper we report on the flux of electrons with energy from ~ 10 - 180 MeV measured with the electron telescope on the Voyager 1 and 2 spacecraft [*Stone et al.*, 1977] in the heliocentric radial range 1 - 22 AU between 1977 and 1984. Jovian electrons were clearly observable between 1978 and 1983 (radial range 2 - 12 AU) at energies below ~ 50 MeV [*Christon et al.*, 1985]. Above ~ 50 MeV the electron intensity exhibited temporal variations generally related to the 11 year modulation of protons > 75 MeV. The overall magnitude of the electron intensity changes between the maximum intensity observed in 1977 and the minimum intensity in 1981 was a factor ~ 2, also comparable to that observed for > 75 MeV protons. By early 1985 the electron intensity had apparently recovered to the level observed in 1977 whereas the proton intensity was still about 20% lower. A detailed interpretation of these electron variations in all energy channels depends on an accurate subtraction of background induced by energetic protons of a few 100 MeV. This subtraction is facilitated by calibration results at several energies. Further results on these temporal variations and limits on possible interplanetary gradients will be reported.

This work was supported in part by NASA under contract NAS 7-918 and grant NGR 05-002-160.

References.

Christon, S. P., A. C. Cummings, E. C. Stone, and W. R. Webber, *19th Internat. Cosmic Ray Conf., La Jolla*, paper SH1.5-18, 1985.

Eraker, J. H., *Ap. J.*, *257*, 862, 1982.

Stone, E. C., R. E. Vogt, F. B. McDonald, B. J. Teegarden, J. H. Trainor, J. R. Jokipii, and W. R. Webber, *Space Sci. Rev.*, *21*, 355, 1977.

GALACTIC COSMIC RAY RADIAL GRADIENTS AND THE ANOMALOUS He COMPONENT NEAR MAXIMUM SOLAR MODULATION AND TO RADII BEYOND 34 AU FROM THE SUN

R. B. McKibben, K. R. Pyle, and J. A. Simpson
Enrico Fermi Institute, The University of Chicago
Chicago, Illinois 60637 (U. S. A.)

ABSTRACT: Radial gradients for relativistic galactic cosmic rays ($E > 70$ MeV) remained nearly constant at ~ 2.5 %/AU from 1978-84, which includes the period of maximum solar modulation in 1981-82. For energies 30-70 MeV/n, gradients decreased at solar maximum to values of 1 %/AU (protons) and 4 %/AU (helium), and appear to be increasing again in 1983-84 toward the values found for solar minimum. The anomalous helium component has not reappeared, either at 1 AU or at Pioneer 10 at $R > 34$ AU.

1. INTRODUCTION: Our observations of the radial and temporal variations of the modulated cosmic radiation and anomalous helium to the time of maximum solar modulation in 1981-82 (McKibben et al., 1983, 1985) showed that, at solar maximum, radial gradients for low energy ($E < 100$ MeV/n) cosmic rays measured between 1 and 31 AU were sharply reduced from their values at solar minimum. At relativistic energies, however, the radial gradient was not strongly affected by the level of solar modulation. We now extend our observations to the end of 1984, by which time the cosmic ray intensity had begun to recover from maximum modulation both at 1 AU and in the outer heliosphere. The Pioneer and IMP instruments used in this study have been described by Simpson et al. (1980), and by Garcia-Munoz et al. (1977). By late 1984, Pioneer 10 had reached a radial distance of > 34 AU from the sun, as shown in Figure 1C.

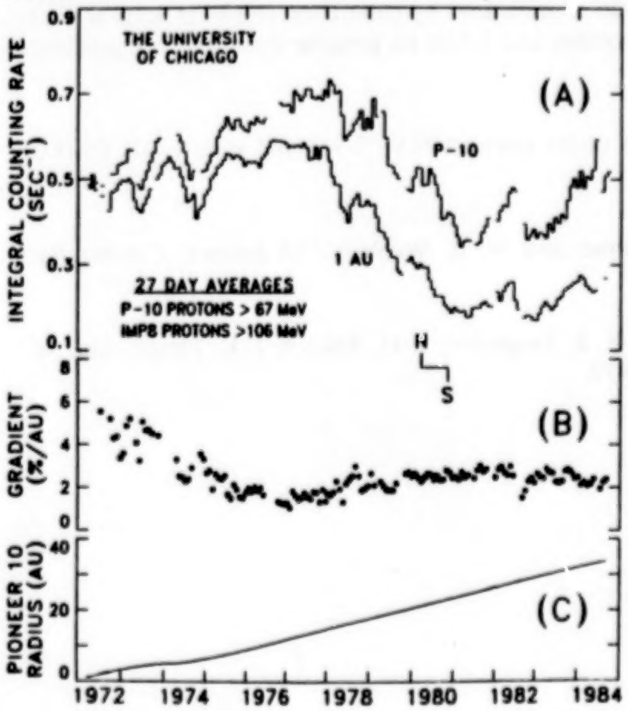

FIGURE 1

2. INTEGRAL GRADIENTS ($E \gtrsim 70$ MeV): Figure 1A shows simultaneous 27 day averages of integral counting rates from Pioneer 10 (protons $\gtrsim 70$ MeV) and IMP 8 (protons $\gtrsim 106$ MeV), selected to exclude contributions from solar particles. These counting rates are dominated by relativistic particles with a mean energy of the order of 2 GeV. The time variations observed at Pioneer 10 remain well correlated with variations at 1 AU after a time shift corresponding to outward propagation at near the solar wind speed (McKibben et al. 1982). In late 1984, the flux at Pioneer 10 at 34 AU was increasing from the maximum modulation observed

C-4

ORIGINAL PAGE IS
OF POOR QUALITY

in 1981-82, but was still not significantly greater than that observed at 1 AU at solar minimum in 1972. Therefore, the flux at Pioneer 10 remained heavily modulated in 1984.

Figure 1B shows the radial gradient of the integral intensity as a function of time. As in McKibben et al. (1983), a 400 km/s propagation delay from 1 AU to Pioneer 10 has been assumed. Although there are significant variations during the near-solar-minimum period (1972-1978), since 1978 the gradient has remained nearly constant at ~ 2.5 %/AU despite large changes in the intensity at both Pioneer and IMP. The transient decrease in the gradient in 1982 is an artifact of the high velocity [$\gtrsim$ 800 km/s (Lockwood and Webber, 1984)] of the shocks which produced the intensity decrease in 1982.

3. LOW ENERGY ($E < 70$ MeV/n) DIFFERENTIAL FLUXES: Figure 2A shows the low energy (30-70 MeV) cosmic ray proton flux as observed at Pioneer 10, Pioneer 11, and IMP 8 starting in 1977, shortly before the onset of renewed solar activity, continuing through solar maximum in 1981-82 and into 1984 when recovery of the cosmic ray flux had begun. After 1979, measurements in this energy range are not available from Pioneer 11 because a detector problem has blocked analysis of particles with energy > 20 MeV/n. As reported earlier (McKibben et al., 1985), at solar maximum (1981-82) for low energy protons, nearly the same flux was measured at Pioneer 10 ($R > 20$ AU) and at 1 AU. At both Pioneer 10 and IMP 8 the proton flux remained essentially constant during 1981-82, and the shocks that produced such strong effects at higher energies had little effect on the low energy proton flux. As the recovery began in 1983-84, the flux at Pioneer 10 once again increased above that at 1 AU.

Figures 2B-D show the 27-day-average radial gradients measured for 30-70 MeV protons, 11-20 MeV/n helium, and 30-70 MeV/n helium. The accuracy of the measurements is reflected in the scatter of the points. All three gradients decrease at solar maximum. The largest decrease is shown by the gradient of 11-20 MeV/n helium and corresponds to the disappearance of the anomalous helium in 1980-81. The shocks in 1982 appear to have produced a further decrease, lasting 6 months or more, in the 30-70 MeV/n helium gradient. No clear corresponding effects are observed for lower energy helium. After maximum modulation, the gradient of 30-70 MeV protons increased slightly, and the data also suggest an increase in gradients for helium.

The observations are summarized in Figures 3A-C, which contain yearly snapshots of the convection-corrected intensity of 30-70 MeV protons, and of 11-20 and 30-70 MeV/n helium. Open

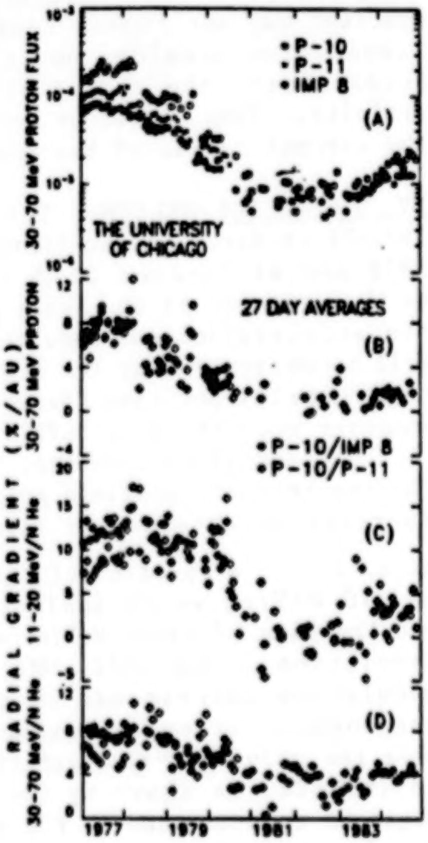

FIGURE 2

ORIGINAL PAGE IS
OF POOR QUALITY

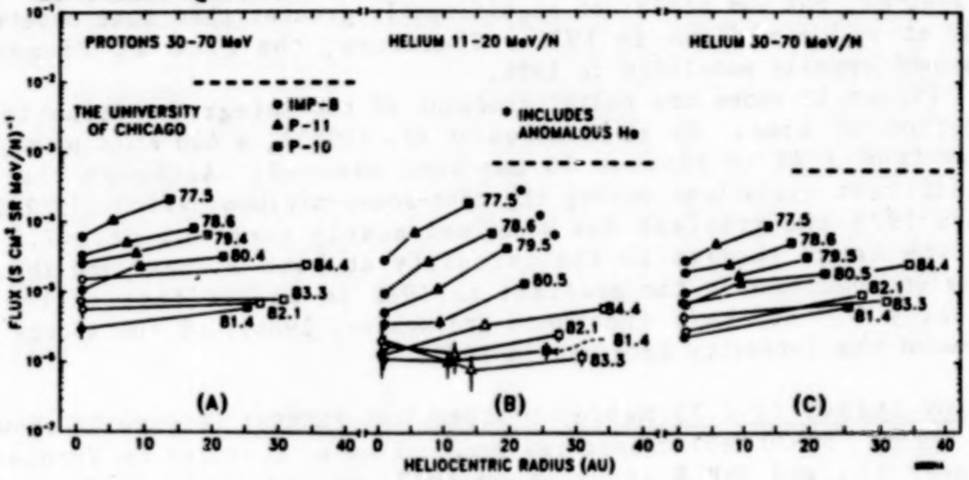

FIGURE 3

symbols correspond to data obtained since maximum modulation in 1981, and the heavy dashed lines indicate estimated interstellar galactic cosmic ray fluxes from the model of Evenson et al. (1983). For all three components, the flux measured in 1984 at Pioneer 10 remains below that measured at 1 AU at solar minimum in 1977. Comparing the observed fluxes in 1984 to the interstellar fluxes, at least 95% of the modulation takes place outside R = 34 AU. Linear extrapolation of the gradients observed in 1984 to the interstellar fluxes suggests modulation boundaries in the range 100-300 AU. However, modulation models suggest that the radial gradient may not remain constant to the boundary, so that linear extrapolation provides no reliable estimate of the boundary location. Furthermore, the radius of the boundary itself may vary with solar activity. Thus, based on our observations to date, we conclude only that the current radius of the modulation region is much larger than 35 AU.

IV. ANOMALOUS HELIUM:

The anomalous helium component was present from 1972-79 at Earth and at Pioneer 10 and 11. It disappeared at 1 AU in 1979 and at Pioneer 10 (R > 20 AU) in 1980-81, at roughly the same time as the reversal of the sun's polar magnetic fields. Alternate models for the acceleration and modulation of this component predict either that it will be observed near the ecliptic only when the north pole of the sun is magnetically positive (Pesses et al., 1981), or that it will be observed whenever modulation is sufficiently weak (Garcia-Munoz et al., 1983).

The anomalous component helium spectrum is significantly softer than the spectrum of modulated galactic cosmic rays. Figure 4 displays the correlation observed at Pioneer 10 between the power law spectral index (i.e. γ for a spectrum of the form $dJ/dE \propto E^{+\gamma}$) for helium between 11 and 70 MeV/n, which indicates the strength of the anomalous component, and the flux of 29-67 MeV/n helium, which measures the level of solar modulation. From 1972-1980, the correlation is well defined, and weaker modulation corresponds to a larger contribution from the anomalous component. At solar maximum in 1981-82, the spectral indices cluster near the value of ~+1.0 expected for normally modulated galactic helium. In 1983-84, as shown by the large unfilled data points, the helium flux began to recover, and by the end of 1984, the helium flux had reached levels where in previous years the spectrum had shown clear evidence of the anomalous component. As of late 1984, however, the spectrum remained consistent with the presence only of galactic cosmic ray helium. These observations show that the presence of the anomalous component near the ecliptic is not a function only of the strength of modulation. Alternatives include 1) existence of a hysteresis effect, in which case the anomalous helium should reappear at Pioneer 10 in the near future, 2) sensitivity of the anomalous helium to the sign of the heliospheric magnetic field, as suggested by Pesses et al. (1981), or 3) dependence of acceleration or modulation of the anomalous helium on some as yet undefined characteristic of heliospheric structure.

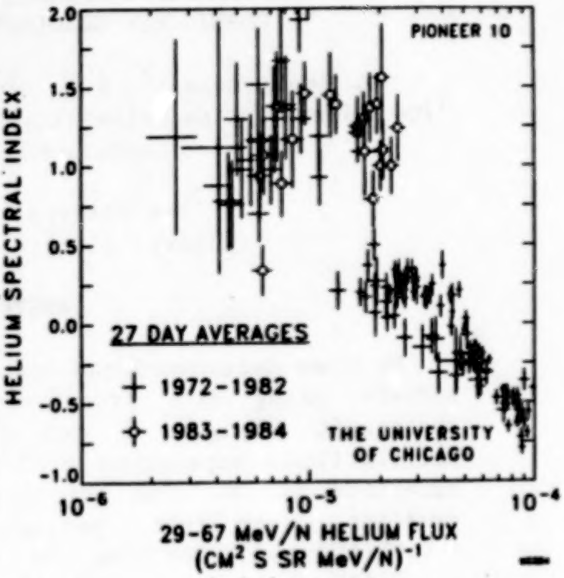

FIGURE 4

4. SUMMARY AND CONCLUSIONS: 1. For relativistic cosmic rays, the radial gradient measured between 1 AU and Pioneer 10 at R > 30 AU was nearly independent of the level of modulation throughout the period 1978-84, remaining approximately constant at ~ 2.5 %/AU.

2. For cosmic rays below 100 MeV/n, the radial gradient was much smaller at maximum modulation than at solar minimum. As the flux increased in 1983-84 after solar maximum, the gradient also began to increase.

3. The cosmic ray flux at Pioneer 10 at > 34 AU remains as heavily modulated as it was at 1 AU in 1972, so that Pioneer 10 is still far from the boundary of the modulation region. Based on estimates of the interstellar spectra, for energies < 100 MeV/n more than 95% of the modulation was occuring beyond 34 AU in 1984.

4. The anomalous helium has yet to reappear at either 1 AU or Pioneer 10.

5. ACKNOWLEDGEMENTS: We are grateful to C. Lopate for his assistance in preparation of the data. This work was supported in part by NASA/Ames Contract NAS 2-11126, and by NASA Contract NAS5-28442.

REFERENCES:

Evenson, P., Garcia-Munoz, M., Meyer, P., Pyle, K.R., and Simpson, J.A., 1983, Ap. J. (Letters), 275, L15.
Garcia-Munoz, M., Mason, G.M., and Simpson, J.A., 1977, Ap. J., 217, 859.
Garcia-Munoz, M., Pyle, K.R., and Simpson, J.A., 1983, Ap. J. (Letters), 274, L93.
Lockwood, J.A., and Webber, W.R., 1984, J. Geophys. Res., 89, 17.
McKibben, R.B., Pyle, K.R., and Simpson, J.A., 1982, Ap. J. (Letters), 254, L23.
________, 1983, Proc. XVIII ICRC, Bangalore, India, 3, 63.
________, 1985, Ap. J. (Letters), 289, L35.
Pesses, M.E., Jokipii, J.R., and Eichler, D., 1981, Ap. J. (Letters), 246, L85.
Simpson, J.A., Bastian, T.S., Chenette, D.L., McKibben, R.B., and Pyle, K.R., 1980, J. Geophys. Res., 85, 5731.

VOYAGER 1 AND 2 MEASUREMENTS OF RADIAL AND LATITUDINAL COSMIC RAY GRADIENTS DURING 1981-84

D. Venkatesan[1,2], R.B. Decker[1] and S.M. Krimigis[1]
[1]The Johns Hopkins University, Applied Physics Laboratory,
Laurel, MD 20707 USA

[2]The University of Calgary
Calgary, Alberta, T2N 1N4 Canada

ABSTRACT

We have determined the cosmic ray radial gradient during 1981-84 using data from very similar detectors onboard spacecraft Voyagers 1 and 2 (radial separation ~ 6 AU, heliolatitude separation ~ 25°)and from the earth-orbiting satellite IMP 8. The principal result is that the radial gradient over this period decreased at the rate ~ 0.4%/AU/year, reaching by the end of 1984 a value of ~ 2.0%/AU between 1 and 16 AU and ~ 0.6%/AU between ~ 16 and 22 AU.

1. Introduction: Measurements of galactic cosmic ray intensity gradients, radial as well as heliolatitudinal, play on important role in guiding theoretical models of cosmic ray propagation in the heliosphere. Determinations of integral radial gradients (for a summary, see Venkatesan et al., 1985) using data from Pioneers 10 and 11, Voyagers 1 and 2, and IMP 8 have revealed relatively small values of 2-4% per AU, thus questioning the concept of a spherically symmetric heliosphere. Decker et al. (1984) have estimated for the first time the heliolatitudinal gradient of galactic cosmic ray intensity during early-1981 through mid-1982, a period coinciding with the initial phase of cosmic ray recovery following the minimum reached in late-1980 to early-1981. They found that for all practical purposes, the heliolatitudinal gradient is 0%/deg over the 16° heliolatitudinal separation in the region 8-13 AU during that period of study. This was based on the assumption that the radial gradient during the 1981-82 recovery period remained at the same ~ 2-4%/AU level as determined from multi-spacecraft measurements during the 1977-80 cosmic ray intensity decay period.

2. Experiment: Our study has used the data from the cosmic ray channel (responding to protons integral above 70 MeV) provided by a heavily shielded solid state detector in the low-energy charged particle (LECP) instrument on both Voyagers. Total counts over a 26 day interval are typically $\gtrsim 2 \times 10^4$; thus the statistical error is $\lesssim 0.7\%$. We have also used the data from the charged particle measurement experiment (CPME) anticoincidence scintillator ($E_p \gtrsim 35$ MeV) on IMP-8. For detector details and analysis refer to Venkatesan et al. (1985).

3. Observations:

(a) Differential Gradient: Figure 1 shows at the top a plot of the 26 day means of the cosmic ray intensity registered by both the Voyagers. Note that the Voyager 1 data has been shifted to the position of Voyager 2 using an average value of 500 km/sec for the solar wind. The convection of cosmic ray features and the appropriateness of such a solar wind speed has been discussed in detail by Venkatesan et al. (1984, 1985). The close correspondence in the two intensity-time profiles is seen.

In the middle of Figure 1 we have plotted the values of the radial gradient G_r given by $G_r = \left[(\ln (R_1/R_2))/\Delta r\right] \times 100\%$, where R_1 and R_2 are the counting rates of Voyagers 1 and 2, and Δr is the radial separation. They are point-by-point computations which assume that the difference in intensity is entirely due to a radial gradient. The points are fitted with the line of least squares; note that G_r decreased from ~ 2.1%/AU to ~ 0.6%/AU over the four year period giving a value for $\dot{G}_r$ of 0.38 (± 0.09)%/AU/year.

In the bottom portion of Figure 1 we have plotted the values of the heliolatitudinal gradient G_ψ given by $G_\psi = \left[(\ln (R_1/R_2))/\Delta\psi\right] \times 100\%$ where $\Delta\psi$ is the latitudinal difference between the two spacecraft. Again, they are point-by-point computations based on the assumption that the difference in intensity is entirely due to a latitudinal gradient. The points are fitted with a line of least squares; note that G_ψ also decreased from ~ 0.42%/deg to ~ 0.13%/deg over the four year period giving a value for $\dot{G}_\psi$ of 0.06 (± 0.02)%/deg/year.

(b) Integral Gradient: We use the terminology "integral gradient" when we use a comparison detector located at 1 AU, such as IMP-8 and "differential gradient" when the two Voyagers are compared with each other. Figure 2 at the top shows the intensity time profiles for IMP-8 and the two Voyagers; the latter data were shifted to 1 AU to compensate for convection of cosmic ray features at the speed of 500 km/sec. Note the similarity among the three profiles.

The middle and lower part of Figure 2 show the integral radial gradient determined from the two pairs, Voyager 1-IMP-8 and Voyager 2-IMP-8. Again these are point-by-point computations and in the case of Voyager 1 (where only it is relevant) the assumption is made that the intensity difference arises entirely from the radial gradient. The values of G_r decreased from ~ 3.5%/AU to ~ 1.5%/AU and from ~ 3.8%/AU to ~ 2.0%/AU respectively; the decreases in the radial gradient are given by $\dot{G}_r$ = 0.48 (± 0.5)%/AU/year and $\dot{G}_r$ = 0.43 (± 0.07)%/AU/year respectively.

4. Discussion and Conclusions: The following points can be made.

(1) The choice of 500 km/sec for the average solar wind speed to correct the data for convection of cosmic ray features (from Voyager 1 to Voyager 2) in the heliospheric region ~ 8 AU to ~ 22 AU during 1981-84 is appropriate since the two intensity-time profiles at the top of Figure 1 agree fairly well.

(2) The similarity in the long-term trend of G_r and G_ψ in Figure 1 is indicative of the fact that the heliosphere, at least up to a radial distance of ~ 22 AU and heliolatitude of 25°, responds to cosmic ray modulation rather similarly. This is not surprising since it is clear from an earlier study (Decker et al., 1984) that no significant

latitudinal gradient exists. This is still our view, by virtue of the fact that the radial gradient G_r of ~ 2.0%/AU is evident from other multispacecraft studies as well.

(3) A decrease in the radial gradient as a function of increasing radial distance is clearly seen. Comparing the middle part of Figure 1 with the bottom portion of Figure 2, we see for example, at the end of 1984, we have IMP-8 (at 1 AU), Voyagers 1 and 2 at radial distances of 16 and 22 AU respectively. We find that the radial gradient G_r in the region 1-16 AU (IMP8-Voyager 2 pair) is ~ 2%/AU and that in the region 16-22 AU (Voyager 2-Voyager 1 pair) is ~ 0.6%/AU, a lower value. This clearly demonstrates that a comparison of integral radial gradient, over larger distances and at the same time later periods in the solar cycle is somewhat questionable. A value of say 2.0%/AU for the radial gradient over a complete solar cycle and out to a heliocentric distance of over 32 AU (Van Allen and Randall, 1985) could very well consist of the mean of the radial gradient G_r over different regions at different times including a 0.0%/AU gradient in the outermost region at the time of the approaching solar minimum. It is appropriate to mention that McKibben et al. (1985) have also observed a similar decrease in the radial gradient for low energy cosmic rays ($10 < E < 70$ MeV).

(4) The trend of G_r shows that we may be approaching a region of $G_r = 0.0$%/AU either at greater distances or at the sunspot minimum (~ 1987-88) at which time Voyager 2 would be at ~ 22-25 AU and Voyager 1 at ~ 30-31 AU. If the trend persists and our interpretation is correct, we may well be seeing the boundary of cosmic ray modulation at the solar minimum. We note that Voyager 1 is generally moving in the direction of the solar apex, while Pioneer 10 although at a greater radial distance, is moving in the opposite direction. It should be pointed out that this is the first time gradient measurement is being reported during the recovery period of the cosmic ray intensity eleven-year cycle at such large radial distances.

In summary, it seems reasonable to conclude that the region of cosmic ray modulation shrinks and expands possibly in step with the solar activity cycle (minimum and maximum). McDonald et al. (1981) have suggested the dominant source of solar cycle modulation as the "pile up" of propagating shocks in the outer heliosphere.

Acknowledgements: This work was supported in part by NASA under Task I of Contract N00024-78-C-5384 and by NSF under grant ATM-8305537.

References

1. Decker,R.B., S.M.Krimigis & D.Venkatesan, Ap. J., 278, L122, 1984
3. McDonald,F.B., N.Lal, J.H.Trainer,M.A.I. Van Hollebeke & W.R.Webber, Ap. J., 249, L71, 1981
4. McKibben,R.B., K.R.Pyle, & J.A.Simpson, Ap. J., 289, L35, 1985.
5. Van Allen,J.A., & B.A.Randall, J.G.R., 90, 1399, 1985
6. Venkatesan,D., R.B.Decker & S.M.Krimigis, J.G.R., 89, 3735, 1984
7. Venkatesan,D., R.B.Decker, S.M.Krimigis & J.A.Van Allen, J.G.R., 90, 2905, 1985

ORIGINAL PAGE IS
OF POOR QUALITY

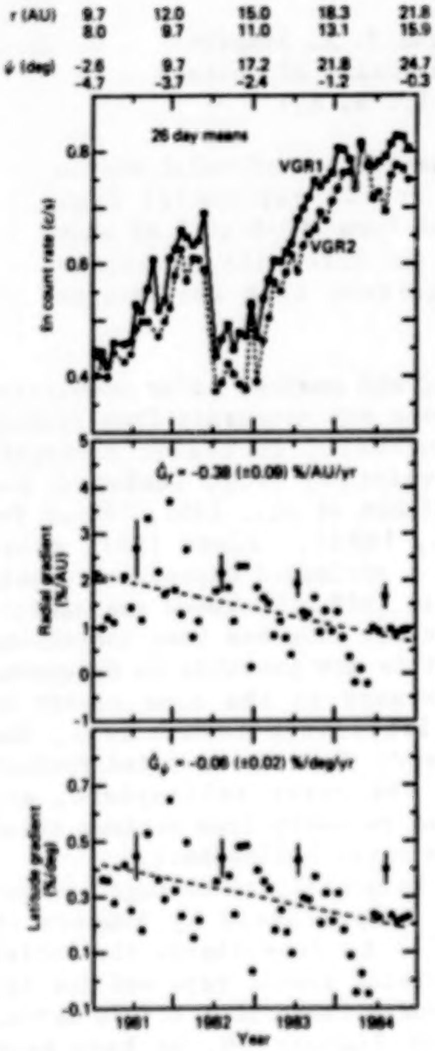

Figure 1

Intensity-time profiles of cosmic ray intensity at Voyagers 1 and 2; Voyager 1 data has been shifted to position of Voyager 2 using a solar wind speed of 500 km/sec. The middle and bottom portions provide the radial and heliolatitudinal gradients between the Voyagers.

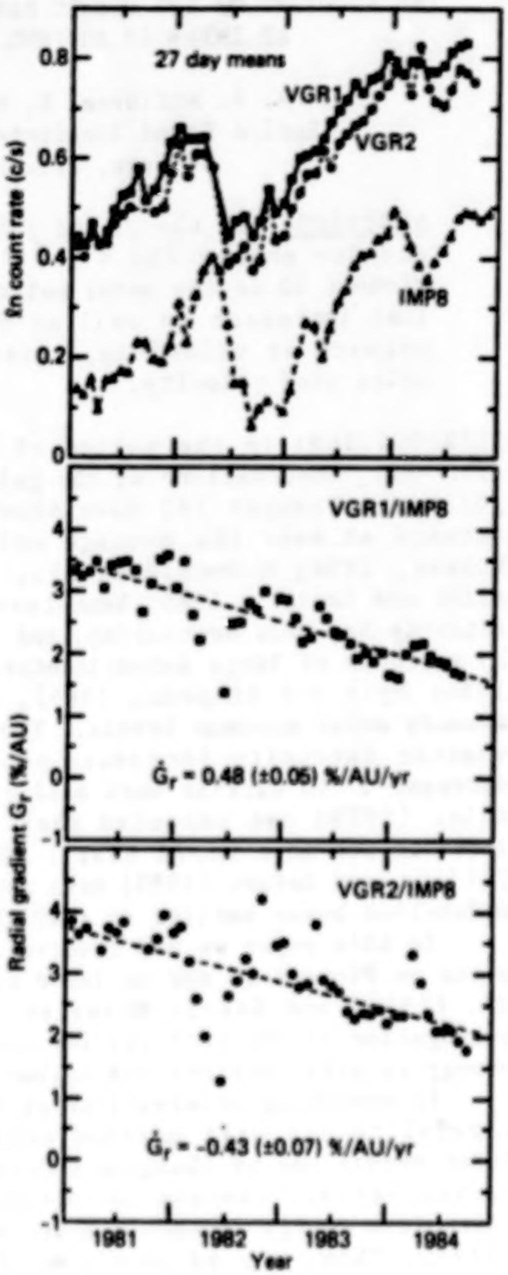

Figure2

Intensity-time profiles of cosmic ray intensity at the Voyagers duly shifted to 1 AU using a solar wind speed of 500 km/sec and IMP 8; the radial gradients are between Voyager 1 and IMP 8 and Voyager 2 and IMP 8.

N85-35052

SH 4.7-7

THE RECOVERY OF THE COSMIC RAY FLUX FROM MAXIMUM SOLAR MODULATION AT IMP-8 (1 AU) AND AT PIONEER 10 (R > 30 AU)

R. B. McKibben, K. R. Pyle, and J. A. Simpson
Enrico Fermi Institute, The University of Chicago
Chicago, Illinois 60637 (U. S. A.)

__ABSTRACT:__ In the period 1980-84, observations of relativistic and low energy ($30 \lesssim E \lesssim 70$ MeV/n) cosmic ray nuclei from Pioneer 10 in the outer heliosphere and from IMP-8 at 1 AU show that increases as well as decreases in intensity propagate outward at velocities equal to or greater than the average solar wind velocity.

__INTRODUCTION:__ In the period of increasing and maximum solar modulation (1977-81), observations of the galactic cosmic ray intensity from Pioneer 10/11 and Voyager 1/2 have shown that intensity decreases propagate outward at near the average solar wind velocity (e.g. Lockwood and Webber, 1984; McDonald et al., 1981; McKibben et al., 1982, 1985a; Van Allen and Randall, 1985; Venkatesan et al., 1985). Since 1981, solar activity has been decreasing, and following a prolonged depression caused by a series of large interplanetary shocks in 1982, (Lockwood and Webber, 1984; Pyle and Simpson, 1985), the cosmic ray flux has been increasing towards solar minimum levels. Therefore, it is now possible to determine whether intensity increases propagate outward in the same manner as decreases. In earlier work dealing with relativistic cosmic rays, Van Allen (1979) has reported that the recovery from an isolated Forbush decrease was more rapid near 1 AU than in the outer heliosphere, and Fillius and Axford (1985) have reported that recovery from maximum solar modulation began earlier at 1 AU than in the outer heliosphere.

In this paper we use observations from University of Chicago instruments on Pioneer 10 and on IMP 8 (described respectively by Simpson et al. (1980) and Garcia-Munoz et al. (1977)) to investigate the radial propagation of the recovery for both relativistic cosmic rays and for low energy galactic protons and helium in the energy range $30 < E < 70$ MeV/n.

In comparing observations at 1 AU and at Pioneer 10, we have been careful to use well matched energy intervals from the two spacecraft. Under conditions of changing modulation, even at one location significant delays between changes in intensity for particles of different energies arise from energy dependent hysteresis effects (e.g. Cooper and Simpson, 1979). Thus, use of poorly matched energy intervals may lead to confusion between phase shifts caused by radial propagation and shifts arising from the energy dependent hysteresis.

__RADIAL DEPENDENCE OF THE RECOVERY:__ In Figure 1A, we compare simultaneous 27 day gradient-corrected averages of the integral intensity of cosmic rays above 67 MeV from Pioneer 10 and above 106 MeV from IMP 8 in the period 1980-84. These counting rates are dominated by relativistic cosmic rays with a mean energy of ~ 2 GeV. During the period shown, Pioneer 10 moved outward from ~ 20 to ~ 34 AU from the sun. As a result of this motion, and of the measured radial gradient of 2.5 %/AU for the relativistic particles (McKibben et al. 1985b), increases in intensity in uncorrected data from Pioneer 10 are caused partly by Pioneer 10's outward motion, and partly by the decreasing level of solar

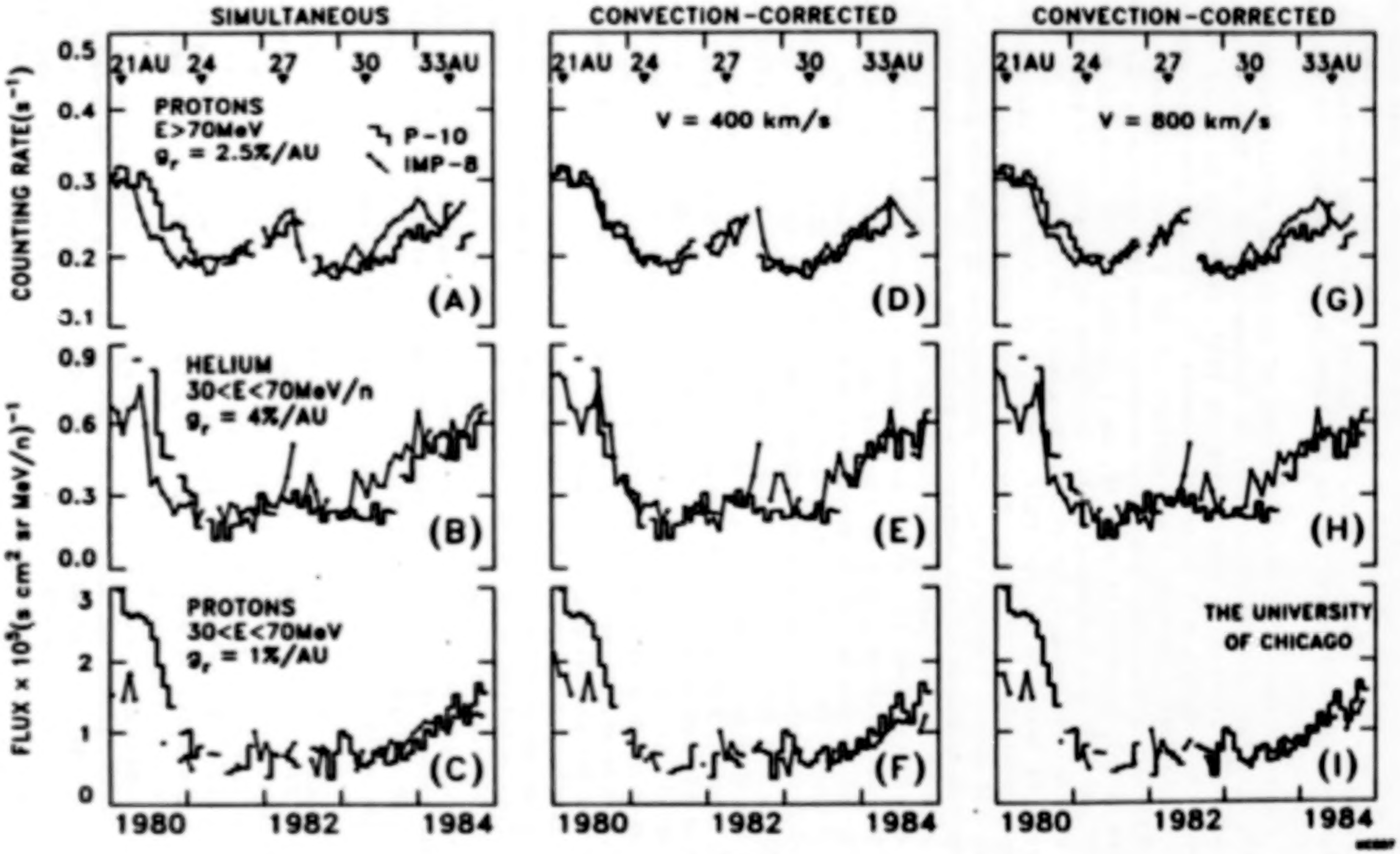
SIMULTANEOUS
CONVECTION-CORRECTED
CONVECTION-CORRECTED
21AU
24
27
30
33AU
PROTONS
E>70MeV
g_r = 2.5%/AU
P-10
IMP-8
V = 400 km/s
V = 800 km/s
COUNTING RATE(s^{-1})
0.5
0.4
0.3
0.2
0.1
(A)
(D)
(G)
HELIUM
30<E<70MeV/n
g_r = 4%/AU
0.9
0.6
0.3
0.0
(B)
(E)
(H)
FLUX × 10^5(s cm^2 sr MeV/n$)^{-1}$
PROTONS
30<E<70MeV
g_r = 1%/AU
THE UNIVERSITY
OF CHICAGO
3
2
1
0
(C)
(F)
(I)
1980
1982
1984

FIGURE 1

ORIGINAL PAGE IS
OF POOR QUALITY

modulation. To reduce the effects of the radial motion, we have extrapolated the intensity measured at Pioneer 10 back to 1 AU assuming a gradient of 2.5 %/AU. Thus, in Figure 1A we have plotted $I(1) = I(R)\exp(-0.025(R-1))$ where $I(R)$ is the counting rate measured by Pioneer 10 at radius R AU.

Figure 1A shows that during periods of increasing modulation (1980, 1982), intensity changes occur later at Pioneer 10 than at IMP 8. During the period of decreasing modulation in 1981, there is no clear delay between the recovery at 1 AU and at Pioneer 10, although the data suggest that the intensity increase began earlier at IMP 8 than at Pioneer 10. In 1983-84, on the other hand, the recovery from the effects of the 1982 shocks clearly began first at 1 AU, as reported by Fillius and Axford (1985) and Pyle and Simpson (1985). In Figure 1D, we show the same data, but with the IMP measurement shifted in time by an amount $\Delta t = (R-1)/V$, where V is taken to be 400 km/s, and Δt is taken to be the nearest integral multiple of 27 days. Over the period shown, Δt increases from 81 to 135 days. Compensating for propagation in this way greatly improves the agreement of the intensity profiles at the two spacecraft. The main exceptions are 1) the period of decreasing modulation in 1981-82, where agreement is better using simultaneous observations than shifted observations, and 2) the period in 1982 immediately following passage of the shocks, which propagated more rapidly than 400 km/s.

Figure 1(B, E) shows the same analysis for 30-70 Mev/n helium, assuming a constant gradient of 4 %/AU. As reported by McKibben et al. (1985b), the radial gradient was larger before the middle of 1980, so that the gradient correction is inadequate for the earlier data. After 1980, however, the gradient was nearly constant at ~ 4 %/AU, and agreement between the intensity profiles for low energy helium at 1 AU and at Pioneer 10 is improved by assuming that all changes in modulation, both increases and decreases, propagate outward with a velocity of about 400 km/s. However, in 1982, there is a large increase in the helium flux at 1 AU that has no analogue at Pioneer 10.

Similar analysis for 30-70 MeV protons is shown in Figure 1(C, F), for a gradient of 1 %/AU. This value of the radial gradient was observed only from mid-1980 until late 1983, after which the gradient began a gradual increase (McKibben et al., 1985b). Therefore, since we have used a constant gradient of 1 %/AU to correct the Pioneer data to 1 AU, comparison between the gradient-corrected intensity profiles is meaningful only from mid-1980 to late 1983. In this period the low energy proton flux was nearly constant, and no conclusions can be drawn.

DISCUSSION: The observations may be summarized as follows. In the recovery from the modulation produced by the shocks in 1982, the intensity increase occurred first at 1 AU and propagated outward with a velocity near 400 km/s both for relativistic cosmic rays and for low energy (30-70 MeV/n) helium. In 1981-82, however, when the modulation was not dominated by any single event, the recovery was more nearly simultaneous at 1 AU and at Pioneer 10.

In considering the propagation of changes in modulation in the heliosphere, Forman and Jones (1985) have pointed out that for models in which the modulation at any point is produced by numerous scattering centers convected outward by the solar wind and distributed along the radial path of a particle inward from a fixed boundary of the modulation region, the recovery from maximum modulation should begin first in the inner heliosphere. Their arguments show that individual features propagate outward at the solar wind velocity but that the overall pattern propagates twice as fast. These conclusions are also implicit in the work of Perko and Fisk (1983). Figure 1(G-I) repeats the analysis of Figure 1(D-F) using a convection velocity of 800 km/s. In 1981-82, when modulation was most likely produced by many disturbances between 1 AU and the boundary, assuming a velocity of 800 km/s significantly improves the agreement between profiles for the relativistic particles at 1 AU and at Pioneer 10. In 1982-84, however, when modulation was dominated by a single event, the data are better organized by a velocity of 400 km/s. The accuracy of the measurements does not allow similar conclusions to be drawn for lower energy particles. For 30-70 MeV protons, agreement is improved in 1983-84 for a velocity of 800 km/s, but, as noted above, changes in the gradient after 1983 make such a conclusion questionable.

An alternative model for explaining outward propagation of the recovery involves 3-dimensional propagation of particles in the heliosphere, leading to the filling in of the inner heliosphere from regions off the ecliptic plane (e.g., Van Allen, 1979). In this model, the radial gradient in the ecliptic could become negative, whereas a negative radial gradient would be inconsistent with the model of Forman and Jones. We find, however, that radial gradients were positive at all times (McKibben et al., 1985b, cf. also Fillius and Axford, 1985).

Our observations of the outward propagation of the recovery from maximum solar modulation are consistent with either the model of Forman and Jones (1985), or with propagation from regions off the ecliptic plane to the inner heliosphere. A definitive observational test to discriminate between the two models must await further explorations by spacecraft off the ecliptic plane.

ACKNOWLEDGEMENTS: This work was supported in part by NASA/Ames Contract NAS 2-11126 and by NASA Contract NAS5-28442.

REFERENCES:

Cooper, J.F., and Simpson, J.A., 1979, Proc. 16th ICRC, Kyoto, Japan, 16, 176.
Fillius, W., and Axford, I., 1985, J. Geophys. Res., 90, 517.
Forman, M.A., and Jones, F.C., 1985, Bull. Am. Phys. Soc., 30, 779.
Garcia-Munoz, M., Mason, G.M., and Simpson, J.A., 1977, Ap. J., 217, 859.
Lockwood, J.A., and Webber, W.R., 1984, J. Geophys. Res., 89, 17.
McDonald, F.B., Lal, N., Trainor, J.H., Van Hollebeke, M.A.I., and Webber, W.R., 1981, Ap. J. (Letters), 249, L71.
McKibben, R.B., Pyle, K.R., and Simpson, J.A., 1982, Ap. J. (Letters), 254, L23.
__________, 1985a, Ap. J. (Letters), 289, L35.
__________, 1985b, Proc. 19th ICRC, La Jolla, Ca., U.S.A., Paper SH4.7-5.
Perko, J.S., and Fisk, L.A., 1983, J. Geophys. Res., 88, 9033.
Pyle, K.R., and Simpson, J.A., 1985, Proc. 19th ICRC, La Jolla, Ca., U.S.A., Paper SH 4.7-9.
Simpson, J.A., Bastian, T.S., Chenette, D.L., McKibben, R.B., and Pyle, K.R., 1980, J. Geophys. Res., 85, 5731.
Van Allen, J.A., 1979, Geophys. Res. Lett., 6, 566.
Van Allen, J.A., and Randall, B.A., 1985, J. Geophys. Res., 90, 1399.
Venkatesan, D., Decker, R.B., Krimigis, S.M. and Van Allen, J.A., 1985, J. Geophys. Res., 90, 2905.

N85-35053

THE LARGE-SCALE MODULATION OF COSMIC RAYS IN MID-1982: ITS DEPENDENCE ON HELIOSPHERIC LONGITUDE AND RADIUS.

K. R. Pyle and J. A. Simpson

Enrico Fermi Institute, The University of Chicago,
Chicago, Illinois 60637 (USA)

ABSTRACT. Near solar maximum, a series of large radial solar wind shocks in June and July 1982 provided a unique opportunity to study the solar modulation of galactic cosmic rays with an array of spacecraft widely separated both in heliocentric radius and longitude. By eliminating hysteresis effects we can begin to separate radial and azimuthal effects in the outer heliosphere. We have been able to show that, on the large scale, changes in modulation (both the increasing and recovery phases) propagate outwards at close to the solar wind velocity, except for the near-term effects of solar wind shocks, which may propagate at a significantly higher velocity. We show that, in the outer heliosphere, azimuthal effects are small in comparison with radial effects for large-scale modulation at solar maximum.

INTRODUCTION. The radially-propagating shock events of mid-1982 provide an exceptional opportunity to examine the dynamic response of the heliosphere to a large, sudden increase in modulation and to study the modulation onset and recovery mechanism as a function of magnetic rigidity and heliospheric radius and longitude. This large series of solar events has been studied intensively over the past several years, both in its modulation effects (e.g. Lockwood and Webber, 1984) and in the shock acceleration of energetic charged nucleons and electrons as far as 28 AU from the sun (Pyle et al. 1984). Observations from a variety of instruments aboard the Pioneer and Voyager spacecraft demonstrate that modulation increases propagate outwards at approximately the solar wind velocity (Pyle et al. 1979; Lockwood and Webber, 1984; McDonald et al. 1981). Fillius and Axford (1985) have reported an outward propagation of recovery from modulation in the 11-year solar cycle, based on a comparison of neutron monitor intensity at 1 AU with Pioneer relativistic cosmic ray measurements. The outward progression of recovery could be due to off-ecliptic fluxes or, as in the model of Perko and Fisk (1983), due to the longer intervals between shocks during the declining phase of solar activity. In a companion paper at this Conference (McKibben et al. 1985) we also discuss the large-scale propagation of solar modulation, showing that both modulation increases and decreases propagate outwards.

In this paper we examine the 1982 large-scale modulation event and its recovery, using a counting rate responding to CNO-Fe nuclei in the approximate energy range 200-1000 MeV/n, measured by identical instruments on Pioneers 10 and 11. We show that for both the onset and recovery of this large modulation event the dominant effect is one of outward propagation at approximately the solar wind velocity, and is relatively independent of heliospheric longitude.

INSTRUMENTATION AND TRAJECTORY. It is well-established that during relatively rapid changes in modulation there is a hysteresis effect whose magnitude is dependent on magnetic rigidity (Simpson 1963; Cooper and

ORIGINAL PAGE IS
OF POOR QUALITY

Simpson 1979). Therefore, to eliminate this rigidity-dependent effect, we have used the F2 counting rate from the two identical Fission Cells developed to measure the intense fluxes of protons during the Pioneer 10 and 11 encounters with Jupiter, and later, Pioneer 11 with Saturn. In interplanetary space these counting rates are sensitive to a variety of galactic cosmic ray species, (H-He 1%, C-Ne 14%, Na-V 28%, and Cr-Ni 56%) (see Simpson et al., 1974 and especially McKibben,1983 for a detailed discussion of the Fission Cell response). The energy interval for response is ~200-1000 MeV/n (~1-3 GV rigidity). These counting rates provide relatively good statistics and permit a fairly precise measure of modulation changes. The overall elemental response is expected to be insensitive to any long-term instrumental drifts.

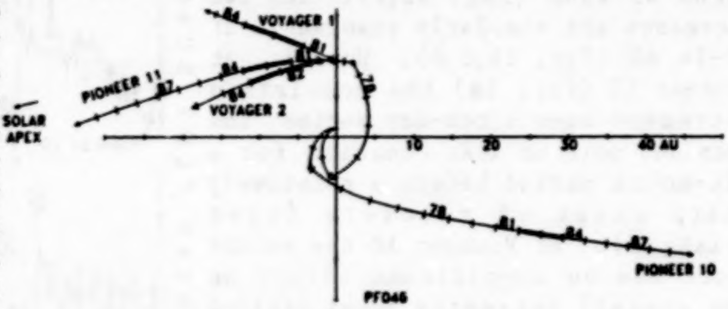

--- FIGURE 1 ---

For comparison we have used the Voyager 1 and 2 counting rates for nucleons >75 MeV (Stone et al., 1977), kindly made available by the Voyager CRS experimenters.

In Figure 1 we have plotted the trajectories of Pioneers 10/11 and Voyagers 1/2, projected onto the ecliptic plane. Pioneer 10, alone among the 4 spacecraft, is moving away from the solar apex, in the direction of the heliospheric tail. The time interval studied here, 1982-3, is indicated by the heavy lines along the trajectories.

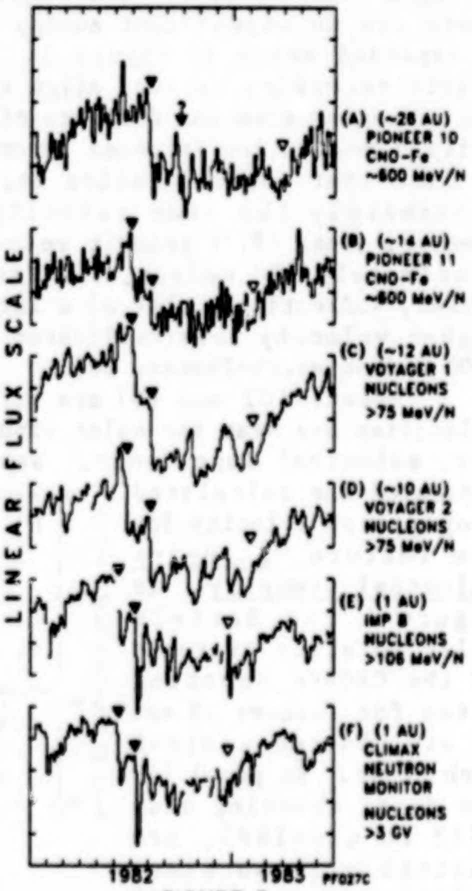

--- FIGURE 2 ---

OBSERVATIONS. In Figure 2 we have plotted 3-day averages of counting rates, showing the behavior of the event at various radii and longitudes in the heliosphere. The two large Forbush decreases seen at 1 AU in mid-1982 (Fig. 1 E,F) are the result of intense solar activity early in June and early in July, 1982. The first of these is apparently caused by the large solar wind shock associated with a flare occurring on 3 June, on the back side of the sun as seen from the earth (Pyle et al. 1984). The longitude of this flare placed it almost directly "under" Pioneer 10. The second decrease (in July), originated with a large solar flare event visible from Earth. In the Figure we have indicated (filled triangles) the outward progression of the modulation. The outward propagation of the recovery is indicated by the open triangles. At 1 AU the two intensity decreases are distinct in time and superimposed on a general downward trend of flux (Fig. 1E,F). The two decreases are similarly resolvable at 10-14 AU (Fig. 1B,C,D). However, at Pioneer 10 (Fig. 1A) the modulation increased over a ten-day period, and remained more or less constant for a six-month period before a relatively sharp onset of recovery (open triangle). At Pioneer 10 the second shock has no significant effect on the overall intensity level (filled triangle with "?").

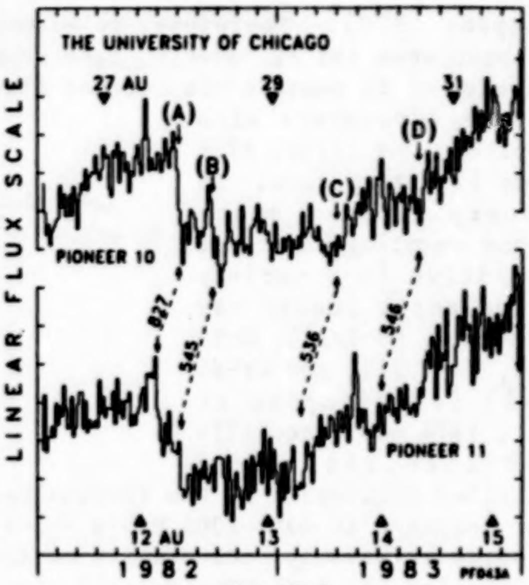

--- FIGURE 3 ---

It is clear from Figure 2 that both the initial Forbush decreases as well as the subsequent rise from the depressed flux levels (open triangles) propagate outwards. Calculation of an accurate value for the radial velocity of the increase, based on this Figure, is difficult owing to the possibility of hysteresis between many of the counting rates shown. To accurately determine the outward velocities we have isolated the two identical CNO-Fe 3-day averaged counting rates from Pioneer 10 and Pioneer 11, between which there are no significant energy hysteresis effects, and plotted them on an expanded scale in Figure 3. The dashed arrows indicate the time shifts necessary to best align the four intensity changes labelled A-D. The triangles show the distance of the two spacecraft from the sun. The initial modulation increase (event (A)) is nearly azimuthally symmetric: we find that the modulation increase propagates outward with approximately the same velocity towards Pioneer 11 and Pioneer 10. However, event (B)'s transit velocity from Earth to Pioneer-11 is approximately 700 Km/sec, but from Pioneer 11 to Pioneer 10 only 545 Km/sec, indicating either a) a large deceleration or b) a significantly higher velocity towards Pioneer 11 (700 Km/sec) than towards Pioneer 10 (600 Km/sec earth-Pioneer 10).

Events (C) and (D) are intensity recoveries where the propagation velocities are near the solar wind velocity, indicating a very small, if any, azimuthal dependence. Near each dashed line in Figure 3 we have indicated the calculated propagation velocity for the feature, assuming azimuthal symmetry. In Figure 4 the Bartels solar rotation averages of the CNO-Fe counting rates for Pioneer 10 and 11 are plotted against each other. In panel (A) the data, covering mid-1982 to mid-1983, are plotted with no time-shifting; in panel (B)

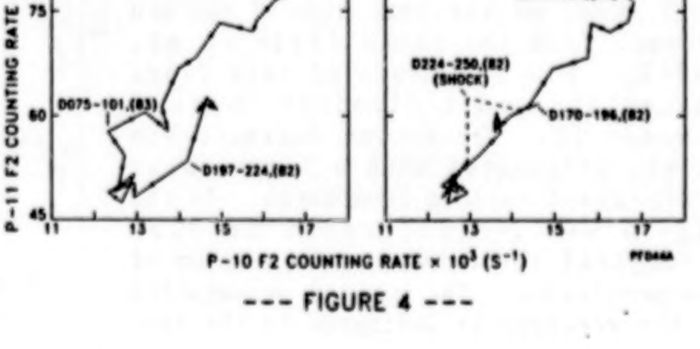

--- FIGURE 4 ---

the Pioneer-11 data have been shifted two solar rotations, equivalent to a solar wind velocity of ~500 Km/sec. This time-shift has placed all of the data points on the same regression line except the one corresponding to the large modulation increase associated with the high-velocity, radial shock. Thus, the assumptions of a) azimuthal symmetry and b) outward propagation at near the solar wind velocity result in a near-perfect alignment of the data at the two spacecraft, differing by ~16 AU in heliospheric radius and by nearly 180 degrees in longitude.

SUMMARY AND CONCLUSIONS. In order to determine the outward velocity of the onset and recovery from modulation of galactic cosmic rays in the heliosphere it is essential to eliminate all magnetic rigidity dependent effects so that rigidity-dependent hysteresis in the heliosphere does not lead to erroneous conclusions.

We have, therefore, selected sets of nucleon-intensity data whose magnetic rigidity ranges are close to each other. The solar-flare generated series of radially-propagating shocks which passed outward through the heliosphere in 1982 provide a unique test of the dynamical processes resulting in large-scale heliospheric modulation.

We have shown that major increases and decreases in solar modulation are primarily radially dependent and not strongly azimuthally dependent.

Not only is the increase in solar modulation an outward propagating effect, as has been shown earlier (e.g. Lockwood and Webber, 1984; Fillius and Axford, 1985) but the recovery from the 1982-3 enhanced modulation period also propagates outward at the approximate solar wind velocity.

ACKNOWLEDGEMENTS. We thank R. Vogt, Principal Investigator on the Voyager CRS experiments, E. Stone, and A. Cummings for making available the Voyager >75 MeV/n nucleon counting rates. This work was supported in part by NASA/Ames Contract NAS 2-11126, by NASA Contract NAS5-28442, and by NSF Grant ATM 84-12382.

REFERENCES:

Cooper, J.F., and Simpson, J.A., 1979, Proc. 16th ICRC, Kyoto, 12, 176.
Fillius, W., and Axford, I., 1985, J. Geophys. Res., 90, 517.
Lockwood, J.A., and Webber, W.R., 1984, J. Geophys. Res., 89, 17.
McDonald, F.B., Lal, N., Trainor, J.H., Van Hollebeke, M.A.I., and Webber, W.R., 1981, Ap. J. (letters), 249, L71.
McKibben, B., 1983, Enrico Fermi Institute Preprint no. 83-21, The University of Chicago.
McKibben, R.B., Pyle, K.R., and Simpson, J.A., 1985, Proc. 19th ICRC, La Jolla, Paper SH4.7-7.
Perko, J.S., and Fisk, L.A., 1983, J. Geophys. Res., 88, 9033.
Pyle, K.R., Simpson, J.A., Mihalov, J.D., and Wolfe, J.H., Proc. 16th ICRC, Kyoto, 5, 345.
Pyle, K.R., Simpson, J.A., Barnes, A., and Mihalov, J.D., 1984, Astrophys. J. (letters), 282, L107.
Simpson, J.A., 1963, Pont. Acad. Sci. Scripta Varia, (Vatican) 25, 363.
Simpson, J.A., Hamilton, D.C., McKibben, R.B., Mogro-Campero, A., Pyle, K.R., and Tuzzolino, A.J., 1974, J. Geophys. Res., 79, 3522.
Stone, E.C., Vogt, R.E., McDonald, F.B., Teegarden, B.J., Trainor, J.H., Jokipii, J.R., and Webber, W.R., 1977, Sp. Sci. Revs., 21, 355.

N85-35054

SH 4.7-10

NONSTATIONARY MODULATION OF GALACTIC COSMIC RAYS IN A NONLINEAR MODEL

V.KH.BABAYAN, M.B.BAGDASARIAN

Yerevan Physics Institute, Markarian st. 2
375036, Yerevan, Armenia, USSR

L.I.DORMAN

Institute of Terrestrial Magnetism,
Ionosphere and Radio Wave Propagation
Moscow Region, Troitsk, USSR

ABSTRACT

An automodel equation for the solar wind velocity is obtained in the self-consistent model. The solution of the convection-diffusion equation is obtained for the density of galactic cosmic rays at a definite dependence of the diffusion coefficient and solar wind velocity on the rigidity and distance.

In studying the propagation of galactic cosmic rays (GCR) in the interplanetary space, properties of the solar wind are considered, independent of the CR intensity. Though it should be noted that the influence of GCR on the supersonic solar wind is comparable with that of other factors (galactic magnetic field etc.).

Then, while investigating the GCR modulations by the solar wind, one should take into account the fact that with the variation of the GCR intensity in time and space, the influence of GCR on the solar wind varies, which in its turn results in the variation of the solar wind velocity. That is, the self-consistent problem should be solved.

In the spherically symmetrical case nonstationary equations of hydrodynamics for the solar wind with account of the GCR influence have the form

$$\frac{\partial u}{\partial t} + u\frac{\partial u}{\partial r} + \frac{1}{\gamma}\left(\frac{\partial c^2}{\partial r} + c^2\frac{\partial}{\partial r}\ln\rho\right) + \frac{1}{\rho}\frac{\partial P}{\partial r} = 0$$

$$\frac{\partial}{\partial t}(\ln\rho) + u\frac{\partial}{\partial r}(\ln\rho) + \frac{\partial u}{\partial r} + \frac{2u}{r} = 0 \qquad (1)$$

$$\frac{\partial c^2}{\partial t} + u\frac{\partial c^2}{\partial r} + (\gamma-1)c^2\left(\frac{\partial u}{\partial r} + \frac{2u}{r}\right) = 0$$

where u, ρ are the velocity and the density of the solar wind, c^2 is the sound velocity, γ is the polytropic index, r is the heliocentric distance, and P is the GCR pressure equal to $P = \frac{1}{3}\int_0^\infty N(r,R,t)\,p v\,dR$ (here N is the concentration of particles with the rigidity R ; p, v are the momentum and the velocity of GCR particles, respectively).

The variation of the spectrum N is determined by the character of GCR modulation in the interplanetary space, i.e. it is defined in the end by the velocity of solar wind and diffusion coefficient   via nonstationary equation of diffusion with account of convection and GCR energy variation /1,2/

$$\frac{\partial N}{\partial t} - \vec{\nabla}(\varkappa\nabla N) + (\vec{u}\,\vec{\nabla})N - (\vec{\nabla}\,\vec{u})\,\frac{R}{3}\,\frac{\partial N}{\partial R} \qquad (2)$$

Let us introduce as in /3/ new dimensionless dependent variables x and y by means of relations $u = x\frac{r}{t}$, $c^2 = y\frac{r^2}{t^2}$ and dimensionless independent variables $\ln t$ and $\ln r$, then the system (1) will have the form

$$\dot{x} - x + x^2 + x' + \frac{1}{\gamma}\left[y' + 2y + y(\ln\rho)'\right] + yp' = 0$$

$$(\ln\rho) + x(\ln\rho)' + x' + 3x = 0 \qquad (3)$$

$$\dot{y} + xy' + 2(x-1)y + (\gamma-1)y(x' + 3x) = 0$$

where, in calculating the last term in the first equation, it is approximately assumed $(\gamma - 1) \approx 1$.

Let us assume that x and y are the function of one independent variable $z = r t^{-a_1}$, where a_i - const. Let us require that r and t do not enter explicitly in (2), then the density should have the form $\rho = t^{a_2} \xi(z)$. Since $\partial/\partial(\ln t) = -a_1 \, d/d(\ln z)$; $\partial/\partial \ln r = d/d \ln z$ the system (3) will take the form

$$
\begin{aligned}
& x'(x-a_1) + x^2 - x + \frac{1}{\gamma}\left(2y + y' + y(\ln\xi)'\right) + yP' = 0 \\
& (\ln\xi)'(x-a_1) + a_2 + x' + 3x = 0 \\
& y/y'(x-a_1) + (\gamma-1)x' + [2(\gamma-1) + (\gamma+1)]x - 2 = 0
\end{aligned}
\tag{4}
$$

where the dash means $\partial/\partial \ln z$.

Eliminating $d(\ln\xi)$ from the first two equations of the system, one may rewrite (4) as

$$
\frac{d \ln z}{dx} = \frac{(a_1 - x)\dfrac{d \ln y}{dx} - (\gamma - 1)}{(3\gamma - 1)x - 2} =
$$

$$
= \frac{(a_1 - x)^2 - y}{y\left[\dfrac{2(a_1-1)+a_2}{\gamma} + 3x + F(a_1 - x)\right] - x(1-x)(a_1 - x)}
\tag{5}
$$

where it is assumed $F = d\rho/d\ln z$

As it is seen, the problem of integration of the initial set of equations in partial derivatives of the first order is reduced to the integration of a first order ordinary differential equation of the form

$$
\frac{dy}{dx} = y \, \frac{F_1(x,y)}{F_2(x,y)}
$$

and to two quadratures.

To define N one should solve eq.(2) which in the spherically symmetric case in dimensionless variables has the form

$$\frac{\partial N}{\partial \tau} - b\varkappa\frac{\partial^2 N}{\partial \rho^2} + \left(au - \frac{2\varkappa b}{\rho} - b\frac{\partial \varkappa}{\partial \rho}\right)\frac{\partial N}{\partial \rho} - \frac{2}{3}\,\frac{au}{\rho}\,\frac{dN}{\partial \rho} - \frac{1}{3}a\xi\,\frac{\partial N}{\partial \xi} = 0 \quad (6)$$

here $\rho = r/r_0$, $\xi = R/R_0$, $\tau = t/T$, $a = T/r_0$, $b = T/r_0^2$
where r_0 is the dimension of the modulating volume, R_0 is the minimum rigidity of particles, T is the time which the solar wind spends to reach the boundary of the modulating volume.

In order to obtain the analytical solution of eq.(6), one should choose the dependence of the diffusion coefficient and the solar wind velocity in the form

$$\varkappa = \varkappa_0\, \rho^{2(1-\alpha)}\, \xi^{2P} \; ; \qquad u = u_0\, \rho^{-2-\frac{3\alpha}{\beta}}$$

where α and β are the arbitrary constants.

Let us search for a solution with boundary conditions

$$N(\rho,\xi,\tau)/_{\rho=0} < \infty \; ; \quad N(\rho,\xi,\tau)/_{\rho=1} = K\xi^{-\gamma}$$

Passing to the variable $\chi = \rho^{\alpha}\xi^{-\beta}$ and using the separation of the variables $N(\chi,\tau) = \varphi(\tau)\psi(\chi)$ we have from (6)

$$\frac{\partial \varphi}{\partial \tau} = -K^2\varphi \, , \qquad \varphi = c\,e^{-K^2\tau}$$

$$\chi\frac{\partial^2\psi}{\partial \chi^2} + \left(\frac{3}{\alpha} - 1\right)\frac{\partial \psi}{\partial \chi} + \frac{K^2}{\alpha^2 b \varkappa_0}\psi = 0 \qquad (7)$$

where K^2 is the separation constant.

The solution of eq.(7) is

$$\psi = c_1\chi^{\nu} J_{\nu}\left(\sqrt{1/\alpha^2 b\varkappa_0}\; K\chi\right) + c_2\chi^{\nu} Y_{\nu}\left(\sqrt{1/\alpha^2 b\varkappa}\; K\chi\right) \qquad (8)$$

where J_{ν} and Y_{ν} are the Bessel functions of type 1 and 2, and $\nu = 1 - \frac{3}{2\alpha}$. After satisfying the boundary conditions we have

$$N = \frac{2}{[Y_{n}(\mu_n)]^2}\sum_{l=1}^{\infty} \chi^{-n} e^{\alpha\sqrt{b\varkappa_0}\,(1-\tau)} J(\mu_l\chi)\left(\int_0^1 \chi_n(\mu_l\eta)\,\eta^{\frac{\gamma}{\beta}+n+1}\,d\eta\right)$$

REFERENCES

/1/ Parker E.N., Planet and Space Sci.,1965,13,9.
/2/ Dolginov A.Z., Toptigin I.N.,Izv.AN SSSR,ser.fiz.,1967, 31, 1269.
/3/ Stanjukovich K.P. Unsteady Motions of Continuum. Moskva, Nauka, 1970, 90 p.
/4/ Kamke E. Handbook of Ordinary Differential Equations. Moskva, Nauka, 1976, 401 p.

DIMENSIONS OF THE SOLAR WIND CAVITY AND OF THE REGION OF INTERPLANETARY COSMIC RAY MODULATION

Dorman I.V.
Institute of History of Science and Technology of the USSR Academy of Sciences. Moscow I030I2, Staropansky per.I/5, USSR

Abstract. We discuss the problem of determining effective dimensions of the region of global galactic cosmic ray modulation from the data on II-year CR variations and the data on the parameters of the solar activity and the solar wind.

I. Effects limiting solar wind propagation. CR propagation is limited to the following effects: I) Pressure of interstellar medium (according to the estimates /I/ this gives $r_{sw} \sim$ I000 A.U. for the boundary between helio-magnetosphere and solar wind); 2) Pressure of the galactic magnetic field $H_G \sim 3\ 10^{-6}$ G (this gives $r_{sw} \sim$ I00 A.U. in the direction perpendicular to the field /2/); 3) Deceleration both by CR and due to charge exchange of interstellar neutral hydrogen (according to nonlinear theory of modulation /3, 4, 5/ this gives $r_{sw} \sim$ 50-I00 A.U. depending on the CR energy density in interstellar space and on the interstellar hydrogen concentration in the vicinity of the Sun). We should emphasize here that we do not know the effects capable of limiting solar wind to $r_o \sim$ I0-20 a.e. Meanwhile, investigating the correlation between CR intensity variations and solar activity variations, many researchers concluded earlier that the dimensions of the modulation region are extremely small ($r_m \approx$ I0-20 A.U. and even $r_m \approx$ 2-3 A.U.). Moreover, many papers have recently appeared which suggest, as before, that $r_m \approx$ I0-20 A.U. Let us try to explain the reason for such a difference and to understand whether the solar wind dimensions can generally coincide with the effective solar wind dimensions, i.e. $r_{sw} \approx r_m$.

2. Estimation of effective dimensions of the interplanetary CR modulation region and investigation of the structure of this region; time and energy hystereses. This estimate can be obtained from calculation of the delay of the observed galactic CR modulation with respect to the processes on the Sun (time hysteresis). Indeed, as shown in /2/, the hysteresis between the total number W of solar spots on the solar disk and the intensity variations of the CR neutron component (observed on the stations Ottawa - the geomagnetic cutoff rigidity R=I.2 GV, Chicago - I.8 GV, Climax - 3.2 GV, and Huankayo - I3.5 GV) is explained well by the convective diffusion model of global galactic CR modulation with an account of the delay $\Delta t \sim r/u$ (u is the mean velocity of the solar wind /2,6/) of the electromagnetic conditions in interplanetary space at a distance r from the Sun with respect to the corresponding processes on the Sun. From the comparison between calculations and observations it follows that I) For particles with a rigidity of several

GV the radius of the modulation region $r_m \sim 100$ A.U.; 2) the effective free path for scattering $\Lambda \backsim R$, where R is particle rigidity (in the region where R exceeds several GV), it decreases as $\Lambda \backsim W^{-1/3}$ with an increase of the solar activity; 3) For CR with high rigidities (tens of GV) r_m decreases approximately as $r_m \backsim R_{ef}^{-1}$, where R_{ef} is the effective rigidity of primaty CR registered by a given device; 4) At very small rigidities the delay in the recovery of CR intensity exceeds the theoretical value as the solar wind activity weakens. This indicates the presence, besides the convective-diffusion modulation region (with $r_m \sim 100$ A.U.), also of a "buffer" layer between solar wind and interstellar medium in which the wind velocity is close to zero but there exists an interplanetary magnetic field amplified due to a permanent pumping by the solar wind. In this layer there is no convective CR outflow, but the delay in the recovery of CR intensity inside the modulation region increases due to a comparatively slow diffusion of low-energy particles. The estimation of the thickness of this diffusion layer gives $L_D \sim 100$ A.U. (the influence of this layer on particles of high rigidities can be neglected due to relatively small magnetic fields there). It was shown in /6/ that in the buffer layer particles can be accelerated to comparatively small energies, which can explain the appearance of an anomalous CR component. Note that at small distances CR are scattered by magnetic inhomogeneities of solar wind, whereas at large distances the main role in CR scattering and their convective outflow must be played by large solar wind perturbations of the type of shock waves.

We believe that r_m is close to r_{sw} only for particles of rather small rigidities. At large r_m distant regions of heliosphere will not modulate particles with rigidities of tens of GV because the azimuthal component of the interplanetary magnetic field decreases with distance ($\backsim r^{-1}$); this fact leads to a decrease of R (corrolary 3).

Corrolaries 3 and 4 discussed above lead to the energy hysteresis which has been thoroughly investigated in recent years.

3. The shift of helio-latitude of active regions within a cycle of solar activity and the dimension of the modulation region. In many papers attempts have been made to explain time hysteresis by the shift of the effective helio-latitude of solar activity from higher to lower values in the course of an 11-year cycle (see, for example, /7-9/). In this case the hysteresis disappears in a first approximation, and so the authors have concluded that the modulation region is very small. In our opinion, such a conclusion is to a great extent groundless. A more accurate account of the helio-latitude shift by means of the HL-index /10/ shows that hysteresis disappears only for an effective angular flux width $\theta \approx 5$-10°. But in this case there is a sharp contradiction between the observed /11/ and the calculated

annual variations. The results are in agreement only for $\theta \sim 30$-50°, but in this case the time hysteresis does not disappear and leads to the results discussed in 3.

4. Short-time variations of solar activity and the dimension of the effective modulation region. The study of the socalled "stepwise" variations in the solar activity and their manifestations in cosmic ray variations /I2/ has led to the conclusion that the corresponding delay in CR with respect to the processes on the Sun makes up I-2 months, which gives $r_M \sim$ 7-IO A.U. But as shown in /I3/, during short-time variations of solar activity only a small part of the modulation region nearest to the Sun takes part in the modulation, and the smaller the characteristic period of solar activity variations, the smaller part of the modulation region is involved in the formation of a corresponding CR variation.

5. Anisotropic diffusion model and the dimension of the modulation region. More accurate calculations of the CR intensity modulation in the framework of the anisotropic diffusion model with an account of polarity reversal of the total magnetic field of the Sun also give large dimensions of the modulation region ($r_M \sim$ 50-IOO A.U.) (see e.g. /I4/).

6. Measurements in space and the dimension of the modulation region. The recent measurements of long-term CR variations and their radial gradient (on a cosmic apparatus (CA) Pioneer IO and II, and on Voyager I and 2) give at least $r_M >$ 65 A.U. /I5/, and according to /I6/, /I7/, the calculations which made use of the same data and took into account the CA measurements near the Earch as well as the ground-based neutron monitor measurements (for elimination of CR time variations) give $r_M \sim$ IOO a.e.

Conclusions: I. Dimensions of the effective modulation region r_M for low-energy (less than several GeV) particles are close to the solar wind dimensions r_{sw} , where $r_M \sim r_{sw} \sim$ IOO a.e. 2. As the particle rigidity R increases, the value of r_M decreases, so that in this case r_M can be much smaller than r_{sw} . The value of r_M also decreases with a decrease of the characteristic period of CR variation (it reaches the maximum value only for long-term variations, such as II- and 22-year ones). 4. The region of effective modulation and solar wind is surrounded by a buffer layer which causes the delay in the recovery of CR intensity. 5. The energy hysteresis is caused by two factors: the dependence of r_M on R and the presence of a buffer layer (the time of diffusion through this layer essentially increases as the particle energy decreases).

REFERENCES

I. Parker E.N. 1963, Interplan. dynamic.proc, New York - London.

2. Dorman I.V., Dorman L.I., I967, J.Geoph.Res., 72, I513.
3. Dorman I.V., Dorman L.I., I968. Geomagnetism and aeronomy, 8, 8I7, I008.
4. Dorman I.V., Dorman L.I., I969, Izv. AN SSR, ser. fiz., 33, I908.
5. Babayan V.Kh., Dorman L.I., I979. Proc. I6-th ICRC, Kyoto, v.3, II7, I23.
6. Dorman I.V., Dorman L.I., I967, Izv. ANSSSR , ser.fiz., 31, I239, I273.
7. Quenby J.J., I965. Proc. 6-th ICRC London, v.I, 3.
8. Kudo S., Wada M., I968. Report of Ionosph. and Sp.Res. in Japan, 22, I37.
9. Stozhkov Yu.I., Charakhchyan T.N., I969, Geomagnetism i aeronomy, 9, 803.
10. Gushina R.T., Dorman I.V., Dorman L.I., Pimenov I.A., I970, Izv. AN SSSR, ser.fiz., 34, 2426, 2434.
11. Dorman L.I., Luzov A.A., Manrukova V.P., I967, DAN SSSR, I72, 839, Izv. AN SSSR, ser. fiz., 3I, I368.
12. Charkhchyan A.N., Charkhchyan T.N., I967. Izv. AN SSSR, ser.fiz., 3I, I3I3.
13. Dorman L.I., I967. Cosmic rays.N 8, 305.
14. Alaniya M.B., Dorman L.I., I98I. "Spatial distribution of the density and flux of galactic cosmic rays". Tbilisi.
15. Mc Kibben R.B., Ryle K.R., Simpson Y.A., I982, Astroph. J. 254, 23-27.
16. Webber W.R., Lockwood J.A., I98I, J. Geophys.Res., 86, II458-II462.
17. Lockwood J.A., Webber W.R., I984, Astroph. J., 279, N I, Pt. I, I5I-I56.

DRIFT AND FORBUSH DECREASES

H. Moraal and M.S. Mulder

N85-35056

PU-CSIR Cosmic Ray Research Unit,
Department of Physics,
Potchefstroom University for CHE,
Potchefstroom, 2520.
South Africa.

ABSTRACT

Evidence is presented that the drift effect on the modulation of galactic cosmic rays can be seen on Forbush decreases observed by the Deep River and Hermanus neutron monitors.

1. Introduction

Since the description of drift effects on the modulation of galactic cosmic rays (Jokipii, Levy, and Hubbard, 1977) its significance has been controversial. Lee and Fisk (1981) argued that the topology of, and fluctuations in the Interplanetary Magnetic Field (IMF) might render drift effects quite ineffective. Jones (1983) remarked that observable drift effects seem hard to find. Current drift models (e.g. those of Jokipii and Thomas; 1981, and Potgieter and Moraal; 1985) however are now in agreement that there should be a small effect on near-Earth observations. In addition, Potgieter and Moraal also showed that despite small observable effects, the dynamics of the modulation in consecutive solar cycles (IMF directions reversed), may be drastically different. These authors also summarised a score of independent observations reflecting drift effects.

Figure 1 shows that after a blast wave has passed Earth, the drift velocity field in the 1970 to 1980 IMF configuration should cause a Forbush decrease to reset faster than during the 1959 to 1969 configuration. In this paper we investigate this hypothesis with data from the Deep River and Hermanus neutron monitors.

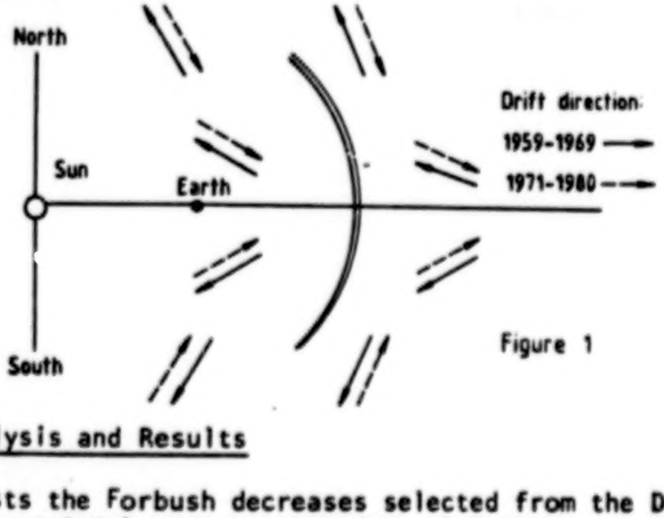

Figure 1

2. Data Analysis and Results

The Table lists the Forbush decreases selected from the Deep River (cutoff rigidity $P_c = 1{,}0$ GV) and Hermanus ($P_c = 4{,}7$ GV) neutron monitors. The time of onset is given as a two digit number for the year, a three digit number for the day, and a two digit number for the hour. The selection criteria for the 109 Hermanus decreases were rather loose. This means that about 15% of them are contaminated by other decreases in the onset phase, reset phase, or both. For Deep Rivier even more decreases were included for a total of 131, but the 85 marked with an asterisk are clear, uncontaminated decreases that reach a clear minimum within 12 hours of onset time.

Figure 2a shows the averages of these decreases for Hermanus. The solid curve is for the period 1959 to 1969 and the dashed one for the period 1971 to 1980. The drift effect predicted from figure 1 is clearly visible. Note that the sharp peaks at onset time (hour 48) and diurnal variations are due to subjectivity of selection of the hour of onset: One is inclined to select a high counting rate at onset time, and this automatically favours the peak of the diurnal variation. The drift effect is even more clearly visible on Figure 2b, which shows the five hour running average of the ratio of 1971-1980 decreases relative to 1959-1969 decreases. Figures 3a and 3b repeat this analysis for all 131 Deep River decreases, while Figures 4a and 4b are for the 85 uncontaminated Deep River decreases only.

Hermanus

5900916	6.6	6905907	6.5
5902618	6.5	6908312	8.7
5904516	7.4	6910212	5.3
5909918	5.1	6911710	9.0
5911320	5.2	7127823	4.8
5913122	12.2	7135118	7.0
5916212	7.0	7204906	5.5
5923124	9.0	7215113	5.8
5929218	6.0	7217114	3.7
5933706	5.7	7230516	8.3
6009110	7.8	7312714	4.5
6010614	5.6	7313815	5.4
6012116	10.4	7318917	3.5
6014314	7.0	7321213	4.3
6019620	10.6	7402516	2.7
6022712	6.1	7406424	3.5
6028005	5.9	7501513	3.7
6110614	4.7	7508515	3.0
6114122	5.5	7511012	3.9
6120712	5.9	7513916	4.1
6127320	4.5	7518909	3.0
6201018	4.1	7522516	2.9
6203604	5.6	7529118	2.5
6214718	4.7	7530817	3.7
6223316	3.8	7532609	3.6
6227304	6.5	7605121	2.0
6229106	6.1	7611807	2.5
6306916	4.1	7612411	3.2
6310820	5.8	7623619	2.4
6318514	4.1	7631904	2.3
6321312	3.8	7702911	3.0
6326506	7.2	7709712	3.3
6330212	6.6	7800318	5.1
6425418	3.5	7802914	4.8
6502102	4.6	7806916	7.0
6510911	3.8	7810012	7.4
6516621	3.8	7812105	16.4
6519924	4.7	7815312	7.5
6522721	3.3	7819409	5.7
6527919	3.7	7831601	4.6
6624606	6.5	7835512	5.1
6625810	8.9	7900613	5.0
6629913	4.5	7903412	3.8
6701305	6.5	7906304	3.5
6703822	5.5	7908712	8.2
6714515	7.4	7909501	7.4
6730218	4.7	7911506	7.1
6802620	5.8	7915719	6.2
6807016	5.0	7918711	7.7
6816218	6.1	7921305	4.4
6816823	4.4	7927916	5.4
6819205	5.8	7931505	5.5
6832108	7.7	8003701	6.0
6834012	6.2	8007912	4.8
6902613	5.1		

Deep River

5900919	6.5	*	6608212	6.5	*	7720918	3.7	*
5902621	9.1		6615122	4.3		7726420	10.4	*
5904510	9.1		6618919	5.1	*	7734704	4.0	*
5909917	5.4	*	6624208	8.4		7800320	6.4	
5911320	6.4	*	6626619	6.1	*	7810017	5.7	
5913121	16.0	*	6628818	5.0	*	7812106	16.5	*
5916209	6.6		6629905	3.9	*	7815311	8.4	*
5919812	21.4		6632117	4.1	*	7823021	5.3	*
5923703	9.6	*	6634716	5.3		7831604	5.0	*
5924621	8.4	*	6701312	5.8	*	7834802	6.7	
5926123	9.5		6704622	5.2	*	7804520	20.3	*
5933704	9.2		6712115	6.2		7908712	7.9	
6009110	12.7	*	6718515	5.0	*	7909503	7.4	
6012722	4.8	*	6720216	5.6		7915718	7.6	*
6012124	14.3		6732602	3.8	*	7918722	8.5	*
6014321	7.2		6802623	4.7		7924104	10.1	*
6014924	6.6		6809622	4.8		7927918	5.6	*
6017923	5.6	*	6811702	3.7	*	7908706	9.6	
6015619	7.9	*	6814202	2.9		8003702	6.1	*
6022718	6.6	*	6830221	12.6		8006606	7.5	*
6028005	8.8	*	6901419	3.6	*	8007916	5.7	*
6104624	5.1		6904115	3.7	*			
6110407	6.6	*	6908219	13.6	*			
6114103	4.8	*	6910301	5.0	*			
6120719	9.9	*	7110819	4.4	*			
6127319	8.4	*	7113716	5.2	*			
6130115	5.5		7127823	4.6	*			
6133517	7.6	*	7135116	7.2	*			
6201004	4.5	*	7206619	4.4				
6203520	6.6		7211401	5.0	*			
6207922	3.9	*	7213619	5.8	*			
6208924	5.1	*	7215119	5.7	*			
6211108	6.3	*	7216909	5.9	*			
6227303	5.6		7221721	22.8	*			
6306917	4.9	*	7230518	10.3	*			
6308122	3.5		7235716	3.5	*			
6310903	2.5		7225718	4.9	*			
6312222	5.7		7229215	4.5				
6318720	4.1		7301921	4.1	*			
6325918	10.3	*	7321213	4.5	*			
6326517	5.2	*	7406418	3.1				
6330214	7.8		7412705	6.1	*			
6332920	3.4	*	7428718	5.8	*			
6402820	3.7	*	7501522	3.4				
6425020	2.5	*	7511012	4.0				
6426520	3.0	*	7518905	2.6	*			
6432023	7.4		7506518	5.7				
6502016	3.0		7508520	3.9	*			
6510918	3.2		7522517	2.7	*			
6516615	3.9	*	7612322	5.2	*			
6515317	2.8		7604720	3.1	*			
6520902	2.3	*	7702915	3.6	*			
6522719	2.5	*	7709716	3.4				
6533912	2.9	*	7717017	3.9				
6602815	2.8	*	7717902	3.4				

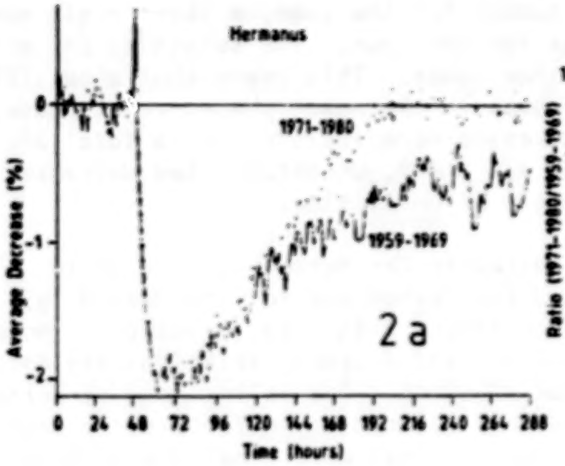

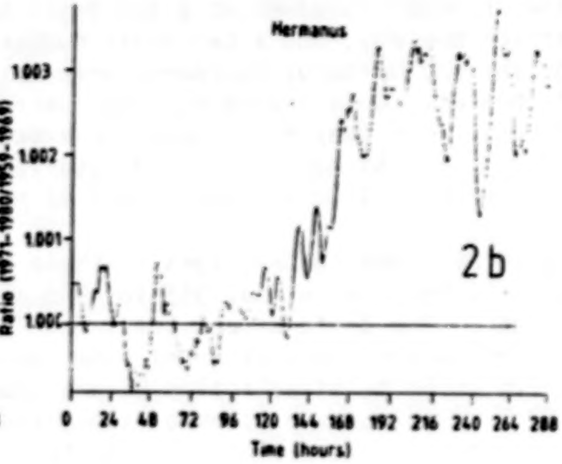

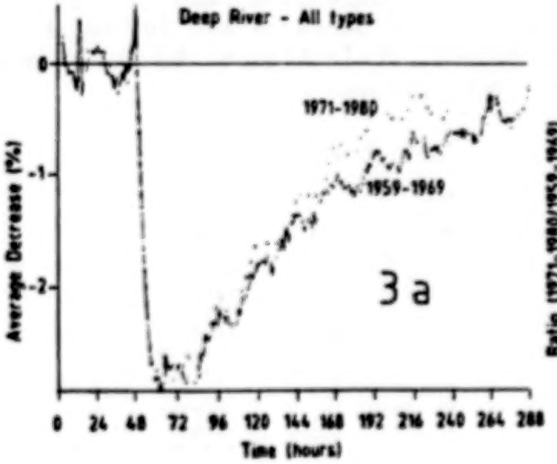

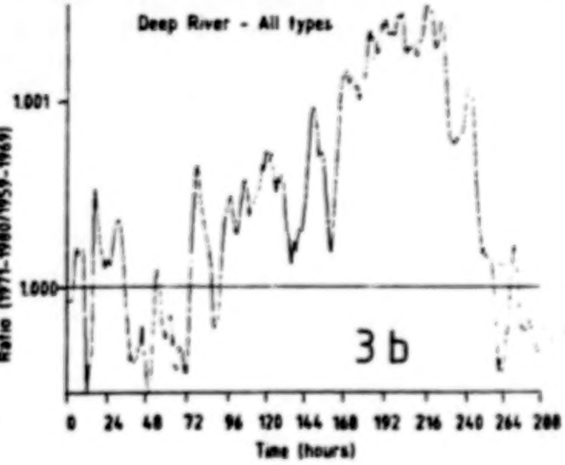

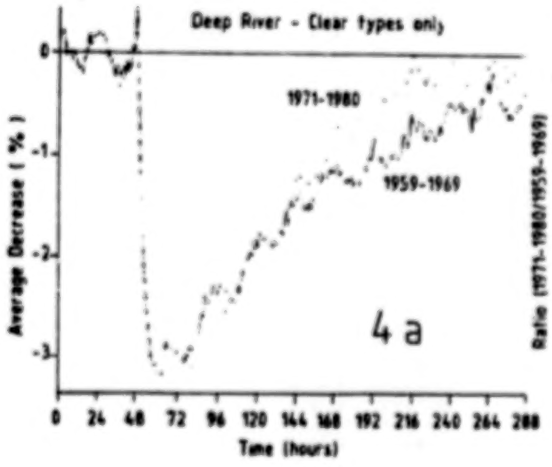

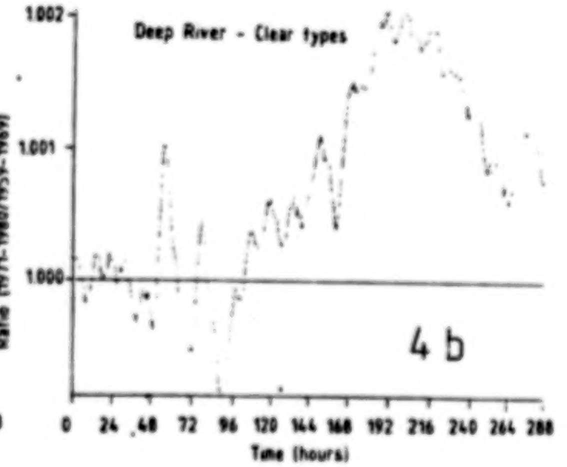

In all cases the effect builds up at approximately the same rate towards maximum at hour 192 (6 days after onset), but on Deep River (Figure 3b) it starts to disappear at about hour 240 (8 days after onset). The Deep River effect is also about a factor two smaller than on Hermanus. Figure 4b shows however that when the contaminated decreases are omitted the effect on Deep River increases somewhat in magnitude and becomes more persistent.

3. Interpretation and Significance

If $\langle\underline{v}_d\rangle$ denotes the omnidirectional drift velocity and U the differential cosmic ray density, then the divergence of the drift flux is

$$\underline{\nabla}.(\langle\underline{v}_d\rangle U) = \langle\underline{v}_d\rangle.\underline{\nabla}U,$$

because $\underline{\nabla}.\langle\underline{v}_d\rangle = 0$. Now $\langle\underline{v}_d\rangle \propto P$ (rigidity) and Potgieter (1984) has shown from his numerical drift model calculations that $\langle\underline{v}_d\rangle.\underline{\nabla}U$ is a rapidly increasing function of P. This qualitatively explains why the Hermanus effect may be larger than the one on Deep River. Quantitative comparison with observations requires that the calculations of Potgieter must be weighted over the response functions of the respective neutron monitors. Such steady state drift calculations can however not explain why the Hermanus effect is more persistent than the Deep River one.

To test the significance of these results, the following tests were performed:

(a) The three largest decreases (5919813, 722172, 7804520 for Deep River and 5913122, 7812105 for Hermanus) were omitted to see whether these had an undesirable weighting effect. This caused no change in the results.
(b) The Hermanus calculations were repeated separately for decreases greater and smaller than the median. Both sets showed the effect, but it was much more significant on the large decreases.
(c) The chronological order of the Hermanus decreases was scrambled randomnly. In this case the effect completely disappeared.

From these tests we think that the drift effect is real and significant. We are presently extending the analysis to additional low, mid, and high latitude neutron monitors to confirm this and to establish a rigidity depence of the effect.

References

Jokipii, J.R., Levy, E.H., and Hubbard, W.G.: 1977, Ap. J., 213, 861.
Jokipii, J.R., and Thomas, B.: 1981, Ap. J., 243, 1115.
Jones, F.C.; 1983, Rev. Geophys. Space Phys., 21, 318.
Lee, M.A., and Fisk, L.: 1981, Ap. J., 248, 836.
Potgieter, M.S.: 1984, Ph.D.-thesis, Potchefstroom University.
Potgieter, M.S., and Moraal, H.: 1985, Ap. J., 294, (July 15 issue).

N85-35057

SH 5.1 - 3

ANOMALOUS SHORT-TERM INCREASES IN THE GALACTIC COSMIC RAY INTENSITY: ARE THEY RELATED TO INTERPLANETARY MAGNETIC CLOUD-LIKE STRUCTURES ?

N. IUCCI, M. PARISI, C. SIGNORINI, M. STORINI and G. VILLORESI
Istituto di Fisica dello Spazio Interplanetario del C. N. R.
Dipartimento di Fisica - Università "La Sapienza"
Piazzale Aldo Moro, 2 - 00185 ROMA, ITALY

Thirty-one short-term increases (time duration < 24 hours and amplitude up to 5%) in the galactic cosmic ray intensity, occurring inside Forbush decreases events, have been identified over the period 1966 - 1977. These increases are highly anisotropic and occur after the compression region following the shock; the interplanetary medium /1/ is characterized by intense (≥ 10 nT) and higly fluctuating magnetic field $\vec{B}$, high velocity, low density and temperature (flare ejecta piston ?) as it can be seen in the examples given in Figures 1, 2, 3 and in the average behaviours of Figure 4. These $\vec{B}$-fluctuations seem to be ordered variations /2/ which could be representative of magnetic clouds /3/; this structure is particularly evident for the 7 cases given in the Table for which the data were always present and $\lambda_3 < 0.5\,\lambda_2$ and $\lambda_3/\lambda_2 \leq \lambda_2/3\lambda_1$ (for the definition of λ_i see /2/); the average behaviour of these events is given in Figure 5. Also the large cosmic ray increase occurring on 17-18 September 1979, already analyzed by other authors /4, 5/, belongs to this category of events as it is shown in Figures 6, 7. In Figure 8 we show the time variations of $\vec{B}$ in the plane (X', Y') of maximum variance and in the plane (X', Z'), Z' being the minimum variance direction.

The analysis of these events is still in progress; the study of further events occurring during 1978 - 1979 and analytical refinement are necessary to understand the origin of the cosmic ray increases observed inside these magnetic clouds.

MAGNETIC CLOUD					ISOTROPIC C. R. INCREASE		
Start D - M - Y	Start H	Duration (h)	λ_3/λ_2	λ_2/λ_1	Start D - M	Start H	Amplitude (%)
23-09-66	21-22	18	.17	.50	24-09	00-01	1.5
13-12-66	20-21	26	.07	.48	14-12	02-03	2.3
13-01-67	19-20	36	.07	.56	13-01	19-20	1.0
29-07-67	20-21	10	.12	.34	29-07	21-22	1.5
24-03-69	17-18	20	.07	.35	24-03	23-24	1.3
09-11-69	04-05	14	.06	.62	09-11	04-05	2.1
15-05-72	20-21	12	.15	.49	16-11	01-02	0.6

ORIGINAL PAGE IS
OF POOR QUALITY

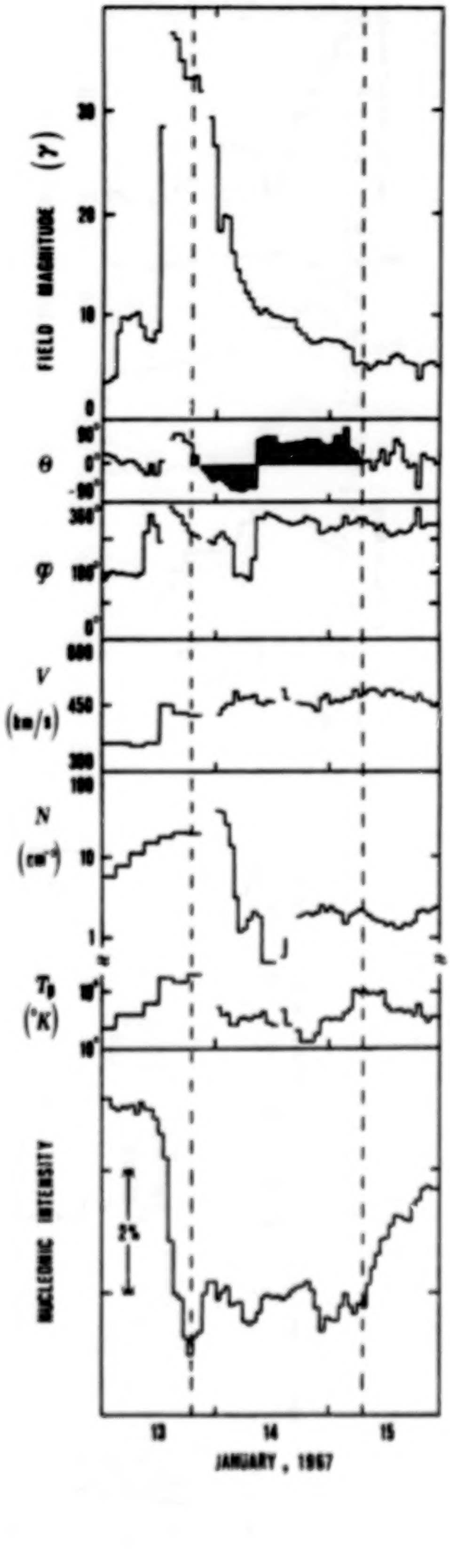

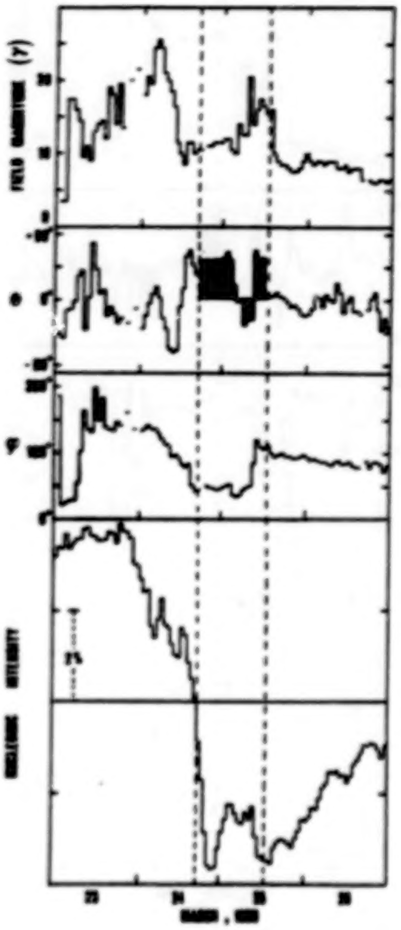

Figure 2 - (see Fig. 1)

Figure 1: Magnetic field, flow parameters and isotropic (average NM-64 intensity of Alert, Deep River, Goose Bay, Inuvik, Kerguelen, Kiel, McMurdo) nucleonic intensity associated with the magnetic cloud which is between the two vertical broken lines.

ORIGINAL PAGE IS
OF POOR QUALITY

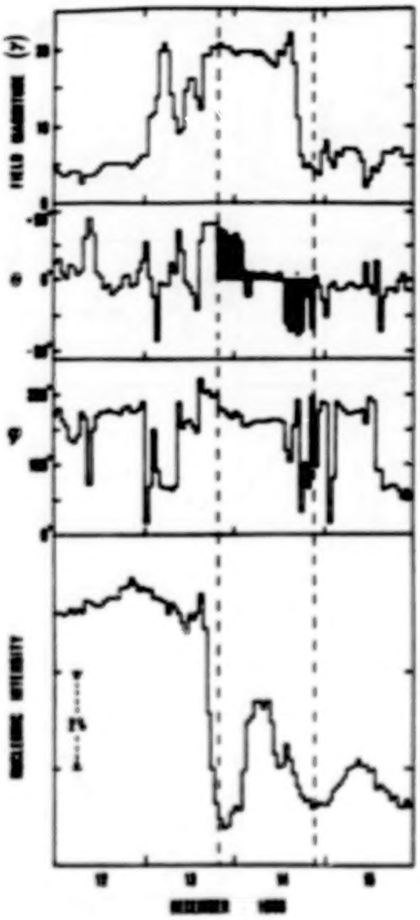

Figure 3 - (see Fig. 1)

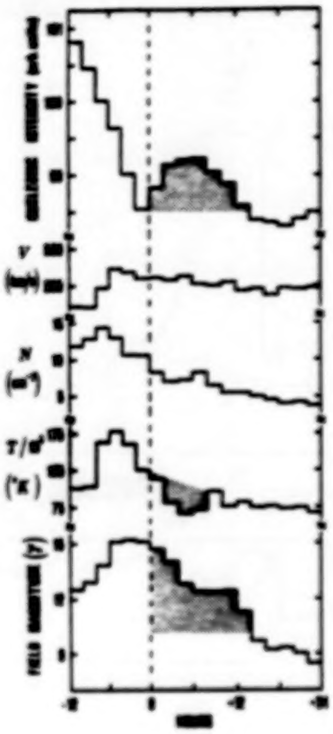

Figure 4

Figure 4: Superposed epoch analysis of interplanetary parameters and average (see the caption of Fig. 1) nucleonic intensity for 31 cosmic ray increases. The epoch time (zero hour) is the first hour of the increase.

Figure 5: a) The same as in Fig. 4 for 7 cosmic ray increases for which it was possible to identify the magnetic cloud structure.
b) The time durations of the 7 magnetic clouds relative to the epoch time are marked by horizontal bars.

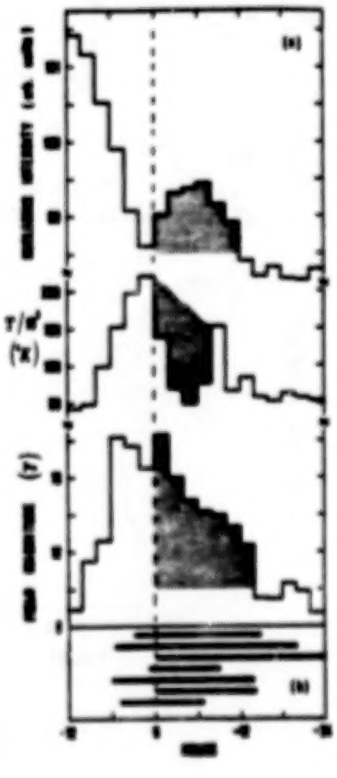

Figure 5

ORIGINAL PAGE IS
OF POOR QUALITY

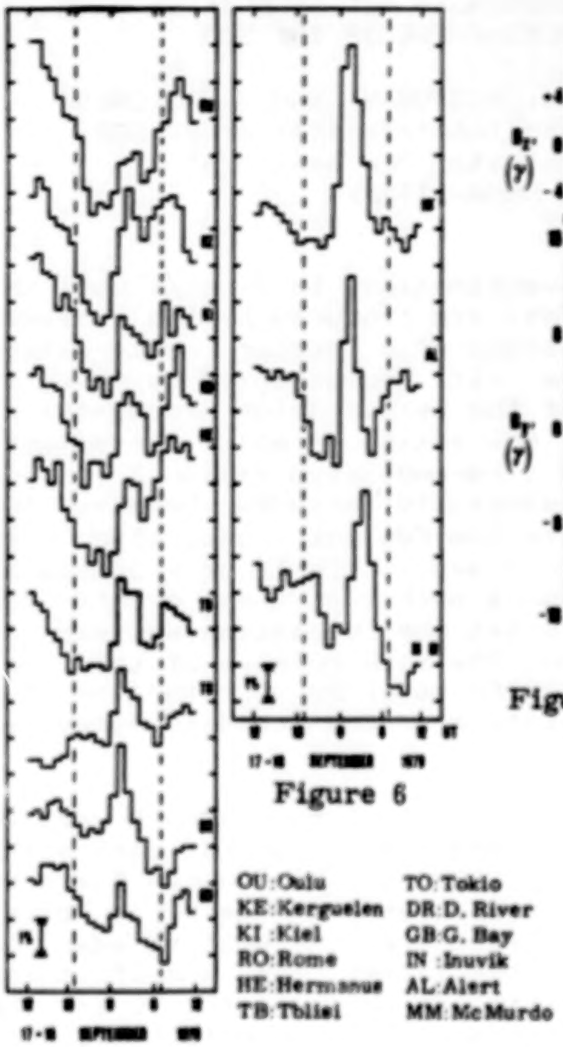

Figure 6

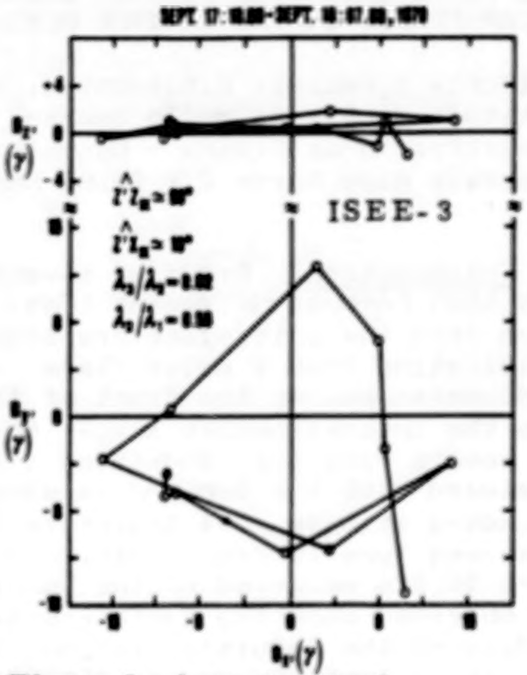

Figure 8 - (see the Text)

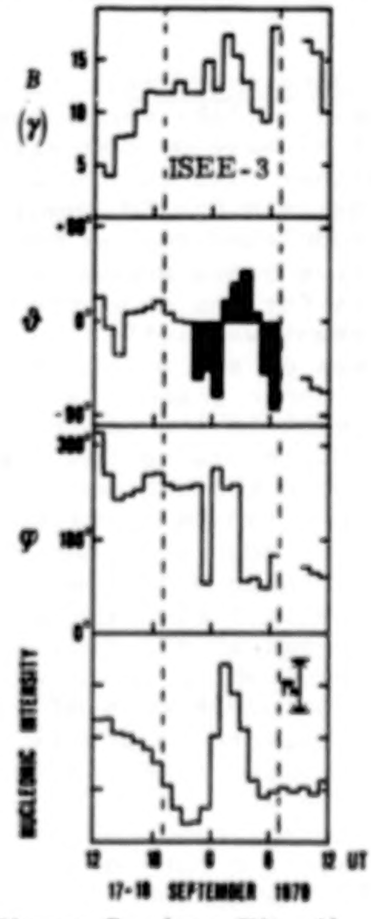

Figure 7 - (see Fig. 1)

References

1) J.H. King: "Interplanetary Medium Data Book", NSSDC/WDC-A-R & S 77-04 (1977), 79-08 (1979).
2) G.L. Siscoe and R.W. Swey: J. Geophys. Res. 77, 1321, 1972.
3) L.W. Klein and L.F. Burlaga: J. Geophys. Res. 87, 613, 1982.
4) S.P. Agrawal and D. Venkatesan: J. Geophys. Res. 87, 9201, 1982.
5) D. Venkatesan et al.: J. Geophys. Res. 86, 4836, 1981.

THE FLARE ORIGIN OF FORBUSH DECREASES NOT ASSOCIATED WITH SOLAR FLARES ON THE VISIBLE HEMISPHERE OF THE SUN

N.IUCCI, M.PARISI, C.SIGNORINI, M.STORINI and G.VILLORESI
Istituto di Fisica dello Spazio Interplanetario del CNR
Dipartimento di Fisica - Universita' 'La Sapienza'
Piazzale Aldo Moro, 2 - 00185 ROMA, ITALY

1. Introduction. Previous investigations (e.g. /1/) have shown that Forbush decreases (Fds) are produced by the propagation into the interplanetary space of a strong perturbation originating from a solar flare (Sf) accompanied by Type IV radioemission. As the front of the perturbation propagates into the interplanetary space, the region in which the galactic cosmic rays are modulated (Fd-modulated region) rotates westward with the Sun and is generally included between two boundary streams /2/; therefore the Fds not associated with observed Type IV Sfs (N.Ass.Fds) are likely to be produced by Type IV Sfs occurred on the Sun's backside; these events can be observed when the Earth crosses the corotating Western boundary of the modulated region. The main purpose of this paper is to support our empirical Fd-model by studying the origin of N.Ass.Fds and the corotation of the boundary streams.

2. Data analysis. It is very likely that the strong active regions (SAR) producing great flare-associated Fds during their passage on the visible hemisphere of the Sun can flare up further Type IV Sfs when they are located on the Sun's backside; a N.Ass.Fd should be observed when the Western edge of a modulated region produced by the flares from one of these active zones encounters the Earth. We think that this is the case for the majority of N.Ass.Fds. In order to test this statement we plotted in Figure 1 the distribution of the onset-times of all (~140) N.Ass.Fds (amplitude ⩾ 1.5% in the polar nucleonic intensity over the period 1957-1979 /1,3,4/) with respect to the central meridian passage (CMP) of 120 SAR /5/ producing large Fds (amplitude ⩾ 3% for Type IV Sfs located between E90-W45 and ⩾ 1.5% for W45-W90 /1/). We notice that, over a random distribution, large peaks come out between -4 and +2 days from the 27-day recurrences of the CMP of SAR ; i.e. these N.Ass.Fds are found to begin some days before the magnetic field line connected with the SAR crosses the Earth. The peak at +27 days appears to be the most pronounced as expected, while the peak amplitude at the CMP of SAR is reduced by the occurrence of large Fds, produced by Type IV Sfs in the Eastern quadrant, which mask the contemporary presence of N.Ass.Fds. Moreover we found that ~60% of the ~140 N.Ass.Fds are related with the CMP of SAR or its +27-day recurrence; on the other hand 58% of the 120 SAR analyzed are related to a N.Ass.Fd occurring near the +27-day CMP recurrence, while for 23% of them the possible N.Ass.Fds are masked by the occurrence of flare-associated Fds.

ORIGINAL PAGE IS
OF POOR QUALITY

In conclusion it seems that the majority of N.Ass.Fds ($\geqslant$ 60%) are produced by intense Type IV Sf activity from long-living SAR; therefore we may expect that most of the remaining N.Ass. Fds could be produced by energetic Type IV Sfs occurring on the Sun's backside in active regions not included in SAR.
Figure 2 shows a Bartels display of CMP dates of SAR (•) together with their 27-day recurrences (o); the arrows indicate the N.Ass.Fd onset-times. The time interval between the +27-day recurrence of CMP of SAR and the beginning of N.Ass.Fds may be explained by two effects: the heliolongitude distance between the active region and the solar source of the Western stream and the speed of the Western stream itself. The Table shows that, as an average, the more the N.Ass.Fd onset-time (t_1) precedes the CMP or its +27-day recurrence (t_0), the more the solar wind speed at the Fd-onset is found to increase. This result may account for about a half of the broadening of the recurrent peaks; therefore the solar source of the Western stream seems to be located, from case to case, between ~40° and ~75° in the West of the active region which is, as expected, the half longitudinal extension of the Fd-modulated region.

$t_1 - t_0$ (days)	V (km/s)	Number of Events
-4 ÷ -2	570	13
-2 ÷ 0	465	17
0 ÷ +2	380	10

The corotation with the Sun of the Fd-modulated region is better shown if the boundary streams are found to recur. The interplanetary data /6/ are used to investigate the recurrence of these perturbations. Periods of enhanced magnetic field intensity (B $\geqslant$ 10nT), not associable either with interaction regions between high-speed streams ejected from coronal holes and the ambient solar wind, or with interplanetary perturbations produced by energetic Type IV Sfs in the visible hemisphere of the Sun, have been identified. The average behaviour of the interplanetary magnetic field intensity B and proton density N for 160 of those perturbations are shown in Figure 3 together with the average behaviour of B and N about ± 27 days (b) and ± 54 days (c). The day of the sharp increase in B was chosen as epoch-time. The results show that there is a high probability that these interplanetary structures corotate with the Sun, being the lifetime $\geqslant$ 2 solar rotations.

3. Conclusions. The parent active regions of most N.Ass.Fds are found to be the ones showing an intense Type IV Sf activity during their passage on the visible hemisphere of the Sun, namely those which are most likely able to produce Type IV Sfs also on the Sun's backside. Type IV Sfs emitted at different times by the same active region will depress the cosmic ray intensity in the same portion of the interplanetary space corotating with the Sun; therefore the Fd-effect will be observed also in the interplanetary regions which were not swept by the front of the perturbation, as it should happen for the N.Ass.-Fds. These results give a further support to the experimental

ORIGINAL PAGE IS
OF POOR QUALITY

Fd-model developed by our group (e.g./2/).

References.

/1/ N.IUCCI et al.: Nuovo Cimento 2C, 1, 1979.
/2/ N.IUCCI et al.: Nuovo Cimento 7C, 467, 1984.
/3/ J.F.STELJES:'Cosmic ray NM-64 data' AECL-Canada 1965-1972.
/4/ M.D.WILSON and M.BERCOVITCH: 'Cosmic ray NM-64 data' AECL-Canada 1973-1979.
/5/ H.V.DODSON and E.R.HEDEMAN: WDC-A(Boulder) Reports UAG-14, 1971, UAG-52, 1975 and UAG-80, 1981.
/6/ J.H.KING: 'Interplanetary Medium Data Book', NSSDC/WDC-A-R & S 77-04 (1977), 79-08 (1979) and 83-01 (1983).

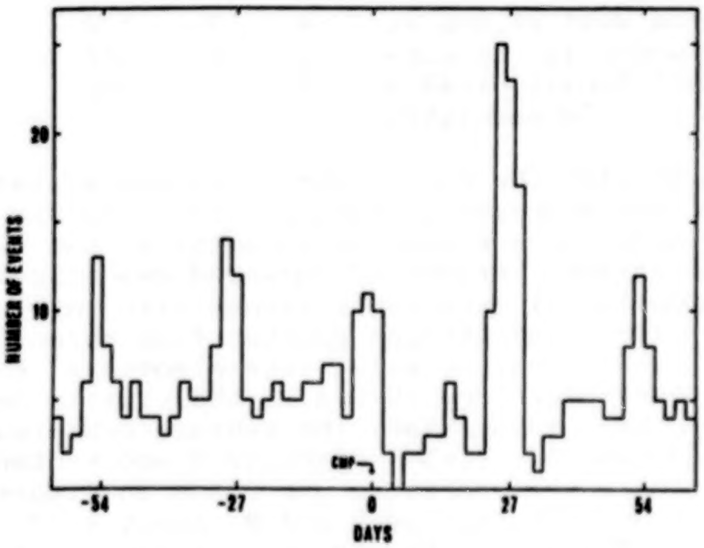

Figure 1: Distribution of the onset times of the N.Ass.Fds with respect to the Central Meridian Passage (CMP) of the active regions producing energetic Type IV Sfs and associated with great Fds (see the Text).

ORIGINAL PAGE IS OF POOR QUALITY

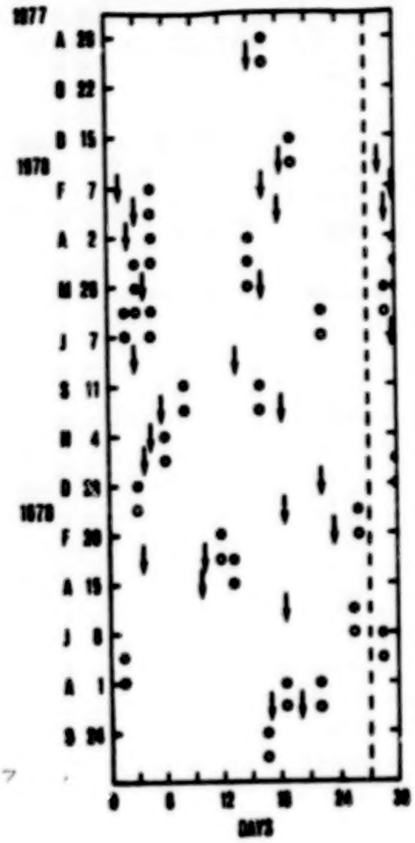

Figure 2: Bartels display of CMP dates of SAR (●) together with their 27-day recurrences (○); the arrows indicate the N.Ass.Fd onset-times.

Figure 3: (a)- Superposed epoch analysis of the interplanetary magnetic field magnitude and proton density for 160 interplanetary perturbations during 10 days centered about the time t_0 of the sharp increase in B which is chosen as epoch time; (b)- the same as in (a) using as epoch time: $t_0 \pm 27$ days; (c)- the same as in (a) using as epoch time: $t_0 \pm 54$ days.

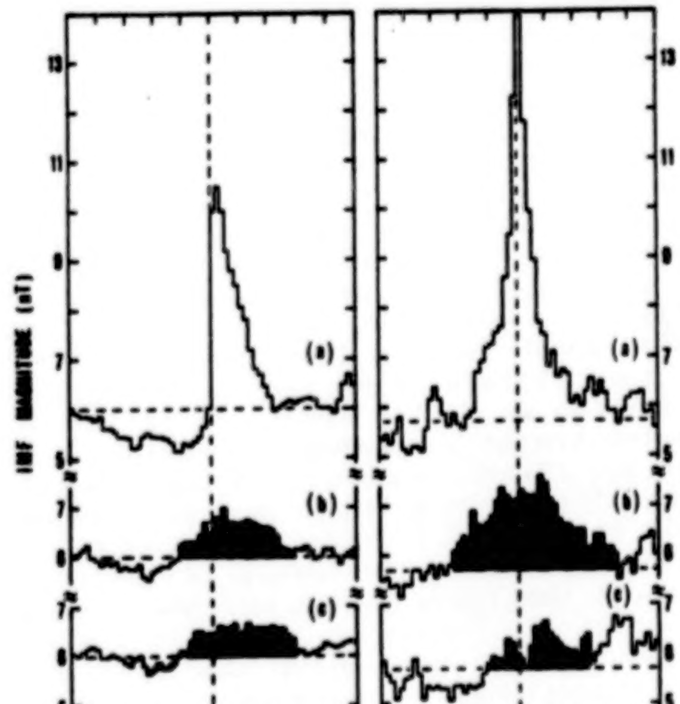

N85-35059

SH 5.1 - 5

LONGITUDINAL DEPENDENCE OF THE INTERPLANETARY PERTURBATION PRODUCED BY ENERGETIC TYPE IV SOLAR FLARES AND OF THE ASSOCIATED COSMIC RAY MODULATION

N.IUCCI, M.PARISI, M.STORINI, G.VILLORESI and S.PINTER (*)
Istituto di Fisica dello Spazio Interplanetario del CNR
Dipartimento di Fisica - Universita' 'La Sapienza'
Piazzale Aldo Moro,2 - 00185 ROMA, ITALY

(*) Geophysical Institute - Slovak Academy of Sciences
947 01 HURBANOVO, CZECHOSLOVAKIA

1. Introduction. One of the most significant features of the flare-associated Forbush decreases (Fds) in the galactic cosmic ray (c.r.) intensity is the so-called East-West asymmetry /1-5/ : the solar flares (Sfs) observed in the Eastern or central region of the solar disk exhibit a higher probability to cause large Fds than the Sfs occurring in the Western portion of the disk. In particular IUCCI et al./5,6/ showed that the interplanetary perturbations generated by Type IV Sfs depress the c.r. intensity in a vast spiral cone-like region (modulated region) which extends along the interplanetary magnetic field from the neighbourhood of the active region to the advancing perturbation, and that, immediately after the flare-generated perturbation, the maximum c.r. modulation is observed between 0° and 40° W (see Figures 4 and 13 in IUCCI et al./5/) of the meridian plane crossing the flare site at time of flare (flare's meridian plane). This asymmetric c.r. modulation could be due to a longitudinal asymmetry in the interplanetary perturbation producing Fds, as suggested by AKASOFU and YOSHIDA /2/ . This expected asymmetry seems to be, at a first glance, in contradiction with the results obtained by PINTER /7/ on the base of multiple spacecraft plasma and magnetic field observations, which indicate that the flare-generated shock waves expand on a broad front which is not spherical but nearly symmetrical with respect to the flare's meridian plane . In fact, if a flare-generated shock wave, displayed symmetrically with respect to the flare's meridian plane, is the only agent responsible for Fds we could hardly explain the observed East-West asymmeytry of the modulated region.

IUCCI et al. /8,6/ showed that the front edge perturbation 'strength' made up by the shock and magnetic blob effects, is well correlated (correlation coeff. 0.96) with the observed Fd-amplitude. Therefore if the shock is almost symmetrical about the flare longitude, the asymmetry of the Fd-modulated region is likely to be due to the magnetic perturbation following the shock which should be displayed asymmetrically in longitude, as suggested by HAURWITZ et al/9/.

BARNDEN/10/ found that the descending phase of some Fds exhibits a clear two-step structure which is located inside the associated interplanetary disturbance.The magnetic field intensity and solar wind plasma parameters indicate that the first step begins with the shock passage at the Earth/10,6/; the second step occurs generally near a discontinuity located inside the magnetic blob and followed by the flare ejecta or driver gas, this second decrease can be often connected to the entry of the Earth into a region with loop-like magnetic field configuration (e.g./11/ and ref. therein).

The main purpose of the present paper is to verify experimentally that an asymmetric perturbation (magnetic blob and discontinuities) following the shock is indeed responsible for the longitudinal asymmetry of the c.r. modulation; this will be done by studying statistically the separate contributions of the shock front and the following magnetic perturbation on the amplitude of the first and second step of Fds as a function of the associated Sf longitude.

2.The influence of shock and magnetic perturbation following the shock on the Fd-amplitude at 1 AU. An example of a two-step Fd time behaviour and associated parameters of the interplanetary medium is given in Figure 1.

First of all we analyzed,over the period 1964-1982, the total Fd-amplitudes as a function of the heliolongitude of the associated Sfs. Figure 2 shows that the total Fd-amplitude depends on the longitudinal position of the parent flare on the Sun; this result shows in particular that the maximum Fd-amplitude is observed when the flare is located $\sim 20^\circ$ East of the central meridian of the solar disk, in other words when the Earth enters the Fd-modulated region at $\sim 20^\circ$ West of the flare's meridian plane.

We next analyzed the relation between the amplitude of the first step of Fds and the longitudinal position of the parent Sfs. Figure 3 shows that, as an average, the highest amplitudes are observed near the flare's meridian plane, in agreement with the results obtained by PINTER /7/.
By means of the envelope curves of Figures 2 and 3 we can determine the large-scale characteristics of the two-step Fds; the polar diagram given in Figure 4 represents the heliolongitude dependence, relative to the flare longitude, of the total amplitude together with the amplitudes of the first and second steps of Fds. The asymmetric second step of Fds may be due to the longitudinal asymmetry of the magnetic perturbation following the shock /9,2/ : the magnetic field compression produced by a nearly symmetric shock, sustained by the driver gas and expanding into the Archimedean interplanetary magnetic field, will be more pronounced somewhere in the West of the flare's meridian plane, but not too far from this plane on which the shock exhibits the highest velocities. This asymmetry is shown in Figure 5 where the parameter $\langle B \rangle . \Delta t$ of the magnetic blob following the shock is plotted against the heliolongitude of the parent Type IV Sf, where Δt is the time duration and $\langle B \rangle$ the average field magnitude during the blob .

3. Relation between the Fd-amplitude and the associated interplanetary perturbation. IUCCI et al./8,6/ found that when the observed interplanetary perturbation is produced by a Type IV Sf the Fd-amplitude is well correlated with an empiric perturbation parameter which is the sum of two parameters: the shock 'strength' P_s and the magnetic blob 'strength' P_b. If we assume that the magnetic blob 'strength' is representative of the magnetic perturbation following the shock, the two parameters will correspond to the two effects reported above and therefore they can be separately correlated with each of the two steps of Fds. On the other hand a shock plus a magnetic blob were recently proved /12/ to form a suitable semipermeable obstacle to particle motion in order to produce the observed Fds. We investigated first the correlation between the total Fd-amplitude and the total perturbation parameter P_0 defined as:

$$P_0 = P_S + A.P_h = V_L + (V_1 - V_0) + 40[(N_1 - N_0)/N_0 + (B_1 - B_0)/B_0] + A(\langle B\rangle \Delta t),$$

where V_L is the local shock velocity (not considered in IUCCI et al. /8,6/) in km/s computed by using the flux conservation equation: $V_L = (V_1 N_1 - V_0 N_0) / (N_1 - N_0)$; indexes 0 and 1 refer to the pre- and post-shock values respectively. The coefficient $A = 1/3600$ $km.s^{-1}.nT^{-1}$ was estimated by making $\langle P_s\rangle = A.\langle P_b\rangle$ as indicated by the similar average amplitudes of the two steps of Fds (see Figure 3). For 21 two-step Fds an accurate estimate of P_s and P_b was possible; in Figure 6 the correlation plot between P_0 and the total Fd-amplitude confirms the results obtained by IUCCI et al./8,6/ (correlation coefficient 0.96); moreover the first step of the decrease is rather well correlated with the shock parameter P_s (correlation coeff. 0.88) as shown in Figure 7, this lower correlation may be attributed to the lower accuracy in the estimate of the first-step amplitudes.

References

/1/ S.YOSHIDA and S.I.AKASOFU: Plan.Sp.Sci. 13,435,1965.
/2/ S.I.AKASOFU and S.YOSHIDA: Plan.Sp.Sci. 15,39,1967.
/3/ Z.SVESTKA: Bull.Astr.Czech. 18,55,1967
/4/ S.GOPASYUK and L.KRIVSKY: Bull.Astr.Czech. 18,125,1967.
/5/ N.IUCCI et al.: Nuovo Cimento 2C, 1 , 1979 .
/6/ N.IUCCI et al.: Nuovo Cimento 7C, 467, 1984.
/7/ S.PINTER: Space Sci. Rev. 32, 145 , 1982 .
/8/ N.IUCCI et al.: Proc. 17th Int. C.R. Conf. 10,151,1981.
/9/ M.W.HAURWITZ et al.: J. Geophys. Res. 70, 2977 , 1965 .
/10/ L.R.BARNDEN: 'Proc. 13th Int. C.R. Conf. 2,1277,1973.
/11/ R.D.ZWICKL et al: 'Proc. SOLAR WIND FIVE', 711,1983.
/12/ B.T.THOMAS and R.GALL: J. Geophys. Res. 89, 2991,1984.

N85-35060

ORIGINAL PAGE IS
OF POOR QUALITY

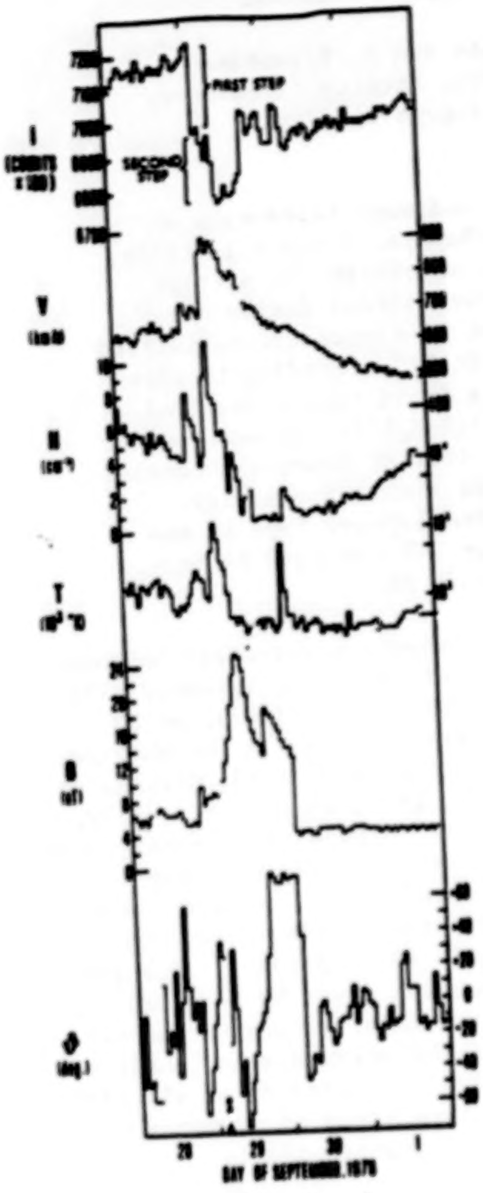

Figure 1

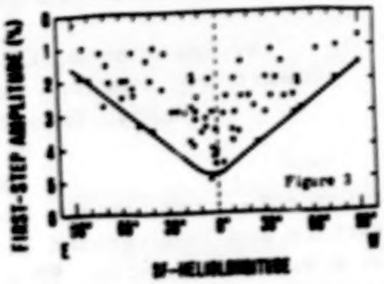

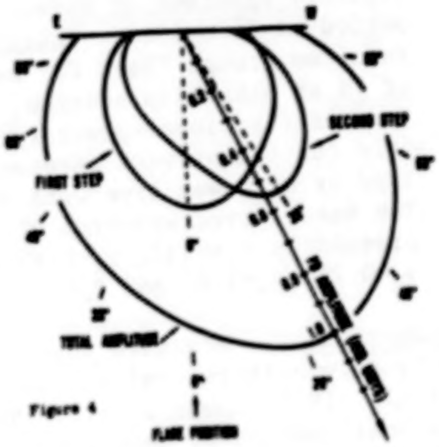
E
W
SECOND STEP
FIRST STEP
TOTAL AMPLITUDE
Figure 4
FLARE POSITION

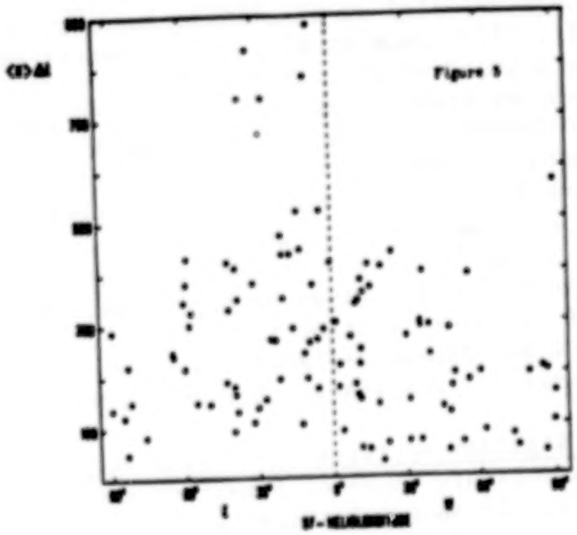

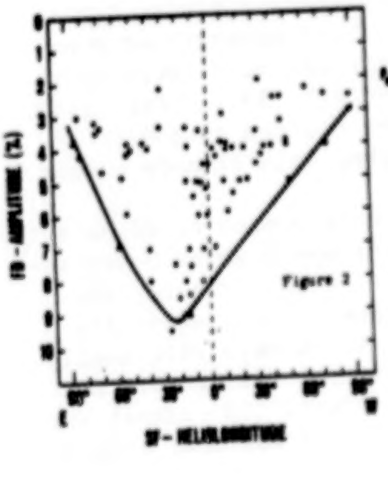

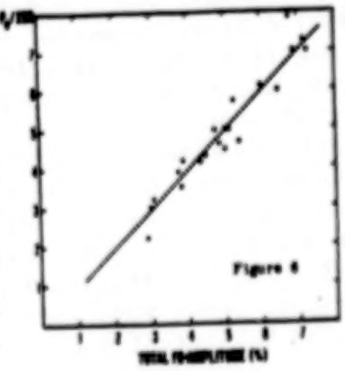

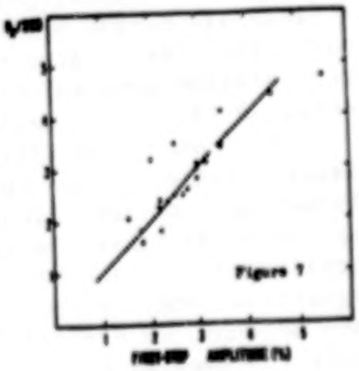

N85-35060

SH 5. 1-6

RIGIDITY SPECTRUM OF FORBUSH DECREASE

S. Sakakibara, K. Munakata and K. Nagashima
Cosmic Ray Research Laboratory, Faculty of Science,
Nagoya University, Nagoya 464 Japan

ABSTRACT

Using data from neutron monitors and muon telescopes at surface and underground stations(Nagoya, 0 m.w.e.; Misato, 34 m.w.e.; Sakashita, 80 m.w.e.), we obtain the average rigidity spectrum of Forbush decreases(Fds) during the period of 1978-1982. Thirty eight Fd-events are classified into two groups "Hard Fd" and "Soft Fd" according to size of Fd at Sakashita station. It is found that a spectral form of fractional-power type($P^{-\gamma_1}(P+P_C)^{-\gamma_2}$) is more suitable for the present purpose than that of power-exponential type or of power type with an upper limiting rigidity. The best fitted spectrum of fractional-power type is expressed by $\gamma_1=0.37$, $\gamma_2=0.89$ and $P_C=10$GV for Hard Fd and $\gamma_1=0.77$, $\gamma_2=1.02$ and $P_C=14$GV for Soft Fd.

1. Introduction. Rigidity spectrum of Forbush decrease(Fd) has been studied by many authors, using neutron monitor data(e.g. Lockwood, 1971; Iucci et al., 1979; Lumme et al., 1983; Fenton et al., 1983), or by adding a small amount of underground muon data to those in the above(e.g. Thambyahpillai et al., 1965; Andreis-Sandrucci et al., 1968; Mishima et al., 1973; Suda et al., 1977; Krymsky et al., 1979; Wada et al., 1979; Sakakibara et al., 1979; Wada and Suda, 1980). These studies have been made by assuming apriori a definite form of the spectrum and have tried to determine parameters involved in the spectral form. In the present paper, we make a comparative study of the spectral forms of Fd, using plenty of data in wide range of primary cosmic ray rigidity. For the muon telescope data, we use the response function given by Murakami et al.(1979,1981). For the neutron monitor data, we choose the response function given by Nagashima(1980) for the maximum solar activity out of three functions(Lockwood and Webber,1967; Aleksanyan et al.,1981; Mori and Nagashima,1984), based on a comparative study of response functions(S.Sakakibara et al.,1984; S.Mori and K.Nagashima,1984).

2. Rigidity spectrum of Forbush decrease. Data used for the present analysis are those of 8 neutron monitors(median primary rigidity $P_m=21 \sim 35$GV), 17 muon telescopes at Nagoya($P_m=60 \sim 119$GV), 9 underground muon telescopes at Misato($P_m=145 \sim 209$GV) and 3 underground muon telescopes at Sakashita($P_m=330 \sim 567$GV) during the period of Feb. 1978 - Feb. 1983. Fourty five Fds greater than 2% in depression for neutron intensity at Alert station were selected, but because of missing data of muon components, 38 Fds were finally adopted.

Fig.1 shows the rigidity dependence of the development of Fd on daily basis, obtained by superposing those 38 Fds at the epoch which 0-day includes the occurence time of SC. As can be seen in this figure, the depression at Sakashita is about 0.15% on the average and statiscally significant, but individual Fd at the station is not always statiscally significant and, in some cases, shows some increase. Taking this fact into account, we classify the Fds into two groups "Hard"(23 events) and "Soft"(15 events) according to size of Fd of Sakashita vertical component.

ORIGINAL PAGE IS
OF POOP QUALITY

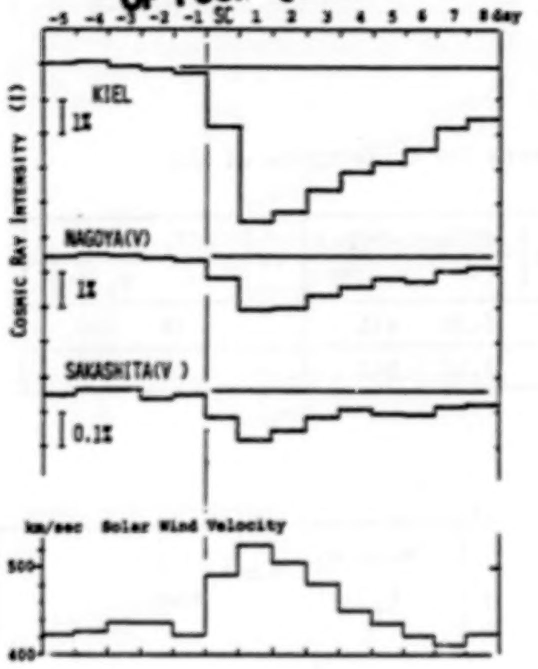

Fig.1 Averaged daily development of 38 Forbush decreases, superposed at the epoch day including SC, and that of the corresponding solar wind velocities.

The magnitude(ΔI) of each Fd is defined by the difference between daily mean intensities on +1 day and -3 day(cf. Fig.1). The boundary of two groups is set at the magnitude(ΔI=0.05%) of Sakashita vertical component, which corresponds to the statistical error for the component.

We made a comparative study of the rigidity spectrum of Fd, using the following three types of the spectrum.

PW : Power type

$$\Delta I \propto \begin{cases} P^{-\gamma} & \text{for } P \leqslant P_u \\ 0 & \text{for } P > P_u \end{cases}$$

PE : Power-Exponential type

$$\Delta I \propto P^{-\gamma} \exp(-P/P_0)$$

FP : Fractional-Power type

$$\Delta I \propto P^{-\gamma_1}(P+P_c)^{-\gamma_2} \qquad \text{.....} \ (1)$$

Corresponding to the parameters involved in Eq.(1), the expected values ΔI_{exp}'s for muon components and neutron monitors are calculated, respectively, from the differential coupling coefficients by Fujimoto et al. (1984) and from those by Mori and Nagashima(1984). By the least squares method, we found that FP-type spectrum in Eq.(1) can produce the expected values ΔI_{exp}'s most compatible with the observations. To demonstrate the coincidence between the observation and ΔI_{exp}'s, we use a diagram whose ordinate represents the observed magnitude of Fd and whose abscissa expresses the corresponding magnitude ΔI_{exp} calculated by using a rigidity spectrum of Fd. We call this the correlation diagram of Fd. If ΔI_{exp} is calculated by using the spectrum determined from the observed data by the least squares method, we call the diagram the best fitted correlation diagram of Fd. In this case, all points on the graph must lie on a line inclined by 45° from the abscissa. Such diagrams of Hard and Soft Fd's are shown in Fig.2, for the FP-type spectrum. It is noted that, in case of Soft Fd, the least squares method was applied to those data excluding those of Sakashita station.

The rigidity dependence of Fd's can be expressed more plainly if we use an effective primary rigidity(P_E) for Fd, which is defined as the median rigidity of a function obtained by multiplying the response function by the best fitted rigidity spectrum of the Fd. Fig.3 shows the P_E-dependence of Hard and Soft Fd's. The average magnitudes $\langle\Delta I\rangle$'s can line up systematically on this graph.

In Table I, we show the best fitted parameters of three types of the

ORIGINAL PAGE IS
OF POOR QUALITY

rigidity spectrum.

Table I. The best fitted parameters for three types of the rigidity spectrum.

Spectral type / Group	FP $P^{-\gamma_1}(P+P_C)^{\gamma_2}$			PE $P^{-\gamma}\exp(-P/P_0)$		PW $P^{-\gamma}$, $(P \leqslant P_U)$	
	γ_1	γ_2	P_C(GV)	γ	P_0(GV)	γ	P_U(GV)
Hard Fd	0.37	0.89	10	0.90	471	0.98	400
Soft Fd	0.77	1.02	14	1.17	145	1.26	100

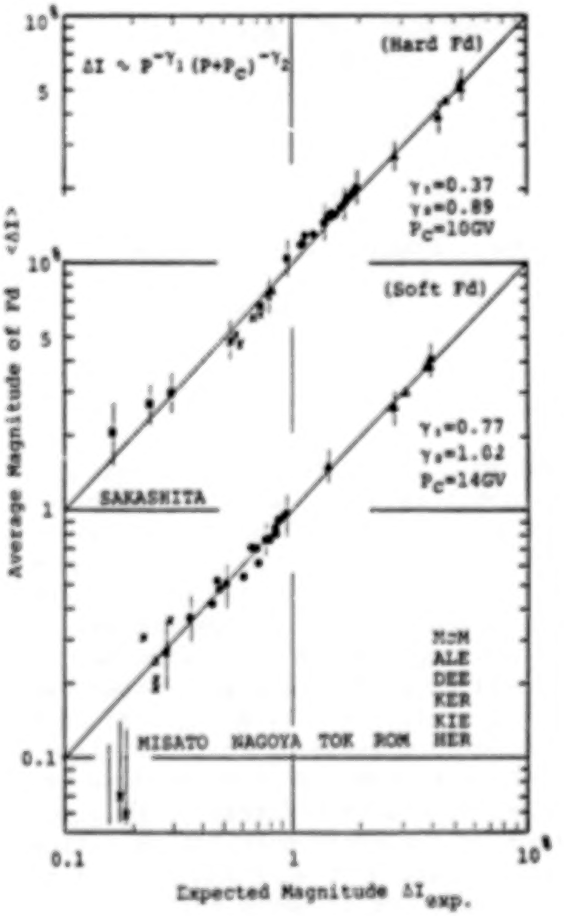

Fig.2 The best fitted correlation diagram of Hard and Soft Fds. ΔI_{exp} is calculated by using the fractional-power type spectrum with parameter shown in the figure, and in case of neutron monitors the NAGASHIMA-response function is selected for the calculation.

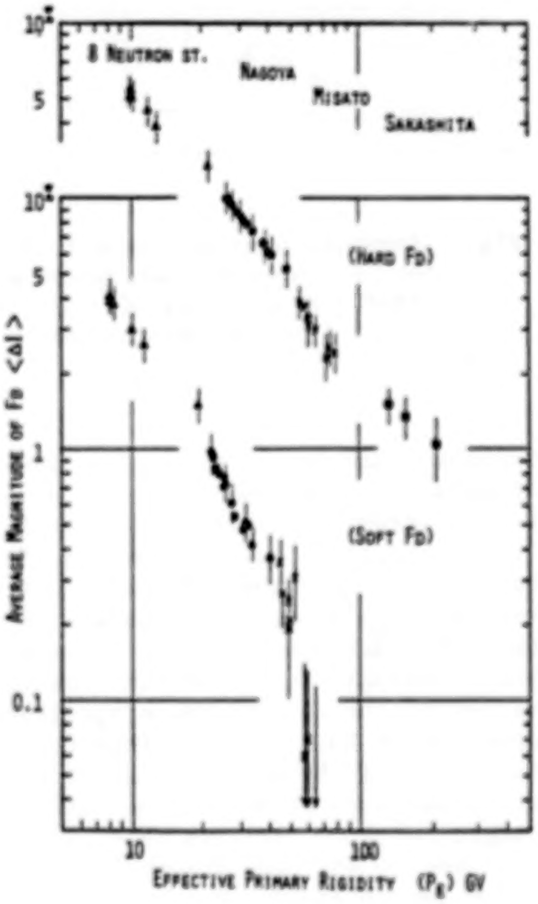

Fig.3 P_E -dependence of average magnitude <ΔI> of Hard and Soft Fds. The effective primary rigidity P_E for Fd defined in the text is calculated under the same conditions as in Fig.2. Errors are derived from the dispersion of individual Fds.

3. Conclusion. It is concluded that the FP-type spectrum is more suitable than PE-type or PW-type to express the observed rigidity dependence of Forbush decrease. However, in case of the Soft Fd, one cannot select the best spectral form out of the three types, by reason of the insufficient accuracy of the observed data in the higher rigidity range.

4. Acknowlegement. The authors are very grateful to Prof. S.Mori and his colleagues, Shinshu University, for providing their data from Misato underground station and also to Dr. M.Wada, Director of WDC-C2, Itabashi, Tokyo, for supplying us neutron monitor data. The authors wish to express their sincere thanks to Prof. I.Kondo, Tokyo University, for his helpful suggestion and discussion.

References

Aleksanyan,T.M., V.M.Beduazhevosky, Ya.L.Bloch, L.I.Dorman, N.S.Kaminar and F.A.Starkov (1981). Proc. 17th Int. Cosmic Ray Conf., (Paris), 3, 225.

Andreis-Sandrucci,L., G.Cini-Castagnoli and M.A.Dodero (1968). Annales de Geophysique, T.24, fasc.3, p.889.

Fenton,A.G., K.B.Fenton and J.E.Humble (1983). Proc. 18th Int. Cosmic Ray Conf., (Bangalore), 10, 164.

Fujimoto,K., A.Inoue, K.Murakami and K.Nagashima (1984). Rep. of Cosmic Ray Research Laboratory, Nagoya Univ., No.9.

Iucci,N., M.Parisi, M.Storini, G.Villoresi and N.L.Zangrilli (1979). Nuovo Cimento, 2C, 411.

Krymsky,G.F., P.A.Krivoshapkin, V.V.Klimenko, A.I.Kuzmin, S.I.Prokopjev, G.V.Skripin, N.P.Chirkov, G.V.Shafer and Yu.G.Shafer (1979). Proc. 16th Int. Cosmic Ray Conf., (Kyoto), 3, 395.

Lockwood,J.H. and W.P.Webber (1967). J.G.R., 72, 3395.

Lockwood,J.A. (1971). Space Sci. Reviews 12, 658.

Lumme,M., M.Nieminen, J.Peltonen, J.J.Torsti, E.Vainikka and E.Valtonen (1983). Proc. 18th Int. Cosmic Ray Conf., (Bangalore), 3, 237.

Mishima,Y., K.Murakami, M.Wada and Y.Miyazaki (1973). Proc. 13th Int. Cosmic Ray Conf., (Denver), 2, 1289.

Mori,S. and K.Nagashima (1984). Proc. Intern. Symp. Cosmic Ray Mod. in the Heliosphere, Morioka, Japan, p.219.

Murakami,K., S.Sagisaka, A.Inoue, Y.Mishima and K.Nagashima (1979). Nuovo Cimento, 2C, [illegible].

Murakami,K., S.Sagisaka, Y.Mishima, A.Inoue and K.Nagashima (1981). Rep. of Cosmic Ray Research Laboratory, Nagoya Univ., No.6.

Nagashima,K. (1980). personal communication.

Sakakibara,S., H.Ueno, K.Fujimoto, Z.Fujii and K.Nagashima (1979). Proc. 16th Int. Cosmic Ray Conf., (Kyoto), 3, 407.

Sakakibara,S., K.Munakata and K.Nagashima (1984). Proc. Intern. Symp. on Cosmic Ray Modulation in the Helioshpere, Morioka, Japan, p.212.

Thambyahpillai,T. and J.C.Dutt (1965). Proc. 9th Int. Cosmic Ray Conf., (London), 1, 257.

Suda,T., Y.Mishima, K.Murakami and M.Wada (1977). Proc. 15th Int. Cosmic Ray Conf., (Plovdiv), 3, 312.

Wada,M., S.Mori, K.Nagashima, S.Sakakibara and S.Yasue (1979). Proc. 16th Int. Cosmic Ray Conf., (Kyoto), 3, 390.

Wada,M. and T.Suda (1980). Sci. Papers I.P.C.R., 74, 1.

N85-35061

SH 5.1-7

SPECTRAL ANALYSIS OF THE FORBUSH DECREASE OF JULY 13, 1982

E. Vainikka, J.J. Torsti, E. Valtonen, M. Lumme,
M. Nieminen, J. Peltonen, and H. Arvela

Department of Physical Sciences, University of Turku, and
Wihuri Physical Laboratory, University of Turku
SF-20500 Turku, Finland

ABSTRACT

The maximum entropy method has been applied in the spectral analysis of high-energy cosmic-ray intensity during the large Forbush event of July 13, 1982. An oscillation with period of about 2 hours and amplitude of 1 - 3 % was found to be present during the decrease phase. This oscillation can be related to a similar periodicity in the magnetospheric field. However, the variation was not observed at all neutron monitor stations.

In the beginning of the recovery phase, the intensity oscillated with a period of about 10 hours and amplitude of $\lesssim 3$ %.

1. INTRODUCTION

One of the largest Forbush decreases (FDs) was observed on July 13, 1982. It was caused by a solar flare of type 3B on July 12 at 0916 UT at position 11 N, 37 E. The arrival of the shock front was indicated by a sudden commencement (SSC) at 1618 UT on July 13. The magnetic disturbance generated the largest geomagnetic storm ever observed in Finland. At Nurmijärvi Geomagnetic Observatory (60.5 N, 24.7 E), the horizontal component of the geomagnetic field reduced 20 % within a few hours, and returned to its predecrease level in 12 hours.

The decrease of high-energy cosmic rays began at about 1620 UT on July 13, and the recovery phase lasted several days. The amplitude of the decrease was of the order of 20 % as measured by the Turku double neutron monitor and other high-latitude monitors.

In order to find out possible periodicities in the cosmic-ray intensity during this FD, we applied the Maximum Entropy Method (MEM), proposed by Burg in 1967, in analyzing data from nine neutron monitor stations. The advantage of MEM is that it leads to much better resolution than the conventional Blackman-Tukey method. It also gives more realistic power spectral estimates, especially for short data records.

2. DATA AND METHOD OF ANALYSIS

The neutron monitor data used in our analysis are displayed in Figure 1. Before the frequency analysis, long-term trends (period > 12 hours) were removed by using the moving average method.

The power spectral density, P(f), was estimated from the equation

$$P(f) = \Delta t \, P_{M+1} \left| 1 + \sum_{k=1}^{M} \alpha_{Mk} \exp(-2\pi i f k \Delta t) \right|^{-2},$$

ORIGINAL PAGE IS
OF POOR QUALITY

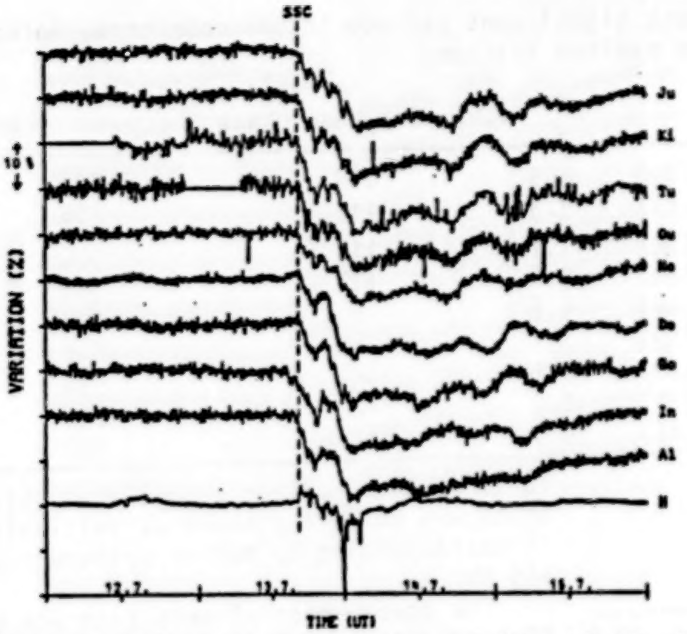

Fig. 1. Neutron monitor counting rates on July 12-15, 1982, at nime stations (see table 1 for the abbreviations). The lowest curve shows the horizontal component of the geomagnetic field as measured at Nurmijärvi station in Finland.

where f is the frequency, Δt is the time interval between the data points, and M is the length of the prediction error filter. The constant P_{M+1} and the coefficients α_{Mk} were determined from the matrix equation

$$\begin{pmatrix} \phi_o & \phi_1 & \cdots & \phi_n \\ \phi_1 & \phi_o & \cdots & \phi_{n-1} \\ \cdot & \cdot & \cdots & \cdot \\ \cdot & \cdot & \cdots & \cdot \\ \phi_n & \phi_{n-1} & \cdots & \phi_o \end{pmatrix} \begin{pmatrix} 1 \\ \alpha_{M1} \\ \cdot \\ \cdot \\ \alpha_{MM} \end{pmatrix} = \begin{pmatrix} P_{M+1} \\ 0 \\ \cdot \\ \cdot \\ 0 \end{pmatrix}$$

where ϕ_l $(l=0,\ldots,n)$ is the autocorrelation with time lag nΔt (for details of the method, see e.g. Ulrych and Bishop 1975). The time interval Δt was 5 or 15 min, and M was determined in the standard way ($M \leq N/3$, N = number of data points).

3. RESULTS AND DISCUSSION

3.1. Decrease phase. The decrease phase started at about 1620 UT. However, at Inuvik the onset time was about 1430 UT. The explanation is that the asymptotic directions of Inuvik rotate with the Earth so that at 1430 UT Inuvik receives particles from the direction of the interplanetary magnetic field-line. But these particles were strongly scattered by the arriving shock front, and thus their intensity decreased earlier.

The only significant variation in the frequency range $3 \cdot 10^{-5} - 10^{-3}$ Hz occurred with periods between 112 and 126 min (Table 1). The amplitude was largest at the mountain station Jungfraujoch (≈ 3 %, as reported also by Debrunner et al. 1983). At Finnish stations (Turku and Oulu), the amplitude was $\lesssim 2$ %. An analysis of the neutron-multiplicity data of the

ORIGINAL PAGE IS
OF POOR QUALITY

Table 1. The most significant periods in the cosmic-ray intensity at various neutron monitor stations.

Station		R_c^{vert} (GV)	Period (min) Decrease phase	Period (min) Recovery phase
Jungfraujoch	(Ju)	4.5	118	716
Kiel	(Ki)	2.3	115	706
Turku	(Tu)	1.1	115	706
Oulu	(Ou)	0.8	112	788
Hermanus	(He)	4.6	-	430
Deep River	(De)	1.1	-	640
Goose Bay	(Go)	0.6	-	596
Inuvik	(In)	0.2	126	540
Alert	(Al)	0.0	(119)	702

Turku neutron monitor showed that this variation was no more present at multiplicities ≥ 4 corresponding to median primary rigidities ≤ 35 GV.

The power spectral densities are shown in Figure 2. It is noteworthy that the 2-hour periodicity was practically absent at Hermanus Deep River, and Goose Bay. Further, the period 119 min of Alert is not statistically significant.

In Figure 3, the power spectral density is presented in more details around the 2-hour peak. The superiority of MEM to the conventional Blackman-Tukey method is evident.

The origin of these oscillations is clearly in the strong variation of the magnetospheric field as can be seen in Figure 4, where the observations of the satellite GOES-2 are reproduced.

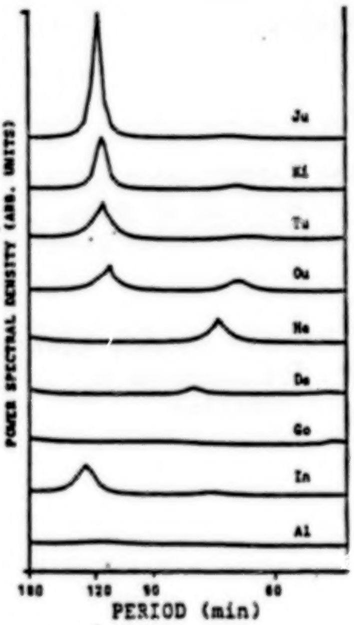

Fig. 2. Power spectral densities of the cosmic-ray intensity observed at various stations during the decrease phase.

3.2. Recovery phase. In the beginning of the recovery phase, rather strong oscillations were observed at all stations. The only remarkable variations occurred with a period of about 10 hours and amplitude of 3 % (Table 1 and Figure 5). A similar periodicity was found by Chirkov et al. (1983) as they analyzed data from several stations. This periodicity could be explained by the activity of the Sun. Another possibility could be successive reflections of galactic cosmic rays on

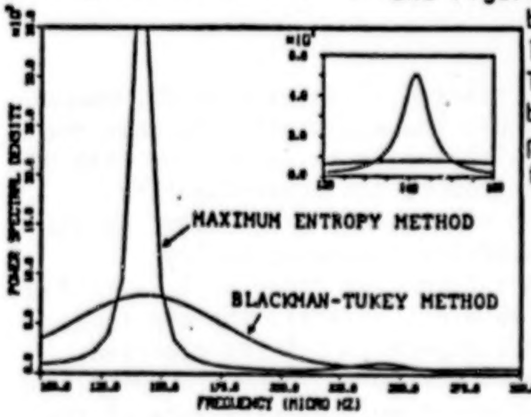

Fig. 3. Power spectral density of the cosmic-ray intensity observed at Jungfraujoch during the decrease phase. The small figure shows the density around the 2-hour peak.

ORIGINAL PAGE IS
OF POOR QUALITY

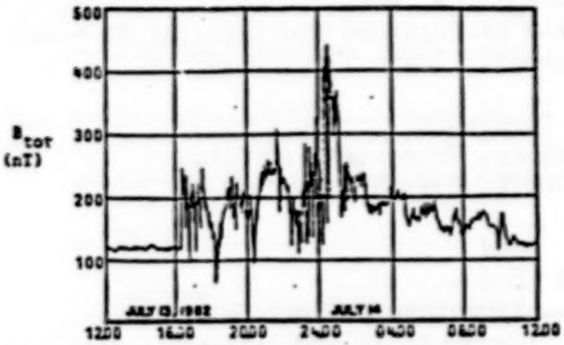

Fig. 4. The total magnetic field as measured by the satellite GOES-2 (from Parsignault et al. 1983).

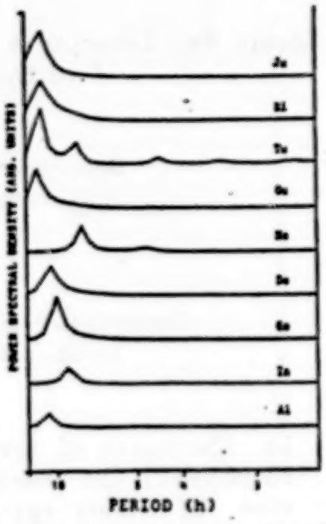

Fig. 5. Power spectral densities during the recovery phase.

the shock front.

Inspection of Figure 1 reveals some phase shifts of a few hours in the 10-hour variation (e.g. Deep River and Goose Bay vs. European stations). This feature is understood in terms of differences in the asymptotic directions of the stations.

4. CONCLUSIONS

The unusual periodicity of 2 hours during the decrease phase of the FD of July 13, 1982, is a direct consequence of strong oscillations in the magnetospheric field. The mechanism of the interactions between the solar wind and the Earth's magnetosphere leading to these oscillations requires further studies.

5. ACKNOWLEDGEMENTS

We are grateful to the following persons for providing us the neutron monitor data: G. Sebor (Jungfraujoch), K. Röhrs (Kiel), H. Kananen (Oulu), P. Stoker (Hermanus), and M. Bercovitch (Deep River, Goose Bay, Inuvik, and Alert). We also thank C. Suchsdorff for the magnetometer data of Nurmijärvi Geophysical Observatory.

REFERENCES

Chirkov, N.P., Filippov, A.T., and Yanchukovsky, V.L., Proc. 18th Int. Cosmic Ray Conf. 3, 245 (1983)

Debrunner, H., Flückiger, E., Golliez, A., Neuenschwander, H., Schubnell, M., and Sebor, G., Proc. 18th Int. Cosmic Ray Conf. 3, 257 (1983)

Parsignault, D.R., Feynman, J., and Rothwell, P., Proc. 18th Int. Cosmic Ray Conf. 10, 266 (1983)

Ulrych, T.J. and Bishop, T.N., Rev. Geophys. Space Phys. 13, 183 (1975)

N85-35062

TRANSIENT COSMIC RAY INCREASE ASSOCIATED WITH A GEOMAGNETIC STORM

S. Kudo and M. Wada
Cosmic Ray Laboratory, Institute of Physical and Chemical Research
7-13 Kaga-1, Itabashi, Tokyo 173, Japan

P. Tanskanen
Department of Physics, University of Oulu
Linnanmaa, SF-90570, Oulu 57, Finland

and
M. Kodama
Department of Physics, Yamanashi Medical College
Tamaho, Nakakoma, Yamanashi 409-38, Japan

ABSTRACT

On the basis of worldwide network data of cosmic ray nucleonic component, the transient cosmic ray increase due to the depression of cosmic ray cutoff rigidity during a severe geomagnetic storm has been investigated in terms of the longitudinal dependence. Multiple correlation analysis among isotropic and diurnal terms of cosmic ray intensity variations and Dst term of the geomagnetic field is applied to each of various station's data. It is shown that the amplitude of the transient cosmic ray increase associated with Dst depends on the local time of the station, and that its maximum phase is found in the evening sector. This fact is consistent with the theoretical estimation based on the azimuthally asymmetric ring current model for the magnetic DS field.

1. Introduction. The depression of cosmic ray cutoff rigidities and the alteration of the asymptotic direction of approach of cosmic rays during geomagnetic storms have been widely investigated by several authors throuth analysis of cosmic ray data or using trajectory-tracing technique (Yoshida et al., 1968; Debrunner et al., 1979; Flückiger et al., 1981). A particular interest is paid to the longitudinal or local time asymmetry of the cutoff rigidity depression or the storm-time cosmic ray increase, in connection with the asymmetric ring current which causes disturbed daily variation of geomagnetic field (Cummings, 1966; Kudo et al., 1984).

In this paper the storm-time cosmic ray increase for mountain stations is analyzed using 28 severe geomagnetic storm events occurred in 1966-1978. In this way the multiple correlation analysis is applied among isotropic and diurnal components of cosmic ray intensity and geomagnetic Dst term, and then the cosmic ray modulation term due to other origins except the lowering of cutoff rigidity is composed. The amplitude is obtained as a function of longitude of the stations.

2. Method of Analysis. The first step of the analysis is to separate the storm-time increase from other kinds of cosmic ray variations during geomagnetic storms. In the previous paper (Tanskanen et al. 1983) we reported that the observed cosmic ray variation during severe geomagnetic storms, CR(t), is reasonably separated into three components, i.e., the diurnal and the isotropic components A(t) and Iso(t), and the Dst depen-

dent component, Dst(t).

$$CR(t)=A(t)+c\cdot Iso(t)+d\cdot Dst(t)$$
$$\text{where}\quad A(t)=a\cdot\cos\omega t+b\cdot\sin\omega t\qquad \omega=2\pi/24hr$$

The isotropic component Iso(t) is an average of neutron monitor data from Thule and McMurdo to analyze the data from the sea-level stations. An average of Thule and Alert is used to analyze the data from the mountain stations since they are all distributed in the northern hemisphere. The coefficients a,b,c and d are obtained by the multiple correlation analysis based on one hour values covering three days centered at the Dst minimum day. The composed cosmic ray intenstiy, CR'(t), is defined by using some of the coefficients as follows.

$$CR'(t)=A(t)+c\cdot Iso(t)$$

The storm-time increase, STI, in unit of %/100nT is determined subtracting CR'(t) from CR(t). Some examples are shown in Figure 1.

3. Local Time Asymmetry of the Storm-Time Increase. The local time dependence of STI is analyzed by using the cosmic ray data from a number of stations distributed over a whole range of longitude on the earth. In the previous paper (S.Kudo et al., 1984), the sea-level stations below 5GV cutoff rigidity are used. After excluding the rigidity dependence of STI we obtained the local time asymmetry of STI from about 30 stations.

The phase and amplitude of the local time asymmetry of the storm time increase are obtained for six events. The histograms of the frequecy distribution of phases of the six events show that the asymmetry is located in the evening sector in the interval of several hours close to the Dst minimum time. The amplitude of the asymmetry averaged over the six events is kept almost constant at 1%/100nT for the same interval of time.

In Figure 2 the observed storm-time increases of the six events are illustrated together with the theoretical expectations. The black circles are the average values of observed STI of the stations with 4 GV cutoff rigidity, and the arrows denote the amplitudes of the asymmetry. The white circles are the theoretical estimations of the average storm time increase for Kiel, Jungfraujoch and Rome, which are obtained from the theoretical curve for the rigidity dependence of the storm-time increase (Kondo,1961). The theoretical values of the amplitude of asymmetry are estimated by using the result of Flückiger et al.'s work (1981), in which they calculated the depression of cutoff regidity based on a partial ring current model. It is seen that the observed values of STI are comparable with the theoretical expectations in magnitude.

4. Analysis on Mountain Stations. The local time dependence of STI on mountain stations is analyzed by using 28 events which occur in various UT hours. The method adopted for the sea-level stations is not applicable for mountain stations because they have various altitudes and the number of stations are limited. In this paper 28 events listed in Table 1 are used.

A typical example is shown in Figure 3, where STI in unit of %/100nT are plotted against UT of the Dst minimum time. Three hour average values of STI centered at the Dst minimum time are used in the present analysis.

The conversion of unit from % to %/100nT is made by multipling STI(%) by 100/ΔDst, where ΔDst is the difference of Dst between its flat level and the average over three hours around the Dst minimum time. The large increase near 18h LT(the arrow) show the local time asymmetry of STI. The other European mountain stations with between 4 and 5 GV cutoff rigidity, Lomnicky-Stit, Zugspitze, Pic-du-Midi, have the same tendency in the local time dependence. On the other hand the mountain stations with higher or lower cutoff rigidities, for example Mt.Norikura(11.4 GV) and Climax(3.0 GV), do not show such an evident asymmetry of the storm-time increase. The STI of Rome is also plotted in Figure 3. The phase of the asymmetry is close to 18h LT.

5. Discussion and Summary. We have obtained the local time asymmetry of the storm-time increase from the worldwide neutron monitor data. In section 2 the method for analyzing the data from a number of sea-level stations with cutoff rigidity lower than 5 GV has been shown briefly. The amplitudes of the asymmetry are consistent with the theoretical expectations, and the phases are located in the evening sector. In section 3 another method has been used to analyze the data from mountain stations or individual stations. The two methods are mutually connected with an equation between LT, UT and the longitude of stations, *LT=UT+(longitude/15degrees)*. It is evident that the data from European mountain stations show the local time asymmetry in the storm-time increase, and that the observed amplitude of asymmetry of Jungfraujoch and Rome are consistent with the theoretical expectations shown in Figure 2. We are making further analysis of the data from individual stations.

6. Acknowledgements. The authors express their sincere thanks to all the stations for sending neutron monitor data to WDC-C2. The present analysis is made on these invaluable data.

References

Cummings, W.D., 'Asymmetric ring currents and the low-latitude disturbance daily variation', J.Geophys.Res., 71, 4495(1966).

Dubrunner, H., and E.Flückiger, H.von Mandach and M. Arens, 'Determination of the ring current radii from cosmic ray neutron monitor data for the 17 December 1971 magnetic storm', Planet.Space Sci., 27, 577(1979).

Flückiger, E.O., D.F.Smart and M.A.Shea, 'On the effect of magnetospheric current systems on cosmic ray cutoff rigidities', Proc.17th ICRC, 4, 244(1981).

Kondo, I., 'On cosmic ray intensity increase during geomagnetic storm', Rep.Ionos.Space Res. Japan, 15, 319(1961).

Kudo,S., M.Wada, P.Tanskanen, H.Kananen and H.Komori, 'Local time asymmetry of the storm-time increases in cosmic rays', Proc.Int.Symp. Cosmic Ray, Morioka, 204(1984).

Sugiura, M., and D.J.Poros, 'Hourly values of equatorial Dst', NASA-GSFC Publications and Solar geophysical data.

P.Tanskanen, H.Knanen, S.kudo, M.Wada and H.Komori, 'Cosmic ray increases during severe geomagnetic storms', Proc.18th ICRC, 3, 217(1983).

Yoshida, S., S.-I. Akasofu and P.C. Kendall, 'Ring current Effects on Cosmic Rays', J.Geophys.Res., 73, 3377(1968).

ORIGINAL PAGE IS
OF POOR QUALITY

EVENT NUMBER	DATE YEAR	MONTH	DAY	Dst MINIMUM UT(hour)	nT
1	1966	3	14	6	-132
2	1966	5	26	23	-112
3	1966	8	30	24	-111
4	1966	9	4	3	-229
5	1967	1	14	6	-176
6	1967	2	16	14	-120
7	1967	5	26	4	-418
8	1967	6	6	3	-172
9	1968	4	5	23	- 95
10	1969	2	2	24	-175
11	1969	3	24	2	-240
12	1969	9	30	3	-132
13	1970	3	8	23	-268
14	1970	12	14	10	-142
15	1971	12	17	21	-167
16	1972	6	18	4	-190
17	1972	8	9	12	-154
18	1972	9	14	6	-146
19	1973	4	1	23	-188
20	1974	9	15	20	-149
21	1974	10	13	15	-105
22	1975	11	9	19	-114
23	1976	1	10	24	-164
24	1976	3	26	9	-229
25	1976	4	1	9	-221
26	1978	7	4	17	-114
27	1978	8	28	10	-242
28	1978	9	29	11	-241

Table 1 List of severe geomagnetic storms from 1966 to 1978.

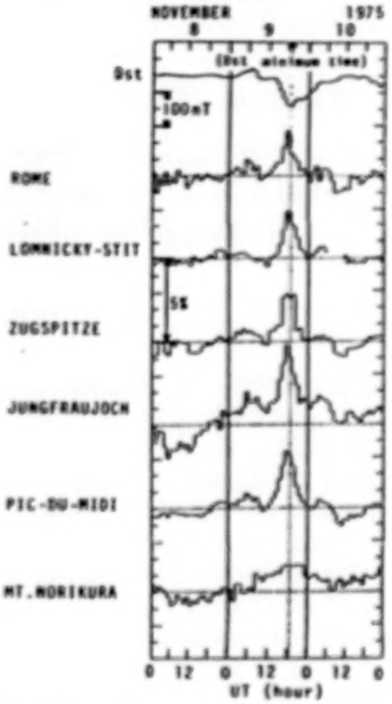

Fig. 1 The storm time increase (STI) for some stations during the geomagnetic storm in November 9, 1975. The topmost curve is the time variation of the geomagnetic Dst(t) (Sugiura).

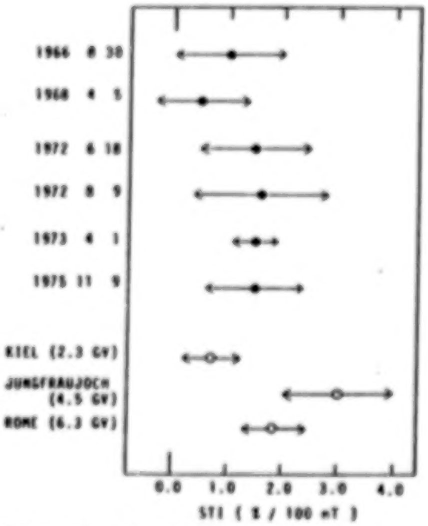

Fig. 2 The observed storm time increase of six events and the theoretical expectations for Kiel, Jungfraujoch and Rome.

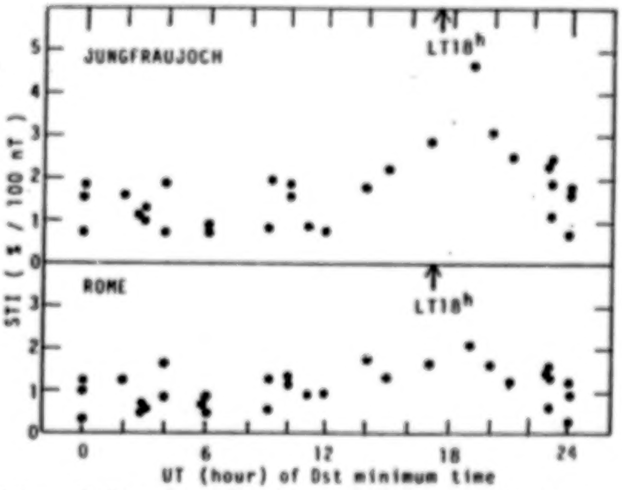

Fig. 3 The local time dependence of the storm time increase for Jungfraujoch and Rome obtained from 28 events listed in Table 1.

N85-35063
SH 5.1-9

GALACTIC COSMIC RAY CURRENTS AND MAGNETIC FIELD IRREGULARITY DEGREE IN HIGH-SPEED SOLAR WIND STREAMS

A.I.Kuzmin

Yakutsk State University, 677007 Yakutsk, USSR

I.S.Samsonov, Z.N.Samsonova

Institute of Cosmophysical Research & Aeronomy
Lenin Ave., 31, 677891 Yakutsk, USSR

ABSTRACT

Currents of galactic cosmic rays (GCR) obtained by global survey method are analyzed. The cases of almost total disappearance of GCR currents are compared with the results of direct measurements of the solar wind parameters. The conclusion is made on a restricted application of the convective-diffusive mechanism of the GCR modulation by the solar wind during the occurence of stationary and regular magnetic fields in the interplanetary medium.

1. Introduction. The cases of almost total disappearance of the GCR currents in a body of the recurrent high-speed streams of the solar wind during three rotations of the Sun for 1974 were indicated in [1] . Here we consider in detail the above phenomenon using the results of direct measurements of the solar wind and interplanetary magnetic field parameters [2] .

2. Results. We used hourly values of the GCR currents obtained by the global survey method [3] on neutron monitor world net data.

As it is known [4] 1973-1974 were characterized by the existence near the Earth of very wide and stable high-speed streams of the solar wind from polar coronal holes. In January - March 1974 the two-sector structure of IMF with noticeably predominance of the negative sector were observed. At this time there were no significant flare origin disturbances of the wind. The GCR intensity was close to the almost unmodulated level which is characteristic for the solar activity minimum in 1976 and it then began to decrease probably due to the solar activity increase.

In the Figure the solar wind speed V , strength H and signs of IMF, intensity I and diurnal values of the GCR currents $\mathcal{Z}_\perp$ for one rotation of the Sun for 1974 are shown. The $\mathcal{Z}_\perp$ are shown as arrows the direction and length of which coincide with the direction and value of currents in the solar-earth coordinate system (scale is at the top). The Earth's position with respect to the neutral IMF sheet during one rotation of the Sun is schematically shown. The

ORIGINAL PAGE IS
OF POOR QUALITY

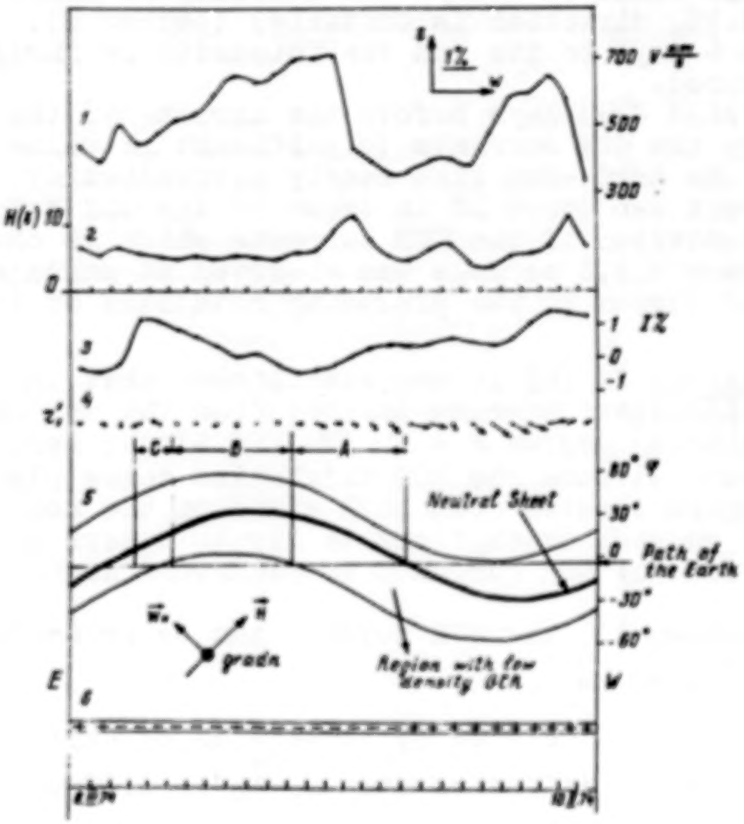

The parameters of the solar wind, IMF and GCR for February 10 and March 8, 1974.
1 - solar wind speed, 2 - IMF strength,
3 - isotropic GCR intensity, 4 - GCR currents in the solar-earth coordinate system, 5 - a scheme of a modulation region of GCR in the solar wind high-speed streams, 6 - the signs of IMF

Earth's heliolatitude corresponds to the analyzed period. The maximum heliolatitude of the neutral sheet was observed to be +30° [5] and it corresponds to the largest removal of the Earth's orbit by 0.5 AU in the meridional plane. In the first narrow high-speed stream the Earth is within the modulation region and the currents behave themselves usually. Therefore we consider here the behaviour of the GCR currents only in the second, wider streams. The velocity of the solar wind stream up to values ~700 km/s the IMF strength increases up to 10 γ and the GCR intensity insignificantly (~ 1%) decreases.

According to the behaviour of the GCR currents the whole considered period can be divided into three parts (Figure, A, B, C). During period A when the Earth enters the high-speed stream an is in the region of the decreased GCR density, the currents have the usual azimuthal direction and the value according to the convective-diffusion mechanism. In 3 days after the IMF disturbance the GCR currents almost completely disappear (their value is within the accuracy of hourly measurements $\sim 0.1\%$, direction is unstable) (period B). This period lasts ~ 6 days to its end the intensity is insignificantly re-recovered.

During period C ~ 3 days before the arrival of the next sector boundary the GCR currents (significant in value) are eastward from the Earth-Sun line nearly perpendicular to IMF force line (about 5-6 hours LT in terms of the GCR anisotropy).

Similar behaviour of the GCR currents which is characteristic for each A,B,C periods was observed at passage of the same high-speed stream in two preceding rotations of the Sun [1].

3. Discussion. In [6] it was established that in the body of recurrent high-speed streams emitted from the coronal holes the IMF irregularity degree $F = D_{\perp}/D_{\parallel}$ is almost zero. Therefore on such streams the GCR modulation takes place only in a narrow region located from both sides of the neutral IMF surface. Based on such conceptions we try to understand the observed behaviour of GCR currents in recurrent high- speed streams.

As it is known [3] the GCR current can be presented as follows: $\vec{W} = \vec{W}_c + \vec{W}_d + \vec{W}_H$,

where $\vec{W}_c$ is the current caused by convection of particles by the solar wind, $\vec{W}_d$ is diffusive stream, $\vec{W}_H$ is diffusion caused by perpendicular density gradient known as the Hall's current.

In part A, in the region with the decreased density the GCR currents are due to convection and diffusion according to the above expression. In region B which is mostly remoted from the neutral sheet in equatorial and meridional planes the Earth falls into the regular and stationary IMF where there are no any scattering centers. In such a field by [7] the convection and the diffusion are absent and the Hall's current [3] appears only when there are density gradients. In the case of the regular field the GCR density gradients will exist at the distance of only one Larmor radius from the boundary of region with decreased density (in our case $\rho \approx 0.04$ AU). As it is seen from the Figure in the region B the GCR density gradient and therefore the Hall's current will not be observed.

In region C the approach of the next sector boundary or of the neutral sheet will be manifested as the Hall's current occurence on a scheme shown in the bottom of the Figure. And the current of the aligned diffusion in this region will be absent while the next sector boundary will arrive since IMF force lines connect the Earth with the west undisturbed hemisphere of the Sun.

For a totally regular field we can write [3] :

$$\vec{W}_H = \left[\frac{\vec{H}}{H} \times \nabla_{\perp} I\right] .$$

If the value of GCR currents in region C is known one can estimate the value of the GCR density gradient perpendicular to ecliptic plane ($\nabla_\perp I \approx 8\%/AU$).

On the other hand, if the stream is stationary then a radial density gradient at the next disturbance of GCR intensity estimated on $\frac{\partial I}{\partial t} = - \nabla_z \vec{V}$ is $\nabla_z I \approx 4\%/AU$.

Both obtained values of gradients do not contradict each other if to take into account the flattening of the GCR modulation region to the neutral sheet.

4. Conclusion. From the above one can conclude the following:

a) In recurrent solar wind high-speed streams from polar coronal holes observed in 1973-1974 the IMP inhomogeneities causing GCR modulation are located only in a relatively narrow region near the neutral sheet. In some favourable cases (January - March 1974) when this sheet is located far enouth, the Earth can get into the region of IMF with superhigh regularity degree where the GCR modulation is practically absent.

b) In such fields the GCR currents (anisotropy) are absent since neither convection nor diffusion of particles exist. At approach of the neutral sheet the Hall's current can occur because of occurence of perpendicular density gradients.

References.

1. Samsonov, I.S. et al., (1981), Proc.17-th ICRC, Paris, 3, 310.
2. King, I.H., (1977), Interplanetary Medium Data Book, Greenbelt.
3. Krymsky, G.F. i dr., (1981), Kosmicheskie luchi i solnechnyi veter, Novosibirsk, Nauka.
4. Kovalenko, V.A., (1983), Solnechnyi veter, Moskwa, Nauka.
5. Samsonov, I.S. et al., (1979), Proc.16-th ICRC, Kyoto, 3, 481.
6. Korzhov, N.P., (1982), Karty polyarnostei globalnogo magnitnogo polya Solntsa i konfiguratsiya mezhplanetnogo tokovogo sloya v 1971-1978. Irkutsk.
7. Stern, D., (1964), Planet.Space Sci., 12, 973.

ORIGINAL PAGE IS
OF POOR QUALITY

ORIGINAL PAGE IS
OF POOR QUALITY

N85-35064

STUDY OF DOMINATING PARAMETERS OF HIGH SPEED SOLAR PLASMA STREAMS IN RELATION TO COSMIC RAY AND GEOMAGNETIC STORMS

B.L. Mishra
Govt. Engineering College,
Rewa (M.P.)486001,India.

and

S.P. Agrawal
Physics Department(Vikram Space Physics Centre)
A.P.S.University, Rewa(M.P.)486003,India.

ABSTRACT

The high speed solar wind streams observed near earth are generally associated with the solar features, such as solar flares and coronal holes. Past studies of these streams from the two sources have revealed distinctly different effects on cosmic ray intensity, whereas the effect is similar for geomagnetic disturbances. Moreover, the effect of the magnitude of the high speed streams (V) and its rate of increase (dv/dt) has also been a subject of investigation to understand their relative contribution in producing geomagnetic disturbances. From the analysis of some of the fast streams presented here, it is difficult to predict, which one of the two (V, dv/dt) is more effective in producing geo-magnetic disturbances. Further, in most of the cases, no substential decrease in cosmic ray intensity is observed.

1. Introduction. The high speed solar wind streams are now known to be associated with energetic solar flares during the period of high solar activity, and with large area solar coronal holes during the declining phase of solar activity. Their distinctly different effects on short-term cosmic ray intensity decreases has been recently pointed out (Venkatesan et.al.1982). Lindblad and Lundstedt (1981, 1983) have compiled the list of high speed solar wind streams for the period 1964-78. Reference is also made in the same reports, that geo-magnetic activity is more closely associated with a large positive time derivative (dv/dt) than with large velocity. Moreover, it has been reported that geo-magnetic activity maximises earlier than solar wind velocity at the earth. (Ballif et.al.1969; Sawyer and Haurwitz, 1976). However, from a critical review of literature, it is not possible to make a positive statement that dv/dt is better associated with geo-magnetic activity than with V. In this paper, we have considered some of those streams which show a very smooth and sharp rise in velocity, to find out the

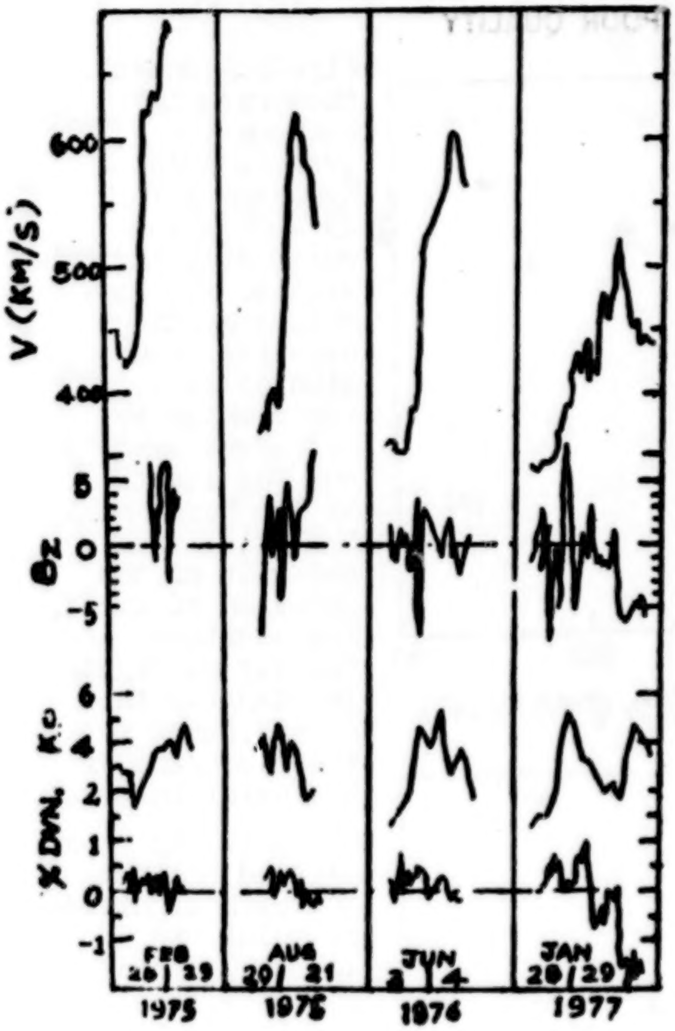

Fig.1 Shows the time intensity plot for three fast rise, high speed solar wind stream events selected from the catalogue published by Lindblad and Lundstedt (1983; see text for details) during the interval 1975-78; in all 25 events were selected. The fourth event (Jan. 28-30, 1977) represents a slow V but smooth rise in solar wind speed with relatively low value of maximum velocity. The Bz component of the interplanetary magnetic field as well as the Kp indices, and the percent deviation of cosmic ray intensity (Deep River neutron monitor) are also shown for each event.

effect of dv/dt and V on geo-magnetic disturbance index Kp, and cosmic ray intensity.

2. Selection of events. For the selection of events, we have made use of the catalogue published by Lindblad and Lundstedt (1983) and the Interplanetary Medium Data Book, Supp. 1 (No. 79-08; Dec. 1979). Moreover, the following conditions were imposed on the solar wind speed profile.

1. The initial velocity of the solar wind, before the start of the event, should be below or around 400 kms/sec.

2. Only that portion of the stream is considered for calculating dv/dt, during which the velocity monotonically increases.

3. The peak value of the solar wind stream is taken within 24-hours of the last hour of the dv/dt. For each event we have selected the maximum value of the 3-hourly Kp-indices for the duration of dv/dt, as well as the maximum value of 3-hourly Kp-indices during the 6-hours on either side of the hour of maximum V. Based on this selection criteria,

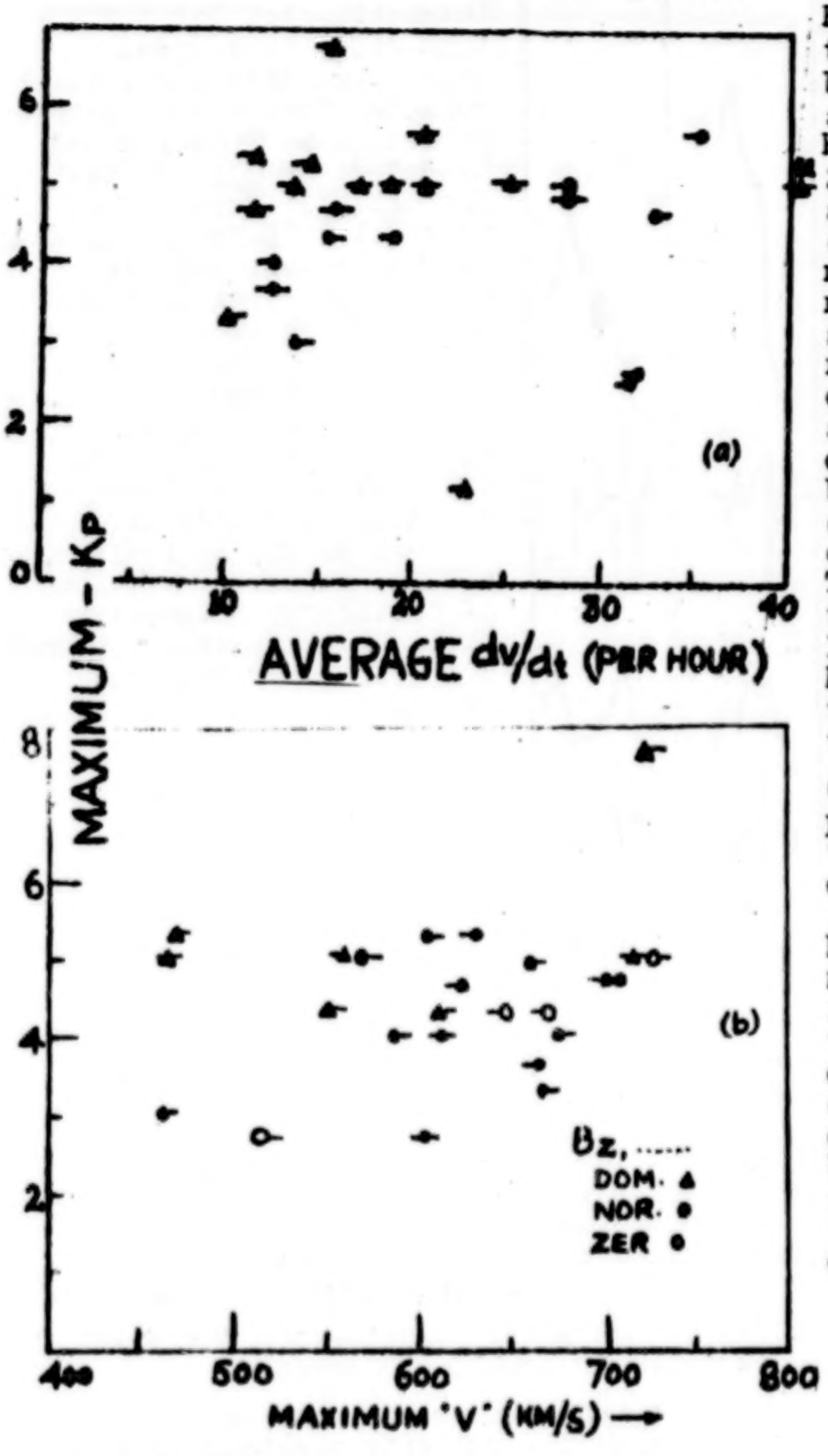

Fig. 2(a) Shows the crossplot between the average dv/dt & Kp-maximum for 25 high speed solar wind stream events. The magnitude of the negative excursion of Bz is represented by different symbols, and the length of the horizontal bars give the estimate of the duration of dv/dt. The position of the bar on right/left depicts the Kp max. being in the start/end of the dv/dt interval.

(b) Shows Kp max. plotted against the peak magnitude of solar wind speed(V) symbols have the same meaning as in fig 2(a). The position of the bar on right/left depicts the time of Kp max. being before/after within six-hours on either side of peak value of V.

we have identified 25 high speed stream events to investigate the effect of dv/dt and maximum-V, on Kp.

3. Analysis and results. Out of 25 high speed streams selected, three representative cases of high dv/dt and large V are depicted in figure 1. In the same figure we have also shown an event of low dv/dt and V, but associated

with highly negative values of Bz. It may be noted that all the three high dv/dt and "V" cases are associated with different conditions of other parameters (Bz, Kp and % deviation of cosmic ray intensity at Alert). From the first 3 cases depicted in figure 1, it can be inferred that Kp is high only when Bz is negative, and is affected equally both during dv/dt and V. This statement is further justified from the plot showing the case of low value of dv/dt and low V, where again for highly negative value of Bz, we find a moderate to high values of Kp. Any significant change in the cosmic ray intensity during the interval of high dv/dt and high V is not observed. On the contrary, a small decrease is associated with the last case of low V and dv/dt, which may be due to other causes.

In figure 2 and 3, we have shown all the 25 cases, correlating the observed maximum value of Kp with the value of dv/dt and V separately. The difference in the magnitude of Bz is also represented in the figure by plotting the value by different symbols. Moreover, the duration of dv/dt is represented by the length of the horizontal bars. The occurrence of maximum value of Kp at the start, middle or end of dv/dt is also represented. Similarly, in the case of V, the occurrence of maximum Kp, before or after the time of maximum V is also depicted.

From both the plots, it is clear that the maximum value of Kp is usually high for all the events (i.e. for maximum V and for average dv/dt), and does not show any significant relationship either with V or dv/dt. This is seen even when we divide the events for various categories of Bz. However, in most of the cases, Kp approaches maximum value either at the end of dv/dt interval, or just before V reaches to maximum values. We have also noticed that the maximum V and dv/dt are loosely correlated with each other, and that could be the reason why maximum Kp is seen in both the cases. Therefore, from the analysis presented here, we conclude that the value of Kp is generally high both during maximum V and high dv/dt and has no preferrence to occur during the interval of dv/dt.

4. References.

Ballif, J.R.; Jones, D.E. and Coleman, P.J., 1969. J.Geophy. Res. 74 p. 2289.

Lindblad, B.A.; Lundstedt, H., 1981. Solar Physics 74 p. 197.

Lindblad, B.A.; Lundstedt, H; 1983. Solar Physics 88 p. 377.

Sawyer, C. and Haurwitz, M.; 1976, J. Geophy. Res. 81 p. 2435.

Venkatesan, D. Shukla, A.K. and Agrawal, S.P. 1982 Solar Physics, 81, p. 375.

N85-35065

SH 5.1-12

INFLUENCE OF MAGNETIC CLOUDS ON COSMIC RAY INTENSITY VARIATIONS

Badruddin, R.S. Yadav and N.R. Yadav
Space Science Group, Dept. of Phys., A.M.U. Aligarh (India).

S.P. Agrawal
Dept. of Phys., A.P.S. Univ., Rewa (M.P.).

ABSTRACT

Neutron monitor data has been analysed to study the nature of galactic cosmic ray transient modulation associated with three types of interplanetary magnetic clouds -clouds associated with shocks, stream interfaces and cold magnetic enhancements.

1. Introduction. It is well known that interplanetary magnetic field is of basic importance in the modulation of galactic cosmic rays. Most of the earlier studies of transient cosmic ray intensity modulations in relation to IMF are confined to the field strength, irrespective of the origin of change in it and other associated properties (Barouch & Burlaga, 1975; Duggal et al., 1983). Recently 46 magnetic clouds were identified in the interplanetary data obtained near the earth between 1967-78 and classified into three classes - shock associated clouds, a stream interface and a cold magnetic enhancement. The Max. field strength is found to be approximately the same and the temperatures are low in all the three types of clouds. The physical characteristics of the magnetic clouds and their role of occurrence suggest that many or all the clouds might be related to coronal mass ejections(Klein and Burlaga, 1982).

Newkirk et al. (1981) have suggested that the interplanetary manifestation of coronal mass transients(ejection) may play an important role in galactic cosmic ray modulation and Burlaga (1983) has observed that the detailed studies of the relations between magnetic clouds and cosmic rays have not been made, but they are worth taking.

In view of the known characteristics of magnetic clouds in relation to magnetic and plasma properties for different classes of clouds and their association with CMEs, it seems important to investigate, in detail, the cosmic ray intensity variations in relation to these clouds of different classes.

2. Analysis. Three types of clouds mentioned above are observed to be moving high magnetic field structures in the interplanetary space. In earlier studies of transient cosmic ray modulations related to interplanetary magnetic field intensity enhancements, most of them are confined to their relationships irrespective of the origin of their enhancement and their other physical properties. We have performed the superposed epoch analysis, using Deep River super neutron monitor data and the date of the cloud observation at the earth as the epoch day, for three classes of clouds seperately. Some individual events have also been studied for more specific investigations.The various interplanetary parameters associated with these clouds are then used to study the time profile and other characteristics of large amplitude transient decreases(Fd-type) in cosmic ray intensity,which are generally associated with shock associated clouds.

3.Magnetic clouds and Cosmic ray intensity Variations. In Fig. I,We have shown the superposed epoch plots of cosmic ray intensity data from Deep River for three classes of clouds.It is found that the decrease in cosmic ray intensity,with the clouds preceded by a shock,is higher in comparision to the decreases observed inassociation with other two types of clouds and the decrease starts earlier than the arrival of the clouds.The recovery is complete nearly ina week time.The decrease in cosmic ray intensity associated with the cloud followed by a stream interface is much smaller than the one mentioned above.The decrease time is also elevated and the onset of the decrease takes place on the arrival of the cloud. The decrease observed in association with the clouds associated with cold magnetic enhancement is still smaller in amplitude and duration,but the decrease in cosmic ray intensity starts when the clouds arrives at the earth.

4.Magnetic clouds following shocks and cosmic ray intensity variation. We have plotted the cosmic ray intensity data in relation to some individual shock associated clouds(Fig.2). Whenever the shock arrival time is not available we have used the sudden commencement of geomanetic storms(SSC)data,since SSC can be regarded as the geomagnetic signature of the arrival time of the interplanetary shocks.We can see from Fig.2 that ,in general,the Forbush-type decrease starts at time of arrival of the shock wave at the earth.However, there are a few cases when no appreciable decrease in cosmic ray intensity is observed,with the shock associated clouds.suggestions have been made in the past that the Forbush-type decrease is caused by the entry of the earth into a loop or tongue of IMF field lines that are fresly ejected from the sun.Cosmic ray density in such loops was considered to be depressed because these field lines do not reach boundary regions of the the heliosphere and also because particles are cooled as the loop expands.We found(Fig.I&2) that in case of shock associated clouds decrease in cosmic ray intensity starts,at the earth ,not at the arrival of the cloud,but at the arrival of the shock that precedes the cloud by few hours.It is difficult to follow the exact time history of the events in detail, because cosmic ray profiles vary significantly with the longitude and latitude of the observing stations.However, it is likely,that the magnetic regime that contained the lowest density of galactic cosmic rays was a portion of the magnetic cloud.These results are in agreement with the view expressed by Palmer et al.(I978).

5.Physical Properties of shock associated magnetic clouds and associated cosmic ray variations .

We have seen that the transient modulation of cosmic ray intensity is related,ingeneral,to the clouds of all the three classes.However,the time profile and amplitude of cosmic ray modulation for three types of clouds is different.Forbush-type transient modulation is related,generally,with the cloud preceded by a shock.We have thus used the cloud and shock parameters to further study the various features of associated modulation.

Fig.3 shows the relation between the duration of the cloud near the earth and the total time taken for a forbush decrease to recover to pre-decrease level from the start of the event.It seems that the total duration of the forbush decrease increases as the cloud duration increases.However, as shown in Fig.4,the time taken by the decrease from the onset time to reach the minimum value of intensity does not depend on the duration of the cloud.But the recovery time of these decreases seems dependent on the duration of the clouds (Fig.5),it is larger for larger duration clouds.Though our results show the above mentioned behaviour,still there is needto have more data to varify this result conclusively.The observed duration of the cloud will depend upon the size and/or speed of the cloud.Since the clouds are observed to be expanding to distances of at least 4AU,they are more likely to be important at larger distances as far as the recovery time is concerned.From the study of cosmic ray intensity at IAU,6.97AU,& I5.9IAU and the findings that a magnetised plasma cloud moved outward and that the recovery time at these distances were,respectively- 6, 22,and I50 days,it may be possible that some of the cloud move to such large distances;they might also be expanding while moving to such distances.It has beenmentioned by Lockwood and Webber(I977)that the modulation regions associated with Forbush decreases were propagating several astronomical units beyond earth.

6.Amplitude of decrease and its relation to the speed of shock associated clouds. We have also studied the amplitude of decrease in relation to maximum solar wind velocity increase observed in association with these shock associated clouds(Fig.6).In general the increase in amplitude is larger when the cloud speed is larger.

References.

Barouch,E.and Burlaga,L.F.(I975),J.Geophys.Res.,80,449.
Burlaga,L.F.,(I983),Proc. I8th ICRC,I2,2I.
Duggal,S.P.,Pomerantz,M.A.,Schaefer,R.K.and Tsao,C.H.,(I983), J.Geophys.Res.,88, 2973 .
Klein,L.W.and Burlaga,L.F.,(I982),J.Geophys.Res.,87,6I3.
Lockwood,J.A.and Webber,W.R.,(I977),J.Geophys.Res.,82,I906.
Newkirk,G.Jr.,Hundhausen,A.J.and Pizzo,V.,(I98I),J.Geophys. Res.,86,5387.
Nishida,A.,(I982),J.Geophys.Res.,87,6003.
Palmer,I.D.,Allum,F.R.and Singer;S.,(I978),J.Geophys.Res; 83, 75.

ORIGINAL PAGE IS
OF POOR QUALITY

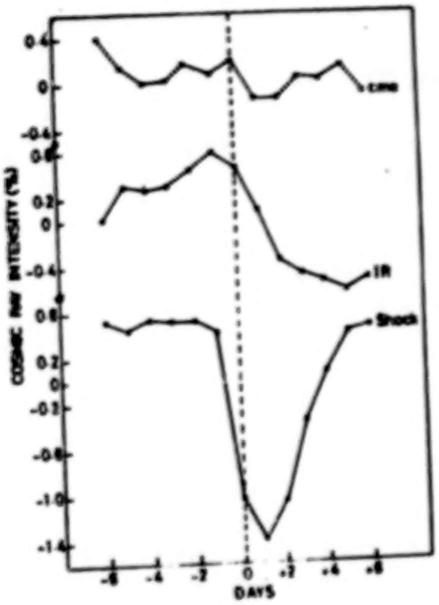

Fig.-1

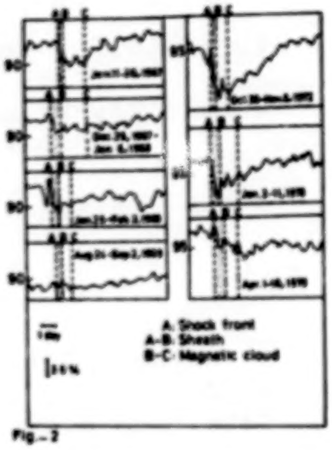

Fig.-2

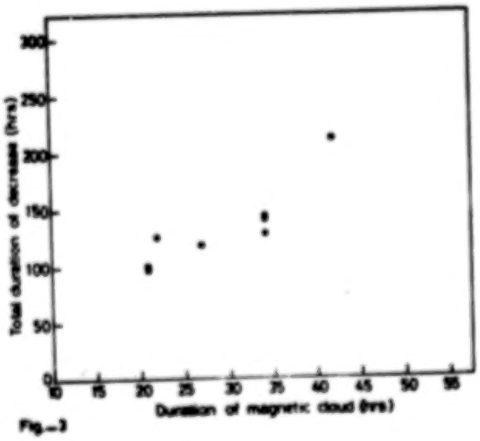

Fig.-3

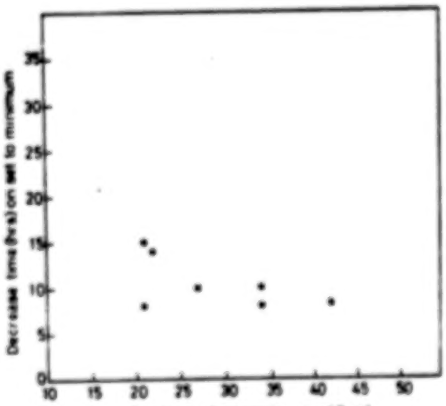

Fig.-4

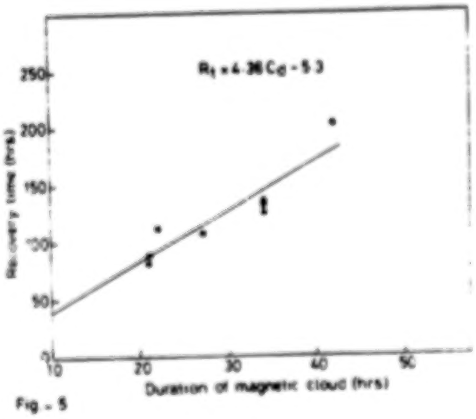

Fig.-5

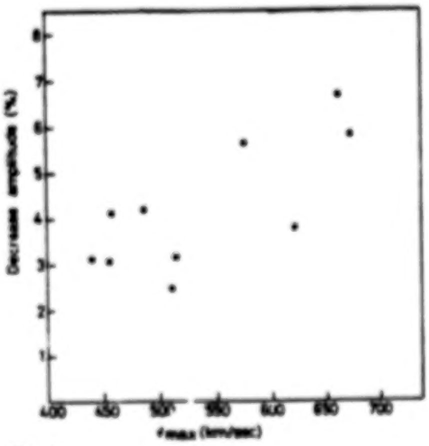

Fig.-6

N85-35066

SH 5.1-13

The Solar Wind Effect on Cosmic Rays and the Solar Activity

Fujimoto,K., Kojima,H.* and Murakami,K.

Cosmic Ray Reserch Laboratory, Nagoya University,
Chikusa-ku, Nagoya 464, Japan

*School of Hygiene, Fujita Gakuen Health University,
Toyoake, Aichi 470-11, Japan

ABSTRACT

The relation of cosmic ray intensity to solar wind velocity is investigated, using neutron monitor data from Kiel and Deep River. The analysis shows that the regression coefficient of the average intensity for a time interval to the corresponding average velocity is negative and that the absolute effect increases monotonously with the interval of averaging,τ, that is, from -0.5% per 100km s^{-1} for $\tau=1$ day to $\sim$-1.1% per 100km s^{-1} for $\tau=27$ days. For $\tau>27$ days the coefficient becomes almost constant independently of the value of τ. The analysis also shows that this τ-dependence of the regression coefficient is varying with the solar activity.

1. Introduction

The relation of cosmic ray intensity to solar wind velocity has been studied by several authors. Duggal et al. (1977) pointed out the effect of high speed wind upon cosmic ray intensity, using neutron monitor data. Iucci et al. (1979) showed the coefficient to be -0.5% per 100km s^{-1}, applying Chree epoch method to neutron monitor data for the period from 1964 to 1974. Munakata et al. (1979) showed that there is a significant correlation between cosmic ray intensity and solar wind velocity. Fujimoto et al. (1983) pointed out that the solar wind effect depends on the solar activity ; its regression coefficient is about -0.8% per 100 km s^{-1} in the maximum activity and -0.2% per 100km s^{-1} in the minimum and the average value over a solar cycle is the same as the coefficient obtained by Iucci et al. (1979).

In the above-mentioned analysis, they used daily mean values for cosmic ray intensity and solar wind velocity. In the present paper, we tried to confirm whether the regression coefficient is determined irrespectively of the time interval of averaging,τ, or not. Cosmic ray intensity is varying sometimes in relation with the solar rotation, while the dominant periodicity in solar wind velocity is of 13.5 days. Then, the regression coefficient was examined for the averaging time interval from $\tau=1$ day to 91 days, covering the wide range around 27 or 13.5 days.

2. Analysis and Result

Data used for the present analysis are daily mean values of neutron intensity at Kiel (1965-78) and Deep River (1965-76). These values (I,%) are measured from their one-year running average level to eliminate the long term variation, they are divided by a time interval τ, and a time series of τ-day averages $\langle I\rangle_{\tau,i}$ $(i=1,2,\ldots.n)$ are arranged. Then, the correlations between cosmic ray intensity $\langle I\rangle_{\tau,i}$ and the corresponding averages $\langle V\rangle_{\tau,i}$ of solar wind velocity are caluculated for various values of τ. Fig. 1 shows the τ-dependence of the regression coefficient (β_τ) of $\langle I\rangle_{\tau,i}$ to $\langle V\rangle_{\tau,i}$. It is clearly seen in the figure that the absolute value of β_τ increases monotonously with τ and becomes almost constant for $\tau>27$ days. The numerical values of β_τ and of the correlation coefficient r_τ are listed in Table 1, in which the error for β_τ is of significance level of 67 %.

Next, data at Kiel are divided into two groups corresponding to the solar activity, that is, a group for the period of the solar maximum (1966-72) and another for the period of the minimum (1973-77). For both the groups the τ-dependence of β_τ are analyzed. Fig. 2 shows the result and one can see that the critical time intervalτ_c beyond which β_τ becomes constant is different from each other between both the periods of the solar maximum and the minimum.

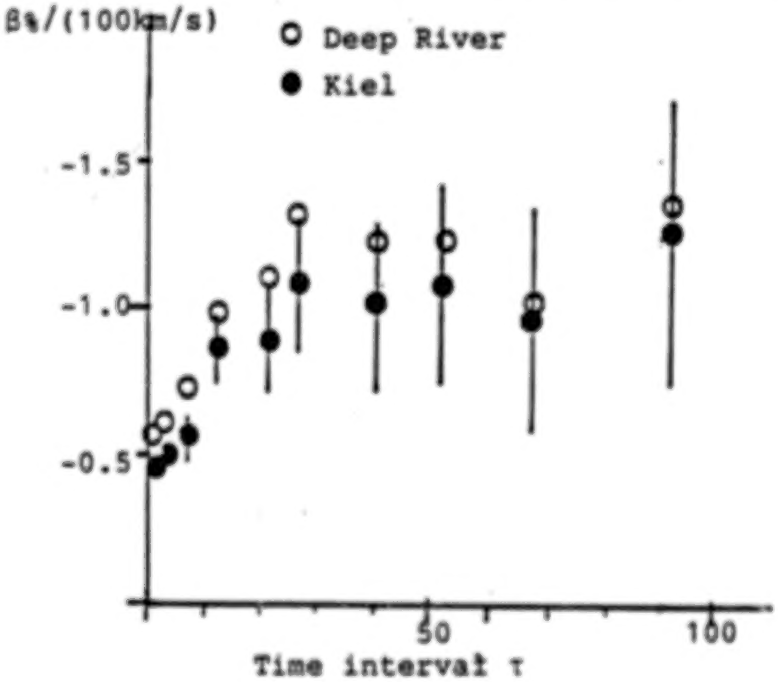

Fig. 1
The regression coefficients as a function of the time interval τ

Table 1 τ-dependence of the regression coefficient (β%/(100km/s)) and of the correlation coefficient (r) of neutron intensity to solar wind velocity, for Kiel (1966-1977) and Deep River (1965-June 1976). n expresses the number of independent data.

		KIEL			DEEP RIVER	
τ (days)	n	β_τ	r_τ	n	β_τ	r_τ
1	3585	-0.45±0.024	-0.29	2687	-0.57±0.031	-0.33
3	1226	-0.49±0.044	-0.30	925	-0.61±0.056	-0.33
7	545	-0.56±0.081	-0.28	406	-0.72±0.10	-0.32
13	301	-0.86±0.13	-0.35	223	-0.98±0.17	-0.35
21	184	-0.88±0.20	-0.31	136	-1.10±0.27	-0.33
27	145	-1.07±0.25	-0.33	107	-1.30±0.34	-0.34
41	97	-1.00±0.31	-0.31	73	-1.20±0.45	-0.30
51	78	-1.07±0.38	-0.30	59	-1.21±0.53	-0.29
67	60	-0.95±0.41	-0.29	45	-0.98±0.56	-0.26
91	45	-1.22±0.49	-0.35	34	-1.33±0.68	-0.32

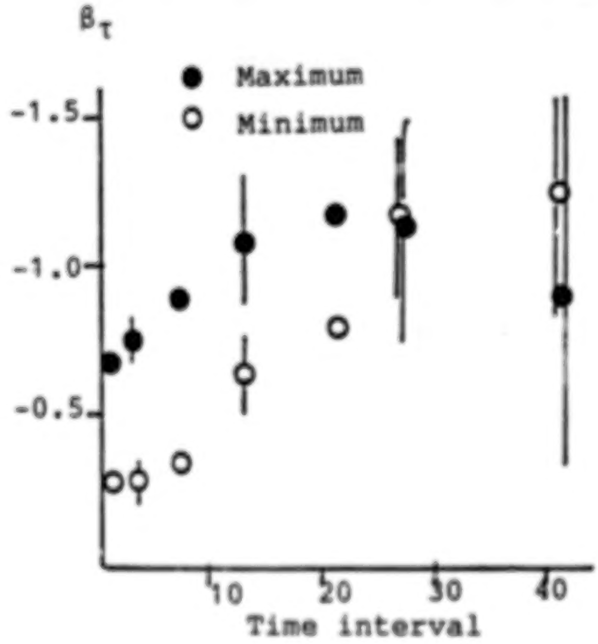

Fig. 2
The regression coefficient (β_τ) as a function of the time interval τ.
Solid circle is β_τ in the maximum period (1966-72) and open circle is β_τ in in the minimum (1973-77).

3. Discussion and Conclusion

As can be seen in Fig. 1, the absolute value of the regression coefficient of neutron intensity to solar wind velocity increases with τ and becomes almost constant for $\tau>27$ days. As the conclusion, at first, we like to emphasize that the regression coefficient has the τ-dependence; the coefficient β_{27} is twice as large as β_1 in magnitude.

The τ-dependence of the correlation can be interpreted when we suppose that the variation of cosmic ray intensity at the earth is reflecting the integrated effect of electromagnetic condition over the interplanetary space within a distance r_c $(=V\cdot\tau_c)$ from the earth. The variations of cosmic ray intensity with periods shorter than T_c $(=k\cdot\tau_c)$ give little contribution to the variation of $\langle I\rangle_\tau$, while the variations with periods longer than T_c contribute to the intensity variation, where k is a constant close to unity. Therefore the effect β is expected to increase with τ up to τ_c, and the effect does not vary so much with τ beyond τ_c.

Second, as seen in Fig. 2, the τ-dependence of the correlation varies with the solar activity. The critical time interval τ_c is shorter than 27 days in the solar maximum and is fairly shorter than the critical interval in the solar minimum.

Why the regression coefficient depends so much upon the solar activity has been left as a question which we shall solve, since we pointed out that dependence in Bangalore Conference. In the previous paper we showed that the coefficient varies over a wide range from -0.2 % per 100km s^{-1} at the solar minimum to -0.8 % per 100km s^{-1} at the solar maximum. Fig. 2 also shows the same dependence. If such a wide variation of the coefficient could be explained by particle diffusion coefficient varied with the solar activity, it would be necessary to consider the diffusion coefficient varying by a factor 2 between the solar minimum and maximum. Such a big change of the diffusion coefficient, however, can not be accepted in the comprehension of the eleven-year cosmic ray intensity variation. Therefore, it will be necessary to connect the solar wind effect β with the above-mentioned change of τ_c through the solar cycle.

Acknowledgment

We express thanks to prof. Nagashima for his variable discussion and suggestions.

References

Duggal, SP. and Pomerantz, MA.,
15th ICRC, Plovdiv, 4, 370 (1977)
Iucci, N., Parisi, M., Storisi, M. and Villoresi, G.,
16th ICRC, Kyoto, 3, 491, 496 (1979)
Munakata, Y. and Nagashima, K.,
16th ICRC, Kyoto, 4, 530 (1979)
Fujimoto, K., Kojima, H. and Murakami, K.,
18th ICRC, Bangalore, 3, 267 (1983)

N85-35067

SH 5.1-14

A RELATION BETWEEN THE SHORT TIME VARIATIONS OF COSMIC RAYS AND GEOMAGNETIC FIELD CHANGE

Takasuke SAKAI and Masahito KATO

Physical Science Laboratories,
College of Industrial Technology, Nihon University,
Shin-ei, Narashino-shi, 275, Japan

ABSTRACT

First, we report an event of ~37min. periodicity in cosmic ray intensity observed at Akeno(38°47'N, 138°30'E, 900m above s.l., cutoff 10.4 GV) during 1300-1900 UT on April 25th, 1984, just a day before Forbush decrease of April 26th. This event seemed to be followed by the periodic variations of the geomagnetic field observed at Kakioka(36°23'N, 140°18'E). The regression coefficient between them was obtained ~-0.07%/10nT.

Second, we show that in general the power spectral density of cosmic rays in the frequency of 10^{-4}-10^{-3}Hz correlates positively with the fluctuations of geomagnetic field(Dst field) around ~1.2×10^{-4}Hz. From the analysis of 47 days data(April 14th to June 13th, 1984), the regression curve was obtained as $y=0.275x^{0.343}$ with the correlation coefficient of 0.48, where x and y mean Fourer components of Dst field summed over 1.04 ~1.39×10^{-4}Hz and cosmic ray power spectral density averaged over 10^{-4}-10^{-3}Hz respectively.

1.Introduction. Dhanju and Sarabhai(1967, 1969) first discussed the cosmic ray power spectrum. They showed that the general frequency dependence of the power spectra in the frequency range of 10^{-6}-10^{-3}Hz and also several periodicity in 1.67-8 $\times10^{-3}$Hz. But Fujii et al(1975) argued against their result obtained in 10^{-4}-10^{-3}Hz. Theoretically, Owens and Jokipii(1972,1974), Toptygin and Vasilijev(1977) discussed the power spectra in the relation to the random magnetic field in the interplanetary space or in the magnetosheath. However, the validity of their model are limitted to the frequency range less than ~10^{-5}Hz.

On the other hand, the existence of short time variations of cosmic rays(10^{-4}-10^{-3}Hz) are reported by several authors by the exhibition of the enhancement in the power spectra after subtracting the poisson noise level or clear vissible oscillations in cosmic ray counting rates(Slade,1972; Kodama et al.,1975; Kozlov et al., 1975; Attolini et al.,1979; Debrunner et al., 1983). However, no clear relation to some other interplanetary or geomagnetic field parameters(e.g., Kp, Dst etc.) has been found.

In this paper, at first, we briefly report the periodic variations of cosmic ray intensity of ~37min. period observed on April 25th, 1984, which seems anticorrelated well to the geomagnetic field change observed at Kakioka(Sakai et al., 1985).

The above event may suggest that the cosmic ray power spectral density around 10^{-4}-10^{-3}Hz are affected by the fluctuations of geomagnetic field, especially Dst field around the same frequency. Thus, we analysed both data of 47days and found that the level of cosmic ray power spectral density in the frequency range of 10^{-4}-10^{-3}Hz are related to the Dst field around 10^{-4}Hz with the correlation coefficient of 0.48.

2. Results. We show 3 minute data of cosmic rays, together with the H-component of the geomagnetic field observed at Kakioka from the time of 1200 to 1900 UT on April 25th in Fig.1. In the figure, errors of the cosmic ray are derived from counting rates.

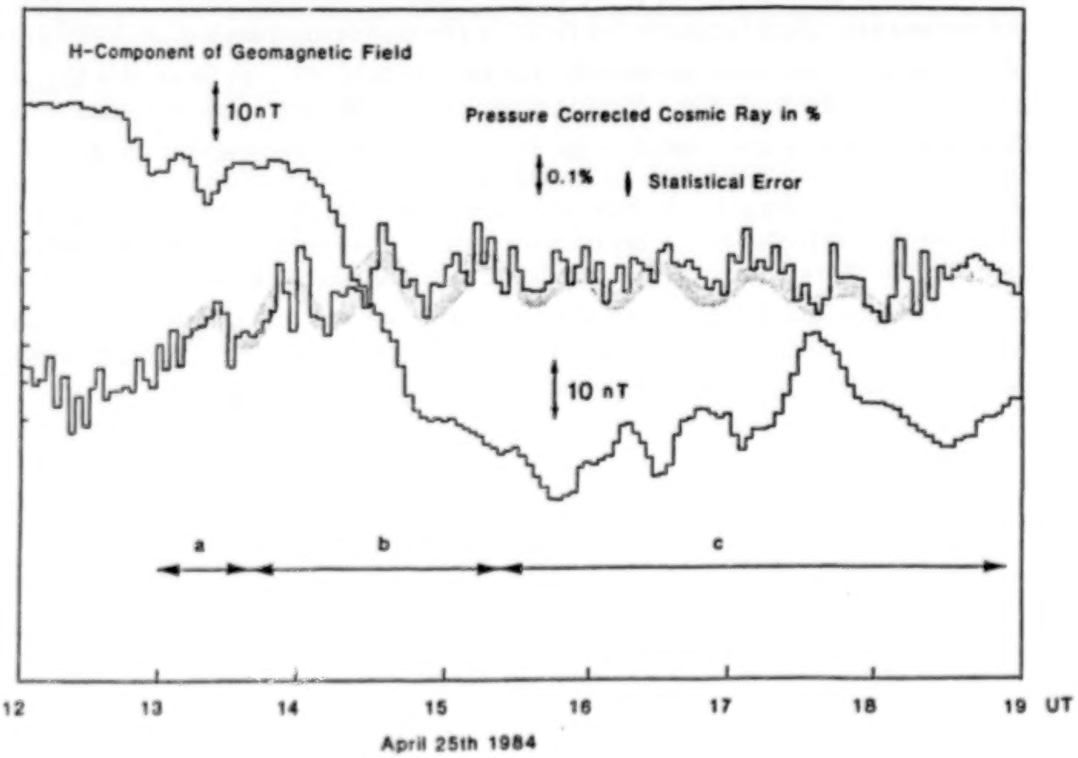

Figure 1. The cosmic ray data of 3 minute value are plotted together with the H-component of the geomanetic field observed at Kakioka from the time period of 1200 UT to 1900 UT on April 25th. The clear oscillations of the cosmic ray counting rates (dotted screen) are seen in anti-correlation with the H-component.

It is clear from the figure that, as shown by a wavy dotted screen, the counting rate of cosmic rays oscillates in anti-correlation with the change of the H-component, especially in the intervals indicated with a letter a and c in the figure. During the time of 1600 -1700 UT, the oscillating part of the geomagnetic field has an amplitude of -10nT in p-p(peak-to-peak). At the same time, the counting rates of cosmic rays change -0.07% in p-p, almost out of phase with the change of the H-component.

From this, we can estimate changing ratio (hereafter refferd to as geomagnetic coefficient) of cosmic rays to the H-component at -0.07%/10nT. More detail discussion are seen in Ref.10.

Also, we can estimate a value of the geomagnetic coefficient following Obayashi(1961) by supposing that the cosmic ray counting rates may be changed by the change of cut off rigidities due to Dst field. The obtained geomagnetic coefficient was -0.3%/10nT. This may be consistent with the observed value if we consider that we don't know about Dst field shorter than 1-hour data. Thus, it seems reasonable that the observed oscillations in cosmic ray counting rates with the period of ~37 min. are mainly due to the change of geomagnetic field.

Further, if we suppose that the above good relationship between cosmic ray intensity and geomagnetic field (probably Dst field) in the frequency range of 10^{-4}-10^{-3}Hz in general exist for not only special days, but also all days, we come to an idea that the power spectral density in the frequency of 10^{-4}-10^{-3}Hz may closely related to the fluctuation of Dst field around the same frequency range. We analysed the data of 47 days through April 14th to June 13th, 1984. The power spectral density of cosmic rays are calculated by using 1-min. data on each day. On the other hand, the data of Dst field, which is available for us, are unfortunately 1-hour data only. 24 data points for a day are too short to get a significant power spectral density around ~10^{-4}Hz. Hence we Fourier analysed 1-day Dst field after running average of 5 hours. and computed the components corresponding to the frequency of 1.04 ~1.39 x 10^{-4}Hz. Fig.2 shows a correlation between the cosmic ray power spectral density averaged

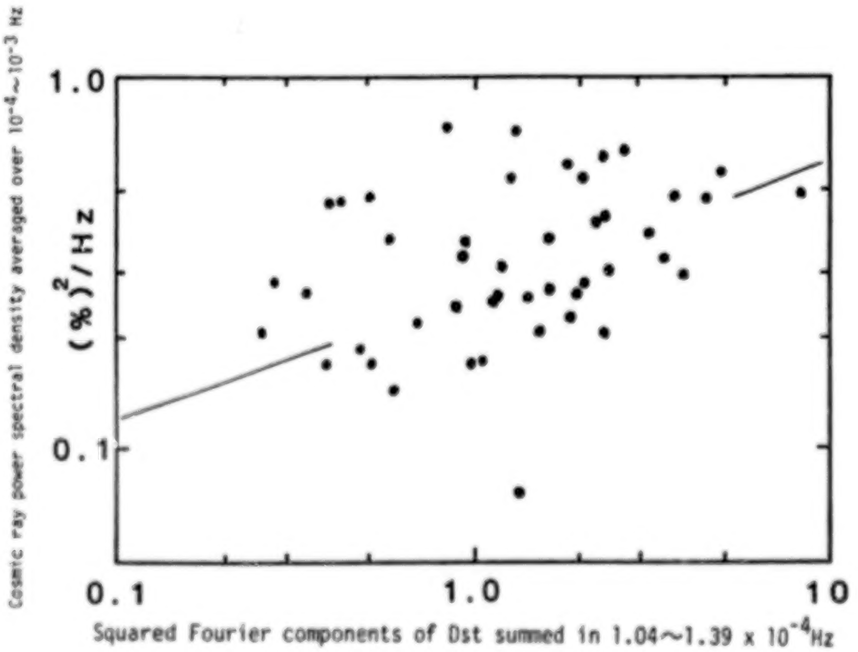

Figure 2. Cosmic ray power spectral density averaged over 10^{-4}~10^{-3} Hz (= y) v.s. squared Fourier components of Dst summed over 1.04~1.39 x 10^{-4} Hz (= x) are shown. The days of analysis are from April 14th to June 13th, 1984. The regression curve is expressed by $y = 0.275\ x^{0.343}$ with the correlation coefficie-t of 0.48.

over 10^{-4}-10^{-3}Hz (=y) and the Fourier components summed in the frequency of 1.04-1.39×10^{-4}Hz (=x). The relation is expressed by the power law of $y=0.275x^{0.343}$ with the correlation coefficient of 0.48.

3. Conclusions.

1) ~37 minutes periodical oscilations with amplitude of ~0.1% in p-p was observed during the time of 1300 to 1900 UT on April 25th, 1984. This oscilation seems to have good correlation with the geomagnetic field change at Kakioka. The geomagnetic coefficient is ~-0.07%/10nT, consistent with the theoretically estimated value. Hence we conclude that the oscilation occured by the change in cut off rigidities due to Dst field.

2) From the fact of 1), we can expect that the power spectral density of cosmic rays in the frequency range of 10^{-4}-10^{-3}Hz is partly caused by the fluctuation of Dst field. Hence we examined the relation between the power density of cosmic rays and the fluctuations of Dst field around 10^{-4}-10^{-3}Hz by using 1 minute data and 1 hr data respectivery. The regression curve is expressed by $y=0.275x^{0.343}$ with the correlation coefficient of 0.48.

3) From 2), the power spectral density of cosmic rays in the frequency range of 10^{-4}-10^{-3}Hz may be one of good indicators of the fluctuations of Dst field at the same frequency.

4) More reliable conclusion about the correlation will be obtained by increasing day of analysis and also by using other stations.

4. Acknowlegements. The authors wish to thank to Prof. Kamata, Prof. Tanahashi and also their colleagues for facilitating the apparatus at Akeno observatory.

5. References.

1. Debrunner, H., et al., *18th Intern. Cosmic Ray Conf. Bangalore*, **3**, 257, 1983.
2. Dhanju, M.S. and V. A. Sarabhai, *Phys. Rev. Lett.*, **19**, 252, 1967.
3. Dhanju, M.S. and V. A. Sarabhai, *11th Intern. Cosmic Ray conf. Budapest*, **2**, 237, 1969.
4. Fujii et al., *13th Intern. Cosmic Ray Conf. Denver*, **2**, 783, 1973.
5. Kato, M., T. Sakai, and M. Wada, *16th Intern. Cosmic Ray Conf. Kyoto*, **5**, 1, 1979.
6. Kodama, M., et al., *13th Intern. Cosmic Ray Conf. Denver*, **3**, 803, 1973.
7. Kozlov, V. I. and N. P. Chirkov, *14th Intern. Cosmic Ray Conf. Munchen*, **3**, 1129, 1975.
8. Obayashi, T., *J. Geomag. Geoelectr.*, **13**, 26, 1961.
9. Slade, D. V., *12th Intern. Cosmic Ray Conf. Hobart*, **3**, 876, 1971.
10. Sakai, T., and M. Kato, *J. Geomag. Geoelectr.*, **37**, 61, 1985.

ORIGINAL PAGE IS
OF POOR QUALITY

SH 5.1-15

ANOMALOUS LOW LEVEL OF COSMIC RAY INTENSITY DECREASES OBSERVED DURING 1980

N85-35068

A.K.Jain, P.K.Pandey and S.P.Agrawal
Physics Department(Vikram Space Physics Centre)
A.P.S.University,Rewa (M.P.) 486003, India

ABSTRACT

Past studies have revealed solar cycle changes in the sunspot activity, as well as in many other solar parameters, such as, solar flares and solar coronal holes. These solar features in turn produce the observed cyclic variations in the interplanetary plasma and fields. Both the cosmic ray intensity as well as the intensity of geomagnetic disturbances are affected by the interplanetary changes and produce 11/22 years periodicity. During the period of high solar activity, solar flares are more abundent, and are expected to produce large Forbush type cosmic ray decreases as well as intense geomagnetic disturbances. An anomalous situation has been noticed during the year 1980 (period of high sunspot activity), when both the geomagnetic disturbance index Ap, as well as the magnitude and number of Forbush decreases are small. Such an anomaly occurs, inspite of the fact that both the sunspot numbers and the energetic solar flares are almost maximum during the present solar cycle. Further investigations reveal that the observed solar flares in 1980 are also situated in favourable longitudes, and hence the cause for such an observed anomalous low values of Ap and the cosmic ray decreases, is presently not understood.

1. Introduction.

The long term variation in the solar activity is generally represented by sunspot numbers, which shows a recurrent tendency with a period of eleven years. Many other associated solar parameters, such as solar flares, coronal holes, also show 11/22 year cyclic variations (see e.g. review, Rao, 1972). Intense solar flares generally produce high speed solar wind streams, which in turn produce geomagnetic disturbances as well as significant decreases in cosmic ray intensity (see, e.g. review, Lockwood, 1971; Agrawal and Singh, 1976). It is therefore, expected that more number of Forbush decreases with larger magnitudes should be observed during the period of high solar

ORIGINAL PAGE IS
OF POOR QUALITY

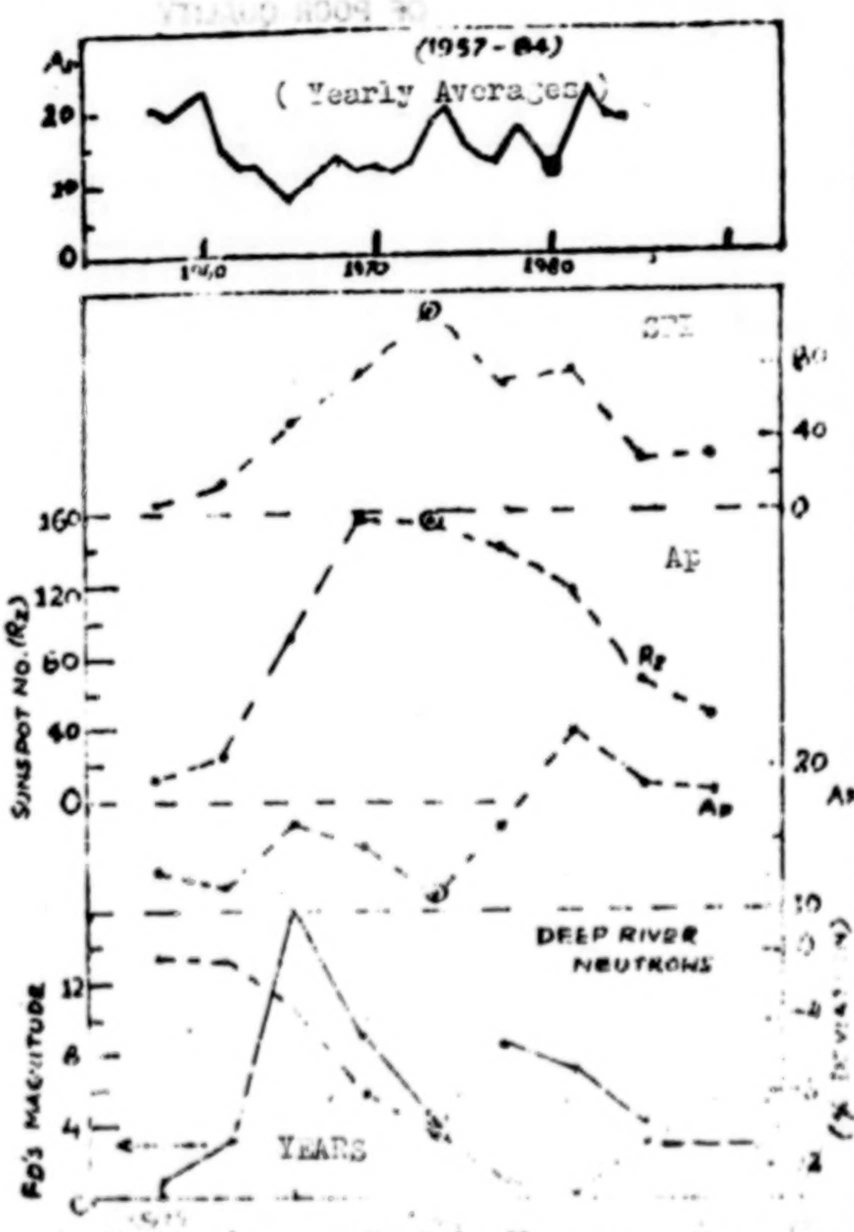

Fig. 1 (top) shows the yearly average variation of the geomagnetic disturbance index Ap, for the years 1957-84. The values for the year 1980 is encircled in this plot as well as in other plots of this figure to clearly identify the anomaly. (bottom) The yearly average values of the solar flare index (see text for details for the computation of SFI), The sunspot number, the Ap index, the Forbush decrease index (see text for details), and the cosmic ray intensity deviation from its max. value observed during Sept.-Nov. 1976, are also shown in the fig. for the years 1976-84. In some cases, the average values for 1984 are derived from 8-10 months data.

activity (e.g. 1979-81). Moreover, the geomagnetic disturbance index Ap should also be high during such periods. In this context, an anomalous situation is observed during the year 1980, when both the Ap index, as well as the number and magnitude of Forbush decreases are quite low. In this paper, we investigate this anomaly to understand, why larger number of energetic solar flares observed in the year 1980 are in-effective in producing geomagnetic disturbances as well as Forbush decreases.

ORIGINAL PAGE IS
OF POOR QUALITY

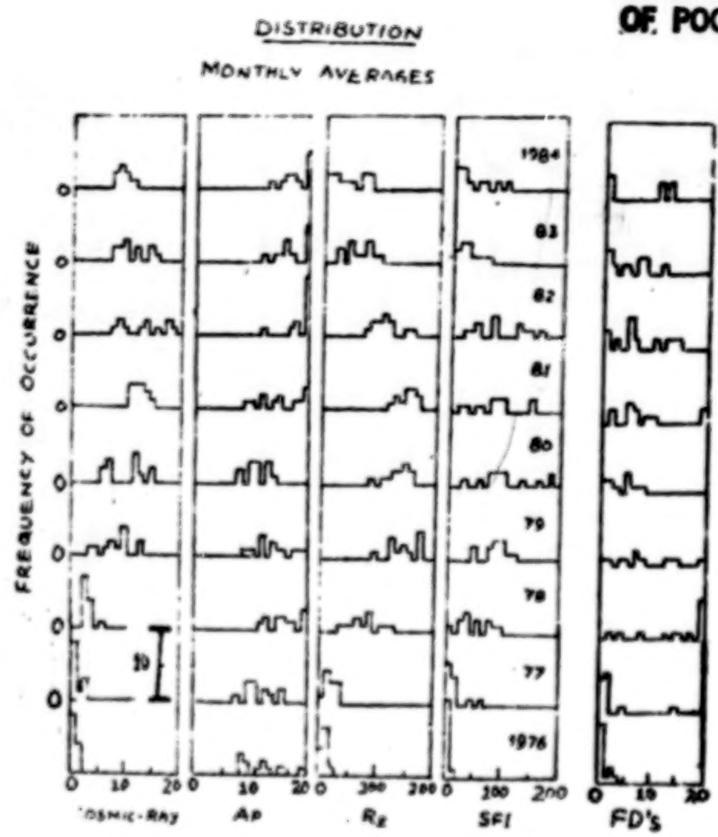

Fig.2 Shows the distribution of monthly averages for all the five parameters for which the yearly averages are shown in figure I. The anomalous low value of Fd's and of Ap index, for the year 1980, is clearly evident.

2. Computation of solar flare and Forbush decrease index.

In another paper (SH 4.4-12) we have described the computation of the solar flare index (S.F.I.) from the list of observed energetic solar flares of importance ≥1, published in prompt reports of solar Geophysical Data. Briefly, SFI has been computed by giving weight to the importance of the solar flare by its numerical value, and also by considering weights for the brightness of the flare. Similarly, the Forbush decrease index has been computed for each month, by numerically adding the magnitude of all the Forbush decreases observed in that month. A decrease in cosmic ray intensity is considered only when its magnitude is ≥1.5%, and the decrease is clearly seen in at-least two high latitude neutron monitor stations. The derived Fd's index has been denoted as Fd's Σmagnitude, and has been used in the diagrams presented later in this paper.

3. Results and Discussion.

The long-term variation of the geomagnetic disturbance index Ap for the years 1957-84 is plotted in figure 1 (top portion of the figure). We note that the yearly average value of Ap index is quite low during the year 1980. The plot

ORIGINAL PAGE IS
OF POOR QUALITY

also shows the minimum value of Ap observed during 1965, the year of minimum solar activity. Other solar and geophysical parameters are plotted in the bottom part of figure 1. Both, the sunspot numbers, as well as the solar flare indices are at their peak value during the year 1980, whereas the Ap index is at its minimum value. We also note that the long term cosmic ray intensity decrease shows a smooth decline starting in 1977 with a minimum in 1982. However, the Forbush decrease index shows a very low value in 1980 as compared to the adjacent values. Thus the low values of Ap and Fd's are quiet anomalous, particularly when one observes the large number of energetic solar flares represented by SFI. To further analyse the distribution of the five parameters represented in figure 1 on yearly basis, we have generated a frequency histogram for each year, and for each parameter, using their monthly values. Such a distribution is plotted in figure 2, for the years 1976-84. Thus, even on a monthly average basis the anomaly of the low values of Ap index, as well as of the Fd's is apparent. To ascertain that the low values of Ap index and of Fd's during 1980, is not due to any large asymmetry in the longitudnal distribution of the solar flares, we have plotted in figure 3, the frequency histrogram for all the solar flares of importance ≥ 1. From the figure, it is seen that there is no deficiency in the number of solar flares in the longitude region 60° East to 30° West for the year 1980, as compared to the years 1979 and 1981. Such an observation, therefore, rules out the possibility, that the solar flares during 1980 are unfavourably placed to be geoeffective. From the results presented here, we therefore note that even-though we have demonstrated the anomaly in terms of low geo-effectiveness of the energetic solar flares during 1980, however, we have not been able to identify the cause for such an anomaly. It is expected that other characteristics of the cosmic ray time variation might be able to provide some clue to understand the reported anomaly.

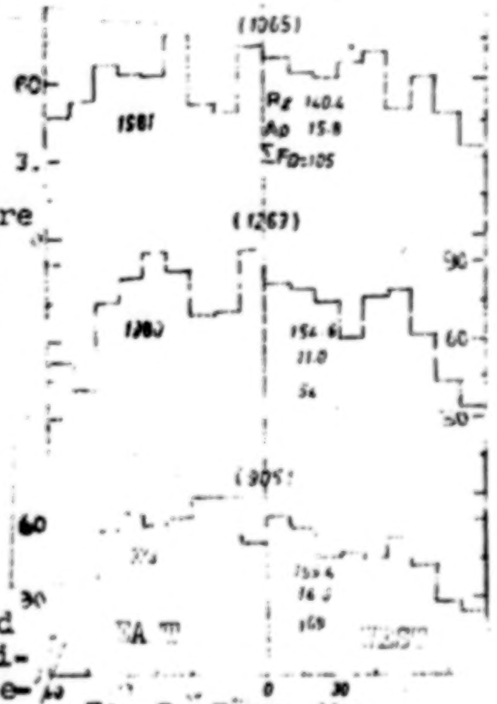

Fig.3 Shows the frequency distribution with heliolongitude of the individual solar flares of importance ≥ 1, for the years 1979,80 & 81. The yearly average values of Rz, Ap and Fd index (Σ Fd) are also mentioned in the fig. alongwith the total number of solar flares for each year.

4. References.

Agrawal, S.P. and Singh, R.L., 1976, Ind.J.Radio & Sp.Phy.5 p.330.
Lockwood, J.A., 1971, Space Sci. Rev. 12 p.658.
Rao, U.R., 1972, Space Sci. Rev. 12 p.719.

N85-35069

SH 5.1-16

OBSERVATIONS OF COSMIC-RAY MODULATIONS IN THE FALL 1984

Torsti, J.J., Nieminen, M., Valtonen, E., Arvela, H.,
Lumme, M., Peltonen, J., and Vainikka, E

Wihuri Physical Laboratory, University of Turku,
and Department of Physical Sciences, University
of Turku, SF-20500 Turku, Finland

ABSTRACT

Modulation of cosmic-ray energy spectrum was studied by using the Turku double neutron monitor. The multiplicity region of detected neutrons produced by cosmic ray hadrons in the monitor was divided into seven categories corresponding to mean energies 0.1, 0.3, 1.0, 3.2, 8.6, 21, and 94 GeV of hadrons at sea level. Based on 24-hour frequencies, a statistical analysis showed that modulation of the intensity in all categories occurred during several periods in the fall 1984. The magnitude of the variation was a few per cent.

1. Introduction. The Turku double neutron monitor enables studies of modulation of energy spectrum of cosmic-ray hadrons. The accuracy of the modulated spectrum, particularly at high energies, is dependent on the duration of the disturbance. Measurements at high energies can be made reliably only in such cases when the disturbance continues for a few days.

In this work, cosmic-ray modulation in the time scale of several days is studied. In order to eliminate the daily variation, 24-hour frequencies of neutron multiplicities were used as the basic data. In order to cover a wide energy range, counting rates of multiplicities from 1 to 200 were analysed.

The present preliminary analysis concerns measurements accomplished during the period from September 1, 1984 to January 8, 1985. No drastic variation of cosmic-ray intensity, such as large Forbush decreases or proton flares, occurred during this period.

2. Cusum plots. The analysis is based on cumulative-sum of observed frequencies in neutron monitor. The entire multiplicity range was divided into seven categories as shown in table 1. The average daily counting rates, f_{ave}, are also given in the table. The median hadron energies represent estimates based on a Monte Carlo model of hadron cascades in the atmosphere and in the monitor /2/.

The daily counting rates in categories 5-7 are so small that the statistical error is more than 1 %. Therefore, it is quite difficult to see from the simple frequency versus time plot whether there exists systematic variation in the course of time. In purpose to separate the real modulation from statistical fluctuations, we use cumulative-sum curves of relative frequencies:

Table 1. Daily counting rates, f_{ave}, and median energies of cosmic-ray hadrons in the Turku double neutron monitor

category	neutron multiplicities	f_{ave} (events/day)	median hadron energy (GeV) at sea level	median hadron energy (GeV) in free space
1	1	786 700	0.1	16
2	2-4	400 300	0.3	24
3	5-8	88 800	1.0	70
4	9-16	16 900	3.2	160
5	17-24	2 890	8.6	310
6	25-48	864	21	540
7	49-200	304	94	1100

$$F_K = \sum_{k=1}^{K} \frac{f_k - f_{ave}}{f_{ave}} \qquad \text{for all days } K = 1,\ldots,122 \;,$$

where f_k represents the pressure-corrected observed frequency for day k . The cusum curves for six multiplicity categories are given in fig. 1.

It is seen that the cusum curves show certain similarities. Changes in the slopes of the curves occur approximately at the same time. The absolute magnitude of the variation tends to increase with increasing multiplicity.Noteworthy is that the curve of the highest category (49-200) shows systematic variation.

3. Periods of constant counting rates. The statistical cusum test reveales which changes in the cusum plots are significant /1/. The risk level of 5 % was used. In the case of the September data, the cusum test showed that multiplicity categories 2, 3, and 4 had two significant changes. The first occurred on the 5th and the second on the 12th of September. In category 1, no statistically significiant changes were found.

Between October 2nd - January 8th, the significance test revealed 4-11 slope changes. The smallest number of changes was obtained in category 7. The poor statistics is a more probable explanation for the small number than physical reasons.

Based on the results obtained from categories 2-4, we conclude that during the following nine periods the daily frequencies do not show significiant changes, i.e., the counting rates can be considered at least roughly constant:

I: September 1-5
II: September 6-12
III: September 13-23
IV: October 2-5
V: October 6-12
VI: October 13 - November 1
VII: November 2-22
VIII: November 23 - December 31
IX: January 1-8

These intervals are shown in fig. 1 by dotted lines.